

Final Report: Evaluation of Rainfall-Runoff Trends in the Upper Colorado River Basin (Phase Two)

**TWDB Contract Number
1800012283**

Prepared By

Jordan Furnans, Ph.D., P.E., P.G.
Michael Keester, P.G.
LRE Water, LLC

Kirk Kennedy, P.G.
Kennedy Resource Company

Pursuant to Senate Bill 1 as approved by the 85th Texas Legislature, this study report was funded for the purpose of studying environmental flow needs for Texas rivers and estuaries as part of the adaptive management phase of the Senate Bill 3 process for environmental flows established by the 80th Texas Legislature. The views and conclusions expressed herein are those of the author(s) and do not necessarily reflect the views of the Texas Water Development Board.

September 26, 2019

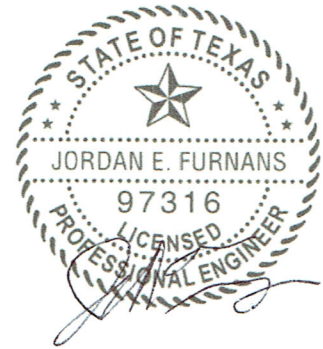
This page is intentionally blank.

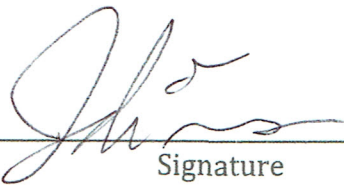
Geoscientist and Engineer Seals

The Texas Water Development Board contracted with LRE Water, LLC, a licensed professional geoscientist firm (Texas License No. 50516) and licensed professional engineering firm (Texas License No. 14368). This report documents the work of the following licensed professional geoscientists and licensed professional engineers in the State of Texas:

Jordan Furnans, Ph.D., P.E., P.G.

Dr. Furnans was the Project Manager for this work and was responsible for all phases of the project.





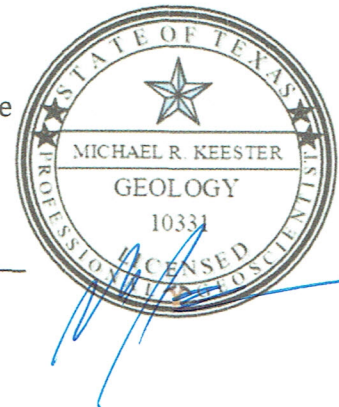
Signature

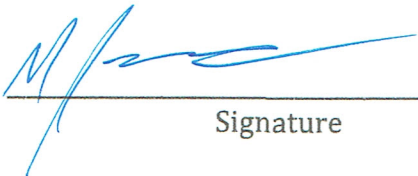


Date

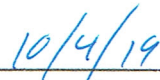
Michael Keester, P.G.

Mr. Keester was responsible for investigating the impact of groundwater on streamflow reductions, and in developing the soil-water-balance modeling which guided project efforts.





Signature



Date

Table of Contents

1	Executive Summary	1
1.1	Materials and Methods.....	1
1.2	Trend Analysis Results.....	2
1.2.1	General Temperature Trends for the Study Area Watersheds.....	2
1.2.2	General Precipitation Trends for the Study Area Watersheds.....	3
1.2.3	General Streamflow Trends for the Study Area Watersheds.....	4
1.2.4	General Soil Moisture Trends for the Study Area Watersheds.....	4
1.2.5	General Land use/Lad Cover Trends for the Study Area Watersheds.....	4
1.3	Non-Statistical Investigation Results	5
1.3.1	Small Pond Analysis for the Study Area Watersheds.....	5
1.3.2	Streamflow Depletion Due To Groundwater Pumping	5
1.3.3	Noxious Brush Identification and Extent Quantification.....	6
1.3.4	Relating Soil Moisture Fluctuations to Runoff	6
1.4	UCWBM Methodology and Results.....	6
1.5	Conclusions.....	7
1.6	Recommendations.....	8
2	Introduction	9
3	Task 1 – Literature Review & Methodology Assessment	14
3.1	Reference Articles.....	14
3.1.1	Crooks and Kay (2015).....	14
3.1.2	Duan et al. (2017).....	14
3.1.3	McAfee et al. (2017).....	15
3.1.4	Woodhouse et al. (2016)	15
3.1.5	Xia et al. (2012)(a).....	15
3.1.6	Xia et al. (2012)(b)	15
3.2	Mann-Kendall Trend Analysis Methods.....	16
3.3	Revision & Updating of Phase I Results.....	21
3.3.1	Updated Study Site Information for Phase II Analysis.....	22
3.3.2	Updated Information for Other Study Sites from Phase I	26
3.3.3	LRE Water’s Opinion regarding Cumulative Mass Plots.....	26
4	Task 2 – Remote Sensing Analysis.....	27
4.1	Small Impoundment Analysis.....	27
4.1.1	National Hydrography Dataset (NHD).....	28
4.1.2	Google Earth Engine (GEE).....	32
4.1.3	US Geological Survey Topographic Maps	34
4.1.4	Manual Data Analysis Using Google Earth (GE).....	35

4.1.5	National Inventory of Dams – NID.....	38
4.2	Small Impoundment Results.....	39
4.3	Noxious Brush & Land Use Analysis.....	46
5	Task 3 – Temperature Trend Analysis.....	54
5.1	Elm Creek Watershed.....	56
5.1.1	Temperatures for Ballinger, TX.....	56
5.1.2	Temperatures for Abilene, TX.....	62
5.2	San Saba Watershed.....	67
5.2.1	Temperatures for Brady, TX.....	69
5.2.2	Temperatures for Eldorado.....	74
5.3	South Concho Watershed.....	79
5.3.1	Temperatures for San Angelo, TX:.....	82
5.4	North Concho Watershed.....	87
5.4.1	Temperatures for Big Spring, TX:.....	91
5.4.2	Temperatures for Sterling City, TX.....	95
5.4.3	Trend Comparisons within the North Concho Watershed.....	99
5.5	Temperature Analysis - Summary.....	101
6	Task 4 – Streamflow Trend Analysis.....	103
6.1	Elm Creek Watershed.....	104
6.2	San Saba Watershed.....	106
6.2.1	San Saba River at Menard.....	106
6.2.2	Brady Creek at Brady.....	108
6.2.3	San Saba River at San Saba.....	111
6.3	South Concho Watershed.....	113
6.4	North Concho Watershed Flow Analysis.....	114
6.5	Streamflow Trend Analysis Summary.....	117
7	Task 5 – Precipitation Trend Analysis.....	119
7.1	Full Precipitation Record Analysis.....	121
7.1.1	Elm Creek Watershed.....	121
7.1.2	Elm Creek Watershed Precipitation Summary & Comparison.....	124
7.1.3	San Saba Watershed.....	125
7.1.4	South Concho Watershed.....	129
7.1.5	North Concho Watershed.....	134
7.2	Runoff-Generating Precipitation Trend Analysis.....	143
7.2.1	Elm Creek Watershed – Ballinger.....	144
7.2.2	San Saba Watershed – San Saba.....	146
7.2.3	South Concho Watershed – Christoval.....	148
7.2.4	North Concho Watershed – Sterling City.....	151

7.3	Precipitation Trend Summary.....	153
8	Task 6 – Soil Moisture Data Analysis.....	154
8.1	GRACE Data Analysis.....	154
8.2	Google Earth Engine (GEE) Analysis	162
8.3	Soil Water Balance Modeling.....	165
8.3.1	SWB Model Domain and Input Data	165
8.3.2	SWB Model Results	169
9	Task 7 – Groundwater Level Evaluations.....	178
9.1	Shallow Groundwater Flow System.....	178
9.2	Regional Groundwater Flow System.....	191
9.3	Baseflow Analysis	197
9.3.1	Elm Creek Watershed	197
9.3.2	San Saba Watershed	199
9.3.3	South Concho Watershed	205
9.3.4	North Concho Watershed.....	206
9.4	Groundwater Analysis Summary	209
10	Task 8 – Demonstrating Cause and Effect Regarding Rainfall/Runoff Response.....	210
10.1	Methodology	210
10.1.1	UCWBM modeling of rainfall quantity and timing	211
10.1.2	UCWBM modeling of Land Use/Land Cover	211
10.1.3	UCWBM modeling of Small Impoundments.....	214
10.1.4	UCWBM operation.....	214
10.2	UCWBM Results – Full Simulation.....	217
10.2.1	UCWBM results for the Elm Creek watershed	217
10.2.2	UCWBM results for the San Saba Watershed.....	219
10.2.3	UCWBM results for the South Concho Watershed	221
10.2.4	UCWBM results for the North Concho Watershed	223
10.3	UCWBM results – By Watershed Parameter	225
11	Summary and Conclusions.....	227
12	Recommendations.....	230
13	Acknowledgements.....	231
14	References.....	232
15	Appendices.....	A-1

List of Figures

Figure 2-1 – Comparison of rainfall and runoff during the 1947-1957 and 2008-2016 drought periods – Elm Creek watershed.	10
Figure 2-2 – Comparison of rainfall and runoff during the 1947-1957 and 2008-2016 drought periods – San Saba River watershed.	11
Figure 2-3 – Comparison of rainfall and runoff during the 1949-1957 and 2008-2016 drought periods – South Concho River watershed.	12
Figure 2-4– Comparison of rainfall and runoff during drought conditions – North Concho Watershed.	13
Figure 3-1 – Sample dataset showing trends identified by the Mann-Kendall analysis –	19
Figure 3-2 Cumulative mass plot for study site #7 - Elm Creek at Ballinger	23
Figure 3-3 Cumulative mass plot for study site #6 - San Saba at San Saba.....	24
Figure 3-4 Cumulative mass plot for study site #2 South Concho at Christoval	25
Figure 3-5 Cumulative mass plot for study site #1 - North Concho Rv near Carlsbad	25
Figure 4-1 Small pond identification using the National Hydrography Dataset (NHD).	29
Figure 4-2 – Small pond categories –.....	30
Figure 4-3 – Exclusion of NHD “Pools” from small pond datasets.	31
Figure 4-4 – Small pond identification with Google Earth Engine (GEE).	33
Figure 4-5 – Using USGS topographic maps to identify and date small ponds.....	35
Figure 4-6 – Small pond digitization within Google Earth	36
Figure 4-7 – Pond surface area adjustments within Google Earth –	37
Figure 4-8 – Updating small pond creation dates using the National Inventory of Dams (NID)..	38
Figure 4-9 – Small pond locations within the study area.....	39
Figure 4-10 – Small pond time-series data for the Elm Creek watershed.....	41
Figure 4-11 - Small pond time-series data for the San Saba watershed.....	42
Figure 4-12 - Small pond time-series data for the North Concho watershed	43

Figure 4-13 - Small pond time-series data for the South Concho watershed. 44

Figure 4-14 – Estimated 2017 Land Use/Land Cover data from the USGS..... 47

Figure 4-15 – NRCS Soil Hydrologic Groups for the study area (obtained during 2019)..... 48

Figure 4-16 – Time-series of weighted-average curve numbers for each study area watershed 49

Figure 4-17 – Time history of land-use/land cover acreage by category for the Elm Creek watershed for the period from 1940-2016..... 50

Figure 4-18 – Time history of land-use/land cover acreage by category for the San Saba watershed for the period from 1940-2016..... 51

Figure 4-19 – Time history of land-use/land cover acreage by category for the South Concho watershed for the period from 1940-2016. 52

Figure 4-20 – Time history of land-use/land cover acreage by category for the North Concho watershed for the period from 1940-2016. 53

Figure 5-1 Map showing temperature measurement locations..... 55

Figure 5-2 – Temperature data For Ballinger for the period 1940-2016..... 57

Figure 5-3 – Temperature Trends For Ballinger for the period 1940-2016 58

Figure 5-4 Annual Average Temperatures for Ballinger for the period 1940-2016..... 60

Figure 5-5– Temperature Data For Abilene for the period 1940-2016..... 63

Figure 5-6- Temperature trends for Abilene for the period 1940-2016 64

Figure 5-7 - Annual Average Temperatures for Abilene for the period 1940-2016..... 65

Figure 5-8 - Temperature Data For Brady for the period 1940-2016 70

Figure 5-9 - Temperature Trends For Brady, for the period 1940-2016 71

Figure 5-10- Annual Average Temperatures for Brady for the period 1940-2016..... 72

Figure 5-11 – - Temperature Data For Eldorado for the period from 1966-2016..... 75

Figure 5-12 - Temperature Trends For Eldorado for the period 1966-2016 76

Figure 5-13- Annual Average Temperatures for Eldorado for the period 1966-2016..... 77

Figure 5-14– - Temperature Data For San Angelo for the period 1940-2016..... 83

Figure 5-15- Temperature Trends For San Angelo for the period 1940-2016 84

Figure 5-16- Annual Average Temperatures for San Angelo for the period 1940-2016 85

Figure 5-17- - Temperature Data For Big Spring for the period 1948-2016..... 92

Figure 5-18- Temperature trends for Big Spring for the period 1948-2016 93

Figure 5-19- Annual average temperatures for Big Spring for the period 1948-2016..... 94

Figure 5-20- - Temperature data For Sterling City for the period 1964-2016..... 96

Figure 5-21 - Temperature trends for Sterling City for the period 1964-2016..... 97

Figure 5-22- Annual Average Temperatures for Sterling City for the period 1964-2016..... 98

Figure 6-1 – Map of streamflow measurement and analysis locations103

Figure 6-2 – Calendar plot of “zero streamflow” days (BLUE) recorded for Elm Creek at Ballinger, for the period 1940-2016.104

Figure 6-3 – Number of dry (zero streamflow) days per year – Elm Creek at Ballinger.....105

Figure 6-4– Annual flows by year for the period 1940-2016 – Elm Creek at Ballinger.106

Figure 6-5– Calendar plot of “zero streamflow” days (BLUE) recorded for the San Saba River at Menard, for the period 1940-2016.....107

Figure 6-6 – Annual flows by year for the period from 1940 to 2016 – San Saba River at Menard.....108

Figure 6-7 – Calendar plot of dry (zero streamflow) days recorded Brady Creek at Brady, TX.....109

Figure 6-8 - - Number of dry (zero streamflow) days per year for the period 1940-2016 – Brady Creek at Brady110

Figure 6-9 – Annual flows by year for the period 1940-2016 – Brady Creek at Brady110

Figure 6-10 – Calendar Plot of dry (zero streamflow) days recorded the San Saba River at San Saba, TX.....112

Figure 6-11 – Annual Flows by Year – San Saba River at San Saba.113

Figure 6-12– Annual flows by year for the period from 1940-2016 – South Concho River at Christoval.....114

Figure 6-13 – Calendar plot of dry (zero streamflow) days recorded for the North Concho River near Carlsbad115

Figure 6-14 – Number of Dry (zero streamflow) Days per year – North Concho River near Carlsbad.....116

Figure 6-15 – Annual flows by year – North Concho River near Carlsbad.....117

Figure 7-1 Map showing measurement locations identified and used in assessing precipitation trends within the study area watersheds.....120

Figure 7-2 Precipitation data for Ballinger for the period 1940-2016.....122

Figure 7-3 Precipitation Data for Abilene for the period 1940-2016.....123

Figure 7-4 Precipitation Data for Menard for the period 1940-2016126

Figure 7-5 Precipitation Data for Brady, TX127

Figure 7-6 Precipitation Data for San Saba for the period 1940-2016.....128

Figure 7-7 Precipitation Data for Christoval for the period 1940-2016.....131

Figure 7-8 Precipitation Data for San Angelo of the period 1944-2016132

Figure 7-9 Precipitation Data for Big Spring or the period 1948-2016136

Figure 7-10 Precipitation Data for the Upper North Concho region for the period 1949-2016–137

Figure 7-11 Precipitation Data for Sterling City for the period 1940-2016138

Figure 7-12 Precipitation Data for the Lower North Concho area for the period 1947-2016 –139

Figure 7-13 – Rainfall calendar plots for Ballinger.....144

Figure 7-14 Precipitation Data for Ballinger for the period 1940-2016, considering only runoff-producing rain events.....145

Figure 7-15 – Rainfall calendar plots for San Saba–.....147

Figure 7-16 Precipitation Data for San Saba for the period 1940-2016, considering only runoff-producing rain events.....148

Figure 7-17 – Rainfall calendar plots for Christoval–.....149

Figure 7-18 Precipitation Data for Christoval for the period 1940-2016, considering only runoff-producing rain events.....150

Figure 7-19 – Rainfall calendar plots for Sterling City for the period 1940-2016.....151

Figure 7-20 - Precipitation Data for Sterling City for the period 1940-2016, considering only runoff-producing rain events..... 152

Figure 8-1 – Map showing locations of GRACE soil moisture data..... 155

Figure 8-2 – GRACE storage data for Ballinger for late 2002-2016, TX..... 157

Figure 8-3 – GRACE, rainfall, and streamflow data for Ballinger for the period 2002-2016 158

Figure 8-4 - – GRACE, rainfall, and streamflow data for Ballinger for 2007- 159

Figure 8-5 – GRACE, rainfall, and streamflow data for Ballinger for 2012-2013- 161

Figure 8-6 – Sample GLDAS soil moisture data for the study area watersheds..... 163

Figure 8-7 – Mann-Kendall analysis results of GLDAS soil moisture data by watershed 164

Figure 8-8. Available soil-water capacity per NRCS datasets..... 168

Figure 8-9. Annual actual evapotranspiration calculated by the SWB model for 1981-2017 170

Figure 8-10 Annual potential evapotranspiration calculated by the SWB model for 1981-2017. 171

Figure 8-11. Annually averaged daily soil moisture calculated by the SWB model.... 172

Figure 8-12 - Annually averaged groundwater recharge calculated by the SWB model. 173

Figure 8-13. Kendall-Theil trends of potential evapotranspiration for each level 6 hydrologic unit in the study-area watersheds as calculated by the SWB model..... 174

Figure 8-14. Kendall-Theil trends of actual evapotranspiration for each level 6 hydrologic units in the study-area watersheds as calculated by the SWB model..... 175

Figure 8-15. Kendall-Theil trend of average daily soil moisture for each level 6 hydrologic unit in the study-area watersheds as calculated by the SWB model..... 176

Figure 8-16. Kendall-Theil trend of groundwater recharge for each level 6 hydrologic unit in the study-area watershed as calculated by the SWB model. 177

Figure 9-1 – Major aquifers within the study area. 179

Figure 9-2 – Minor aquifers within the study area 180

Figure 9-3 – Map of shallow groundwater wells located in close proximity to streams, as well as wells for which water level data was available..... 181

Figure 9-4 – Data for well #4209502 near Elm Creek 183

Figure 9-5 - Data for well #4149701 near Brady Creek..... 184

Figure 9-6 - Data for well #4263928 near the San Saba River 185

Figure 9-7 - Data for well #4251206 located upstream within the Brady Creek watershed –
 186

Figure 9-8 - Data for well #44309102 located near Sterling City within the North Concho
 watershed 187

Figure 9-9 - Data for well #4416202 located near Sterling City within the North Concho
 watershed 188

Figure 9-10 - Data for well #4408704 located near Sterling City within the North Concho
 watershed 189

Figure 9-11 – Known water wells within the study area watersheds..... 190

Figure 9-12 – Well depths in and within 10 miles of the study area watersheds..... 192

Figure 9-13 – Potentiometric surface from 1970 through 2010 for the Elm Creek watershed
 193

Figure 9-14 – Potentiometric surface from 1970 through 2010 for the San Saba watershed.
 194

Figure 9-15 – Potentiometric surface from 1970 through 2010 for the South Concho
 watershed..... 195

Figure 9-16 – Potentiometric surface from 1970 through 2010 for the North Concho
 watershed..... 196

Figure 9-17 – Calculated annual baseflow in the Elm Creek watershed from USGS 0812700
 Elm Ck at Ballinger, TX streamflow data..... 198

Figure 9-18 – Reported pumping in Runnels and Taylor counties..... 199

Figure 9-19 – Reported pumping in McCulloch, Menard, San Saba, and Schleicher counties .
 200

Figure 9-20 – A) Calculated annual baseflow in the San Saba watershed from USGS
 08144500 San Saba Rv at Menard, TX streamflow data, and B) Percent of total streamflow
 that is baseflow..... 201

Figure 9-21 – A) Calculated annual baseflow in the San Saba watershed from USGS 08145000 Brady Ck at Brady, TX streamflow data, and B) Percent of total streamflow that is baseflow.....202

Figure 9-22 – A) Calculated annual baseflow in the San Saba watershed from USGS 08146000 San Saba Rv at San Saba, TX streamflow data, and B) Percent of total streamflow that is baseflow.....204

Figure 9-23 – A) Calculated annual baseflow in the South Concho watershed from USGS 0812800 S Concho Rv at Christoval, TX streamflow data, and B) Percento of total streamflow that is baseflow.....205

Figure 9-24 – Reported pumping in Schleicher and Tom Green counties206

Figure 9-25 – Calculated annual baseflow in the North Concho watershed from USGS 08134000 N Concho Rv nr Carlsbad, TX streamflow data.....207

Figure 9-26 – Reported pumping in Sterling and Tom Green counties.....208

Figure 10-1 – Computational process included within the UCWBM216

Figure 10-2 – UCWBM results for the Elm Creek watershed – (A) Percentage difference in runoff by year, (B) difference in runoff by year (in acre-ft), (C) computed runoff leaving the watershed as streamflow.....218

Figure 10-3 – UCWBM results for the San Saba watershed – (A) Percentage difference in runoff by year, (B) difference in runoff by year (in acre-ft), (C) computed runoff leaving the watershed as streamflow.....220

Figure 10-4 – UCWBM results for the South Concho watershed – (A) Percentage difference in runoff by year, (B) difference in runoff by year (in acre-ft), (C) computed runoff leaving the watershed as streamflow.....222

Figure 10-5 – UCWBM results for the North Concho watershed.....224

List of Tables

Table 1-1 - Small Pond Data by Watershed.....	5
Table 3-1 – Hypotheses and trends resulting from Mann-Kendall analyses.....	16
Table 3-2 – Updates to Phase I Results	21
Table 4-1 – Small Pond Analysis Results – 2019 Conditions.....	45
Table 4-2 – “Channel Ponds” excluded from the small pond analyses.....	45
Table 4-3 – Runoff curve number for USGS Land Use Classifications.	46
Table 4-4 – Watershed percentage area by hydrologic soil group	48
Table 5-1 – Teamperature measurement stations for the Elm Creek watershed.....	56
Table 5-2 – Temperature Trend Statistics for Ballinger, for the period 1940-2016	62
Table 5-3 – Temperature Trend Statistics for Abilene for the period 1940-2016	66
Table 5-4 – Teamperature measurement stations for the San Saba watershed.....	69
Table 5-5 – Temperature trend statistics for Brady for the period from 1940-2016	74
Table 5-6 – Temperature trend statistics for Eldorado for 1966-2016	78
Table 5-7 – Temperature trend statistics for Eldorado & Brady, 1967-2016.....	79
Table 5-8 – Teamperature measurement stations for the South Concho watershed.....	82
Table 5-9 – Temperature trend statistics for San Angelo for the period 1940-2016.....	86
Table 5-10 – Temperature Trend Statistics for Eldorado & San Angelo, 1966-2016.....	87
Table 5-11 – Teamperature measurement stations for the North Concho watershed.....	91
Table 5-12 – Temperature Trend Statistics for Big Spring for the period 1948-2016	95
Table 5-13 – Temperature trend statistics for Sterling City, TX.....	99
Table 5-14 – Minimum temperature trend statistics for the North Concho watershed, 1964-2016	100
Table 5-15 – Maximum temperature trend statistics for the North Concho watershed, 1964-2016	100
Table 6-1 – Streamflow Trends Analysis	118

Table 7-1 – Precipitation measurement stations for the Elm Creek watershed.....	121
Table 7-2 – Precipitation Trends Elm Creek Watershed.....	124
Table 7-3 – Precipitation measurement stations for the San Saba watershed.....	125
Table 7-4 – Precipitation Trends San Saba Watershed.....	129
Table 7-5 – Precipitation measurement stations for the South Concho watershed.....	130
Table 7-6 – Precipitation Trends South Concho Watershed	133
Table 7-7 – Precipitation measurement stations for the North Concho watershed	134
Table 7-8 – Precipitation Trends – North Concho Watershed for the period 1949-2016...	142
Table 7-9 – Adjustments to curve numbers based on antecedent moisture conditions.....	143
Table 8-1. Description of the TWDB Groundwater Availability Modeling projection system. 167	
Table 9-1 – Mann-Kendall results for baseflow trends, Elm Creek at Ballinger	198
Table 9-2 – Mann-Kendall results for baseflow trends, San Saba River at Menard	201
Table 9-3 – Mann-Kendall results for baseflow trends, Brady Creek at Brady	203
Table 9-4 – Mann-Kendall results for baseflow trends, San Saba River at San Saba	204
Table 9-5 – Mann-Kendall results for baseflow trends, South Concho River at Christoval	205
Table 9-6 – Mann-Kendall results for baseflow trends, North Concho River nr Carlsbad ..	207
Table 10-1 – Rainfall data sources used within the UCWBM	211
Table 10-2 – Adjustments to curve numbers based on antecedent moisture conditions ...	213
Table 10-3 – UCWBM results by watershed parameter, comparing 2016 and 1940 conditions	225
Table 10-4 – UCWBM results as a median percentage of total modeled rainfall.....	226

Abbreviations

ACIS	Applied Climate Information System
cfs.....	Cubic Feet per Second
ft.....	feet (units of measure)
GCM.....	Global Climate Model
GEE.....	Google Earth Engine
GIS	Geographic Information System
GLDAS	Global Land Data Assimilation System
GRACE.....	Gravity Recovery and Climate Experiment
GWDB.....	Groundwater Database
LCRA.....	Lower Colorado River Authority
MSL	Mean Sea Level
NASA	National Aeronautics and Space Administration
NHD	National Hydrography Dataset
NID	National Inventory of Dams
NRCS.....	Natural Resources Conservation Service
PoR.....	Period of Record
SCS.....	Soil Conservation Service
SDR.....	Texas Water Development Board Submitted Drillers Report Database
TCEQ.....	Texas Commission on Environmental Quality
TWDB.....	Texas Water Development Board
UCWBM.....	Upper Colorado Water Balance Model
USGS	United States Geological Survey
WAM.....	Water Availability Model

This page is intentionally blank.

1 Executive Summary

This report presents efforts undertaken in Phase II of the Texas Water Development Board (TWDB) project to evaluate rainfall-runoff trends in the Upper Colorado River Basin of Texas. This report was commissioned in support of the Colorado and Lavaca Rivera and Matagorda and Lavaca Bays Basin and Bay Area Stakeholder Committee (Colorado-Lavaca BBASC) as part of the adaptive management phase of the Senate Bill 3 process.

In the August 2017 Phase I report (KRC, 2017), it was noted that observed flows in the Upper Colorado River watershed declined at all study sites over the period 1940-2016. Declines at the majority of sites were attributed to historical water use and the construction of large upstream permitted reservoirs. Yet for some of the study sites, observed flow declines exceeded the declines that could result from permitted upstream withdrawals and reservoir storage. It was concluded that activities not accounted for in the streamflow naturalization process may have impacted the observed flows. These activities could include: 1) construction of small reservoirs, 2) groundwater use, 3) average temperature changes, 4) changes to rainfall patterns, and 5) land use changes, including the existence of noxious brush. TWDB and the Colorado-Lavaca BBASC convened Phase II efforts specifically to study these activities and assess their impact on streamflow declines. The Phase II efforts were to focus only on the following watersheds:

- San Saba River Watershed
- South Concho River Watershed
- North Concho River Watershed above Carlsbad, TX
- Elm Creek Watershed

This report documents the methodology and results from Phase II efforts. Project updates have been provided as presentations to both the Region F (6/20/2019) and Region K (7/10/2019) regional water planning groups.

1.1 Materials and Methods

The Mann-Kendall statistical analysis technique was used during Phase II to identify significant decreasing, increasing, or stable trends in time series data (Meals, 2011, Mann, 1945, Kendall, 1975).

For assessing temperature trends, daily maximum and minimum temperature records were obtained from stations within or around the study area watersheds. Stations needed to have sufficiently long periods of record to discern trends, and efforts were made to only utilize stations with periods of record spanning both the 1947-1957 and 2008-2016 drought periods. Some stations with shorter periods of record were included in the analyses so that data from at least two stations per watershed were available. By using data from multiple stations within a watershed, it was possible to discern both temporal and spatial trends in each of the properties being analyzed. The following properties were analyzed statistically using the Mann-Kendall technique:

- Air Temperature (maximum and minimum)
- Precipitation
- Streamflow
- Soil Moisture
- Land use/land cover (using curve numbers)

Aside from the Mann-Kendall statistical analyses, additional non-statistical investigations were conducted. These investigations included:

- Quantifying the number, surface area, volume, and approximate creation date of small ponds within each watershed
- Assessing the possibility of streamflow depletion due to local groundwater pumping
- Assessing and quantifying the extent of noxious brush over time within the watersheds
- Assessing how soil moisture fluctuations may be linked to rainfall-runoff response observations.

Lastly, to quantify the effects of changes in watershed parameters on resulting streamflow, the Upper Colorado Water Balance Model (UCWBM) was created. This model performed water budget analyses on watersheds using actual rainfall patterns (for a given “rain year”) with watershed conditions from specified “watershed years.” Each watershed year differed with respect to the watershed land use /land cover (via curve numbers), number of small ponds in existence, and the rates of evaporation water loss from those small ponds.

1.2 Trend Analysis Results

Numerous statistically significant trends were observed throughout the study area watersheds. These trends varied both in time and spatially across watersheds. In many instances, however, data suggested stability, with no significant increasing or decreasing trends evident. It was also common for parameters to show stability in terms of long term trends, while at the same time experiencing increasing variability amongst data points when assessed over only short time periods.

1.2.1 General Temperature Trends for the Study Area Watersheds

Temperature trends (average maximums and minimums) were analyzed using daily data averaged over monthly, seasonal, and annual time periods. Most stations within the study area watersheds exhibited similar trends, however the two stations outside of the study area (Big Spring and Abilene) routinely demonstrated opposite trends to those observed from the watershed-located stations. The Big Spring and Abilene stations were included in this analysis as they are located near the upper reaches of the North Concho and Elm Creek watersheds, respectively, and their inclusion provided sufficient data from which to discern spatial gradients in the data.

Most in-watershed stations indicated decreasing or stable trends for the number of days per year exceeding 100°F. Decreasing trends were also noted for most stations with respect to the number of days per year on which temperatures dropped below freezing. An increasing trend was observed for these stations when considering the number of days per year on which the minimum temperature remained above 60°F.

Monthly and seasonal analyses at each in-watershed station routinely resulted in significant increasing trends for minimum temperatures, with mostly stable trends evident for maximum temperatures. For example, the station from Eldorado, TX (located in the upper reaches of the South Concho watershed) reported increasing minimum temperatures annually, for all seasons, and for all months except April. However significant increases in maximum temperatures for this location were only computed for August, September, October, and the Fall period, with all other periods resulting in stable trends. Similarly, minimum temperatures at Brady, TX (in the San Saba watershed) showed significant increases for nearly all monthly, seasonal, and annual periods, yet showed largely stable trends with respect to maximum temperatures.

In general, the temperature analysis concluded that maximum temperatures are remaining stable or slightly increasing, whereas minimum temperatures are increasing. This suggests that the watersheds are retaining more heat, which may affect evapotranspiration rates and the types of vegetation that can thrive in each environment.

1.2.2 General Precipitation Trends for the Study Area Watersheds

The Mann-Kendall analyses applied to daily precipitation data resulted in numerous statistically significant results. Phase II results confirmed the Phase I conclusion that all stations within the study area watersheds either experienced stability in terms of the total annual rainfall volume, or that the annual volumes have been slightly increasing over time. Analyses also showed that in general, the number of rainy days per year increased at statistically significant levels, and the duration of dry periods between rainfall events correspondingly decreased. These trends, when combined with often static trends in annual total rainfall, indicated that the average (or median) rainfall depth per rain event exhibited a statistically significant decreasing trend. As with the temperature data, precipitation recorded at Big Spring and Abilene did not follow the same trends as that recorded at locations within the study area watersheds.

When considered on a monthly and seasonal basis, other common trends were observed. For example, it was common for stations to report increases in rainfall in March, followed by decreases in April. Increases were also common in the summer months (June-August) and November. Only few stations, such as Sterling City (North Concho Watershed) reported decreases in months other than April. These trends suggest an apparent shift in the timing of rainfall over the calendar year, which could have implications for irrigation, evaporation water loss, and land use/land cover.

1.2.3 General Streamflow Trends for the Study Area Watersheds

As streamflow was largely assessed within the Phase I study, its assessment herein was limited to application of the Mann-Kendall analysis technique. Assessments were made using gauge-recorded, non-naturalized streamflow.

For the North Concho River near Carlsbad, there was an increasing trend in the number of days per year during which the river was dry (i.e. had zero flow). There also was a significant decreasing trend in total annual flows, with an apparent “change point” occurring in 1962, after which point variability in annual flows was largely diminished. In contrast, for the South Concho watershed, it was determined that the river never ran dry, and had a stable total annual flow over the period of record. This suggests that groundwater baseflow may play more of an important role within the South Concho watershed than it does in the North Concho watershed.

For the Elm Creek watershed, data from Ballinger (at the watershed outlet) shows increasing dry days during the drought period, suggesting minimal groundwater influence on creek baseflow. For the San Saba watershed, dry days were only observed during the drought periods prior to 1990, yet total annual flows showed decreasing trends over the entire period of record. It is notable, however, that records for Menard (within the San Saba watershed) indicated increasing trends in March, November, and December, with stable trends calculated for all other periods. This was in contrast to trends recorded elsewhere in the watershed (at San Saba and Brady).

1.2.4 General Soil Moisture Trends for the Study Area Watersheds

Soil moisture data was obtained and analyzed from two sources: 1) GRACE satellite data provided by NOAA and 2) GLDAS data provided by NASA. As the GRACE data was only available from 2002-Present, it was not suitable for use in Mann-Kendall analyses, yet was useful in illustrating the variable rainfall-runoff response under different soil moisture conditions.

GLDAS data was obtained as gridded median annual soil moisture content for the soil section from 20cm depth to 100 cm depth. It should be noted that the GLDAS data is modeled soil moisture content, similar to that described in (Xia, 2012). The GLDAS data was aeriially-weighted by watershed and used to compute trends of the 1948-2018 period of record. Each watershed exhibited an increasing trend in soil moisture, suggesting that soils are steadily building up water content and are likely close to saturation at present, ignoring seasonal fluctuations. Further review of the GLDAS dataset is warranted, including reviewing data for lower soil layers, and review of data other than median annual values.

1.2.5 General Land use/Lad Cover Trends for the Study Area Watersheds

Land Use/Land Cover data for each study area watershed was obtained from the US Geological Survey for the period 1940-2016. Data was clipped and tabulated to acres per watershed of various land use classifications developed by the USGS. These acreages and

classifications were used to determine watershed-average SCS runoff curve numbers, which varied by time and watershed. Curve numbers are a standard parameter used in converting rainfall to runoff, and in general lower curve numbers generate less land surface runoff. Mann-Kendall analyses on the curve numbers suggested that land use/land cover change was minimal within the South Concho, San Saba, and Elm Creek watersheds. Changes of nearly 4 units were observed, however, for the North Concho watersheds.

1.3 Non-Statistical Investigation Results

1.3.1 Small Pond Analysis for the Study Area Watersheds

To assess the potential impact of small ponds on watershed streamflow, pond properties had to be obtained. Ponds were identified and dated using the National Hydrography Dataset (NHD), USGS topographic maps, ArcGIS aerial images, and Google Earth images. Pond areas were manually digitized within AcrGIS and Google Earth, if the aerial extent was not previously accurate as included within the NHD. Pond storage capacities were approximated based on the pond area and the area vs. storage formula used in the Colorado River Basin Water Availability Model (WAM) maintained by the Texas Commission on Environmental Quality. Table 1-1 presents the resulting small pond data by watershed, including all ponds present in 2019.

Table 1-1 - Small Pond Data by Watershed

Watershed	Number of Ponds	Total Pond Surface Area (acres)	Estimated Pond Storage (acre-ft)
San Saba Watershed	7,191	6,401	17,243
Elm Creek Watershed	3,226	2,468	11,855
North Concho Watershed	1,319	1,098	3,125
South Concho Watershed	763	843	3,282

1.3.2 Streamflow Depletion Due To Groundwater Pumping

To assess streamflow depletion potential due to groundwater pumping, TWDB groundwater well databases were queried, identifying shallow wells located within 1 mile of large watercourses, and for which water level data was available over at least a 10-year portion of the period of record. Only seven wells were identified, yet analysis of their data suggested connections between the well water levels and streamflow within nearby rivers. It was impossible to discern, however, if groundwater pumping resulted in reduced streamflow.

Attempts were made to identify non-registered potential domestic and livestock wells along the San Saba River via analysis within Google Earth, yet wells were not easily identifiable.

1.3.3 Noxious Brush Identification and Extent Quantification

Attempts were made to quantify acreage of noxious brush extent over time using LandSAT imagery within the Google Earth Engine programming framework. These attempts were ultimately unsuccessful as identification of the noxious brush (as opposed to other vegetation) was not reliable within the available data.

1.3.4 Relating Soil Moisture Fluctuations to Runoff

Soil moisture data from the GRACE dataset were obtained and processed for all locations within the study area watersheds, with GRACE data available worldwide on an $0.125^\circ \times 0.125^\circ$. Data from Ballinger, TX was compared to both streamflow and rainfall records from the Elm Creek watershed outlet. Comparing the datasets led to identifying times when the soil moisture was high and low rainfall resulted in large volumes of streamflow. There were also instances when the soil moisture was low, and repeated low-intensity rainfall events led to elevated soil moisture without large increases in streamflow. These trends all generally conform with the theory that high soil moisture generates more runoff, but that prolonged moderate rainfall is needed to increase soil moisture without generating runoff.

1.4 UCWBM Methodology and Results

To quantify the effect of land use, small ponds, and rainfall patterns on streamflow, the Upper Colorado Water Balance Model (UCWBM) was created. This model allows for the simulation and quantification of runoff from rainfall (as measured from any user-defined year) on watersheds defined with the land use/land cover properties (i.e. curve number) and small pond properties from a different year. In this way, was possible to assess how much runoff-based streamflow would have resulted from a 2016 rainfall applied to a watershed reflecting 1950 conditions (for example). Model assumptions limit the model's utility for comparing computed and actual streamflow, and the UCWBM is designed only to compare streamflows computed under varying rainfall and watershed conditions. The UCWBM does not simulate groundwater influences on streamflow, and does not limit rainfall infiltration based on soil moisture content.

When applied to the Elm Creek and San Saba watersheds, 2016 watershed conditions resulted in, on average, 20% and 3% less streamflow than 1940 watershed conditions, respectively. This indicates that the relatively large number and cumulative sizes of the small ponds in these watersheds can play a significant role in decreasing streamflow. A similar reduction (15%) in streamflow was computed for the North Concho watershed, yet this reduction was attributed to the decreased in watershed curve number due to land use/land cover change, rather than due to the existence of small ponds.

In contrast, when the UCWBM was applied to the South Concho watersheds (under 2016 watershed conditions compared to 1940 watershed conditions), computed streamflow decreased slightly. For this watershed, land use/land cover changes resulted in an actual increase in computed runoff. Yet this increase was overwhelmed by the decrease in runoff resulting from the small ponds within the watershed.

1.5 Conclusions

The most significant conclusions drawn from this Phase II analysis include that:

- Most temperature gauges throughout the study area watersheds demonstrated increasing minimum temperatures with decreasing or stable maximum daily temperatures.
- Most precipitation stations experienced increasing frequencies of rain events, with the number of annual rainy days increasing. Combined with generally stable total annual rainfall quantities, the resulting median rainfall depth often reports a significant decreasing trend.
- Runoff-generating rainfall events tended to occur with equal frequency and magnitude over the 1940-2016 period of record for this analysis.
- For the North Concho watershed, which has the fewest number of small impoundments, land use change appears to be the biggest driver resulting in reduction in runoff and streamflow.
- For the Elm Creek and San Saba watershed, whose watershed-averaged curve numbers have each decreased by less than one unit over the period of record, small pond usage (and construction) appear to be the drivers of hydrologically significant changes in runoff and streamflow. Streamflow within the South Concho watershed is also reduced due to the existence of small ponds, yet the reduction is mitigated by increased runoff as a result of land use/land cover changes.

The UCWBM results suggest that the impact of small ponds and land use/land cover changes accounts for some (if not all) of the differences between streamflows observed in the 1947-1957 and 2008-2016 drought periods. Permitted diversions, which were not included in this Phase II analysis, when combined with the small pond impacts, may explain most or all of the observed streamflow differences, at least for the San Saba, South Concho, and Elm Creek Watersheds. We do not expect this to be so for the North Concho watershed, where the small ponds do not have a significant impact on resulting streamflow. For this region, we suspect that land use change and possibly noxious brush are playing a significant role in decreasing streamflow.

1.6 Recommendations

Based on the Phase II data, analyses, and results presented herein, we suggest the following additional investigations:

- Develop a semi- or fully- distributed rainfall/runoff model of the study area watersheds, similar to those presented in (Xia, 2012). Such a model would provide spatial variability in model input (which is not included in the UCWBM), and would be able to simulate both surface runoff and subsurface infiltration processes. The model should account for the extent and water usage properties of the noxious brush common to each watershed.
- Further comprehensive study of the potential impacts of noxious brush, likely through modeling and empirical study of results generated from recently completed and published paired watershed studies.
- Additional small pond analysis, including expanding the analysis to the entire Colorado River watershed and defining drainage areas for each pond. This will allow better quantification of each pond's impact to its local portion of the watershed, as well as the watershed outlet.
- Modeling future temperature and precipitation scenarios as derived from Global Climate model data.

2 Introduction

In general, the Upper Colorado River basin watershed is largely rural, consisting mainly of agricultural and ranch land while supporting small to medium-sized communities/cities. The watershed extends north-westerly from Lake Travis, and average annual rainfall decreases westerly from the lake. Therefore the upper reaches of the Upper Colorado River basin typically receive less rainfall than the lower reaches located closer to the Highland Lakes. As such, changes to the rainfall/runoff response in the upper basin may lead to reduced streamflow in an area that is typically already considered a low-streamflow environment.

As stated in (KRC, 2017)

“Observed streamflows in the Colorado River basin upstream of the Highland Lakes have been noted to be lower in recent years than what has been observed in the past”

This sentiment has been stated by many, and was proven in 2017 under TWDB Contract No. 1600012001. That project assessment report identified potential factors that might explain the observed rainfall-runoff relationship. It recommended further study of these factors within key sub-watersheds within the Upper Colorado River Basin so that definitive conclusions could be derived with respect to the attribution of observed rainfall-runoff relationships.

Phase II of this project effort commenced in the Fall of 2018 under TWDB Contract No. 1800012283. The objectives of the Phase II efforts were to determine the plausible causal factors for observed changes in the relationship between rainfall and stream flow, as well as to quantify the streamflow impacts. Phase II efforts were to focus on the following four sub-watersheds within the Colorado River watershed:

- Elm Creek Watershed
- San Saba River Watershed
- South Concho River Watershed
- North Concho River Watershed

This document presents the findings resulting from the Phase II study, including statistical analyses of watershed characteristics, and analyses designed to assess the possible causes of runoff decline identified in the Phase I project report (KRC, 2017). Figure 2-1 through Figure 2-4 provide evidence of the assertion driving this project, namely that recent streamflow is lower than past streamflow despite current rainfall quantities being equal or larger. Each of the following figures was generated for the outlet location of the watersheds included in this Phase II study. The sources of the rainfall data shown in these figures are provided in Section 0 of this report, and streamflow sources are provided in Section 0 of this report. In each of these figures, annual totals are presented for the period between 1947 and 1957, and for the period from 2008 to 2016. These time periods encompass the critical drought periods defined by the Lower Colorado River Authority (LCRA) within their 2015 (LCRA, 2015) and 2019 Water Management Plans (LCRA, 2019).

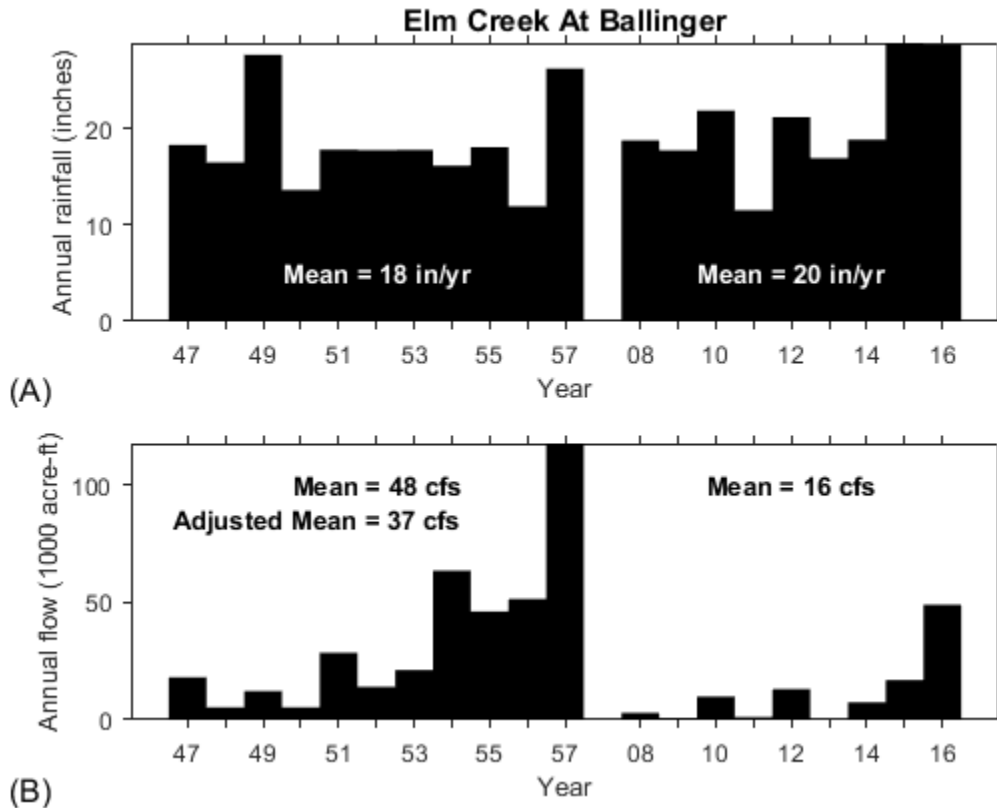


Figure 2-1 – Comparison of rainfall and runoff during the 1947-1957 and 2008-2016 drought periods – Elm Creek watershed.

As shown in Figure 2-1A, rainfall totals for the Ballinger area ranged from between 11.9 inches/year to 27.6 inches per year during the 1947-1957 drought period, with a mean rainfall total of 18 inches per year. In contrast, during the 2008-2016 drought period, rainfall quantities ranged from 11.5 to 28.9 inches per year, with a mean of 20 inches per year. Therefore mean annual rainfall during the more recent drought period exceeded that during the previous drought period by two inches per year. Total annual streamflow, however, decreased during the 2008-2016 drought period (Figure 2-1B) with mean flows of 16 cfs compared to mean flows of 48 cfs during the 1947-1957 drought period. An adjusted mean flow for the period 1947-1956 (excluding the large flood flows that occurred in 1957) results in an adjusted mean flow of 37 cfs, which still more than doubles the mean flow for the 2008-2016 drought period.

It is notable within Figure 2-1A that rainfall in 1949 exceeded the rainfall in 1957, yet streamflow in 1957 was nearly 10x larger than the total annual streamflow in 1949.

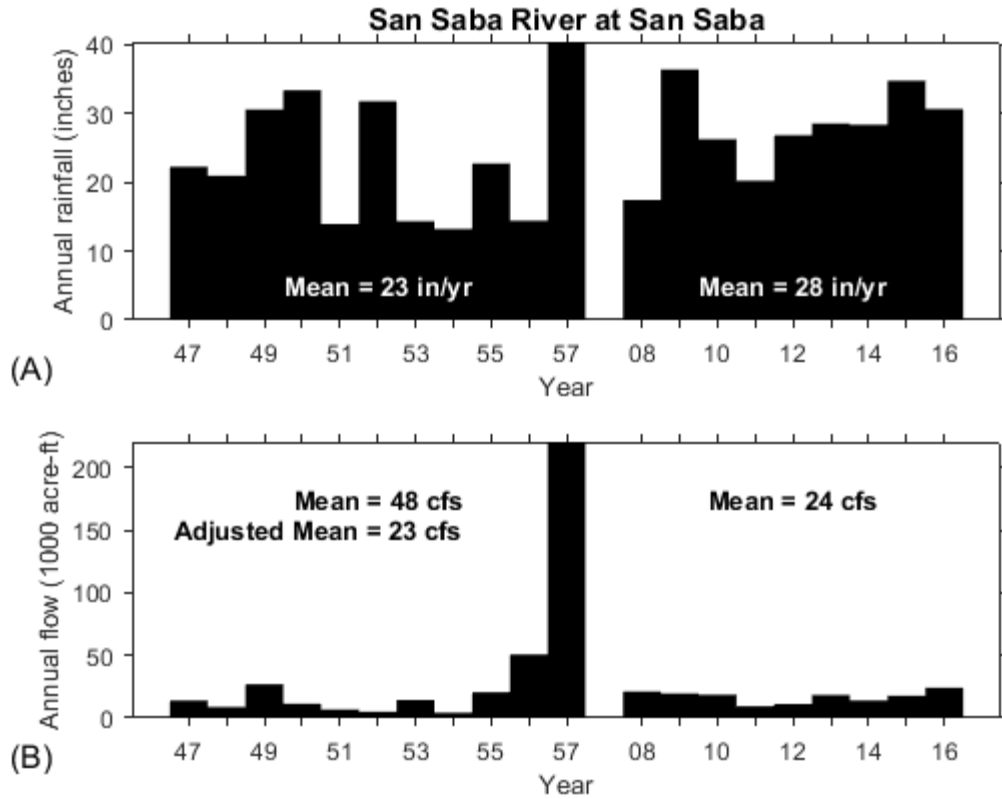


Figure 2-2 – Comparison of rainfall and runoff during the 1947-1957 and 2008-2016 drought periods – San Saba River watershed.

As shown in Figure 2-2A, rainfall totals for the San Saba area ranged from between 13.9 inches/year to 40.3 inches per year during the 1947-1957 drought period, with a mean rainfall total of 23 inches per year. In contrast, during the 2008-2016 drought period, rainfall quantities ranged from 17.4 to 36.3 inches per year, with a mean of 28 inches per year. Therefore mean annual rainfall during the more recent drought period exceeded that during the previous drought period by five inches per year. With this increase in rainfall, the total annual streamflow increased during the 2008-2016 drought period (Figure 2-2B) with mean flows of 24 cfs compared to adjusted mean flows of 23 cfs during the 1947-1956 drought period.

Figure 2-3 displays the annual rainfall and flow totals for the South Concho River at Christoval, with the data presenting a similar pattern to that observed from the San Saba River at San Saba data (Figure 2-2). Mean rainfall during the 2008-2016 period exceeded that from during the 1947-1957 period by five (5) inches per year. Mean streamflow increased by 1 cfs during the 2008-2016 drought, compared to the adjusted mean streamflow from the 1947-1956 period. It is notable that the rainfall in 1957 (33.2 inches) was only 10% higher than that occurring in 1949, yet the resulting streamflow was five times (5x) greater. It is also notable that rainfall in 2016 exceeded that from 1957, yet produced 20% of the annual streamflow from 1957.

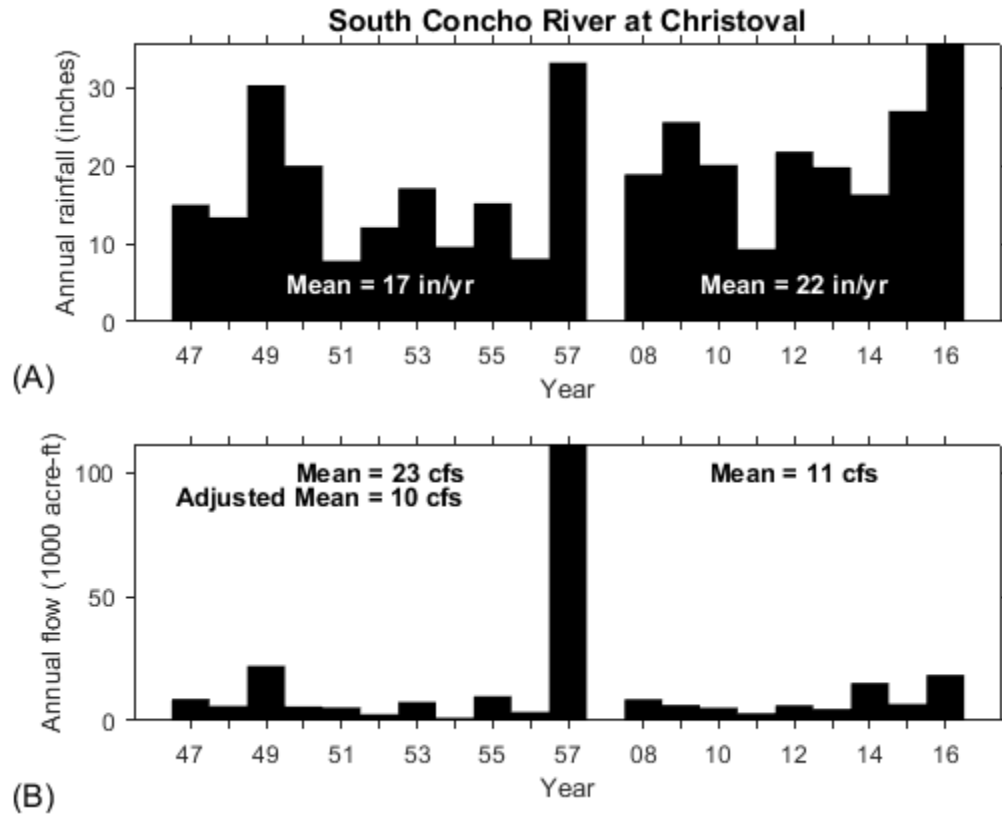


Figure 2-3 – Comparison of rainfall and runoff during the 1949-1957 and 2008-2016 drought periods – South Concho River watershed.

Unlike the patterns observed for the San Saba watershed (Figure 2-2) and South Concho watershed (Figure 2-3), rainfall and streamflow data for the North Concho watershed (Figure 2-4) indicate decreasing streamflow with increasing rainfall. During the 2008-2016 drought period, the mean annual rainfall was 20 inches per year, which exceeded the mean of 17 inches per year for the 1947-1957 period. Adjusted mean streamflow for the 1947-1956 period, however, was approximately five times (5x) higher than the mean streamflow for the 2008-2016 drought period. It is notable that the rainfall recorded in 1957 which resulted in over 150,000 acre-ft of streamflow was exceeded six times within the 1947-1956 and 2008-2016 periods, yet streamflows resulting from those wet years never approached that resulting from the 1957 rainfall.

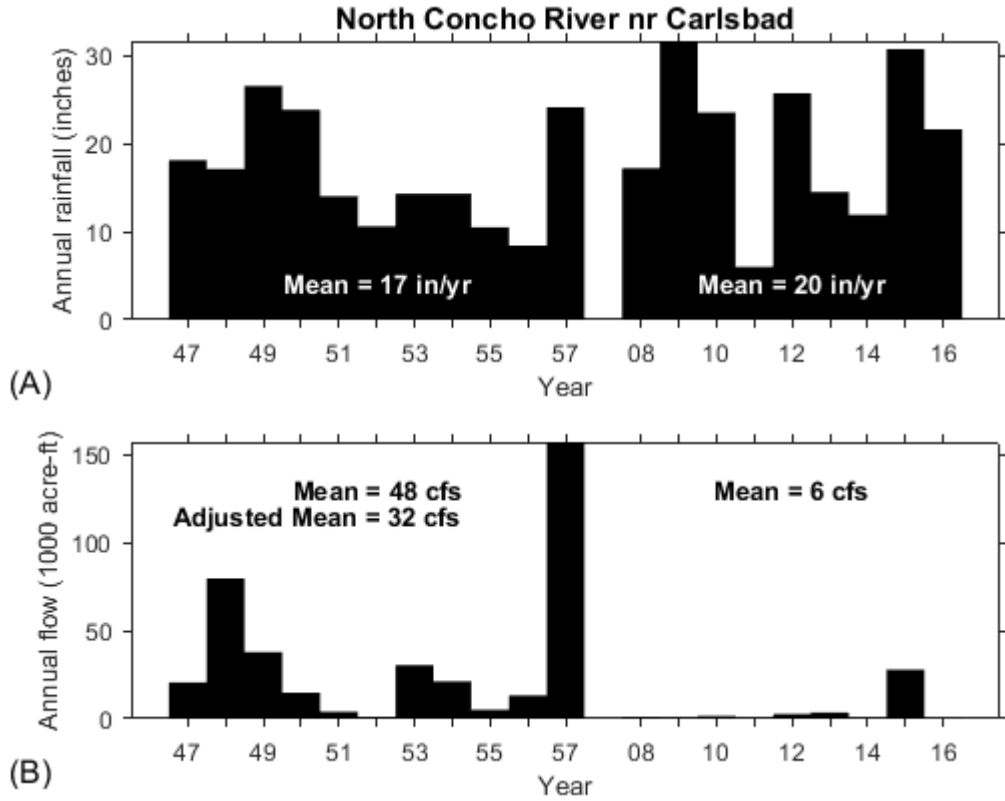


Figure 2-4– Comparison of rainfall and runoff during drought conditions – North Concho Watershed.

In summary, for the four watersheds included within this study, the 2008-2016 drought period resulted in greater average rainfall than in the 1947-1957 drought period, yet produced only slightly increased (for the San Saba and South Concho watersheds) or decreased streamflow (for the Elm Creek and North Concho watersheds).

3 Task 1 – Literature Review & Methodology Assessment

The purpose of this study task was to review similar published study efforts and determine if established analytical techniques and methods could be applied to the study area watersheds during this Phase II project.

3.1 Reference Articles

Prior to commencing this Phase II study, the TWDB identified similar studies from the published literature that may have impacted this study and provided insight into analysis methods and parameters of concern. This section provides brief reviews of each relevant study previously identified by the TWDB. This section does not provide a comprehensive review of all published reports, journal articles, presentations, etc. regarding evaluating changes to the rainfall-runoff response of watersheds overtime.

3.1.1 Crooks and Kay (2015)

In their rainfall-runoff response study of the Thames catchment in southern England, the authors utilize a “Climate and Land-use Scenario Simulation in Catchments” (CLASSIC) model developed (for other purposes) in the mid-1990s. The CLASSIC model was driven with daily precipitation and temperature measurements, modeled potential evaporation estimates, and gridded watershed properties (elevation, land use, soil type, etc.). The model performed a water balance in both the subsurface and surface realms, and computed resulting streamflow. The resulting streamflow compared well with naturalized flow data. The authors did not use their model to assess how rainfall, if applied to a watershed under different conditions, would result in different volumes of streamflow. It appears, however, that such an investigation could have been undertaken using their CLASSIC model. The authors also concluded that evaporation from the watershed plays a “major role” in determining the volume of annual runoff, and they recommend using temperature data and the Blaney-Criddle formula for estimating potential evaporation.

3.1.2 Duan et al. (2017)

In this study, a “Water Supply Stress Index Model (WaSSI)” was developed to examine the roles of climatic variables in altering annual runoff across the United States (Duan, 2017). The model was driven both with historical records and future modeled scenarios derived from Global Climate Models (GCMs). Their modeling efforts suggest that variations in precipitation have driven observed variations in streamflow historically, but that the importance of temperature will surpass that of precipitation if GCM predictions actually occur in the future. They concluded that evaporation increases are likely due to predicted temperature increases, yet will be partially offset by increases in humidity. The WaSSI model was a combination existing snow, evapotranspiration and soil moisture accounting models. The authors did not consider land use change or other terrain-based features in

their analysis, which allowed their methods to be readily applied to the entire continental United States.

3.1.3 McAfee et al. (2017)

In an attempt to improve climate change impact studies, statistical models were used to compute simulated streamflow for the Upper Colorado River Basin from the river headwaters in Wyoming and Colorado to Lee's Ferry in Arizona (McAfee, 2017). The statistical models related monthly average temperatures, monthly total precipitation, and monthly soil moisture data to naturalized flow estimates. From the relationships, future flow estimates were derived using temperature, rainfall, and soil moisture data statistically re-sampled from the historical datasets. Their analysis of the statistical model results indicated that streamflows for a given precipitation change were lower when temperature changes were increasing. Their results yielded greater streamflow variability under warmer and drier conditions.

3.1.4 Woodhouse et al. (2016)

In this study effort, the authors developed empirical relationships between precipitation, temperature, and antecedent soil moisture on Upper Colorado River Basin (in Wyoming, Colorado, Utah, New Mexico, and Arizona) water year streamflow. This study used precipitation as the main driver for streamflow, and then assess how variations in temperature and soil moisture could account for observed differences between the physical and model-predicted streamflow based on the precipitation-streamflow relationship. They concluded temperature differences can explain nearly 40% of the variation in streamflow, with soil moisture playing a less significant and more uncertain role (Woodhouse, 2016).

3.1.5 Xia et al. (2012)(a)

In this study, the authors describe the results from the "North American Land Data Assimilation System" (NLDAS-2), which is a combination of rainfall, infiltration, soil moisture accounting and land surface models capable of computing streamflow. The NLDAS-2 was applied to the continental United States, and the authors compared results from the various modeling option built into the system. One conclusion from the model comparisons was that gridded rainfall datasets such as PRISM better demonstrate the effects of landscape topography than do gauge-based datasets. This suggests that gridded PRISM data should be used when attempting to re-create the rainfall-runoff response for watersheds with rapidly varying terrain (Xia, 2012)(a).

3.1.6 Xia et al. (2012)(b)

In the companion study to (Xia, 2012)(a), the authors presented model validation for the NLDAS-2 system. The compared simulated streamflow to observed streamflow for 961 small basins and 8 major basins within the continental United States, using US Geological

Survey (USGS) records. Their results indicated improving model skill in reproducing gauge flow records when average flows were considered on a monthly and annual basis, rather than on a daily basis. (Xia, 2012)(b)

3.2 Mann-Kendall Trend Analysis Methods

The Mann-Kendall statistical test is an effective way of identifying trends in time-series datasets that do not conform to a normal distribution or any other formal mathematical distribution (Meals, 2011) (Helsel, 2002). The Mann-Kendall analysis as applied herein involves a two-sided test against a “Null Hypothesis” and two “alternate Hypotheses” regarding the existence of trends within the data. Hypotheses used in this application are provided in Table 3-1.

Table 3-1 – Hypotheses and trends resulting from Mann-Kendall analyses

Hypothesis	Trend	Description
Null	Stable	Time series data suggests temporal stability, does not suggest increasing or decreasing trends with a high degree of confidence.
Alternate #1	Increasing	Time series data suggests increasing trends with a high degree of confidence
Alternate #2	Decreasing	Time series data suggests decreasing trends with a high degree of confidence

As applied during this Phase II project, the Mann-Kendall analysis method will test subject datasets to discern whether the data indicates temporal trends, with the default assumption (i.e. “Null Hypothesis”) being that the data is stable over time. The alternative hypotheses are that the data indicates an increasing trend with time, or a decreasing trend with time. Results from the Mann-Kendall analysis will include the identified trend and the confidence level suggesting the trend is correct. The confidence level is an indicator of how likely the alternate hypotheses (increasing or decreasing trends) are likely to be correct, and how likely the Null Hypothesis (stable trend) is to be rejected.

The Mann-Kendall analysis method is implemented mathematically using various steps and equations, each resulting in a statistic that provides insight into the trends suggested by the data. The first computed statistic “S” provides a numerical computation indicative of data trends. The value “S” is calculated via Eq. 3-1:

$$S = \sum_{i=1}^{n-1} \sum_{j=i+1}^n \text{sign}(y_j - y_i)$$

Eq. 3-1

The value “S” is an integer, made up of the sum of a series of comparisons between values in the time series database. For example, if one entry in the database (“y_j”) is greater than the prior entry (“y_i”), then by Eq. 3-1 a value of “1” is added to the previously computed “S.” However if “y_i” were greater than “y_j” then a value of “-1” would be added to the

previously computed “S.” If the values were identical, than “S” remains unchanged. Therefore when applied to all entries in the dataset, the resulting value “S” provides an indication of whether database values are increasing or decreasing. Positive values of “S” indicate increasing trends in the data, and larger the values S indicate stronger trends. Negative values of “S” indicate decreasing trends in the data, and smaller values (or larger magnitudes of S, ignoring the negative sign) indicate stronger decreasing trends.

When utilizing Mann-Kendall analyses, it is important only to consider the sign of the computed “S” value and not compare “S” values derived from different datasets. The computed “S” values really depend on both data trends and the number of values included in the database. Therefore it is inappropriate to compare “S” values computed for different datasets, unless the datasets contain exactly the same number of entries. For this reason, Mann-Kendall analyses and assessments must consider both the computed “S” and the number of entries in the dataset (“n”). This consideration is made through the computed value “τ” which normalizes “S” by the total number of combinations of data points considered in implementing Eq. 3-1. The formula for τ is provided in:

$$\tau = \frac{S}{n(n-1)/2}$$

Eq. 3-2

Possible values for τ range from -1 to 1, with a value of “-1” indicating that every data point in the dataset is lower than the previous data point in the dataset (decreasing trend). Conversely a τ value of 1 indicates that every data point in the dataset is higher than the previous data point in the dataset (increasing trend). Thus values of τ that are closer to -1 or 1 indicate stronger negative or positive trends, respectively, and stable trends are indicated when τ is closer to 0. Defining trends based on τ is therefore somewhat subjective, and for this reason values for τ are not provided throughout this report.

To further determine the likelihood of the trends suggested by the S and τ parameters, the Mann-Kendall technique requires the application of the “Large Sample Approximation” (Helsel, 2002). This approximation assumes that the test statistic used in Eq. 3-1 (i.e. the comparison between two data points) may be closely approximated by a standard normal distribution. With this assumption, it is possible to calculate the value “Z”:

$$Z = \begin{cases} \frac{S-1}{\sigma_s} & \text{if } S > 0 \\ 0 & \text{if } S = 0 \\ \frac{S+1}{\sigma_s} & \text{if } S < 0 \end{cases}$$

Eq. 3-3

With σ_s defined as:

$$\sigma_S = \sqrt{(n/18)(n-1)(2n+5)}$$

Eq. 3-4

Using the computed value “Z,” it is possible to determine the “p” value, which is conceptually considered as the “believability” of the Null Hypothesis (Helsel, 2002). Smaller p-values are stronger indicators of the evidence for rejection of the Null Hypothesis (“Stable” trends) and acceptance of one of the alternative hypotheses (“Increasing” or “Decreasing” trends).

$$p = 2(1 - f(Z))$$

Eq. 3-5

With $f(z)$ referring to the probability of exceedance of Z for a standard normal distribution. Values for $f(z)$ are given by the equation:

$$f(Z) = \frac{1}{2} \left(1 + \operatorname{erf} \left[\frac{|Z|}{\sqrt{2}} \right] \right)$$

Eq. 3-6

With “erf” referring to the error function defined in standard mathematics.

The last step in using the Mann-Kendall analysis in assessing trends is to compare the computed “p” value (Eq. 3-5) to a user-defined threshold “ α ,” which is considered to be an acceptable risk tolerance for incorrectly rejecting the Null hypothesis. Typical values for α are 0.05 or 0.01, which correspond to a 5% or 1% chance, respectively, of incorrectly rejecting the Null hypothesis. For a given value of α , the following conditions apply:

if $p \leq \alpha$ Null hypothesis is rejected, Alternative hypothesis 1 or 2 is accepted

if $p > \alpha$ Null hypothesis is accepted, Alternative hypothesis 1 and 2 are rejected

Eq. 3-7

As an alternative to reporting “p” values, the Mann-Kendall algorithms used in this Phase II effort report “Confidence Levels” given by the equation:

$$\text{Confidence Level} = (1 - p) \cdot 100\%$$

Eq. 3-8

The Confidence Level as defined herein reflects the likelihood that Alternative hypotheses #1 or #2 were properly accepted based on the provided data. Higher confidence levels indicate greater likelihood that the Alternative hypotheses (increasing or decreasing trends) are true given the available data.

For this Phase II effort, the value for α was set to 25%, such that a Confidence Level exceeding 75% indicates an increasing or decreasing trend. Within this Phase II report, Mann-Kendall results will be expressed as the trend and confidence level.

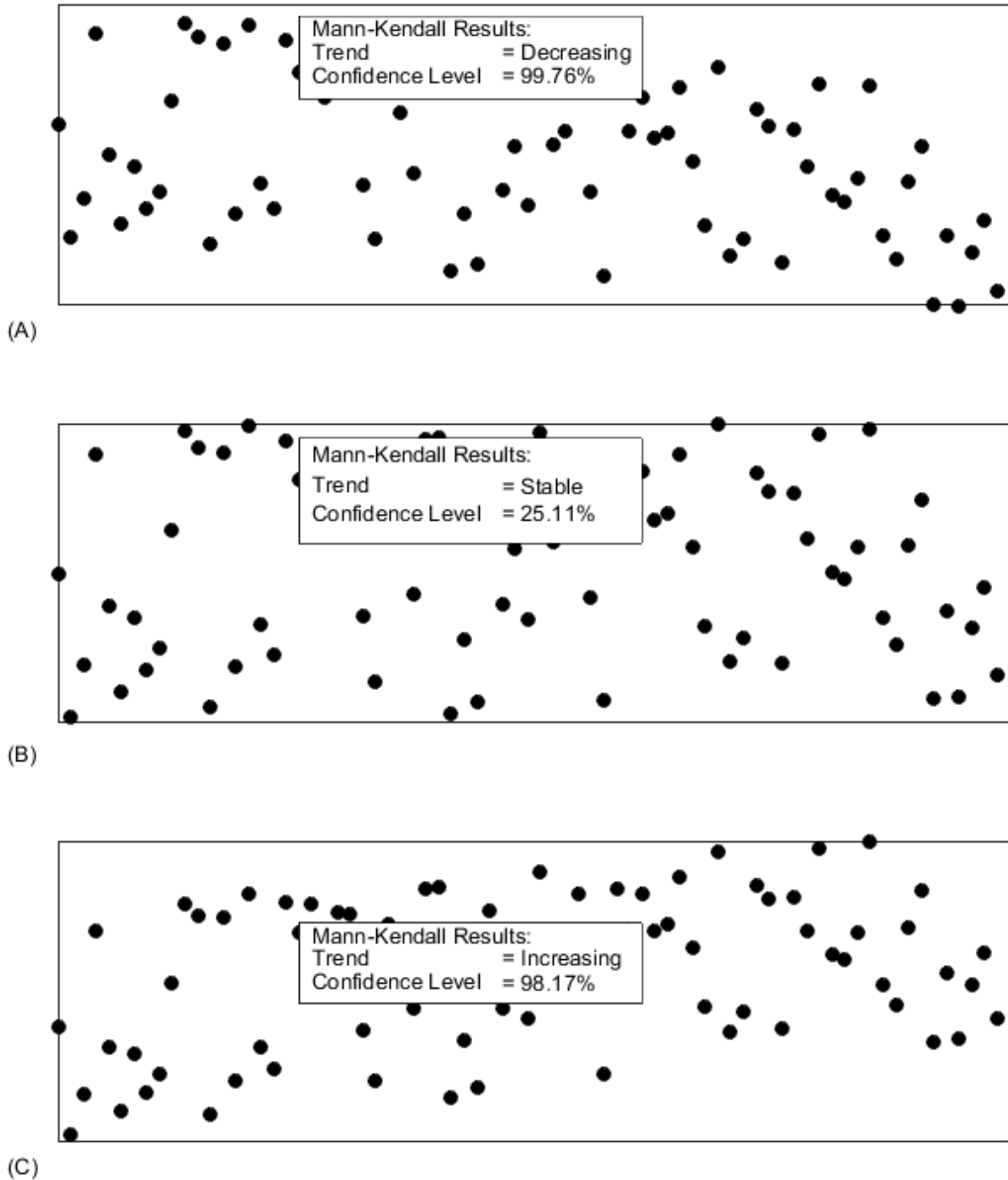


Figure 3-1 – Sample dataset showing trends identified by the Mann-Kendall analysis – (A) a decreasing trend, (B) a stable trend, and (C) an increasing trend.

Figure 3-1 presents examples of the Mann-Kendall analysis applied to a modified randomly generated dataset. Data shown in this example do not require units, and as such both axes on each graphic are left blank and unlabeled. The Mann-Kendall analysis is performed on each dataset, starting from the left-most plotted point and continuing rightward. Data shown on each of the three graphics in Figure 3-1 was derived from the same set of randomly generated numbers.

In Figure 3-1A, the random values are each decreased by 50% of the number-order of the values. For example, if the 10th random entry were given a value “10,” then the plotted value would be “5” as $10 - 10 * 50\% = 5$. Such a dataset is likely, but not guaranteed, to exhibit a decreasing trend. As shown, the Mann-Kendall analysis did conclude there is a decreasing trend in the data, and the confidence level of this conclusion was computed as 99.76%. It is notable that while the trend in the overall dataset is decreasing and the computed confidence level is high, this does not signify that all values will decrease from one entry in the dataset to the next. As shown in Figure 3-1A, there exists variation in values throughout the data, yet as identified through the Mann-Kendall analysis, the overall trend is of decreasing values.

Figure 3-1B demonstrates a stable trending dataset, exhibiting neither increasing or decreasing trends. This dataset was unmodified from the randomly assigned data forming the basis for each of the three datasets displayed in Figure 3-1. As with the dataset with decreasing trends, the stable trending dataset exhibits variation from one data point to the next, yet the variation does not lead the overall dataset to show increasing or decreasing trends.

Figure 3-1C displays a dataset with an increasing trend, which is evident visually as the plotted points tend to be higher toward the right of the graphic. In this dataset, the random values were each increased by 50% of the number-order of the values. For example, if the 10th random entry were given a value “10,” then the plotted value would be “15” as $10 + 10 * 50\% = 15$. Such a modified random dataset is likely, but not guaranteed, to exhibit increasing trends. As with the decreasing and stable trending datasets, the increasing trending dataset exhibits variations and fluctuations in values from one point to the next such that the next point in the dataset is likely but not required to be higher in value than the previous point.

For discussions within the remainder of this report, Mann-Kendall analysis results are always presented as a combination of “Trend” and “Confidence Level” values. The threshold used to determine whether a trend is stable or increasing/decreasing is equivalent to a 75% confidence level. This confidence level suggests that there is a 75% chance the trend is real, but also that there is 25% chance the identified trend is false. Higher confidence levels are better indicators of the likelihood that the identified trend is real.

3.3 Revision & Updating of Phase I Results

Phase I of this project was completed in mid-2017 and utilized the most up to date hydrologic period of record available at that time for 14 locations in the upper Colorado River basin. The study sites used in Phase I of the project are listed below:

- Site #1 – North Concho River near Carlsbad
- Site #2 – South Concho River at Christoval
- Site #3 – Concho River at Paint Rock
- Site #4 – San Saba River at Menard
- Site #5 – Brady Creek at Brady
- Site #6 – San Saba River at San Saba
- Site #7 – Elm Creek at Ballinger
- Site #8 – Pecan Bayou at Mullin
- Site #9 – Llano River at Llano
- Site #10 – Pedernales River near Johnson City
- Site #11 – Colorado River at Colorado City
- Site #12 – Colorado River above Silver
- Site #13 – Colorado River near Ballinger
- Site #14 – Colorado River near San Saba

The current phase of the project (Phase II) performs a more in-depth review of the historical conditions and other factors that may have impacted long term rainfall/runoff conditions for a smaller portion of the study area covered in the Phase I effort. Specifically, the Phase II effort is concentrated in the watersheds of the North Concho, South Concho, San Saba, and Elm Creek which were represented in the Phase II report by the following study sites:

- Site #1 - North Concho at Carlsbad
- Site #2 - South Concho at Christoval
- Site #6 – San Saba at San Saba.
- Site #7 - Elm creek at Ballinger

Since the Phase I report was completed, additional years of hydrologic information have become available and thus the major surface water related inputs to the Phase I analysis were extended to include the most up to date information. The following summarizes the period of record for each of the surface water related information for both the Phase 1 and Phase II periods:

Table 3-2 – Updates to Phase I Results

Phase of Project	I	II
Date of Phase Completion	Mid 2017	Mid 2019
Available Period Of Record for Observed Streamflow	1940-2016	1940-2018
Available Period of Record for Observed Precipitation	1940-2016	1940-2018
Available Period of Record for Naturalized Flow	1940-2013	1940-2016

Although Phase II only concentrates on 4 of the study sites reviewed in the Phase I report, each of the 14 study sites evaluated in Phase I were also updated and reviewed. The process described in the Phase I report was repeated for each study site to update the hydrologic period (2016-2018 for observed flow and precipitation; and 2014-2016 for naturalized flow) and the same process of long term trend analysis was used to evaluate the extended period. Specifically, the information presented in Appendix D (Cumulative Mass Plots) and Appendix E (Double Mass Plots) of the Phase I report were extended to include the new information and plots covering the most up to date period of record were evaluated as to whether the new information changed the trends noted in the Phase I report.

Since the Phase I effort was completed, the entire study area has experienced increased precipitation and observed flow, especially in late 2018. In addition, the naturalized flow information is now available through 2016, which offer new comparison opportunities for the 2014-2016 period. The next section details these results for the study site locations covered in Phase II of the project and the final section provides general observations of results for the study site locations that were used in Phase I but are not part of current Phase II effort.

3.3.1 Updated Study Site Information for Phase II Analysis

Within the Phase I project report, Kennedy Resource Company (2017) used cumulative mass plots to describe patterns in rainfall and streamflow for the period from 1940-2013. Since completion of the Phase I report, additional naturalized flow data has been made available by the Texas Commission on Environmental Quality (TCEQ), extending the period of record to 1940-2016. This period of record is the focus time-period for the Phase II project analysis, and as such we considered it beneficial to extend the Phase I analysis to include the additional flow data. This portion of the Phase II project was undertaken by Kennedy Resource Company.

The cumulative mass plot for each of the four study sites that are covered by the current Phase II effort are presented below along with observations with regard to how the extended hydrologic information relate to long term trends. The time based cumulative mass plots are presented for each of these sites because it facilitates easy comparison of long term quantities of precipitation and flow at the site of interest. Monthly accumulated observed streamflow and naturalized flow are plotted on the left Y axis, with cumulative monthly rainfall plotted on the right Y axis, and time in years on the X axis. Cumulative mass plots provide a means to observe the precipitation trace and both flow traces at the same time and to be able to examine precise periods along with knowledge of major reservoir construction dates, if applicable. Analyses of these plots and their significance were provided in the Phase I report for this project (KRC, 2017).

3.3.1.1 Site #7 - Elm creek @ Ballinger

The complete cumulative mass plot for Elm Creek at Ballinger is presented in Figure 3-2. Review of the plot shows almost identical deflections to those that were observed at study site #6. Again, similar to observations of the study sites #1, #2, and #6, it is clear that these deflections are reflecting the recent increases in precipitation but there is not enough period of record available after these events to make conclusions with regard to long term trend changes.

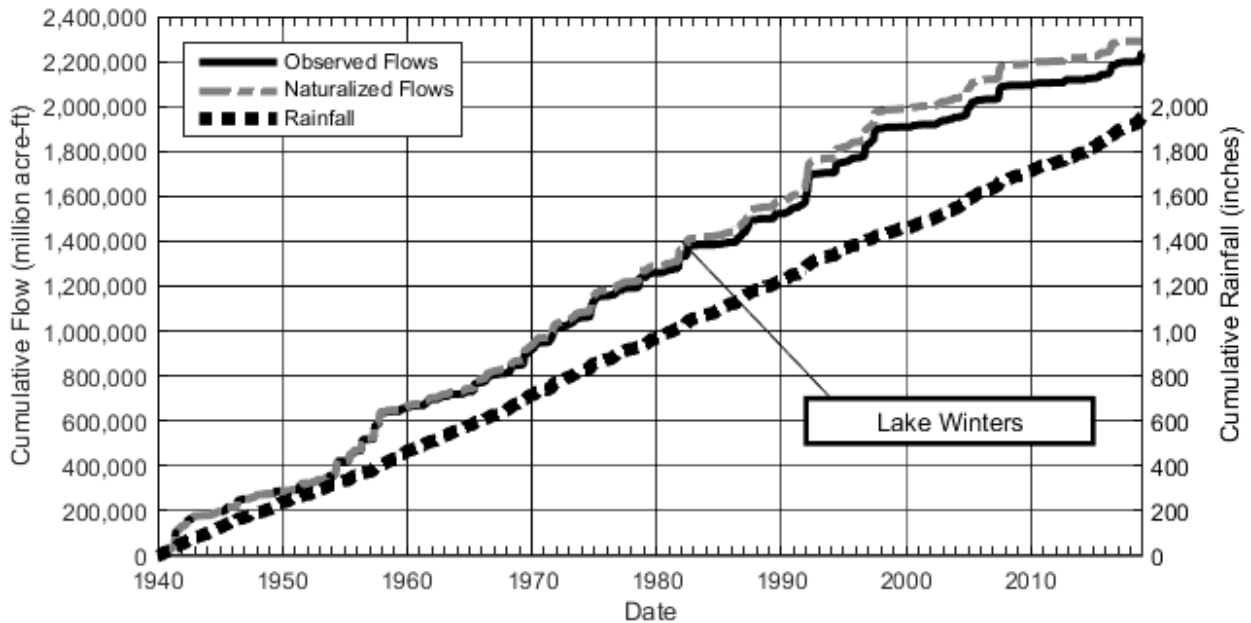


Figure 3-2 Cumulative mass plot for study site #7 - Elm Creek at Ballinger

3.3.1.2 Site #6 – San Saba at San Saba.

The complete cumulative mass plot for the San Saba River at San Saba is presented in Figure 3-3. Review of the plot shows that there was an increase in precipitation in 2018 with a corresponding substantial increase in observed flow, both of which are outside of the period of record for which naturalized flow data are available. This 2018 increase appears to be similar to what is seen at the end of several past drought cycles. In addition, in response to an increase in precipitation, the flow traces show an increase in 2015, which is substantial although not unprecedented. Similar to observations of the study sites #1 and #2, it is clear that these deflections are reflecting the recent increases in precipitation but there is not enough period of record available after these events to conclude much with regard to long term trend changes.

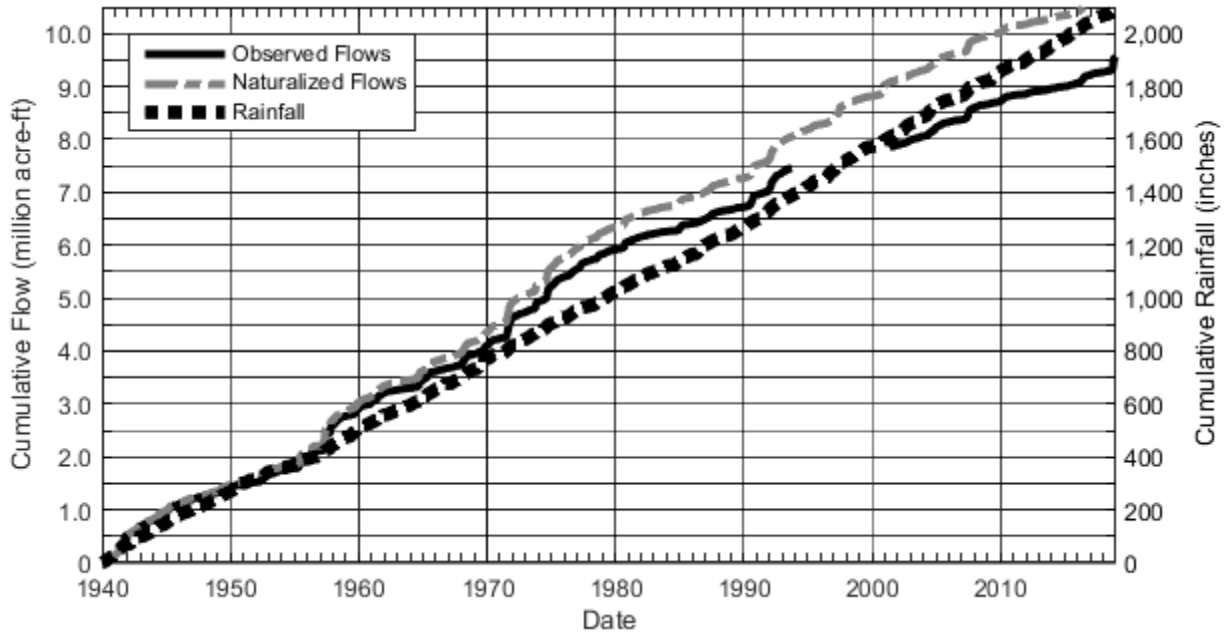


Figure 3-3 Cumulative mass plot for study site #6 - San Saba at San Saba

3.3.1.3 Site #2 - South Concho at Christoval

The complete cumulative mass plot for this site is presented in Figure 3-4. Review of the plot shows that there was a substantial increase in precipitation in 2018 with a corresponding increase in observed flow, both of which are outside of the period of record naturalized flow is available. This 2018 increase appears to be similar to what is seen at the end of the 1950's drought period. In addition, a small increase can be seen in 2014, which shifts the flow curves but does not substantially change the trends. With regard to the major shift in the last few months of the period of record, it is clear that these deflections are reflecting the most recent large rain events but there is not enough period of record after these events to conclude much with regard to long term trend changes.

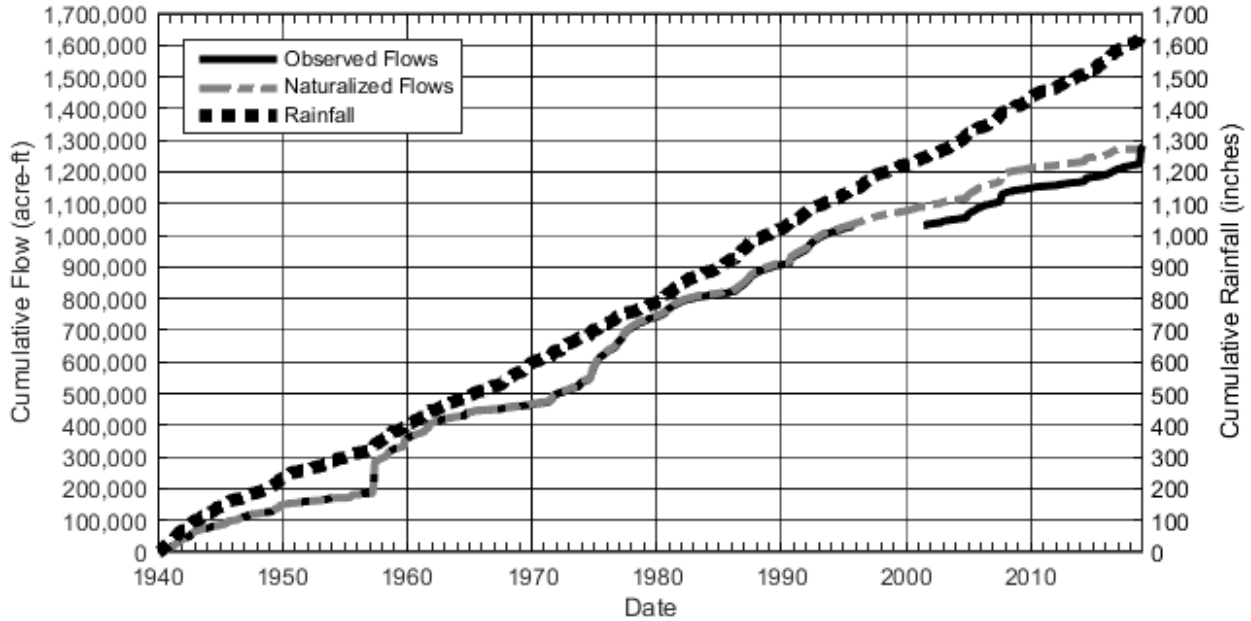


Figure 3-4 Cumulative mass plot for study site #2 South Concho at Christoval

3.3.1.4 Site #1 - North Concho nr Carlsbad

The complete cumulative mass plot for the North Concho River nr Carlsbad is presented in Figure 3-5. Review of the plot shows that precipitation has increased in the late period of record with a corresponding increase in naturalized flow. However, the increases are not inconsistent with other flood events in the past and there does not appear to be a significant change in any of the trends after the large precipitation events ended.

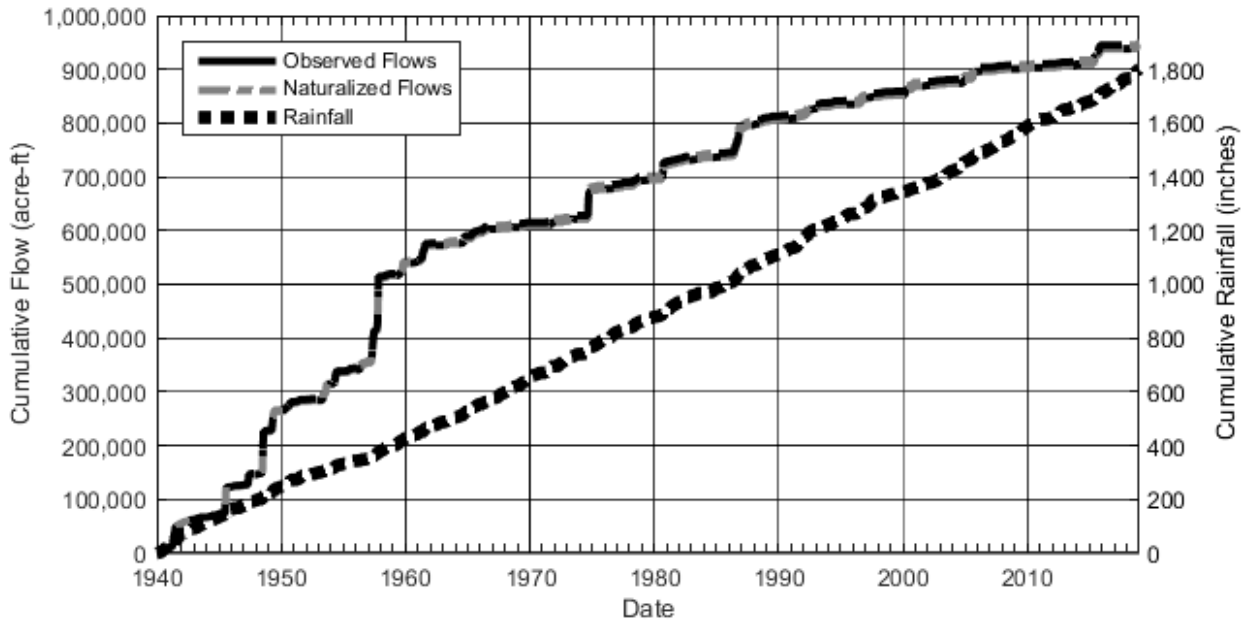


Figure 3-5 Cumulative mass plot for study site #1 - North Concho Rv near Carlsbad

3.3.2 Updated Information for Other Study Sites from Phase I

Similar to the information that has been detailed for the 4 study sites covered in the current Phase II effort, review of the cumulative mass and double mass plots for the other 10 Phase I study sites show varying magnitudes of increases in each of the long term hydrologic indicators for the extended period of record. However, since these increases are only able to be observed for the last couple of years, conclusions regarding changes to the long term runoff trends cannot be made. Nevertheless, these results are encouraging in that they show that since about 2015, both observed streamflow and naturalized flows have increased in response to recent increases in precipitation. Other sections of this report detail an in-depth analysis of many of the factors that are believed to impact quantities of runoff over time for the Phase II study areas and the recent increases in precipitation will be taken into consideration.

3.3.3 LRE Water's Opinion regarding Cumulative Mass Plots

LRE Water has reviewed these plots provided by Kennedy Resource Company, and has concluded that they provide little analytical value with respect to identifying and quantifying trends within the rainfall and streamflow datasets. As shown in Section 3.3.1, the vertical scales of each graphic often make difficult assessing differences between cumulative naturalized streamflow and measured streamflow. We suggest that a better analysis method would be to plot how observed and naturalized flows change with rainfall. This could allow for the identifications of periods in time when the rainfall-runoff response noticeably changed within a given watershed. LRE Water did not perform such analyses as they were outside the scope of work of this Phase II project.

4 Task 2 – Remote Sensing Analysis

4.1 Small Impoundment Analysis

Under this task, data was to be collected regarding the existence, surface area, and storage capacity of small ponds located within the subject watersheds. As used herein, “small ponds” refers to ponds smaller (in both storage capacity and surface area) than those impoundments incorporated into the flow naturalization process (as described by Kennedy, 2017 and others). The flow naturalization process generally involves only the larger impoundments, whose water storage, evaporative losses, and pass-through requirements have a direct, individual impact on streamflow from the watershed. Within the four study area watersheds incorporated into the Phase II analysis, the following “large ponds” were excluded as they are already included in the flow naturalization process:

- Lake Winters (Elm Creek Watershed)
- Lake Nasworthy (South Concho Watershed)
- Twin Buttes Reservoir (South Concho Watershed)
- Brady Reservoir (San Saba Watershed)
- OC Fisher Lake (North Concho Watershed)

In theory, small ponds may retain water that would otherwise travel downstream and contribute to streamflow. The retained water will also likely seep into the local groundwater system through the bottom of the ponds. Portions of the retained water will also be lost to evaporation. It is likely that most small ponds do not have the ability to pass water downstream until the ponds are full, thereby making the ponds an explicit hindrance to downstream streamflow. This is true both for on-channel and off-channel ponds, the later which would receive direct precipitation and diffuse surface runoff in order to fill; this infilling water would otherwise contribute to streamflow if the off-channel pond were not present.

The goal of this task was to quantify the number of ponds currently existing within each study area watershed, to quantify the surface area of the ponds, and to estimate the capacity of each pond and of the collective ponds by watershed. The secondary goal was to determine the approximate date upon which each pond was created. The creation dates of each pond provide knowledge as to when each pond began altering the local hydrology and resulting streamflow from the watershed. For example, ponds created in the year 2000 would not have had any impact on streamflow for years prior to the year 2000. By developing a database of small ponds in this manner, it is possible to quantify the collective impact of the ponds on streamflow, and how that impact changes over time.

To identify small ponds and catalog pond properties, we used a variety of publically available datasets and software programs. The following sections detail the methodology used in pond identification. Identified ponds include both naturally occurring lakes/ponds and impoundments created by human influences on the natural landscape.

4.1.1 National Hydrography Dataset (NHD)

The National Hydrography Dataset (NHD) is a digital representation of the water drainage network and graphically depicts the locations of rivers, streams, canals, ponds, lakes, and other waterbodies. The dataset is currently maintained by the US Environmental Protection Agency (EPA), and is periodically updated when suitably accurate new data is available. NHD data for the State of Texas was obtained from the Texas Natural Resource Information Service (TNRIS) website (<https://tnris.org>) and was processed using ArcGIS software. The NHD data used for this project was last updated in 2002, and thus all polygons within the “NHD_Waterbodies” feature class were initially assigned a creation date of “2002.” The NHD dataset itself does not contain creation dates as a waterbody attribute.

Figure 4-1 is an example of how the NHD and available aerial imagery was used to develop an improved small pond dataset for the study area watersheds. Specifically, the figure depicts a portion of the NHD from the Elm Creek watershed, showing ponds overlain on a “Basemap” aerial land surface image obtained through the ArcGIS system software. The NHD ponds are shown with a red outline, and four ponds are visible on the aerial image. These outlines generally conform to the size and shape of the underlying ponds visible on the aerial image, and therefore did not require revision. For instances when the NHD ponds were smaller in extent than the underlying ponds visible on the aerial image, then the NHD ponds were edited so that each pond’s final shape (and surface area) match that of the pond from the image. For instances when the NHD pond was of a greater extent than the pond visible from the aerial image, the NHD pond was not modified, as it was assumed that the pond extent at the time of the NHD creation (2002) did match the extent of the pond as seen in the original images from which the NHD was created. This larger extent would likely represent the size of the pond at a time when the pond contained more water than was evident in the updated aerial images available within the ArcGIS Basemap databases.

Figure 4-1 also identifies four ponds that are visible within the aerial image yet not included in the NHD. These “non-NHD” ponds would have been incorporated into the project pond database through manual digitization. Digitization was primarily undertaken using imagery and tools available within the Google Earth software (see Section 4.1.4), yet was also performed within ArcGIS if underlying aerial imagery provided metadata listing the date when the imagery was taken. The Basemap used in Figure 4-1 did not include metadata, and as its data was not discernible, ponds were not digitized based on this image. The image is presented here for illustration purposes only.

Figure 4-2 illustrates the different types of ponds that were included in the Phase II small pond evaluation. These pond types included:

- On-Channel Ponds (Figure 4-2A) – ponds that receive direct precipitation, diffuse surface runoff, and concentrated runoff from a defined NHD flowline (creek, stream, river, etc.).

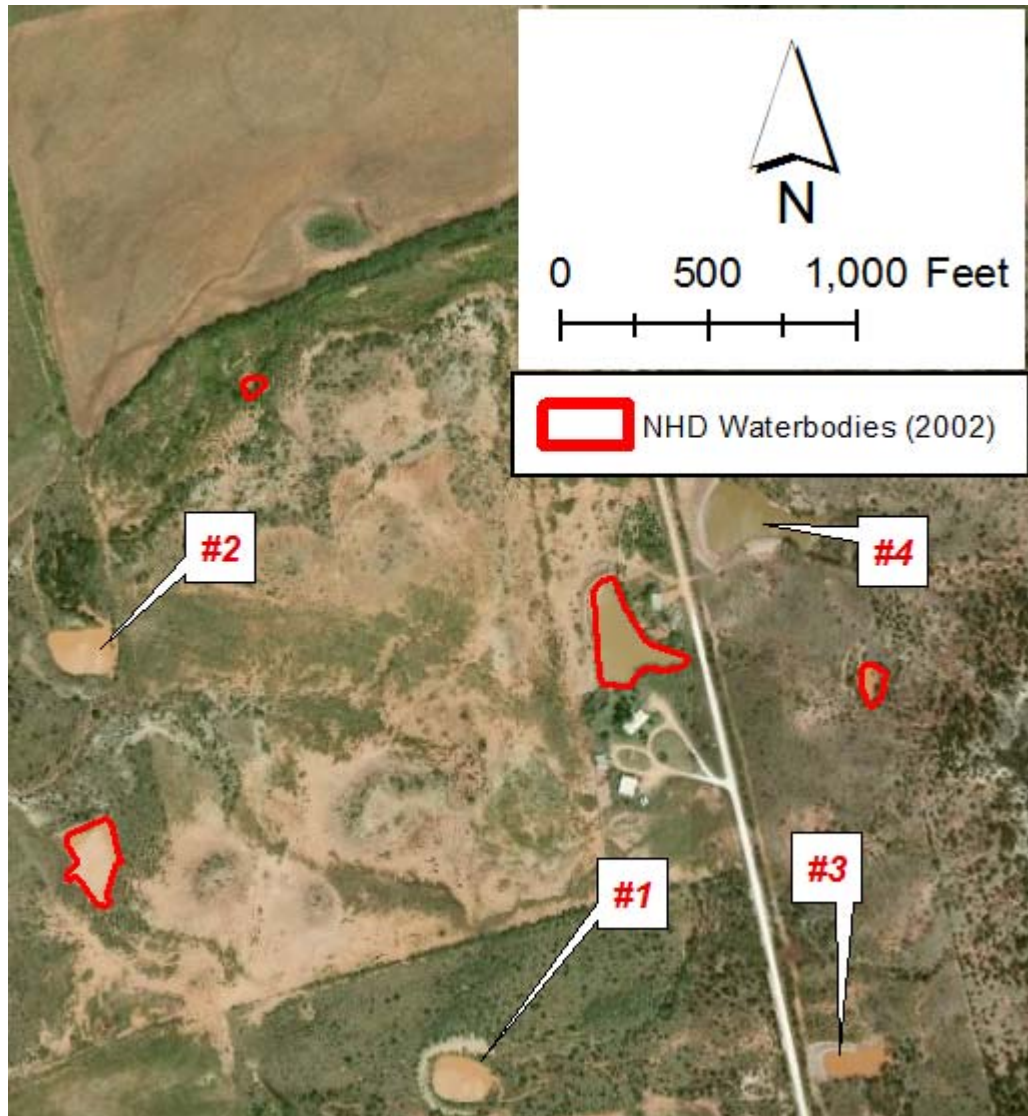


Figure 4-1 Small pond identification using the National Hydrography Dataset (NHD).

- Off-Channel Ponds (Figure 4-2B) – ponds that receive direct precipitation and diffuse surface runoff, but do not receive concentrated runoff from a defined NHD flowline (creek, stream, river, etc.).
- Off-Channel Isolated Ponds (Figure 4-2C) – ponds that receive direct precipitation and inflows pumped from a nearby source (such as a NHD flowline).

Off-channel isolated ponds are likely to be ponds used by municipalities to store diverted surface water from nearby waterbodies, or locally sourced groundwater. The significance of the small pond classification is discussed further in Section 0. During this Phase II project, small ponds were identified and assigned a “creation date,” yet were not assigned a classification into one of the categories displayed in Figure 4-2.

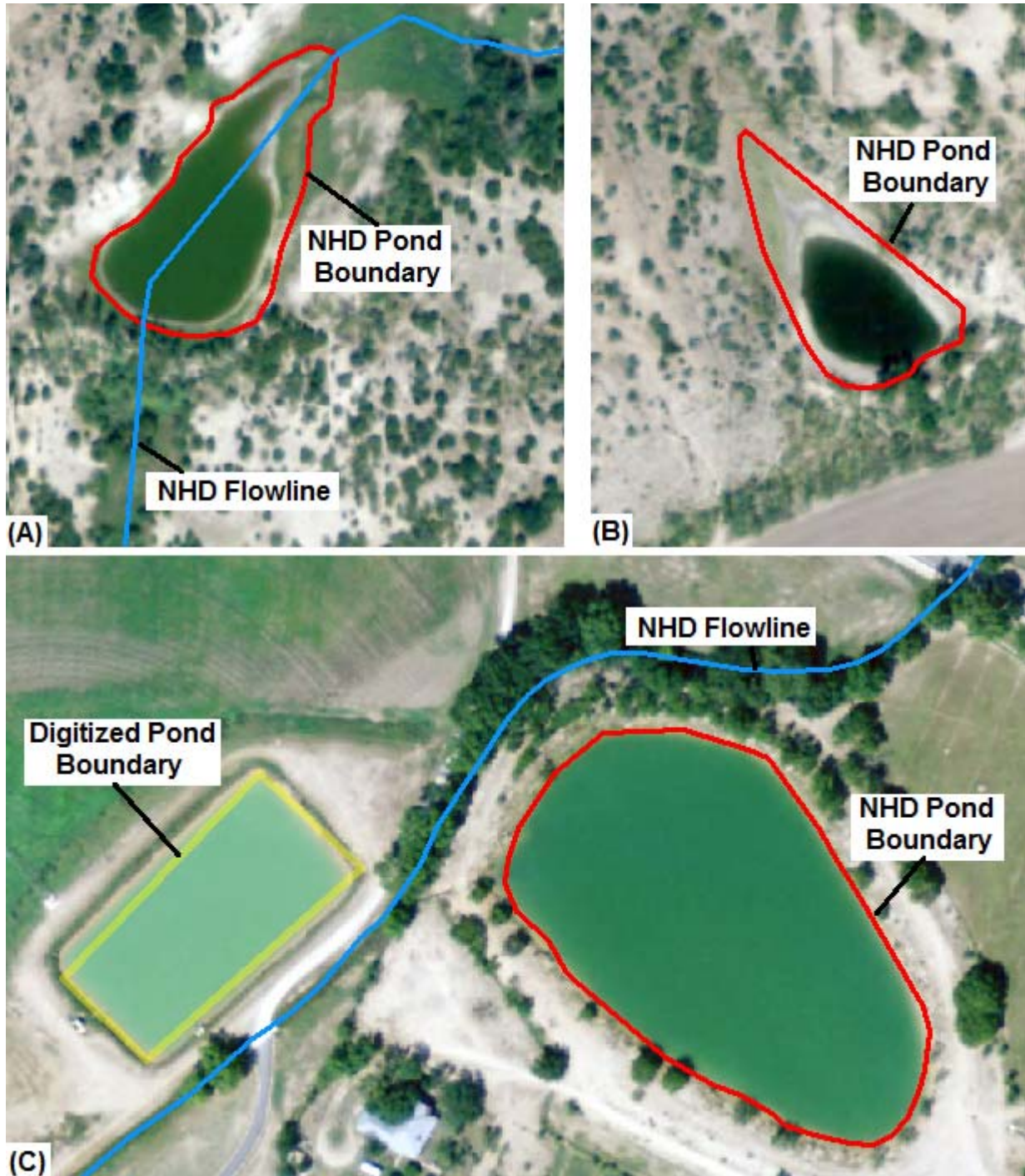


Figure 4-2 – Small pond categories – (A) On-channel ponds, (B) off-channel ponds with contributing watersheds, and (C) off-channel ponds without contributing watersheds. Red pond boundaries are from the NHD, and yellow boundary was manually digitized. Aerial imagery shows portions of Menard County in the San Saba River watershed, with imagery dating from 2008 as obtained from Google Earth.

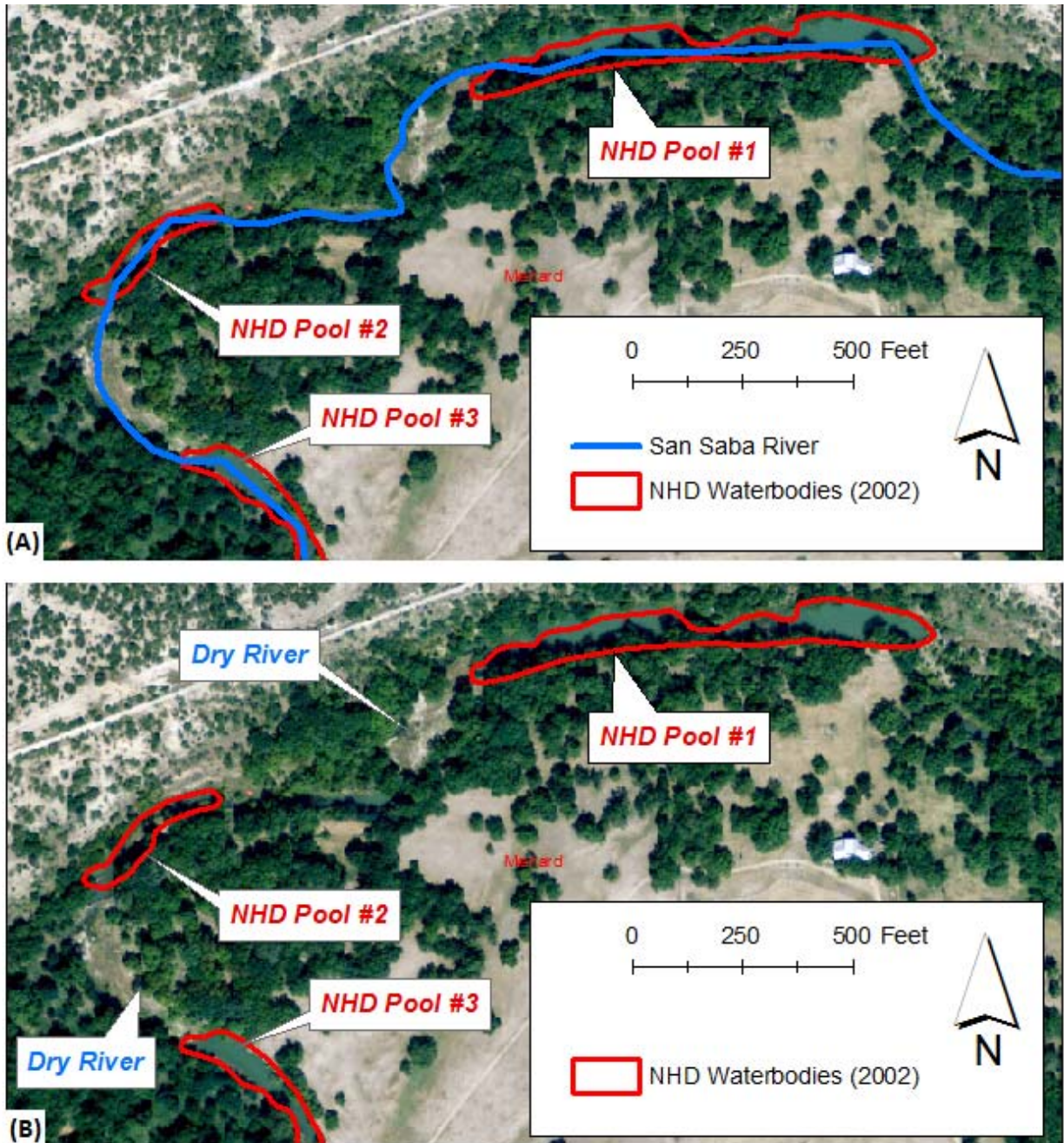


Figure 4-3 – Exclusion of NHD “Pools” from small pond datasets. (A) three pools along the San Saba River are included in the NHD. (B) sections of dry river evident between pools. Aerial image is from 2008.

Figure 4-3 identifies another category of ponds as included within the NHD dataset. These ponds, labeled as “Pools” in the image represent portions of the flowing river that may retain water at times of low streamflow. In Figure 4-3A, three NHD Pools are identified along a portion of the San Saba River east of Menard. Figure 4-3B shows the same image with the removal of the blue line representing the San Saba River. From this image, it is evident that at the time of the aerial image (2008, source TNRIS), the San Saba River was dry in between the identified pools, and that the river was not flowing. All pool

waterbodies located along the main-stem reaches of the larger rivers and creeks within the study area were excluded from the small ponds database created for this Phase II project. The creeks and rivers considered when excluding NHD pools included:

- Elm Creek
- San Saba River (Downstream from Talbot Lake)
- Brady Creek
- North Concho River
- South Concho River

Pools within these creeks and rivers were excluded as it is impossible to determine the extent to which these pools must be full before passing water downstream. The implications of this exclusion are discussed further in Section 4.2 and Section 0. NHD pool waterbodies located on creeks and rivers other than those listed above were included in the small pond dataset. Their inclusion is discussed further in Section 0.

4.1.2 Google Earth Engine (GEE)

In an attempt to avoid manual digitization of all newly identified ponds, we developed processing programs within Google Earth Engine (GEE). These programs make use of publically available LANDSAT data and the analysis capabilities included within Google Earth (Google, 2019) to potentially hasten the pond identification process. The processing programs essentially study the digitized LANDSAT terrain images, which are images of the land surface as captured via satellite. GEE programs were configured to review each image, identify adjacent pixels that represent standing water, and then create a polygon surrounding the adjacent pixels. The resulting polygon therefor represents an estimate of the surface extend of a pond as derived from the LANDSAT image. The LANDSAT data available for use in GEE processing consisted of bi-weekly images from 1986-Present, although not all images were suitable for pond identification due to periodic cloud cover captured at some locations.

Figure 4-4 displays the results of the GEE processing for the same portion of the Elm Creek watershed shown in Figure 4-1. The GEE-identified waterbodies are shown as filled polygons, with different colored polygons denoting identification of the pond(s) in different years. As show, GEE was able to identify the two larger ponds included within the NHD, as well as the non-NHD pond identified as “#1.” However, GEE was unable to properly identify the shapes of these ponds, as the colored polygons did not match the pond extent from the NHD or the aerial image. As such, we determined that GEE was not a viable tool for accurately locating and sizing ponds within the study area watersheds. This is additionally true in recognizing that GEE was unable to identify the smaller ponds labeled as “#2,” “#3,” and “#4” in Figure 4-4. We suspect the difficulty in using GEE for pond identification lies in the similar color of the water in each pond to nearby excavated or barren landscape. Ponds with blue water were more easily identified with GEE.

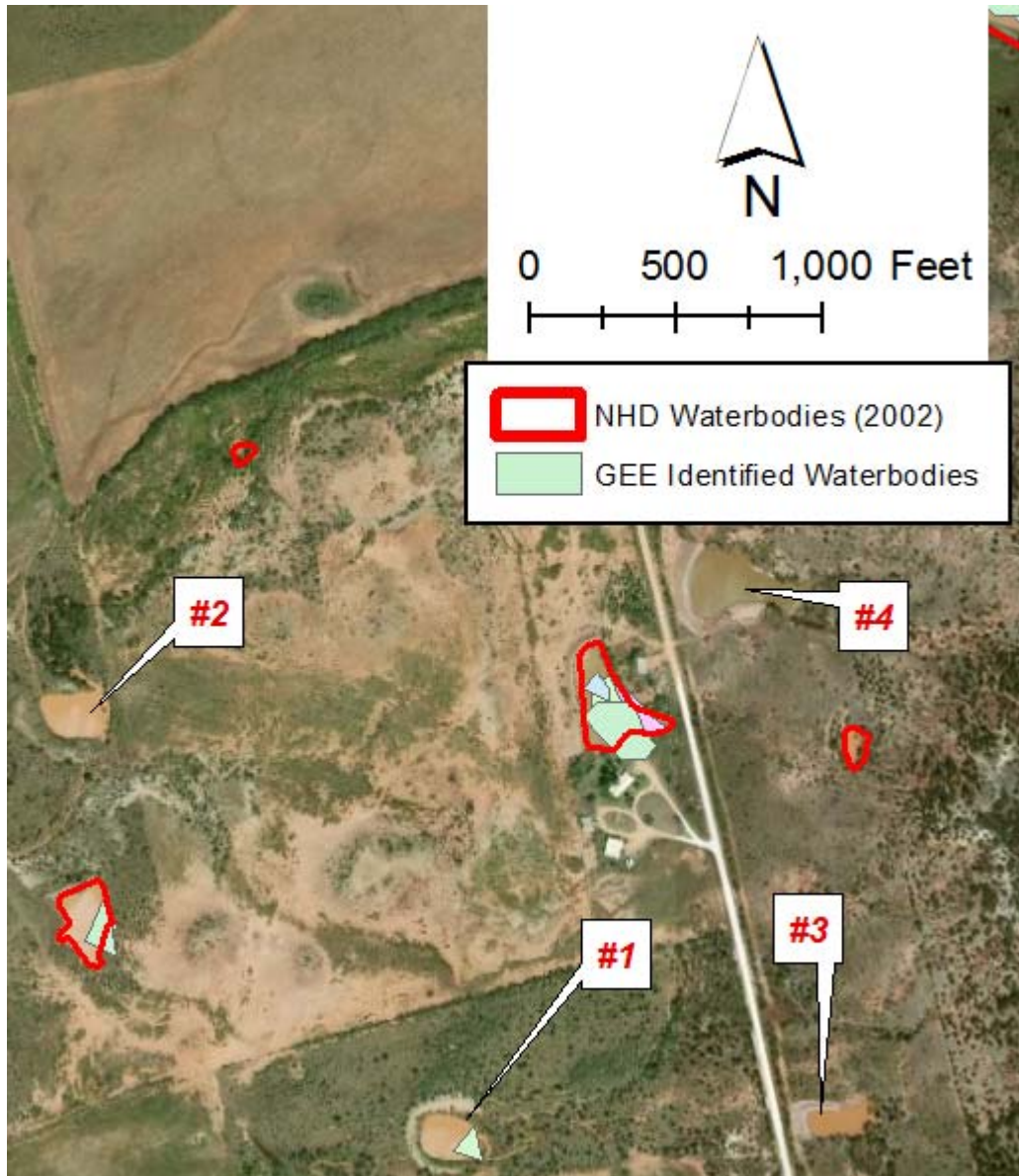


Figure 4-4 – Small pond identification with Google Earth Engine (GEE)

Results from the GEE processing were useful, however, in locating ponds requiring manual digitization, as well as in assigning creation dates to ponds. For the NHD ponds in Figure 4-4 that also have GEE polygons, the pond creation date was changed from “2002” (the NHD creation date) to the earliest date on which GEE identified water in NHD pond extent. Thus GEE usage allows for assigning dates to certain ponds that existed or where created between 1986 and 2002.

4.1.3 US Geological Survey Topographic Maps

Further refinement of pond boundaries and creation dates was achieved through manual review of digitized United States Geological Survey (USGS) topographic maps. These digitized maps are publicly available and accessible for use in ArcGIS processing from the Texas Natural Resources Information System (TNRIS, <https://tnris.org> as of 7/6/2019). Each map displays a date on which the map information represents, and can include additional dates detailing when features on the map were last photorevised. USGS topographic maps were generally created in the 1950s-1960s, with photorevisions occurring when needed in the 1980s. Therefore reviewing of USGS topographic maps allowed for the determination of earlier creation dates than available through the NHD and GEE. In total, review of 149 USGS quadrangle topographic maps was needed to cover all portions of the study area watersheds.

Figure 4-5 shows the USGS topographic map for the same area visible in Figure 4-1 and Figure 4-4. This map shows features present as of 1967 per the date provided on the maps lower left corner (not shown). As shown, the three ponds included in the NHD dataset were in existence in 1967, as indicated by the blue map coloring underneath the NHD and GEE Identified waterbodies. It is also evident that the ponds labeled “#1,” “#2,” “#3,” and “#4” did not exist in 1967; thus the creation date for these ponds could not be updated based on the USGS topographic map.

In utilizing topographic maps to assess the existence and size of small ponds, it is assumed that each map was produced accurately and accurately represents the land surface at the time of the map creation (and photorevision). It is possible that small ponds existed at the time of the topographic map creation, and that the mapmaker deemed them too small or insignificant to be included on the map. As such, it is possible that a small pond that existed in 1967 (for example) was not shown on the topographic map, but was included in the NHD dataset. Under this analysis, such a pond would be assigned a creation date of 2002, rather than 1967. As detailed in Section 10, such an error in the creation date would mean that the hydrologic influence of the pond would not “occur” until the 2002 date, which could lead to mis-interpretation of the impacts the pond historically had on streamflow. For this phase II analysis, it was assumed that all topographic maps were accurate and properly represented the surface hydrology of the terrain at the time of the map creation.

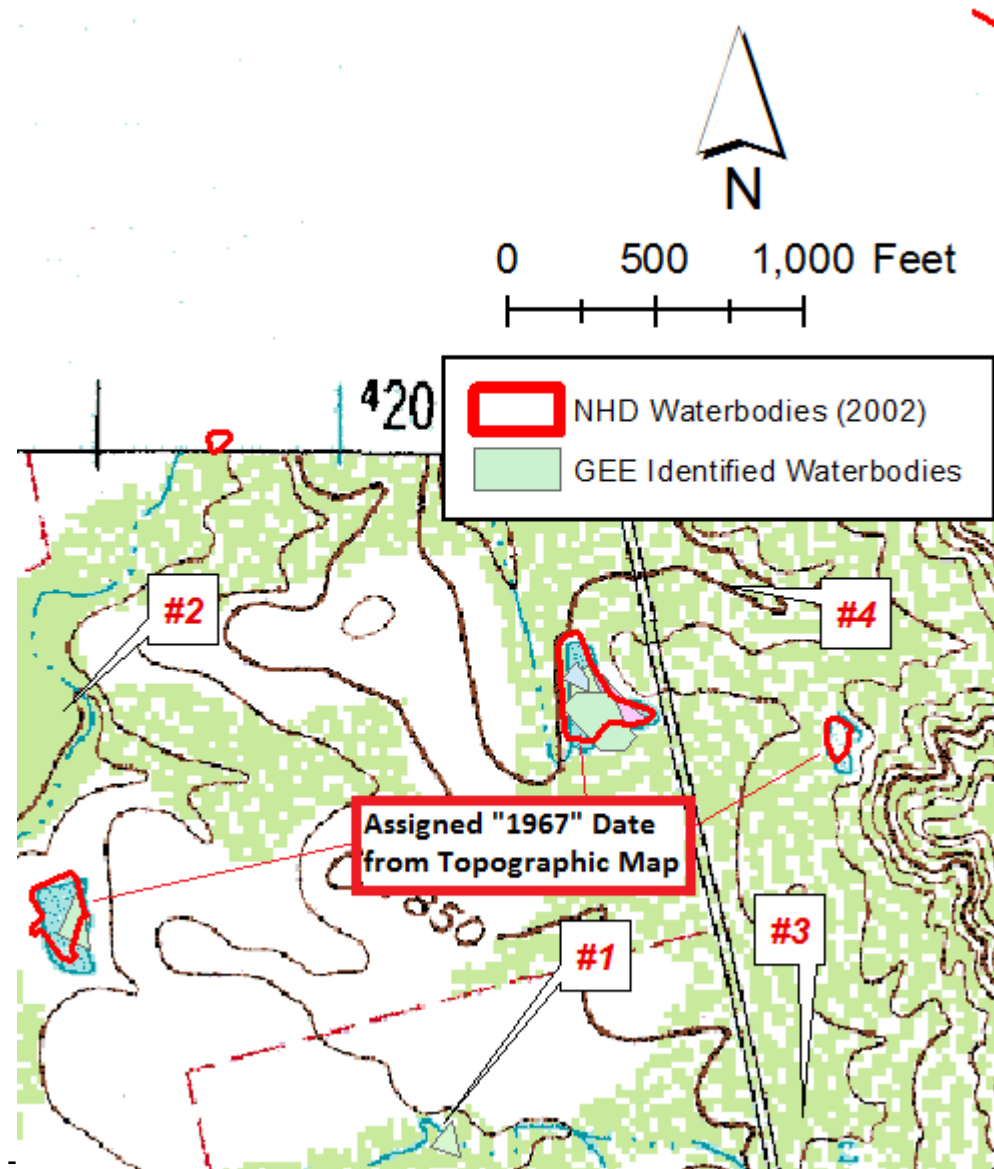


Figure 4-5 – Using USGS topographic maps to identify and date small ponds

4.1.4 Manual Data Analysis Using Google Earth (GE)

The most useful method for identifying “new” small ponds involved manual review of aerial imagery within Google Earth (GE). Use of Google Earth was beneficial in that the aerial imagery available is generally newer than that available within ArcGIS, and each image contained metadata detailing the date of the image. In addition, Google Earth is publicly available (whereas ArcGIS requires a software license), and is therefore available for use by individuals without access to ArcGIS. To use Google Earth for pond identification, the NHD dataset was exported from ArcGIS as a KMZ (Google Earth format) file, and then imported into Google Earth. Ponds identified in Google Earth were manually digitized using the existing Google Earth functionality, and then imported back into ArcGIS for further processing.

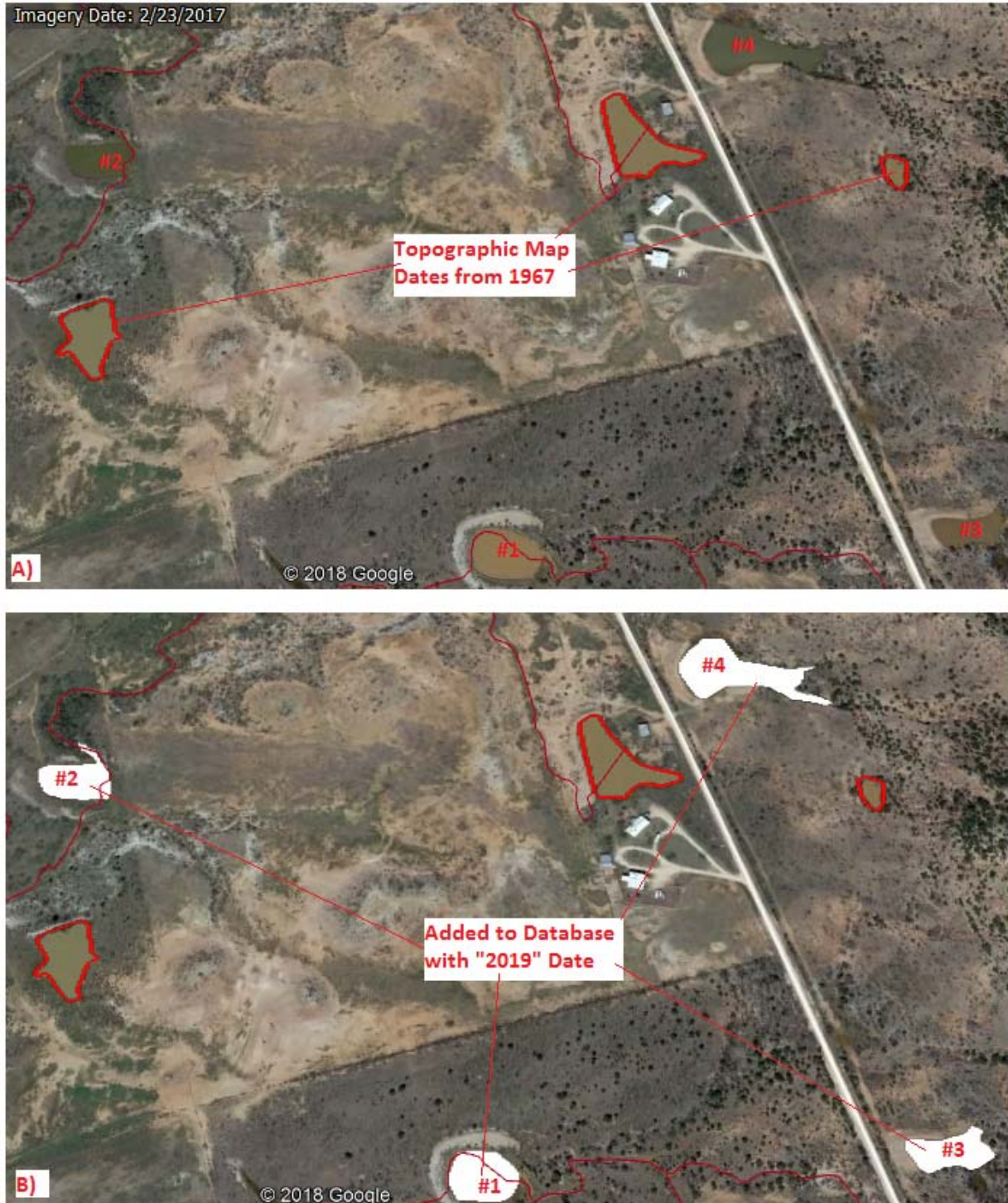


Figure 4-6 – Small pond digitization within Google Earth

Figure 4-6 shows the Google Earth view of the same location within the Elm Creek watershed used in Figure 4-1-Figure 4-5. Specifically Figure 4-6A shows the digitized

ponds from the NHD dataset, assigned a creation date of 1967 based on the USGS topographic map (Figure 4-5). Figure 4-6B shows the ponds #1-#4 digitized within Google Earth, consisting of white polygons. These polygons were imported back into ArcGIS, where they were assigned a creation date of “2019” based on the date of the image used in Google Earth.

All polygons digitized within Google Earth were assigned a creation date of “2019” to denote that they were identified within Google Earth. These creation dates could be further refined using the “Historical Imagery” tool within Google Earth, yet full use of this tool was not possible under the scope of this Phase II project.

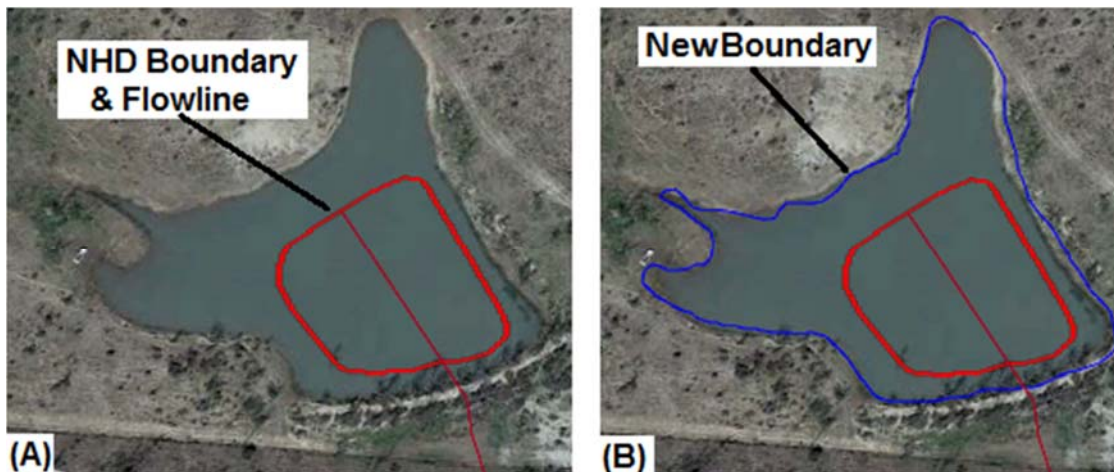


Figure 4-7 – Pond surface area adjustments within Google Earth – (A) pond boundary within NHD is smaller than indicated from the Google Earth image, (B) larger pond boundary (blue) is digitized, and the smaller pond is eliminated from the small pond dataset. Example is from the Elm Creek Watershed.

Figure 4-7 demonstrates how Google Earth was often used to update the existing NHD waterbody dataset to reflect the true size of the identified waterbodies. Within Figure 4-7A, an on-channel pond is identified within the NHD dataset, yet the pond extent is clearly smaller than the physical pond extent evident within the Google Earth image. For such instances, the larger pond extent is digitized within Google Earth (Figure 4-7B) and the new boundary replaces the NHD boundary within the small pond dataset. In contrast, if the pond boundary from the NHD encompassed the pond extent visible within Google Earth, then the pond boundary from the NHD was used in the small pond dataset. This process insured that the small pond dataset represents the ponds at their fullest, largest extent based on data from all available sources. The largest pond extent depicts the capacity of the pond to store water that would otherwise contribute to streamflow had the pond not existed.

4.1.5 National Inventory of Dams – NID

During Phase I of this study, data from the National Inventory of Dams (NID) was used to help assess the impact of small ponds. This data was obtained for inclusion into the Phase II small pond dataset. For each of the 103 NID entries located within the subject watersheds, NHD polygons corresponding to each NID point location were identified. Each NHD polygon was then attributed with the creation date recorded within the NID attributes for each point. Figure 4-8 presents three small ponds that were in the NHD and were assigned a “1970” creation date based on the date of the topographic maps showing the ponds in existence. Data from the NID indicated the ponds existed prior to 1970, and the creation dates for these entries within the small ponds database was adjusted to reflect the “year_Compl” attribute for the corresponding point entry within the NID database.

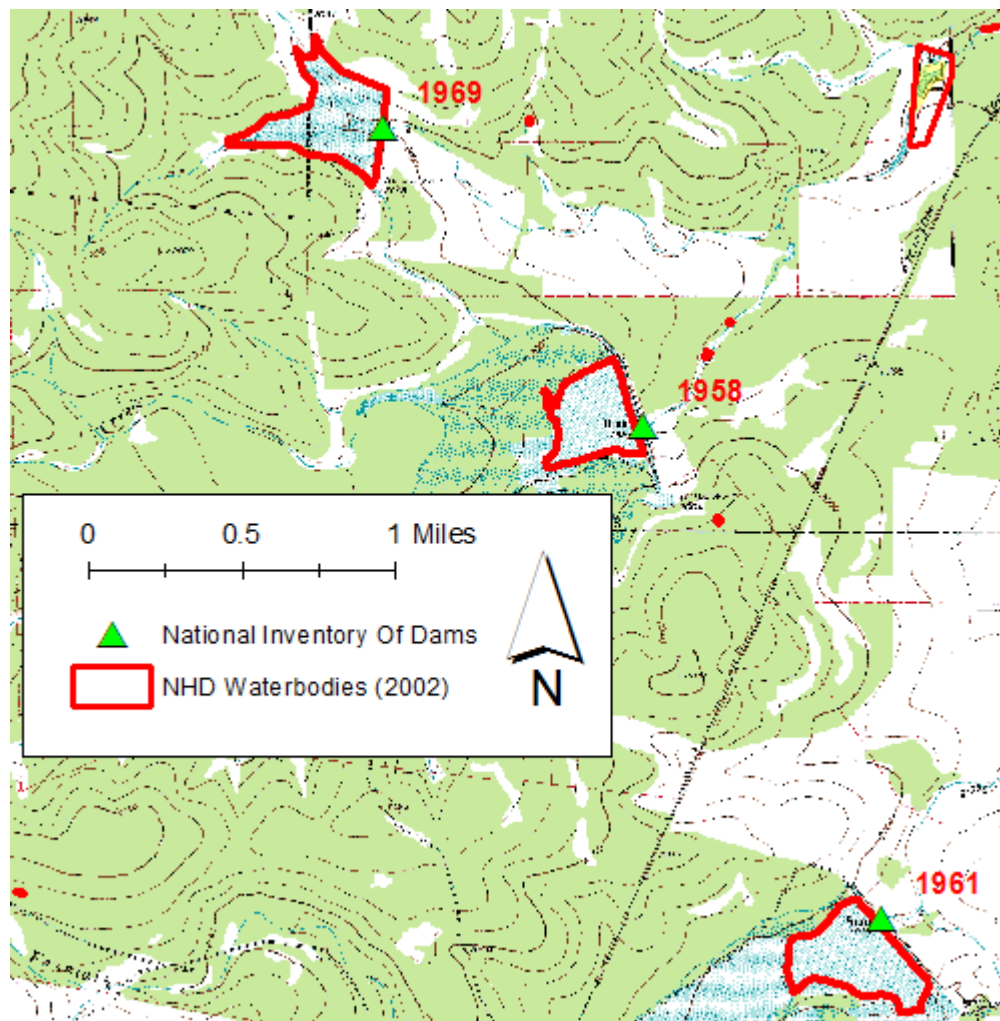


Figure 4-8 – Updating small pond creation dates using the National Inventory of Dams (NID). Shown are three ponds within the San Saba River watershed that were assigned the creation date of “1970” based on the date of the topographic map. These dates were then reduced based on the date of pond creation as stored within the NID.

4.2 Small Impoundment Results

The small pond identification process led to the inclusion of over 1,000 new ponds within the modified NHD project database. Most of these ponds had surface areas ranging from 0-5 surface acres, as most larger ponds were previously included within the NHD yet had their extents modified within Google Earth. Figure 4-9 shows the location of the waterbodies discovered in Google Earth and GEE, as well as waterbodies included in the NHD and channel waterbodies that were in the NHD but excluded from this analysis. The San Saba watershed contained the majority of the younger ponds, with many also found within the Elm Creek watershed. Newer ponds within the South Concho watershed tended to be located in close proximity to the South Concho River, whereas those in the North Concho watershed were found further away from the watershed's larger streams.

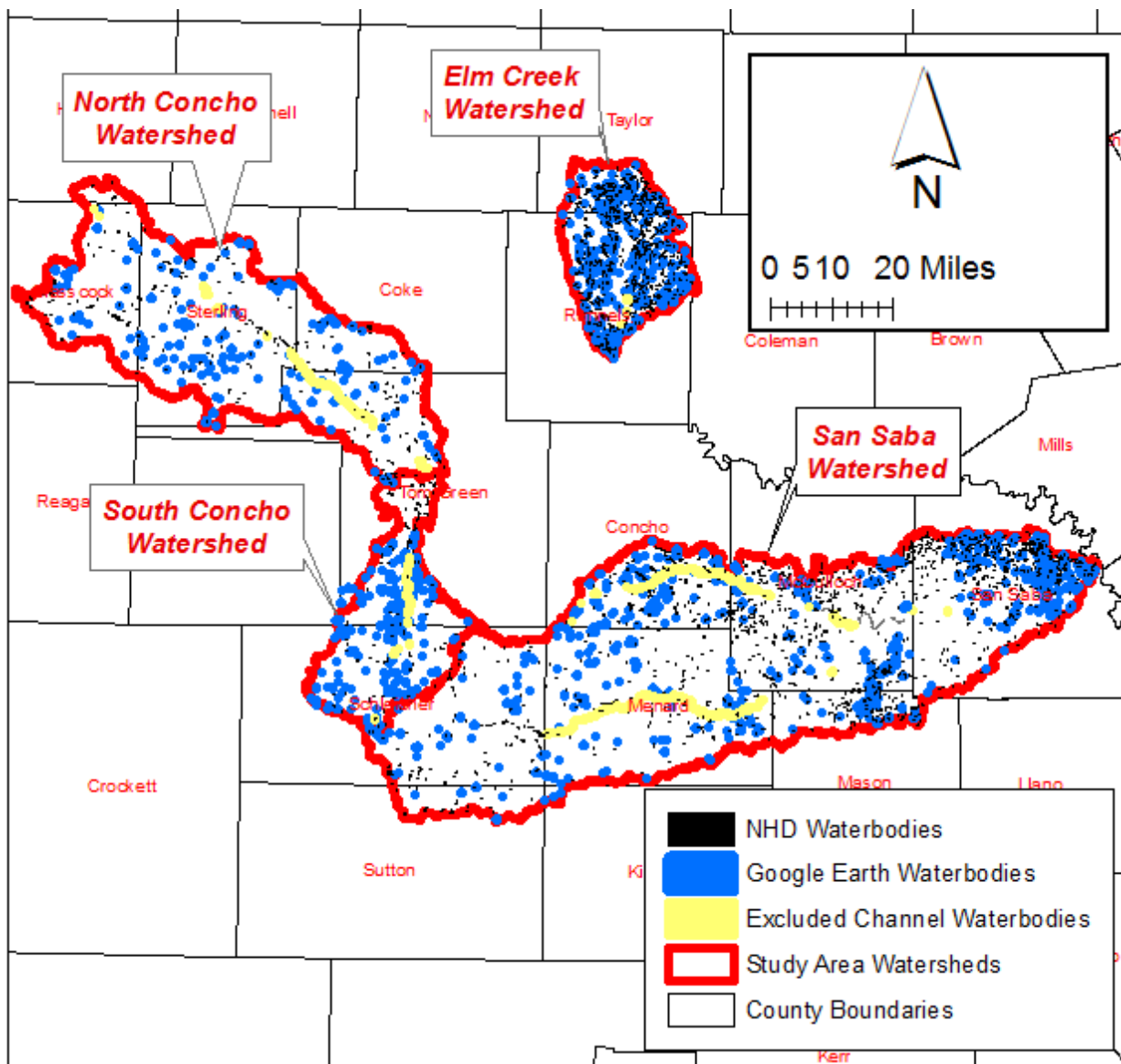


Figure 4-9 – Small pond locations within the study area

Pond surface areas (in acres) were calculated using the “Check Geometry” tool within ArcGIS, with the computed areas being added as a field in the database. Pond volumes were estimated based on the computed pond area, using a formula (Eq. 4-1) included within the Colorado Basin Water Availability Model (WAM) maintained and published by the Texas Commission on Environmental Quality (TCEQ). Within the WAM, Eq. 4-1 is used to determine the approximate surface area of a pond based on its computed storage, so that the WAM may properly compute storage loss or gain due to net evaporation. For this project, Eq. 4-1 is used to compute pond storage (or volume) based on the pond area as calculated within ArcGIS.

Eq. 4-1
$$Area = 0.911(Storage)^{0.695} \rightarrow Storage = \left(\frac{Area}{0.911}\right)^{1/0.695}$$

For this analysis and discussion, the term “storage” refers to the volume of water within a pond at any given moment, and is used interchangeably with the term “volume.” A pond’s “capacity” refers to the maximum storage for the pond, as calculated from Eq. 4-1 when using the maximum pond area as measured within ArcGIS.

Figure 4-10 presents results of the small pond analysis for the Elm Creek watershed. This watershed contains over 3,500 small ponds, with about 50% created after 2002 and over 300 ponds identified within Google Earth that were not contained within the 2002 NHD dataset. All ponds were found to have been created after then 1947-1957 critical drought period. The total surface area for these ponds amounts to 2,073 acres, which is slightly below 1% of the watershed area. The approximated total storage volume of these small ponds is 4,590 acre-ft, with only a small fraction of this capacity resulting from those ponds identified using Google Earth. The majority of the total storage volume within the Elm Creek watershed’s small ponds stem from Soil Conservation Service (SCS) reservoirs created within the 1960’s. The size of these reservoirs was often under-represented within the 2002 NHD. For comparison, Lake Winters (which was not included in the small pond dataset) has an approximate capacity of 8,374 acre-ft (when full), therefore the volume of all small ponds within the watershed amounts to 55% of the capacity of Lake Winters.

Figure 4-11 presents results of the small pond analysis for the San Saba watershed. This watershed contains over 7,000 small ponds, with about 35% created after 2002 and over 600 ponds identified within Google Earth that were not contained within the 2002 NHD dataset. Few of the ponds were created near the end of the 1947-1957 critical drought period, yet the ponds created during that time were typically SCS reservoirs with both larger areas and capacities (compared to the ponds created after 2002). The total surface area for the San Saba Watershed small ponds amounts to just over 5,600 acres, which is approximately 0.3% of the watershed area. The total storage capacity of these small ponds is 17,100 acre-ft. The majority of the total storage capacity within the San Saba watershed’s small ponds stem from Soil Conservation Service (SCS) reservoirs identified on USGS topographic maps dated “1970.” The size of these reservoirs was often under-represented within the 2002 NHD. For purposes of comparison, Brady Creek Reservoir has a surface area of approximately 2,000 acres, and a storage capacity of over 28,800 acre-ft. Therefore the small ponds within the San Saba watershed encompass a surface area 2.5x greater than Brady Creek Reservoir, yet store only 59% as much water.

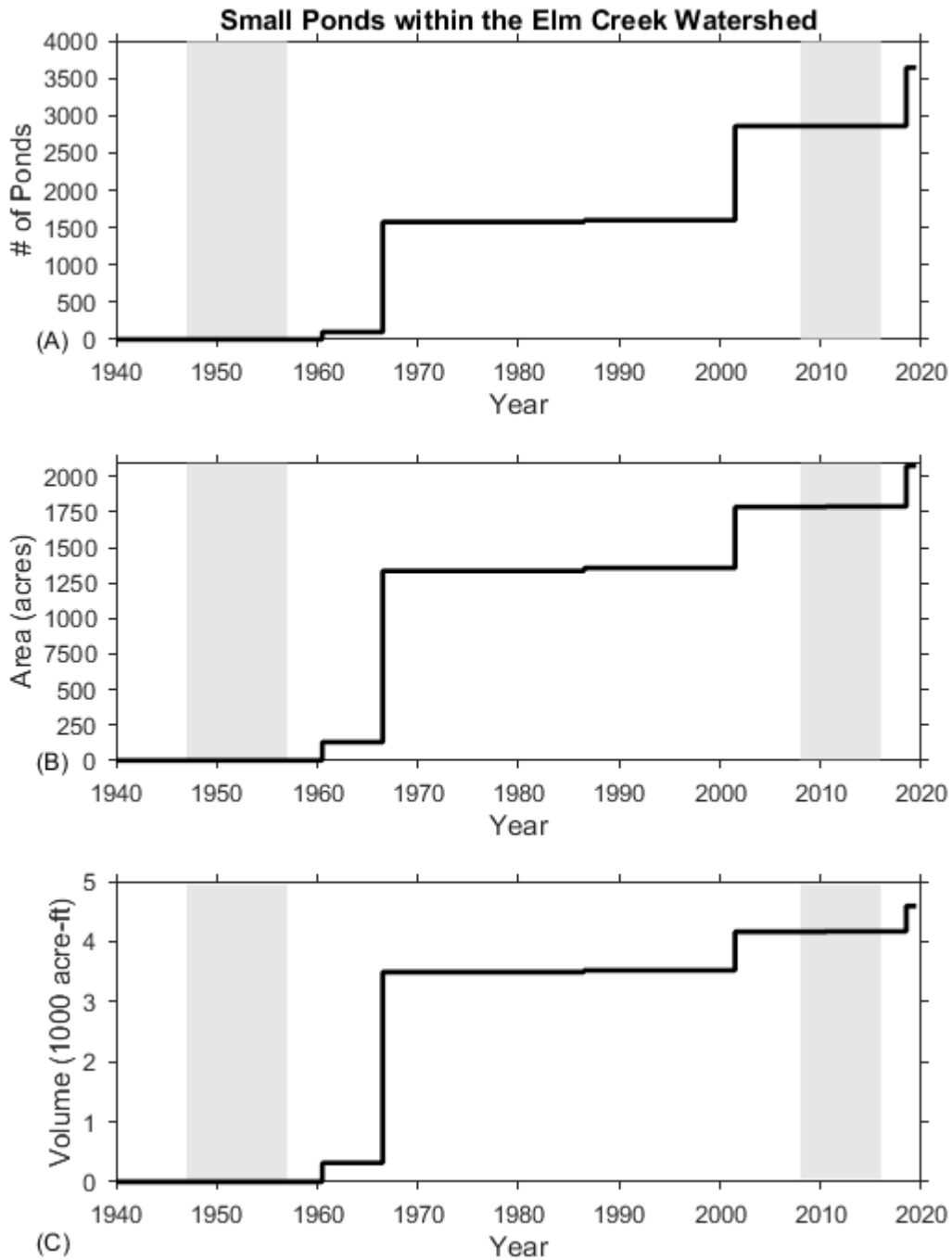


Figure 4-10 – Small pond time-series data for the Elm Creek watershed – (A) Number of ponds, (B) total surface area of ponds (when full), and (C) total volume of ponds (when full). Grey areas denote the 1947-1957 and 2008-2016 critical drought periods.

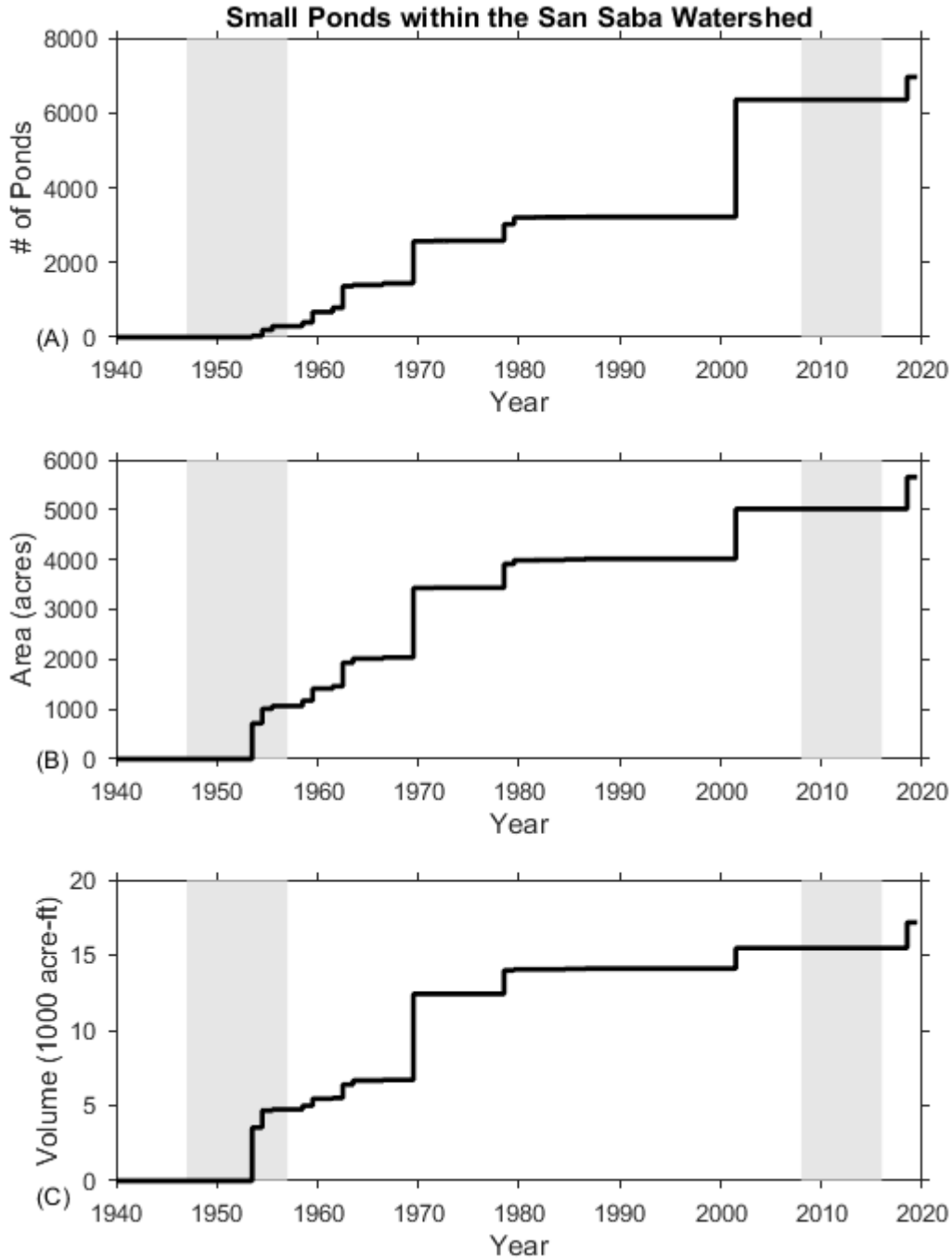


Figure 4-11 - Small pond time-series data for the San Saba watershed – (A) Number of ponds, (B) total surface area of ponds (when full), and (C) total volume of ponds (when full). Grey areas denote the 1947-1957 and 2008-2016 critical drought periods.

Figure 4-12 presents results of the small pond analysis for the North Concho watershed. This watershed contains fewer ponds than are located within the smaller Elm Creek watershed, and a majority of its ponds were created after 2002. Some ponds were created near the end of the 1947-1957 critical drought period, and those ponds tended to be larger ponds both in surface area and capacity. The total surface area for small ponds within the

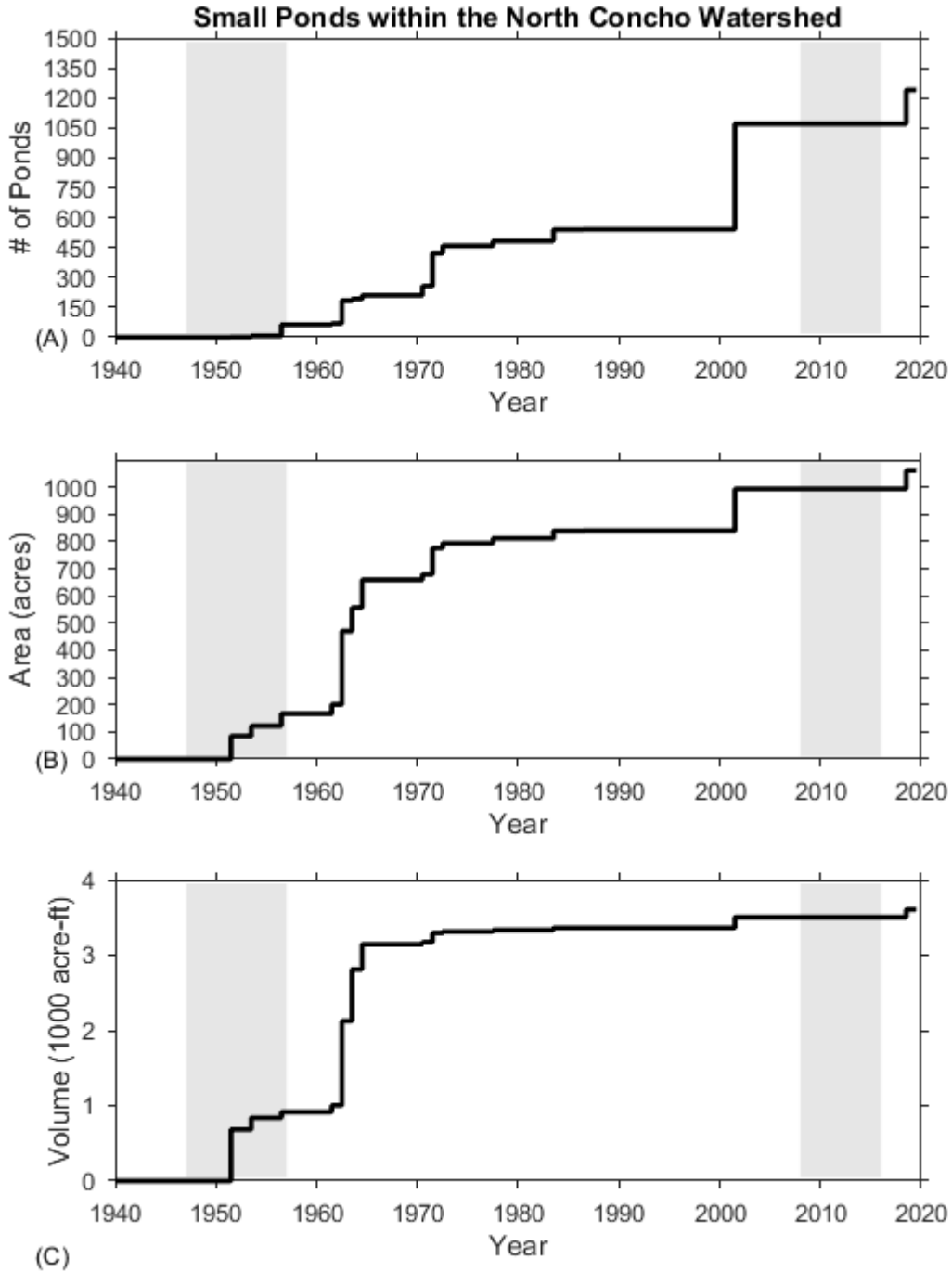


Figure 4-12 - Small pond time-series data for the North Concho watershed – (A) Number of ponds, (B) total surface area of ponds (when full), and (C) total volume of ponds (when full). Grey areas denote the 1947-1957 and 2008-2016 critical drought periods.

North Concho watershed is just over 1,000 acres, which is approximately 0.1% of the watershed area. The approximated total storage capacity of these small ponds is 3,600 acre-ft, with only a small fraction of this capacity resulting from those ponds identified using Google Earth. Over 85% of the watershed’s small pond storage capacity (Figure 4-12C) was created prior to 1965.

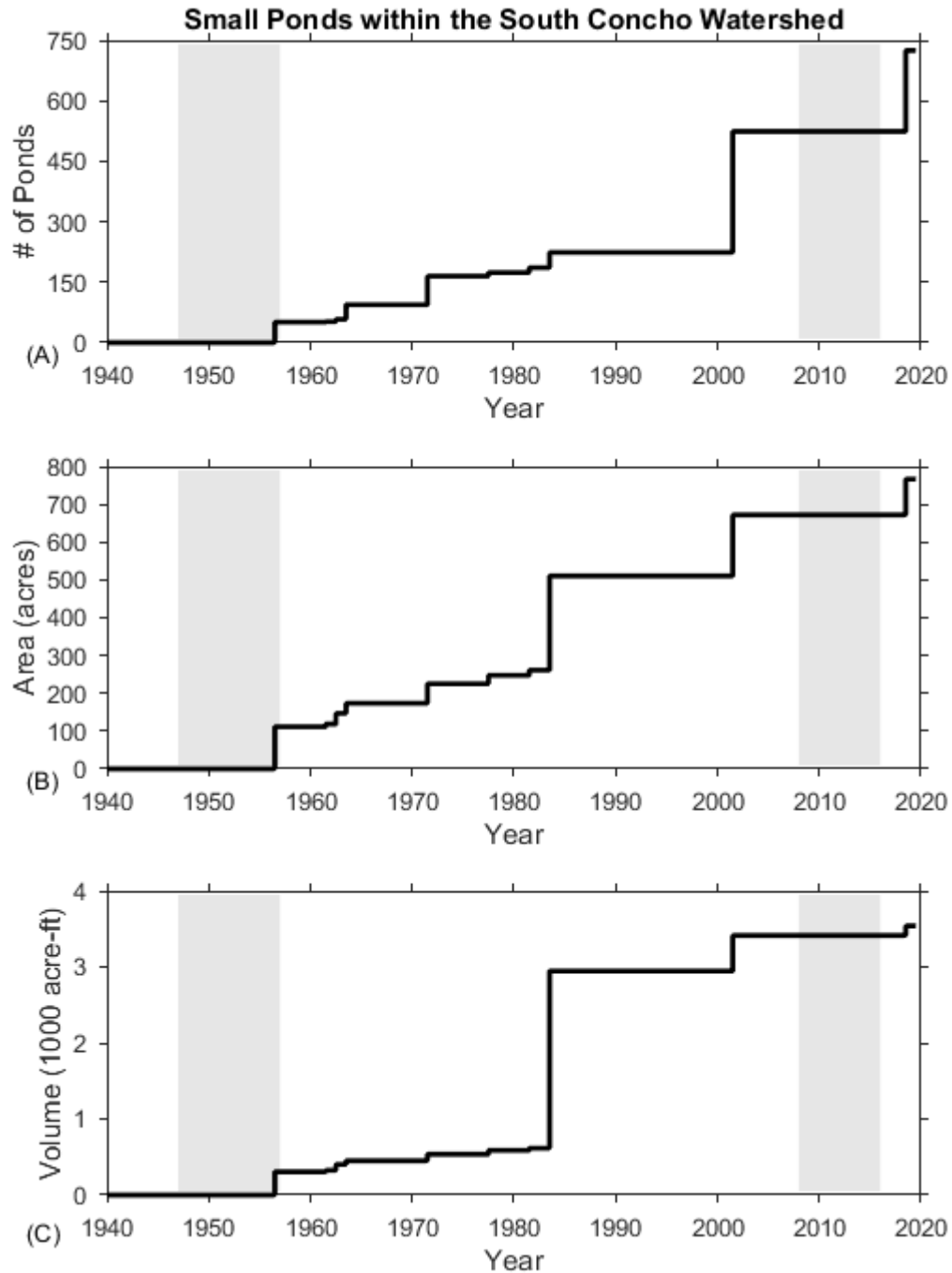


Figure 4-13 - Small pond time-series data for the South Concho watershed – (A) Number of ponds, (B) total surface area of ponds (when full), and (C) total volume of ponds (when full). Grey areas denote the 1947-1957 and 2008-2016 critical drought periods.

Figure 4-13 Figure 4-14 presents results of the small pond analysis for the South Concho watershed. This watershed contains fewer ponds than all other study area watersheds. The total surface area for these ponds amounts to just under 800 acres, which is approximately 0.2% of the watershed area. The approximated total storage capacity of these small ponds is 3,000 acre-ft, with only a small fraction of this capacity resulting from those ponds

identified using Google Earth. The majority of the total storage capacity is found in a small number of ponds first identified on USGS topographic maps dating from 1984.

Table 4-1 – Small Pond Analysis Results – 2019 Conditions

Watershed	Small Ponds Per Watershed			
	Number	Area (acres)	Volume (acre-ft)	Pond Area as Percentage of watershed area
Elm Creek	3,226	2,468	11,855	0.8%
San Saba	6,961	5,654	17,166	0.3%
South Concho	725	766	3,540	0.2%
North Concho	1,240	1,061	3,608	0.1%

Although excluded from this Phase II analysis, channel ponds were identified within each watershed, and their numbers, areas, and volumes are provided by watershed in Table 4-2. Channel ponds are uncommon within the Elm Creek watershed, and likely have negligible impact on the watershed hydrology. In contrast, the San Saba watershed contained 266 identified channel ponds, with a combined area of over 800 acres and volume of over 2,000 acre-ft. Evaporative losses and water storage within these ponds could have a significant effect on the watershed hydrology, and could warrant further investigation and pond classification. This will be discussed further in Section 10.1.3. Channel ponds for the North Concho and South Concho watersheds are not as numerous as in the San Saba watershed, yet could also have an impact on downstream streamflow.

Table 4-2 – “Channel Ponds” excluded from the small pond analyses

Watershed	Channel Ponds		
	Number	Area (acres)	Volume (acre-ft)
San Saba	266	803.2	2279.5
Elm Creek	5	3.2	3.3
North Concho	89	131.5	237.7
South Concho	38	77.2	165.1

4.3 Noxious Brush & Land Use Analysis

The second part of this remote sensing task was to attempt to quantify the extent of noxious brush on land within the four study area watersheds. Per the Phase I report, the existence of noxious brush, which tends to evapotranspire more water than native plants, is likely a prime cause of the reduced streamflow from the subject watersheds (Figure 2-1- Figure 2-4). Quantifying the extent of noxious brush across the study area, and how the extent changes over time since the 1950's, would provide evidence regarding the impact of such thirsty vegetation on local streamflow.

We attempted to utilize GEE and LandSAT images to identify and map the spatial extent of noxious brush over time. However we were unable to distinguish noxious brush (such as mesquite) from other vegetation. As a result, we were able only to track changes in vegetated areas, without having any ability to tie such changes into increased local water usage. As an alternative to the originally-planned noxious brush analysis, we performed an analysis of land-use/land cover data for the study area watersheds.

To discern how landscape changes may affect streamflow overtime, we developed an application of the curve number method created by the Soil Conservation Service (SCS). Full details of this method are presented in Section 10.1.2 of this report. In essence, the curve number method is a mathematical means for assessing how much of water from a given rainfall event will become surface runoff and contribute to streamflow. The method relies upon established properties of the land surface (soil type and vegetation), and each land surface category is assigned a numerical “curve number” to reflect the surface’s ability to generated runoff. Curve numbers range from 0 to 100, with higher numbers indicating that a greater portion of the precipitation will become runoff. Table 4-3 presents runoff curve numbers for the land use categories and soil groups considered in this Phase II analysis.

Table 4-3 – Runoff curve number for USGS Land Use Classifications.

Land Use Description	Runoff Curve Number per Soil Group			
	A	B	C	D
Open Water	100	100	100	100
Developed	65	77	84	88
Mechanically Disturbed	77	86	91	94
Mining	74	83	88	90
Barren	74	83	88	90
Deciduous Forest	38	48	57	63
Evergreen Forest	48	58	73	80
Mixed Forest	43	53	65	72
Grassland	49	69	79	84
Shrubland	35	56	70	77
Cropland	67	78	85	89
Hay/Pasture	49	69	79	84
Herbaceous Wetland	30	58	71	78
Woody Wetland	30	58	71	78

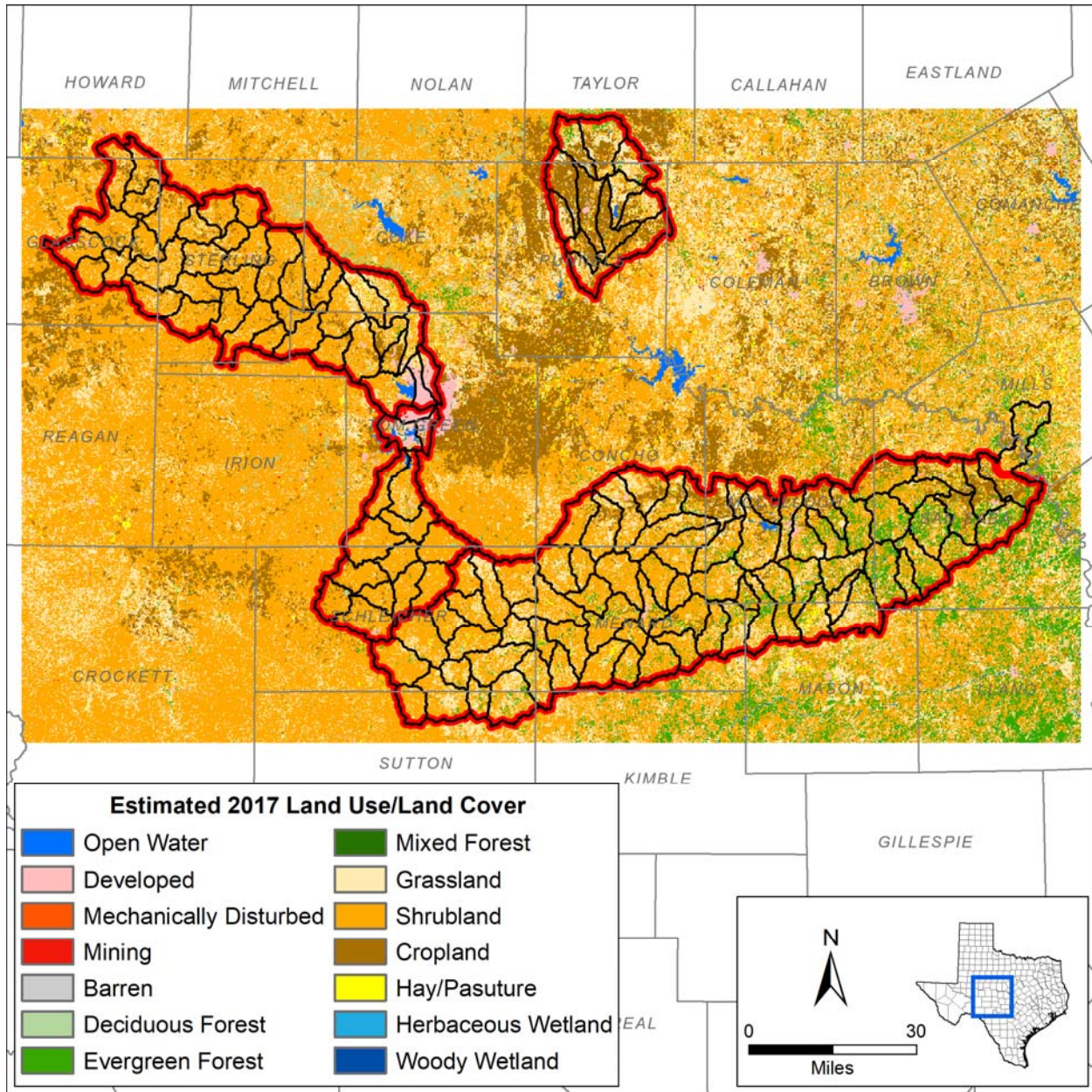


Figure 4-14 – Estimated 2017 Land Use/Land Cover data from the USGS

To determine the appropriate land use category for assigning curve numbers, we obtained annual gridded land use/land cover data from 1940-2016 (Sohl, 2018). This data is available from the USGS from the “ScienceBase Catalog” (www.sciencebase.gov as of 7/6/2019), and is viewable and manageable within ArcGIS software. We developed ArcGIS scripts to clip the conterminous-US files to areas spanning only the four study area watersheds, to quantify the acres of land within each watershed by category, and to produce tables of tabulated data. Figure 4-14 presents the estimated land use/land cover data for the study area for 2017.

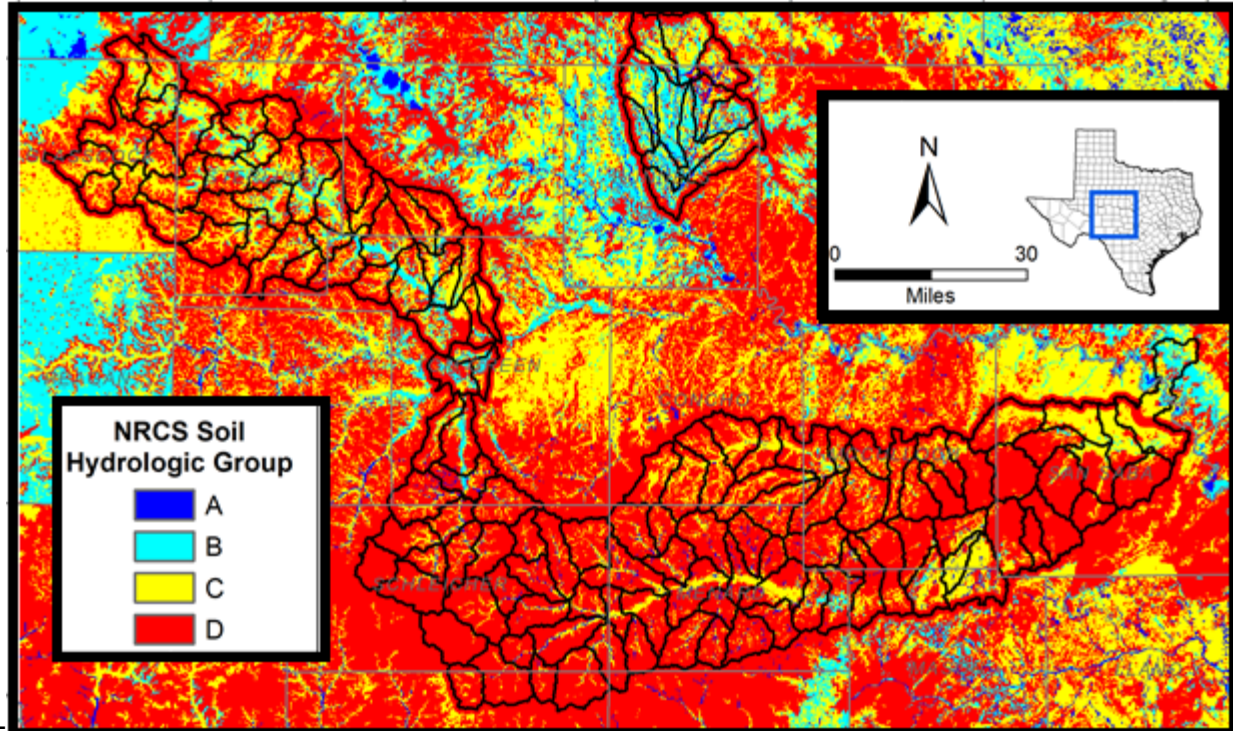


Figure 4-15 – NRCS Soil Hydrologic Groups for the study area (obtained during 2019).

Figure 4-15 presents the soil group data from the National Resources Conservation Service (NRCS). This data was available in grid format, allowing for an automatic assessment of both the soil group and associated Land use/Land Cover classification for each grid cell included within the study area watersheds. Thus through ArcGIS scripting, we determined the area-weighted curve number for each of the study area watersheds on an annual basis for the period from 1940-2016. Table 4-4 presents the tabulated percentage surface area of each watershed by NRCS soil group.

Table 4-4 – Watershed percentage area by hydrologic soil group

Watershed	Percentage Area Per Hydrologic Soil Group			
	A	B	C	D
Elm Creek	4.56%	34.87%	33.74%	26.81%
San Saba	1.27%	0.80%	19.59%	78.32%
South Concho	2.09%	5.15%	15.20%	77.54%
North Concho	0.08%	7.56%	38.67%	53.67%

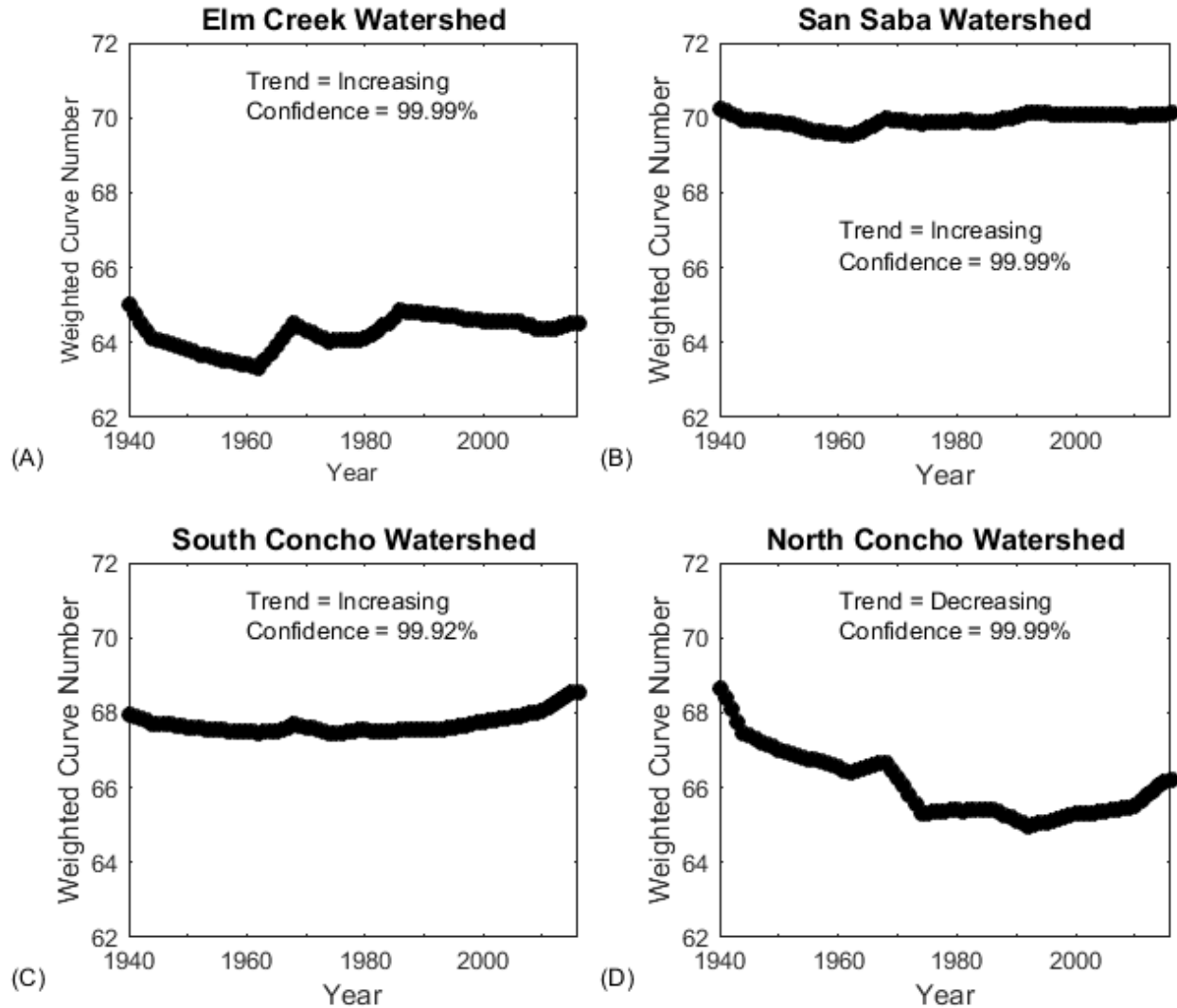


Figure 4-16 – Time-series of weighted-average curve numbers for each study area watershed

Figure 4-16 presents the annual weighted-average curve numbers computed for each watershed, based on the NRCS soil group and land use/land cover data for each given year. The weighted average values were computed based on the surface areas. Tabulated values of land use/land cover by watershed, category, and year are provided in Appendix A. As shown, curve numbers for the Elm Creek, San Saba, and South Concho watersheds have exhibited little net change from 1940-2016, with minor variations from year-to-year based on slight land use changes. Mann-Kendall analyses indicate increasing curve number trends for each of these watersheds, yet the magnitude of the annual increase is small. For the North Concho watershed, curve numbers decreased between 1940 and 2016 due to the variations in land use/land cover that occurred over that time period. Decreasing curve numbers generally signify that the land surface will absorb more water, thereby reducing the amount of water that forms runoff for streams.

Figure 4-17 to Figure 4-20 provide the time-history of land use/land cover acreages for each study area watershed.

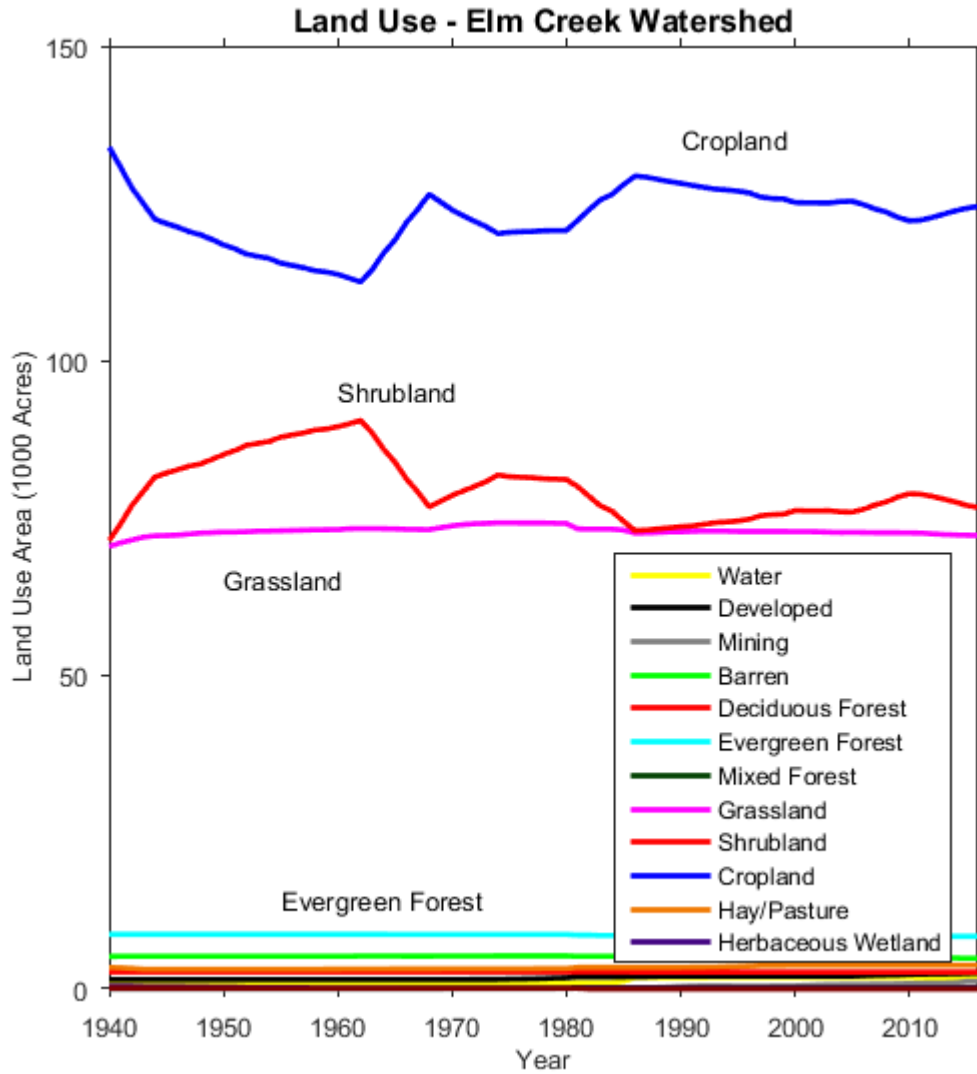


Figure 4-17 – Time history of land-use/land cover acreage by category for the Elm Creek watershed for the period from 1940-2016. Tabulated data is provided in Appendix A.

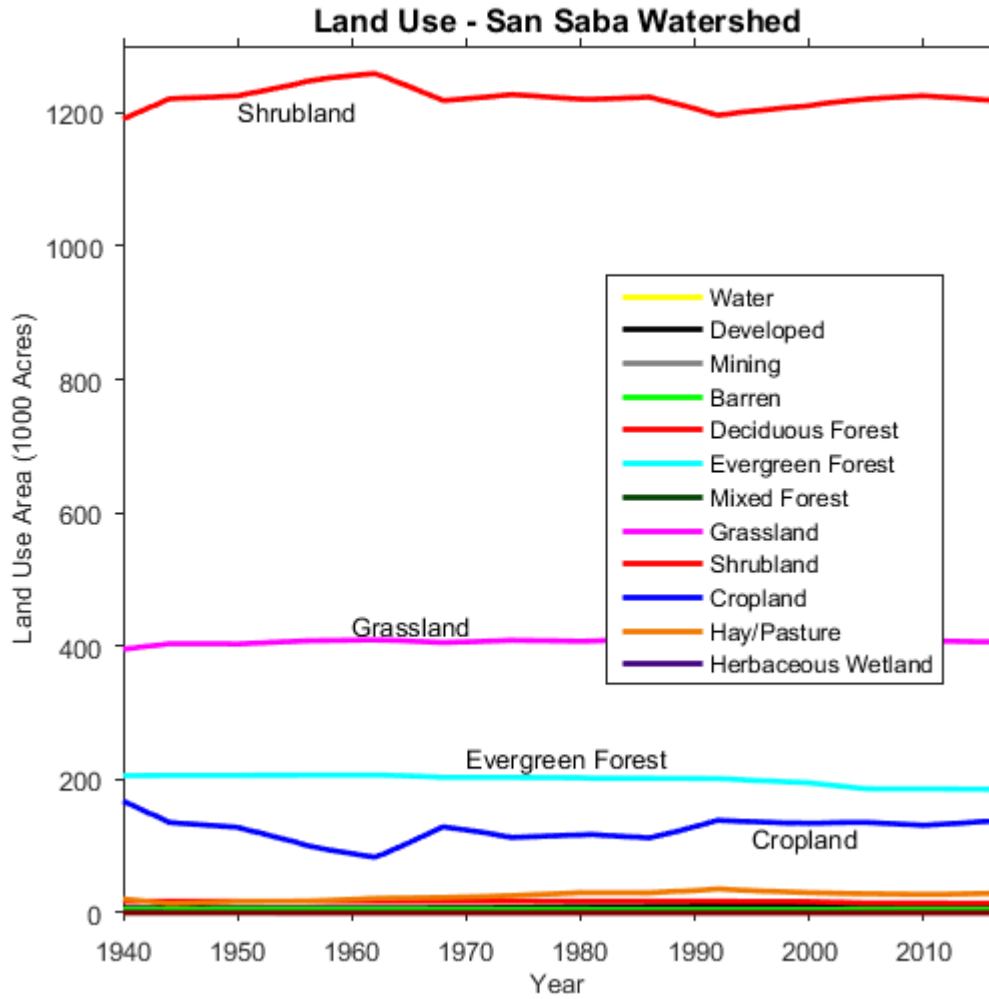


Figure 4-18 – Time history of land-use/land cover acreage by category for the San Saba watershed for the period from 1940-2016. Tabulated data is provided in Appendix A.

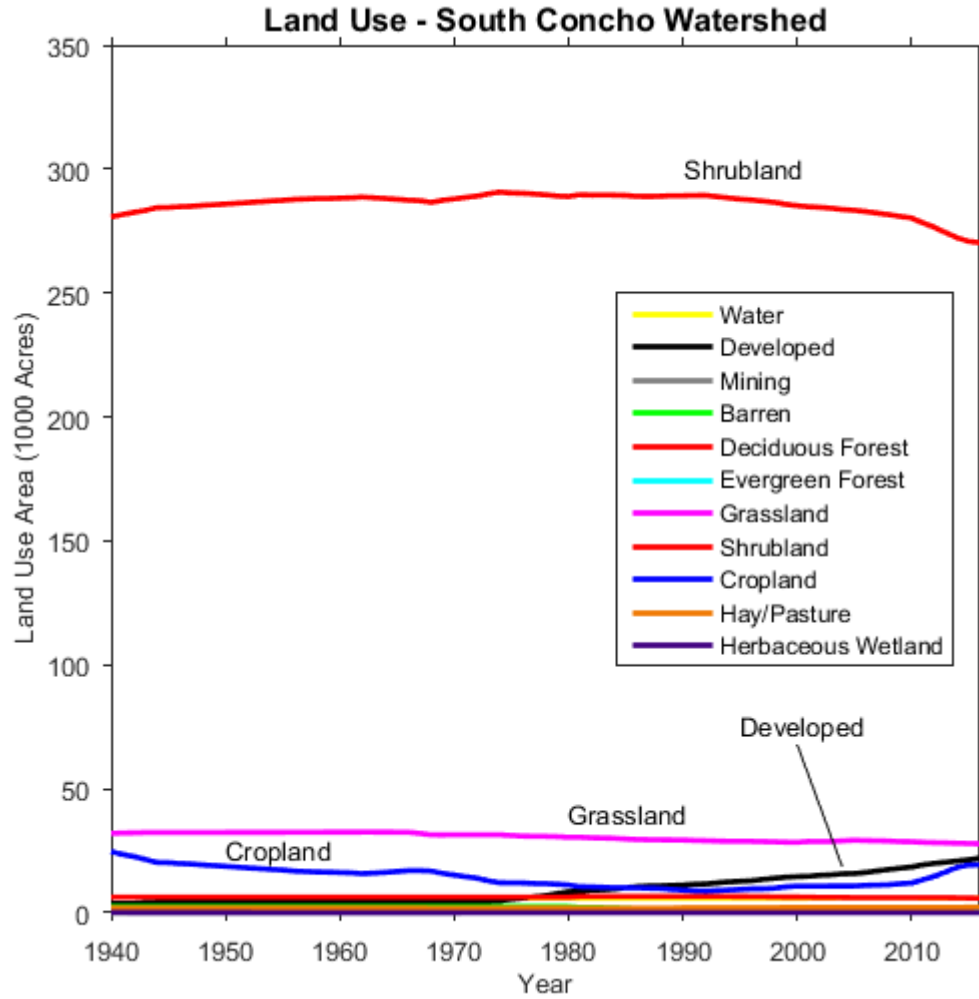


Figure 4-19 – Time history of land-use/land cover acreage by category for the South Concho watershed for the period from 1940-2016. Tabulated data is provided in Appendix A.

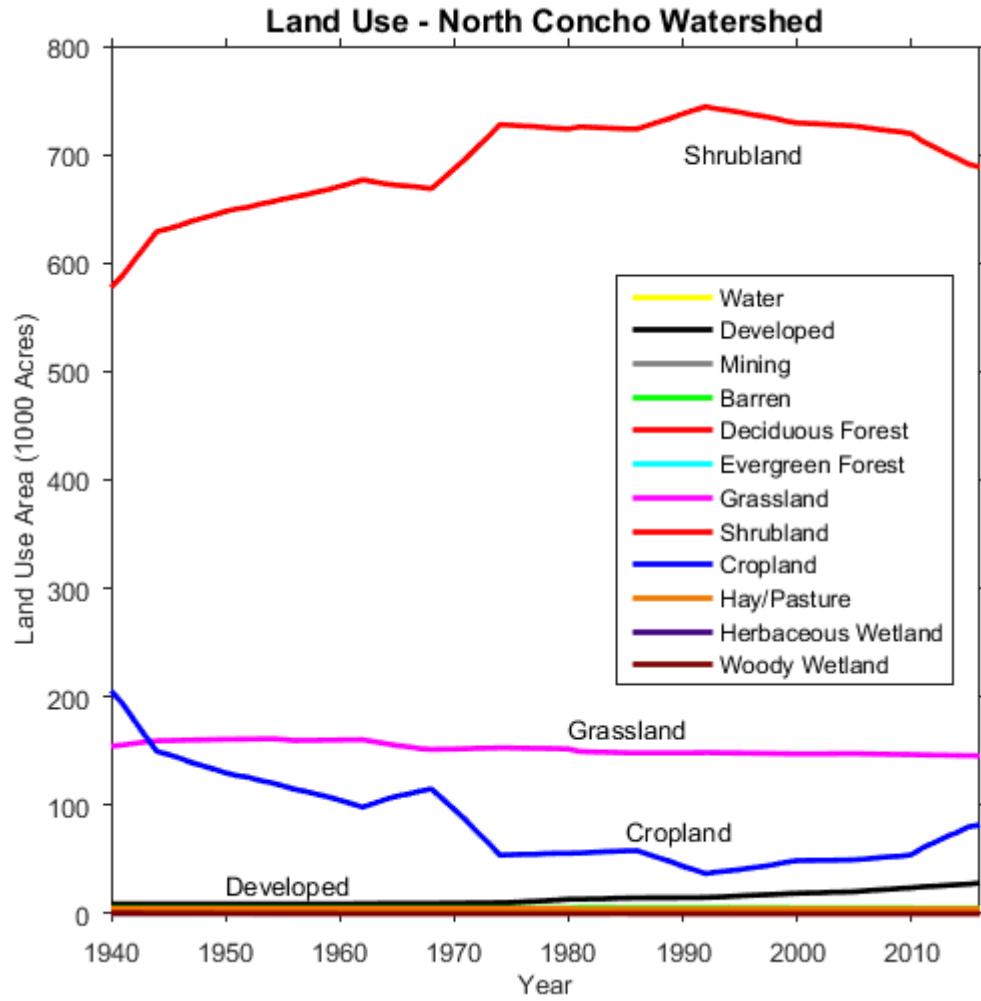


Figure 4-20 – Time history of land-use/land cover acreage by category for the North Concho watershed for the period from 1940-2016. Tabulated data is provided in Appendix A.

5 Task 3 – Temperature Trend Analysis

As identified in the literature review for Phase II (Section 3.1), increasing temperatures are considered to be one of the main causes of decreasing streamflow. This is tempered somewhat by the recognition that subject watersheds from previous studies all tended to be large watersheds with streamflow affected by seasonal snowmelt. Small, rainfall-dominated watersheds like the four in this Phase II study, have yet to be analyzed to assess the temperature-streamflow relationship. Within this section, we present the analysis of temperature trends within each study area watershed.

Figure 5-1 presents a map showing the location of long-term temperature measurement stations within the vicinity of the study area watersheds. Temperature data was obtained using the TSTool software developed by the Openwater Foundation in conjunction with the Colorado Department of Natural Resources and the Colorado Water Conservation Board Division of Water Resources. This tool, publically available at <http://openwaterfoundation.org/software-tools/tstool> as of 7/6/2019, compiles available time series data from a variety of sources, including the State of Colorado, NRCS, USGS, and the US Bureau of Reclamation. We identified 50 temperature data recording stations located within and around the four study area watersheds (Figure 5-1), yet many stations did not report sufficiently long, continuous periods of record for use in statistical analysis. We attempted to identify stations with continuous periods of record from the 1940s to the present, and found individual stations at Sterling City, Ballinger, and Brady which fit this criteria. For other locations, we had to compile data from relatively close geographic areas in order to obtain a reasonably long period of record. Such compilations were required for stations near Big Spring, Abilene, San Angelo, and Eldorado. Stations and station compilations were selected for analysis such that data was available for the upper and lower portions of each subject watershed.

Temperature data were obtained as daily maximum and minimum values for the period of record for each gauge. Data were processed to contain the value “-9999” for instances when data were missing and not available. Statistical analysis of temperature data were only performed on valid data, excluding data containing the “-9999” value. Data analysis was limited to the period of record for this Phase II report, specifically from 1940-2016. Daily data was averaged monthly, seasonally, and annually with the Mann-Kendall technique applied to each dataset to determine and evaluate data trends. For seasonal averaging, monthly data was grouped as follows:

- “Winter” = December, January, and February
- “Spring” = March, April, and May
- “Summer” = June, July, and August
- “Fall” = September, October, and November.

For winter periods, data from December corresponds to the December from the previous year, so that the “Winter 2019” period consists of December 2018, January 2019, and February 2019 data. All annual averages were based on the calendar year.

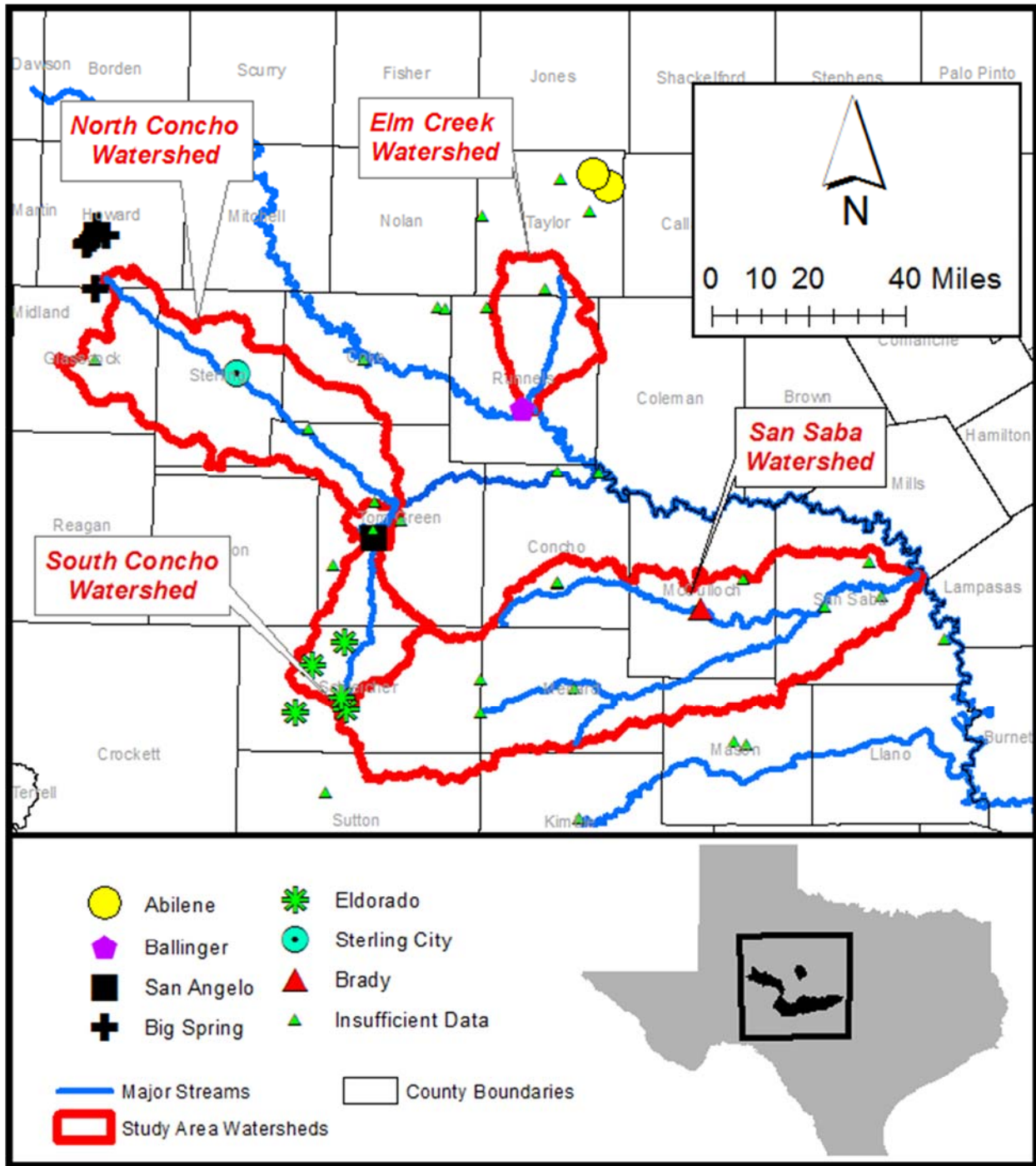


Figure 5-1 Map showing temperature measurement locations

5.1 Elm Creek Watershed

As shown in Figure 5-1, within the vicinity of the Elm Creek watershed two temperature recording locations exist with sufficient data to allow for trend analysis over the 1940-2016 period of record: 1) Ballinger, TX at the watershed outlet, and 2) Abilene, TX which is outside of the watershed but perhaps indicative of temperature that would be experienced within the upper reaches of the watershed. Spatial gradients in temperature across the Elm Creek watershed would be better resolved if data were available from the center of the watershed, likely from Winters. No suitable temperature data were available for the Winters area from sources utilized during this project effort.

Table 5-1 presents information regarding the temperature measurement stations used in assessing trends across the Elm Creek watershed. As shown, data from “Ballinger 2 NW” was available from 1900-2019, yet only data for the period 1940-2016 was used in this analysis. Data from the City of Abilene was compiled from two (2) separate gauge locations within the city limits, with each station providing data at different times. Combined, the period of record of available data for Abilene ran from 9/15/1885 to 4/1/2019, yet only data for the period 1940-2016 was used in this analysis.

Table 5-1 – Temperature measurement stations for the Elm Creek watershed

<u>Station Name</u>	<u>ACIS ID</u>	<u>Latitude</u>	<u>Longitude</u>	<u>Start Date</u>	<u>End Date</u>
Ballinger 2 NW	23597	31.7413N	99.9763W	1/1/1900	4/2/2019
Abilene Regional AP	23787	32.4105	99.6822W	3/1/1944	4/1/2019
Abilene	23801	32.45N	99.7333W	9/15/1885	2/29/1944

** ACIS = Applied Climate Information System

5.1.1 Temperatures for Ballinger, TX

Figure 5-2 presents a calendar plot of temperature data for Ballinger, TX from 1940-2016. Data shown in BLACK reflect periods when data was unavailable (assigned the value “-9999”). RED data in Figure 5-2 indicate days during which the recorded high temperature exceeded 100 °F, which occurred often within the summer months yet occasionally in April, May, September and October. BLUE data indicate days during which the recorded low temperature was below 32 °F, which occurred often from November-February as well as occasionally in March, April, and October. Based on only the visual analysis of Figure 5-2, it is possible to suggest that the frequency of days exceeding 100 °F has decreased over the period of record, although it does appear to have increased during the 2008-2016 drought period, relative to the period from 1970-2005.

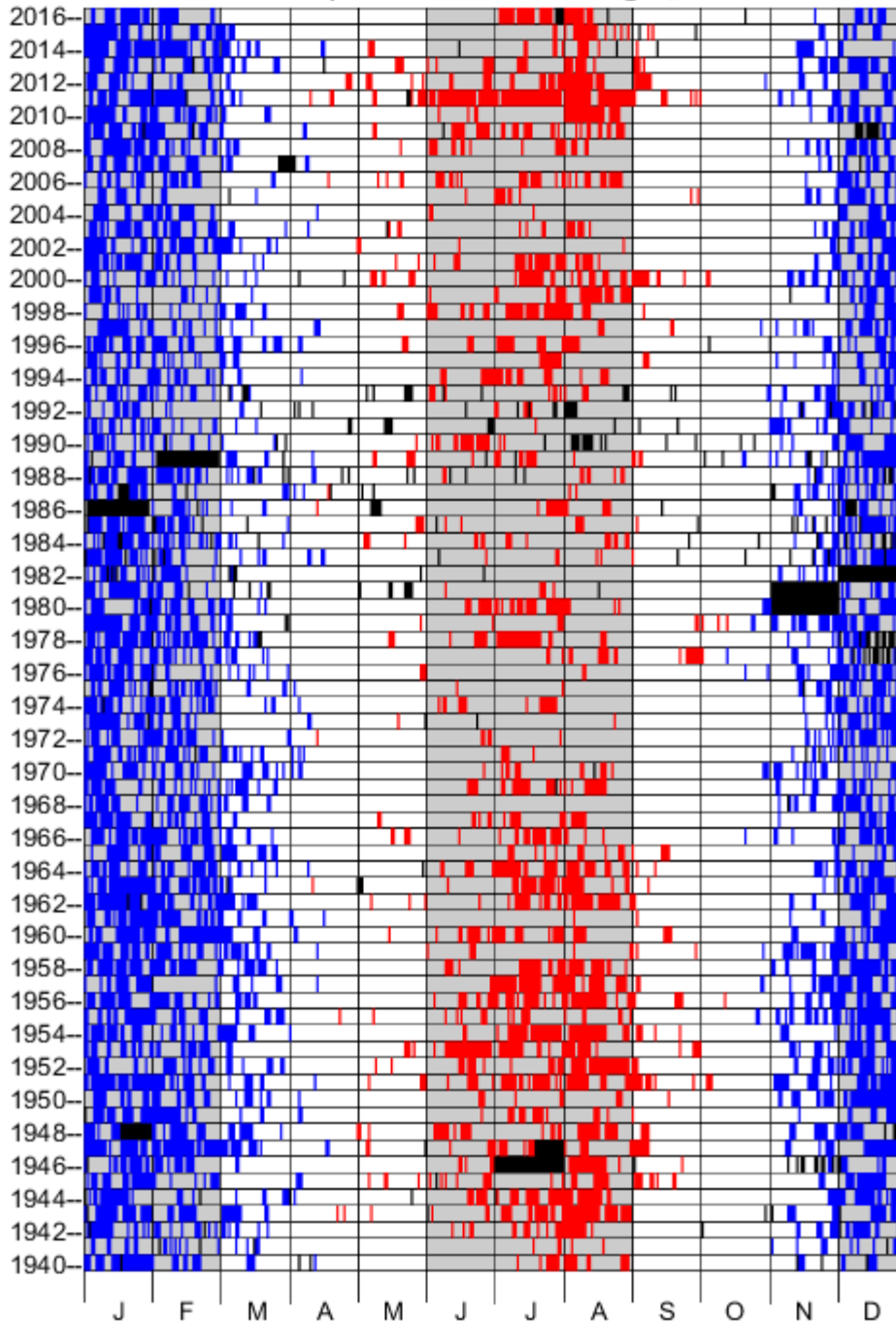


Figure 5-2 – Temperature data For Ballinger for the period 1940-2016 – BLUE showing when minimum temperatures dropped below 32° F, RED showing when maximum temperatures exceeded 100°F. BLACK indicates no valid data was recorded.

Figure 5-3 presents a statistical analysis of the Ballinger temperature data, including Mann-Kendall analysis results. Within Figure 5-3A, the number of 100 °F per calendar year is presented over time, with values ranging from 0 to over 100 days (in 2011). Per the Mann-Kendall analysis, there is a decreasing trend in the data, confirming the visual trend

identified in Figure 5-2. Data shown in Figure 5-3A also confirm the suspicion that the frequency of 100 °F degree days increased during the 2008-2016 drought period when compared to the 1970-2005 period.

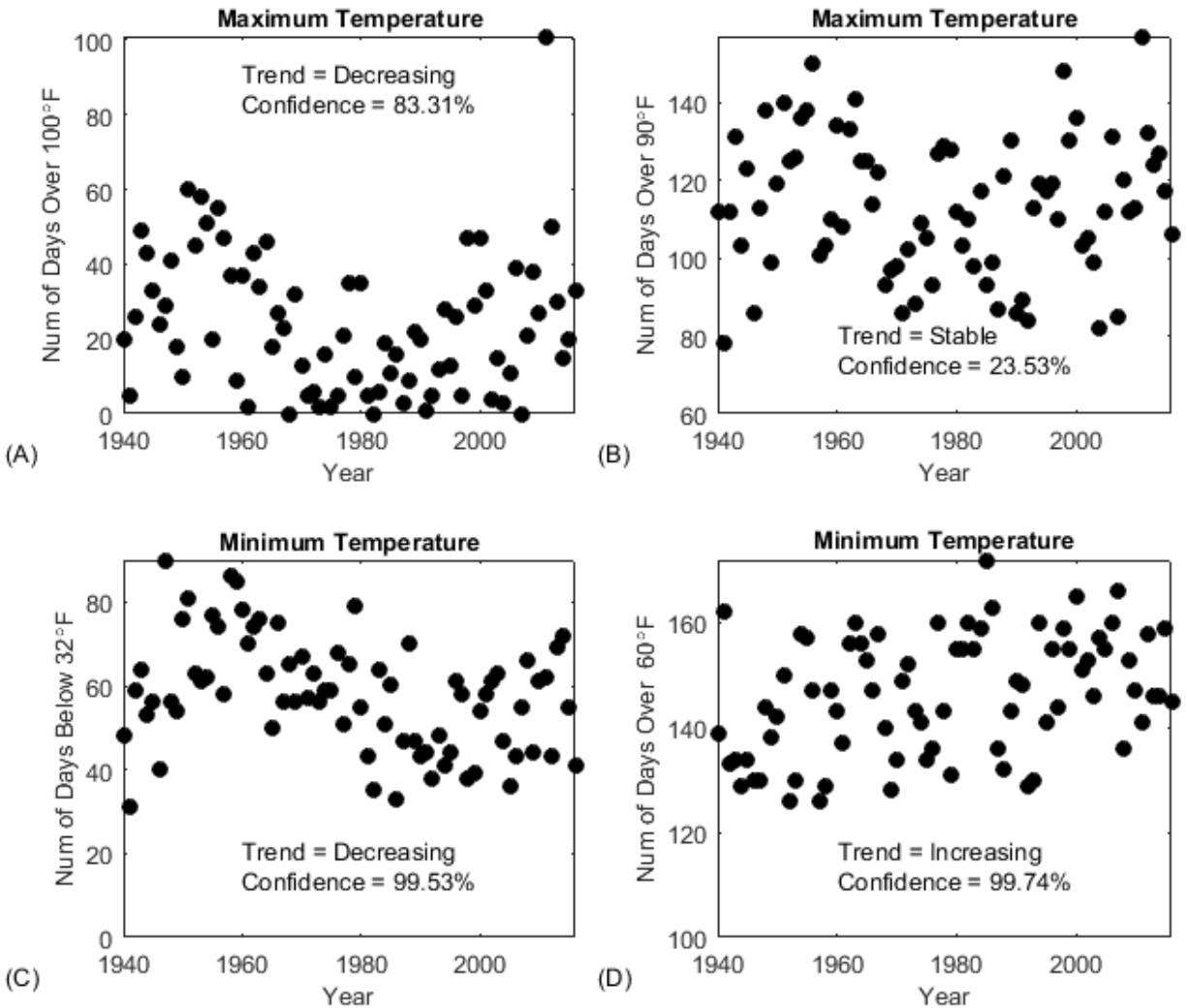


Figure 5-3 – Temperature Trends For Ballinger for the period 1940-2016 – A) Days exceeding 100°F, B) Days exceeding 90°F, C) Days with minimum temperatures below 32°F, D) Days with minimum temperatures exceeding 60°F.

Per Figure 5-3, the number of days per year on which the high temperature exceeded 90°F has remained stable over the period of record. This, combined with the decreasing trend in the number of 100°F days suggests that extreme high temperatures may be occurring less often, yet days with mildly high temperatures are occurring with unchanged frequency.

Figure 5-3C presents the number of days per year during which the minimum recorded temperature dropped below 32 °F. For the period from 1940-2016, the overall trend is decreasing, such that the number of low-temperature days per year is decreasing with time. However for the period from 1940-1960, the number of low-temperature days

appears to have increased, followed by a decrease from 1960-1990 and then another increase from 1990-2016. It is perhaps notable that during both the 1947-1957 and 2008-2016 drought periods, Ballinger experienced increases in the number of days when temperatures decreased below 32 °F.

When quantifying the number of days per year when the minimum temperature exceeds 60 °F (Figure 5-3D), an increasing trend becomes evident. This suggests that Ballinger is experiencing a warming trend, although one that is not evident by tracking only high- and low-temperature extremes.

In general, results from Figure 5-3 indicate that Ballinger, TX is experiencing warming in that the minimum daily temperatures are increasing. Maximum temperatures, as well as the frequency with which temperatures exceed high values, are generally decreasing. Combined, this suggest that Ballinger temperatures are tending to remain high more often, even though extreme high temperatures are occurring less frequently. The areas does not appear to be cooling off as often recently as it had done over the earlier portion of the period of record.

This general observation is further confirmed through an analysis of the annual average maximum and minimum temperatures for Ballinger (Figure 5-4). Annual averages are computed as the arithmetic average of either daily high or daily low temperatures for the calendar year. Mann-Kendall analysis for the average minimum temperatures (Figure 5-4A) reinforces the conclusion derived from Figure 5-3 that minimum daily temperatures are increasing. Maximum daily temperatures, however, do not show any increasing or decreasing trends (Figure 5-4B).

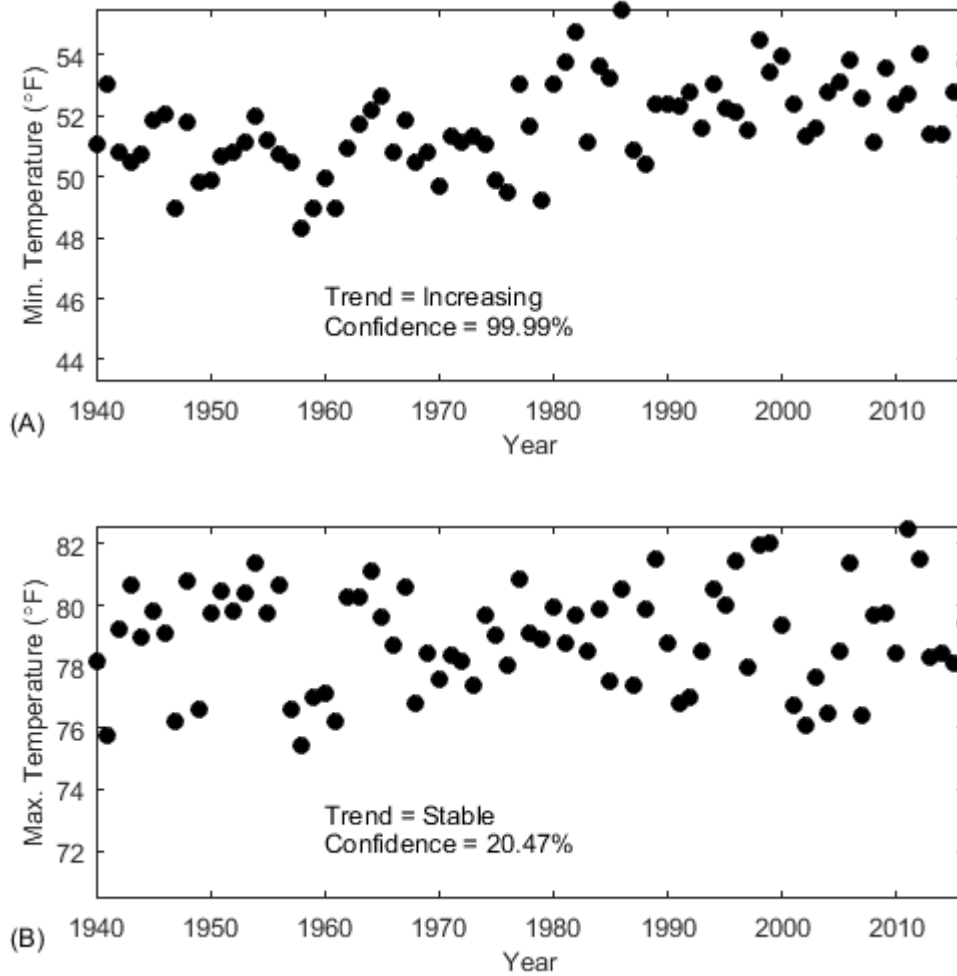


Figure 5-4 Annual Average Temperatures for Ballinger for the period 1940-2016 – A) Average minimum daily temperature, B) Average maximum daily temperature

Table 5-2 presents monthly, seasonal, and annual temperature trends computed for Ballinger. Periods showing increasing or decreasing Mann-Kendall trends are shown with grey shading. Negative trends are indicated in **bold underline**, and positive trends are indicated with ***bold italics***. As shown, average minimum temperatures show increasing trends for all months EXCEPT April and December, as well as for Spring, Summer, Fall, and Annual periods. Maximum temperatures show decreasing trends for July for the Summer period, yet otherwise exhibit stable trends.

Table 5-2 – Temperature Trend Statistics for Ballinger, for the period 1940-2016

Period	Minimum Temperatures		Maximum Temperatures	
	Trend	Confidence	Trend	Confidence
January	<i>Increasing</i>	94.75%	Stable	60.16%
February	<i>Increasing</i>	92.50%	Stable	47.28%
March	<i>Increasing</i>	99.94%	Stable	44.44%
April	Stable	68.40%	Stable	37.46%
May	<i>Increasing</i>	94.76%	Stable	67.33%
June	<i>Increasing</i>	98.84%	Stable	63.28%
July	<i>Increasing</i>	96.38%	<u>Decreasing</u>	76.75%
August	<i>Increasing</i>	99.36%	Stable	64.91%
September	<i>Increasing</i>	96.85%	Stable	6.31%
October	<i>Increasing</i>	96.98%	Stable	50.46%
November	<i>Increasing</i>	99.83%	Stable	69.01%
December	Stable	70.09%	Stable	39.79%
Spring	<i>Increasing</i>	99.89%	Stable	66.05%
Summer	<i>Increasing</i>	99.51%	<u>Decreasing</u>	88.85%
Fall	<i>Increasing</i>	99.95%	Stable	33.27%
Winter	<i>Increasing</i>	95%	Stable	21.33%
Annual	<i>Increasing</i>	99.99%	Stable	20.47%

BOLD, ITALICS, & SHADING = increasing trend

BOLD, UNDERLINE, & SHADING = decreasing trend

5.1.2 Temperatures for Abilene, TX

Figure 5-5 presents a calendar plot of temperature data for Abilene, TX from 1940-2016. Data shown in BLACK reflect periods when data was unavailable (assigned the value “-9999”). RED data in Figure 5-5 indicate days during which the recorded high temperature exceeded 100 °F, which occurred often within the summer months yet occasionally in May and September. BLUE data indicate days when the recorded low temperature was below 32 °F, which occurred often from November-February as well as occasionally in March, April, and October. Based on only the visual analysis of Figure 5-5, it is possible to suggest that the frequency of days exceeding 100 °F has increased over the period of record, reaching a peak during the 2008-2016 drought period.

Figure 5-6 presents a statistical analysis of the Abilene temperature data, including Mann-Kendall analysis results. Within Figure 5-6A, the number of 100 °F per calendar year is presented over time, with values ranging from 0 to over 80 days (in 2011). Per the Mann-Kendall analysis, the data indicates a stable trend over time, refuting the visual trend identified in Figure 5-5. Data shown in Figure 5-6A also confirm the suspicion that the frequency of 100 °F degree days increased during the 2008-2016 drought period when compared to the period from 1990-2000, although upon excluding data from 2011, the data from 2008-2016 is similar to that experienced in the 1930s-1950s.

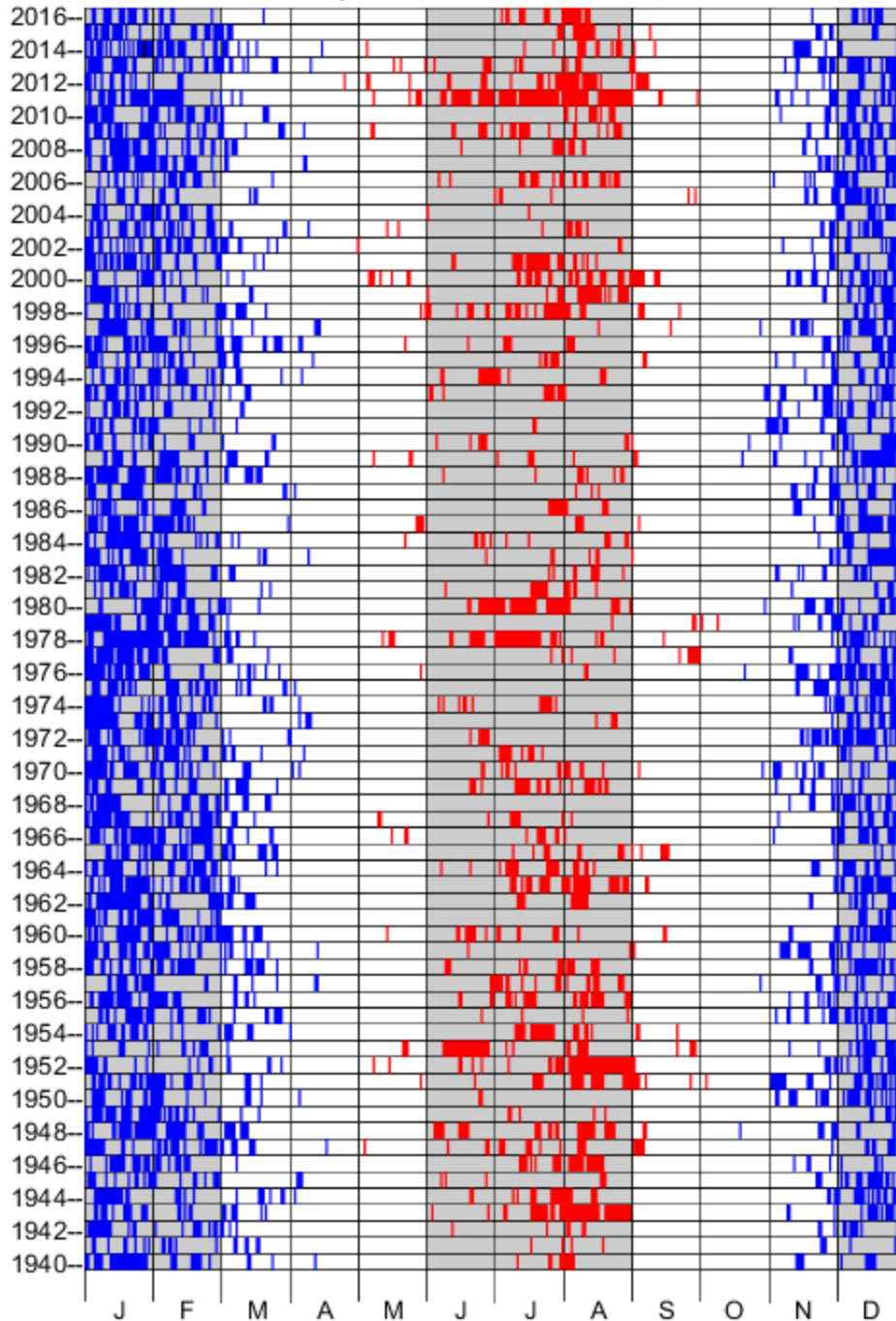


Figure 5-5– Temperature Data For Abilene for the period 1940-2016 – BLUE showing when minimum temperatures dropped below 32° F, RED showing when maximum temperatures exceeded 100°F. BLACK indicates no valid data was recorded.

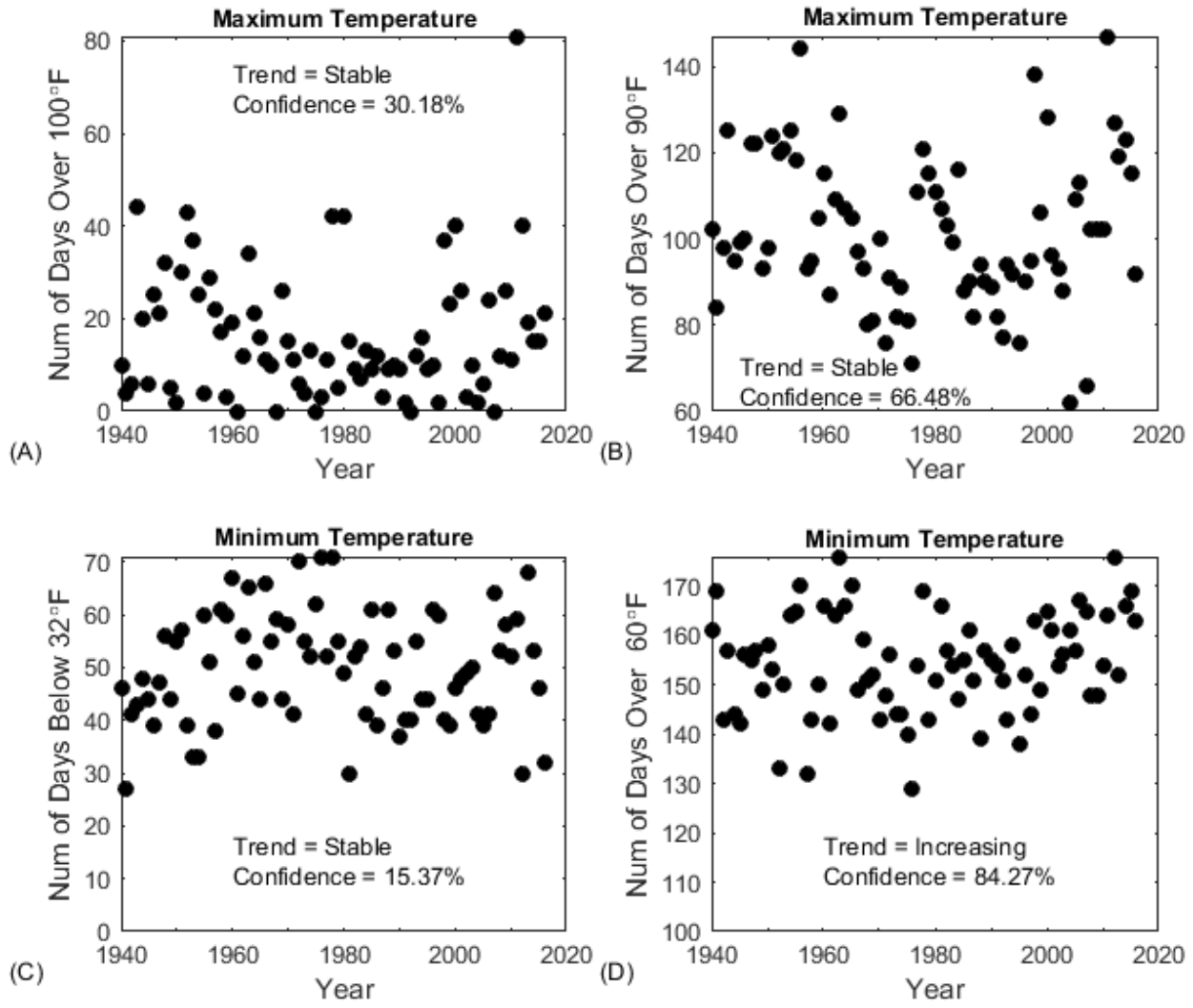


Figure 5-6- Temperature trends for Abilene for the period 1940-2016 – A) Days exceeding 100°F, B) Days exceeding 90°F, C) Days with minimum temperatures below 32°F, D) Days with minimum temperatures exceeding 60°F.

Similar to the results from Ballinger, stable trends were observed when considering the frequency with which daily maximum temperatures exceeded 90 °F (Figure 5-6B). Therefore maximum temperature data indicate that Abilene is not currently experiencing averaged hotter temperatures than it had over the prior period of record.

Figure 5-6C presents the number of days per year during which the minimum recorded temperature dropped below 32 °F. As shown, there is a stable trend over the period of record, indicating that the Abilene area is not likely to experience more freezing days annually now than in the past. It is also notable that there is an apparent variation to the range of data shown in Figure 5-6C, of about 30 days. This suggests that while in general the variation in the number of freezing days in successive years will fall within the 30-day region.

Figure 5-6D, depicting the annual number of days with minimum temperatures above 60 °F, indicates an increasing trend similar to that indicated by the temperature data from Ballinger. This suggests that the Abilene region, while exhibiting stable trends in terms of temperature extremes, is generally experiencing an average warming trend in that the area is not “cooling off” as much in the evenings and mornings (when the daily minimum temperatures are likely to be recorded).

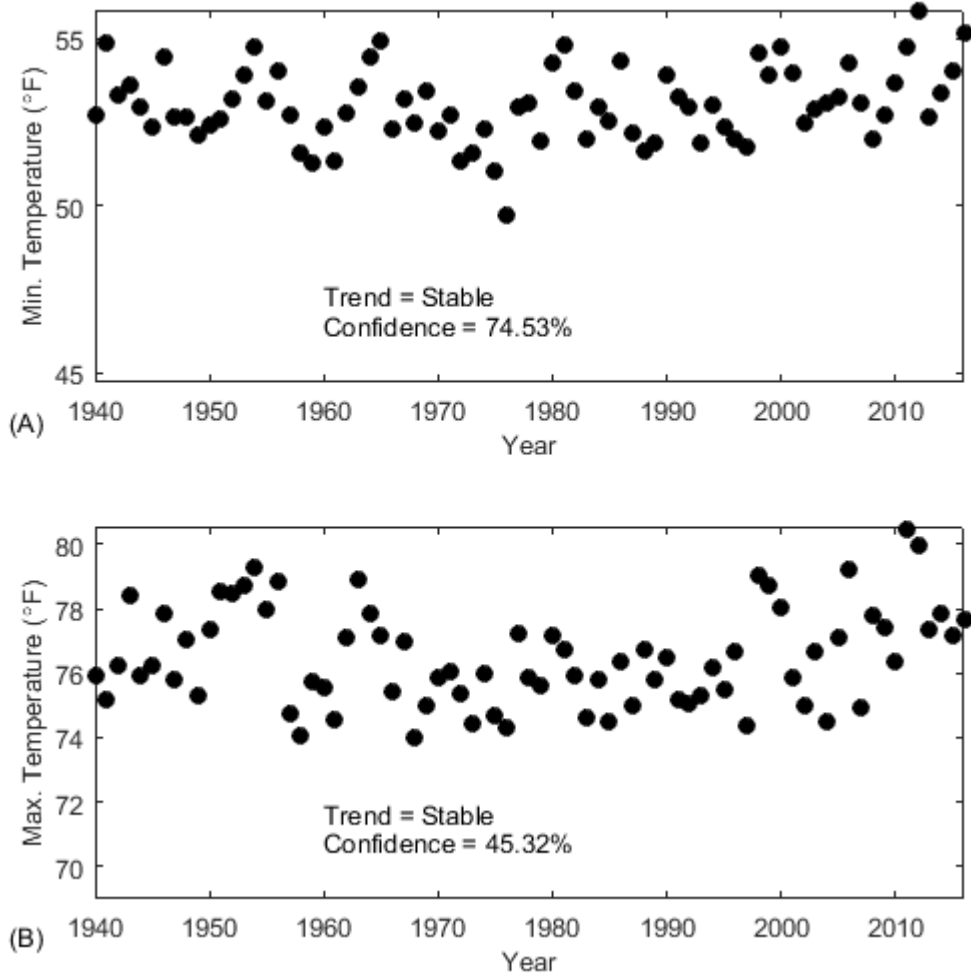


Figure 5-7 - Annual Average Temperatures for Abilene for the period 1940-2016 – (A) Average minimum daily temperature, (B) Average maximum daily temperature

Figure 5-7 provides the annual average minimum and maximum temperatures for Abilene, and demonstrates that both datasets exhibit stable trends over the 1940-2016 period of record. The confidence level in the minimum temperature stable trend is just below the threshold level to indicate trend significance (as used in this Phase II analysis), and the data suggests an increasing trend at lower confidence levels. Thus as with Ballinger, Abilene appears to be experiencing higher minimum temperatures and stable high temperatures.

Table 5-3 – Temperature Trend Statistics for Abilene for the period 1940-2016

Period	Minimum Temperatures		Maximum Temperatures	
	Trend	Confidence	Trend	Confidence
January	<i>Increasing</i>	77.18%	<i>Increasing</i>	81.30%
February	Stable	26.84%	Stable	41.45%
March	<i>Increasing</i>	99.10%	<i>Increasing</i>	76.67%
April	Stable	9.45%	Stable	44.73%
May	Stable	47.06%	Stable	40.23%
June	Stable	35.58%	Stable	38.39%
July	Stable	11.41%	Stable	64.92%
August	Stable	11.05%	Stable	23.96%
September	Stable	9.45%	Stable	19.79%
October	Stable	23.51%	Stable	27.83%
November	Stable	73.61%	Stable	61.14%
December	Stable	60.33%	Stable	20.17%
Spring	<i>Increasing</i>	88.86%	Stable	70.80%
Summer	Stable	3.93%	Stable	66.50%
Fall	Stable	48.77%	Stable	27.17%
Winter	Stable	16.34%	Stable	47.28%
Annual	Stable	74.53%	Stable	45.32%

BOLD, ITALICS, & SHADING = significant increasing trend
BOLD, UNDERLINE, & SHADING = significant decreasing trend

Table 5-3 presents monthly, seasonal, and annual temperature trends computed for Abilene for the period from 1940-2016. Periods showing statistically significant Mann-Kendall trends are shown with grey shading. Negative trends are indicated in **bold underline**, and positive trends are indicated with ***bold italics***. As shown, average minimum temperatures show increasing trends only in January, March, and for the Spring period. Increasing maximum temperatures are indicated for January and March, with all other periods exhibiting stable trends.

Results for Abilene presented in Table 5-3 contrast with those presented for Ballinger in Table 5-2, indicating that a gradient of temperature change trends exists across the Elm Creek watershed. The gradient is such that minimum temperatures are more likely to increase within the lower portion of the watershed (near Ballinger), with the increases becoming less likely toward the upper portion of the watershed near Abilene. Maximum temperature trends appear to remain constant (largely stable) across the watershed between Ballinger and Abilene.

5.2 San Saba Watershed

As shown in Temperature data were obtained as daily maximum and minimum values for the period of record for each gauge. Data were processed to contain the value “-9999” for instances when data were missing and not available. Statistical analysis of temperature data were only performed on valid data, excluding data containing the “-9999” value. Data analysis was limited to the period of record for this Phase II report, specifically from 1940-2016. Daily data was averaged monthly, seasonally, and annually with the Mann-Kendall technique applied to each dataset to determine and evaluate data trends. For seasonal averaging, monthly data was grouped as follows:

- “Winter” = December, January, and February
- “Spring” = March, April, and May
- “Summer” = June, July, and August
- “Fall” = September, October, and November.

For winter periods, data from December corresponds to the December from the previous year, so that the “Winter 2019” period consists of December 2018, January 2019, and February 2019 data. All annual averages were based on the calendar year.

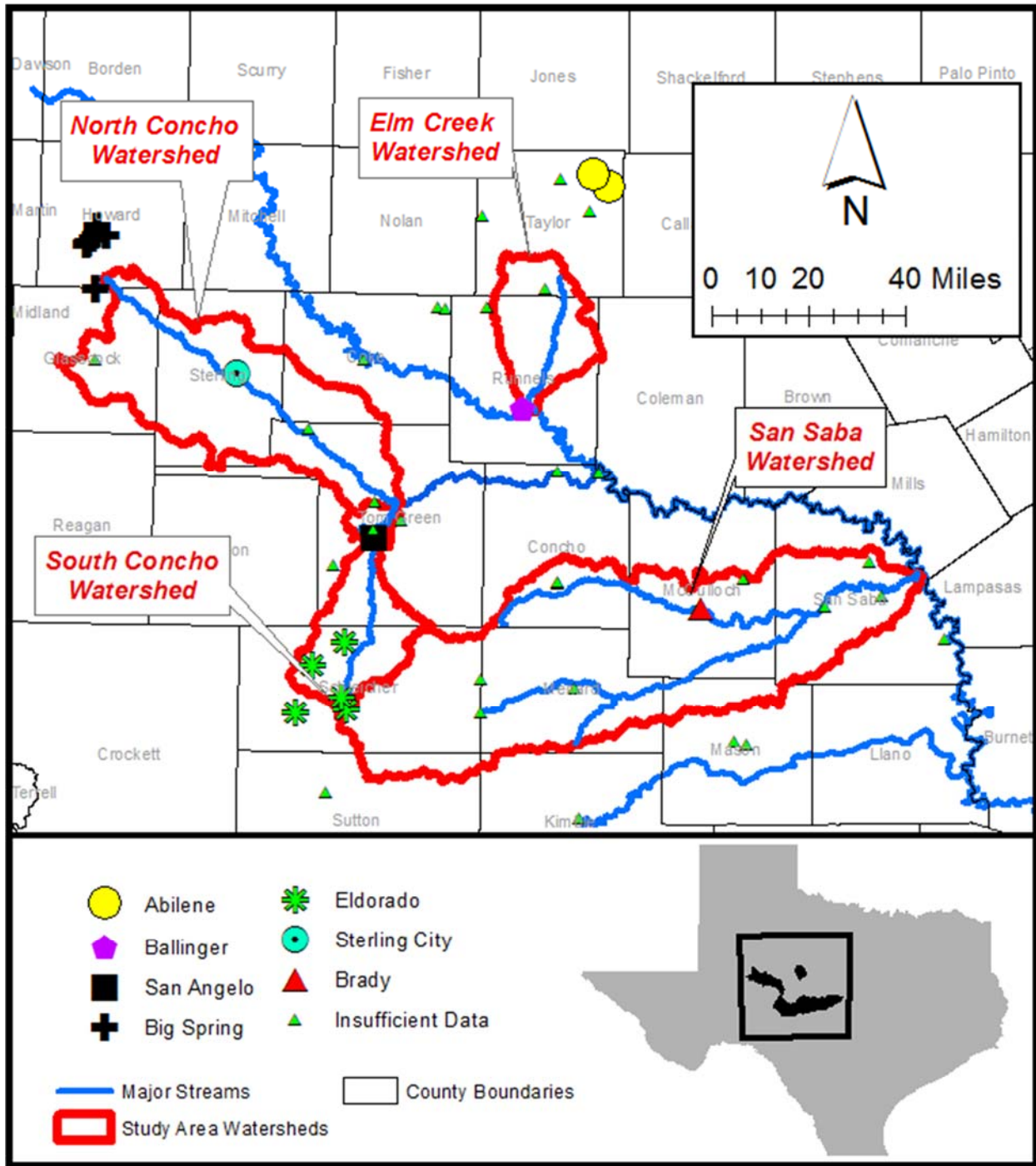


Figure 5-1, the only temperature station with a significantly long record suitable for statistical analysis located within the San Saba watershed was the station in Brady. Sufficient data from Eldorado was also available, and this location outside the western boundary of the San Saba watershed is discussed here to provide insight into temperature trend gradients from West to East across the watershed. Spatial gradients in temperature across the San Saba watershed would be better resolved if data were available from Fort

McKavett, Menard, and San Saba. However insufficient temperature data were available for these locations from sources utilized during this project effort.

Table 5-4 presents information regarding the temperature measurement stations used in assessing trends across the San Saba watershed. As shown, data from “Brady” was available from 1937-2019, yet only data for the period 1940-2016 was used in this analysis. Data from the City of Eldorado was compiled from five (5) separate gage locations within the vicinity of the city, with each location providing data at different times. Combined, the period of record of available data for Eldorado ran from 1/1/1966 to 4/1/2019, yet only data for the period 1967-2016 was used in this analysis.

Table 5-4 – Temperature measurement stations for the San Saba watershed

Station Name	ACIS ID	Latitude	Longitude	Start Date	End Date
Brady	23442	31.14453N	99.34922W	3/4/1937	4/2/2019
ELDORADO 10W	31513	30.8191N	100.7572W	3/1/2003	9/24/2011
ELDORADO 12N	28803	31.03698N	100.59119W	8/1/1999	2/8/2008
ELDORADO 11NW	23373	30.96667N	100.7W	3/1/1966	6/30/1981
ELDORADO	31512	30.8694N	100.5994W	3/1/2003	4/1/2019
ELDORADO 2 SE	24339	30.8333N	100.58333W	9/1/1981	8/22/1989

** ACIS = Applied Climate Information System

5.2.1 Temperatures for Brady, TX

Figure 5-8 presents a calendar plot of temperature data for Brady from 1940-2016. Data shown in BLACK reflect periods when data was unavailable (assigned the value “-9999”). RED data in Figure 5-8 indicate days during which the recorded high temperature exceeded 100 °F, which occurred often within July and August, yet occasionally in May, June, and September. BLUE data indicate days with the recorded low temperatures below 32 °F, which occurred often from November-February as well as occasionally in March, April, and October. Based on only the visual analysis of Figure 5-8, it does not appear that hot or cold days are occurring with greater annual frequency, although the increase in hot days for 2011 is notable.

Figure 5-9 presents a statistical analysis of the Brady temperature data, including Mann-Kendall analysis results. Within Figure 5-9A, the number of 100 °F per calendar year is presented over time, with values ranging from 0 to over 70 days (in 2011). Per the Mann-Kendall analysis, the data exhibits a stable trend, confirming the visual trend identified in Figure 5-8. In contrast, an increasing trend is indicated regarding the number of days per year on which temperatures exceed 90 °F (Figure 5-9B). This could suggest that extreme high temperatures are as likely now as in the past, yet that moderate high temperatures are likely to increase.

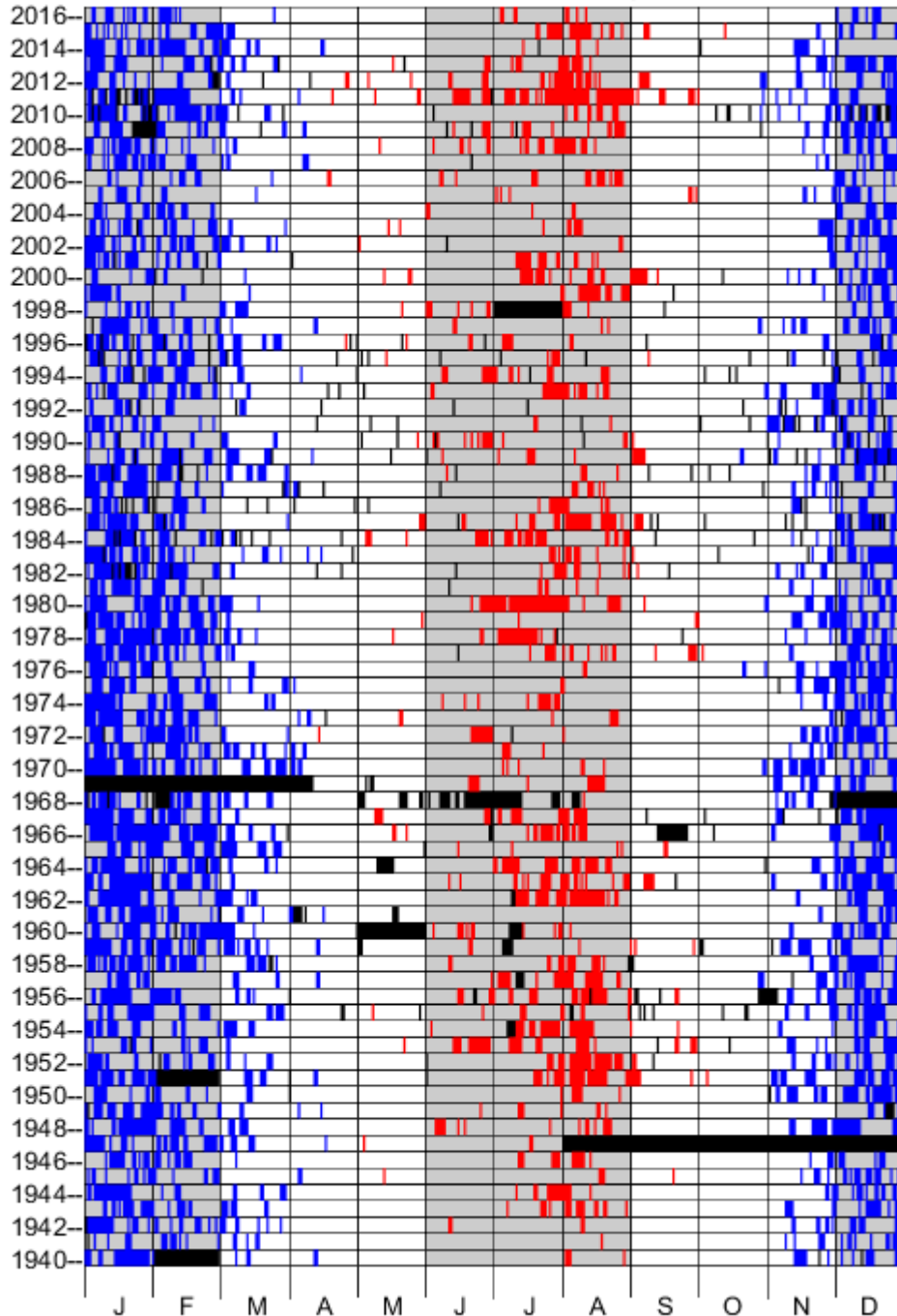


Figure 5-8 - Temperature Data For Brady for the period 1940-2016 – BLUE showing when minimum temperatures dropped below 32° F, RED showing when maximum temperatures exceeded 100°F. BLACK indicates no valid data was recorded.

Trends evident from analysis of Brady minimum temperatures do suggest that the area is warming. There is a decreasing trend in the number of days for which temperatures drop below 32 °F, yet the data also appears to be generally increasing from 1940-1962 and then decreasing from 1965 onward (Figure 5-9C). Similarly when considering the number of

days on which minimum temperatures exceed 60°F (Figure 5-9D), there is an increasing trend. This trend, however, mimics the trend from Figure 5-9C in that from 1940-1965 the number of days appears to decrease, whereas the increase occurs from 1965 to 2016. This suggests that conditions within the Brady area changed in and around 1965, although this date does not appear to indicate changes within the maximum temperature datasets.

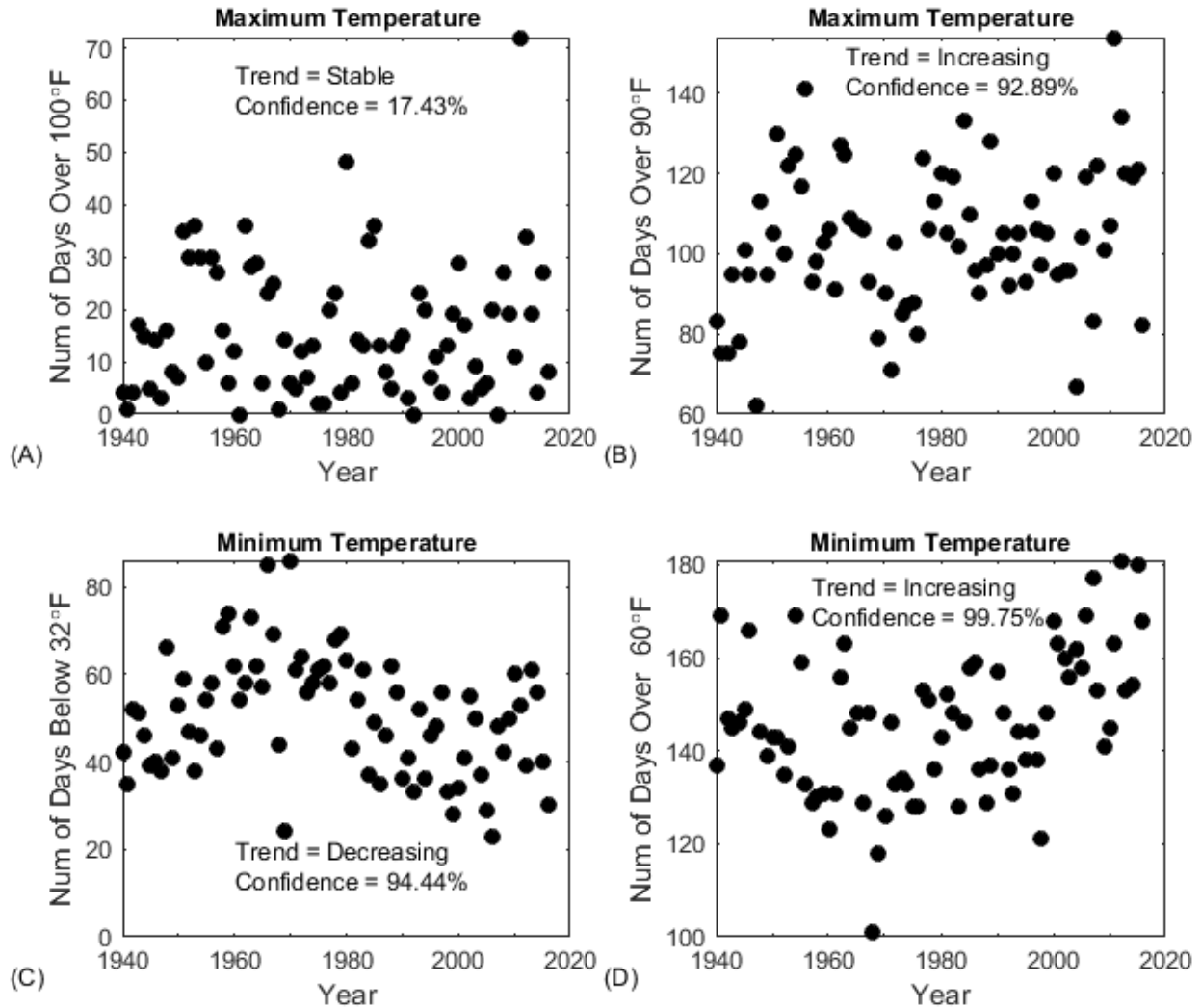


Figure 5-9 - Temperature Trends For Brady, for the period 1940-2016 – A) Days exceeding 100°F, B) Days exceeding 90°F, C) Days with minimum temperatures below 32°F, D) Days with minimum temperatures exceeding 60°F.

Annual average temperatures for Brady (Figure 5-10) show increasing trends in both minimum and maximum temperatures. The annual average minimum temperature also shows a transition from decreasing values for 1940-1965, and increasing values after 1965.

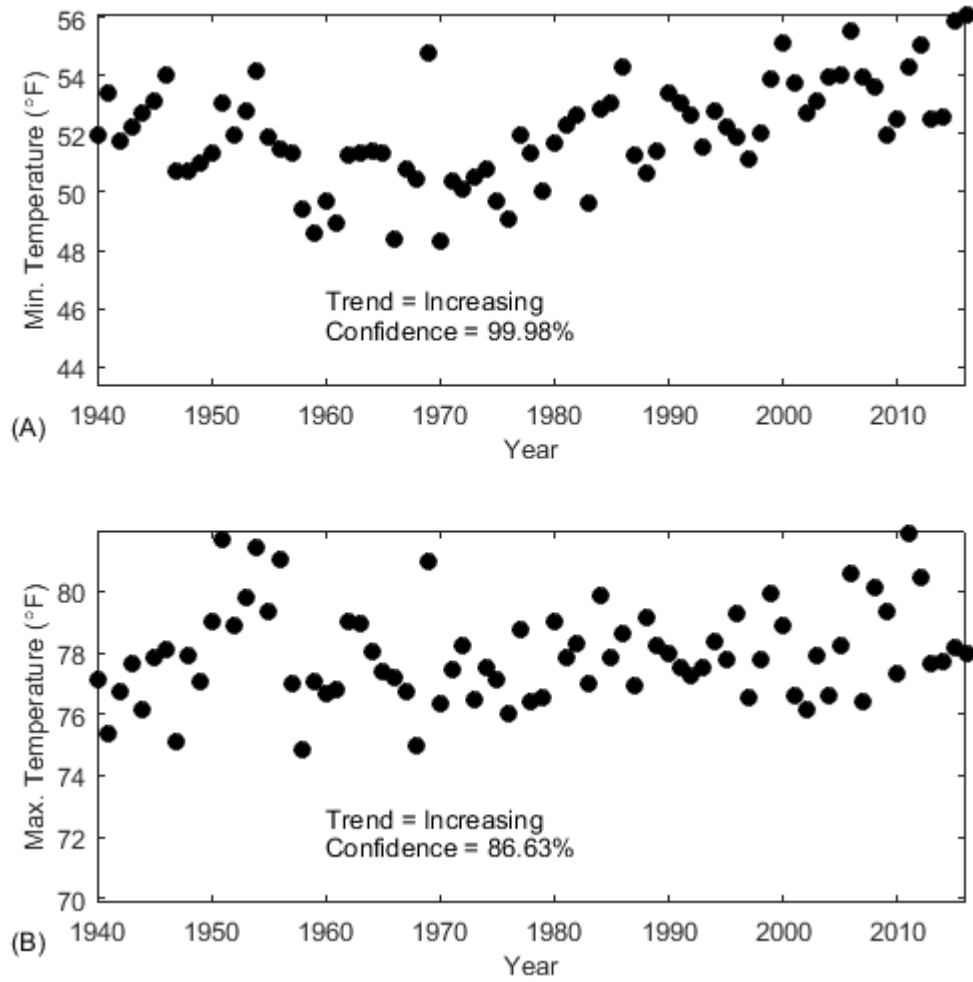


Figure 5-10- Annual Average Temperatures for Brady for the period 1940-2016 – A) Average minimum daily temperature, B) Average maximum daily temperature

Table 5-5 presents monthly, seasonal, and annual temperature trends computed for Brady. Periods showing statistically significant Mann-Kendall trends are shown with grey shading. Negative trends are indicated in **bold underline**, and positive trends are indicated with ***bold italics***. As shown, average minimum temperatures show increasing trends for all computed time periods other than February and April. Analysis of the maximum temperature data identified for most periods, with increasing trends evident for May, October, Spring, and annually. This data suggests that Brady temperatures are becoming less variant, with less cooling occurring throughout the area on a daily, monthly, and seasonal basis. This temperature trend is similar to that exhibited for Ballinger, TX (Table 5-2), and less similar to that observed for Abilene (Table 5-3).

Table 5-5 – Temperature trend statistics for Brady for the period from 1940-2016

Period	Minimum Temperatures		Maximum Temperatures	
	Trend	Confidence	Trend	Confidence
January	<i>Increasing</i>	98.39%	Stable	71.82%
February	Stable	61.46%	Stable	54.19%
March	<i>Increasing</i>	99.80%	Stable	56.22%
April	Stable	70.07%	Stable	61.38%
May	<i>Increasing</i>	98.67%	<i>Increasing</i>	86.11%
June	<i>Increasing</i>	99.30%	Stable	44.15%
July	<i>Increasing</i>	83.42%	Stable	60.77%
August	<i>Increasing</i>	99.01%	Stable	9.10%
September	<i>Increasing</i>	94.89%	Stable	63.02%
October	<i>Increasing</i>	89.06%	<i>Increasing</i>	83.55%
November	<i>Increasing</i>	99.98%	Stable	68.27%
December	<i>Increasing</i>	90.33%	Stable	11.13%
Spring	<i>Increasing</i>	99.54%	<i>Increasing</i>	79.89%
Summer	<i>Increasing</i>	98.88%	Stable	29.80%
Fall	<i>Increasing</i>	99.93%	Stable	73.58%
Winter	<i>Increasing</i>	98.50%	Stable	59.53%
Annual	<i>Increasing</i>	99.98%	<i>Increasing</i>	86.63%

BOLD, ITALICS, & SHADING = significant increasing trend
BOLD, UNDERLINE, & SHADING = significant decreasing trend

5.2.2 Temperatures for Eldorado

Although Eldorado is outside of the San Saba watershed (Figure 5-1), analysis of its temperature records is included in this section to provide information for comparison with data from Brady. This will possibly allow for the assessment of gradients in temperature trends in the W-E direction across the San Saba watershed.

Figure 5-11 presents a calendar plot of temperature data for Eldorado from 1966-2016. Data shown in BLACK reflect periods when data was unavailable (assigned the value “-9999”). RED data in Figure 5-11 indicate days during which the recorded high temperature exceeded 100 °F, which occurred often within July and August, yet occasionally in May, June, and September. BLUE data indicate days during which the recorded low temperature was below 32 °F, which occurred often from November-February as well as occasionally in March, April, and October. None of the gages in the vicinity of Eldorado recorded reliable temperature readings for the period from August 1989 through July 1999, resulting in the black portion in the center of the image. Statistics based on this dataset, even within the 10-years of missing data, are still valid. The statistics could be changed, however, should suitable data become available to fill in the gaps.

Figure 5-12 presents a statistical analysis of the Eldorado temperature data, including Mann-Kendall analysis results. Within Figure 5-12A, the number of 100 °F per calendar year is presented over time, with values ranging from 0 to over 40 days (in 2011). Per the Mann-Kendall analysis, the data exhibits stable trends over time. Similarly, a stable trend is indicated for the number of days with temperatures exceeding 90 °F (Figure 5-12B).

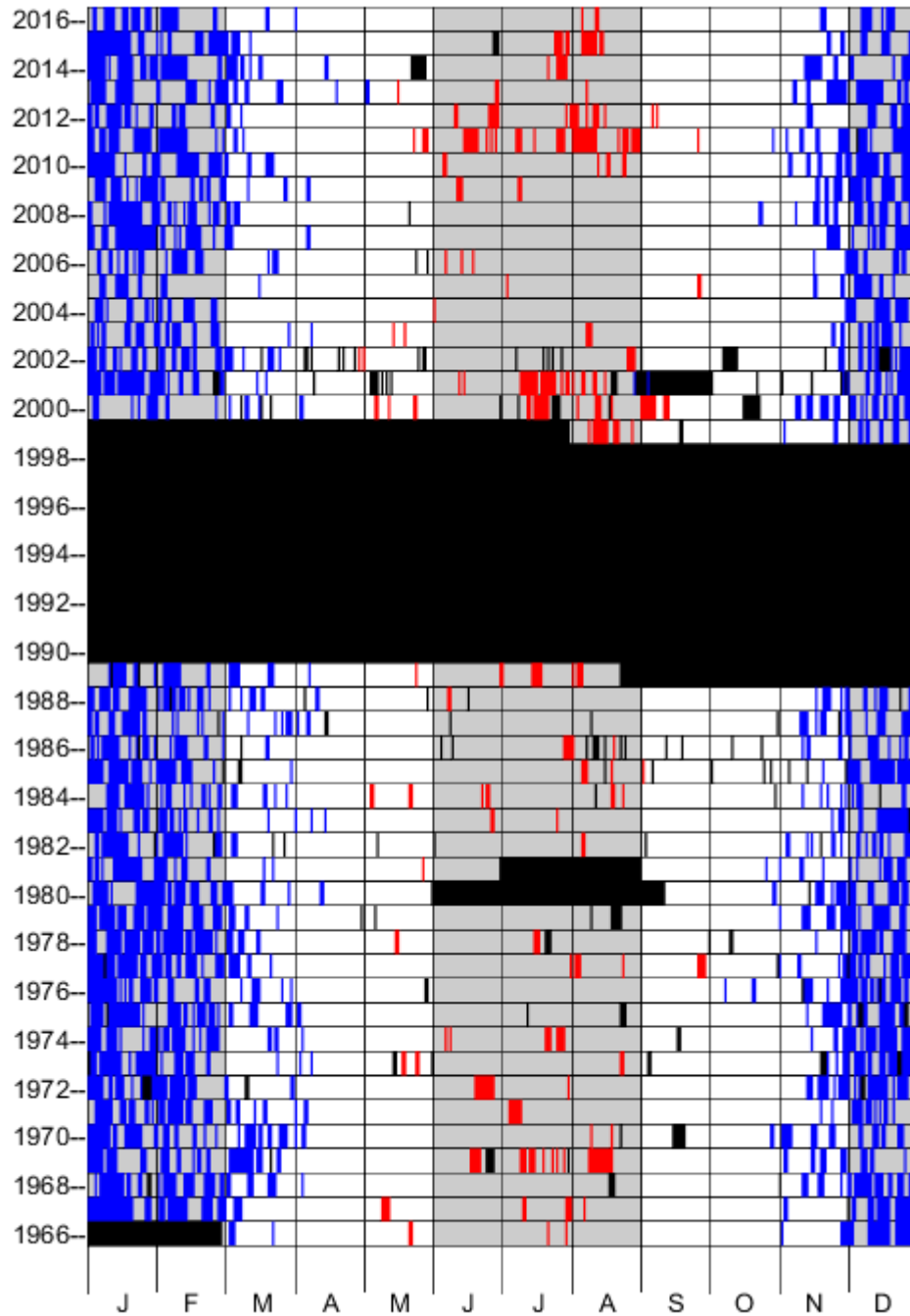


Figure 5-11 -- Temperature Data For Eldorado for the period from 1966-2016 – BLUE showing when minimum temperatures dropped below 32° F, RED showing when maximum temperatures exceeded 100°F. BLACK indicates no valid data was recorded.

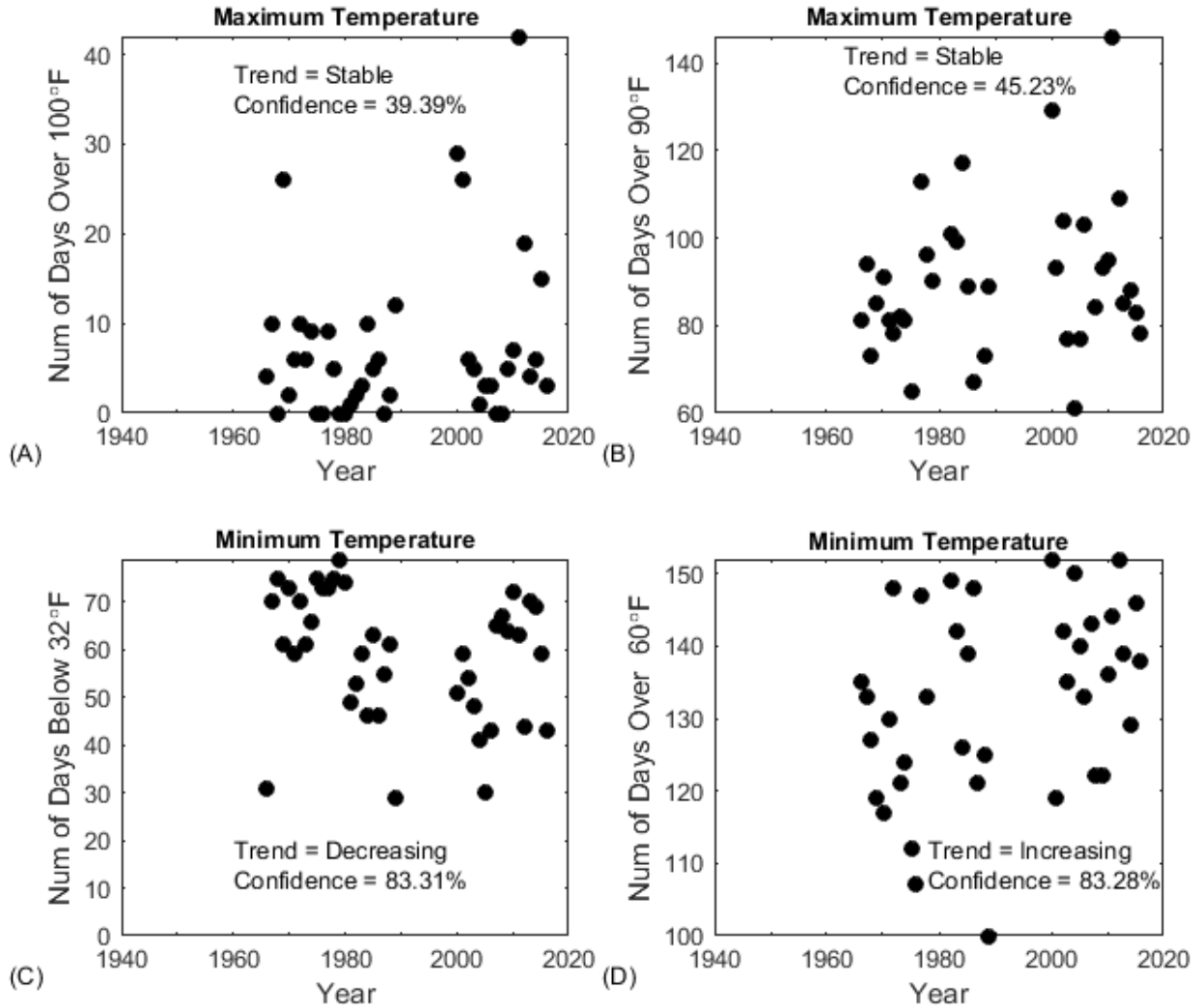


Figure 5-12 - Temperature Trends For Eldorado for the period 1966-2016 – A) Days exceeding 100°F, B) Days exceeding 90°F, C) Days with minimum temperatures below 32°F, D) Days with minimum temperatures exceeding 60°F. Time axis is scaled for 1940-2020 to allow for direct comparisons with Figure 5-9.

Non-stable trends are, however, evident within the data describing minimum temperatures recorded for Eldorado. There is a decreasing trend in the number of days for which temperatures drop below 32 °F, with decreasing values evident from 1967 through 2005, followed by a series of higher values (colder periods) from 2005-2018. During this later colder period, however, some of the years experienced less cold days, following along with the 1967-2005 trend. Similarly when considering the number of days on which minimum temperatures exceed 60°F (Figure 5-12D), there is an increasing trend through the entire dataset, with the variation among the data appearing to diminish over time. This trend suggests that Eldorado, like Brady and Ballinger, is not cooling off to the extent it had previously, even while daily maximum temperatures remain unchanged.

Average annual minimum and maximum temperatures (Figure 5-13) indicate increasing and stable trends, respectively.

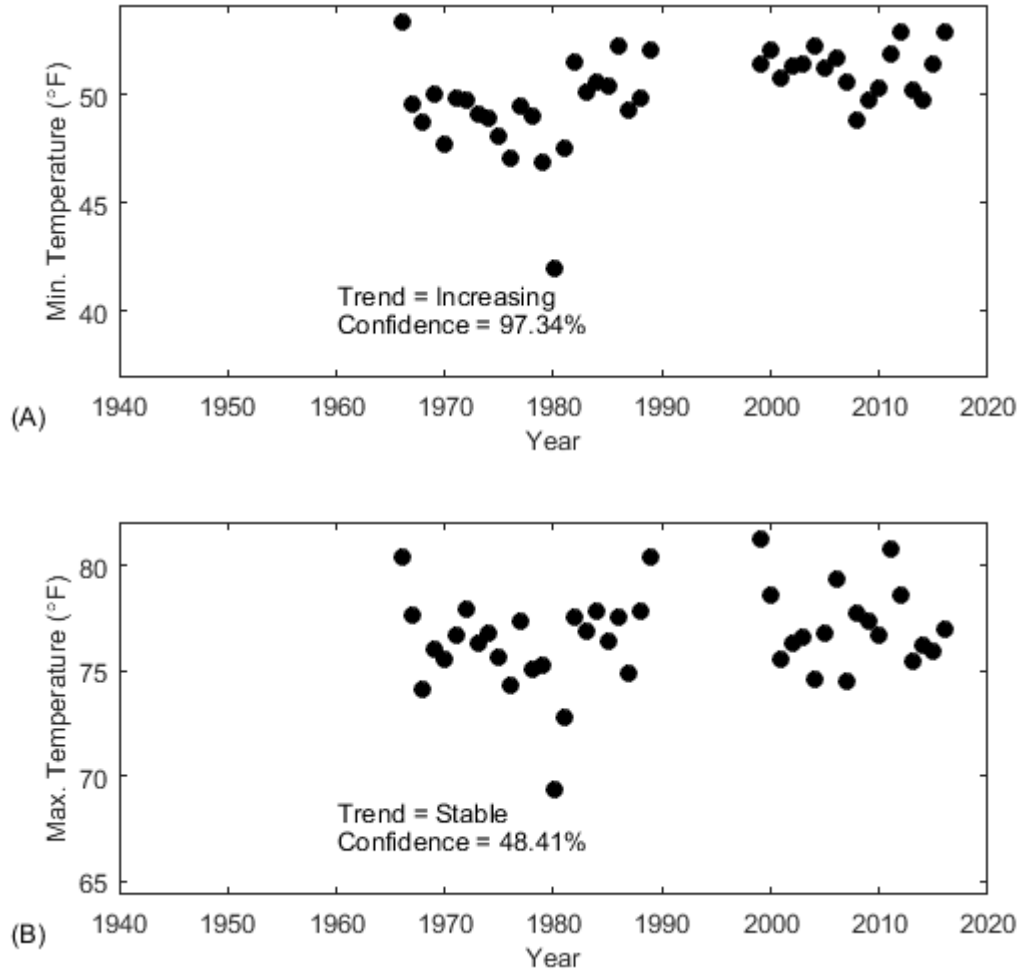


Figure 5-13- Annual Average Temperatures for Eldorado for the period 1966-2016 – A) Average minimum daily temperature, B) Average maximum daily temperature. Time axis is scaled for 1940-2020 to allow for direct comparisons with Figure 5-10.

Table 5-6 presents monthly, seasonal, and annual temperature trends computed for Eldorado, TX. Periods showing statistically significant Mann-Kendall trends are shown with grey shading. Negative trends are indicated in **bold underline**, and positive trends are indicated with ***bold italics***. As shown, average minimum temperatures show significant increasing trends for all computed time periods except April. Maximum temperature data did indicate increasing trends for August, September, October, and the fall season, yet indicated stable trends for all other computed time periods. This data suggests that Eldorado temperatures are becoming less variant, with less cooling occurring throughout the area on a daily, monthly, and seasonal basis. This temperature trend is similar to that exhibited for Ballinger (Table 5-2), and matches well with trends computed for Brady (Table 5-5).

Table 5-6 – Temperature trend statistics for Eldorado for 1966-2016

Period	Minimum Temperatures		Maximum Temperatures	
	Trend	Confidence	Trend	Confidence
January	<i>Increasing</i>	91.10%	Stable	10.19%
February	<i>Increasing</i>	98.25%	Stable	26.45%
March	<i>Increasing</i>	77.91%	Stable	9.83%
April	Stable	12.49%	Stable	24.68%
May	<i>Increasing</i>	91.63%	Stable	5.37%
June	<i>Increasing</i>	99.93%	Stable	0%
July	<i>Increasing</i>	99.89%	Stable	15.94%
August	<i>Increasing</i>	99.99%	<i>Increasing</i>	83.94%
September	<i>Increasing</i>	96.33%	<i>Increasing</i>	93.45%
October	<i>Increasing</i>	92.02%	<i>Increasing</i>	85.88%
November	<i>Increasing</i>	77.91%	Stable	66.59%
December	<i>Increasing</i>	91.32%	Stable	29.93%
Spring	<i>Increasing</i>	90.88%	Stable	2.78%
Summer	<i>Increasing</i>	99.98%	Stable	72.03%
Fall	<i>Increasing</i>	96.98%	<i>Increasing</i>	85.26%
Winter	<i>Increasing</i>	98.85%	Stable	12.03%
Annual	<i>Increasing</i>	97.34%	Stable	48.41%

BOLD, ITALICS, & SHADING = significant increasing trend
BOLD, UNDERLINE, & SHADING = significant decreasing trend

Table 5-7 presents a comparison of Mann-Kendall trends for temperature datasets for Eldorado and Brady, with each dataset limited to the 1967-2016 time period of the Eldorado dataset. By limiting each dataset to the same time periods, comparison between the resulting trends can indicate variations resulting from the data and not from the differing periods of record used in the analysis. For clarity purposes, within Table 5-7, increasing trends are indicated with an up-arrow (“↑”), decreasing trends with a down-arrow (“↓”) and stable trends with a series of dashes (“—”). As shown, both locations exhibit increasing trends for nearly all time periods regarding minimum average temperatures. Maximum temperatures at Brady indicated more increasing trends than those suggested by the Eldorado data, yet both dataset suggested consistent trends for August-October and the Fall time periods. Note: the trends presented for Brady within Table 5-7 are different than those indicated in Table 5-5 due to the differences in the period of records for data used in each analysis.

Table 5-7 – Temperature trend statistics for Eldorado & Brady, 1967-2016

Period	Minimum Temperatures				Maximum Temperatures			
	Eldorado		Brady		Eldorado		Brady	
	Trend	%	Trend	%	Trend	%	Trend	%
January	↑	<i>91.10%</i>	↑	<i>99.94%</i>	---	10.19%	↑	<i>77.24%</i>
February	↑	<i>98.25%</i>	↑	<i>98.81%</i>	---	26.45%	---	64.81%
March	↑	<i>77.91%</i>	↑	<i>92.13%</i>	---	9.83%	---	6.18%
April	---	12.49%	↑	<i>80.80%</i>	---	24.68%	---	29.96%
May	↑	<i>91.63%</i>	↑	<i>99.98%</i>	---	5.37%	↑	<i>82.20%</i>
June	↑	<i>99.93%</i>	↑	<i>99.99%</i>	---	0%	---	59.24%
July	↑	<i>99.89%</i>	↑	<i>99.99%</i>	---	15.94%	---	29.11%
August	↑	<i>99.99%</i>	↑	<i>99.99%</i>	↑	<i>83.94%</i>	↑	85.95%
September	↑	<i>96.33%</i>	↑	<i>99.97%</i>	↑	<i>93.45%</i>	↑	82.46%
October	↑	<i>92.02%</i>	↑	<i>97.28%</i>	↑	<i>85.88%</i>	↑	93.67%
November	↑	<i>77.91%</i>	↑	<i>99.64%</i>	---	66.59%	↑	<i>93.78%</i>
December	↑	<i>91.32%</i>	↑	<i>94.73%</i>	---	29.93%	---	66.29%
Spring	↑	<i>90.88%</i>	↑	<i>99.79%</i>	---	2.78%	---	61.13%
Summer	↑	<i>99.98%</i>	↑	<i>99.99%</i>	---	72.03%	↑	<i>83.16%</i>
Fall	↑	<i>96.98%</i>	↑	<i>99.99%</i>	↑	<i>85.26%</i>	↑	<i>96.63%</i>
Winter	↑	<i>98.85%</i>	↑	<i>99.99%</i>	---	12.03%	↑	<i>92.59%</i>
Annual	↑	<i>97.34%</i>	↑	<i>99.99%</i>	---	48.41%	↑	<i>96.49%</i>

BOLD, ITALICS, & SHADING = significant increasing trend
BOLD, UNDERLINE, & SHADING = significant decreasing trend

5.3 South Concho Watershed

As shown in Temperature data were obtained as daily maximum and minimum values for the period of record for each gauge. Data were processed to contain the value “-9999” for instances when data were missing and not available. Statistical analysis of temperature data were only performed on valid data, excluding data containing the “-9999” value. Data analysis was limited to the period of record for this Phase II report, specifically from 1940-2016. Daily data was averaged monthly, seasonally, and annually with the Mann-Kendall technique applied to each dataset to determine and evaluate data trends. For seasonal averaging, monthly data was grouped as follows:

- “Winter” = December, January, and February
- “Spring” = March, April, and May
- “Summer” = June, July, and August
- “Fall” = September, October, and November.

For winter periods, data from December corresponds to the December from the previous year, so that the “Winter 2019” period consists of December 2018, January 2019, and February 2019 data. All annual averages were based on the calendar year.

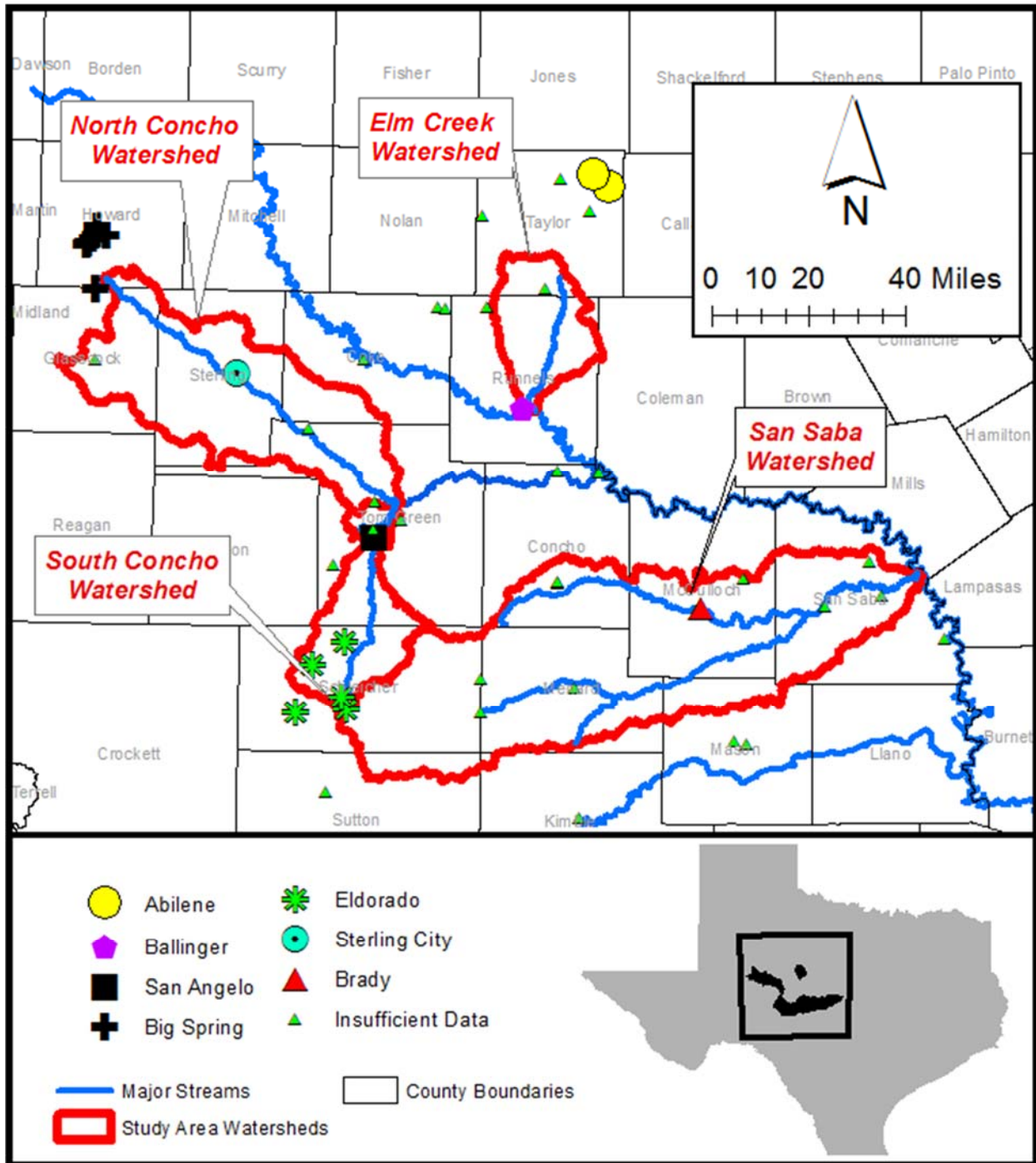


Figure 5-1, within the South Concho watershed sufficient temperature data from the vicinity of San Angelo and Eldorado were available to allow for statistical analysis. These stations are located at the North and South ends of the watershed, respectively. Data from the Eldorado gauges also was used to represent the temperatures for the upper portion of the San Saba watershed, and as such data for the Eldorado location was presented in Section 5.2.2. Similarly, data recorded at San Angelo could reasonably represent temperatures expected within the downstream end of the North Concho watershed.

Table 5-8 presents information regarding the temperature measurement stations used in assessing trends across the South Concho watershed. As shown, data from “San Angelo Mathis Field” was available from 1907-2019, yet only data for the period 1940-2016 was used in this analysis. Data from the City of Eldorado was compiled from five (5) separate gage locations within the vicinity of the city, with each location providing data at different times. Combined, the period of record of available data for Eldorado ran from 1/1/1966 to 4/1/2019, yet only data for the period 1967-2016 was used in this analysis.

Table 5-8 – Teamperature measurement stations for the South Concho watershed

Station Name	ACIS ID	Latitude	Longitude	Start Date	End Date
San Angelo Mathis Field	29769	31.35167N	100.495W	8/1/1907	4/1/2019
ELDORADO 10W	31513	30.8191N	100.7572W	3/1/2003	9/24/2011
ELDORADO 12N	28803	31.03698N	100.59119W	8/1/1999	2/8/2008
ELDORADO 11NW	23373	30.96667N	100.7W	3/1/1966	6/30/1981
ELDORADO	31512	30.8694N	100.5994W	3/1/2003	4/1/2019
ELDORADO 2 SE	24339	30.8333N	100.58333W	9/1/1981	8/22/1989

** ACIS = Applied Climate Information System

5.3.1 Temperatures for San Angelo, TX:

Figure 5-14 presents a calendar plot of temperature data for San Angelo from 1940-2016. Data shown in BLACK reflect periods when data was unavailable (assigned the value “-9999”). RED data in Figure 5-14 indicate days during which the recorded high temperature exceeded 100 °F, which occurred often within June, July, and August, yet occasionally in April, May, September, and October. BLUE data indicate days with the recorded low temperatures below 32 °F, which occurred often from November-February as well as occasionally in March, April, and October. Based on only the visual analysis of Figure 5-14, it does not appear that hot or cold days are occurring with greater annual frequency, although the increase in hot days for 2011 is notable.

Figure 5-15 presents a statistical analysis of the San Angelo temperature data, including Mann-Kendall analysis results. Within Figure 5-15A, the number of 100 °F per calendar year is presented over time, with values ranging from 0 to over 100 days (in 2011). Per the Mann-Kendall analysis, there is a stable trend in the data, indicating that the frequency of 100 °F days is not increasing or decreasing with time. Figure 5-15B suggest a similarly stable trend for the number of days with temperatures exceeding 90 °F. These trends combine to indicate that San Angelo has generally not recently experienced greater or less hot days than it had in the from 1940.

When considering trends resulting from analysis of the minimum temperatures, Figure 5-15 C demonstrates there is an increasing trend for the number of days per year with temperatures below 32°F. In addition, the number of days per year on which San Angelo experienced minimum temperatures exceeding 60°F has exhibited a stable trend. These results regarding minimum daily temperatures are in contrast to those obtained from the Ballinger, Abilene, Brady, and Eldorado datasets.

Average annual maximum and minimum temperatures for San Angelo (Figure 5-16) also exhibit trends that differ from the other locations already discussed in this Phase II report. Specifically, Figure 5-16A indicates a stable annual trend for average minimum temperatures for San Angelo, and Figure 5-16B indicates an increasing average maximum temperature.

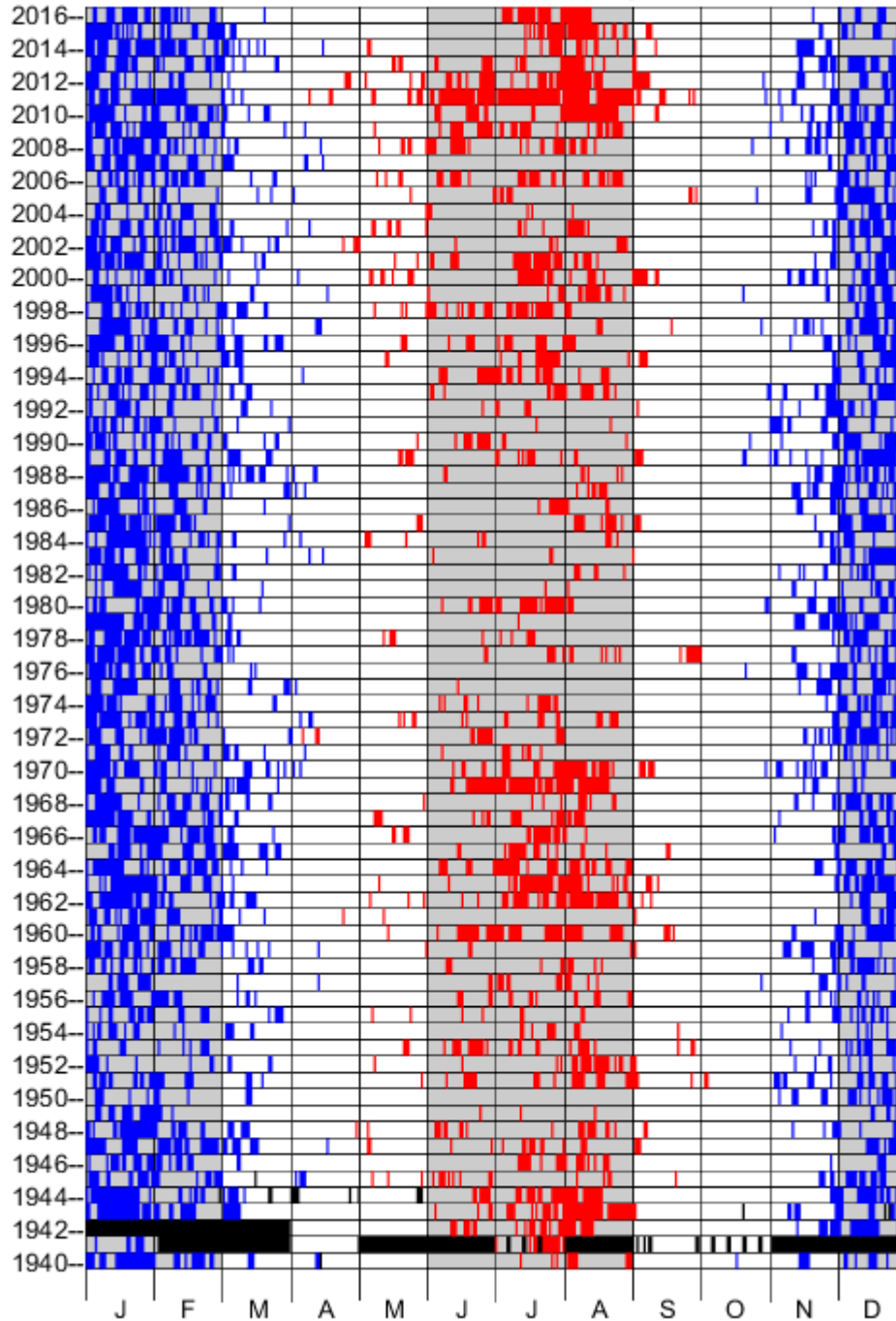


Figure 5-14-- Temperature Data For San Angelo for the period 1940-2016 – BLUE showing when minimum temperatures dropped below 32° F, RED showing when maximum temperatures exceeded 100°F. BLACK indicates no valid data was recorded.

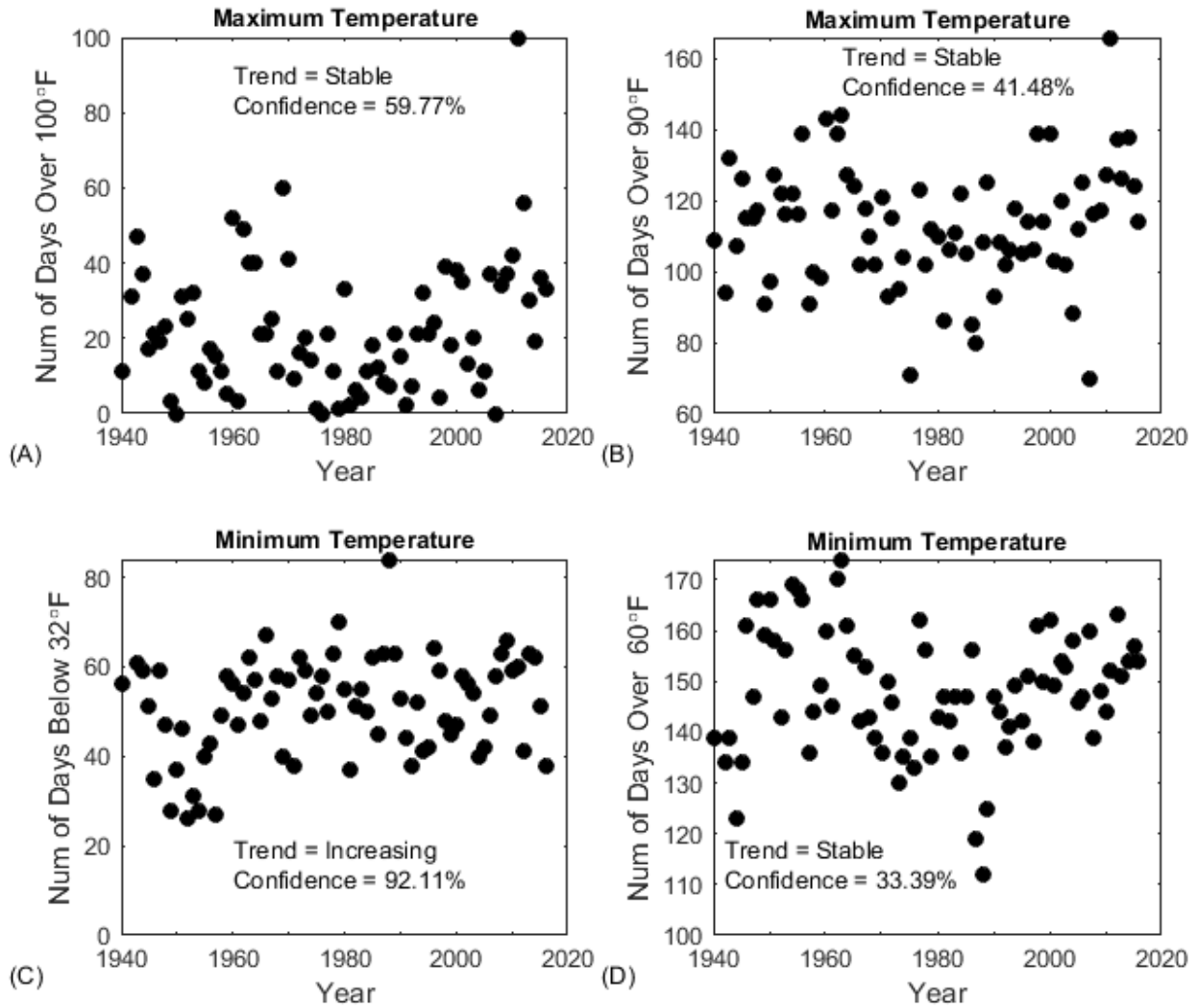


Figure 5-15- Temperature Trends For San Angelo for the period 1940-2016 – A) Days exceeding 100°F, B) Days exceeding 90°F, C) Days with minimum temperatures below 32°F, D) Days with minimum temperatures exceeding 60°F.

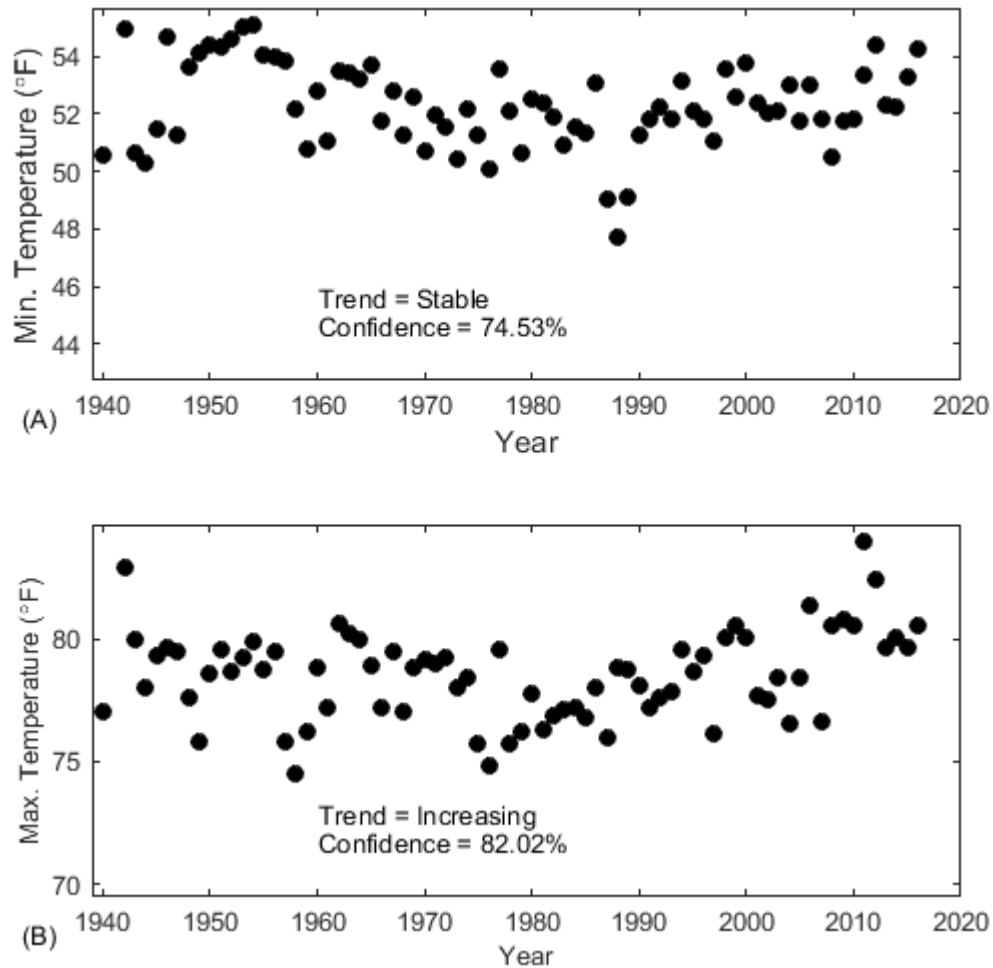


Figure 5-16- Annual Average Temperatures for San Angelo for the period 1940-2016 – A) Average minimum daily temperature, B) Average maximum daily temperature

Table 5-9 presents monthly, seasonal, and annual temperature trends computed for San Angelo, TX. Periods showing increasing or decreasing Mann-Kendall trends are shown with grey shading. Negative trends are indicated in **bold underline**, and positive trends are indicated with ***bold italics***. As shown, average minimum temperatures show significant decreasing trends for October and December only, with stable trends for all other periods. Maximum temperature data indicate increasing trends for January, March, April, May, Spring, Winter, and Annual periods. This data suggest that San Angelo temperatures are becoming increasingly variant, with greater cooling and heating occurring throughout the area on a daily, monthly, and seasonal basis. The general increasing of maximum temperatures over various periods has not been indicated in analysis of the other locations described in this report. Similarly, decreasing minimum temperatures have only been identified for the San Angelo location.

Table 5-9 – Temperature trend statistics for San Angelo for the period 1940-2016

Period	Minimum Temperatures		Maximum Temperatures	
	Trend	Confidence	Trend	Confidence
January	Stable	14.23%	<i>Increasing</i>	<i>94.03%</i>
February	Stable	66.32%	Stable	53.30%
March	Stable	67.68%	<i>Increasing</i>	<i>90.41%</i>
April	Stable	57.40%	<i>Increasing</i>	<i>82.86%</i>
May	Stable	11.76%	<i>Increasing</i>	<i>87.93%</i>
June	Stable	26.68%	Stable	14.94%
July	Stable	36.54%	Stable	9.99%
August	Stable	28.56%	Stable	24.42%
September	Stable	42.65%	Stable	61.62%
October	<u>Decreasing</u>	<u>76.84%</u>	Stable	65.11%
November	Stable	5.36%	Stable	55.51%
December	<u>Decreasing</u>	<u>92.33%</u>	Stable	9.65%
Spring	Stable	11.13%	<i>Increasing</i>	<i>92.22%</i>
Summer	Stable	62.76%	Stable	27.18%
Fall	Stable	37.50%	<i>Increasing</i>	<i>83.56%</i>
Winter	Stable	69.54%	Stable	62.16%
Annual	Stable	74.53%	<i>Increasing</i>	<i>82.02%</i>

BOLD, ITALICS, & SHADING = significant increasing trend

BOLD, UNDERLINE, & SHADING = significant decreasing trend

Trend gradients implied for the South Concho watershed may be reasonably deduced from the San Angelo (North) and Eldorado (south) datasets. Gradient assessment would be improved through analyses of additional temperature data for Christoval, TX, located within the South Concho watershed between San Angelo and Eldorado. Reliable, long period of record data for Christoval was not obtained during the course of this project.

Table 5-10 presents a comparison of Mann-Kendall trends for temperature datasets for Eldorado and San Angelo, with each dataset limited to the 1967-2016 time period of the Eldorado dataset. By limiting each dataset to the same time periods, comparison between the resulting trends can indicate variations resulting from the data and not from the differing periods of record used in the analysis. For clarity purposes, within Table 5-10, increasing trends are indicated with an up-arrow (“↑”), decreasing trends with a down-arrow (“↓”) and stable trends with a series of dashes (“—”).

As shown, changing the analysis period of record for the San Angelo temperature data resulted in changing computed trends for a majority of the computed time periods. With respect to minimum temperatures, both Eldorado and San Angelo experienced increasing trends for May-September, for Spring-Fall, and for the Annual periods. Similarly both locations exhibited increasing maximum temperature trends for August-October and for the Fall period. These common trends across the South Concho watershed from 1967-2016 suggest similar trends would be expected at all locations across the watershed.

Table 5-10 – Temperature Trend Statistics for Eldorado & San Angelo, 1966-2016

Period	Minimum Temperatures				Maximum Temperatures			
	Eldorado		San Angelo		Eldorado		San Angelo	
	Trend	%	Trend	%	Trend	%	Trend	%
January	↑	<i>91.10%</i>	---	73.05%	---	10.19%	↑	88.80%
February	↑	<i>98.25%</i>	---	68.45%	---	26.45%	---	56.83%
March	↑	<i>77.91%</i>	---	74.82%	---	9.83%	↑	83.25%
April	---	12.49%	---	6%	---	24.68%	↑	90.57%
May	↑	<i>91.63%</i>	↑	96.97%	---	5.37%	↑	94.13%
June	↑	<i>99.93%</i>	↑	97.39%	---	0%	---	72.32%
July	↑	<i>99.89%</i>	↑	86.40%	---	15.94%	↑	75.19%
August	↑	<i>99.99%</i>	↑	99.18%	↑	<i>83.94%</i>	↑	97.81%
September	↑	<i>96.33%</i>	↑	83.50%	↑	<i>93.45%</i>	↑	99.40%
October	↑	<i>92.02%</i>	---	33.64%	↑	<i>85.88%</i>	↑	98.47%
November	↑	<i>77.91%</i>	---	62.02%	---	66.59%	↑	92.52%
December	↑	<i>91.32%</i>	---	22.39%	---	29.93%	---	43.06%
Spring	↑	<i>90.88%</i>	↑	94.32%	---	2.78%	↑	98.84%
Summer	↑	<i>99.98%</i>	↑	99.12%	---	72.03%	↑	99.37%
Fall	↑	<i>96.98%</i>	↑	85.44%	↑	<i>85.26%</i>	↑	99.67%
Winter	↑	<i>98.85%</i>	---	42.47%	---	12.03%	↑	91.37%
Annual	↑	<i>97.34%</i>	↑	96.84%	---	48.41%	↑	99.83%

BOLD, ITALICS, & SHADING = significant increasing trend

BOLD, UNDERLINE, & SHADING = significant decreasing trend

5.4 North Concho Watershed

As shown in Temperature data were obtained as daily maximum and minimum values for the period of record for each gauge. Data were processed to contain the value “-9999” for instances when data were missing and not available. Statistical analysis of temperature data were only performed on valid data, excluding data containing the “-9999” value. Data analysis was limited to the period of record for this Phase II report, specifically from 1940-2016. Daily data was averaged monthly, seasonally, and annually with the Mann-Kendall technique applied to each dataset to determine and evaluate data trends. For seasonal averaging, monthly data was grouped as follows:

- “Winter” = December, January, and February
- “Spring” = March, April, and May
- “Summer” = June, July, and August
- “Fall” = September, October, and November.

For winter periods, data from December corresponds to the December from the previous year, so that the “Winter 2019” period consists of December 2018, January 2019, and February 2019 data. All annual averages were based on the calendar year.

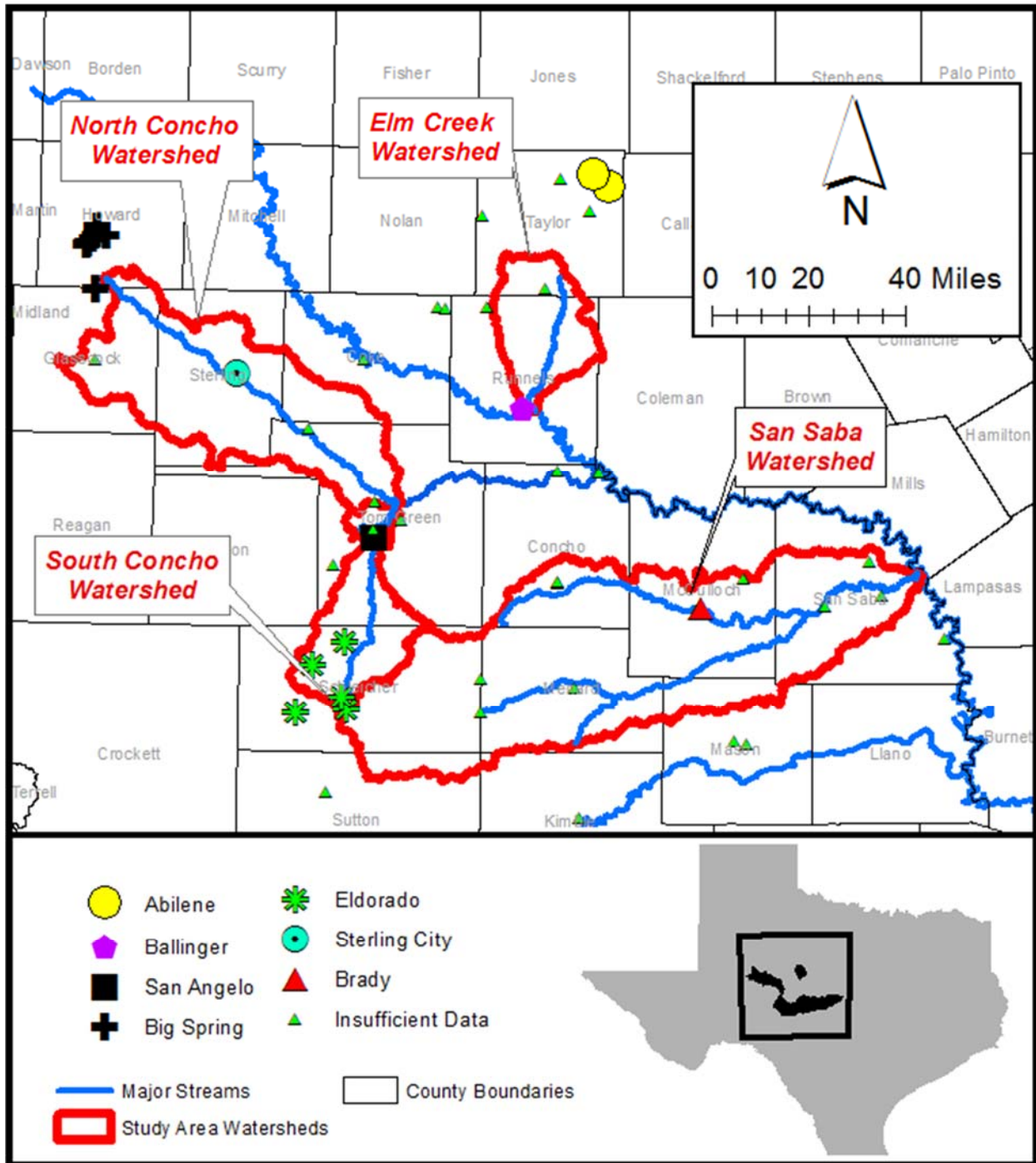


Figure 5-1, within the vicinity of the North Concho watershed sufficient temperature data from Big Spring, Sterling City, and San Angelo were available to allow for statistical analysis. . These stations are located roughly along the NW-SE oriented line traveling through the North Concho watershed, thereby allowing for the establishment of gradients in temperature trends across the watershed. Data from the San Angelo gauges also were used to represent the temperatures for the downstream portion of the South Concho watershed, and as such data for the San Angelo location were presented in Section 5.3.1.

Table 5-11 presents information regarding the temperature measurement stations used in assessing trends across the North Concho watershed. As shown, data from “San Angelo Mathis Field” was available from 1907-2019, yet only data for the period 1940-2016 was used in this analysis. Data from Sterling City were only available from 1963 to the present, so the analysis was limited to the 1964-2016 time period. Data from Big Spring were compiled from six (6) separate gage locations within the vicinity of the city, with each location providing data at different times. Combined, the period of record of available data for Big Spring ran from 1/1/1948 to 4/1/2019, yet only data for the period 1948-2016 was used in this analysis.

Table 5-11 – Teamperature measurement stations for the North Concho watershed

Station Name	ACIS ID	Latitude	Longitude	Start Date	End Date
San Angelo Mathis Field	29769	31.35167N	100.495W	8/1/1907	4/1/2019
Sterling City	23652	31.8347N	100.9827W	9/24/1963	2/28/2019
Big Spring	29762	32.2443N	101.4537W	1/1/1948	3/26/2019
Big Spring	29761	32.23333N	101.5W	1/1/1948	11/15/1953
Webb AFB	32412	32.21667N	101.51667W	11/15/1953	12/9/1970
Lees	31608	32.082N	101.4842W	11/1/2003	9/14/2010
Big Spring McMahan Wrinkle Airport	32300	32.21667N	101.51667W	8/1/2009	4/1/2019
Big Spring Field Station	23753	32.2683N	101.4858W	7/2/2003	6/6/2008

** ACIS = Applied Climate Information System

5.4.1 Temperatures for Big Spring, TX:

Temperature data for Big Spring, TX (Figure 5-17) was compiled by combining records from 5 separate gauges located in and around Big Spring. Specifically data from ACIS ID station #29762 used, with data gaps filled in from valid data recorded at other stations. The resulting dataset spans from 1948 to 2019, yet this Phase II analysis was limited to only 1948-2016 data. Within Figure 5-17, data shown in BLACK reflect periods when data was unavailable (assigned the value “-9999”). RED data in Figure 5-17 indicate days during which the recorded high temperature exceeded 100 °F, BLUE data indicate days during which the recorded low temperature was below 32 °F. Visual inspection of the data suggests that the number of 100 °F days has increased during the 2008-2016 drought period, while the number of freezing days has either remained steady of decreased slightly.

Figure 5-18 presents a statistical analysis of the Big Spring temperature data, including Mann-Kendall analysis results. Within Figure 5-18A, the number of 100 °F per calendar year is presented over time, with values ranging from 0 to over 70 days (in 2011). Per the Mann-Kendall analysis, there is a significant increasing trend in the data, indicating Big Spring has recently experienced a greater frequency of extremely hot days in comparison to most of the period of record. A similar increasing trend was obtained regarding the number of days with temperatures exceeding 90 °F (Figure 5-18B), however the data suggests a decreasing trend from 1948-1975, followed by an increasing trend from 1975 to 2016.

Stable trends were identified within the data describing minimum temperatures recorded for Big Spring. The number of days for which temperatures drop below 32 °F has remained consistently between 20 and 80 days per year across the entire period of record (Figure 5-18). Similarly when considering the number of days on which minimum temperatures exceed 60°F (Figure 5-18D), an overall stable trend was determined for the entire period of record, yet the data appears to exhibit decreasing trends from 1948-1980 and increasing trends from 1980 to 2016.. In general, Big Spring appears to be getting hotter during the summer, yet is maintaining its ability to cool off in the winter and during nighttime hours.

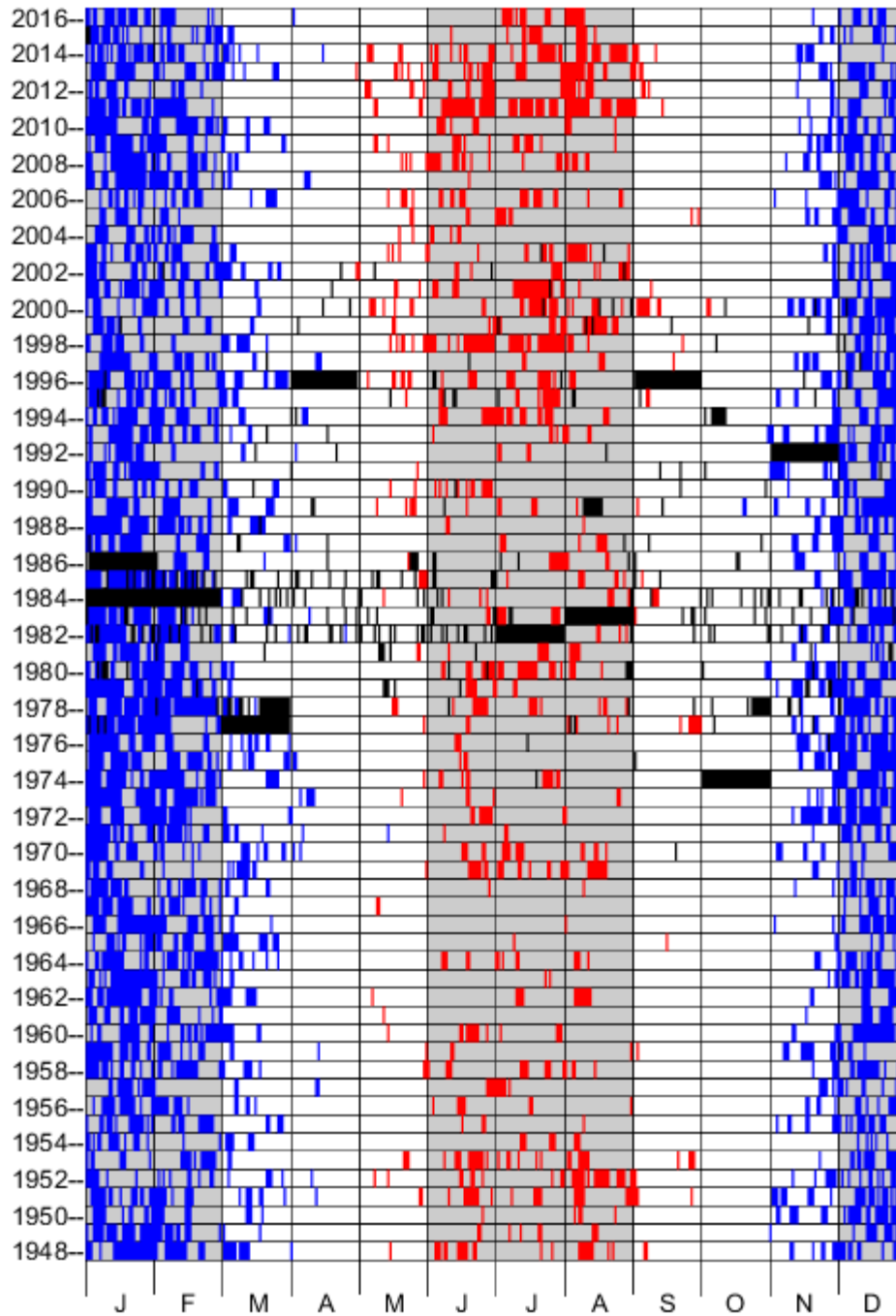


Figure 5-17-- Temperature Data For Big Spring for the period 1948-2016 – BLUE showing when minimum temperatures dropped below 32° F, RED showing when maximum temperatures exceeded 100°F. BLACK indicates no valid data was recorded.

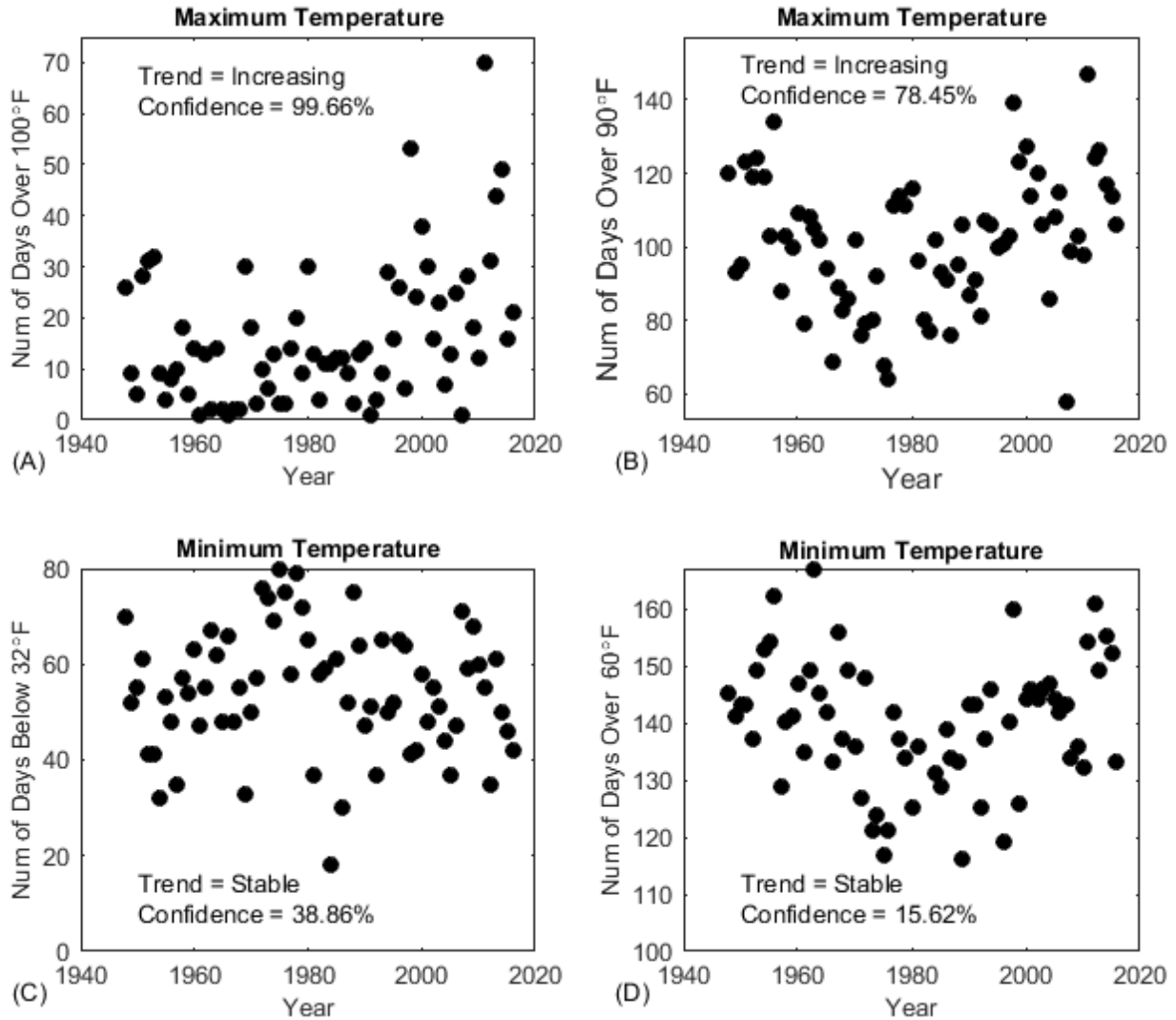


Figure 5-18- Temperature trends for Big Spring for the period 1948-2016 – A) Days exceeding 100°F, B) Days exceeding 90°F, C) Days with minimum temperatures below 32°F, D) Days with minimum temperatures exceeding 60°F.

Mann-Kendall analyses of the average annual maximum and minimum temperatures (Figure 5-19) determined that both datasets suggest increases, signifying that Big Spring is warming. Similar results were obtained for Brady, yet all no other temperature stations reported increasing trends in both annual average minimum and maximum temperatures.

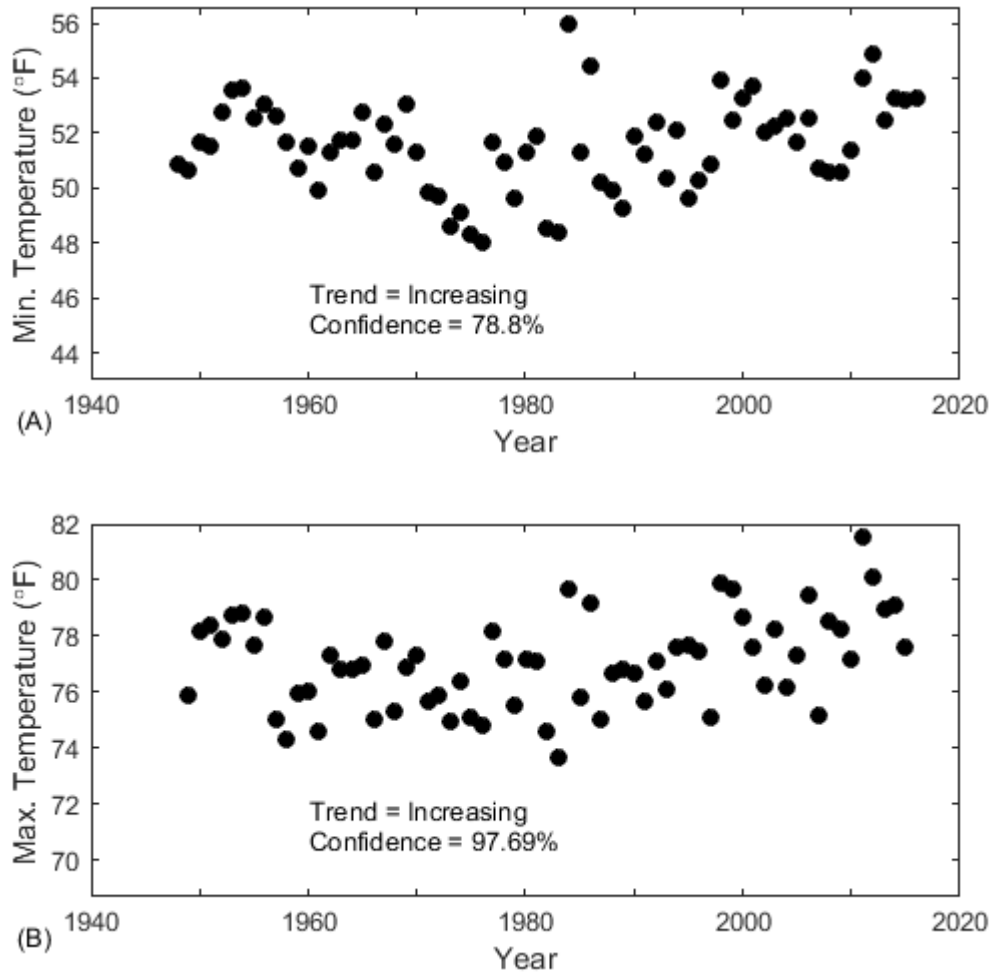


Figure 5-19- Annual average temperatures for Big Spring for the period 1948-2016 – A) Average minimum daily temperature, B) Average maximum daily temperature

Table 5-12 presents monthly, seasonal, and annual temperature trends computed Big Spring, TX. Periods showing statistically significant Mann-Kendall trends are shown with grey shading. Negative trends are indicated in **bold underline**, and positive trends are indicated with ***bold italics***.

As shown, average minimum temperatures show significant increasing trends for January, March, and August as well as for the summer, fall, and annual periods. Analysis of the maximum temperature data indicates increasing trends for the months of March, April, May, August, and November, as well as increasing trends for spring, summer, fall and annual periods.

Table 5-12 – Temperature Trend Statistics for Big Spring for the period 1948-2016

Period	Minimum Temperatures		Maximum Temperatures	
	Trend	Confidence	Trend	Confidence
January	<i>Increasing</i>	<i>75.09%</i>	Stable	71.36%
February	Stable	0%	Stable	68.54%
March	<i>Increasing</i>	<i>92.58%</i>	<i>Increasing</i>	<i>90.55%</i>
April	Stable	18.82%	<i>Increasing</i>	<i>96.99%</i>
May	Stable	18.82%	<i>Increasing</i>	<i>91.76%</i>
June	Stable	47.33%	Stable	67.26%
July	Stable	50.81%	Stable	58.61%
August	<i>Increasing</i>	<i>89.43%</i>	<i>Increasing</i>	<i>77.04%</i>
September	Stable	43.01%	Stable	40.78%
October	Stable	72.08%	Stable	62.23%
November	Stable	73.96%	<i>Increasing</i>	<i>84.69%</i>
December	Stable	58.61%	Stable	61.04%
Spring	Stable	52.81%	<i>Increasing</i>	<i>98.16%</i>
Summer	<i>Increasing</i>	<i>79.29%</i>	<i>Increasing</i>	<i>88.65%</i>
Fall	<i>Increasing</i>	<i>91.37%</i>	<i>Increasing</i>	<i>87.60%</i>
Winter	Stable	14.92%	Stable	42%
Annual	<i>Increasing</i>	<i>78.80%</i>	<i>Increasing</i>	<i>97.69%</i>

BOLD, ITALICS, & SHADING = significant increasing trend
BOLD, UNDERLINE, & SHADING = significant decreasing trend

5.4.2 Temperatures for Sterling City, TX

Temperature data for Sterling City, TX (Figure 5-20) were available from 1964 to 2019. Within Figure 5-20, data shown in BLACK reflect periods when data was unavailable (assigned the value “-9999”), and include most of 1985-1986. RED data in Figure 5-20 indicate days during which the recorded high temperature exceeded 100 °F, BLUE data indicate days during which the recorded low temperature was below 32 °F. Visual inspection of the data suggests that the number of 100 °F days has remained stable over the period of record, while the number of freezing days has either remained steady or decreased slightly.

Figure 5-21 presents a statistical analysis of the Sterling City temperature data, including Mann-Kendall analysis results. Within Figure 5-21A, the number of 100 °F per calendar year is presented over time, with values ranging from 0 to over 50 days (in 2011). Per the Mann-Kendall analysis, there is a stable in the data, indicating Sterling City high temperature days have not changed in frequency over the course of the period of record. In contrast, Figure 5-21B indicates a significant decreasing trend in the number of days (per year) with temperatures above 90° F. The trend suggests a general cooling of the area toward the end of the period of record.

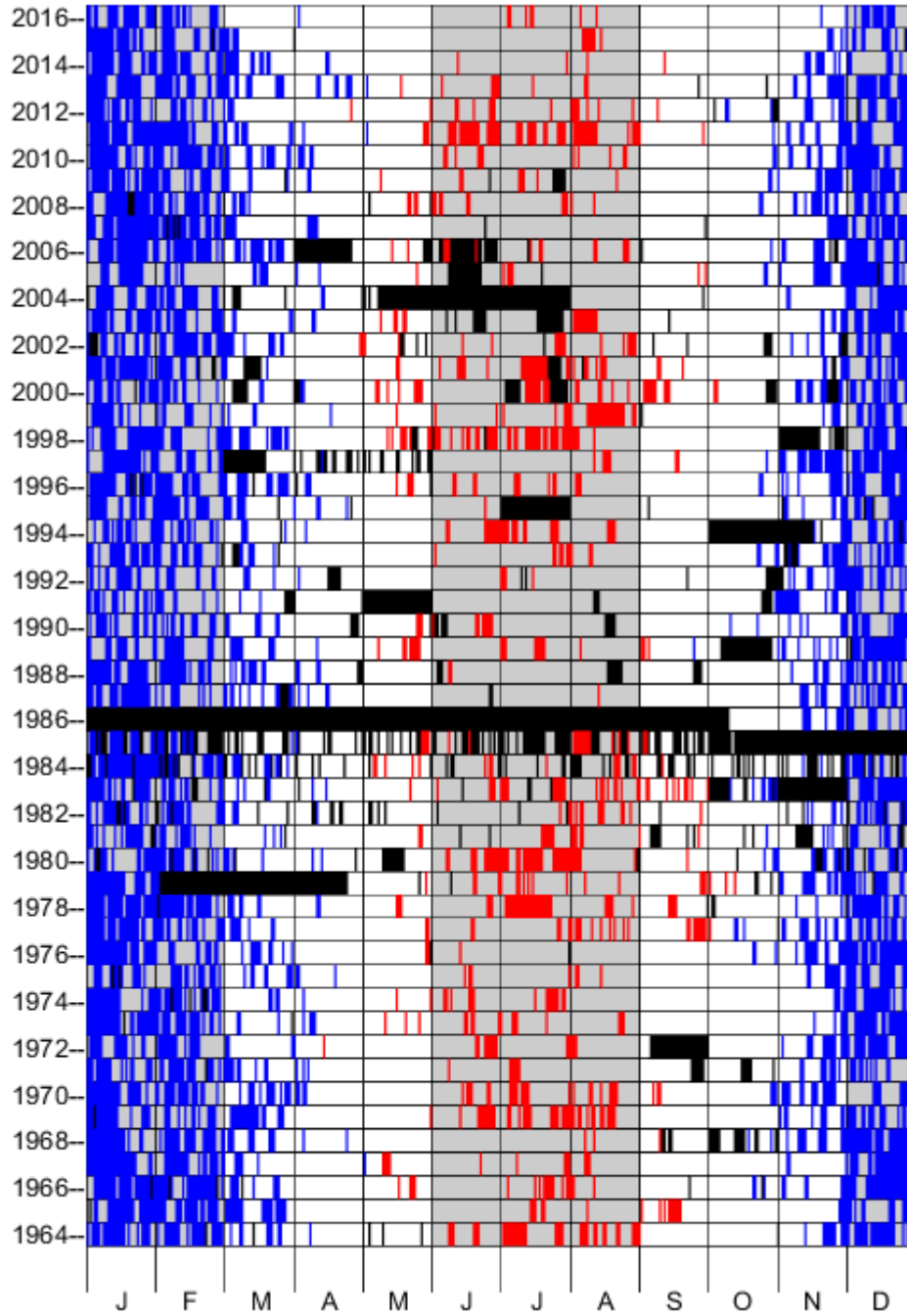


Figure 5-20-- Temperature data For Sterling City for the period 1964-2016 – BLUE showing when minimum temperatures dropped below 32° F, RED showing when maximum temperatures exceeded 100°F. BLACK indicates no valid data was recorded.

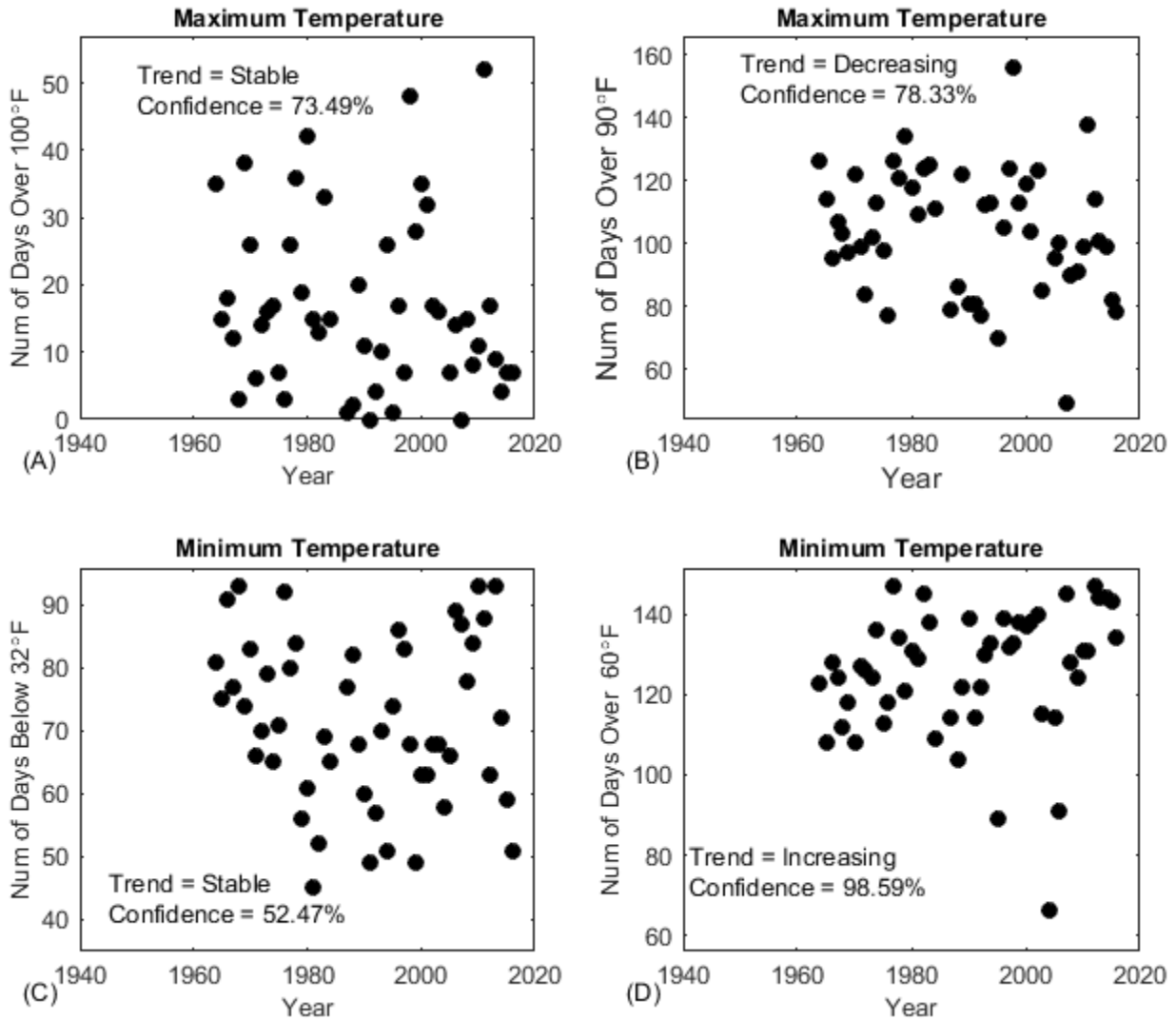


Figure 5-21 - Temperature trends for Sterling City for the period 1964-2016 – A) Days exceeding 100°F, B) Days exceeding 90°F, C) Days with minimum temperatures below 32°F, D) Days with minimum temperatures exceeding 60°F.

A stable trend was apparent within the data describing the number of days per year Sterling City experienced temperatures below 32 °F (Figure 5-21C). As shown, the number of freezing days ranged between approximately 40 and 90 per year, with values at the extremes of this range observed throughout the period of record. In contrast, when considering the number of days on which minimum temperatures exceed 60°F (Figure 5-21D), the data indicates an increasing trend, yet with much variation in data from year to year. This suggests that cooler days are occurring less often while freezing days occur with the same frequency as throughout the period of record.

Average annual minimum temperatures (Figure 5-22A) show both an increasing trend and an increase in the variation of data points from year to year. This suggests that minimum temperatures will be increasing, yet that it is not unlikely to have year-to-year variations that may mask the increase.

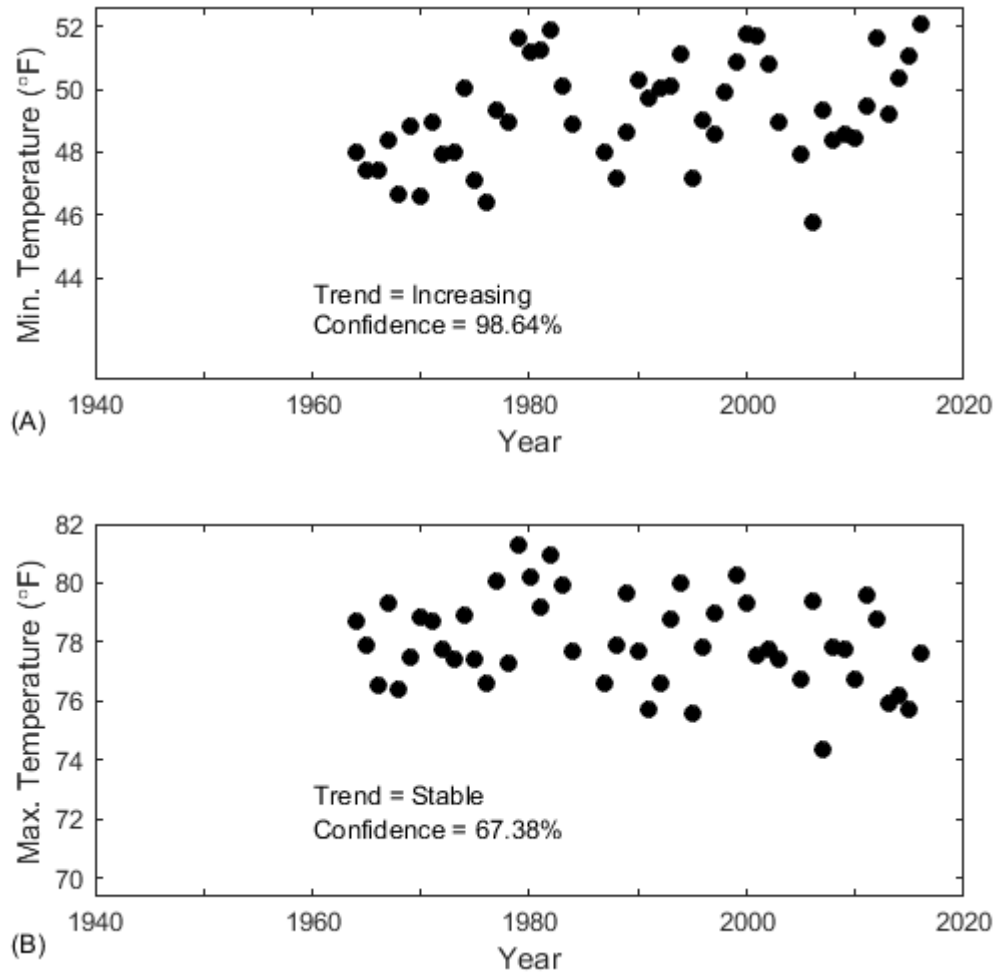


Figure 5-22- Annual Average Temperatures for Sterling City for the period 1964-2016 – A) Average minimum daily temperature, B) Average maximum daily temperature

Average annual maximum temperatures (Figure 5-22B) indicate a stable trend, yet with a seemingly constant variation in year-to-year annual maximum temperatures throughout the period of record.

Table 5-13 presents monthly, seasonal, and annual temperature trends computed Sterling City, TX. Periods showing statistically significant Mann-Kendall trends are shown with grey shading. Negative trends are indicated in **bold underline**, and positive trends are indicated with ***bold italics***. As shown, average minimum temperatures show significant increasing trends for most months, all seasons except spring, and for the annual period. Analysis of the maximum temperature data indicate decreasing trends for the months of July and December, but otherwise indicate stability for all other time periods. These trends in contrast to those observed for San Angelo (Table 5-9), and are similar to those computed for Big Spring (Table 5-12). Additional temperature data from within the Upper North Concho watershed would be beneficial in determining how temperatures might be changing in that region in between Sterling City and Big Spring.

Table 5-13 – Temperature trend statistics for Sterling City, TX

Period	Minimum Temperatures		Maximum Temperatures	
	Trend	Confidence	Trend	Confidence
January	Stable	73.41%	Stable	29.51%
February	<i>Increasing</i>	<i>89.39%</i>	Stable	65.38%
March	Stable	63.81%	Stable	55.84%
April	Stable	44.74%	Stable	36.05%
May	<i>Increasing</i>	<i>96.03%</i>	Stable	21.10%
June	<i>Increasing</i>	<i>98.84%</i>	Stable	57.32%
July	<i>Increasing</i>	<i>97.09%</i>	<u>Decreasing</u>	<u>92.52%</u>
August	<i>Increasing</i>	<i>99.66%</i>	Stable	2%
September	Stable	36.65%	Stable	9.98%
October	<i>Increasing</i>	<i>99.11%</i>	Stable	2.66%
November	Stable	37.83%	Stable	52.29%
December	Stable	7.33%	<u>Decreasing</u>	<u>95.87%</u>
Spring	Stable	66.99%	Stable	44.80%
Summer	<i>Increasing</i>	<i>99.93%</i>	Stable	57.72%
Fall	<i>Increasing</i>	<i>98.52%</i>	Stable	23.71%
Winter	<i>Increasing</i>	<i>82.98%</i>	Stable	52.80%
Annual	<i>Increasing</i>	<i>98.64%</i>	Stable	67.38%

BOLD, ITALICS, & SHADING = significant increasing trend
BOLD, UNDERLINE, & SHADING = significant decreasing trend

5.4.3 Trend Comparisons within the North Concho Watershed

Table 5-14 and Table 5-15, respectively, present a comparison of Mann-Kendall trends for minimum and maximum temperature datasets for Big Spring, Sterling City, and San Angelo. As presented in the table, trends are listed from the northwest to the southeast of the watershed. Trends were assessed for the time period from 1964-2016 as this is the period of record common to all datasets in the analysis. By limiting each dataset to the same time periods, comparison between the resulting trends can indicate variations resulting from the data and not from the differing periods of record used in the analysis. For clarity purposes, within Table 5-7 increasing trends are indicated with an up-arrow (“↑”), decreasing trends with a down-arrow (“↓”) and stable trends with a series of dashes (“—”).

As shown in Table 5-14, minimum temperatures are increasing watershed-wide for February, June, and August as well as for the summer and annual periods. Trends for Sterling City follow a similar pattern to those of Big Spring, and are more likely to be increasing than are the trends indicated by the San Angelo data. This suggests a trend gradient across the watershed, with temperatures more often increasing in the upper reaches of the watershed than in the lower reaches of the watershed.

Data from Table 5-15 indicate that maximum temperatures show similar increasing trends at the ends of the watershed (Big Spring and San Angelo), but show either stable or decreasing trends for Sterling City.

Table 5-14 – Minimum temperature trend statistics for the North Concho watershed, 1964-2016

Period	Big Spring		Sterling City		San Angelo	
	Trend	%	Trend	%	Trend	%
January	↑	96.38%	---	73.41%	---	69.60%
February	↑	92.42%	↑	89.39%	↑	91.56%
March	↑	94.77%	---	63.81%	↑	81.29%
April	---	49.97%	---	44.74%	---	46.05%
May	↑	81.18%	↑	96.03%	---	73.72%
June	↑	98.51%	↑	98.84%	↑	90.86%
July	↑	86.70%	↑	97.09%	---	44.60%
August	↑	99.96%	↑	99.66%	↑	99.28%
September	↑	90.24%	---	36.65%	---	37.11%
October	↑	99.88%	↑	99.11%	---	70.31%
November	---	12.90%	---	37.83%	---	2.44%
December	---	32.72%	---	7.33%	---	31.26%
Spring	↑	94.35%	---	66.99%	↑	77.87%
Summer	↑	99.83%	↑	99.93%	↑	93.51%
Fall	↑	98.54%	↑	98.52%	---	53.38%
Winter	↑	92.38%	↑	82.98%	---	47.72%
Annual	↑	99.65%	↑	98.64%	↑	95.47%

BOLD, ITALICS, & SHADING = significant increasing trend
BOLD, UNDERLINE, & SHADING = significant decreasing trend

Table 5-15 – Maximum temperature trend statistics for the North Concho watershed, 1964-2016

Period	Big Spring		Sterling City		San Angelo	
	Trend	%	Trend	%	Trend	%
January	↑	75.78%	---	29.51%	↑	87.31%
February	↑	93.04%	---	65.38%	↑	88.59%
March	↑	89.22%	---	55.84%	↑	81.80%
April	↑	95.15%	---	36.05%	---	72.06%
May	↑	98.61%	---	21.10%	↑	92.49%
June	↑	98.97%	---	57.32%	---	44.52%
July	---	74.11%	↓	92.52%	---	39.20%
August	↑	99.78%	---	2%	↑	98.46%
September	↑	99.22%	---	9.98%	↑	99.13%
October	↑	90.88%	---	2.66%	↑	98.22%
November	---	57.86%	---	52.29%	---	61.81%
December	---	33.31%	↓	95.87%	---	27.15%
Spring	↑	99.50%	---	44.80%	↑	96.99%
Summer	↑	99.98%	---	57.72%	↑	97.11%
Fall	↑	98.84%	---	23.71%	↑	98.61%
Winter	↑	79.64%	---	52.80%	↑	91.60%
Annual	↑	99.96%	---	67.38%	↑	99.75%

BOLD, ITALICS, & SHADING = significant increasing trend
BOLD, UNDERLINE, & SHADING = significant decreasing trend

5.5 Temperature Analysis - Summary

With the application of the Mann-Kendall analytical technique, we've identified patterns and trends in temperature values for locations throughout the four study-area watersheds. Each watershed had a minimum of two temperature stations located within or near to its boundaries, and the spatial relationship between stations aids in assessing variations in temperature trends.

For the Elm Creek watershed, maximum daily temperatures are generally stable near Ballinger, at the watershed outlet. Maximum temperature decreases are occurring in July and the summer season. Minimum daily temperatures are, on average, increasing for all months but April and December. These trends are in contrast to trends observed for Abilene, TX which is outside of the Elm Creek watershed yet may still be indicative of temperature trends in the upper reaches of the Elm Creek watershed. For Abilene, maximum temperatures are increasing for January and March, yet are stable for all other periods. Minimum temperatures for Abilene are increasing for January, March, and the spring season, but are otherwise stable.

For the San Saba watershed, data recorded at Brady, TX showed increasing trends in minimum daily temperatures, for all months, seasons, and on an annual basis with the exceptions of February and April (which showed stable trends). Analyses of the maximum temperatures recorded at Brady, however, suggested increasing trends in May and October as well as during the spring and annual periods. Similar results were obtained from Eldorado, located to the west of the upper reaches of the San Saba watershed. At Eldorado, minimum temperatures were found to be statistically increasing for all periods except April. Maximum temperatures were found to be increasing for August, September and October, as well as for the fall season. Based on the calculated trends from these two locations, it is likely that minimum daily temperatures are increasing across the entire San Saba watershed, with maximum daily temperatures increasing for some months to a greater degree toward the western edge (upper reaches) of the watershed.

Within the South Concho watershed, daily minimum temperatures recorded at San Angelo (on the downstream edge of the watershed) showed decreasing trends for the months of October and December, with stable trends for all other periods. Increases in maximum daily temperatures were computed for January, March, April, and May as well as for the spring, fall, and annual periods. San Angelo was the only location for which trends suggested minimum temperatures were decreasing while maximum temperatures were increasing. At Eldorado, located near the upper reaches of the South Concho watershed, minimum temperatures were found to be statistically increasing for all periods except April. Maximum temperatures (at Eldorado) were found to be increasing for August, September and October, as well as for the fall season. Therefore within the South Concho watershed, there appears spatial gradient of temperature changes, with the upper reaches of the watershed becoming hotter and the lower basin experiencing lower minimum temperatures and higher maximum temperatures.

Within the North Concho watershed, trends in temperature changes are generally more uniform across the entire watershed. Data from Big Spring, Sterling City, and San Angelo

each indicate increasing minimum temperature trends for February, June, and August as well as for the summer and annual periods. The computed trends in minimum temperatures show stability for more time periods when comparing downstream locations within the watershed to upstream locations. This suggests more moderate temperature changes may be occurring near San Angelo, with greater changes occurring toward the upper reaches of the watershed. Trends in maximum temperatures are nearly identical for Big Spring and San Angelo, with nearly all periods indicating increasing trends. In contrast, data from Sterling City suggests maximum temperatures are stable for all periods other than July and December (when temperatures are decreasing).

It is notable that trends resulting from many datasets analyzed in this portion of the Phase II report often change values depending upon the period of time for which the Mann-Kendall analysis is applied. For example, for assessing common trends within the North Concho watershed, data for San Angelo was limited to the period of 1964-2016. Yet when assessing trends for the South Concho watershed, data from San Angelo for the period from 1966 to 1940 were used. Trends from these analyses were similar and consistent. Yet when assessing trends only from the San Angelo dataset (using the full period of record 1940-2016), most periods were found to be stable, with fewer showing increasing trends. LRE prefers to perform trend analyses on datasets containing larger amounts of valid data. Thus if additional temperature data for the study area watersheds becomes available, it would be beneficial to repeat this trend analysis using the extended datasets.

6 .Task 4 – Streamflow Trend Analysis

Under this task, streamflow records were to be analyzed using the Mann-Kendall technique. The objective of the analyses is to identify trends and determine “change points,” or points in time when significant streamflow changes occurred, if any such change points become evident.

Streamflow data used in this analysis was compiled during Phase I of this study effort. Data was provided as daily-averaged flow rates (in cubic feet per second or “cfs” units) for each day from 1940 through 2016. Methods of data compilation are documented within the Phase I report. Figure 6-1 shows the locations of the six flow measurement locations within the study area watersheds.

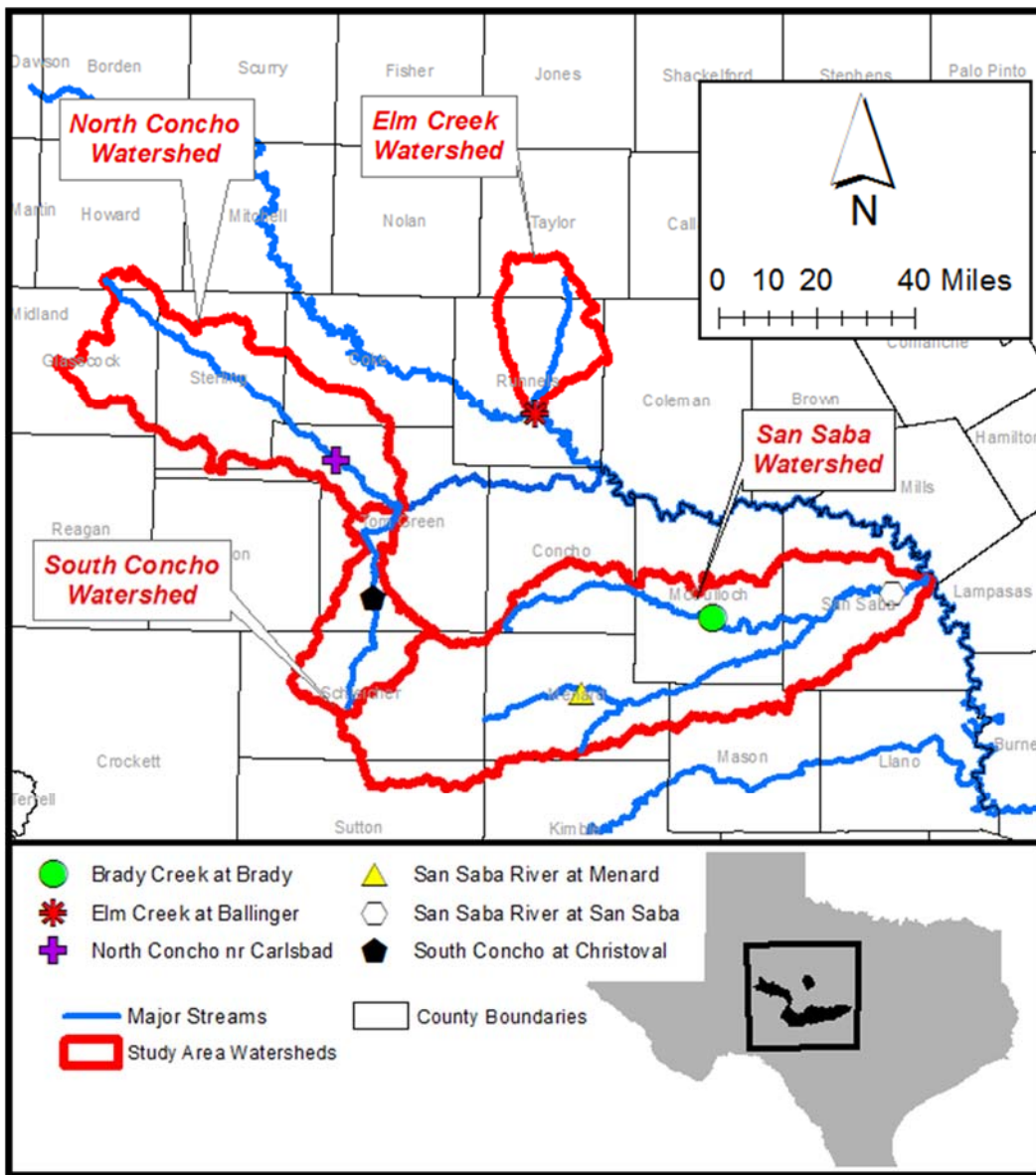


Figure 6-1 – Map of streamflow measurement and analysis locations

6.1 Elm Creek Watershed

Within the Elm Creek watershed, Elm Creek flows southward to the confluence with the Colorado River near the City of Ballinger. Streamflow data has been compiled for Elm Creek at Ballinger. The USGS maintains a stream gauge at this location, with the designation “USGS 08127000 Elm Ck at Ballinger, TX.” Data from this gauge is available for download from the USGS National Water Information System (NWIS), with the gauge period of record listed as between 1932-04-01 and 2019-07-06 (written in YYYY-MM-DD format). For this analysis, streamflow data was limited to the period of 1940-01-01 to 2016-12-31. Data used in this analysis was not directly downloaded from the NWIS system, but rather was obtained (unmodified) from the results of the Phase I analysis for this project.

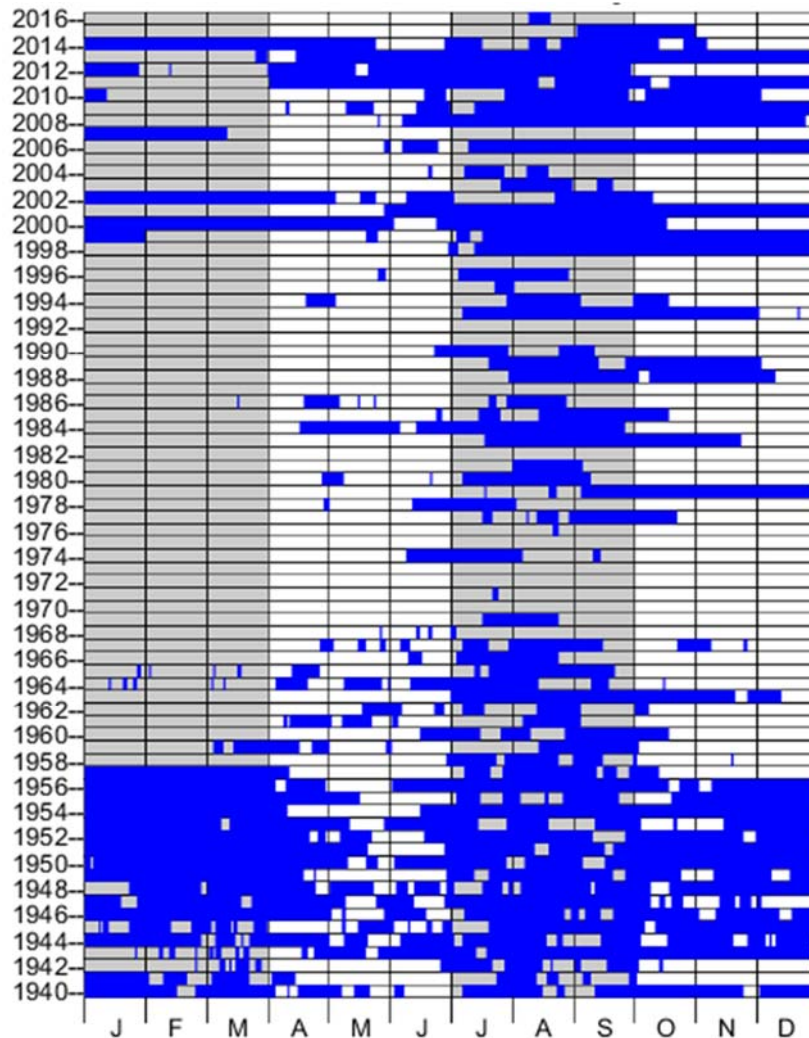


Figure 6-2 – Calendar plot of “zero streamflow” days (BLUE) recorded for Elm Creek at Ballinger, for the period 1940-2016.

Figure 6-2 provides a calendar plot showing when Elm Creek was dry (i.e. had reported streamflows of “0 cfs”). As shown, the creek was frequently dry, especially in July, August, and September. During the 1947-1957 drought period, the river was dry for the majority of

each year. Similar dry extents occurred during the more recent drought from 2008-2016. This periodic dryness indicates that the creek does not always receive an influx of water from the surrounding alluvium, and that flows in Elm Creek are driven by the extent to which local rainfall provides surface runoff and recharges the alluvial aquifer.

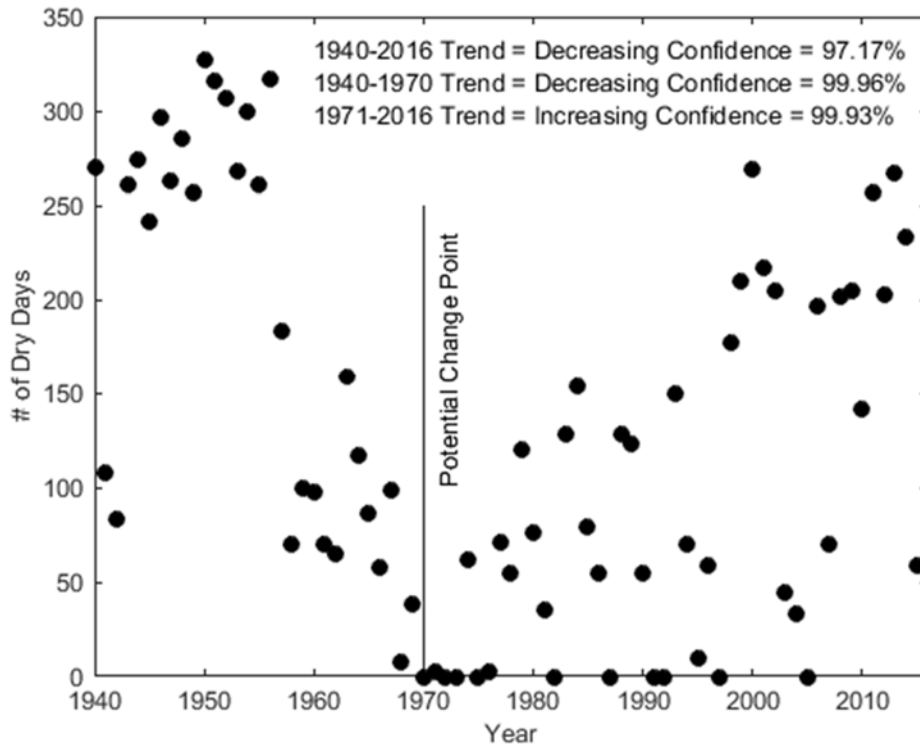


Figure 6-3 – Number of dry (zero streamflow) days per year – Elm Creek at Ballinger.

The Mann-Kendall analysis, applied to the number of dry days per year (Figure 6-3) indicates a decreasing trend for the 1940-2016 period of record, such that fewer dry days are occurring in recent years. This assertion, however, is misleading given that recent years (1975-Present) indicate an increasing trend with large year-to-year variability. Around the year 1970, there is a potential “change point” in the data, indicating a shift from a decreasing to an increasing trend in the number of dry (zero streamflow) days per year.

Similar variability is observed in the Annual Flow dataset for Elm Creek (Figure 6-4). The Mann-Kendall analysis indicates a significant decreasing trend, yet the year-to-year variability in annual flows tends to visually mask the decreasing data trend. As shown in Figure 6-4, Lake Winters was officially impounded in 1983, and annual flow totals before and after this time do not indicate that the reservoir impacted the watershed streamflow.

Streamflow typically consists of a combination of runoff from rainfall events and groundwater entering the river channel as baseflow. Section 9.3.1 contains a discussion of the baseflow component of streamflow within Elm Creek, as well as provides statistics regarding trends in baseflow quantities.

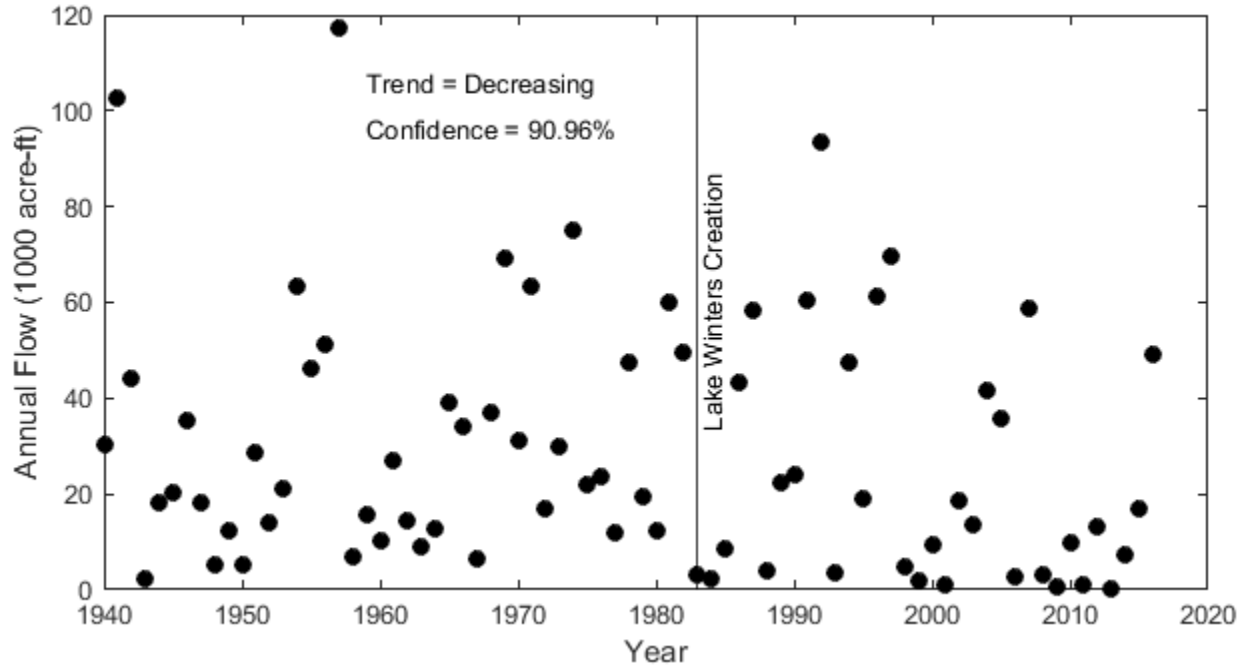


Figure 6-4– Annual flows by year for the period 1940-2016 – Elm Creek at Ballinger.

6.2 San Saba Watershed

As shown in Figure 6-1, three (3) streamflow measurement sites exist within the San Saba watershed. Results from each of these sites will be presented separately, followed by a comparison of results between the three locations. Section 9.3.2 contains a discussion of the baseflow component of streamflow within the San Saba watershed, as well as provides statistics regarding trends in baseflow quantities.

6.2.1 San Saba River at Menard

Within the San Saba watershed, the San Saba River flows eastward toward its confluence with the Colorado River downstream of San Saba, TX. Streamflow data has been compiled for the San Saba River at Menard, which is located within the middle of the watershed. The USGS maintains a stream gauge at this location, with the designation “USGS 08144500 San Saba Rv at Menard, TX.” Data from this gauge is available for download from the USGS National Water Information System (NWIS), with the gauge period of record listed as between 1915-10-01 and 2019-07-06 (written in YYYY-MM-DD format). For this analysis, streamflow data was limited to the period of 1940-01-01 to 2016-12-31. Data is not available from 1993-10-1 to 1997-09-30. Data used in this analysis was not directly downloaded from the NWIS system, but rather was obtained (unmodified) from the results of the Phase I analysis for this project.

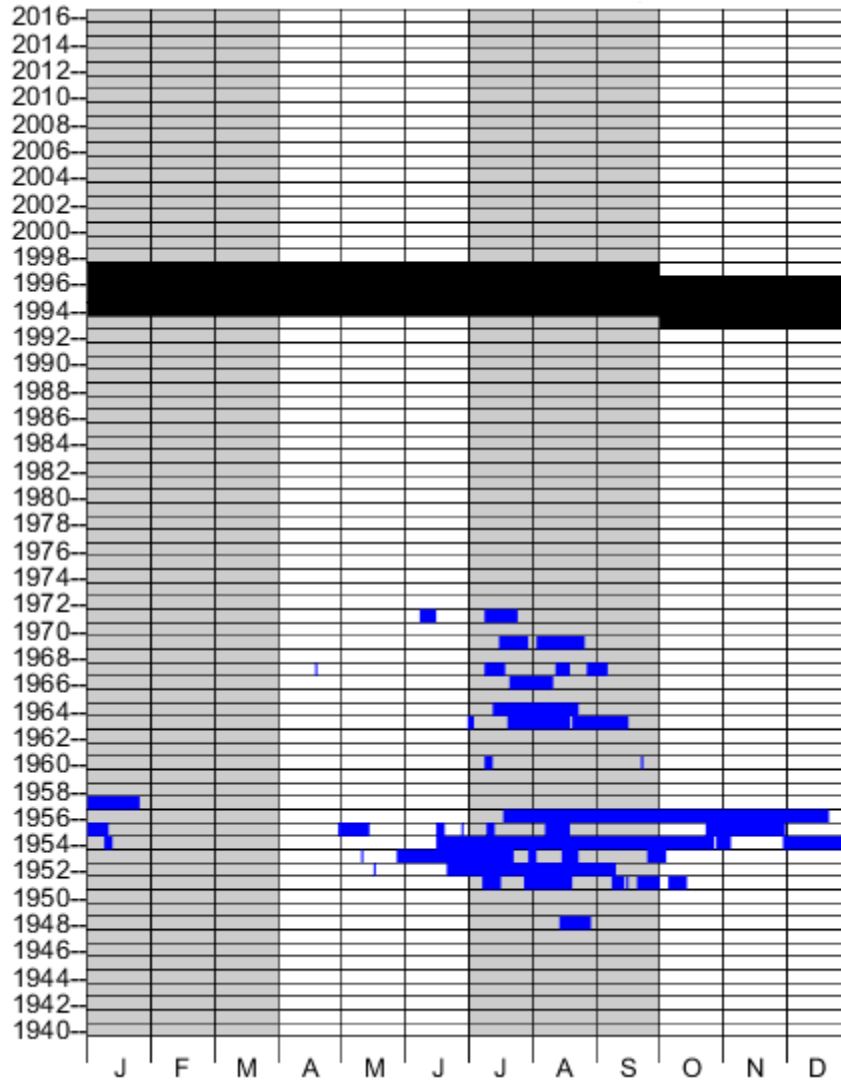


Figure 6-5– Calendar plot of “zero streamflow” days (BLUE) recorded for the San Saba River at Menard, for the period 1940-2016.

Figure 6-5 provides a calendar plot showing when the San Saba River at Menard was dry (i.e. had reported streamflows of “0 cfs”). As shown, the river was dry only during the 1950’s drought period and for periodic summer months between 1960 and 1972. After 1972, the San Saba River at Menard has never been dry, suggesting it likely receives some quantity of baseflow as discharges from a local alluvial aquifer.

Figure 6-6 depicts the annual flow by year for the San Saba River at Menard. Mann Kendall analysis results do not indicate a significant trend in the data. However there does appear to be a periodicity within the data, specifically with periods of 4-5 years of higher flow followed by longer periods of lower flow. This pattern repeats four times over the period of record. It is also interesting to note that periods of high flow occur approximately every 15 years from 1957 through 1992. The pattern is broken in 2005-2007 (which did not contain a high-flow year). The cause for these observed periodicities is unknown.

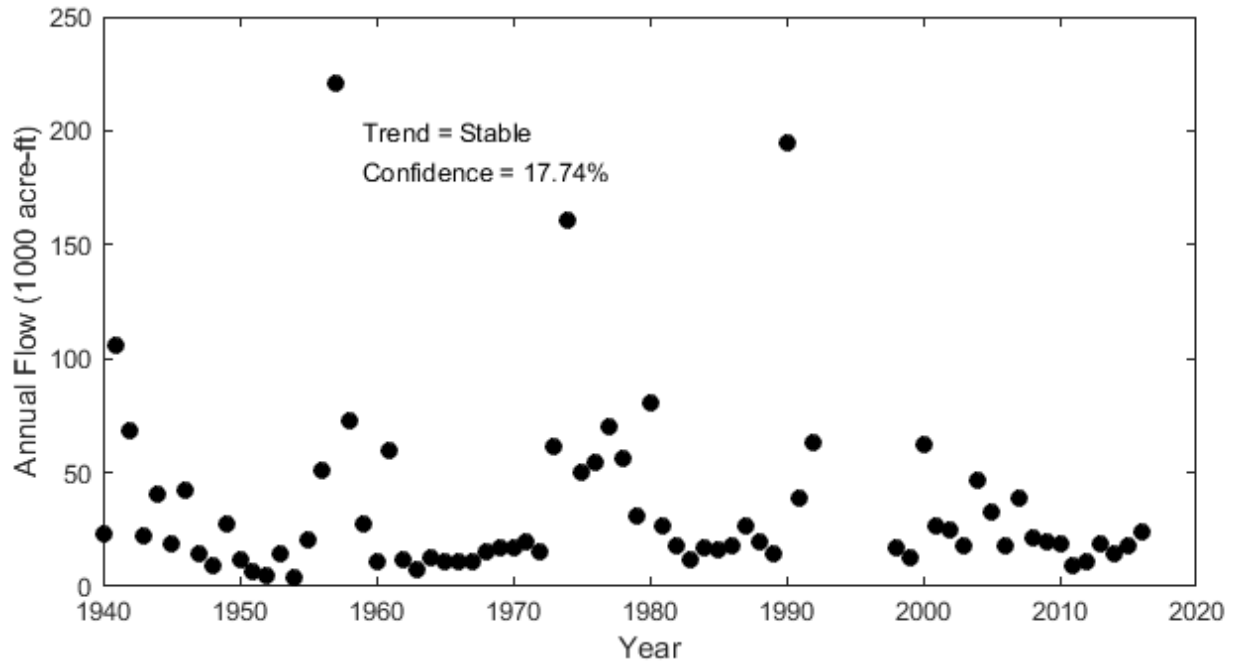


Figure 6-6 – Annual flows by year for the period from 1940 to 2016 – San Saba River at Menard.

6.2.2 *Brady Creek at Brady*

Within the San Saba watershed, Brady Creek flows eastward toward its confluence with the San Saba River upstream of San Saba, TX. Streamflow data has been compiled for Brady Creek at Brady, which is located in the north-eastern portion of the watershed. The USGS maintains a stream gauge at this location, with the designation “USGS 08145000 Brady Ck at Brady, TX.” Data from this gauge is available for download from the USGS National Water Information System (NWIS), with the gauge period of record listed as between 1939-06-01 and 2019-07-06 (written in YYYY-MM-DD format). For this analysis, streamflow data was limited to the period of 1940-01-01 to 2016-12-31. Data is unavailable for the period from 1986-10-01 to 2001-05-01. Data used in this analysis was not directly downloaded from the NWIS system, but rather was obtained (unmodified) from the results of the Phase I analysis for this project.

Figure 6-7 provides a calendar plot showing when Brady Creek at Brady was dry (i.e. had reported streamflows of “0 cfs”). As shown, the river was often dry throughout the period of record, with no patterns discernible within the dates of the dryness. Given the frequency within which the creek is dry, it is unlikely that the creek receives significant and constant baseflow from the local alluvium. Brady Creek likely thrives after local runoff-creating rain events, or after such events recharge the contributing local aquifer.

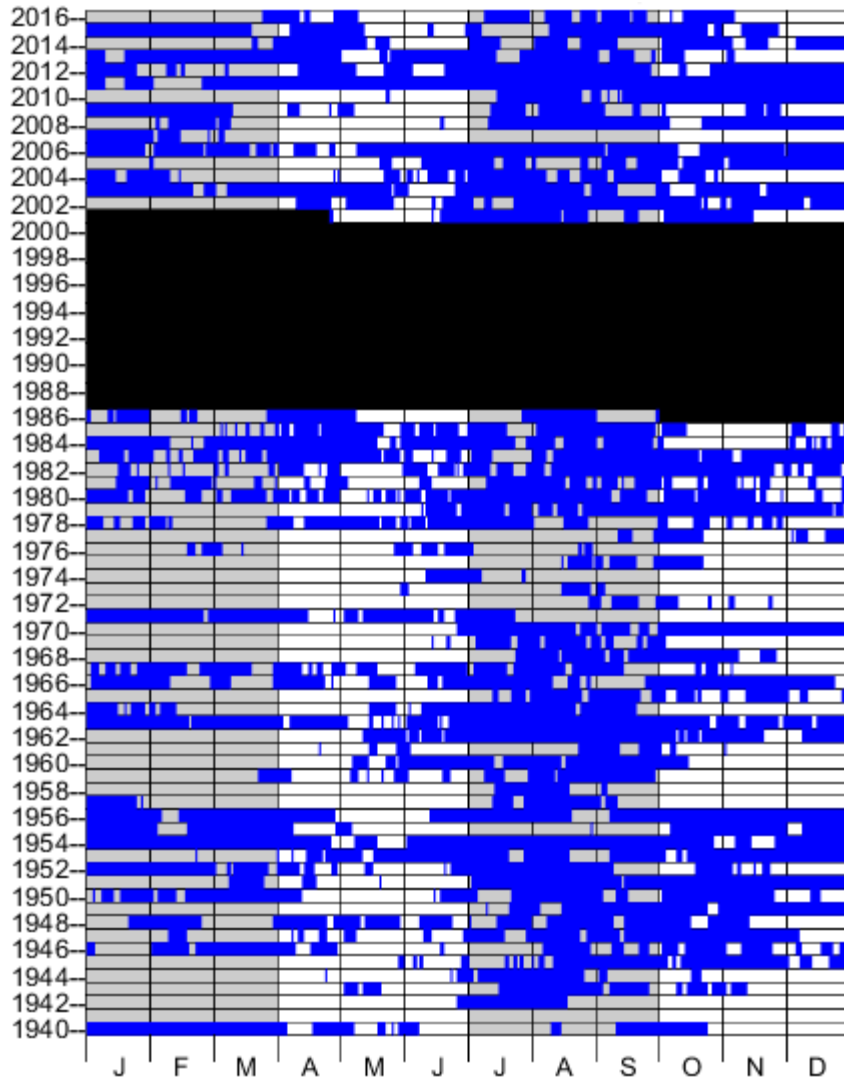


Figure 6-7 – Calendar plot of dry (zero streamflow) days recorded Brady Creek at Brady, TX..

Figure 6-8 presents the number of dry days per year recorded for Brady Creek at Brady. As shown, results are highly variable from year to year, and the Mann-Kendall analysis indicates an increasing trend.

Figure 6-9 presents the annual flow by year for Brady Creek at Brady. Mann-Kendall analysis indicates a decreasing trend, with flows seeming to decrease significantly after 1980 (although missing data makes this claim contentious). Flows also decreased after the 1963 impoundment of Brady Creek Reservoir. It is notable that the annual flows exhibit a periodicity similar to that observed for the San Saba River at Menard, including the pattern of high flows at roughly 15-year intervals.

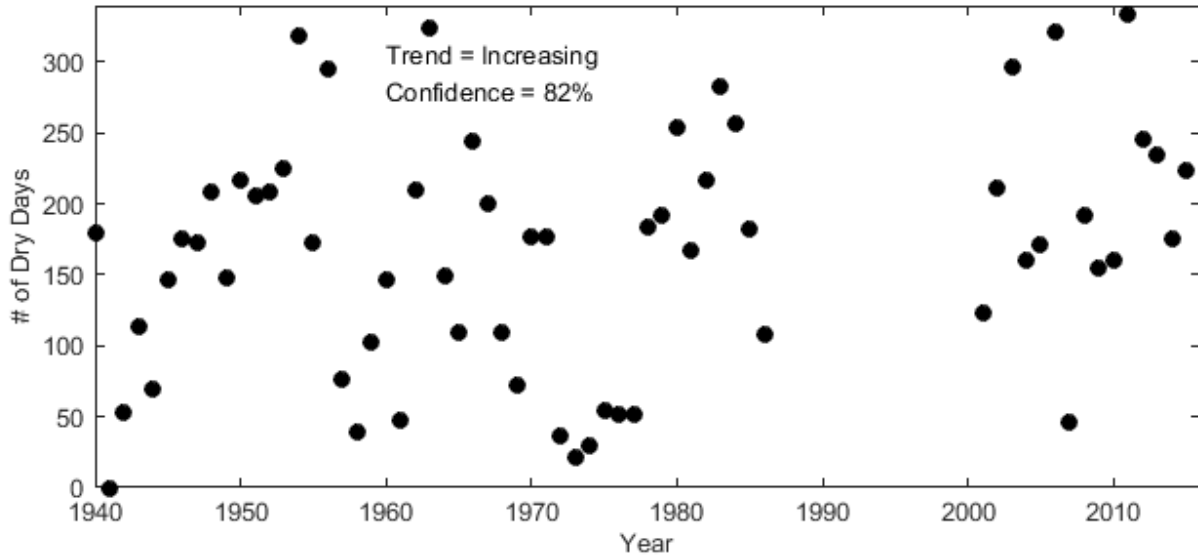


Figure 6-8 -- Number of dry (zero streamflow) days per year for the period 1940-2016 – Brady Creek at Brady

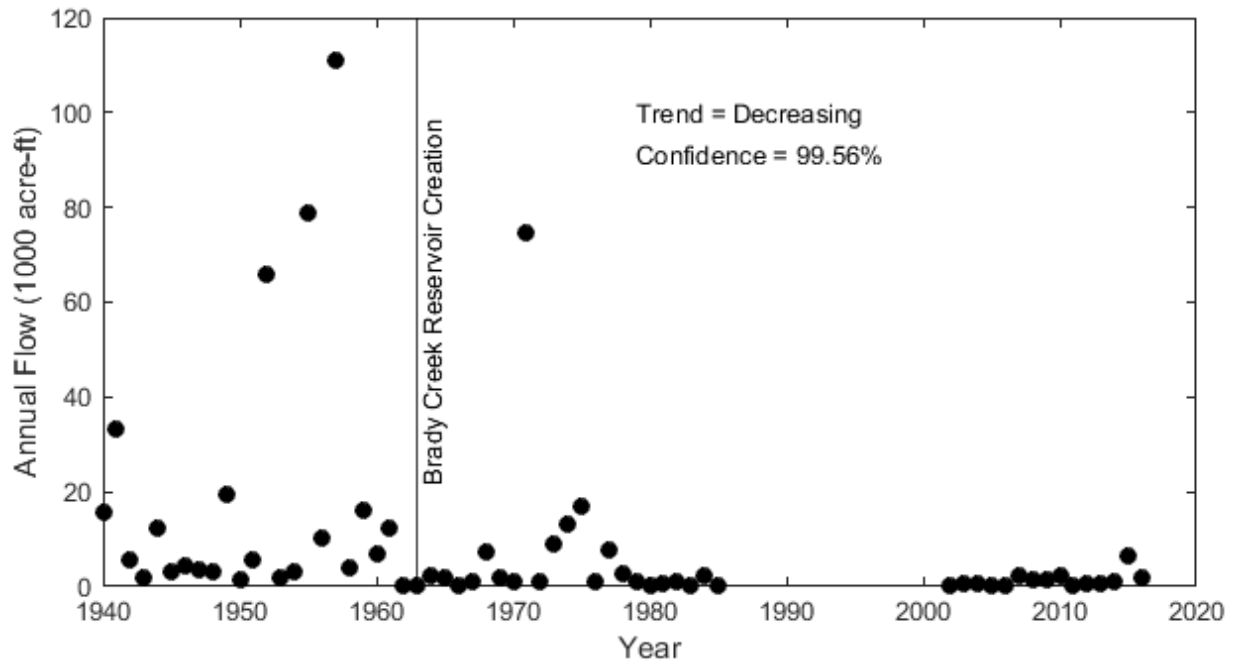


Figure 6-9 – Annual flows by year for the period 1940-2016 – Brady Creek at Brady

6.2.3 San Saba River at San Saba

Within the San Saba watershed, the San Saba River flows eastward toward its confluence with the Colorado River downstream of San Saba, TX. Streamflow data has been compiled for the San Saba River at San Saba, which is located within the lower section of the watershed downstream from the confluence with Brady Creek yet upstream from the confluence with the Colorado River... The USGS maintains a stream gauge at this location, with the designation "USGS 08146000 San Saba Rv at San Saba, TX." Data from this gauge is available for download from the USGS National Water Information System (NWIS), with the gauge period of record listed as between 1915-10-01 and 2019-07-06 (written in YYYY-MM-DD format). For this analysis, streamflow data was limited to the period of 1940-01-01 to 2016-12-31. Data is not available from 1993-10-1 to 1997-09-30. Data used in this analysis was not directly downloaded from the NWIS system, but rather was obtained (unmodified) from the results of the Phase I analysis for this project.

Figure 6-10 provides a calendar plot showing when the San Saba River at San Saba was dry (i.e. had reported streamflows of "0 cfs"). As shown, the river was dry only during short-duration portions the 1950's drought period, during portions of the summer in 1963-1964, and for a brief period in June 1985. The river has not been dry since June 1985, although it may have been dry during the period for which data is unavailable. Notably, the San Saba River at San Saba was not dry during the recent drought period (2008-2016). This suggests the river receives baseflow from the surrounding alluvial aquifer and that the river is not entirely dependent on rainfall runoff to maintain flows. It is notable that flows at San Saba (Figure 6-10) are dry less often than flows recorded upstream at Menard (Figure 6-5). This reflects San Saba's position downstream in the watershed, where it receives baseflow contributions and runoff from a greater portion of the watershed.

Figure 6-11 depicts the annual flow by year for the San Saba River at San Saba. Mann Kendall analysis indicates a decreasing trend in the data. Data also appears to show less periodicity than observed at Menard (Figure 6-6) or in Brady Creek at Brady (Figure 6-9). The periodicity in high flow years that was previously noted for the upstream gauges is still present at San Saba, with high flow years occurring approximately every 15 years (Figure 6-11). The cause for these observed periodicities is unknown, yet it is assumed based on large rainfall events that periodically provide rainfall and runoff to the watershed. It is also possible that the periodicity is related to the rate at which the groundwater supplies recharge the local alluvial system, resulting in greater runoff when storage within the alluvium is full. During this Phase II project, attempts to discern the cause for the observed periodicity were not undertaken. It is also notable that flows resulting from the periodic high-flow years appear to be decreasing with time; flows in 1957 approached 500,000 acre-ft/yr, whereas flows in 2018 reached only 300,000 acre-ft/yr.

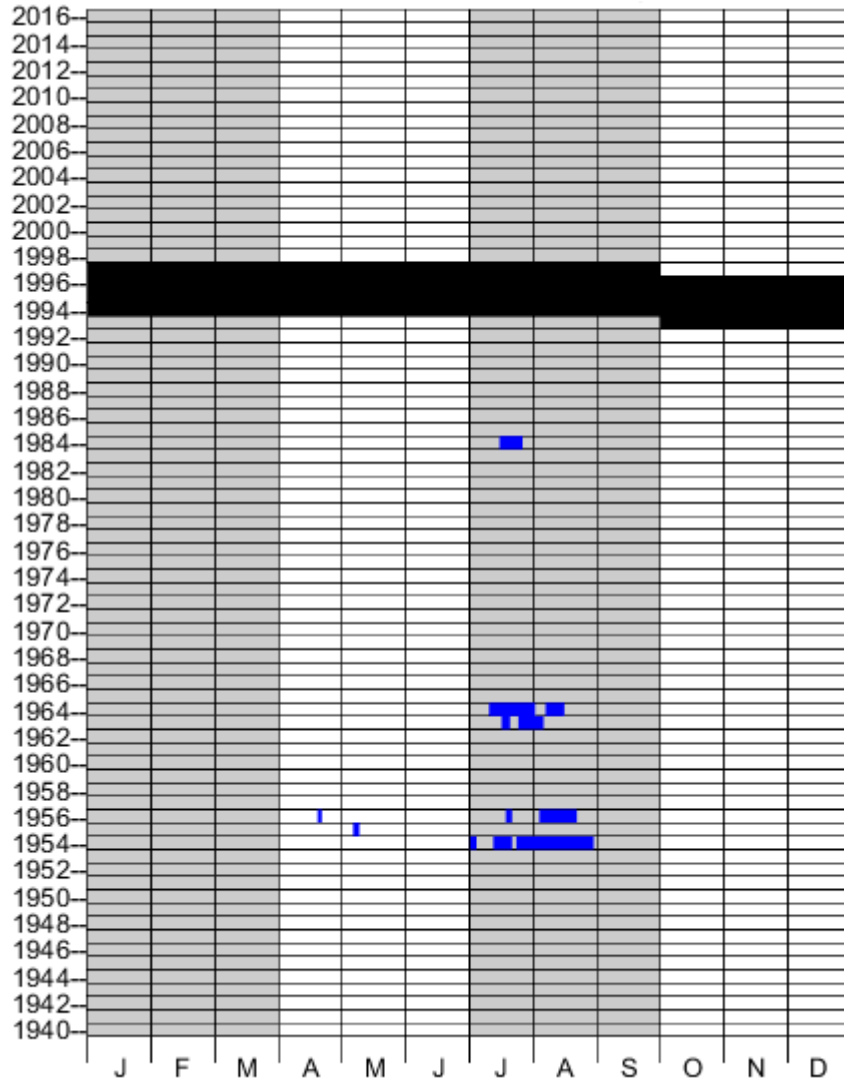


Figure 6-10 – Calendar Plot of dry (zero streamflow) days recorded the San Saba River at San Saba, TX..

Based on the non-high flow years shown in Figure 6-11, the average year produces between 100,000 and 150,000 acre-ft of flow at San Saba. For Brady Creek, the average year produces less than 20,000 acre-ft of flow at Brady (Figure 6-9), and the San Saba River at Menard produces less than 50,000 acre-ft/yr (Figure 6-6). Thus the average gauged flow upstream from San Saba (i.e. Brady PLUS Menard) is less than 70,000 acre-ft/yr, signifying that the San Saba watershed downstream from the Menard and Brady gauges but upstream from the San Saba gauge produces between 30,000 and 80,000 acre-ft of streamflow during an average year. This additional flow from the watershed likely includes both rainfall runoff and additional groundwater input as baseflow.

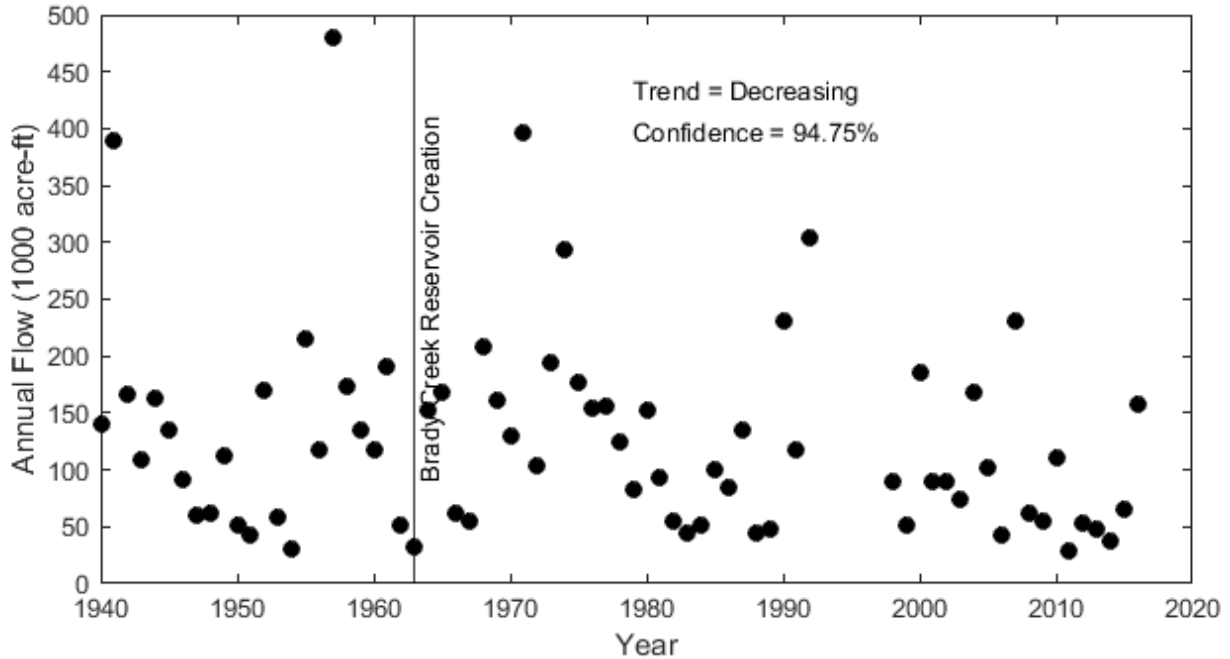


Figure 6-11 – Annual Flows by Year – San Saba River at San Saba.

6.3 South Concho Watershed

Within the South Concho watershed, the South Concho River flows northward into Twin Buttes Reservoir near San Angelo. Streamflow data has been compiled for the South Concho River at Christoval. The USGS maintains a stream gauge at this location, with the designation “USGS 08128000 S Concho Rv at Christoval, TX.” Data from this gauge is available for download from the USGS National Water Information System (NWIS), with the gauge period of record listed as between 1930-03-01 and 2019-07-06 (written in YYYY-MM-DD format). For this analysis, streamflow data was limited to the period of 1940-01-01 to 2016-12-31. Data is not available from 1995-10-1 to 2001-04-30. Data used in this analysis was not directly downloaded from the NWIS system, but rather was obtained (unmodified) from the results of the Phase I analysis for this project.

Data for this location indicate that the South Concho River was never dry during the period of record of this analysis. This suggests that a significant portion of flow within the South Concho River is derived from groundwater entering the river channel; this baseflow remains ever-present, even during long dry periods between rain events that would contribute runoff to the streamflow. Figure 6-12 displays the total annual flow, including the Mann-Kendall results indicating a stable streamflow trend over the period of record. The largest flows occurred in 1957 at the end of the 1947-1957 drought period. Baseflow for this location are analyzed and discussed in Section 9.3.3. It is noted that there is evidence of a 15-year periodicity in the annual flow totals in Figure 6-12, similar to the periodicity in streamflow recorded at streamflow gauges within the San Saba watershed.

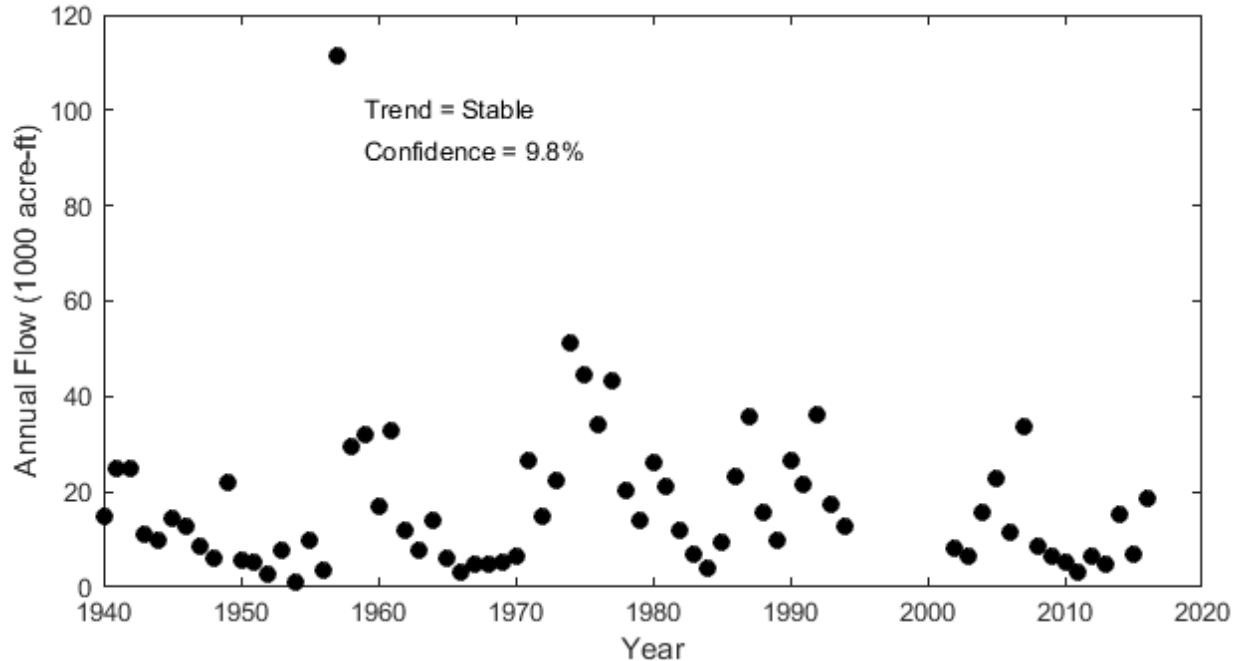


Figure 6-12– Annual flows by year for the period from 1940-2016 – South Concho River at Christoval.

6.4 North Concho Watershed Flow Analysis

Within the North Concho watershed, the North Concho River flows to the south east and into OC Fisher Lake near San Angelo. Streamflow data has been compiled for the North Concho River near Carlsbad, which is located upstream of where the river enters into OC Fisher Lake. The USGS maintains a stream gauge at this location, with the designation “USGS 08314000 N Concho Rv nr Carlsbad, TX.” Data from this gauge is available for download from the USGS National Water Information System (NWIS), with the gauge period of record listed as between 1924-04-01 and 2019-07-06 (written in YYYY-MM-DD format). For this analysis, streamflow data was limited to the period of 1940-01-01 to 2016-12-31. Data used in this analysis was not directly downloaded from the NWIS system, but rather was obtained (unmodified) from the results of the Phase I analysis for this project.

Figure 6-13 provides a calendar plot showing when the North Concho River near Carlsbad was dry (i.e. had reported streamflows of “0 cfs”). As shown, the river is frequently dry, especially in July, August, and September. During 1964-1974, the river was dry for the majority of each year. Similar dry extents occurred during the more recent drought from 2011-2016. It is notable that during the 1947-1957 drought period, the North Concho River was not dry as often as it was during the 1964-1974 period or during the 2011-2016 drought period.

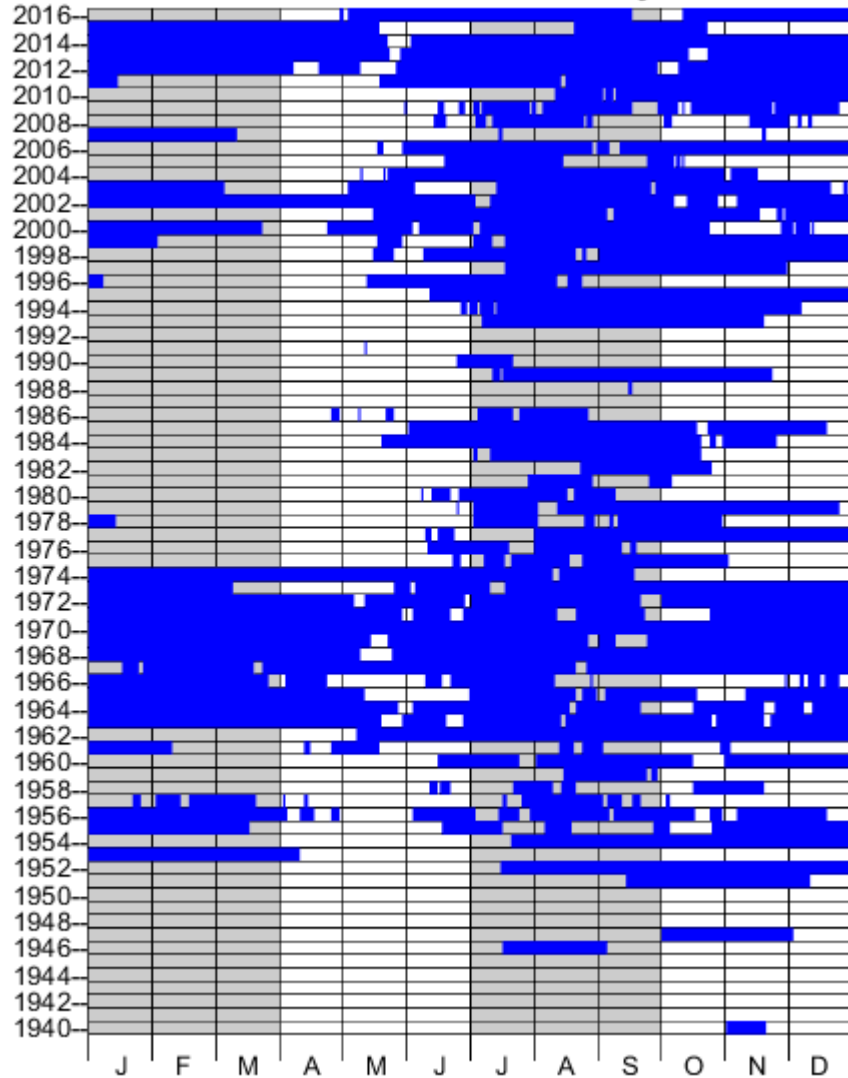


Figure 6-13 – Calendar plot of dry (zero streamflow) days recorded for the North Concho River near Carlsbad.

Figure 6-14 presents the number of days per year on which the North Concho River was dry at the Carlsbad gauge location. Dry days per year range from zero to 365, and the Mann-Kendall analysis results indicate there is a significant increasing trend over the entire period of record. It is notable, however, that there seems to be an abrupt reduction in dry days that occurred in 1974. The cause of this reduction, which could simply be due to increased rainfall, is unknown. After 1974, there appears to have been a general increase in the number of dry days per year, with year-to-year variations.

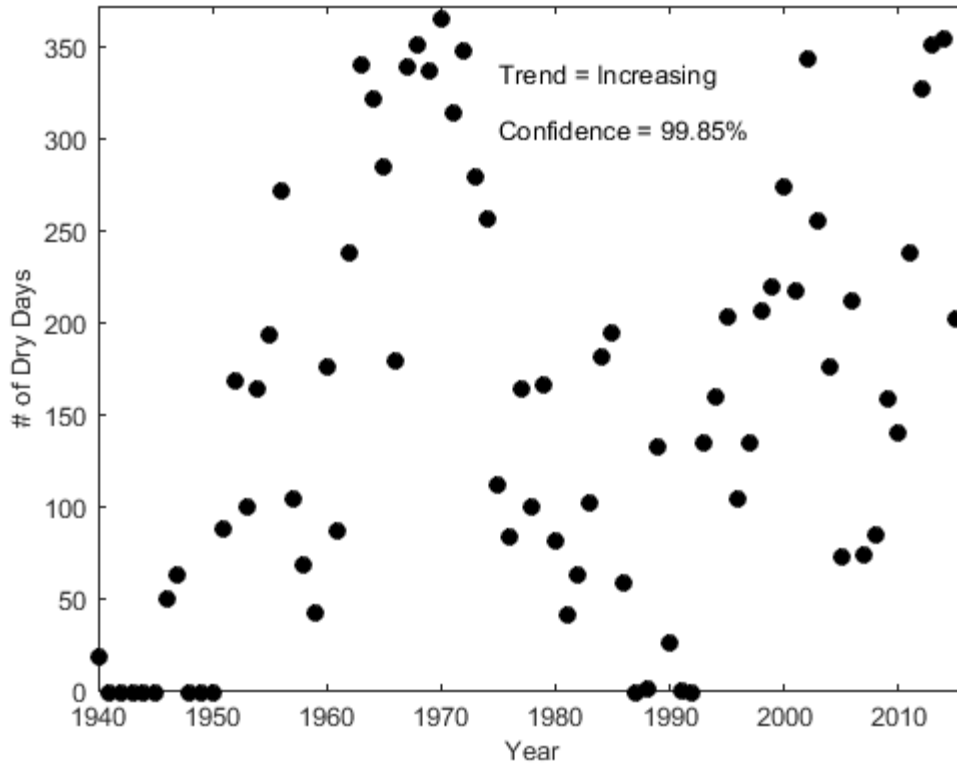


Figure 6-14 – Number of Dry (zero streamflow) Days per year – North Concho River near Carlsbad.

Figure 6-15 presents the total annual streamflow for the 1940-2016 period of record. As indicated, prior to 1964, there exists a wide range of annual flow totals. After 1964, however, the majority of years experienced lower streamflow and lower variation between one year and the next. For the period from 1964 to 2016, there exist 8 years when the total annual flow was noticeably larger than the flows from preceding and following years. These larger flow years appear more as anomalies and likely result from increased rainfall occurring in each year. However the relatively equal temporal spacing between the large flow years is similar to the periodic nature of the flows recorded in the San Saba and South Concho watersheds (although of higher frequency). The Mann-Kendall analysis identified a decreasing trend within the annual flow data.

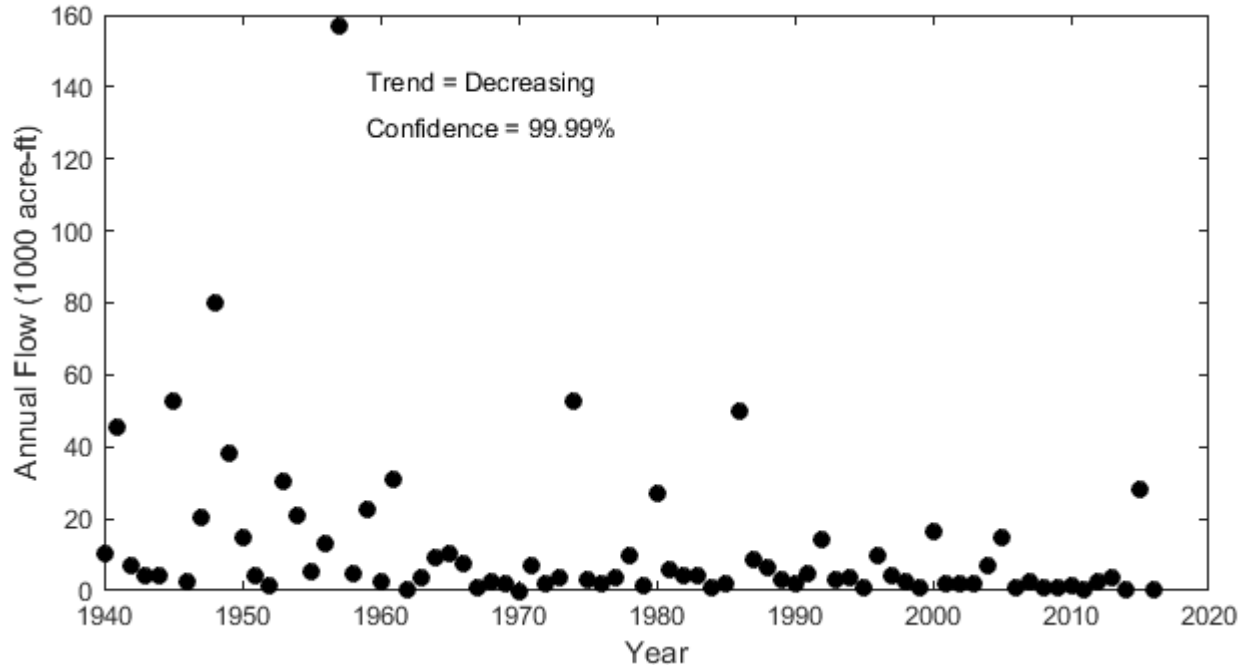


Figure 6-15 – Annual flows by year – North Concho River near Carlsbad

6.5 Streamflow Trend Analysis Summary

Table 6-1 presents a summary of computed Mann-Kendall trends for streamflow data from each of the 6 streamflow gauge locations presented in this section of the report. Periods showing increasing or decreasing Mann-Kendall trends are shown with grey shading. Decreasing trends are indicated in **bold underline**, and increasing trends are indicated with ***bold italics***. Presented together in Table 6-1, trends from all 6 sites allows for comparison of data between sights, and provides insight to the variable streamflow changes present throughout the study area.

For example, streamflow within the North Concho River near Carlsbad demonstrates decreasing trends for all periods. Decreasing streamflow trends were also computed for Elm Creek, Brady Creek, and the gauges on the San Saba River, yet the decreasing trends for these locations were not as prevalent (by period) as for the North Concho River location. In contrast, flows within the South Concho River at Christoval were not found to demonstrate any increasing or decreasing trends, for any period (months, seasons, or annually). Trends for Brady Creek and the San Saba River at San Saba were similar, occurring for the same periods and all indicating decreasing streamflow. Yet for the San Saba River at Menard, the only computed significant trends were for increasing streamflow in March, November, and December. Such increasing trends were only present elsewhere in the Elm Creek data from Ballinger, which was also the only site for which both increasing and decreasing trends were computed.

Table 6-1 – Streamflow Trends Analysis

	North Concho Rv nr Carlsbad		South Concho Rv. at Christoval		Elm Creek at Ballinger	
Period	Trend	Confidence	Trend	Confidence	Trend	Confidence
January	<u>Decreasing</u>	<u>83.79%</u>	Stable	40.23%	<u>Increasing</u>	<u>95.51%</u>
February	<u>Decreasing</u>	<u>91.19%</u>	Stable	18.77%	Stable	74.81%
March	<u>Decreasing</u>	<u>78.72%</u>	Stable	13.27%	<u>Increasing</u>	<u>98.52%</u>
April	<u>Decreasing</u>	<u>96.01%</u>	Stable	31.42%	Stable	74.60%
May	<u>Decreasing</u>	<u>99.37%</u>	Stable	20.47%	<u>Decreasing</u>	<u>99.92%</u>
June	<u>Decreasing</u>	<u>99.88%</u>	Stable	39.62%	<u>Decreasing</u>	<u>75.82%</u>
July	<u>Decreasing</u>	<u>99.96%</u>	Stable	26.51%	Stable	44.43%
August	<u>Decreasing</u>	<u>99.94%</u>	Stable	44.14%	<u>Decreasing</u>	<u>83.69%</u>
September	<u>Decreasing</u>	<u>99.91%</u>	Stable	4.55%	<u>Decreasing</u>	<u>91.35%</u>
October	<u>Decreasing</u>	<u>88.39%</u>	Stable	30.77%	Stable	71.37%
November	<u>Decreasing</u>	<u>77.07%</u>	Stable	55.59%	Stable	49.92%
December	<u>Decreasing</u>	<u>98.86%</u>	Stable	56.63%	Stable	73.24%
Spring	<u>Decreasing</u>	<u>99.85%</u>	Stable	5.61%	<u>Decreasing</u>	<u>99.50%</u>
Summer	<u>Decreasing</u>	<u>99.99%</u>	Stable	47.63%	<u>Decreasing</u>	<u>80.09%</u>
Fall	<u>Decreasing</u>	<u>81.77%</u>	Stable	2.80%	<u>Decreasing</u>	<u>91.48%</u>
Winter	<u>Decreasing</u>	<u>95.81%</u>	Stable	42.65%	Stable	53.64%
Annual	<u>Decreasing</u>	<u>99.99%</u>	Stable	9.80%	<u>Decreasing</u>	<u>90.96%</u>
San Saba River at San Saba						
	San Saba Rv at Menard		Brady Creek at Brady		San Saba River at San Saba	
Period	Trend	Confidence	Trend	Confidence	Trend	Confidence
January	Stable	70.27%	Stable	29.35%	Stable	70.68%
February	Stable	27.17%	Stable	55.35%	Stable	73.03%
March	<u>Increasing</u>	<u>84.83%</u>	Stable	7.74%	Stable	18.43%
April	Stable	23.17%	<u>Decreasing</u>	<u>97.76%</u>	<u>Decreasing</u>	<u>87.08%</u>
May	Stable	9.80%	<u>Decreasing</u>	<u>97.15%</u>	<u>Decreasing</u>	<u>97.53%</u>
June	Stable	42.65%	<u>Decreasing</u>	<u>80.73%</u>	Stable	73.79%
July	Stable	67.76%	Stable	37.81%	Stable	25.85%
August	Stable	70.48%	Stable	30.44%	Stable	70.68%
September	Stable	59.66%	Stable	58.89%	<u>Decreasing</u>	<u>78.67%</u>
October	Stable	49.90%	Stable	54.97%	Stable	54.80%
November	<u>Increasing</u>	<u>77.69%</u>	Stable	10.99%	Stable	23.17%
December	<u>Increasing</u>	<u>98.26%</u>	Stable	65.60%	Stable	32.39%
Spring	Stable	22.50%	<u>Decreasing</u>	<u>98.97%</u>	<u>Decreasing</u>	<u>96.08%</u>
Summer	Stable	38.70%	<u>Decreasing</u>	<u>89.54%</u>	Stable	71.48%
Fall	Stable	52.11%	Stable	63.51%	Stable	69.45%
Winter	Stable	74.90%	Stable	62.57%	Stable	59.91%
Annual	Stable	17.74%	<u>Decreasing</u>	<u>99.56%</u>	<u>Decreasing</u>	<u>94.75%</u>

BOLD, ITALICS, & SHADING = significant increasing trend
BOLD, UNDERLINE, & SHADING = significant decreasing trend

7 Task 5 – Precipitation Trend Analysis

Under this task, precipitation records were to be analyzed using the Mann-Kendall technique, with records evaluated by season and month as well as other pertinent periods. The objective of the analyses is to identify trends and determine any possible “change points,” or points in time when significant precipitation changes occurred.

Figure 7-1 presents a map showing the location of long-term precipitation measurement stations within the vicinity of the study area watersheds. Precipitation data was obtained from two sources: 1) the TSTool software and 2) data compiled during Phase I of this study.

The TSTool software was developed by the Openwater Foundation in conjunction with the Colorado Department of Natural Resources and the Colorado Water Conservation Board Division of Water Resources. This tool, publically available at <http://openwaterfoundation.org/software-tools/tstool> as of 7/6/2019, compiles available time series data from a variety of sources, including the State of Colorado, NRCS, USGS, and the US Bureau of Reclamation. From the TSTool software and database, we identified 171 precipitation recording stations located within and around the four study area watersheds (Figure 7-1), yet many stations did not report sufficiently long, continuous periods of record for use in statistical analysis. We attempted to identify stations with continuous periods of record from 1940 to 2016, and found individual stations at Ballinger, Brady, and Menard which fit this criteria. For other locations, we had to compile data from relatively close geographic areas in order to obtain a reasonably long period of record. Such compilations were required for stations near Big Spring, Abilene, Sterling City, and San Angelo. Station compilations were also needed for the area between Big Spring and Sterling City (labeled as “Upper North Concho”) as well as the area between Sterling City and San Angelo (labeled as “Lower North Concho”). Stations and station compilations were selected for analysis such that data was available for the upper and lower portions of each subject watershed.

Data compiled during the Phase I portion of this project consisted of daily precipitation totals (in inches) for the period between January 1, 1940 and December 31, 2018. This data was used for the Christoval and San Saba locations (Figure 7-1).

Precipitation data was obtained as daily values (in inches of depth) for the period of record for each gauge. Data were processed to contain the value “-9999” for instances when data was missing and not available. Within many datasets obtained from the TSTool, data were missing from one gage record on a given day, yet included in the record of a nearby gauge on that same day. In such instances, the data records were combined to “fill-in” gaps within the time-series record for the given location. Statistical analysis of precipitation data was only performed on valid data, excluding data containing the “-9999” value. Daily data was averaged monthly, seasonally, and annually, with the Mann-Kendall technique applied to each dataset to determine and evaluate data trends.

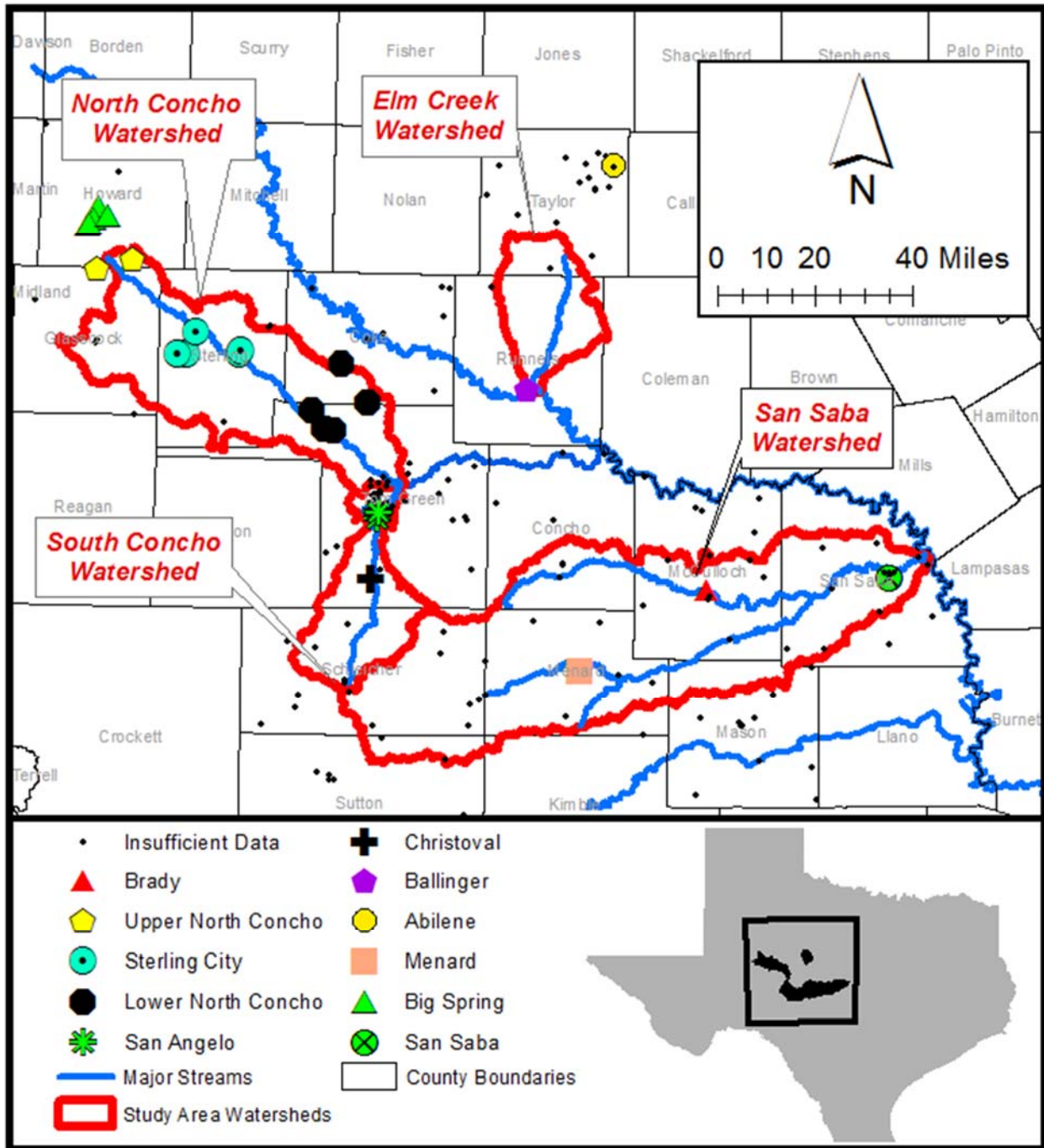


Figure 7-1 Map showing measurement locations identified and used in assessing precipitation trends within the study area watersheds.

For seasonal averaging, monthly data was grouped as follows:

- “Winter” = December, January, and February
- “Spring” = March, April, and May
- “Summer” = June, July, and August
- “Fall” = September, October, and November.

For winter periods, data from December corresponds to the December from the previous year, so that the “Winter 2019” period consists of December 2018, January 2019, and February 2019 data. All annual averages were based on the calendar year.

Within this Phase II analysis, precipitation data is analyzed in two separate ways. The first method involves considering all rainfall readings recorded at each gage. In this way, annual rainfall totals reflect the sum of all measurements for the year recorded at the gage. The second method involves filtering out small rainfall events which were not likely to contribute runoff to local watercourses. The methods and results are provided in Section 7.1 and Section 7.2 respectively.

7.1 Full Precipitation Record Analysis

7.1.1 Elm Creek Watershed

As shown in Figure 7-1, within the vicinity of the Elm Creek watershed two precipitation stations exist with sufficient data to allow for trend analysis over the 1940-2016 period of record: 1) Ballinger, TX at the watershed outlet, and 2) Abilene, TX which is outside of the watershed but perhaps indicative of precipitation that would fall on the upper reaches of the watershed. Spatial gradients in precipitation across the Elm Creek watershed would be better resolved if data were available from the center of the watershed, likely from Winters. No suitable precipitation data was available for the Winters area from sources utilized during this project effort.

Table 7-1 presents information regarding the precipitation stations used in assessing trends across the Elm Creek watershed. As shown, data from “Ballinger 2 NW” was available from 1900-2019, yet only data for the period 1940-2016 was used in this analysis. Data from the City of Abilene was compiled from two (2) separate gauge locations within the city limits, with each station providing data at different times. Combined, the period of record of available data for Abilene ran from 1/1/1886 to 4/1/2019, yet only data for the period 1940-2016 was used in this analysis.

Table 7-1 – Precipitation measurement stations for the Elm Creek watershed

Station Name	ACIS ID	Latitude	Longitude	Start Date	End Date
Ballinger 2 NW	23597	31.7413N	99.9763W	1/1/1900	4/2/2019
Abilene	23801	32.45N	99.73333W	1/1/1886	2/29/1944
Abilene Regional AP	23787	32.4105N	99.6822W	3/1/1944	4/1/2019

** ACIS = Applied Climate Information System

7.1.1.1 Ballinger

Precipitation data for Ballinger, TX was available for the period from 1900-2019, yet only data from 1940-2016 was included in this analysis. Figure 7-2A provides the annual rainfall totals for Ballinger, which range from 10 to 35 inches. Mann Kendall Analysis suggests stability in the rainfall totals, without increasing or decreasing trends across the entire 77-year period of record. Year to year variation in rainfall totals spans up to 15 inches, and the median annual rainfall total is 22 inches.

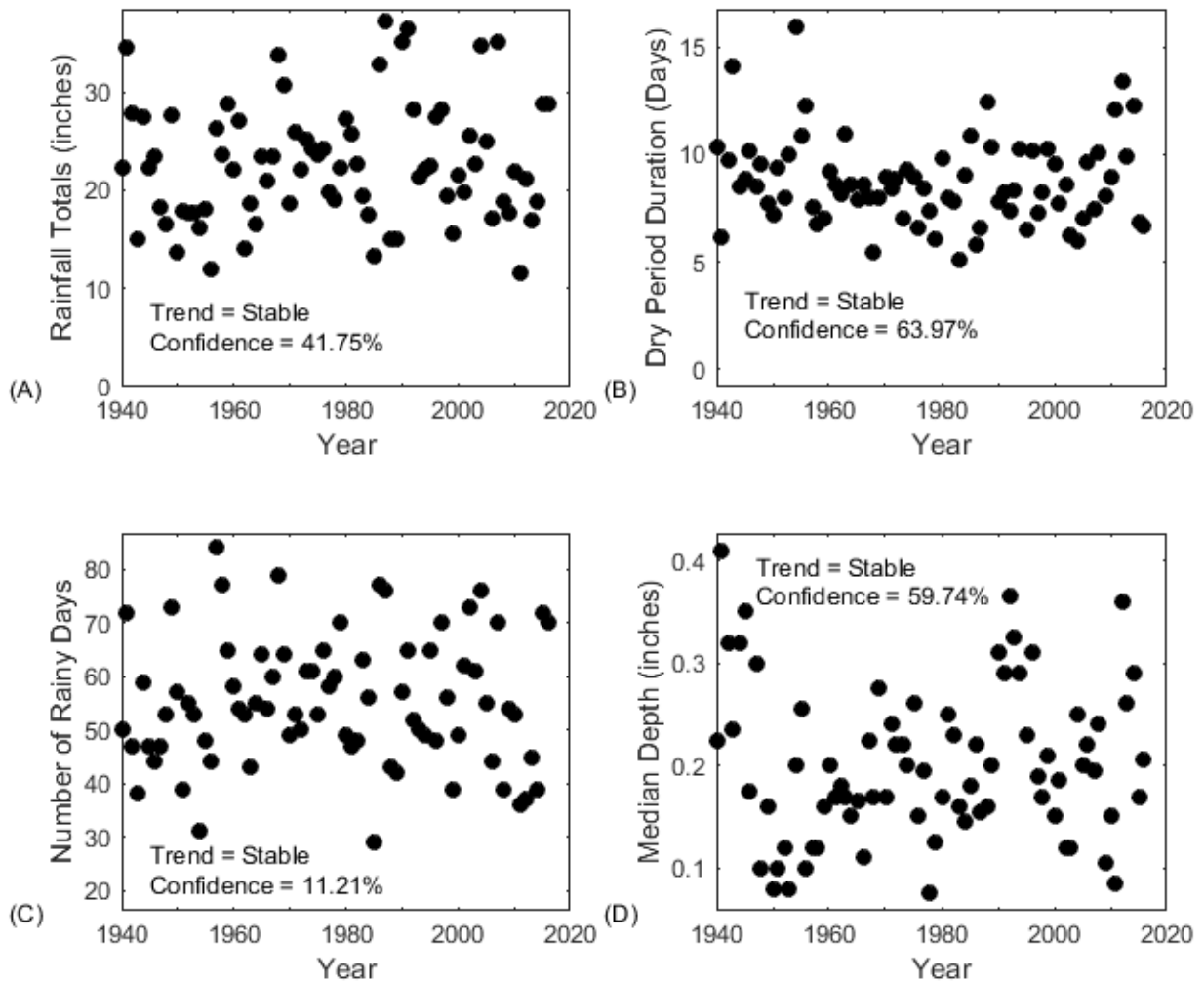


Figure 7-2 Precipitation data for Ballinger for the period 1940-2016 – A) Annual rainfall totals, B) average duration of dry periods, C) number of rainy days per year, D) median rainfall depth per year.

Figure 7-2B presents the average dry period duration per year, and indicates a stable trend. This suggests that Ballinger has not experienced a change in the frequency of rainfall events, which is confirmed by the stable trend indicated in Figure 7-2C.

The stable trends for the number of rainy days per year, coupled with the stable annual precipitation totals, leads to a stable trend the median rainfall depth for Ballinger (Figure 7-2D). Median depths per year range from 0.4 in to 0.08 inches, with no discernible change in rainfall patterns from year to year.

7.1.1.2 Abilene

As shown in Figure 7-1, precipitation data for Abilene, TX was compiled from records of 2 gauges within the City of Abilene. In compilation, precipitation data is available for the period from 1886-2019, yet data analysis presented herein is limited to the period from 1940-2016.

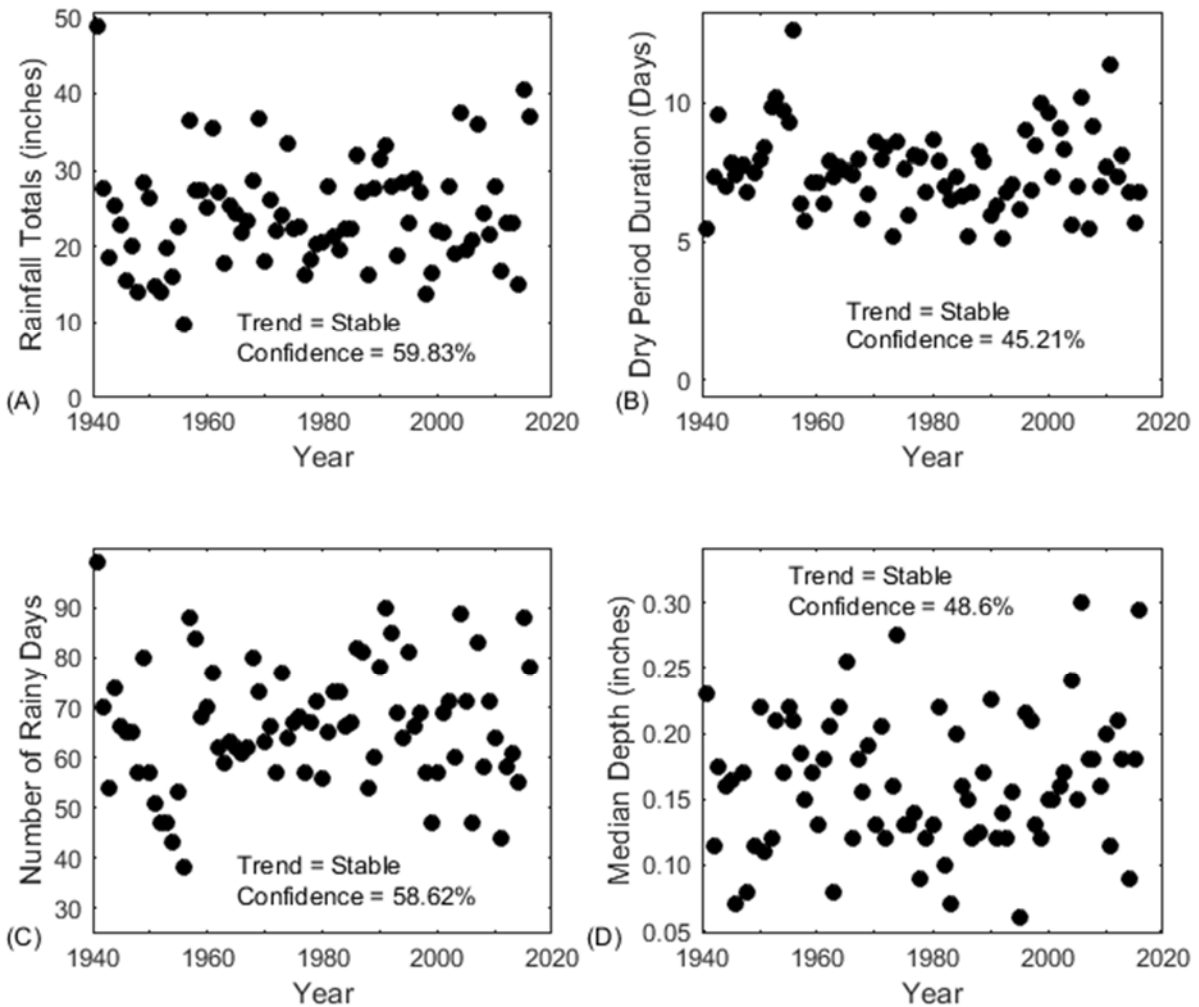


Figure 7-3 Precipitation Data for Abilene for the period 1940-2016 – A) Annual rainfall totals, B) average duration of dry periods, C) number of rainy days per year, D) median rainfall depth per year.

Figure 7-3A presents the total annual precipitation for Abilene, indicating a stable trend over the period of record. Annual totals range from 10 inches to 49 inches, with a median value of 23 inches/year.

Figure 7-3B present the time-history of annual average dry durations, showing neither increasing or decreasing trends. The data does appear to spread vertically in recent years, suggesting that year-to-year variability may be increasing even if the average dry period duration (7-8 days) remains stable.

Figure 7-3C indicates that the number of rainy days per year shows a stable trend, yet with large year-to-year variability. A similarly stable trend in median annual rainfall depth is evident for the period of record data (Figure 7-3D).

7.1.2 Elm Creek Watershed Precipitation Summary & Comparison

Precipitation analysis results for the gages in the vicinity of the Elm Creek watershed suggest that similarly stable conditions may be found spatially across the watershed. At the watershed outlet (Ballinger, TX), total precipitation has remained stable over the 77 year period of record of this analysis, and similar stability was computed for Abilene d. Stability in rainfall frequency and median depth was also computed for both locations.

Table 7-2 presents Mann-Kendall analysis results for both the Ballinger and Abilene locations, broken down by month, season, and annual periods. Both stations show identical monthly trends, with increased March and June precipitation and decreased precipitation in April and May. Summer precipitation in increasing in each location as well. These changes in the monthly pattern of rainfall may affect streamflow based on the consumption of water by flora during the growing season.

Table 7-2 – Precipitation Trends Elm Creek Watershed

Period	Ballinger		Abilene	
	Trend	Confidence	Trend	Confidence
January	Stable	25.98%	Stable	31.02%
February	Stable	52.39%	Stable	60.59%
March	<i>Increasing</i>	<i>99.33%</i>	<i>Increasing</i>	<i>98.23%</i>
April	<u>Decreasing</u>	<u>92.86%</u>	<u>Decreasing</u>	<u>83.14%</u>
May	<u>Decreasing</u>	<u>89.63%</u>	<u>Decreasing</u>	<u>83.82%</u>
June	<i>Increasing</i>	<i>82.30%</i>	<i>Increasing</i>	<i>75.46%</i>
July	Stable	50.75%	Stable	43.10%
August	Stable	33.04%	Stable	62.54%
September	Stable	42.35%	Stable	56.48%
October	Stable	42.35%	Stable	37.50%
November	Stable	11.91%	Stable	67.87%
December	Stable	38.79%	Stable	10.34%
Spring	Stable	74.72%	Stable	72.61%
Summer	<i>Increasing</i>	<i>93.46%</i>	<i>Increasing</i>	<i>79.56%</i>
Fall	Stable	22.50%	Stable	56.21%
Winter	Stable	36.60%	Stable	13.88%
Annual	Stable	41.75%	Stable	59.83%

BOLD, ITALICS, & SHADING = significant increasing trend

BOLD, UNDERLINE, & SHADING = significant decreasing trend

7.1.3 San Saba Watershed

As shown in Figure 7-1, within the San Saba watershed three suitable precipitation stations were identified: 1) Menard, within the Upper-middle portion of the watershed, 2) Brady, within the lower-middle portion of the watershed, and 3) San Saba, near the watershed outlet. Spatial gradients in precipitation across the San Saba watershed would be better resolved if data were available from the upper reaches of the watershed near Fort McKavett or Eldorado. Available data from these areas, however, was not of sufficient duration to be suitable to assess long-term precipitation trends.

Table 7-3 presents information regarding the precipitation stations used in assessing trends across the San Saba watershed. As shown, data from each station was available outside of the period of record of this Phase II analysis. Data from the rainfall station at San Saba was not obtained directly from the TSTool, yet was obtained from the precipitation database developed during Phase I of this study.

Table 7-3 – Precipitation measurement stations for the San Saba watershed

<u>Station Name</u>	<u>ACIS ID</u>	<u>Latitude</u>	<u>Longitude</u>	<u>Start Date</u>	<u>End Date</u>
Menard	23356	30.9044N	99.7863W	1/1/1900	4/2/2019
Brady	23442	31.14453N	99.34922W	3/4/1937	3/31/2019
San Saba^^	23439	31.18333N	98.71667W	1/1/1901	4/1/2019

** ACIS = Applied Climate Information System

^^ Data for San Saba was obtained from Phase I project results.

7.1.3.1 Menard

Precipitation data for the Menard location was obtained from the TSTool database, and is available for the period from 1900-2019. Analyses presented herein, however, were limited to the period of record from 1940-2016.

As shown in Figure 7-4A, rainfall totals recorded at Menard range from 10 inches/year to 35 inches per year, which is similar to those measured at Ballinger, Christoval, and San Angelo. The Mann-Kendall analysis indicates that annual rainfall totals are stable, and not exhibiting increasing or decreasing trends.

In contrast, Figure 7-4B indicates a statistically significant decreasing trend in the average duration of dry periods for Menard. Durations decreased from an average of 10 days in 1940 to just 7 days in 2016, yet with some year-to-year variations disrupting the overall decreasing trend.

With the decrease in the duration of dry periods (Figure 7-4B), the number of rainy days per year experienced by Menard should generally increase. This trend is confirmed in Figure 7-4C, which shows an increasing trend in the number of rainy days per year observed at Menard. The year-to-year variation also appears to be increasing, with the record low having occurred during the recent drought in 2011.

The stable rainfall totals combined with increasing numbers of rainy days requires a reduction in the average depth of each rain event. This is evident in Figure 7-4D, which shows a decreasing trend in median rainfall depths. Based on the data presented, it appears

that median depths decreased rapidly from 1940-1955, and then more gradually from 1955-2016, yet this assessment is hampered by missing data from the early 1950's. Median depths appear to have been reduced from 0.3 inches per event to 0.15 inches per event.

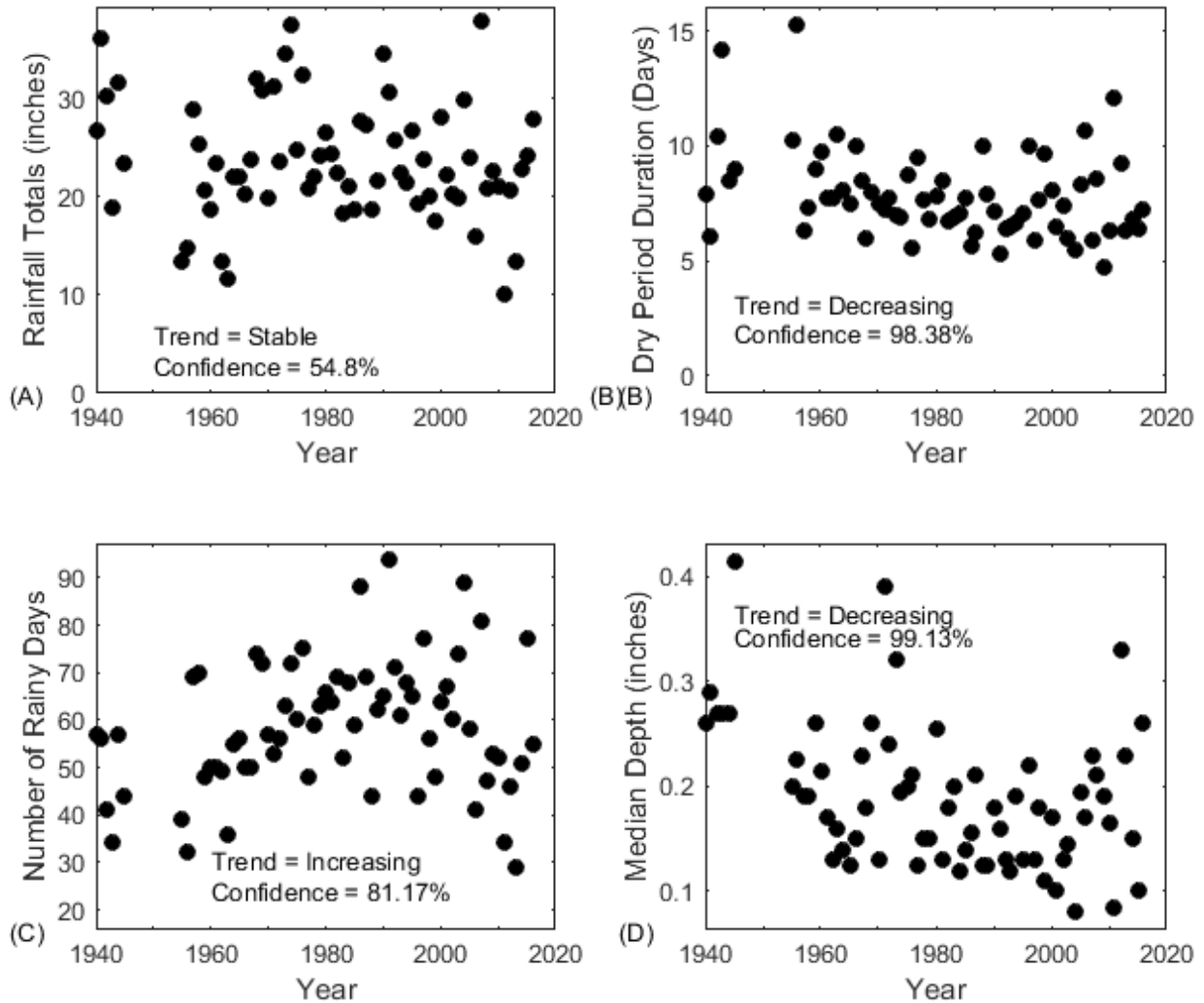


Figure 7-4 Precipitation Data for Menard for the period 1940-2016 – A) Annual rainfall totals, B) average duration of dry periods, C) number of rainy days per year, D) median rainfall depth per year.

7.1.3.2 *Brady*

Precipitation data for Brady was obtained from the TSTool database, and is available for the period from 1937-2019. For this analysis, only data from 1940-2016 was included.

As shown in Figure 7-5A, total annual precipitation for Brady indicates an increasing trend. Rainfall totals range from 8 inches per year to 35 inches per year, with a median value of 25 inches/yr. Year-to-year variation is also evident, and has varied by up to 15 inches between successive years. Such variations can mask smaller increasing trends evident over the entire period of record.

Figure 7-5B shows a decreasing trend in the duration of dry periods recorded at Brady. The average dry duration appears to have dropped from 9 to 7 days over the period of record, although the year-to-year variation in data makes such estimates difficult and inaccurate. The year-to-year variation appears to have remained constant over the period of record.

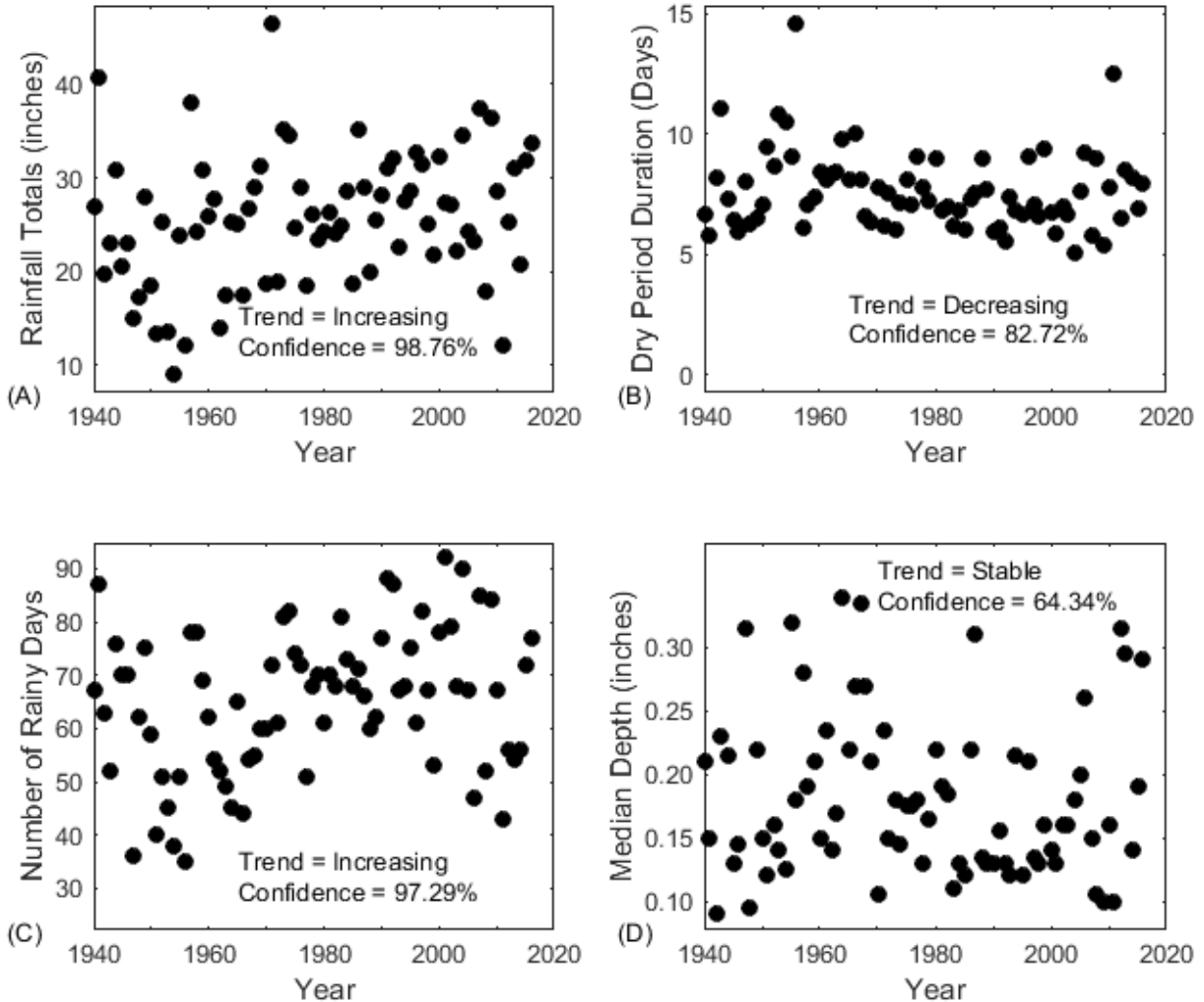


Figure 7-5 Precipitation Data for Brady, TX – A) Annual rainfall totals, B) average duration of dry periods, C) number of rainy days per year, D) median rainfall depth per year.

The number of rainy days experienced each year in Brady (Figure 7-5C) shows an increasing trend, yet with a large variation in the year-to-year values. The increase in both the annual rainfall totals and the number of rainy days per year combines to result in a stable trend in the median rainfall depth (Figure 7-5D). While remaining stable over the period of record, the year-to-year variation in median depth is large, which visually masks the stable trend within the data. The range in median depths (0.1-0.3 inches) is also a large portion of the median depths themselves, indicating great variability in the data.

7.1.3.3 San Saba

Precipitation data for the San Saba location was obtained from the databases developed during Phase I of this project. The data is available for the period 1940-2018, yet only data for 1940-2016 was used in this analysis.

As shown in Figure 7-6A, annual rainfall totals have been relatively stable and do not indicate increasing or decreasing trends. Values range from 13 inches per year to 45 inches per year, with a median value of 27 inches per year.

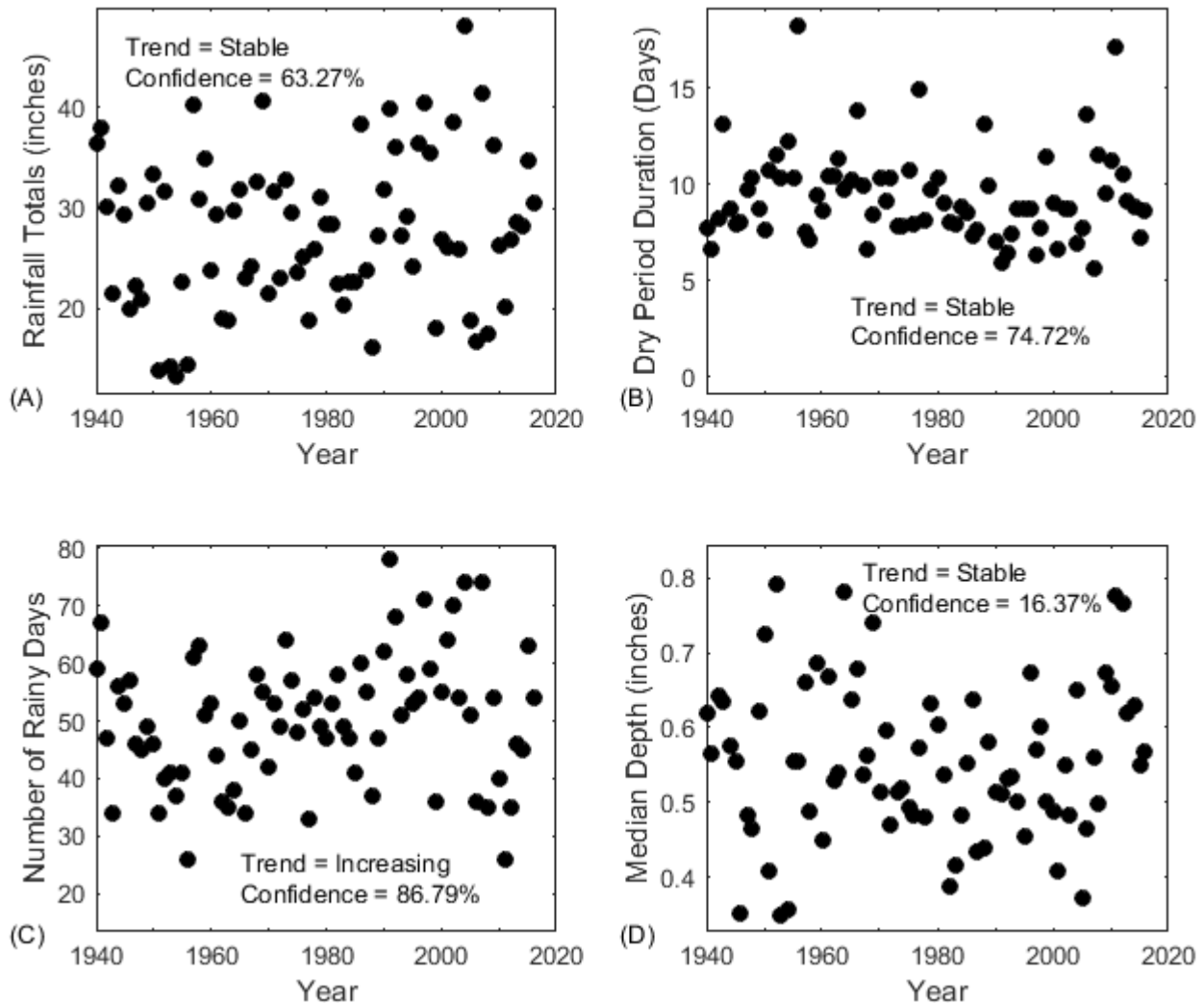


Figure 7-6 Precipitation Data for San Saba for the period 1940-2016 – A) Annual rainfall totals, B) average duration of dry periods, C) number of rainy days per year, D) median rainfall depth per year.

Figure 7-6B indicates that the duration of dry periods for San Saba has also remained stable over the period of record, with high points in the data corresponding to the 1956 and 2011 severe drought years. The Mann-Kendall analysis of the number of rainy days per year for San Saba (Figure 7-6C) indicates an increasing trend. Stability is also indicated for the average rainfall depth (Figure 7-6D).

7.1.3.4 San Saba Watershed Precipitation Summary & Comparison

Rainfall data collected at Menard, TX indicate that the frequency of rainfall events is increasing while the average rainfall depth is decreasing. The number of rainy days recorded at Menard and San Saba show similar increasing trends, yet the median rainfall depths at these stations have remained stable over the period of record. Total annual rainfall for both Menard and San Saba has been stable, yet has increased for Brady. The data from the three stations suggests that spatial gradients in precipitation patterns exist across the San Saba watershed.

Table 7-4 – Precipitation Trends San Saba Watershed

Period	Menard		Brady		San Saba	
	Trend	Confidence	Trend	Confidence	Trend	Confidence
January	Stable	52.14%	Stable	53.21%	Stable	39.75%
February	Stable	58.92%	Stable	43.25%	Stable	23.20%
March	<i>Increasing</i>	<i>95.12%</i>	<i>Increasing</i>	<i>99.61%</i>	<i>Increasing</i>	<i>99.40%</i>
April	<u>Decreasing</u>	<u>99.05%</u>	<u>Decreasing</u>	<u>89.35%</u>	<u>Decreasing</u>	<u>99.30%</u>
May	Stable	74.71%	Stable	72.46%	Stable	61.39%
June	Stable	50.73%	Stable	66.23%	<i>Increasing</i>	<i>90.37%</i>
July	<i>Increasing</i>	<i>82.47%</i>	<i>Increasing</i>	<i>83.95%</i>	<i>Increasing</i>	<i>87.09%</i>
August	Stable	10.84%	Stable	73.04%	Stable	60.22%
September	<u>Decreasing</u>	<u>97.39%</u>	Stable	7.01%	Stable	8.06%
October	Stable	20.47%	Stable	57.40%	<i>Increasing</i>	<i>78.22%</i>
November	Stable	62.83%	<i>Increasing</i>	<i>96.60%</i>	Stable	31.47%
December	Stable	42.66%	Stable	48.22%	Stable	55.65%
Spring	Stable	42.95%	<i>Increasing</i>	<i>77.01%</i>	Stable	31.43%
Summer	<i>Increasing</i>	<i>82.16%</i>	<i>Increasing</i>	<i>95.31%</i>	Stable	73.79%
Fall	Stable	73.23%	Stable	68.82%	Stable	47.93%
Winter	Stable	55.07%	Stable	32.40%	Stable	52.44%
Annual	Stable	54.80%	<i>Increasing</i>	<i>98.76%</i>	Stable	63.27%

BOLD, ITALICS, & SHADING = significant increasing trend

BOLD, UNDERLINE, & SHADING = significant decreasing trend

Watershed presents Mann-Kendall statistics for precipitation recorded at the three locations within the San Saba watershed, by month, season, and on an annual basis. As shown, each station reports an increasing trend in March precipitation, and a decreasing trend in April precipitation. Increases in July precipitation are also indicated for each location, yet with only Menard and Brady demonstrating increases for the summer periods. Each location reports stable precipitation trends for January, February, May, and December, as well as for the Fall and Winter seasons.

7.1.4 South Concho Watershed

As shown in Figure 7-1, the South Concho watershed contains two precipitation recording stations: 1) Christoval, located near the middle of the watershed, and 2) San Angelo, located near the watershed outlet. Precipitation data from Eldorado, TX (located near the upper reaches of the watershed) was unavailable for a suitably long and complete period of record analysis.

Table 7-5 presents information regarding the precipitation stations used in assessing trends across the South Concho watershed. As shown, data from each station was available outside of the period of record of this Phase II analysis. Data from the rainfall station at Christoval was not obtained directly from the TSTool, yet was obtained from the precipitation database developed during Phase I of this study.

Table 7-5 – Precipitation measurement stations for the South Concho watershed

Station Name	ACIS ID	Latitude	Longitude	Start Date	End Date
Christoval 3SSW	83717	31.17084N	100.51555W	1/1/1940	3/23//2019
San Angelo Mathis Field	29769	31.35167N	100.495W	8/13/1907	4/1//2019

** ACIS = Applied Climate Information System

^^ Data for Christoval was obtained from Phase I project results.

7.1.4.1 Christoval

Precipitation data for the Christoval location were obtained from the databases developed during Phase I of this project. The data are available for the period 1940-2018, yet only data for the period from 1940 to 2016 were used in this analysis.

As shown in Figure 7-7A, annual rainfall totals for Christoval have remained stable, without showing significant increasing or decreasing trends over the period of record. The year-to-year variation in totals can span up to 15 inches, yet long-term stability in total rainfall is indicated. Rainfall amounts range from 8 inches to 40 inches, with median value of approximately 20 inches/year.

Figure 7-7B presents the duration of dry periods within the Christoval area, and indicates no significant increasing or decreasing trends. The range in dry days seems to increase at the beginning and toward the end of the period of record, with values ranging from 7-11 days for the majority of the middle portion of the data (1960-2000). It is notable that the significant droughts for this area occurred in the 1950's and 2008-2016, which is where Figure 7-7B shows increased dry period durations. Therefore during drought conditions, it appears that Christoval experiences rainfall less often than during non-drought periods.

Figure 7-7C presents the number of rainy days per year recorded at Christoval, and demonstrates no significant increasing or decreasing trends. Similarly the median rainfall depth (Figure 7-7D) has remained relatively stable over the period of record.

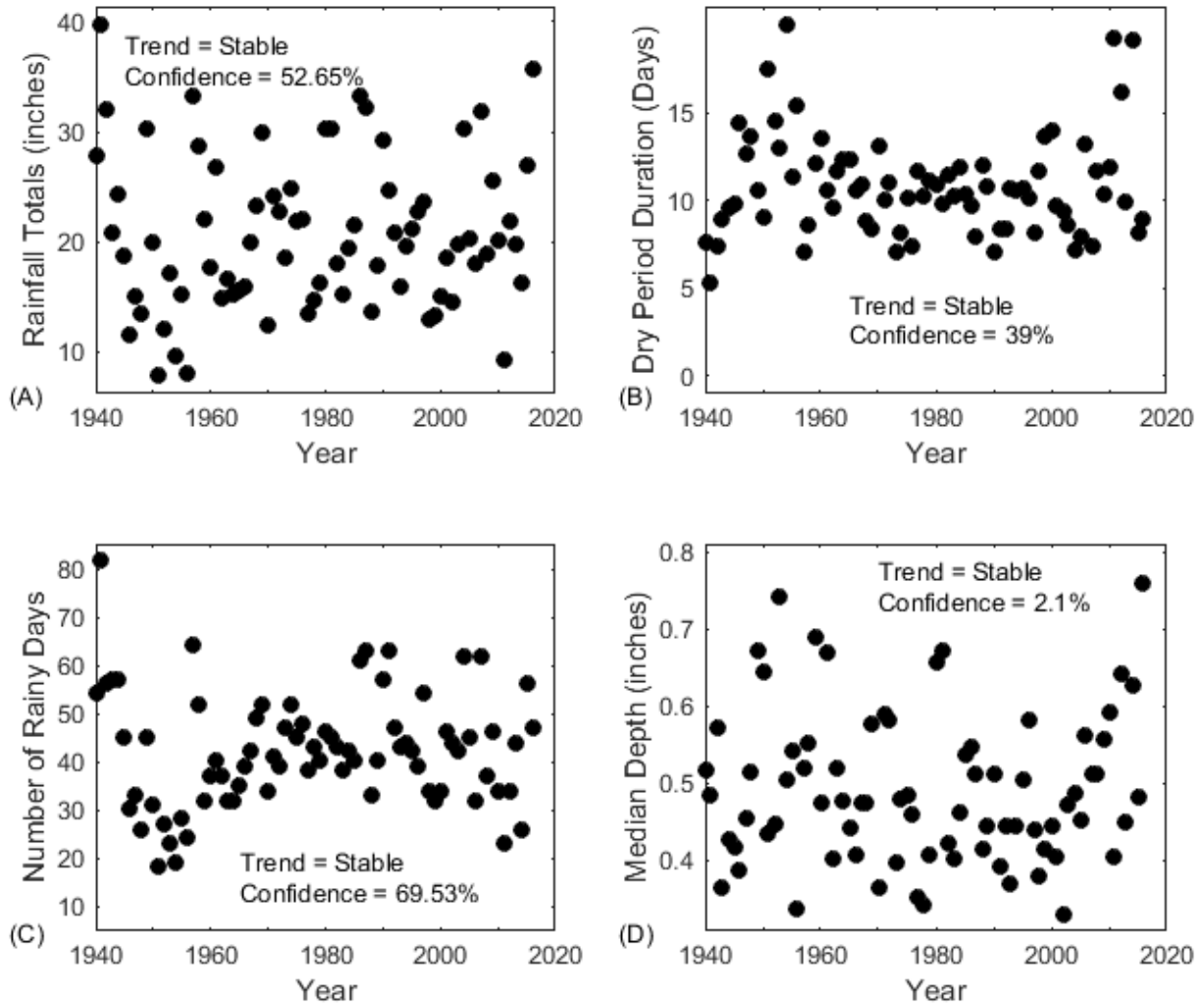


Figure 7-7 Precipitation Data for Christoval for the period 1940-2016 – A) Annual rainfall totals, B) average duration of dry periods, C) number of rainy days per year, D) median rainfall depth per year.

7.1.4.2 San Angelo

The gauge sites which combined to form San Angelo precipitation data are all located in the lower reaches of the South Concho watershed, just upstream of where the North and South Concho Rivers merge to form the Concho River. Data is available for 1944 to the present, yet only data from 1944-2016 is included within this analysis.

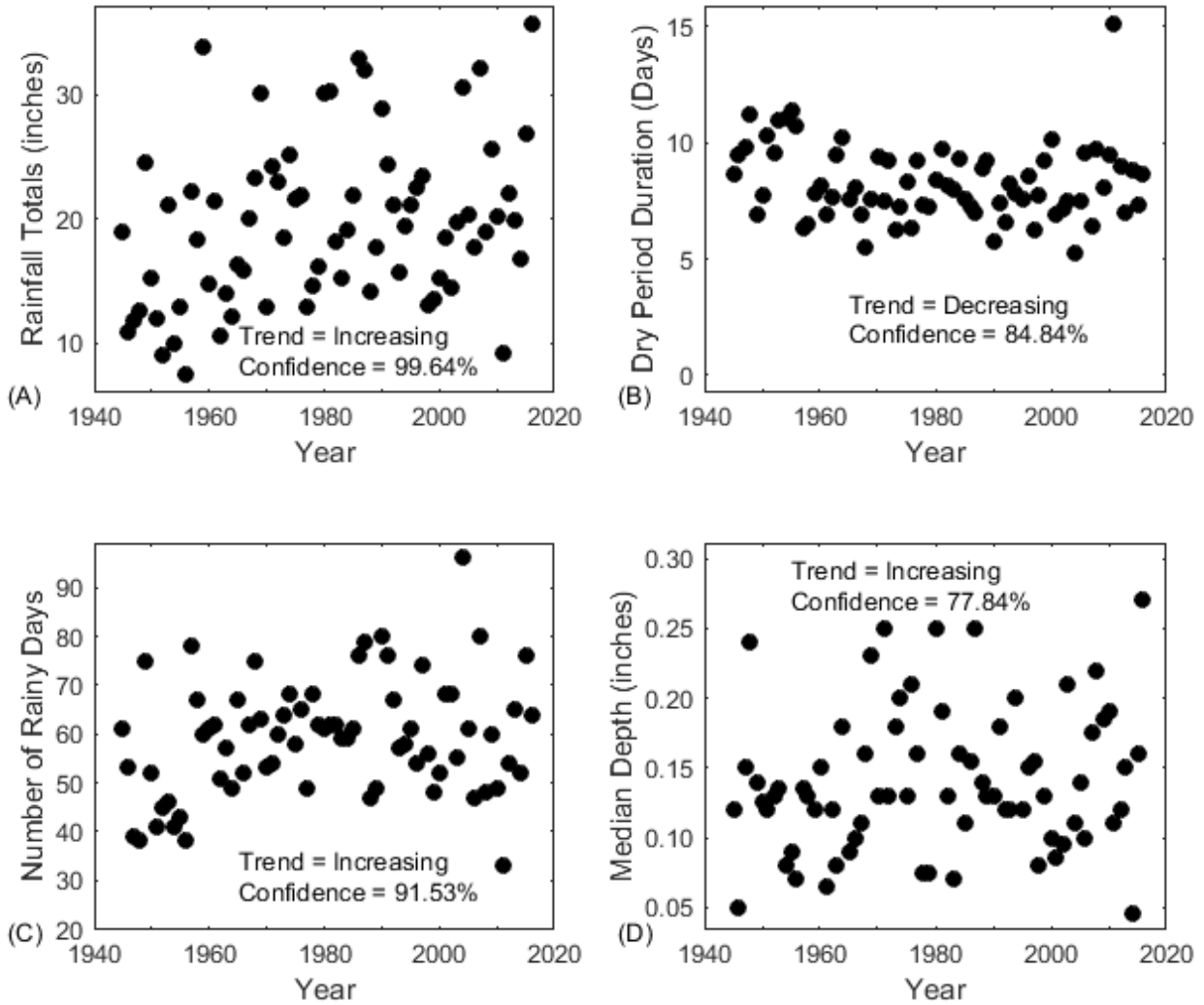


Figure 7-8 Precipitation Data for San Angelo of the period 1944-2016– A) Annual rainfall totals, B) average duration of dry periods, C) number of rainy days per year, D) median rainfall depth per year.

As indicated in Figure 7-8, annual rainfall totals for San Angelo show an increasing trend, yet maintain large year-to-year variations. Rainfall totals range from 7 to 35 inches per year, and it is common for totals to vary by over 10 inches from one year to the next.

Figure 7-7B shows a decreasing trend in the number of dry days between rainfall events. The decrease is runs from approximately 10 days in 1944 to 7 days in 2019. Figure 7-7C also demonstrates that there is an increasing trend in the number of rainy days per year, with large year-to-year variations evident.

Figure 7-7D presents the median rainfall depth per year at the San Angelo location. Mann-Kendall analysis on this dataset indicates that the median rainfall depth per rain event is increasing. Thus for San Angelo, data indicates increasing trends in total annual rainfall, the frequency of rainfall events, and the median depth of rainfall events.

7.1.4.3 South Concho Watershed Precipitation Summary

Data from the San Angelo and Christoval sites indicate that both locations experienced similar precipitation totals, yet only San Angelo experienced increasing totals over time. San Angelo also experiences lower median rainfall depths than those recorded at Christoval (0.15 inches versus 0.5 inches). Christoval also receives rainfall on approximately 20 more days per year than does San Angelo.

Table 7-5 presents Mann-Kendall analysis results for both stations within the South Concho watershed, by month, season, and on an annual basis. As shown, both stations indicate increasing precipitation in March, with decreasing precipitation in April. Both stations also indicate increasing precipitation in August. Only San Angelo exhibits increasing precipitation on a seasonal and annual basis. This indicates that across the South Concho basin, similar precipitation patterns are to be expected, yet slight spatial gradients in precipitation trends will exist. Additional data from Eldorado would provide insight into the trends in precipitation in the upper reaches of the South Concho watershed.

Table 7-6 – Precipitation Trends South Concho Watershed

Period	Christoval		San Angelo	
	Trend	Confidence	Trend	Confidence
January	Stable	2.13%	Stable	59.15%
February	Stable	0%	Stable	67.15%
March	<i>Increasing</i>	<i>98.95%</i>	<i>Increasing</i>	<i>99.90%</i>
April	<u>Decreasing</u>	<u>89.38%</u>	<u>Decreasing</u>	<u>80.57%</u>
May	Stable	5.96%	Stable	64.43%
June	Stable	30.79%	<i>Increasing</i>	<i>86.18%</i>
July	Stable	66.12%	Stable	5.42%
August	<i>Increasing</i>	<i>88.80%</i>	<i>Increasing</i>	<i>97.93%</i>
September	Stable	14.31%	Stable	38%
October	Stable	38.42%	Stable	68.33%
November	Stable	19.80%	<i>Increasing</i>	<i>83.19%</i>
December	Stable	19.79%	<i>Increasing</i>	<i>83.44%</i>
Spring	Stable	41.76%	<i>Increasing</i>	<i>92.31%</i>
Summer	Stable	1.05%	<i>Increasing</i>	<i>91.29%</i>
Fall	Stable	18.09%	<i>Increasing</i>	<i>90.06%</i>
Winter	Stable	22.21%	Stable	70.44%
Annual	Stable	52.65%	<i>Increasing</i>	<i>99.64%</i>

BOLD, ITALICS, & SHADING = significant increasing trend
BOLD, UNDERLINE, & SHADING = significant decreasing trend

7.1.5 North Concho Watershed

As shown in Figure 7-1, precipitation data was collected and analyzed for 5 locations within the vicinity of the North Concho watershed, which each location located roughly along the NW-SE axis of the watershed. The locations, listed from the North West (upper reaches of the watershed) to the south east (lower reaches of the watershed) are:

- Big Spring, TX (Outside of the watershed)
- Upper North Concho (Upper reaches of the watershed)
- Sterling City
- Lower North Concho (between Sterling City and San Angelo)
- San Angelo (lower reaches of the watershed, near the outlet)

Table 7-3 presents information regarding the precipitation stations used in assessing trends across the North Concho watershed. As shown, only data from the San Angelo location is available for the full period of record for this Phase II analysis (1940-2016). For locations other than San Angelo, all analyses presented in this section include the earliest available location data through 2016.

Table 7-7 – Precipitation measurement stations for the North Concho watershed

Location	Station Name	ACIS ID	Latitude	Longitude	Start Date	End Date
Big Spring	Big Spring	29761	32.23333N	101.5W	1/1/1948	11/15/1953
	Big Spring	29762	32.2443N	101.4537W	1/1/1948	3/26/2019
	Webb AFB	32412	32.21667N	101.51667W	11/15/1953	12/31/1970
	Big Spring Field Station	23753	32.2683N	101.4858W	7/2/2003	4/2/2019
	Big Spring 1.5E	69819	32.2412N	101.4538W	3/24/2013	10/22/2015
	Big Spring McMahon Wrinkle Airport	32300	32.2125N	101.52139W	8/1/2009	4/1/2019
Upper North Concho	Lees	31608	32.082N	101.4842W	11/1/2003	3/1/2019
	Forsan	23720	32.11167N	101.36417W	4/9/1949	9/30/2008
Sterling City	Sterling City 9 NW	23668	31.9N	101.13333W	7/1/1949	8/31/1960
	Sterling City	23652	31.8347N	100.9827W	4/1/1926	2/28/2019
	Garden City 16 E	23634	31.83333N	101.2W	4/12/1949	9/30/1951
	Sterling City 0.7 NE	64946	31.8462N	100.9781W	12/6/2011	3/22/2019
	Bade Ranch	23633	31.83333N	101.16667W	6/1/1948	10/22/1948
Lower North Concho	Water Valley 11 ENE	23632	31.8136N	100.6286W	2/1/1959	3/13/2019
	Water Valley 11 ENE	23599	31.7N	100.53333W	4/2/1949	7/31/1958
	Water Valley	23585	31.67253N	100.72832W	1/1/1947	4/2/2019
	Sanatorium	23574	31.61667N	100.65W	9/28/1945	6/30/1953
	Carlsbad 2.4 WNW	64952	31.6205N	100.6798W	10/22/2011	3/13/2019
San Angelo	San Angelo Mathis Field	29769	31.35167N	100.495W	8/13/1907	4/1/2019

** ACIS = Applied Climate Information System

^^ Data for Christoval was obtained from Phase I project results.

7.1.5.1 Big Spring

Located to the north and west of the North Concho watershed, Big Spring serves as the upper location for assessing the watershed's spatial and temporal variation in precipitation. Figure 7-9 presents the statistical analysis of rainfall within the vicinity of Big Spring.

In Figure 7-9A, annual rainfall totals are presented overtime. As shown, rainfall ranges from 5 in/yr (2011) to nearly 35 in/yr (2005), with the majority of years having rainfall totals of 15-25 inches. Mann-Kendall analysis of the data indicated an increasing trend over the 1940-2016 period of record.

In Figure 7-9B, the annual average duration of "Dry Days" (defined as the number of days between rainfall events) is plotted by year. Increasing dry durations could indicate greater rainfall absorption potential by the soil, and could then suggest less resulting streamflow. As shown, Mann-Kendall analysis indicated an increasing trend in average dry day duration, suggesting that the timing between rainfall events is increasing for this area.

Figure 7-9C presents the number of days per year during which rainfall was recorded. As shown, the number of rainy days increased from 1948-1957, decreased from 1957-1980, and increased from 1980 to 2018. The overall trend from 1948-2018 is decreasing, yet trends over the shorter periods are also clear. Combined with the notion that total annual rainfall (Figure 7-9A) also increased, the result of increasing the number of rainy days is that the median (and average) rainfall depth per event must also increase.

Figure 7-9D presents the median rainfall depth per year, displaying an increase in values for the 1957-1980 period when the number of rainy days decreases. The recent (2008-2016) drought period shows relative large numbers of rainy days per year, resulting in lower median rainfall depths per rain event over this time period. Over the entire 1948-2016 period of record, the median depth of rainfall per rain event shows an increasing trend.

In general, Figure 7-9C and Figure 7-9D show long-term trends over the entire dataset yet also demonstrate contrasting visual trends over shorter portions of each dataset. Conceptually, if the total annual rainfall is increasing and the number of rainy days per year is decreasing, then the median rainfall depth per rain event should also increase. Figure 7-9 results fit this pattern. Yet increasing median rainfall depth per rain events should lead to increased runoff, which is not evident from stream gauge records from the North Concho watershed (Section 6.4). However it is also possible that as the Big Spring location is outside of the North Concho watershed, its rainfall patterns and trends will not have influence on flows within the watershed.

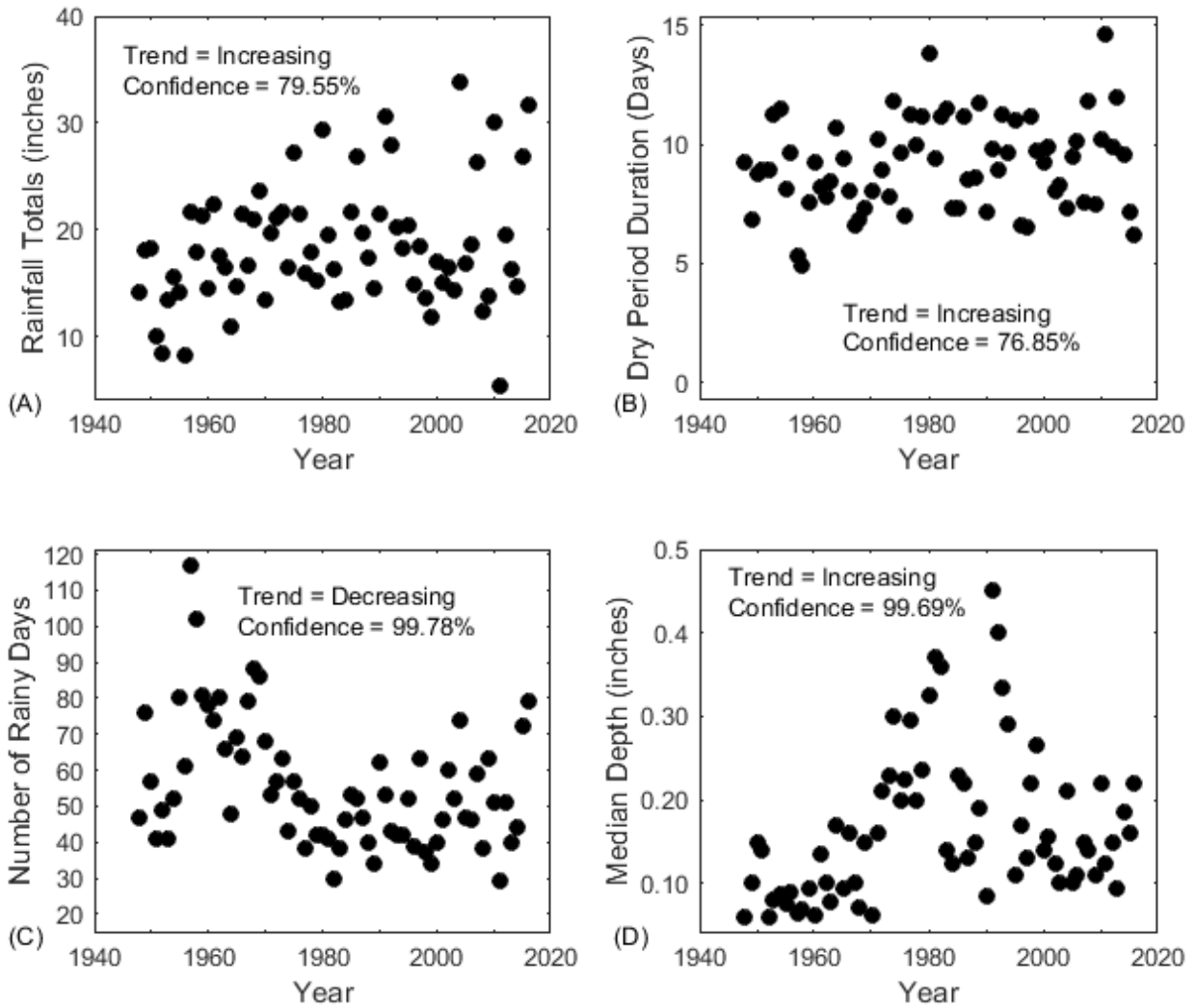


Figure 7-9 Precipitation Data for Big Spring for the period 1948-2016 – A) Annual rainfall totals, B) average duration of dry periods, C) number of rainy days per year, D) median rainfall depth per year.

7.1.5.2 Upper North Concho Watershed

As shown in Figure 7-1, rainfall stations located in the extreme upper reaches of the North Concho watershed were compiled into the Upper North Concho dataset. The gauging sites are generally located between Big Spring and Sterling City.

Figure 7-10A presents the annual rainfall totals for the Upper North Concho region. As shown, recent (1990-2016) data show a wide variation in totals from year to year, yet the Mann-Kendall analysis does not indicate overall increasing or decreasing trends. Rainfall totals are similar to those recorded at Big Spring, although in general the Upper North Concho region receives more rain per year.

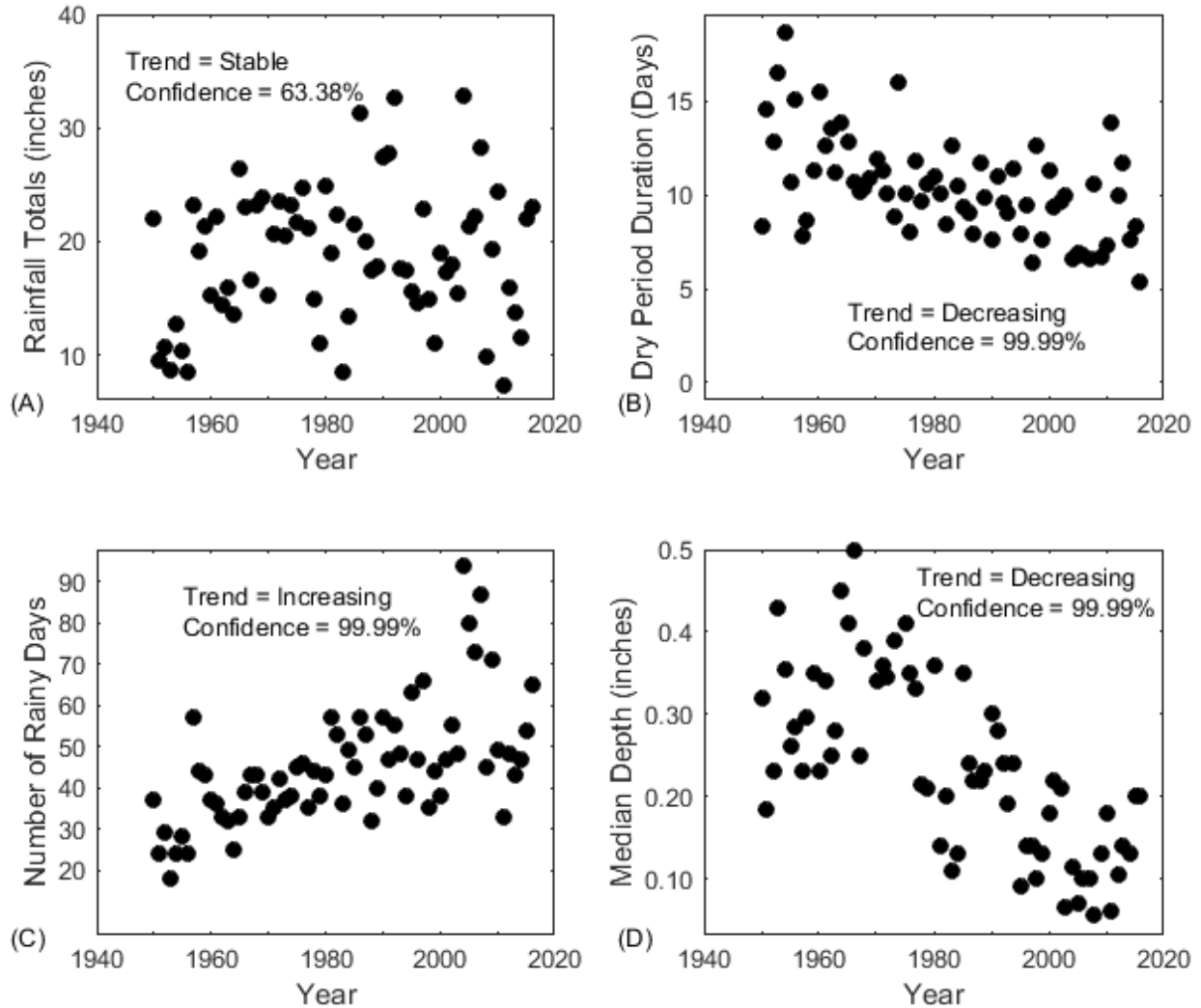


Figure 7-10 Precipitation Data for the Upper North Concho region for the period 1949-2016– A) Annual rainfall totals, B) average duration of dry periods, C) number of rainy days per year, D) median rainfall depth per year.

In Figure 7-10B, the annual average duration of “Dry Days” (defined as the number of days between rainfall events) is plotted by year. As shown, Mann-Kendall analysis indicates a decreasing trend, suggesting that rainfall is occurring more frequently in recent years. This result is corroborated in Figure 7-10C, where the number of rainy days per year shows an increasing trend.

The stable rainfall totals and increasing number of rainy days per year for the Upper North Concho watershed suggests that rainfall depths should show decreasing trends. This is confirmed in Figure 7-10D, where median depths decrease from near 0.5 inches to 0.1 inches over the period of record.

7.1.5.3 Sterling City

Sterling City is located generally in the middle of the North Concho watershed (Figure 7-1), and is downstream from the Upper North Concho gauging sites. Rainfall data is available at this location from 1926-2019, representing a longer period of record than is available from Big Spring or the Upper North Concho sites. For this analysis, only data from 1940-2016 were included.

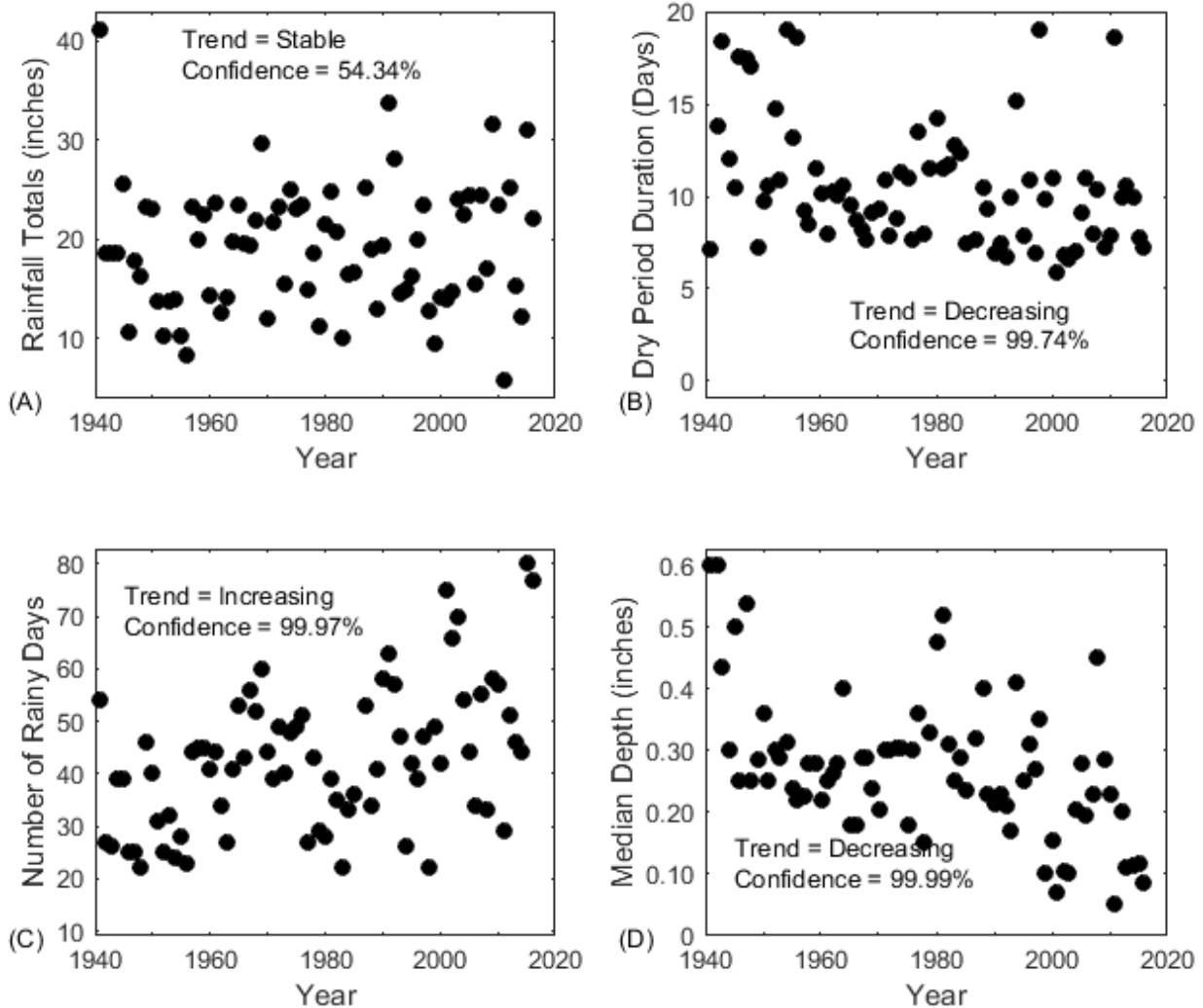


Figure 7-11 Precipitation Data for Sterling City for the period 1940-2016 – A) Annual rainfall totals, B) average duration of dry periods, C) number of rainy days per year, D) median rainfall depth per year.

Similarly to the findings from the Big Spring and Upper North Concho analyses, Figure 7-11A demonstrates that total annual rainfall within the Sterling City region remains neither increasing or decreasing on a statistical basis, yet the year-to-year rainfall variation seems to be increasing.

Figure 7-11B denotes a decreasing trend in the average dry duration between rain events. This result is corroborated by the increasing trend in the number of rainy days per year (Figure 7-11C), resulting in decreasing trend in the median rainfall depth (Figure 7-11D).

At Sterling City, the median rainfall depth decreased from 0.5 inches per rain event to under 0.1 inches per rain event over the period of record. These trends are similar to that observed within the Upper North Concho dataset and within the later portion of the Big Spring dataset.

7.1.5.4 Lower North Concho Watershed

The gauge sites which combined to form the Lower North Concho precipitation data are all located roughly between Sterling City and San Angelo, thereby representing the lower portion of the North Concho watershed (Figure 7-1). Rainfall data is available at this location from 1947-2019, yet only data from 1947-2016 is included in this analysis.

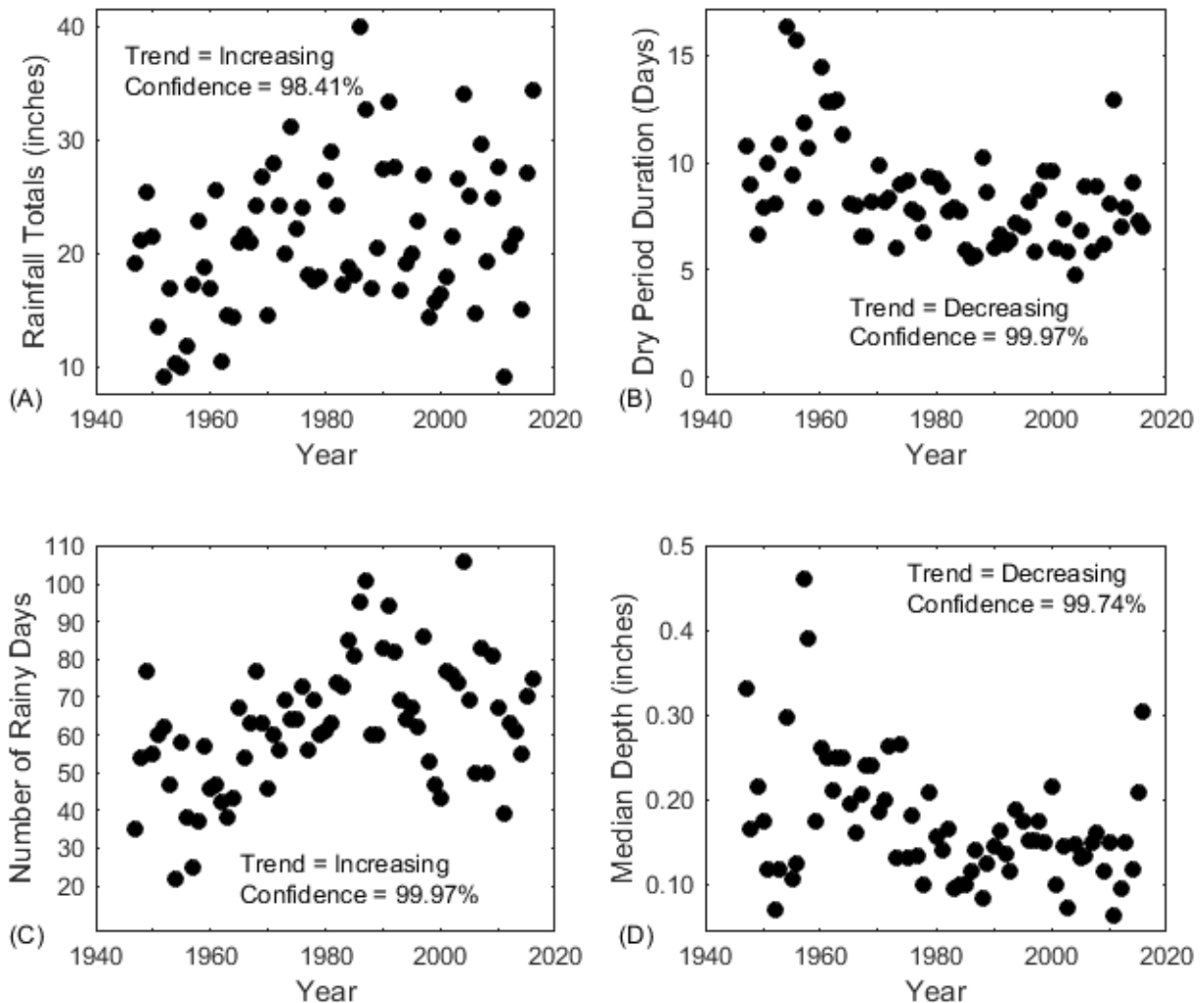


Figure 7-12 Precipitation Data for the Lower North Concho area for the period 1947-2016 – A) Annual rainfall totals, B) average duration of dry periods, C) number of rainy days per year, D) median rainfall depth per year.

Figure 7-12A presents the annual rainfall totals for the Lower North Concho region. Unlike results for Big Spring, Upper North Concho, and Sterling City, rainfall totals for the Lower

North Concho region show an increasing trend, per the Mann-Kendall analysis. The variation in year-to-year rainfall values also appears to be increasing.

Figure 7-12B presents the average dry duration for the region, demonstrating a decreasing trend. This indicates that rainfall is occurring more frequently during more recent years than during the earlier portion of the period of record.

Figure 7-12C presents the number of rainy days per year for the Lower North Concho region. As shown, the number of rainy days generally increased from 1947-1990, and then decreased (with variability from year-to-year) from 1990 to 2016. The overall Mann-Kendall trend, however, is that the number of rainy days is increasing with a high confidence level.

Figure 7-12D presents the median rainfall depth per year, and indicates that the depths are decreasing with time to a statistically significant degree. This trend was identified in data from the Upper North Concho and Sterling City sites, as well as for the Big Spring site post 1990, making this trend ubiquitous across the watershed.

The Lower North Concho precipitation data differs from that of the other North Concho watershed sites located upstream in that it shows an increasing trend in annual rainfall totals. Yet the increasing totals combined with an increasing number of rainy days still resulted in a decreasing trend in the median rainfall depth.

7.1.5.5 San Angelo

As discussed in Section 7.1.4.2, the gage sites which combined to form San Angelo precipitation data are all located in the lower reaches of the South Concho watershed, just upstream of where the North and South Concho Rivers merge to form the Concho River. This location also is in the vicinity of the downstream end of the North Concho watershed, and as such trends derived from this data may be useful in assessing spatial variability in precipitation trends across the North Concho watershed. Data is available for 1944 to the present, yet only data from 1944-2016 is included within this analysis.

Figure 7-8 shows that for San Angelo, annual rainfall totals are increasing, while the average duration between rain events is decreasing. The number of rainy days per year is also increasing, yielding a net decrease in median rainfall depth per rain event. This trend is similar to that observed for all precipitation stations within the North Concho watershed, and for the later portion of the Big Spring data period of record.

7.1.5.6 North Concho Watershed Precipitation Summary

As presented in Sections 7.1.5.1-7.1.5.5, numerous trends exist within the watershed's precipitation datasets. These trends are informative for their specific locations, but also must be considered geographically with respect to the entire watershed.

It is notable that the two downstream-most precipitation stations within the watershed each suggest increasing annual precipitation, whereas the three other stations upstream indicate stable annual values. Thus when considering annual rainfall trends, an NW-SE

gradient across the watershed exists, ranging from stable to increasing rainfall totals. A similar gradient exists for decreasing median rainfall depths, ranging from recently decreasing (at Big Spring) to decreasing at Upper North Concho through to San Angelo.

All sites other than Big Spring expressed increasing trends in the number of rainy days per year, and decreasing trends in the number of dry days between rain events. However considering Big Spring is not actually located within the North Concho watershed, it is accurate to say that across the entire watershed the frequency of rainfall events in increasing.

Table 7-8 presents Mann-Kendal analyses of rainfall data for each of the 5 sites attributed to the North Concho watershed, with analysis periods broken down by month, season, and annually. Periods showing statistically significant Mann-Kendall trends are shown with grey shading. Negative trends are indicated in **bold underline**, and positive trends are indicated with ***bold italics***. Sites are listed starting upstream (Big Spring) and moving in downstream order until the San Angelo site at the watershed outlet. The period of record included in Table 7-8 is from 1949-2016, which is the period of record common for all sites shown in the Table. This ensures that comparisons drawn from the data provided are based on the data contents, and not skewed by some sites utilizing more data than others. As such, the trends and confidence levels presented in Table 7-9 may differ from those previously discussed.

As shown in Table 7-8, consistent trends were often observed for most of the sites across the watershed. For example, increasing rainfall trends were computed for the month of March for all sites except Sterling City. Also for the month of April, the upper-most watershed sites (Big Spring and Upper North Concho) exhibited decreasing trends. Lower watershed sites (Sterling City, Lower North Concho, and San Angelo) exhibited stable trends for April, yet with higher confidence values approaching the 75% threshold needed to be deemed a non-stable trend. Considering the general trend of increasing rainfall in March followed by decreasing rainfall in April, it appears that the annual pattern of rainfall timing may be shifting, causing additional rain earlier in the calendar year. This identical set of trends in rainfall patterns for March and April was evident in data from all of the gage sites included in this Phase II analysis.

For three out of the five sites, August precipitation shows significant increases. This increase in precipitation during a typically hot summer month may yield tempered changes in August runoff as water losses to evaporation and evapotranspiration are generally increased during hotter periods. This is especially concerning given that August minimum temperatures within the North Concho watershed are generally increasing (Table 5-11). All sites reported stable trends for February, May, and September.

Table 7-8 – Precipitation Trends – North Concho Watershed for the period 1949-2016

Period	Big Spring		Upper North Concho Watershed		Sterling City	
	Trend	Confidence	Trend	Confidence	Trend	Confidence
January	Stable	15.61%	Stable	68.72%	Stable	16.91%
February	Stable	15.53%	Stable	5.61%	Stable	41.47%
March	<i>Increasing</i>	<i>96.06%</i>	<i>Increasing</i>	<i>97.33%</i>	Stable	65.41%
April	<i>Decreasing</i>	<i>76.53%</i>	<i>Decreasing</i>	<i>78.31%</i>	Stable	66.33%
May	Stable	39.97%	Stable	15.86%	Stable	47.87%
June	<i>Increasing</i>	<i>76.63%</i>	Stable	43.01%	Stable	32.34%
July	Stable	1.26%	Stable	29.53%	Stable	68.89%
August	<i>Increasing</i>	<i>97.23%</i>	<i>Increasing</i>	<i>80.78%</i>	Stable	62.33%
September	Stable	47.48%	Stable	0.43%	Stable	13.18%
October	Stable	19.26%	Stable	48.74%	Stable	9.99%
November	Stable	41.48%	Stable	56.94%	Stable	15.42%
December	Stable	10.18%	Stable	59.02%	Stable	53.87%
Spring	Stable	34.72%	Stable	3.88%	Stable	45.81%
Summer	<i>Increasing</i>	<i>95.04%</i>	Stable	70.12%	Stable	41.88%
Fall	<i>Increasing</i>	<i>86.31%</i>	Stable	63.09%	Stable	56.21%
Winter	Stable	11.45%	Stable	51.82%	Stable	56.85%
Annual	Stable	71.74%	Stable	63.38%	Stable	54.34%

Period	Lower North Concho Watershed		San Angelo	
	Trend	Confidence	Trend	Confidence
January	Stable	46.84%	<i>Increasing</i>	<i>88.48%</i>
February	Stable	22.35%	Stable	62.81%
March	<i>Increasing</i>	<i>99.52%</i>	<i>Increasing</i>	<i>99.93%</i>
April	Stable	59.43%	Stable	55.77%
May	Stable	38.78%	Stable	25.45%
June	<i>Increasing</i>	<i>97.77%</i>	<i>Increasing</i>	<i>83.73%</i>
July	<i>Increasing</i>	<i>92.73%</i>	Stable	13.32%
August	Stable	73.31%	<i>Increasing</i>	<i>89.43%</i>
September	Stable	35.90%	Stable	0.86%
October	Stable	20.01%	<i>Increasing</i>	<i>76.40%</i>
November	<i>Increasing</i>	<i>94.57%</i>	Stable	51.05%
December	Stable	49.43%	<i>Increasing</i>	<i>86.35%</i>
Spring	Stable	52.52%	<i>Increasing</i>	<i>91.07%</i>
Summer	<i>Increasing</i>	<i>99.30%</i>	<i>Increasing</i>	<i>86.89%</i>
Fall	<i>Increasing</i>	<i>83.97%</i>	<i>Increasing</i>	<i>77.86%</i>
Winter	Stable	43.06%	<i>Increasing</i>	<i>75.56%</i>
Annual	<i>Increasing</i>	<i>98.41%</i>	<i>Increasing</i>	<i>98.79%</i>

BOLD, ITALICS, & SHADING = significant increasing trend
BOLD, UNDERLINE, & SHADING = significant decreasing trend

7.2 Runoff-Generating Precipitation Trend Analysis

To determine a minimum rainfall threshold likely to contribute to watershed runoff, principles of the SCS curve number method were employed. This method is described in detail in Section 10 yet introduced here. The SCS curve number method has become a standard technique for estimating runoff for rainfall events, and is included in most introductory hydrology textbooks. Method presentation herein follows that included in (Lindeburg, 2003).

According to the SCS curve number methodology, runoff occurs when the rainfall quantity “P” exceeds the initial abstractions “I_a,” which represents the water lost to canopy interception prior to the rainfall reaching the ground surface. The parameter I_a is therefore the threshold rainfall depth which must be exceeded for a rain event to produce runoff. Values for I_a are computed using Eq. 7.1 and Eq. 7.2 as follows:

Eq. 7-1 $I_a = 0.2S$

Eq. 7-2 $S = \frac{1000}{CN} - 10$

Where “S” is the portion of the rainfall that is lost to the groundwater system and “CN” is the curve number for the watershed. Values for CN for each watershed vary from year-to-year as the land use/land cover of each watershed changes over time. These CN values were computed and presented in Section 4.3 and Figure 4-16.

Prior to use in computing I_a using Eq. 7-1 and Eq. 7-2, the CN values must be adjusted to reflect antecedent moisture conditions. Adjustments are necessary to reflect the principle that previously wet ground will produce more runoff from a given rainfall event, and previously dry ground will produce less runoff as more of the rainfall infiltrates into the groundwater system. Curve number adjustments to account for antecedent moisture conditions are made according to Table 7-9, with “RT” referring to the total rainfall for the previous 5 days.

Table 7-9 – Adjustments to curve numbers based on antecedent moisture conditions

Condition	Formula	5-Day Antecedent Rainfall Criteria	
		Growing Season March 15-October 15	Dormant Season October 16-March 14
I - Dry	$CN_I = \frac{4.2CN}{10 - 0.058CN}$	RT < 1.4 in	RT < 0.5 in
II - Average	“CN” From Section 4.3	1.4 in ≤ RT ≤ 2.0 in	0.5 in ≤ RT ≤ 1.0 in
III - Wet	$CN_{III} = \frac{23CN}{10 + 0.13CN}$	RT > 2.0 in	RT > 1.0 in

RT = Total rainfall for the previous 5-days

The following sections provide analysis of runoff-generating rainfall events only for the locations used in modeling rainfall-runoff response for each study area watershed (Section 10).

7.2.1 Elm Creek Watershed – Ballinger

Precipitation data for Ballinger, in the Elm Creek Watershed (Section 7.1.1.1), was modified to include only rain events that would generate runoff, per the SCS curve number method. Results are shown in Figure 7-13.

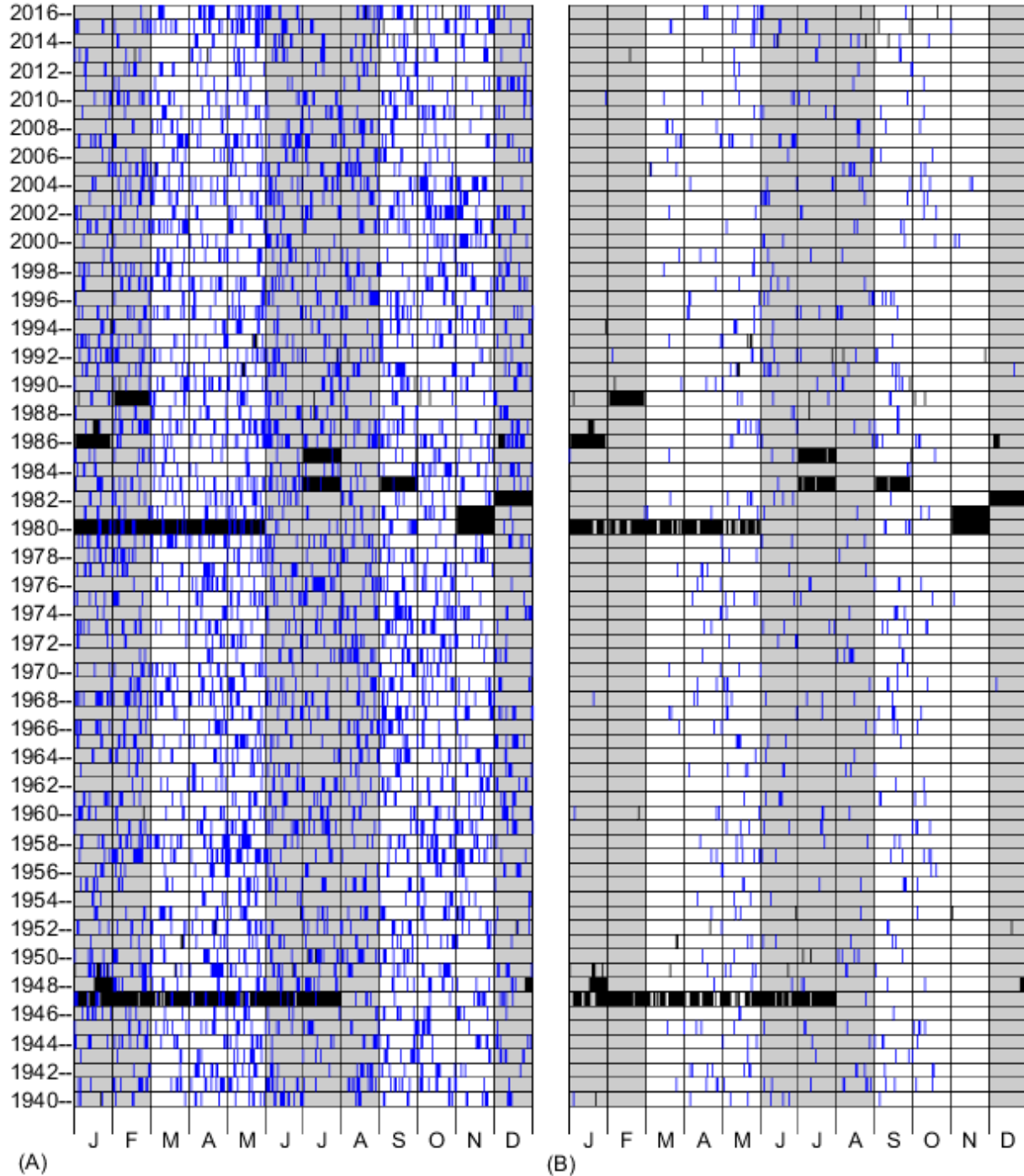


Figure 7-13 – Rainfall calendar plots for Ballinger – A) All recorded rainfall, B) Only runoff-generating rainfall. BLUE bars indicate days when rainfall occurred. BLACK bars indicate days with missing data.

Figure 7-13 presents calendar plots of rain events from the Ballinger location, showing when rain occurred for each year from 1940-2016. Blue lines indicate days when rain was recorded, and black lines represent days when data was unavailable. Grey shading indicate the winter and summer months, as previously defined. Figure 7-13A shows all days when rainfall was recorded, with this data previously analyzed in Section 7.1.1.1. Figure 7-13B shows only the days in which the recorded rainfall was sufficient to generate runoff, per the SCS curve number method. As shown, runoff-generating rain events are less frequent and tend to occur more often from April through October.

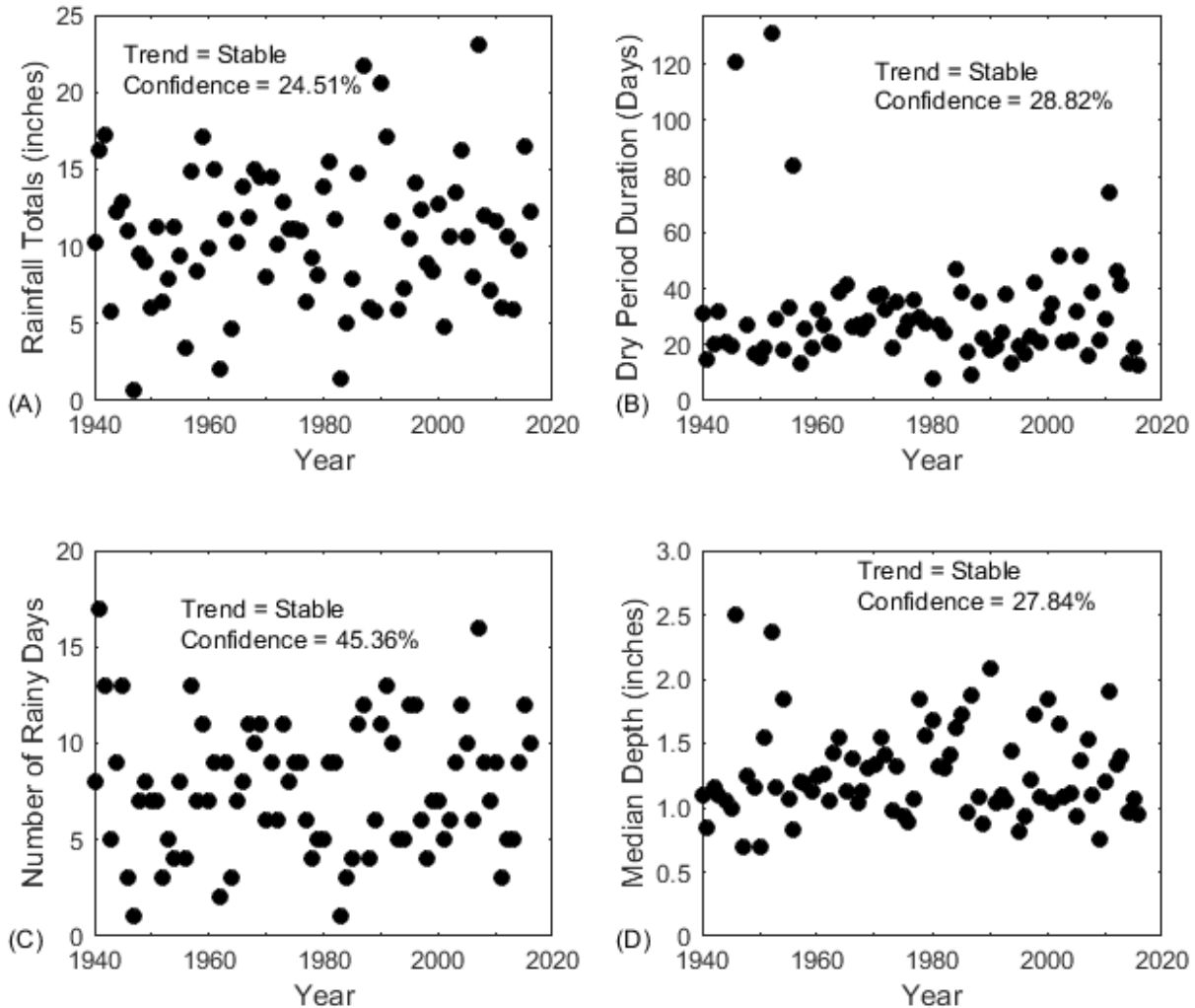


Figure 7-14 Precipitation Data for Ballinger for the period 1940-2016, considering only runoff-producing rain events – A) Annual rainfall totals, B) average duration of dry periods, C) number of rainy days per year, D) median rainfall depth per year.

Figure 7-14 presents the statistical analysis of annual rainfall-related data, considering only rainfall events that would generate runoff. As shown, total annual runoff-generating rainfall ranged from 1 to 24 inches per year, with stable trends indicated over the 1940-2016 period of record (Figure 7-14A). Stable trends were also indicated for the average duration of dry periods between rainfall events (Figure 7-14B), although an increasing trend would

be evident if the three outlier data points from prior to 1960 were excluded from the analysis. The outliers were caused by a low number of runoff-generating rain events occurring in those years. Stable trends were also reported for the number of rainy days per year (Figure 7-14C) and the median depth of rainfall during the rainy days (Figure 7-14D).

7.2.2 San Saba Watershed – San Saba

Precipitation data for San Saba, in the San Saba Watershed (Section 7.1.3.3), was modified to include only rain events that would generate runoff, per the SCS curve number method. Results are shown in Figure 7-15.

Figure 7-15 Figure 7-14 presents calendar plots of rain events from the San Saba location, showing when rain occurred for each year from 1940-2016. Blue lines indicate days when rain was recorded, and black lines represent days when data was unavailable. Grey shading indicate the winter and summer months, as previously defined. Figure 7-15A shows all days when rainfall was recorded, with this data previously analyzed in Section 7.1.3.3. Figure 7-15B shows only the days in which the recorded rainfall was sufficient to generate runoff, per the SCS curve number method. As shown, runoff-generating rain events are less frequent and tend to occur more often from April through October. In comparison with similar data from the Ballinger location (Figure 7-13), runoff-generating events at San Saba appear to occur more frequently during the winter months, and occur more often over most years.

Figure 7-16 presents the statistical analysis of annual rainfall-related data for San Saba, considering only rainfall events that would generate runoff. As shown, total annual runoff-generating rainfall ranged from 5 to 35 inches per year, with increasing trends indicated over the 1940-2016 period of record (Figure 7-16A). Stable trends were also indicated for the average duration of dry periods between rainfall events (Figure 7-16B), although an increasing trend would be evident if the three outlier data points from prior to 1960 were excluded from the analysis. As within the Ballinger data, the San Saba outliers were caused by a low number of runoff-generating rain events occurring in those years. Stable trends were also reported for the number of rainy days per year (Figure 7-16 C), yet an increasing trend was identified in the median depth of rainfall during the rainy days (Figure 7-16 D). Figure 7-16 indicates that for the San Saba watershed, recent rainfall patterns result in greater runoff-generating events, which should correspond with increasing runoff, depending upon the timing of the rain events.

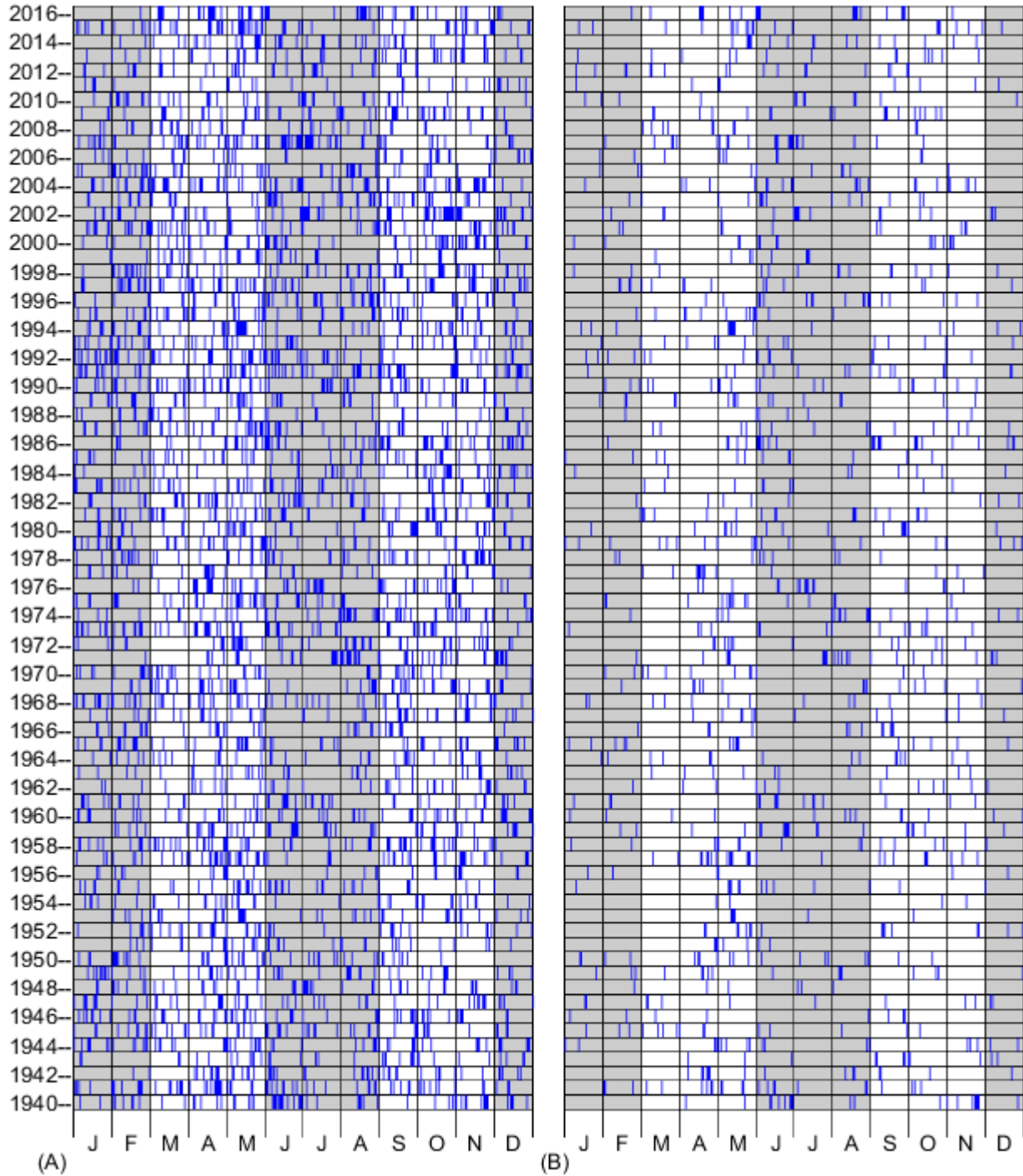


Figure 7-15 – Rainfall calendar plots for San Saba– A) All recorded rainfall, B) Only runoff-generating rainfall. BLUE bars indicate days when rainfall occurred. BLACK bars indicate days with missing data. Grey shading separates seasons (Winter, Spring, Summer, and Fall).

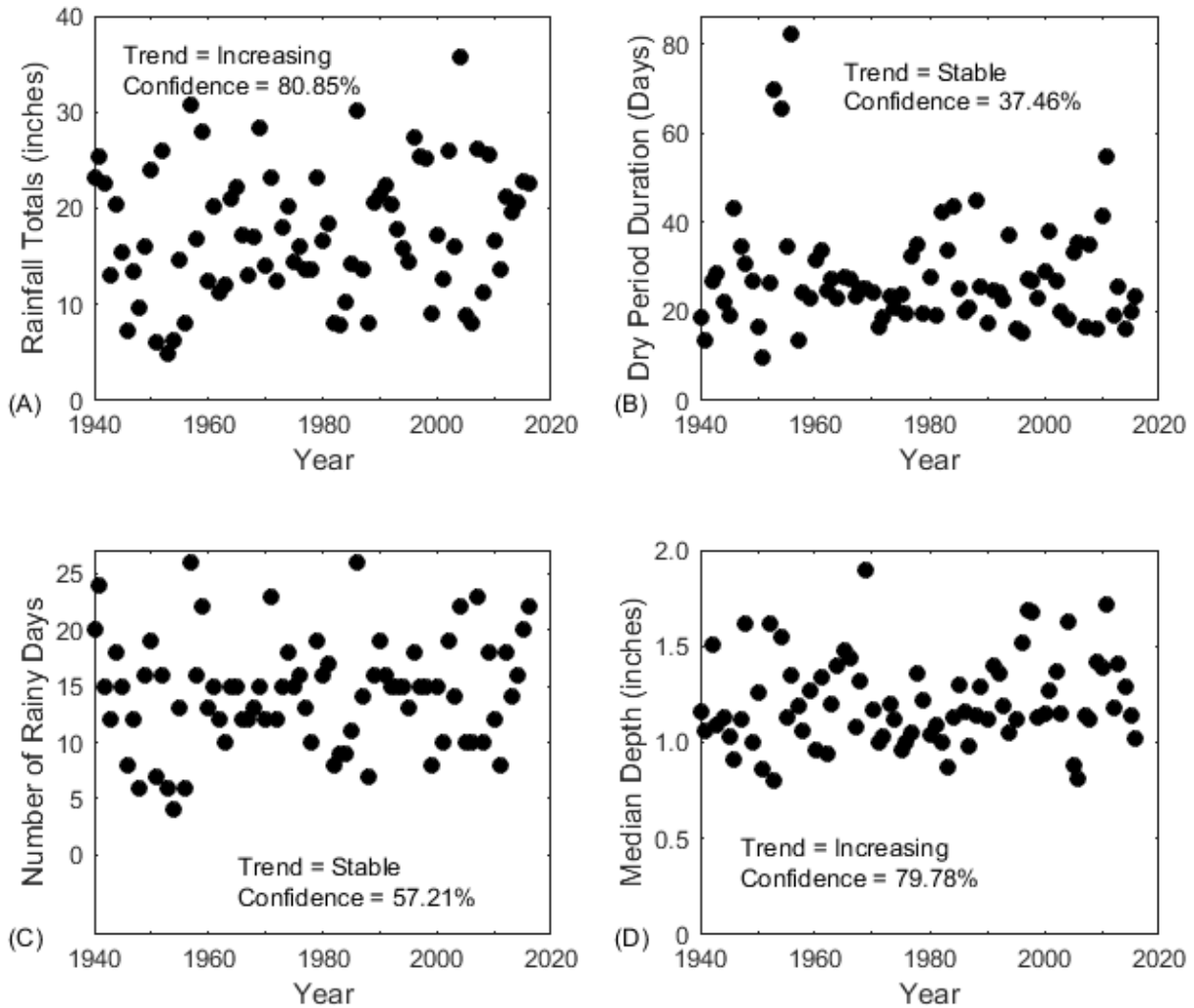


Figure 7-16 Precipitation Data for San Saba for the period 1940-2016, considering only runoff-producing rain events – A) Annual rainfall totals, B) average duration of dry periods, C) number of rainy days per year, D) median rainfall depth per year.

7.2.3 South Concho Watershed – Christoval

Precipitation data for Christoval, in the South Concho watershed (Section 7.1.4.1), was modified to include only rain events that would generate runoff, per the SCS curve number method. Results are shown in Figure 7-17.

Figure 7-17 Figure 7-14 presents calendar plots of rain events from the Christoval location, showing when rain occurred for each year from 1940-2016. Blue lines indicate days when rain was recorded, and black lines represent days when data was unavailable. Grey shading indicate the winter and summer months, as previously defined. Figure 7-17A shows all days when rainfall was recorded, with this data previously analyzed in Section 7.1.4.1. Figure 7-17B shows only the days in which the recorded rainfall was sufficient to generate runoff, per the SCS curve number method.

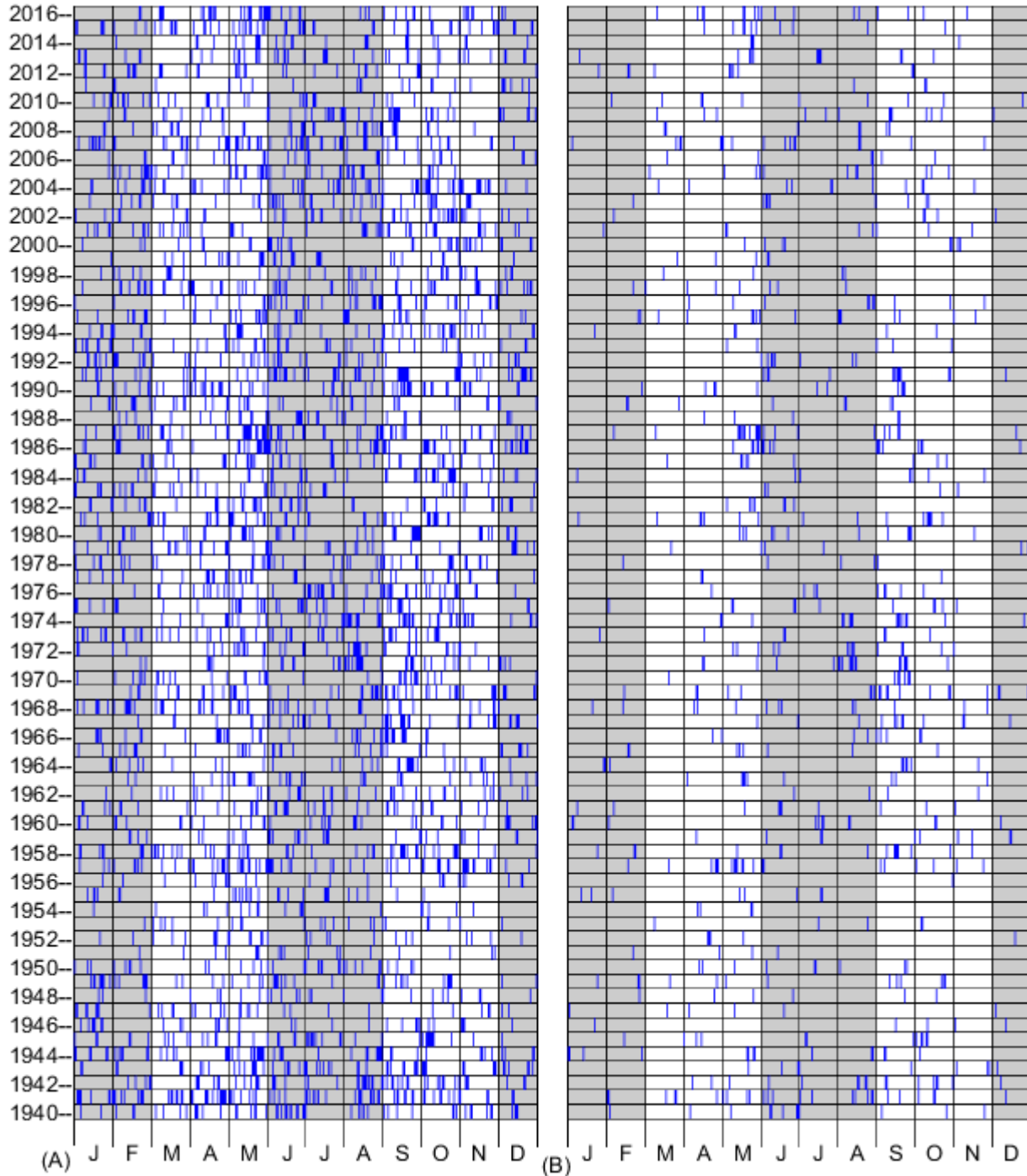


Figure 7-17 – Rainfall calendar plots for Christoval– A) All recorded rainfall, B) Only runoff-generating rainfall. BLUE bars indicate days when rainfall occurred. BLACK bars indicate days with missing data. Grey shading separates seasons (Winter, Spring, Summer, and Fall).

As shown in Figure 7-17, runoff-generating rain events are less frequent and tend to occur more often from April through October. The timing and frequency of runoff-generating events seems to compare better to that from San Saba (Figure 7-15) than from Ballinger (Figure 7-13).

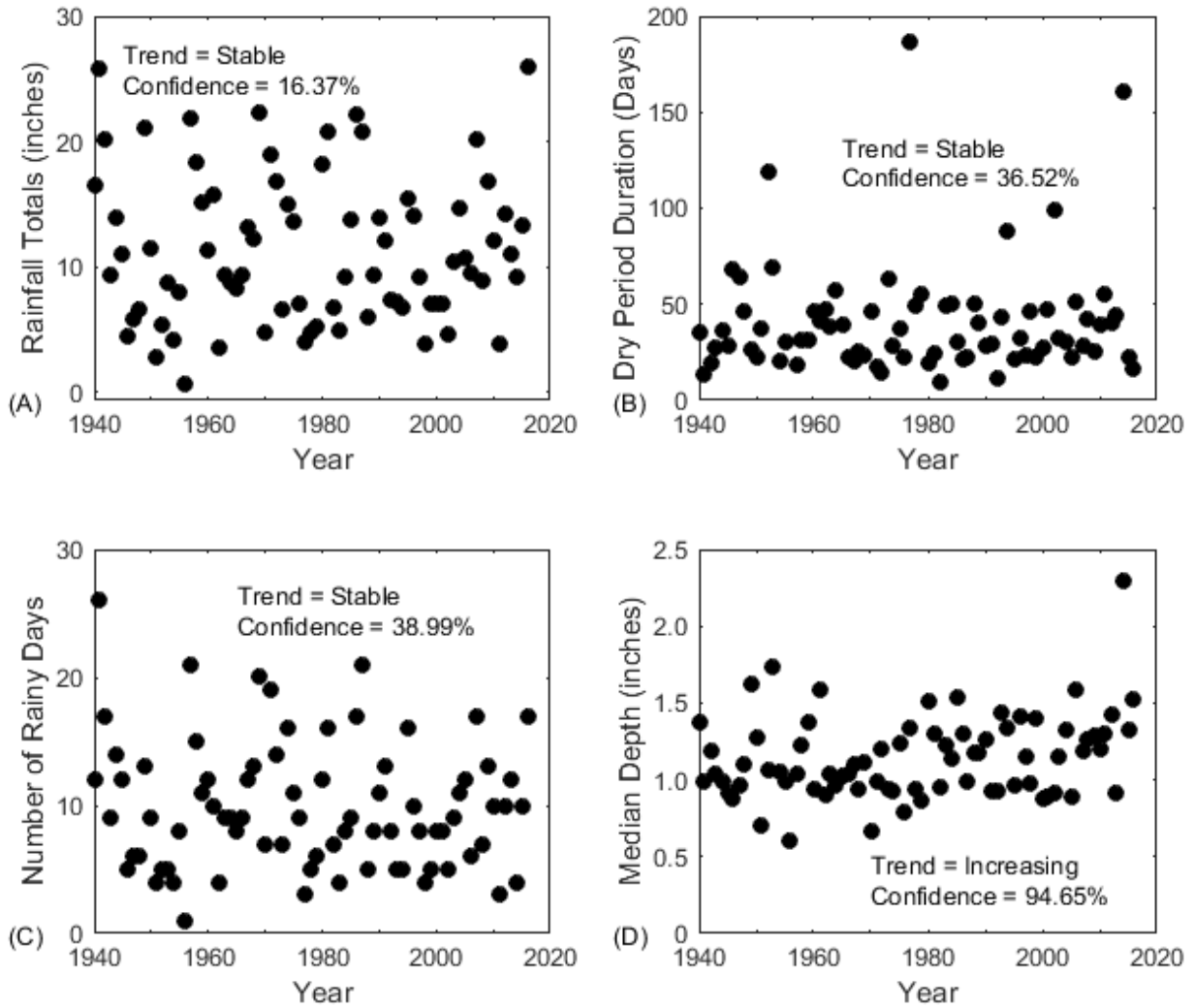


Figure 7-18 Precipitation Data for Christoval for the period 1940-2016, considering only runoff-producing rain events – A) Annual rainfall totals, B) average duration of dry periods, C) number of rainy days per year, D) median rainfall depth per year.

Figure 7-18 presents the statistical analysis of annual rainfall-related data for Christoval, considering only rainfall events that would generate runoff. As shown, total annual runoff-generating rainfall ranged from 1 to 26 inches per year, with a stable trend indicated over the 1940-2016 period of record (Figure 7-18A). Stable trends were also indicated for the average duration of dry periods between rainfall events (Figure 7-18B), yet as with data from Ballinger and San Saba there are general outliers during the driest years. A stable trend was also reported for the number of rainy days per year (Figure 7-18 C), yet an increasing trend was identified in the median depth of rainfall during the rainy days (Figure 7-18 D). This increasing trend is likely influenced by the outlier median depth computed for the year 2014, during which only 3 runoff-generating events occurred. Without this outlier, it is likely that the data would exhibit a stable trend with respect to median rainfall depth.

7.2.4 North Concho Watershed – Sterling City

Precipitation data for Sterling City, in the North Concho watershed (Section 7.1.5.3), was modified to include only rain events that would generate runoff, per the SCS curve number method. Results are shown in Figure 7-19.

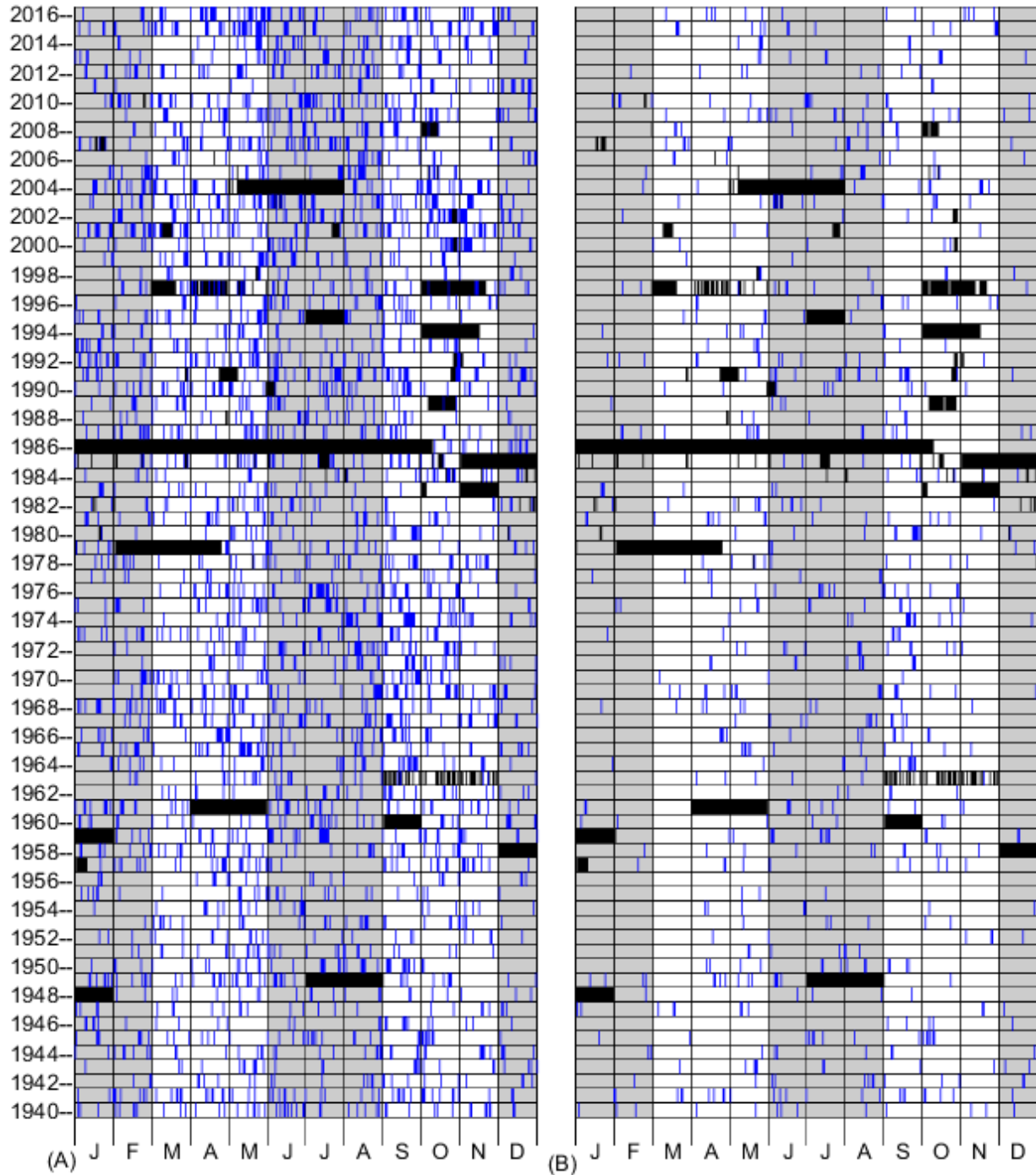


Figure 7-19 – Rainfall calendar plots for Sterling City for the period 1940-2016 – A) All recorded rainfall, B) Only runoff-generating rainfall. BLUE bars indicate days when rainfall occurred. BLACK bars indicate days with missing data. Grey shading separates seasons (Winter, Spring, Summer, and Fall).

Figure 7-19 Figure 7-14 presents calendar plots of rain events from the Sterling City location, showing when rain occurred for each year from 1940-2016. Blue lines indicate days when rain was recorded, and black lines represent days when data was unavailable. Grey shading indicate the winter and summer months, as previously defined. Figure 7-19A shows all days when rainfall was recorded, with this data previously analyzed in Section 7.1.5.3. Figure 7-19B shows only the days in which the recorded rainfall was sufficient to generate runoff, per the SCS curve number method.

As shown in Figure 7-19, runoff-generating rain events are less frequent and tend to occur more often from April through October. The timing and frequency of runoff-generating events seems to be less than those computed for each of the other study area watersheds.

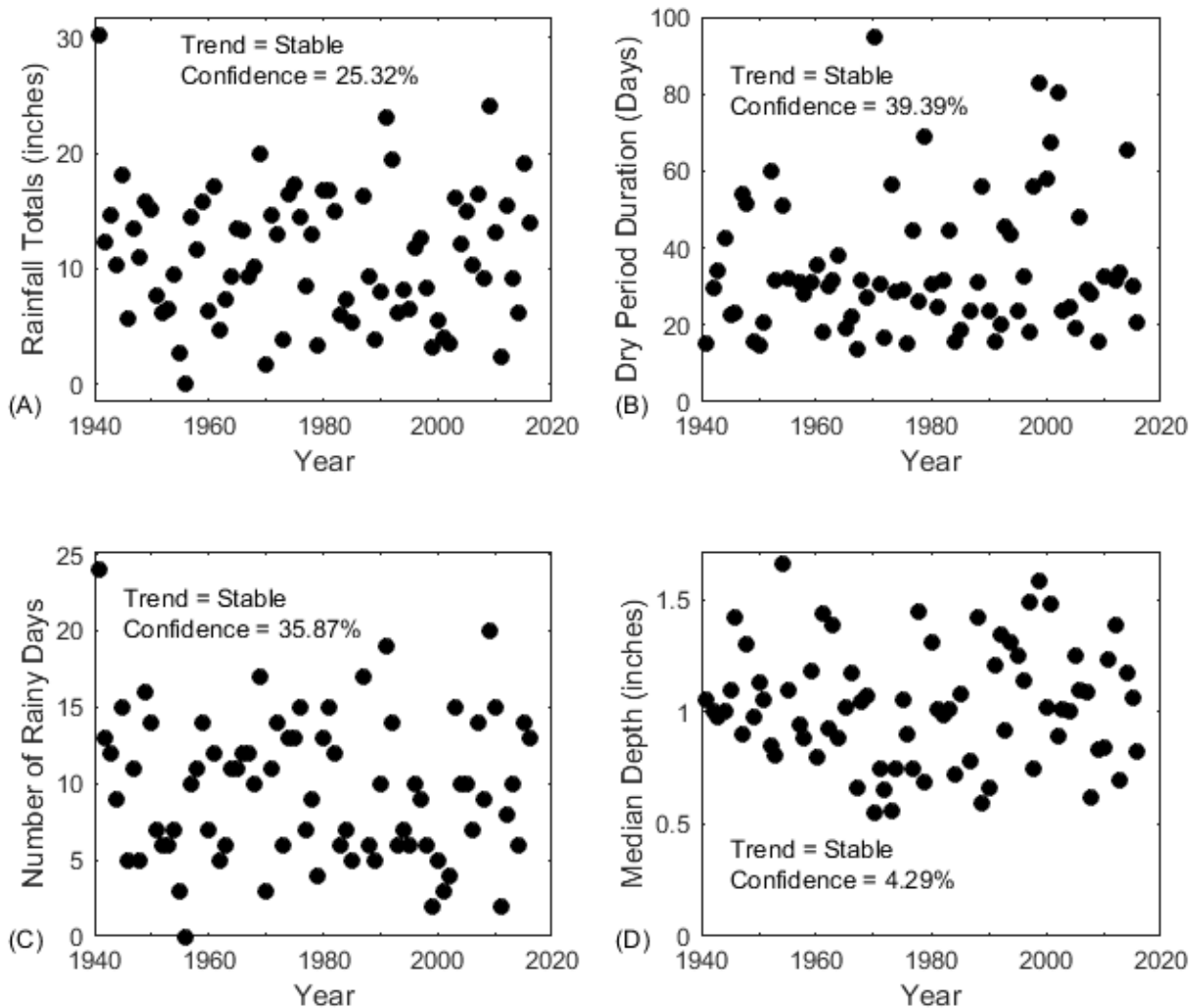


Figure 7-20 - Precipitation Data for Sterling City for the period 1940-2016, considering only runoff-producing rain events – A) Annual rainfall totals, B) average duration of dry periods, C) number of rainy days per year, D) median rainfall depth per year.

Figure 7-20 presents the statistical analysis of annual rainfall-related data for Sterling City, considering only rainfall events that would generate runoff. As shown, total annual runoff-generating rainfall ranged from 0 to 30 inches per year, with a stable trend indicated over the 1940-2016 period of record (Figure 7-20A). Stable trends were also indicated for the average duration of dry periods between rainfall events (Figure 7-20B), for the number of rainy days per year (Figure 7-20 C), and for the median depth of rainfall during the rainy days (Figure 7-20D). This general stability in time for rainfall patterns within the North Concho watershed should indicate that any changes in streamflow would not be due only to changes in rainfall amounts or temporal patterns.

7.3 Precipitation Trend Summary

As outlined in Sections 7.1.3-7.2, many precipitation stations indicate stable annual rainfall totals combined with increasing numbers of rainy days and decreasing median rainfall depths. This trend is evident most often within the North Concho watershed, and at both Menard and Brady within the San Saba watershed. No stations reported decreasing trends in annual total rainfall.

Many stations reported a shift in the timing of rainfall events during the spring months. In general, increasing rainfall totals were recorded in March, with corresponding decreasing totals reported for April. Increasing rainfall totals were also often reported for August.

For most locations, rainfall totals for winter months (December, January, and February) remained stable.

When considering only the larger rainfall events that will typically produce surface runoff, all watersheds seem to exhibit stable trends with respect to total annual rainfall and the frequency of rain events. Median rainfall depths show increasing or stable trends. The stability of runoff-generating rainfall events and totals over the period of record suggests that changes in rainfall patterns are not likely to be a main cause of observed changes in streamflow quantities.

8 Task 6 – Soil Moisture Data Analysis

Under this task, available soil moisture data for the study area watersheds was to be obtained and evaluated. The goal of this task was to determine the existence of trends in soil moisture for the subject watersheds, and ultimately to link the trends toward any observed trends in precipitation (Section 0) and streamflow (Section 0). In undertaking this task, soil moisture data from the Gravity Recovery and Climate Experiment (GRACE) satellite mission as well as from the Global Land Data Assimilation System (GLDAS) were obtained and analyzed.

8.1 GRACE Data Analysis

The Gravity Recovery and Climate Experiment (GRACE) is a project developed and maintained by the U.S. National Aeronautics and Space Administration (NASA). The project uses twin satellites which continuously orbit the earth measuring slight variations in local gravity. From these variations, in conjunction with land surface models, scientists are able to quantify and map groundwater and soil moisture indicators in support of weekly drought monitoring applications (Houborg, 2012). It is noted that output from GRACE data sources stems from vertical integration of the measure of water content, and therefore encompasses fluctuations in groundwater storage (deep and shallow), near-surface soil moisture, and surface water storage. Some researchers have noted there is uncertainty within the GRACE data that could mask the fluctuations in any of these vertically-integrated water storage entities, making accurate assessments of soil moisture content difficult to discern (Di Long, 2014). For the purposes of this Phase II assessment, the GRACE data processing methodology was not reviewed, and GRACE results were assumed to accurately represent soil moisture conditions within the subsurface of the study area watersheds. Conclusions drawn from analyses resulting from the GRACE satellite data are provided in reference to this assumption and the uncertainty attributed to GRACE results by some (but not all) researchers. Evaluating the validity of GRACE soil moisture data was outside the scope of this Phase II project.

GRACE Data is publically available and downloadable from numerous NASA websites. For this project, GRACE data was downloaded from <https://nasagrace.unl.edu/data/> in April of 2019. GRACE soil moisture data was downloaded and processed to provide bi-weekly assessments of soil moisture conditions on a 0.125° x 0.125° grid across the study area (Figure 8-1). Data was available for the time period from April 1, 2002 to April 29, 2019.

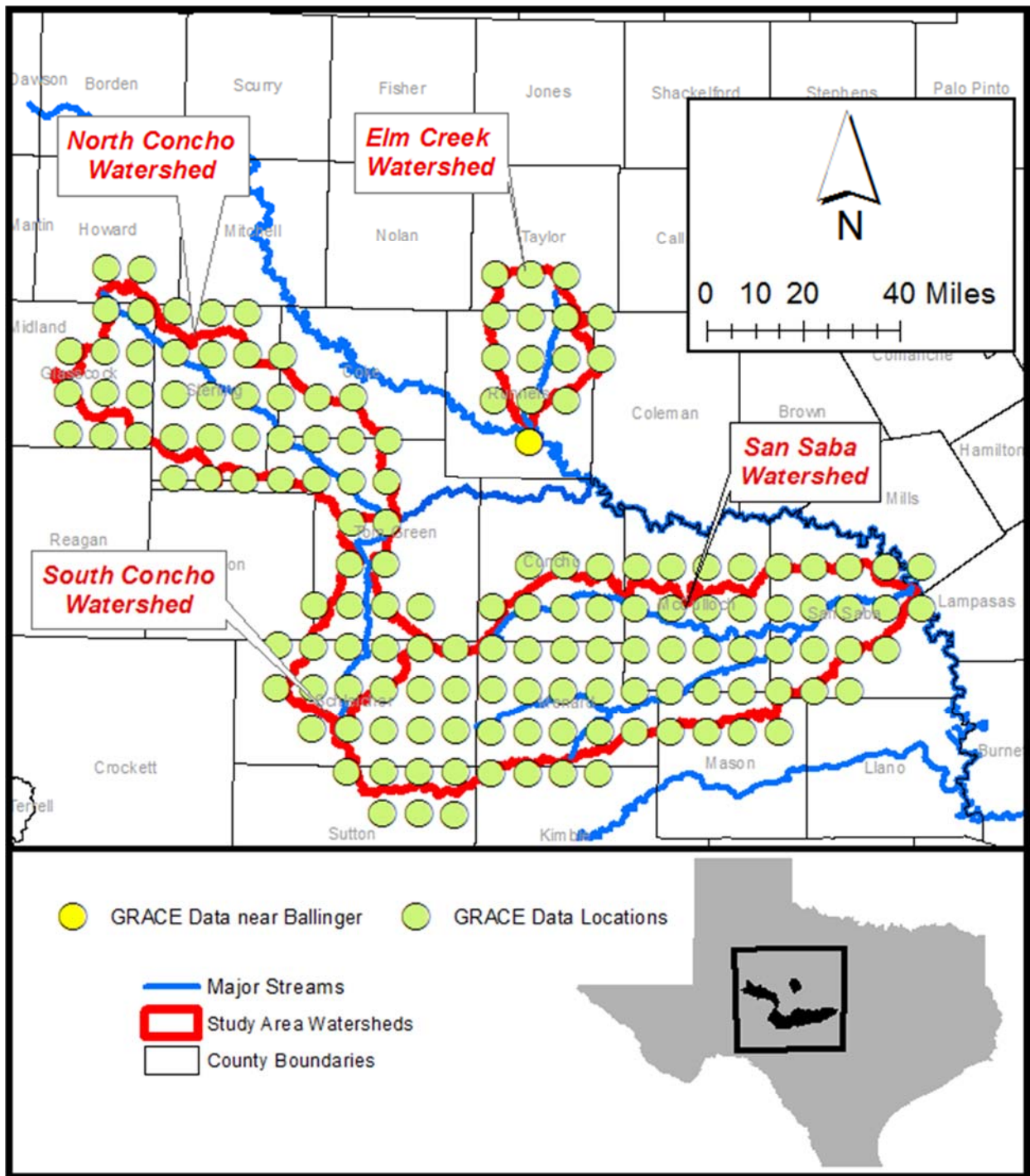


Figure 8-1 – Map showing locations of GRACE soil moisture data.

Figure 8-2 plots GRACE-derived soil moisture data for the location nearest to Ballinger at the southern end of the Elm Creek watershed (shown in YELLOW in Figure 8-1). GRACE data output for each location consists of the computed water storage content in the surface zone, root-zone, and as deeper groundwater storage. Storage in the surface zone reflects water content near the ground surface, and root-zone storage reflects water content below

the surface zone. Storage in the groundwater zone includes a total representation of water storage in the groundwater system, extending deeper than the portion of the surface aquifer that may contribute groundwater as baseflow to streams.

Figure 8-2 provides the time-series plots of storage in the surface, root-, and groundwater zones below Ballinger for the time period from late 2002 through 2016. Storage in each zone is plotted as a percentage of the maximum (and minimum) zone storage content computed over the period of record. Therefore instances where storage is shown as “100%” indicate that at that time, the GRACE data resulted in the largest storage quantity for the particular zone over the period of record. As such, as additional data is added to the period of record analysis, storage values could be updated if the new data suggest greater or lesser storage content than the previous maximum and minimum storage, respectively.

As shown in Figure 8-2A, storage within the surface zone fluctuates rapidly, and often changes from near 0% full to near 100% full within 1-2 bi-weekly satellite passes. This suggests that storage in the surface zone would quickly adjust based on recharge quantities from rain events, as well as evapotranspiration from the ground to the atmosphere.

Fluctuations within storage within the root-zone (Figure 8-2B) also occur rapidly, but not as rapidly as in the surface zone. Storage content within the root-zone shows similar patterns to that within the surface zone, likely indicating that root-zone content is also tied to groundwater recharge events and evaporative losses.

Fluctuations within the groundwater storage content are longer in time with respect to those within the surface and root-zones (Figure 8-2C). This likely reflects the concept that groundwater levels will respond more slowly to recharge events and evapotranspirative losses. However general trends within the groundwater storage time-series also tend to correspond to similar (but more rapid) fluctuations within the surface and root zones.

Within Figure 8-2, the time period labeled “#1” indicates an instance of groundwater replenishment that is common to all three datasets. Within this time from late 2011 to mid-2012, the storage content of all three zones increased from near record low values to high storage percentages. Storage within the surface water and root-zones increased from near 0% to near 100%, with fluctuations occurring over the time period. Storage within the groundwater zone increased from 10% to 80%, without the fluctuations evident in the data from the surface and root-zones. This indicates that overall groundwater replenishment can occur with replenishment within the surface and root zones, but that groundwater replenishment may not be to the same degree or with the same rapidity.

The time period labeled “#2” in Figure 8-2 shows a period where storage in all three zones decreased rapidly and then increased to levels greater than the original level at the beginning of the selected time period. The decrease and increase in surface and root-zone storage again occurred more rapidly than in the groundwater storage, and the overall change in groundwater storage was of a lessor magnitude than the storage changes in the other zones. This supports the notion that surface and root-zone water content will respond quicker to surface conditions (such as rainfall and evapotranspiration).

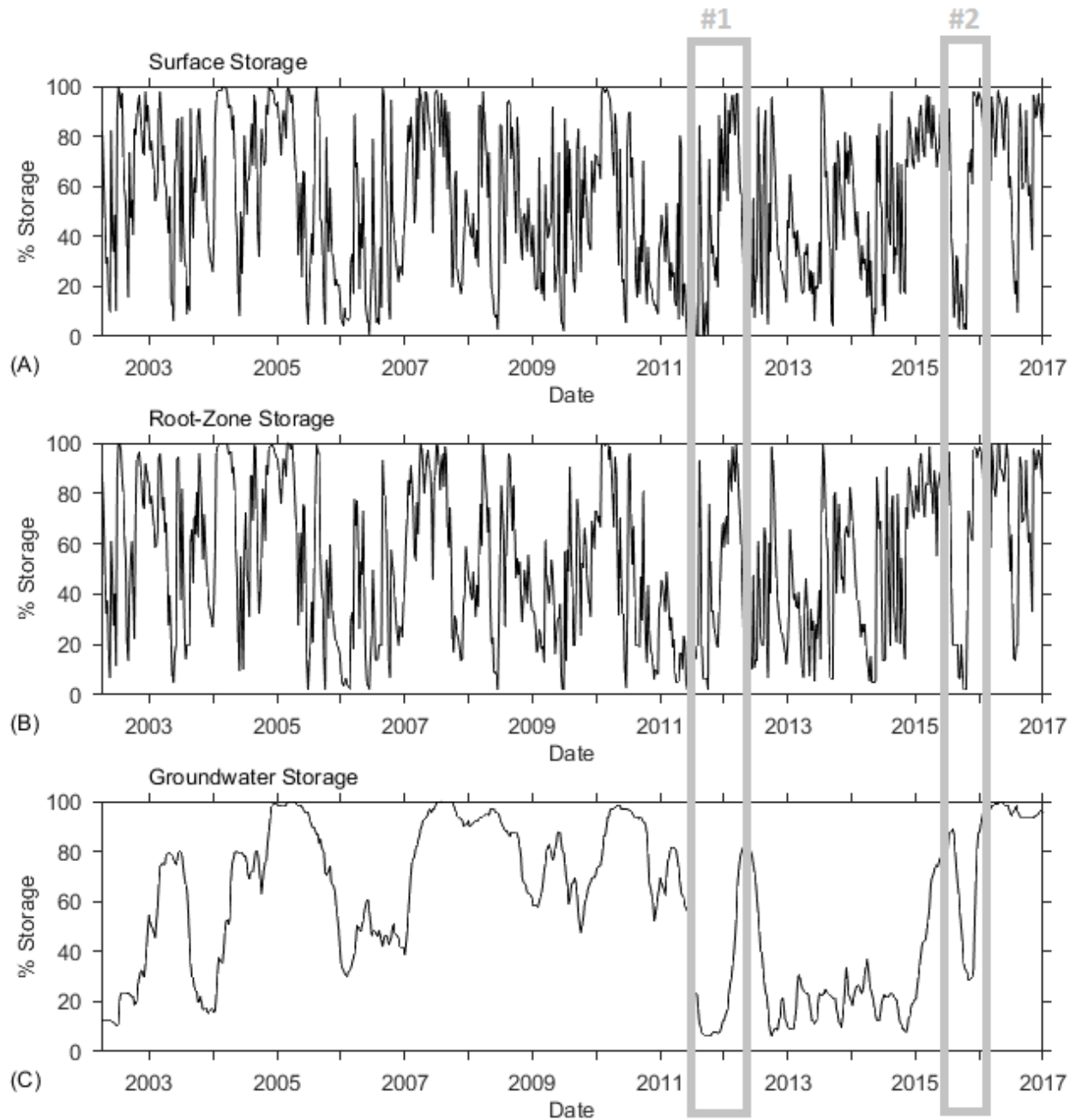


Figure 8-2 – GRACE storage data for Ballinger for late 2002-2016, TX – A) surface storage, B) root-zone storage, C) groundwater storage

Figure 8-3 presents the GRACE surface storage data from Ballinger (Figure 8-2A) with time series of rainfall (Section 7.1.1.1) and streamflow (Section 6.1). As shown, during the 2002-2016 period for which GRACE data is available, there were 8 instances when Elm Creek streamflow exceeded 1000 cfs. In general, the times of these higher streamflow events corresponded with times of higher recorded rainfall, yet not all high rainfall events produced runoff. The times of the higher streamflow events also corresponded to times when the GRACE data indicated that surface storage was high (above 80%).

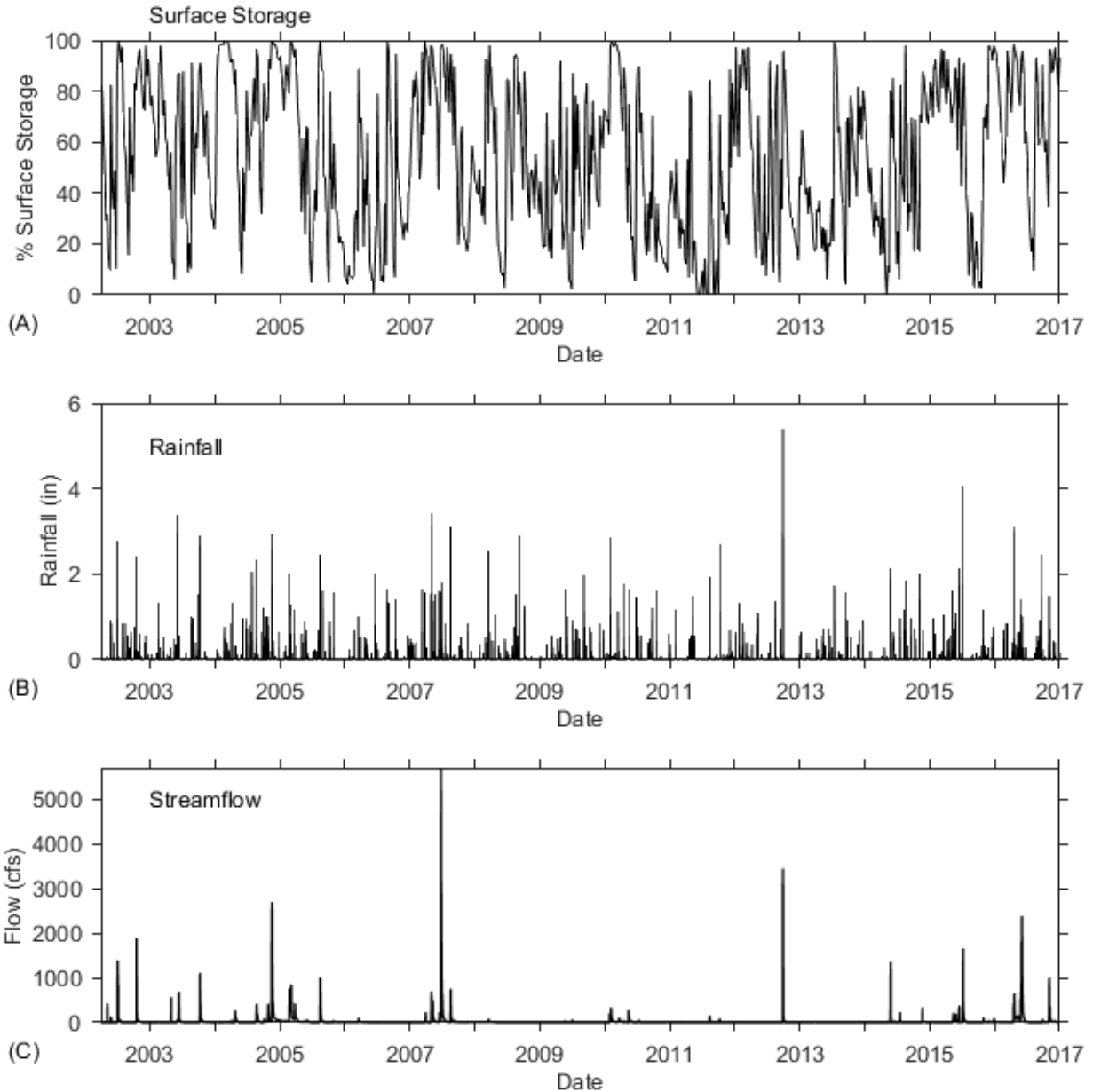


Figure 8-3 – GRACE, rainfall, and streamflow data for Ballinger for the period 2002-2016 – A) GRACE surface storage data, B) rainfall data from Ballinger, C) streamflow data from Elm Creek at Ballinger

Figure 8-4 presents the same data as included in Figure 8-3, yet focuses on year 2007 which contained the largest streamflow event occurring during the period for which GRACE data are available. During 2007, the surface storage started at 0% and then increased to 80% due to rainfall events in January. These rainfall events only replenished the surface storage, as they did not result in any streamflow increases. Lack of rain in February caused the reduction in surface storage and the continued low quantity of streamflow. Rains in March caused surface storage to refill, and resulted in an increase in streamflow at the end of the month. The timing of the increased streamflow corresponds to a larger rainfall event and to the filling of the surface storage at the end of March.

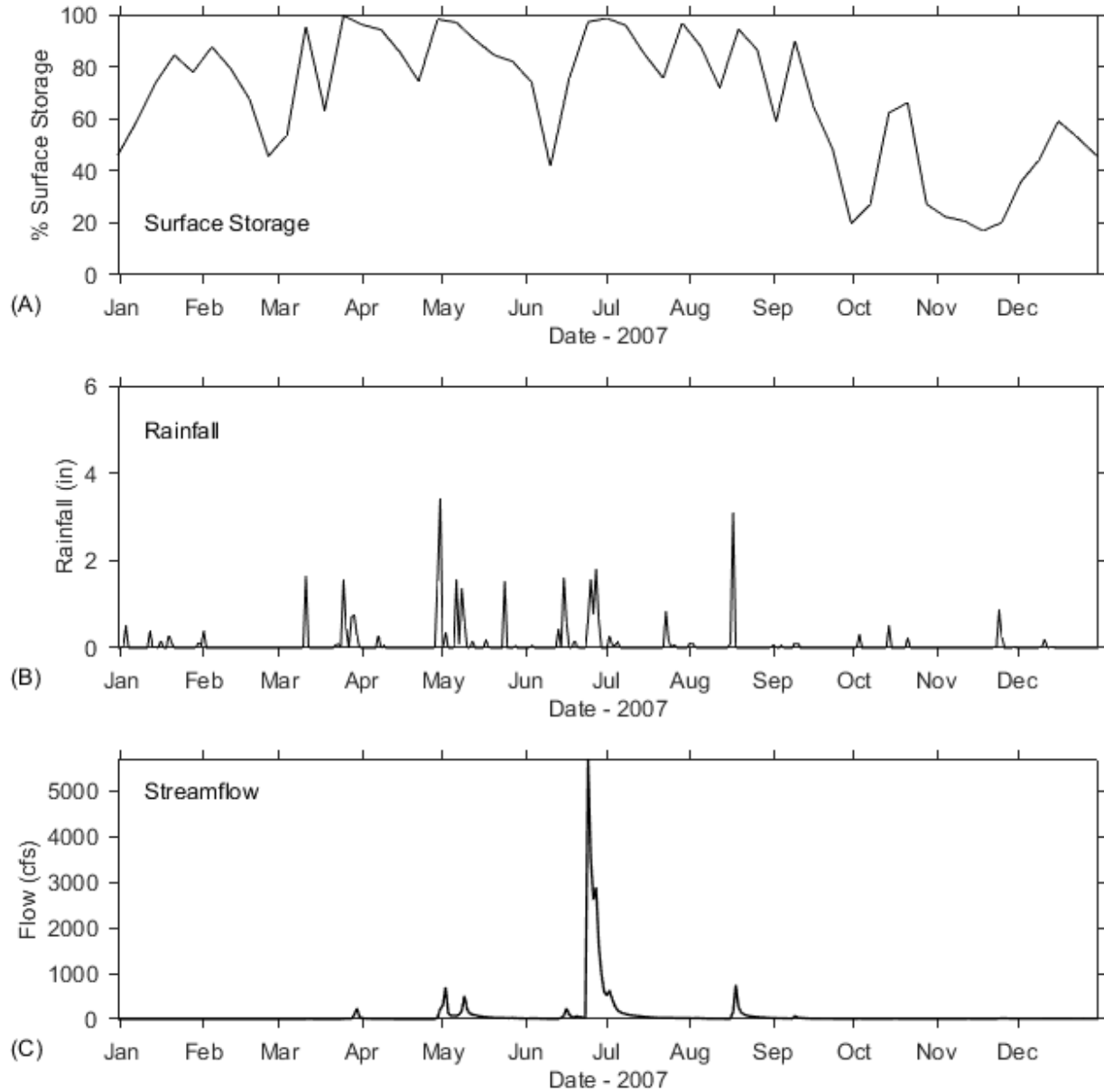


Figure 8-4 -- GRACE, rainfall, and streamflow data for Ballinger for 2007-- A) GRACE surface storage data, B) rainfall data from Ballinger, C) streamflow data from Elm Creek at Ballinger

A dry April causes a reduction in surface storage, which was replaced in early May as the result of a runoff-generating rainfall event that contributed to a streamflow increase. Surface storage continued to decrease in May despite the frequent rainfall events, which may be indicative of increased evapotranspiration losses due to increased May temperatures. By June, surface storage had returned to its January level (40%) only to increase rapidly due to a 1.5-inch rainfall event occurring in mid-month. This rain event was followed by successive days of sustained 1.5-inch/day rainfall, which resulted in the filling of the surface storage and the rapid increase in streamflow to over 5,000 cfs. After the high flow event, surface storage decreased and increased due to periodic dry and wet

periods. It is notable that the 3-inch rain-event which occurred in mid-August was insufficient to refill the surface storage, and only resulted in a streamflow of approximately 1000 cfs. Smaller rain events from September-December 2007 did little to refill the surface storage, and did not result in increases in streamflow.

Figure 8-3 highlights the connection and interplay between soil moisture content, rainfall, and streamflow for the Ballinger area, and demonstrates how high soil moisture content is needed to generate streamflow from short-duration, low intensity rain events. It also demonstrates how decreases in surface storage in the GRACE data correspond to time periods without rainfall or significant streamflow.

Figure 8-5 presents the same surface storage, rainfall, and streamflow data for Ballinger as presented in Figure 8-3, yet for the time period from January 2012 to December 2013. As shown, streamflow during this period was low, with the exception of a large flow event that occurred around October 1, 2012. This large streamflow event (3,500 cfs) resulted from a 5-inch rainfall in late September 2012. At the time of the rainfall event, surface storage was increasing, from a low (5%) in early September and had reached 40% just prior to the rainfall event. The large rainfall event resulted in the increase in surface storage to near 100%, and caused the increase in streamflow. After the October 2012 rain event, and extended dry period resulted in the reduction in surface storage, which continued through small rainfall events throughout 2013. A larger rainfall event in July 2013 was able to refill surface storage, but was insufficient to result in increased streamflow at Ballinger.

In comparing Figure 8-4 and Figure 8-5, it is evident that it is the interplay between surface storage and rainfall that results in larger streamflow events. During 2007, the 5,000 cfs streamflow event was generated by a prolonged 1.5 inch/day series of rainfall events, which also commenced at a time when surface storage was above 75% and increasing. In contrast, in 2012 a more-intense, shorter duration rainfall event resulted in a short-lived increase in streamflow only after surface storage levels were replenished. The intense rain event occurred at a time when GRACE data indicated the surface storage was at 40% and decreasing. Had the storage been higher prior to the intense rainfall event, it is likely that the resulting streamflow would have been higher.

The GRACE data shown in Figure 8-2 to Figure 8-5, with the corresponding analysis, demonstrates the relationship between surface storage content, rainfall, and runoff for the Ballinger area. Further study of the GRACE data could be undertaken to assess the data utility for runoff prediction. Trends in the GRACE data are not readily analyzable with the Mann-Kendall technique. This fact, combined with the lack of data prior to 2002 negated the utility in applying further analyses to the GRACE datasets. The GRACE datasets, however, did provide useful insight into the interaction between the soil moisture levels and rainfall in order to produce runoff and increase streamflow. It demonstrates, for the Ballinger TX area at least, that the study area creates runoff when soil moisture levels are high, and that the generated runoff will increase only after the surface storage is sufficiently refilled.

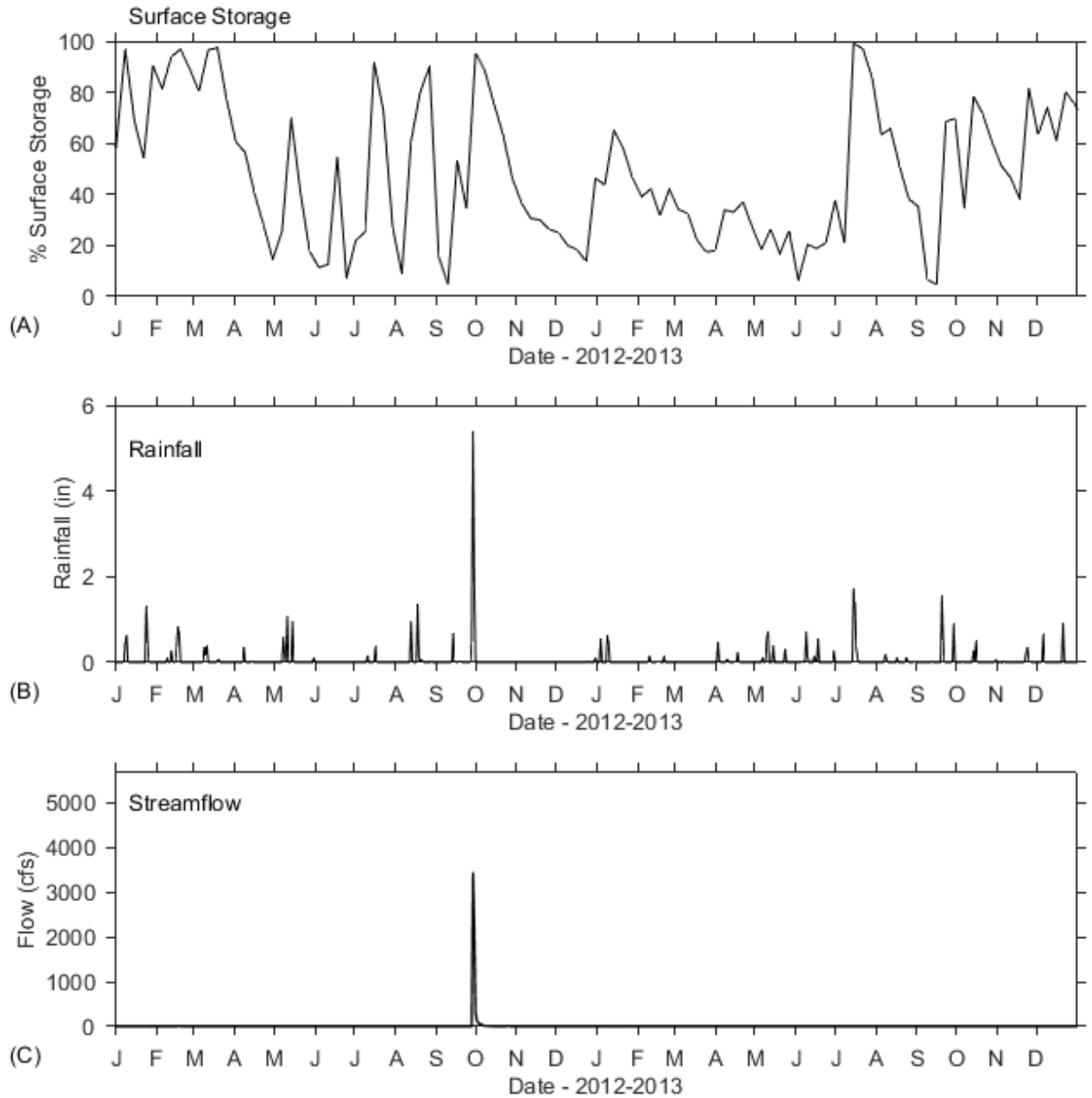


Figure 8-5 – GRACE, rainfall, and streamflow data for Ballinger for 2012-2013– A) GRACE surface storage data, B) rainfall data from Ballinger, C) streamflow data from Elm Creek at Ballinger

Given the general agreement between GRACE data, rainfall, streamflow, and hydrologic theory, LRE Water concludes that the GRACE data may provide reliable evidence of soil moisture within the study area watersheds, despite the conclusions of selected researchers (Di Long, 2014). LRE Water has not thoroughly investigated the GRACE dataset and processing methodologies, however, and has not conducted the level of research into GRACE that has been undertaken by other GRACE users and researchers.

8.2 Google Earth Engine (GEE) Analysis

As identified during the small pond detection portion of Task 2 (Section 4.1.2), Google Earth Engine (GEE) is a powerful processing software package capable of extracting spatially variable data from large georeferenced databases. To better assess soil moisture trends within the study areas, GEE was utilized to obtain and process Global Land Data Assimilation System (GLDAS) data. Data was then transferred into georeferenced TIF format files suitable for display and query within ArcGIS system software. Additional information regarding the GLDAS data is available at <https://ldas.gsfc.nasa.gov/gldas> (as of 7/6/2019).

GLDAS data was available for the study area from 1948-2019, yet obtaining this complete set of data required extracting data from two separate GLDAS databases. Specifically the Reprocessed GLDAS 2-0 dataset yielded data from 1948-2000, and the GLDAS 2.1 dataset yielded data for 2001-2019. Combining data from separate GLDAS databases was not expected to yield inconsistencies in the analysis results. Data was extracted using customized GEE scripts as median annual soil moisture values, reported in kg/m² of surface area. The data exported from GEE corresponds to the soil moisture content found at depths between 40cm and 100cm.

Figure 8-6 provides a map view of the GLDAS soil moisture data for 2011. Data is provided along a regular 0.25° x 0.25° grid, clipped to the extent of the study area watersheds. Values shown for the San Saba watershed in Figure 8-6 range from between 45 kg/m² to 140 kg/m², with the higher values located in the western portion of the watershed. This indicates that spatial variability in soil moisture is likely within the watershed, at least according to the GLDAS models. Figure 8-6 indicates that even during an extremely dry year like 2011, the upper reaches of the San Saba watershed, as well as the entire South Concho watershed and lower portions of the North Concho watershed, retained significant quantities of water within the upper soil layers. This result is consistent the fact that the South Concho River at Christoval never ran dry (Section 7.1.4.1). It is also notable that the greatest soil moisture content shown in Figure 8-6 is located in areas of large reservoirs that typically are not full. These reservoirs include Twin Buttes Reservoir, Lake Nasworthy, and OC Fisher Lake.

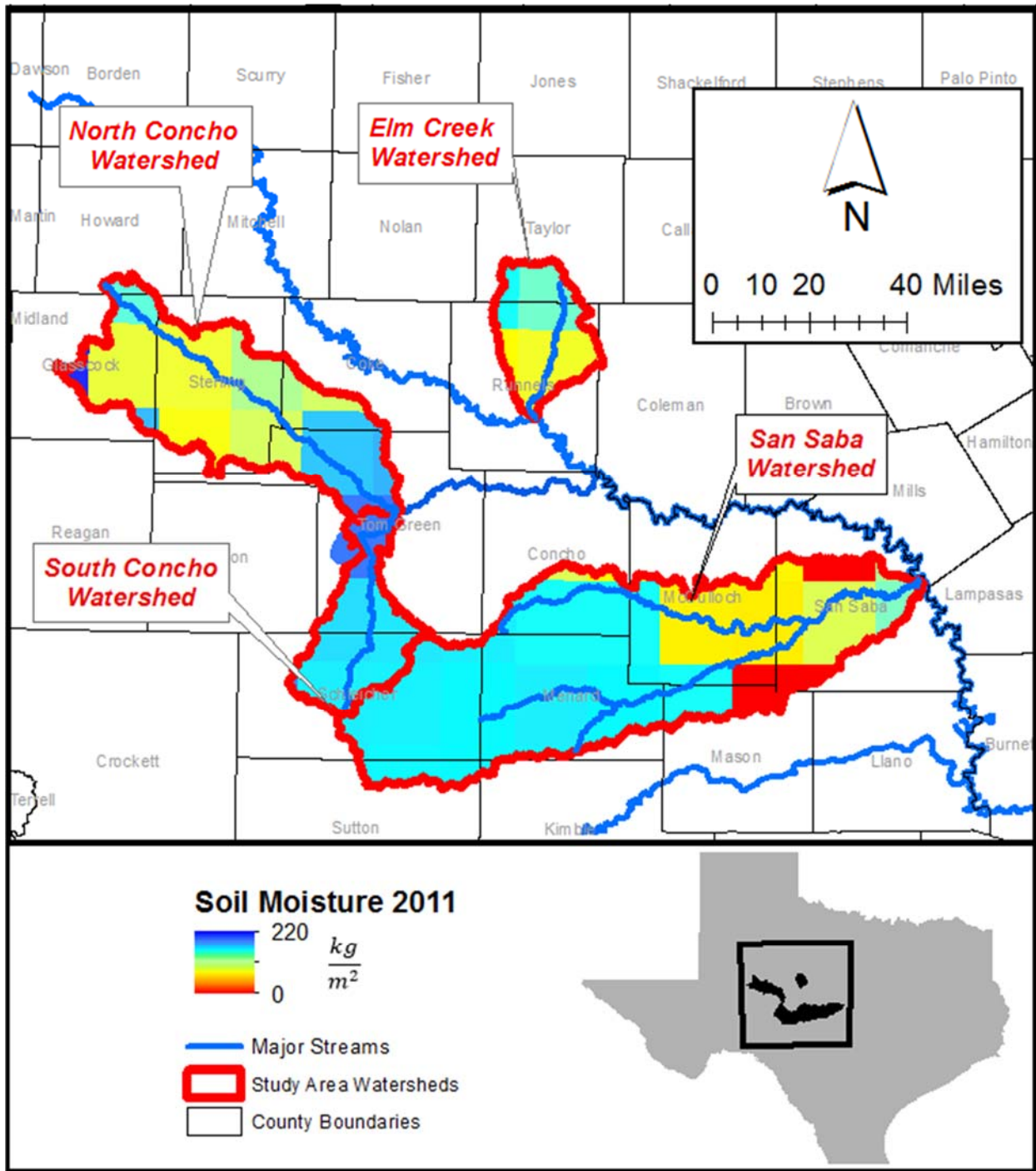


Figure 8-6 – Sample GLDAS soil moisture data for the study area watersheds.

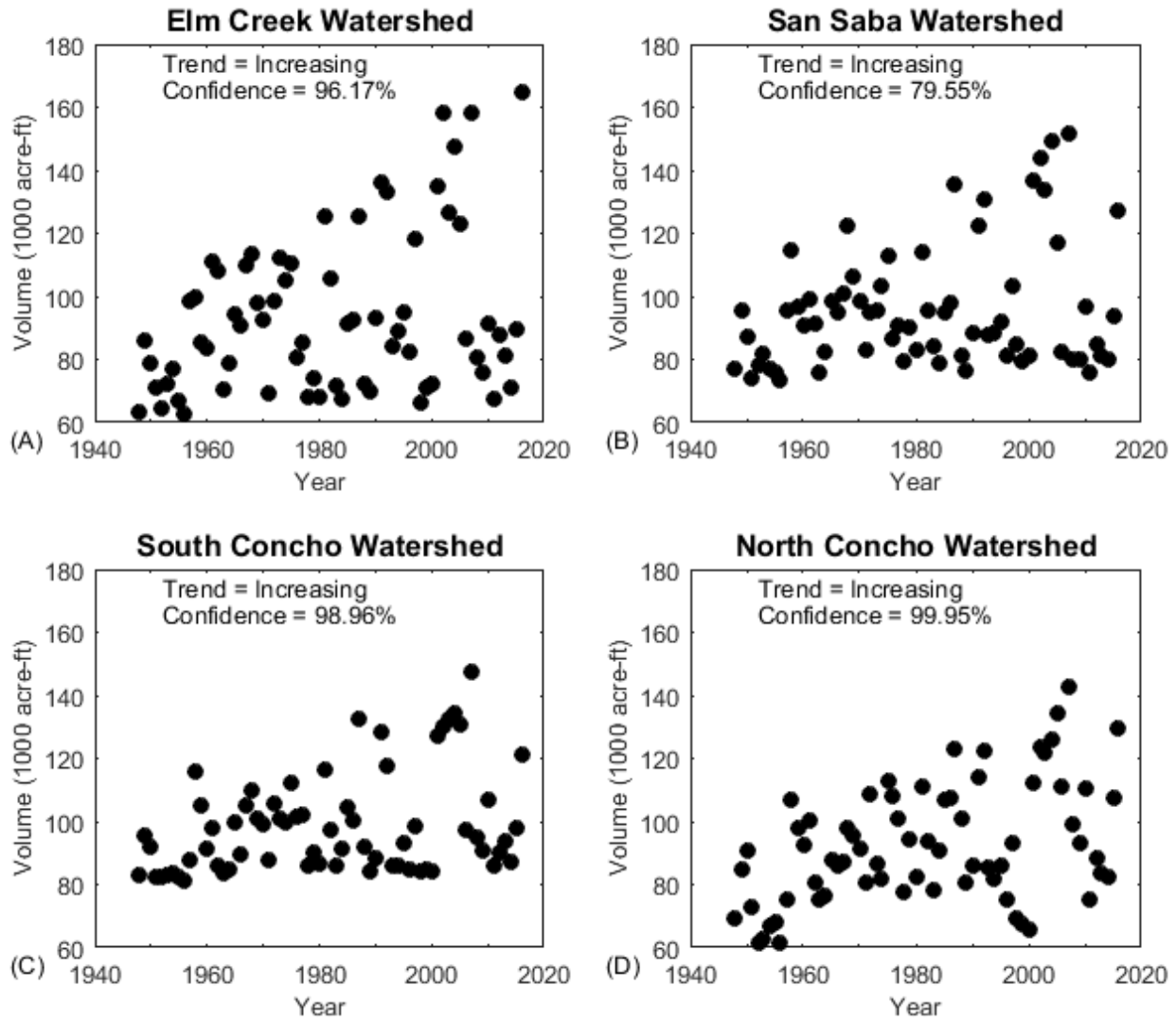


Figure 8-7 – Mann-Kendall analysis results of GLDAS soil moisture data by watershed

Figure 8-7 presents the area-weighted average soil moisture content by year for each study area watershed. GLDAS data output was processed within ArcGIS to convert the mass per land surface area values into volumes of water, assuming a water density of 1000 kg/m². As shown, all watersheds show increasing trends in soil water volume from 1948-2019. Each watershed also demonstrates year-to-year variability in the soil water volume values, reflecting that conditions will adjust rapidly due to rainfall, evapotranspiration, infiltration, and potential usage, diversion, or transport of the shallow groundwater. It is notable that for each watershed, the lowest soil water volumes were computed for the 1950's drought, rather than for the more recent 2008-2016 Colorado River Basin drought.

8.3 Soil Water Balance Modeling

To supplement our analysis of soil moisture data, we also developed a soil-water-balance (SWB) model for the period from January 1, 1981 through December 31, 2017. This effort was not included in the Phase II scope of work, yet was undertaken in addition to all other tasks in order to evaluate the SWB. For the model we used the SWB code developed by the USGS to evaluate the spatial and temporal variations in potential groundwater recharge (Westenbroek and others, 2010). The SWB code uses a combination of gridded and tabular data to calculate potential groundwater recharge separately for each grid cell within a model domain. The SWB code evaluates the sources and sinks of water within each grid cell at and near land surface and then calculates recharge as the difference between the change in soil moisture and the sources and sinks. Sources for recharge include precipitation and inflow (surface runoff from an adjacent grid cell) while sinks include evapotranspiration, outflow (surface runoff to an adjacent grid cell), and interception (rainfall trapped and used by vegetation and evaporated or transpired from plant surfaces).

Westenbroek and others (2010) indicate that the SWB code uses a modified form of the Thornthwaite-Mather soil-water accounting method (Thornthwaite and Mather, 1957) to calculate the potential groundwater recharge. One of the key components in the recharge equation is the change in soil moisture. Using precipitation and calculated evapotranspiration, the SWB code models the amount of soil moisture in each grid cell with amounts greater than the soils' maximum water-holding capacity being converted to potential groundwater recharge (Westenbroek and others, 2010)¹.

8.3.1 SWB Model Domain and Input Data

We set up the SWB model domain to include all four study area basins. We then divided the model domain into a regular grid of 1,000 columns and 600 rows with each model cell side being 1,000 feet and covering an area of 1,000,000 square feet (approximately 23 acres). We defined the location of the grid using the TWDB Groundwater Availability Modeling projection system (see The SWB model requires gridded data for the hydrogeologic soil group, land-use/land-cover, available soil-water capacity, and surface-water flow direction. In addition, the model requires climate data such as daily precipitation, daily minimum temperature, and daily maximum temperature in either a tabular or gridded format. For our model we used the gridded climate data obtained from the PRISM Climate Group . The SWB model also requires standard tables defining soil-moisture accounting and land use characteristics for performing the calculations.

¹ We have provided a very brief representation of the SWB code. Please refer to the SWB code documentation for the complete details on the calculation of the water-balance components.

Table 8-1) with the lower-left corner of the grid located at coordinates 4400000.0 easting and 19440000.0 northing.

The SWB model requires gridded data for the hydrogeologic soil group, land-use/land-cover, available soil-water capacity, and surface-water flow direction. In addition, the model requires climate data such as daily precipitation, daily minimum temperature, and daily maximum temperature in either a tabular or gridded format. For our model we used the gridded climate data obtained from the PRISM Climate Group (PCGOSU, 2018). The SWB model also requires standard tables defining soil-moisture accounting and land use characteristics for performing the calculations.

Table 8-1. Description of the TWDB Groundwater Availability Modeling projection system.

Parameter	Value
Geographic Coordinate System	North American 1983
Angular Unit	Degree (0.0174532925199433)
Prime Meridian	Greenwich (0.0)
Datum	North American 1983
Spheriod	GRS 1980
Semimajor Axis	6378137.0
Semiminor Axis	6356752.314140356
Inverse Flattening	298.257222101
Projection	Albers
False Easting	4921250.0
False Northing	19685000.0
Central Meridian	-100.0
Standard Parallel 1	27.5
Standard Parallel 2	35.0
Latitude of Origin	31.25
Liner Unit	Foot (0.3048006096012192)

The land-use lookup table provides information regarding the Natural Resources Conservation Service (NRCS) curve number, rooting depth, interception, and maximum daily recharge specific to a land-use type. The second standard input is the Thornthwaite-Mather soil moisture retention table which is provided with the SWB code. The second input required no modification, but we did update the land-use lookup table for the runoff curve number, maximum recharge, and interception for the study area using NRCS publication “Urban Hydrology for Small Watersheds” (1986).

We obtained land-use/land cover data for the years 1992 (Vogelmann and others, 2001), 2001 (Homer and others, 2007), 2006 (Fry and others, 2011), and 2011 (Homer and others, 2015) from the Multi-Resolution Land Characteristics (MRLC) Consortium (<http://www.mrlc.gov/>, accessed July 2018). The gridded data provides a classification of the land use at a spatial resolution of 30 meters (about 100 feet). To match the model grid resolution, we re-sampled the grid to the coarser resolution by assigning the land-use classification that compromises the greatest area within the larger grid cell. We then simplified the land use types into 14 categories from the MRLC datasets. Figure 4-14 illustrates the land use/land cover SWB model input for 2017 and Table 4-3 provides the runoff curve number for each land use description.

We developed the hydrogeologic soil group and soil-water capacity data from datasets available from the NRCS (2018). Like the land-use/land-cover data, we used the model grid dimensions to calculate the area of each cell that intersected a defined hydrogeologic soil group and assigned the group covering the most area of the cell as the single cell integer value. We used the same process to assign the soil-water capacity values as a real number to create a gridded dataset. Figure 4-15 illustrates the hydrologic soil group designations in the study area and Figure 8-8 illustrates the available water capacity for each SWB model cell.

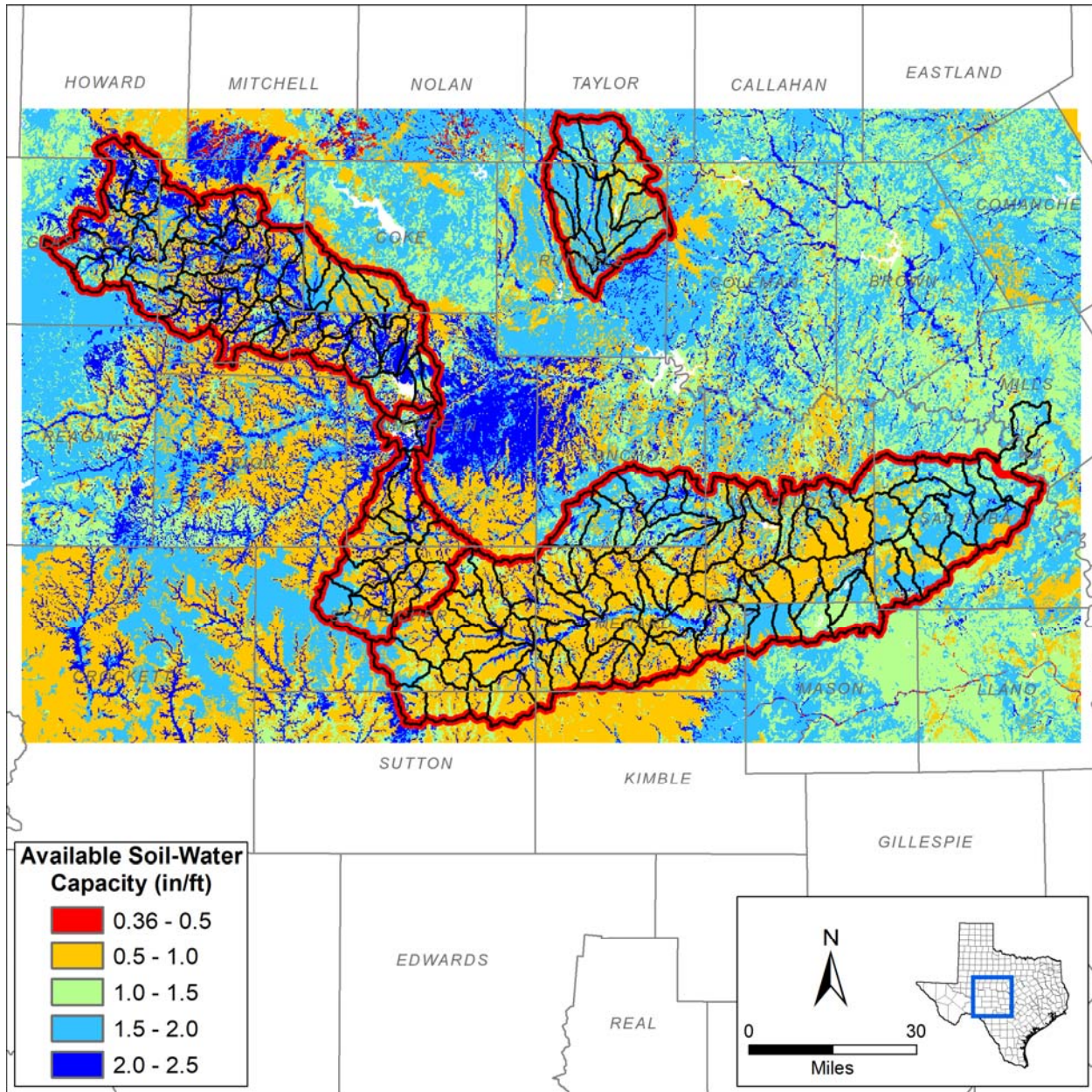


Figure 8-8. Available soil-water capacity per NRCS datasets.

As mentioned above, the SWB model can use either gridded climate data or tabular data from a single station. To better represent the climate across the study area, we used gridded temperature and precipitation data obtained from the PRISM Climate Group (PCGOSU, 2018). After obtaining datasets for daily precipitation, daily minimum temperature, and daily maximum temperature from January 1, 1981 through December 31, 2017 from the PRISM Climate Group, we clipped and re-sampled the grids to match our model domain and cell size. We limited our data collection from the PRISM Climate Group to no earlier than 1981 because earlier years only have datasets representing a monthly time period. Also, we did not collect data beyond 2017 as this year represent the last full year of “stable” daily data (PCGOSU, 2018). Note: within the SWB we used the PRISM data

in order to evaluate the impacts of temporal and spatial variation on SWB results. As such, the SWB timeframe is limited to 1981 to 2017. An alternative approach would be to utilize the temperature and precipitation data discussed in Section 5 and Section 7, respectively, to apply the SWB calculations over the full 1940-2016 project period of record. Doing so, however, would have limited the spatial variability in the model results.

Within the SWB model, we selected the Hargreaves-Samani method to calculate potential evapotranspiration. The Hargreaves-Samani method is the only method where the SWB model code will produce a spatially variable estimate of potential evapotranspiration (Westenbroek and others, 2010). While other options are available for estimating potential evapotranspiration within the model, the other methods produce a spatially uniform estimate of potential evapotranspiration across the entire model domain.

8.3.2 SWB Model Results

We performed the SWB simulation to represent the period from January 1, 1981 through December 31, 2017. The SWB model code provides results at a daily time scale. However, when considering groundwater recharge Westenbroek and others (2010) advise that limitations of the method make it most appropriate to present results as monthly or annual estimates at the small catchment scale. As such, we limited our interpretation of the SWB model results to trends in the simulated conditions at an annual scale to assess how the changes may affect conditions in the study-area watersheds. We also computed results for each of the level 6 hydrologic units within the study area watersheds.

Figure 8-9 is a chart of the annual actual evapotranspiration within the study area watersheds. Mann-Kendall analysis indicates that actual evapotranspiration exhibits stable trends for each watershed over the 1981-2017 modeled period of record. Actual evapotranspiration values for the watersheds range from 6 to 30 inches/year. While the rate of actual evapotranspiration is relatively stable during the first 15 years of the simulation, the year-to-year variation in values appears to increase from 1995 onward. These results for later years reflect greater volatility in the modeled climatic conditions (rainfall and temperature).

Figure 8-10 is a chart of the annual potential evapotranspiration within the study area watersheds. Mann-Kendall analysis indicates that potential evapotranspiration exhibits stable trends for each watershed over the 1981-2017 modeled period of record. Potential evapotranspiration values for the watersheds range from 54 to 67 inches/year. While the rate of potential evapotranspiration is relatively stable during the first 15 years of the simulation, the year-to-year variation in values appears to increase from 1995 onward. These results for later years reflect greater volatility in the modeled climatic conditions (rainfall and temperature).

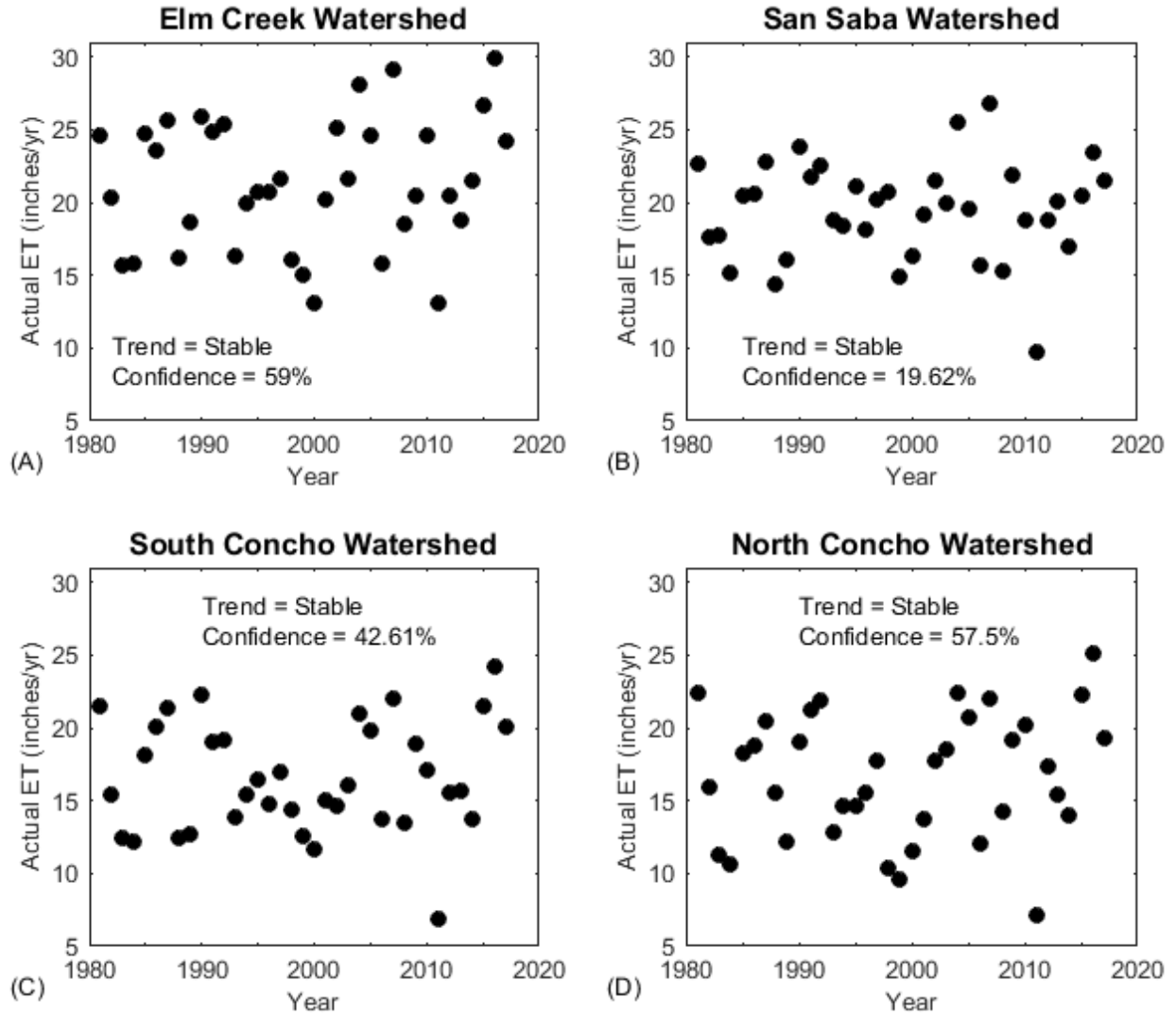


Figure 8-9. Annual actual evapotranspiration calculated by the SWB model for 1981-2017 – A) Elm Creek watershed, B) San Saba watershed, C) South Concho watershed, D) North Concho watershed.

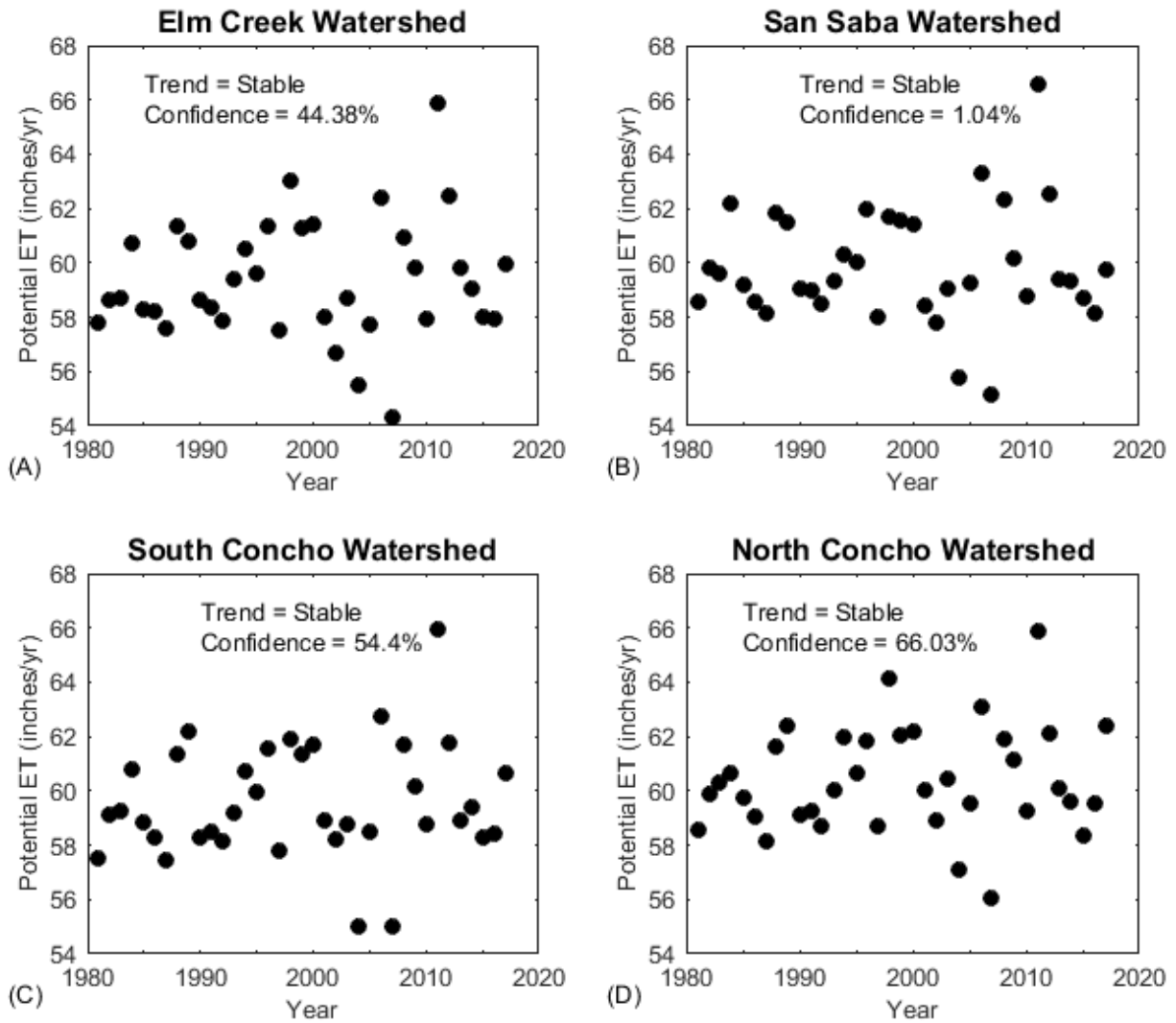


Figure 8-10 Annual potential evapotranspiration calculated by the SWB model for 1981-2017 – A) Elm Creek watershed, B) San Saba watershed, C) South Concho watershed, D) North Concho watershed.

The SWB model-calculated soil moisture (Figure 8-11) estimates mimic the potential and actual evapotranspiration estimates. Soil moisture averages 0.66 inches per day for all watersheds, and is typically less than 0.80 inches per day. Mann-Kendall analyses indicate stable soil moisture trends for all watersheds over the 1981-2017 time period.

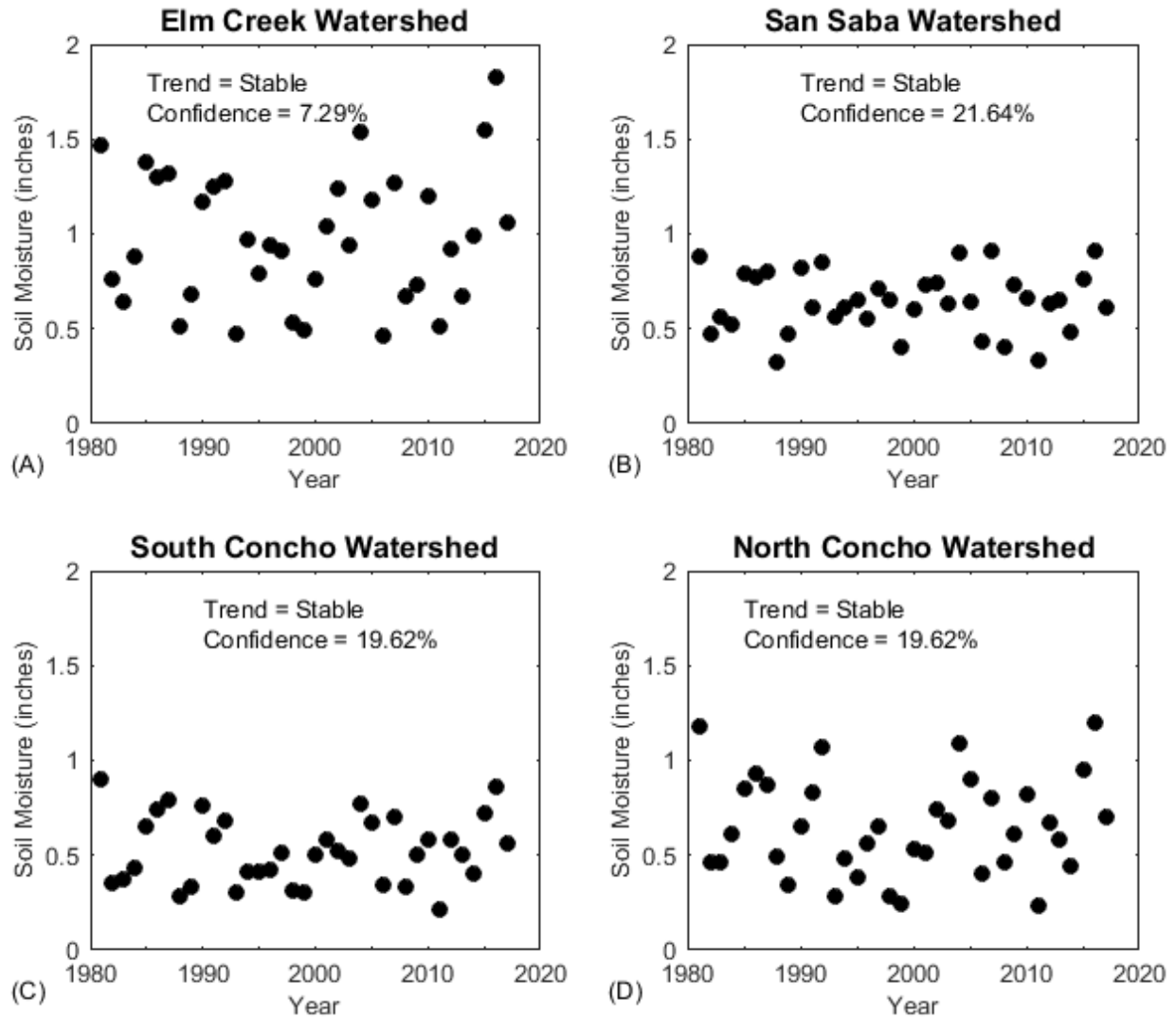


Figure 8-11. Annually averaged daily soil moisture calculated by the SWB model. – A) Elm Creek watershed, B) San Saba watershed, C) South Concho watershed, D) North Concho watershed.

The SWB model calculated annual groundwater recharge estimates (Figure 8-12) average less than 1.0 inches per year for all watersheds, and exhibit stable trends for all watersheds except the South Concho watershed. Within the South Concho watershed, the SWB indicates an increasing trend in groundwater recharge over time.

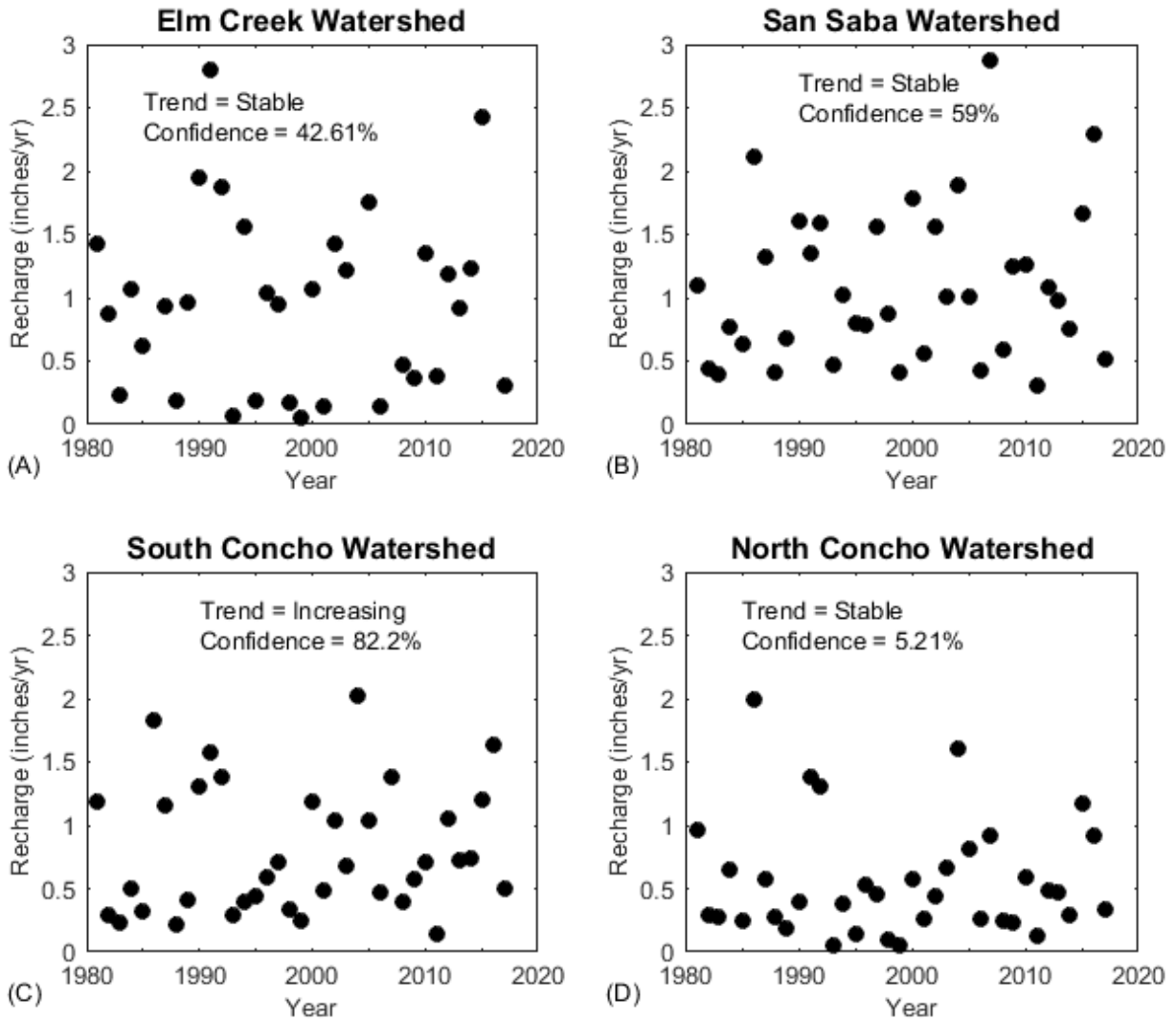


Figure 8-12 - Annually averaged groundwater recharge calculated by the SWB model. – A) Elm Creek watershed, B) San Saba watershed, C) South Concho watershed, D) North Concho watershed.

In addition to analyzing the trends for the study-area basins as a whole, we also analyzed the results for each level 6 hydrologic unit delineation. Specifically, we applied the Mann-Kendall analysis method to assess the existence of any increasing or decreasing trends, and then used a Kendall-Theil regression calculation to quantify the rate at which an identified non-stable trend is either increasing or decreasing (Granato, 2006).

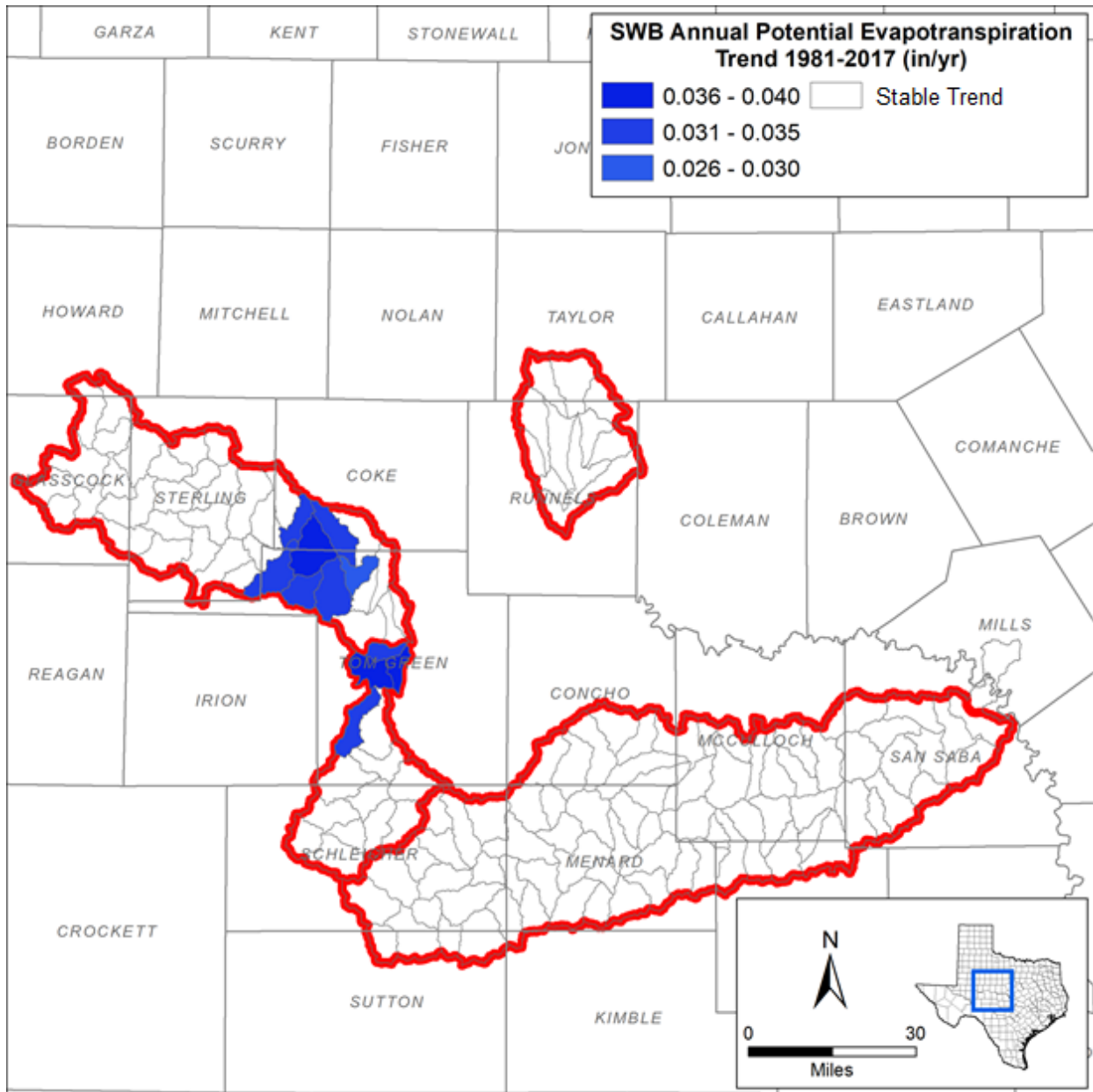


Figure 8-13. Kendall-Theil trends of potential evapotranspiration for each level 6 hydrologic unit in the study-area watersheds as calculated by the SWB model.

Figure 8-13 illustrates the trends (by HUC-6) in estimated potential evapotranspiration across the study areas. As the figure shows, the all sub-watersheds within the Elm Creek and San Saba watersheds show stable trends in potential evapotranspiration. Only for portions of the North Concho watershed (near Carlsbad) and the South Concho watershed near San Angelo were increasing trends evident from the potential evapotranspiration data.

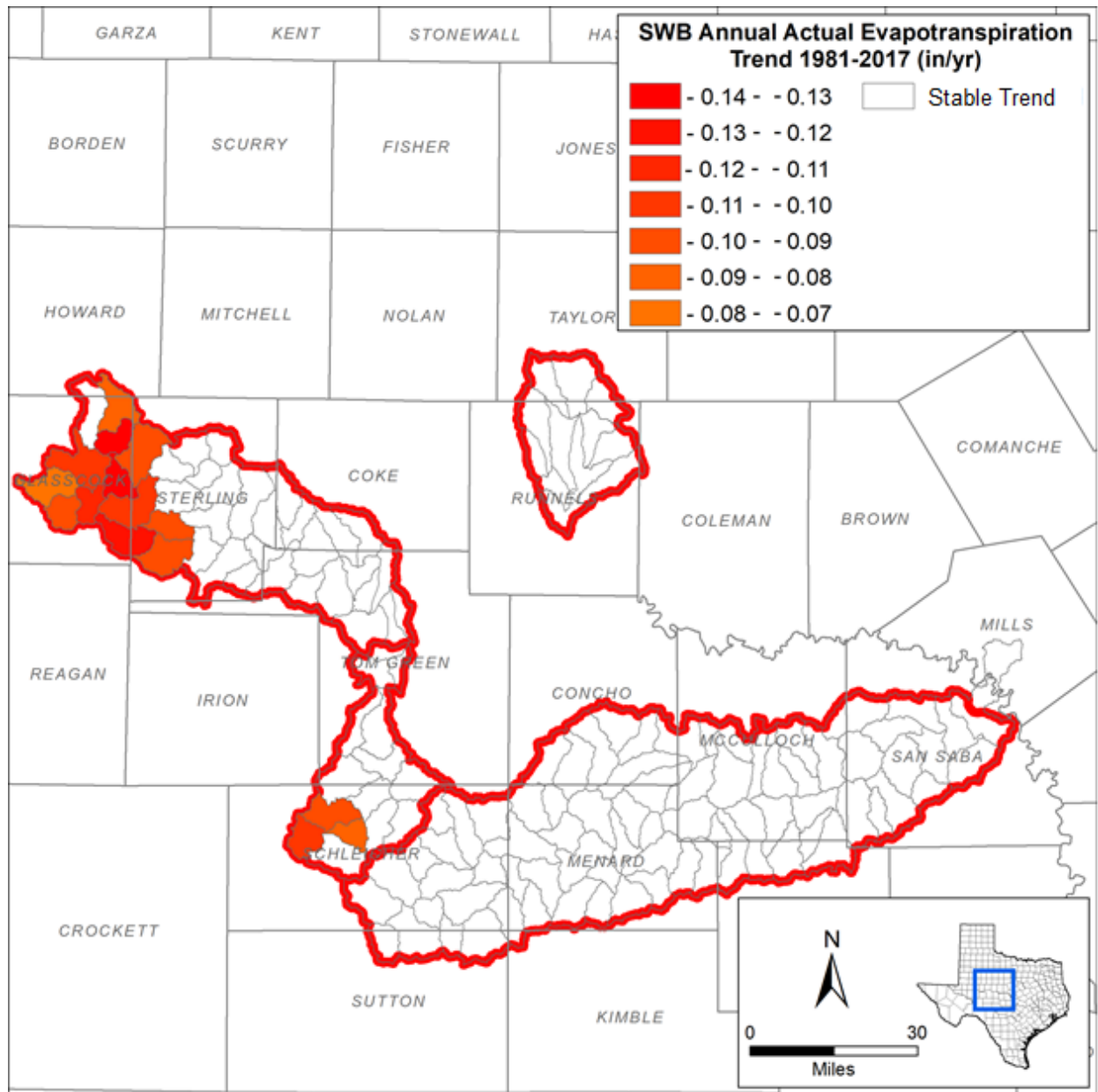


Figure 8-14. Kendall-Theil trends of actual evapotranspiration for each level 6 hydrologic units in the study-area watersheds as calculated by the SWB model.

Figure 8-14 illustrates the trends (by HUC-6) in estimated actual evapotranspiration across the study areas. As the figure shows, the all sub-watersheds within the Elm Creek and San Saba watersheds show stable trends in actual evapotranspiration. Only for portions of the North Concho watershed (near between Big Spring and Sterling City) and the South Concho watershed near Eldorado were decreasing trends evident from the actual evapotranspiration data.

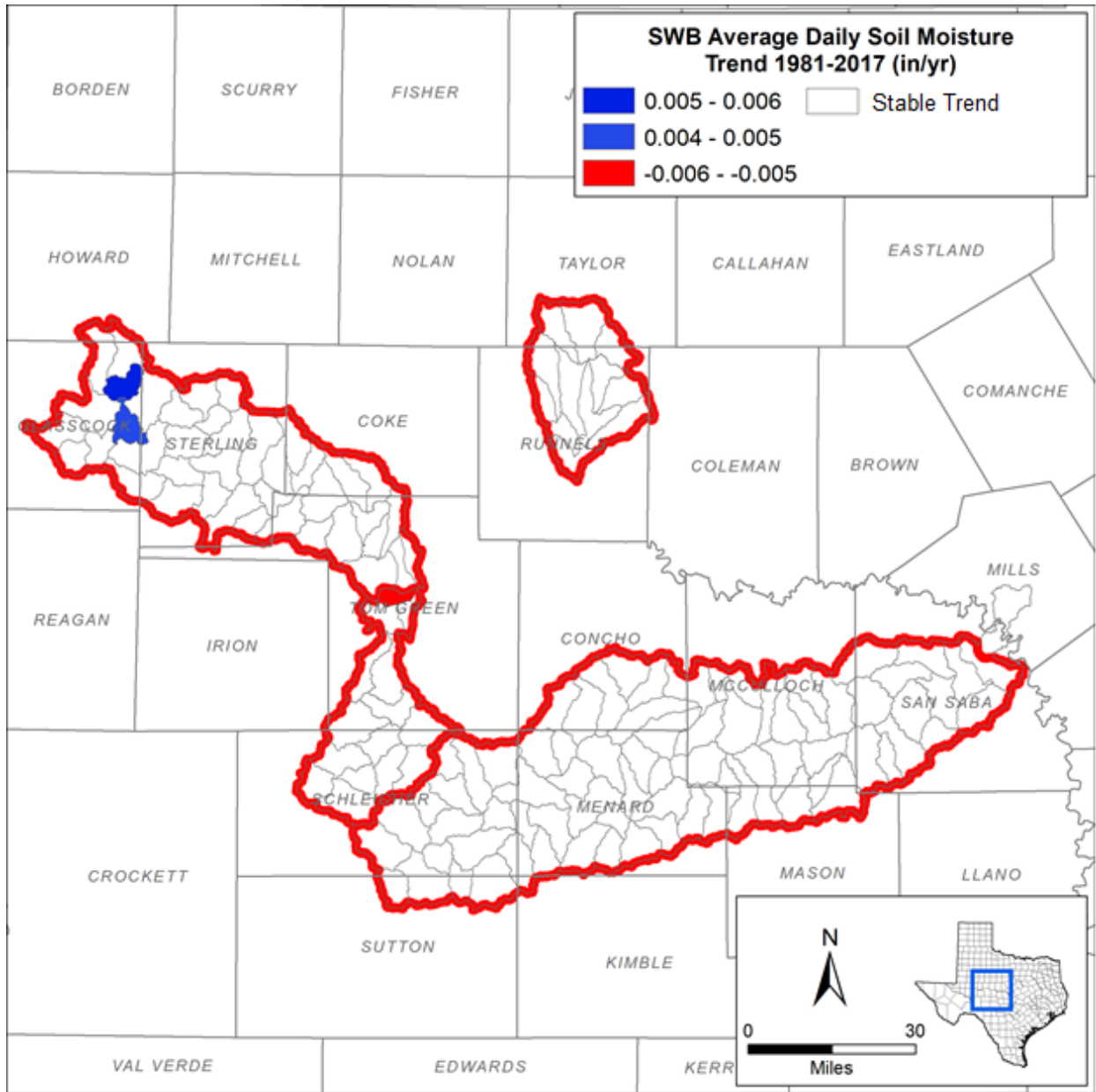


Figure 8-15. Kendall-Theil trend of average daily soil moisture for each level 6 hydrologic unit in the study-area watersheds as calculated by the SWB model.

Figure 8-15 illustrates the trends (by HUC-6) in estimated soil moisture across the study areas. As the figure shows, the all sub-watersheds within the Elm Creek and San Saba watersheds show stable trends in soil moisture. Only portions of the North Concho watershed (near between Big Spring and Sterling City) show increasing trends in soil moisture, and a single HUC-6 subwatershed within the South Concho watershed exhibits a decreasing soil moisture trend. These soil moisture results are in contrast to the results obtained through analysis of the GLDAS data (Figure 8-7).

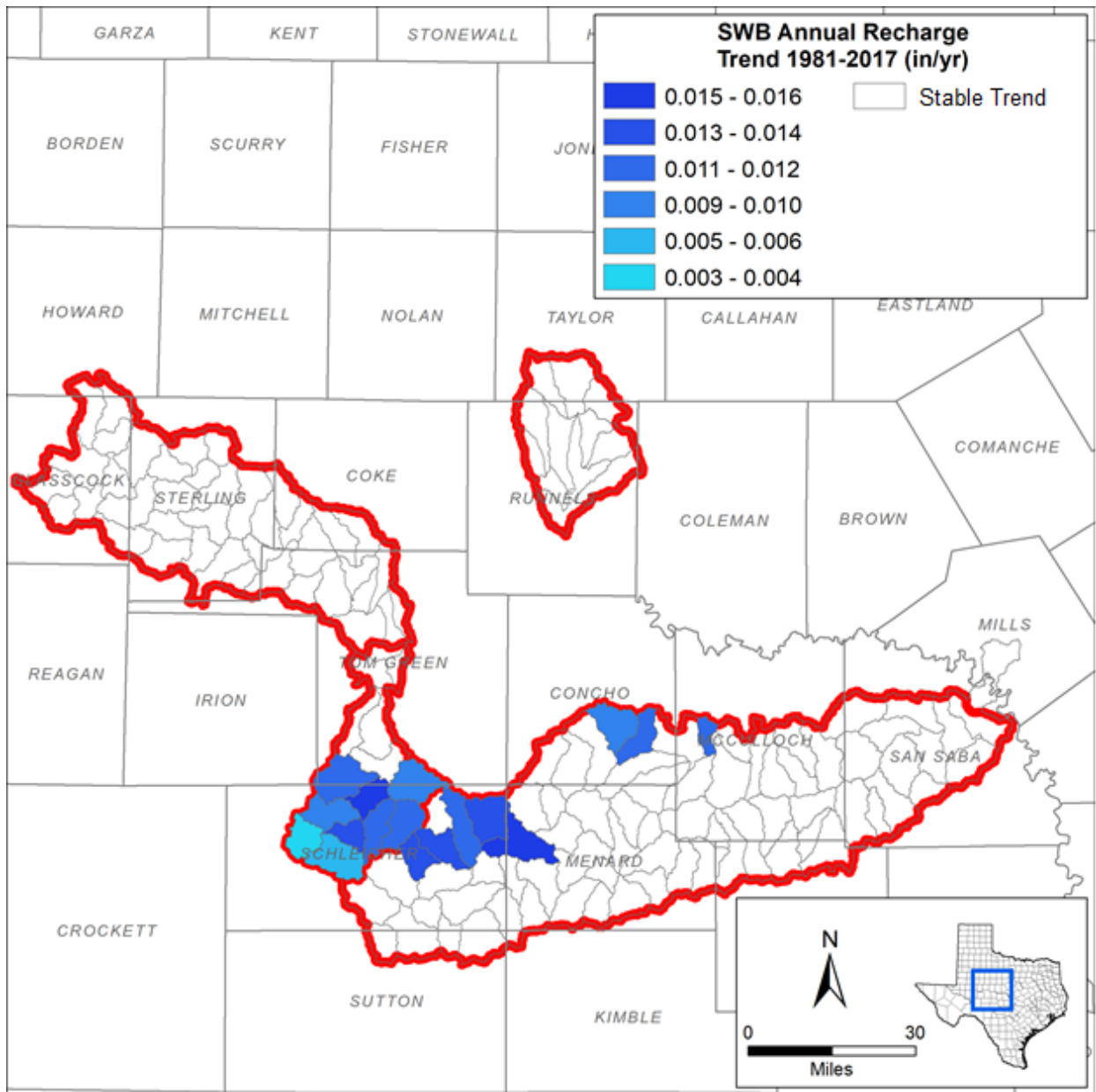


Figure 8-16. Kendall-Theil trend of groundwater recharge for each level 6 hydrologic unit in the study-area watershed as calculated by the SWB model.

Figure 8-16 illustrates the trends (by HUC-6) in estimated groundwater across the study areas. As the figure shows, the all sub-watersheds within the Elm Creek and North Concho watersheds show stable trends in soil moisture. Only portions of the South Concho watershed (near Eldorado) and San Saba watershed show increasing trends in recharge.

9 Task 7 – Groundwater Level Evaluations

The objective of this task was to consider the extent to which groundwater withdrawals may be reducing streamflow in nearby water courses. The study area is located within the Edwards Plateau as described by Mace and Angle (2004). There is one major aquifer (Edwards-Trinity (Plateau)) and six minor aquifers (Lipan, Dockum, Marble Falls, Ellenburger, Hickory, and Cross Timbers) within the study area watersheds. Figure 9-1 and Figure 9-2 illustrate the major and minor aquifers in the study area, respectively.

Generally, the local subsurface geology is comprised of shallow Quaternary age deposits overlying the Cretaceous age rocks of the Edwards-Trinity (Plateau) Aquifer. In most of the study area, these Cretaceous age rocks unconformably overlie older Paleozoic formations (Willis, 1954). The Paleozoic formations outcrop in the eastern portion of the study area and dip below the Cretaceous and Quaternary formations in the western part of the study area (Baker and Baum, 1965).

Within the North Concho watershed, the alluvial deposits and Leona Formation are incised into the Cretaceous rocks and are in direct contact with Paleozoic age limestones (Beach and others, 2004). These formations form the Lipan Aquifer within the North Concho and South Concho watersheds. Within the San Saba watershed the aquifers are, from youngest to oldest, the Edwards-Trinity (Plateau), Cross Timbers, Marble Falls, Ellenburger-San Saba, and Hickory; however, these aquifers are not well-connected in the subsurface being separated by low permeability confining units. Within the Elm Creek watershed, the Cross Timbers Aquifer is prevalent with a small portion of the Edwards-Trinity (Plateau) Aquifer present at the northern end of the watershed.

9.1 Shallow Groundwater Flow System

Our evaluation began by reviewing wells completed within the study area watersheds by querying wells from the TWDB groundwater data base (GWDB) and submitted drillers reports database (SDR). Our initial evaluation focused on wells that were located within the study area watersheds, had depths less than 150 feet, and were located less than a mile from study area flow lines as included in the TCEQ WAM geographic information system (GIS) files for the Colorado River Basin. The resulting wells are mapped in Figure 9-3.

We focused on the shallow groundwater system in the areas near the streams as these are the areas where water-level decline would most affect baseflow to streams. As stated by Mace and others (**Unsupported source type (ConferenceProceedings) for source Mac07.**), “the interaction of a stream and an aquifer is an intimate affair that occurs locally on the order of feet to tens of feet.” The shallow flow zone is the primary conduit in the real physical aquifer system for much of the recharge that enters the groundwater system to move relatively quickly to discharge locations in the aquifer’s outcrop, which includes seeps, springs, and surface water bodies” (Young and others, 2018). In addition, deeper wells are more likely to represent deeper flow systems with local confining units that limit the connection to the shallow water table (Young and others, 2018). Water-level

observations in shallow wells near the streams are more likely to represent the local water table conditions, and may be affecting baseflow to streams.

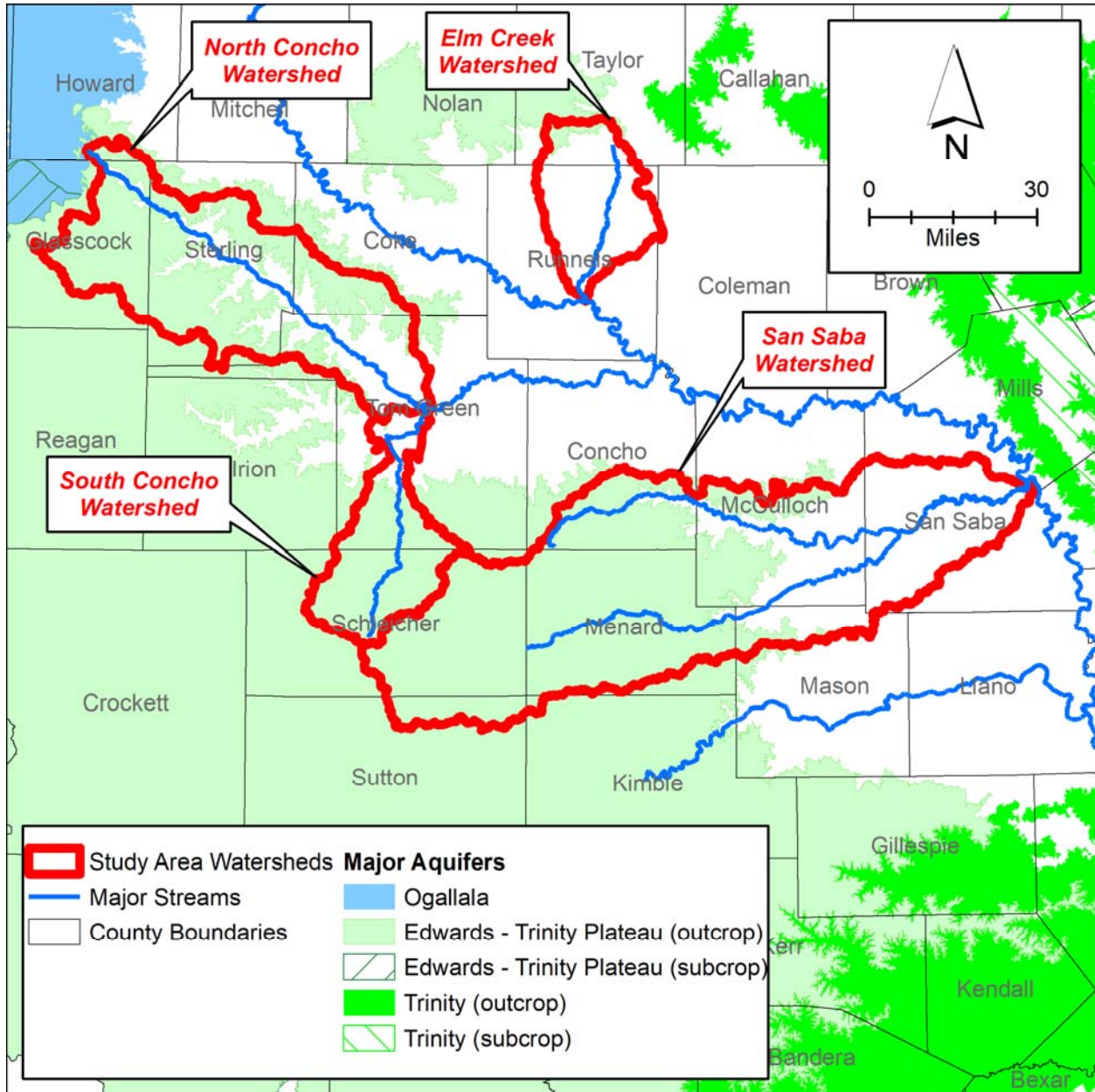


Figure 9-1 – Major aquifers within the study area.

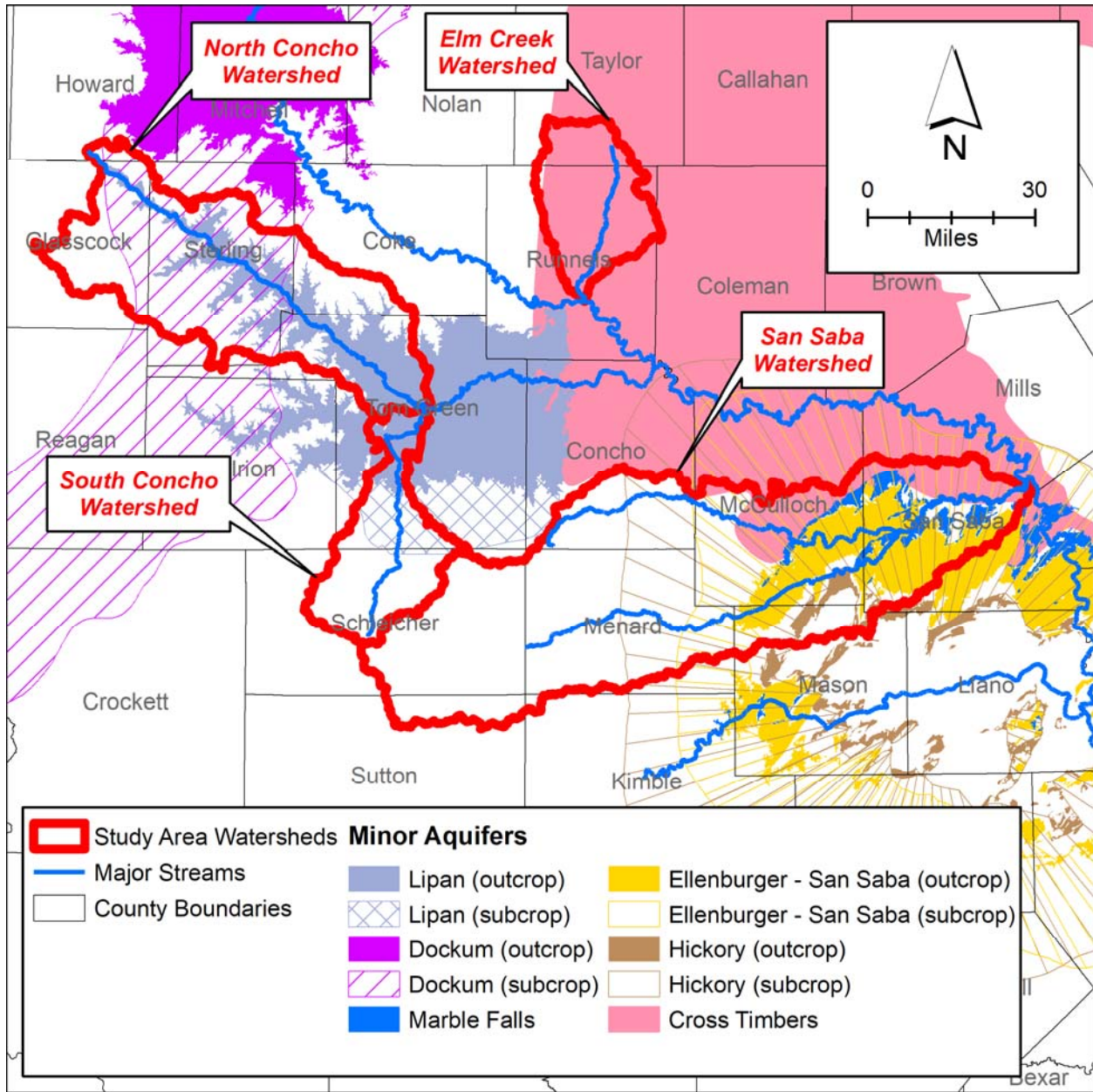


Figure 9-2 – Minor aquifers within the study area.

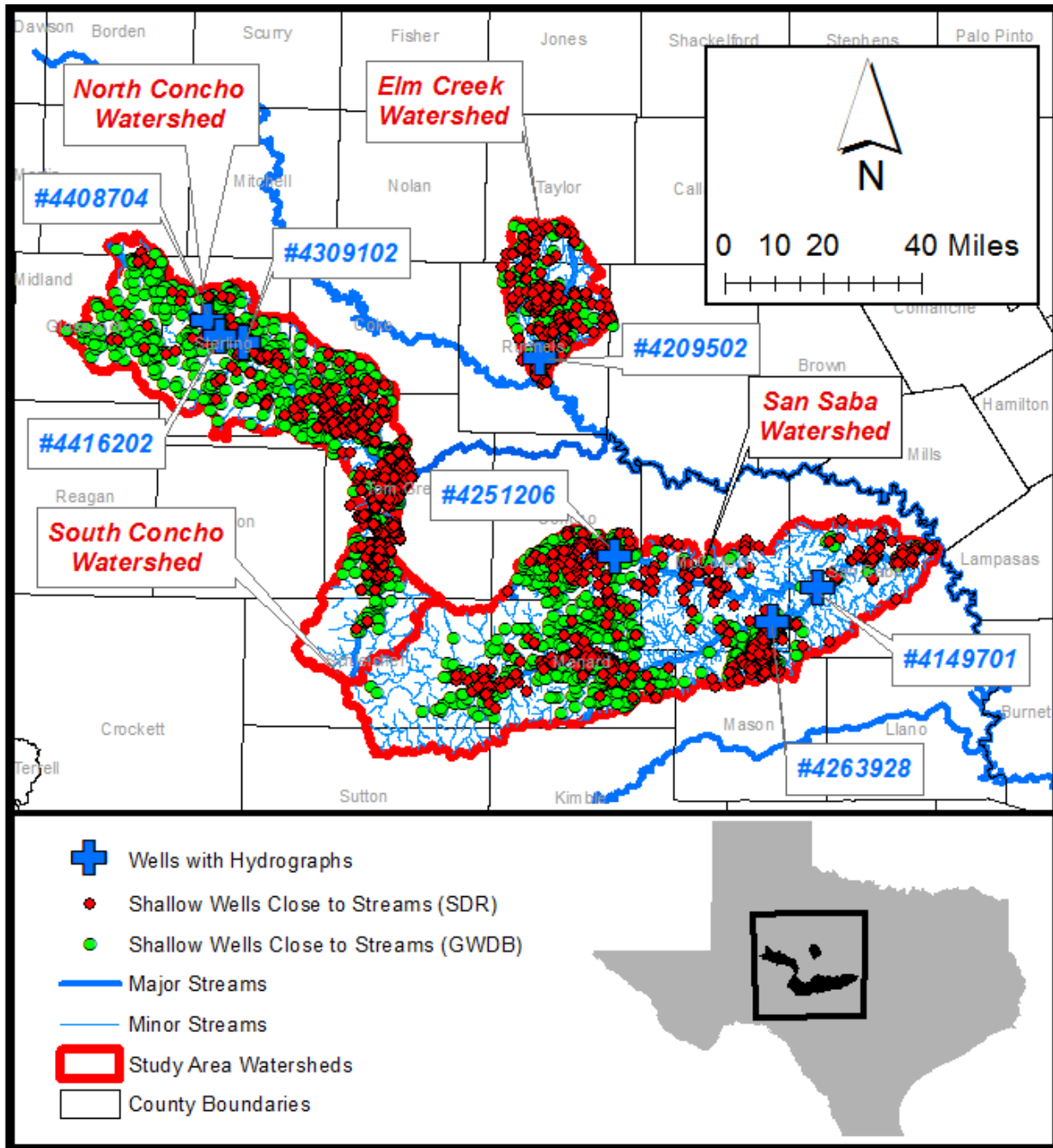


Figure 9-3 – Map of shallow groundwater wells located in close proximity to streams, as well as wells for which water level data was available.

Attempts were made to identify un-registered personal “Domestic and Livestock” wells along the San Saba River through visual inspection of aerial imagery within Google Earth. These attempts were undertaken after discussion with Carolyn Runge of the Menard County Underground Water District, who expressed concern that such wells were draining streamflow out of the San Saba River. Upon review of the Google Earth images, it was determined that wells were likely too small to be properly resolved and identified from the

available imagery. The identification process could likely be improved through the use of drones, flown and controlled from the river preferably during winter months with less vegetation along the river banks.

Of the 1687 TWDB GWDB wells and 4511 SDR wells shown on Figure 9-3, TWDB databases contained water level time-histories for only 7 identified wells. These seven wells are labeled with blue crosses on Figure 9-3, and the well identification number is provided in blue labels.

Figure 9-4 shows the available water levels (in ft above Mean Sea Level or MSL) for well #4209502, a water level observation well maintained by the Lipan-Kickapoo Water Conservation District. The well is located approximately $\frac{3}{4}$ of a mile from Elm Creek upstream from Ballinger. Water levels in the well fluctuated between elevations 1667 ft and 1687 ft, with a net decrease in levels between 2004 and 2012. Figure 9-4B presents the streamflow recorded downstream from the well for Elm Creek at Ballinger (USGS gage #0812700). The streamflow record consists of numerous higher flow events interspersed with low or zero flow periods (Figure 9-4B and Figure 6-2), with annual streamflows showing a decreasing trend (Figure 6-4). Figure 9-4C presents the rainfall recorded in Ballinger and discussed in Section 7.1.1.1.

As labeled with grey lines and numbers on Figure 9-4 are four time periods of interest for comparing streamflow, well water levels and rainfall. Period #1 occurred in late 2004, when Elm Creek had flow event exceeding 2500 cfs. This flow event occurred at a time when well water levels were increasing from 1670 ft to 1687 ft over approximately 1-year, suggesting that the high flow event could be either contributing to aquifer recharge or could be caused (in part) from increased baseflow from the aquifer. Rainfall prior to period #2 was rather frequent and in excess of 1 inch (per day), which could indicate that sufficient water was available to recharge the local groundwater system and cause well water levels to rise without also producing large runoff events. The larger runoff event denoted by period #1 could have resulted from the local groundwater system being saturated and unable to absorb as much of the rainfall event at that time.

Following mid-2005, streamflows decline and well water levels generally decline, reaching a nadir in early 2006. Rainfall during this period does tend to be lower, with higher rainfall amounts interspersed with longer periods of lower rainfall totals. Water levels then increase to mid-2007 (period #2), yet the increase does not appear to be connected to an increase in streamflow until the large streamflow event in mid-2007. The large streamflow event (period #2) occurred at a time when rainfall was approximately 1-inch. Yet prior to the large streamflow event, a 3-inch rainfall event produced only a small streamflow event. This suggests that the large streamflow event denoted as period #2 resulted from previous rainfall events saturating the local surficial aquifer, which would result in increased runoff from smaller rainfall events.

The period #2 high streamflow event also marked the change in water level trends from rising to declining, which could support the theory that the large streamflow was generated as a result of the local alluvium being saturated and unable to accommodate more recharge.

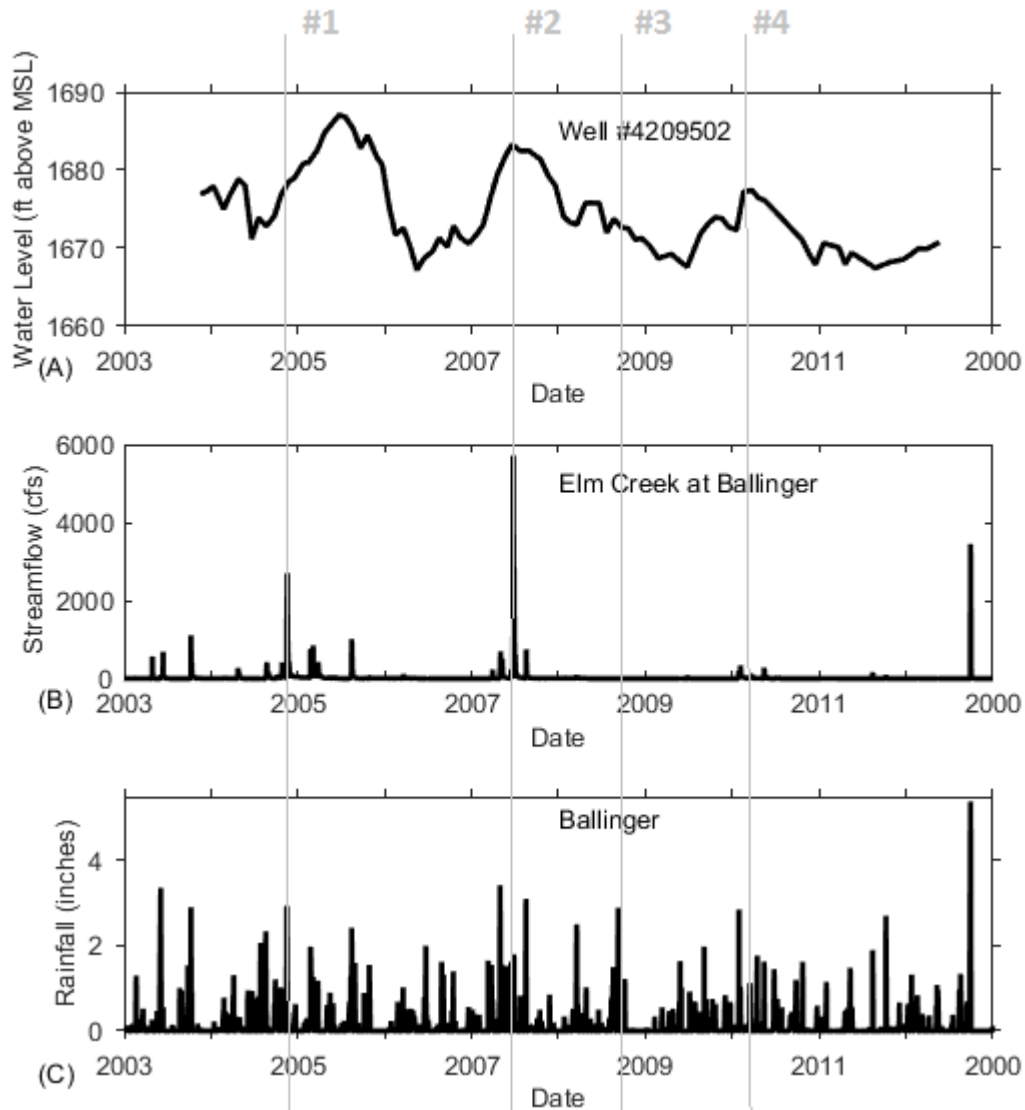


Figure 9-4 – Data for well #4209502 near Elm Creek – A) water levels, B) nearby streamflow, C) local rainfall

Period #3 marks a time of prolonged low streamflow and water level declines in the well, yet rainfall events occurring between period #2 and period #3 include 3 events exceeding 3 inches per day. It is possible that the low-rainfall events within this time period allow the surficial aquifer to dry out and absorb bigger rainflow events without generating large streamflow.

Period #4 notes the increase in water levels around the time of small peaks in streamflow, which occur after a rain event exceeding 3-inches. This could indicate, as with Period #2, that the local alluvium became saturated and led to increases in streamflow.

Pumping records for wells in the vicinity of well #4209502 are not available, and as such we cannot discern how local well use effects the recorded water levels.

In general, Figure 9-4 suggests that large flow events can occur at times when water levels are rising within well #4209502. It is likely that the rainfall events leading to the high-streamflow events shown in Figure 9-4B also contributed to local groundwater recharge, which would tend to increase well water levels. This recharge would also likely contribute to baseflow increases for a time period following the rainfall/high streamflow event. This theory is supported by the observation labeled as period #1. Observations labeled as period #2 and period #4 suggest that well water level increases may peak when alluvium becomes saturated, resulting in increased runoff resulting from rain events. Period #3 suggests that declines in water levels can occur when streamflow is low, yet the data presented does not indicate whether water level declines are the cause or result of low streamflow. The frequency of higher-intensity rainfall events, as well as duration of drier periods between larger rainfall events, may play an important role in regulating both well water levels and streamflow within the Elm Creek watershed.

Figure 9-5 presents water level data and nearby streamflow data for well #4149701 located near Brady Creek at Brady. Streamflow was recorded at the USGS gage #0814500 ("Brady Ck at Brady, TX), and is discussed in detail in Section 6.2.2. Well water levels are shown from 1990-2012, yet a single well level reading from 1973 was similar to that recorded in 1992 (without any other recordings made between 1973 and 1992). Streamflow data for Brady Creek was unavailable for the period 1990-2002.

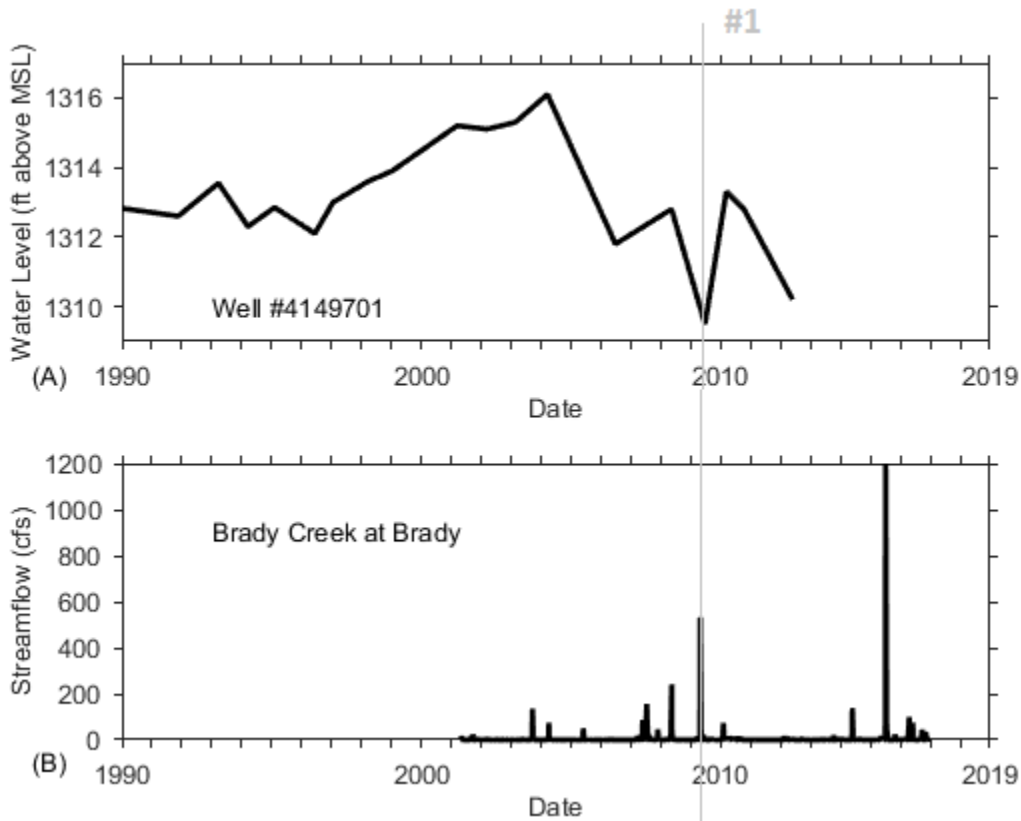


Figure 9-5 - Data for well #4149701 near Brady Creek – A) water levels, B) nearby streamflow

Water levels in well #4149701 generally increased from 2002-2004, and may have increased more rapidly as a result of the smaller streamflow event occurring in late 2004. After this time, however, streamflow levels decreased until 2006, followed by a slight increase and decrease in 2009. At the end of this decrease (labeled as period #1), a larger streamflow event occurred, and this event likely contributed to the water level increase that occurred during 2010. As pumping data are unavailable for well #4149701, it is not possible to discern how well pumping affected the well hydrograph shown in Figure 9-5A. In general, the streamflow and water level time-series data presented in Figure 9-5 suggest a linkage between the local groundwater and surface water systems, but insufficient data are available to fully confirm or refute this linkage.

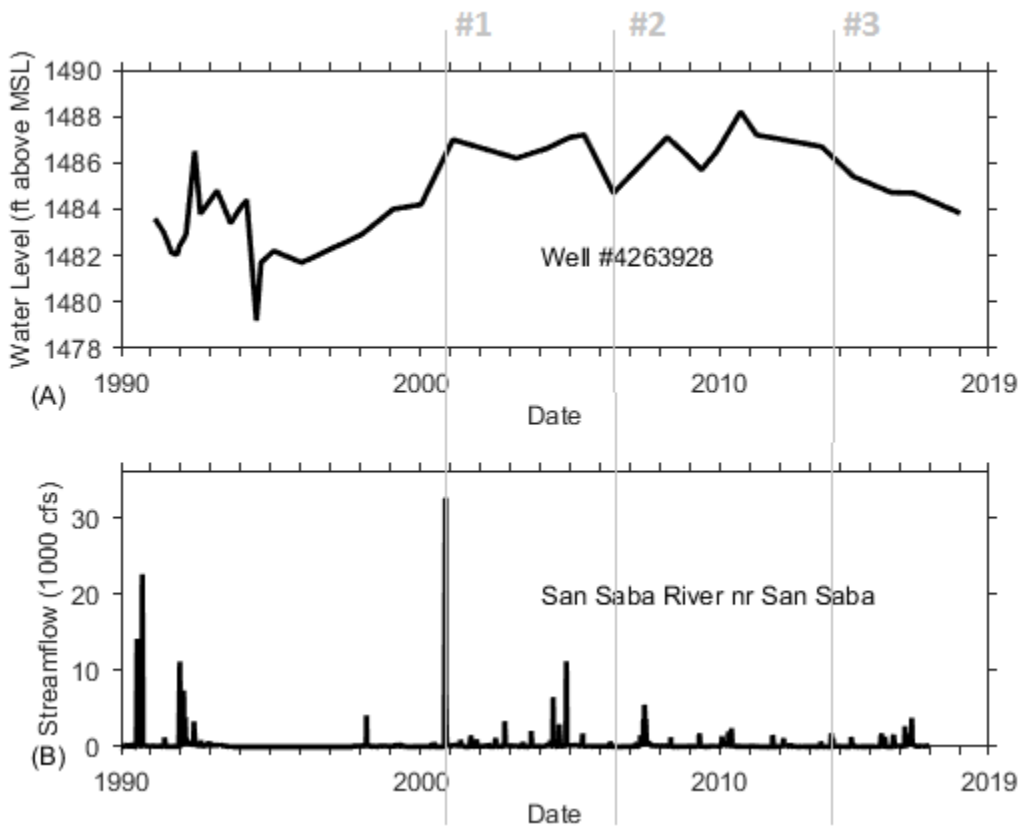


Figure 9-6 - Data for well #4263928 near the San Saba River – A) water levels, B) nearby streamflow

Figure 9-6 presents well water levels for well #4263928, located along the San Saba River downstream yet upstream of the confluence with Brady Creek. Streamflow in Figure 9-6B is provided from the USGS gage on the San Saba River near San Saba (USGS gage #08146000) and is discussed in Section 6.2.3. As shown, well water levels have fluctuated by up to 10-feet over the period of record, and have shown a net increase over this time. Period #1 depicts a high-streamflow event occurring at the same time when well water levels are increasing and reaching a peak level. This may indicate that the surficial aquifer system has been recharging due to previous rainfall events, and that the large streamflow event occurred only when the local groundwater system was nearly saturated. Period #2 denotes a decrease in well water levels during a period of prolonged low

streamflows. Period #3 also denotes a period of prolonged well water level decreases concurrent with periods of low streamflow.

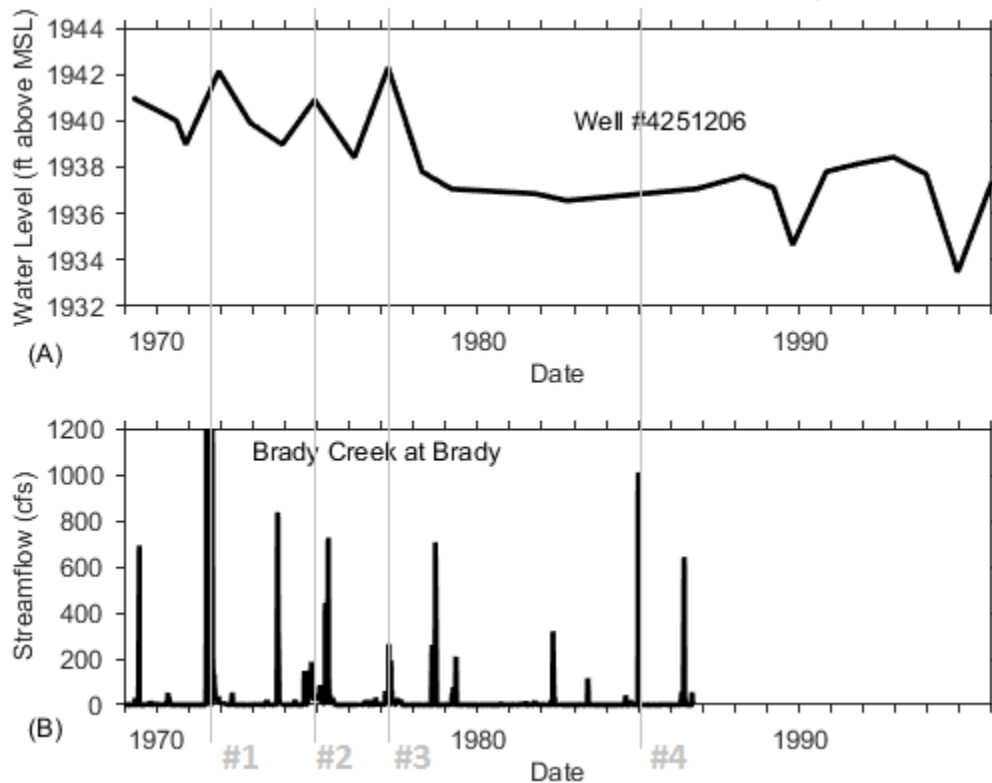


Figure 9-7 - Data for well #4251206 located upstream within the Brady Creek watershed – A) water levels, B) streamflow recorded downstream from the well.

Figure 9-7 presents water level data from well #4251206 within the upper reaches of the Brady Creek watershed, with streamflow recorded at the USGS gage #0814500 located near the downstream end of the watershed. Due to the geographical difference between the well and the streamflow gage, relationships between the two datasets may not be clear. Periods #1, #2, and #3 mark instances of relatively rapid increases in well water levels at times during which high streamflow events were recorded. In contrast, period #4 occurs during a high streamflow event at a time when well water levels remained constant for nearly 10-years (1979-1989). In general, data from Figure 9-7 fit the theory that high streamflow events occur when well water levels are higher as the local aquifer is unable to absorb as much of the rainfall. However, Figure 9-7 does not provide conclusive evidence of a linkage between well water levels and streamflow, in part likely due to the geographical separation between the well and the gage.

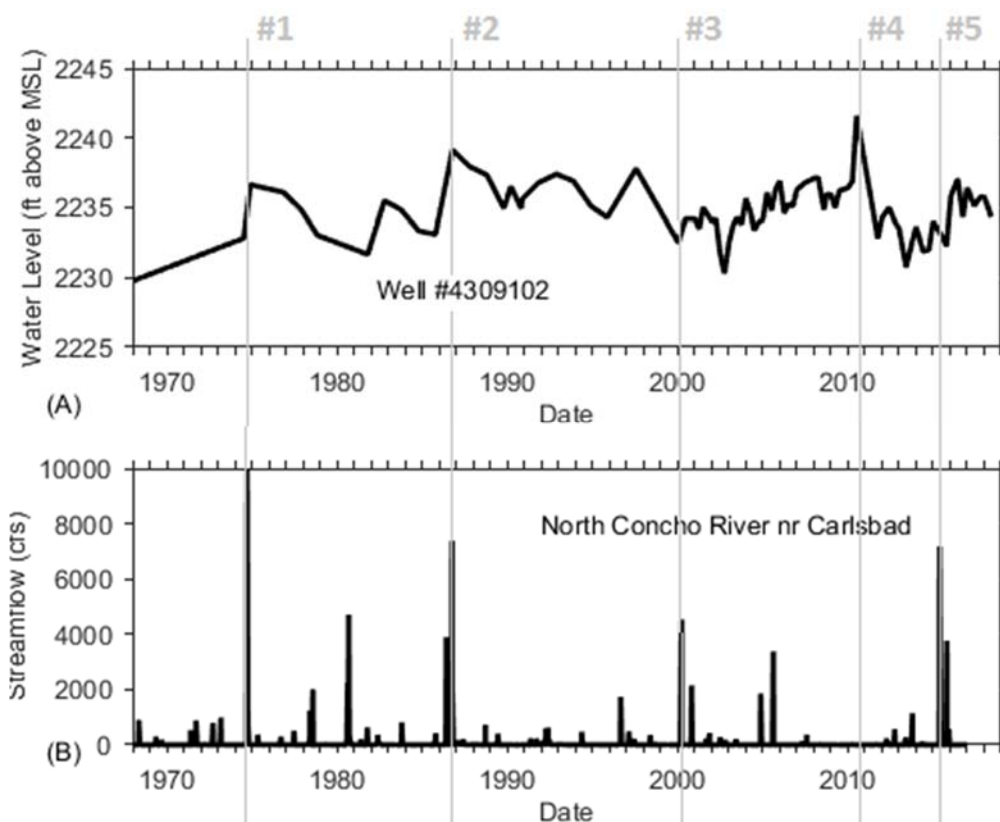


Figure 9-8 - Data for well #44309102 located near Sterling City within the North Concho watershed – A) water levels, B) streamflow recorded for the North Concho River near Carlsbad.

Well water levels and streamflow for locations within the North Concho watershed are presented in Figure 9-8, Figure 9-9, and Figure 9-10. Each of the wells is located upstream of the USGS gage on the North Concho River near Carlsbad (USGS gage #08314000), whose streamflow record is discussed in Section 6.4. Data from each of these wells spans over 40 years, providing useful insight into water level trends with respect to streamflow. Within Figure 9-8, labeled periods #1 and #2 represent large streamflow events that occur after rapid increases in well water levels. This possibly indicates that the local groundwater system was recharging prior to the high-streamflow event, and the event occurred when the local system could no longer rapidly absorb available rainfall. Period #3 (Figure 9-8) indicates a large streamflow event which occurred at the end of a decline in water levels. This may indicate that the streamflow event contributed to the local groundwater recharge, effectively reversing the declining trend in well water levels. Period #4 denotes a peak in well water levels without any corresponding local peak in streamflow. It is possible that this water level measurement is erroneous, or that factors other than rainfall and streamflow are influencing well water levels at this time. Period #5 denotes the beginning of a 3-ft rise in water levels around the time of a 7000 cfs flow event, which suggests that the high streamflow event could be contributing to local groundwater recharge.

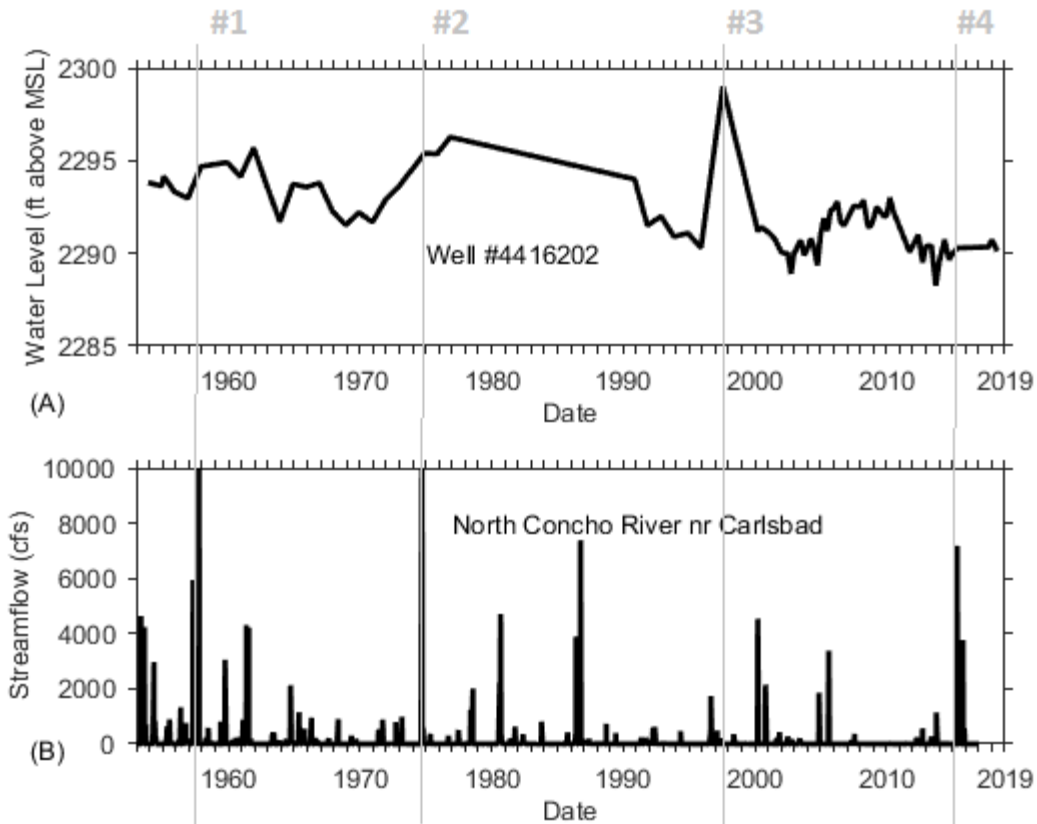


Figure 9-9 - Data for well #4416202 located near Sterling City within the North Concho watershed – A) water levels, B) streamflow recorded for the North Concho River near Carlsbad.

Similar to Figure 9-8, Figure 9-9 labeled periods #1 and #2 represent large streamflow events that occur after rapid increases in well water levels. For period #1, there were several high streamflow events prior to the period and the local soil conditions were likely saturated. However, for period #2, water levels had been generally rising since 1970. While pumping data are not available, the long-term rise in water levels is likely associated with a decline in pumping in the area. Period #3 denotes a peak in well water levels without any significant peak in streamflow. It is possible that this water level measurement is erroneous, or that factors other than rainfall and streamflow are influencing well water levels at this time. Period #4 identifies a high streamflow event without a corresponding rise in water level. The lack of change in water level suggests the rainfall may have occurred downstream of the well or there was little opportunity for recharge to the local groundwater system.

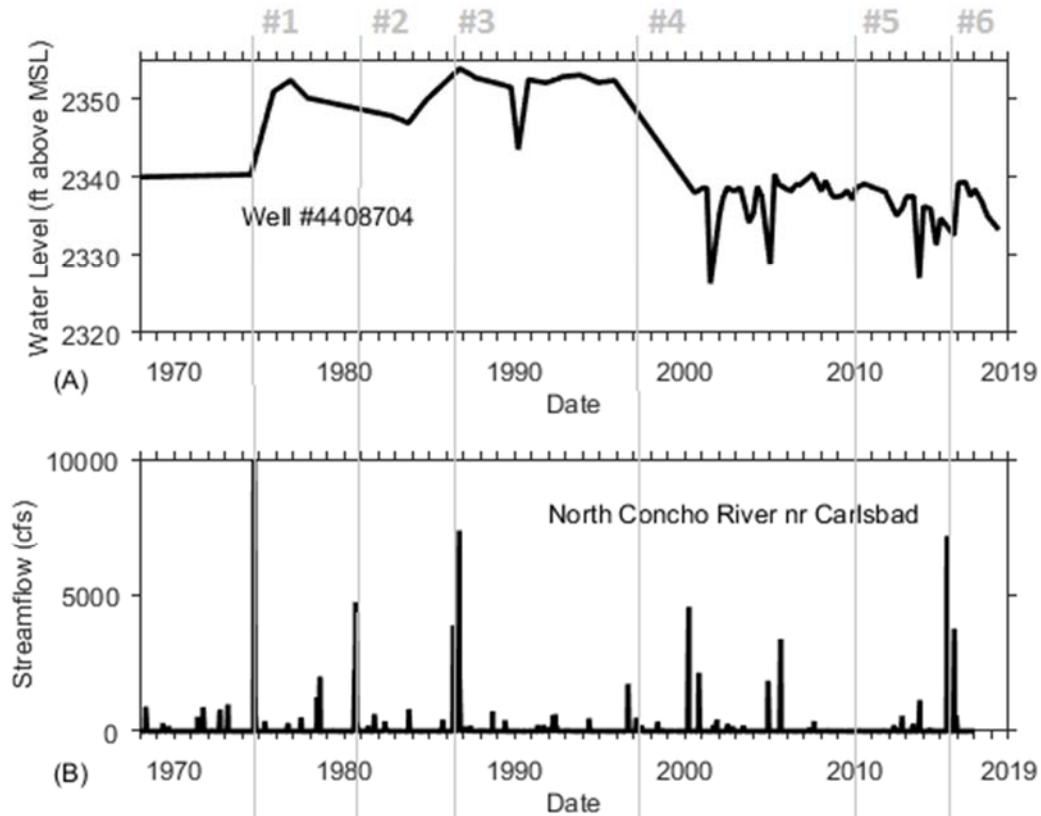


Figure 9-10 - Data for well #4408704 located near Sterling City within the North Concho watershed – A) water levels, B) streamflow recorded for the North Concho River near Carlsbad.

Figure 9-10 illustrates the water levels in the most upstream well of the three wells in the North Concho watershed that are discussed. Period #1 denotes the beginning of a more than 10-foot rise in water levels from 1974 to 1976 that corresponds to a high streamflow event. It is possible this streamflow event contributed to aquifer recharge. Period #2 identifies a period of general water level decline between 1977 and 1982. While there is a high streamflow event at period #2, there are not any corresponding water level measurements near the time of the event to determine if there was an associated change in water level. Period #3 denotes the end of a period of general rise in water levels followed by relatively stable water levels until 1995. The water level peak at period #3 follows high streamflow events that likely contributed recharge to the local aquifer. From the end of 1995 to mid-2000, no water levels are reported for the well. During this 5-year period only one high streamflow event occurred as denoted by period #4 and water levels reportedly declined by over 10 feet. Up until period #5, water levels remained relatively constant and then began to decline. At period #6 there was a high streamflow event with a corresponding rise in water levels in the well. The rise could be due to recharge to the local aquifer from the stream or a reduction in pumping associated with the rainfall event. The rapid water level decline following period #6 suggests local recharge occurred followed by discharge back to the stream via baseflow.

Figure 9-11 presents the cumulative number of known water wells within the study area watersheds, shown by year. This graphic only contains wells for which the drilling date was known and included within the source databases. Figure 9-3 and Figure 9-11 do not contain any of the SDR wells registered with TCEQ prior to 2001. These well reports are all available from the TCEQ, yet not in a format easily query-able such as Excel or ArcGIS, making them difficult to include in this analysis. Figure 9-11 also does not include any un-registered domestic and livestock wells that potentially exist within the study area watersheds.

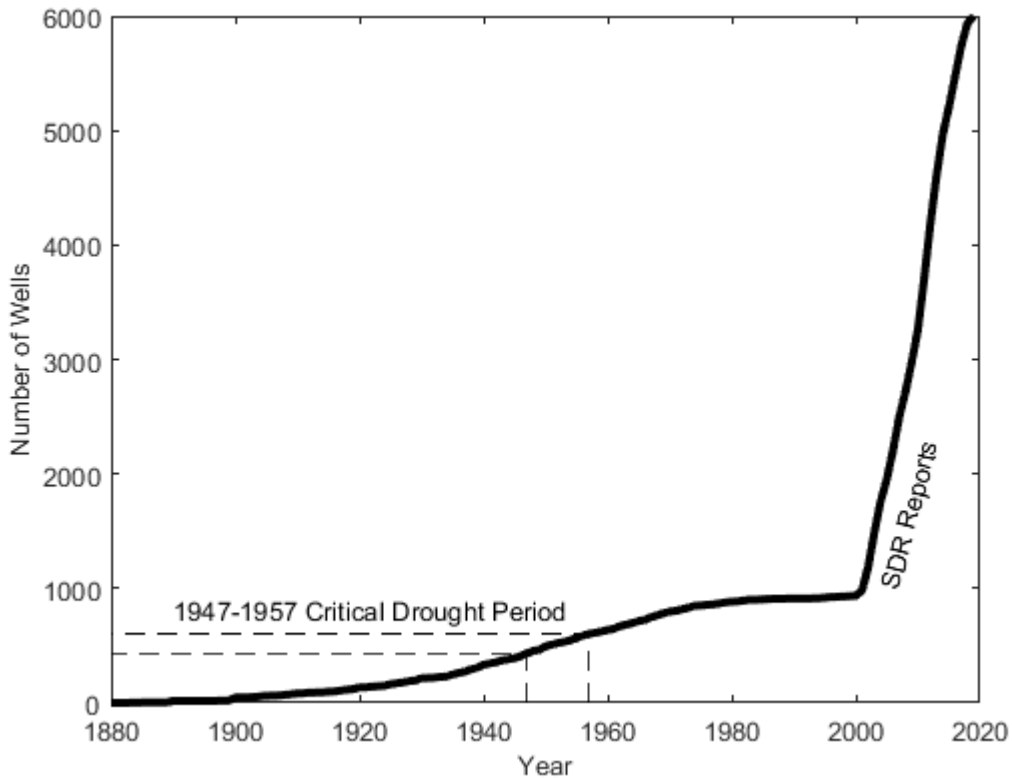


Figure 9-11 – Known water wells within the study area watersheds

The purpose of Figure 9-11 is to point out that the number of known groundwater wells with the study area watersheds has greatly increased since the 1947-1957 critical drought period (LCRA, 2015). The collective pumping rates of these wells over time are unknown, and therefore the true impact of these wells on the local stream system cannot accurately be deduced. As a result of the lack of available data for assessing the potential linkage between groundwater withdrawals and reduced streamflow, no further analyses were conducted.

9.2 Regional Groundwater Flow System

With the limited available data for the shallow groundwater flow system, we expanded our review to include a greater area with deeper wells. Including these wells creates a dataset that includes both the shallow and deeper aquifer systems. As discussed above it is important to note that deeper wells can be essentially hydraulically isolated from the water table near land surface (Young and others, 2018). However, it is necessary to include these wells to develop potentiometric surfaces of the formations and regional flow system beneath the study area watersheds.

To develop potentiometric surface maps of the formations beneath the watersheds, we selected wells from the TWDB GWDB that are located within a polygon extending outward 10 miles of each study area watershed boundary. From these wells, we removed wells that did not have any water level measurements and that did not have an assigned aquifer code. We then prepared histograms of the well depths associated with each watershed.

As Figure 9-12 illustrates, except in the San Saba watershed, most of the wells with available water level measurements are less than 150 feet deep with nearly all wells being less than 400 feet deep. In the San Saba watershed, we identified more deep wells that are associated with the deeper aquifers in the eastern part of the watershed. To limit the depth from which we considered water levels, we only used wells that were 300 feet deep or less in the North Concho watershed, 200 feet deep or less in the Elm Creek watershed, and 400 feet deep or less in the South Concho and San Saba watersheds.

After filtering the dataset to the wells that would best represent the regional groundwater flow system near each watershed, we then obtained the reported water level data for each well from the TWDB GWDB. We limited the water levels used in our evaluation to those marked as “publishable” within the database. We reviewed the number of available measurements per year and found the number of measurements increased significantly from 1970 onward which led us to limit our evaluation of groundwater levels to begin in 1970. We further limited the water levels we used in the evaluation to those collected between the beginning of October for year of interest and end of February for the following year (for example, 10/1/1970 through 2/28/1971) with the goal of using water level measurements from a period when groundwater pumping is typically less. For wells with more than one measurement during the period, we used the average water level.

Using the water level data for each watershed, we prepared potentiometric surface maps from the available data. Figure 9-16 through Figure 9-14 illustrate the calculated potentiometric surfaces for each watershed. Importantly, the number of data points available for the interpolation of the potentiometric surface varies significantly between some of the datasets. This variance can greatly influence the interpolation and care should be taken when drawing conclusions from the results.

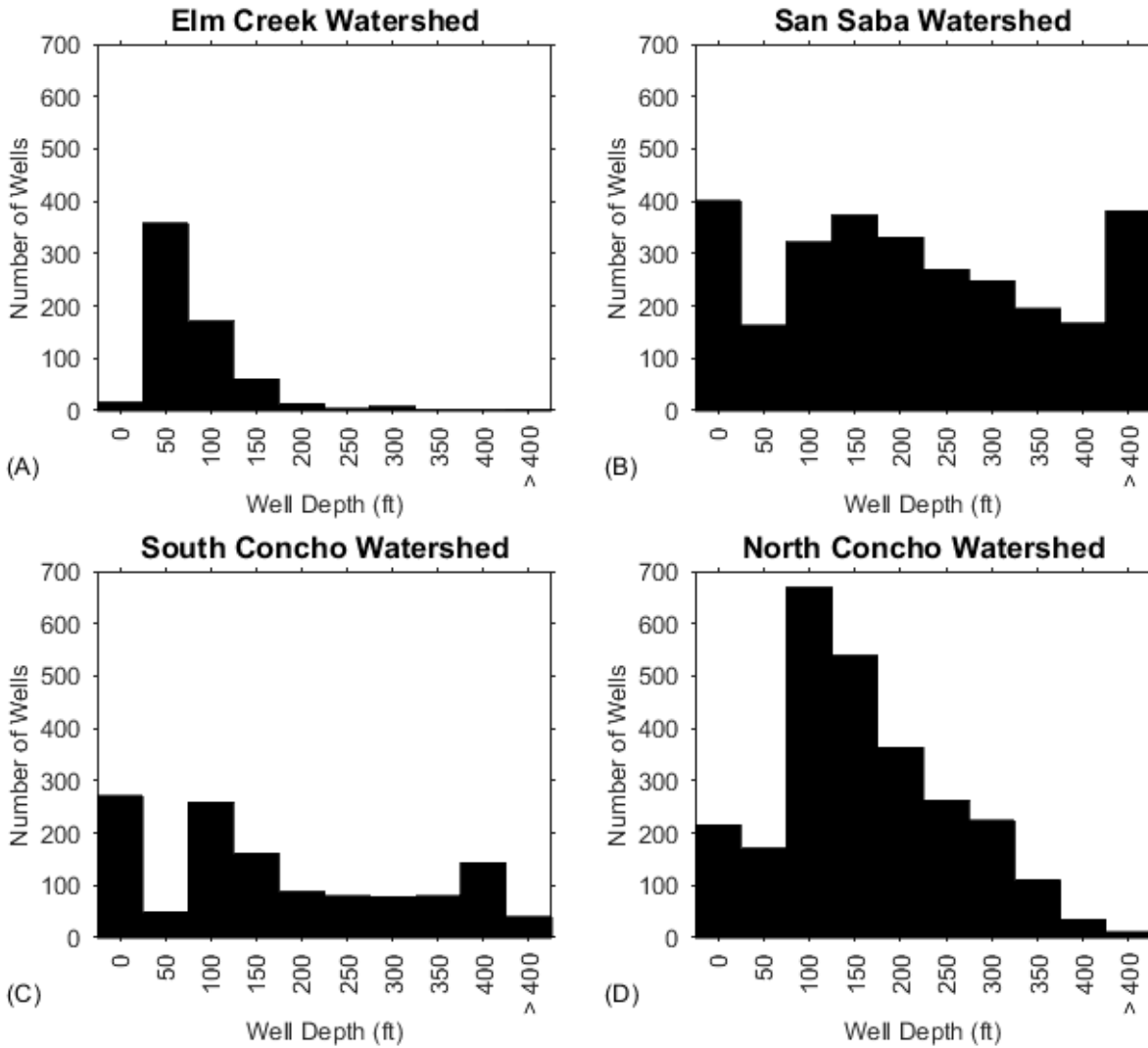


Figure 9-12 – Well depths in and within 10 miles of the study area watersheds.

In the Elm Creek watershed (Figure 9-13), the variations in data availability make drawing clear conclusions difficult. The patterns for 1990 and 2010 are similar as measured water levels are available in approximately the same locations for each period. These patterns (from the 1990 and 2010 datasets) suggest there may a small decline in water levels over time, but it is unclear and inconclusive. Water level contours derived from 1970, 1980, and 2000 datasets do not follow a pattern similar to those obtained from the 1990 and 2010 datasets. Lack of consistent spatial data availability makes discerning potentiometric surface trends impossible.

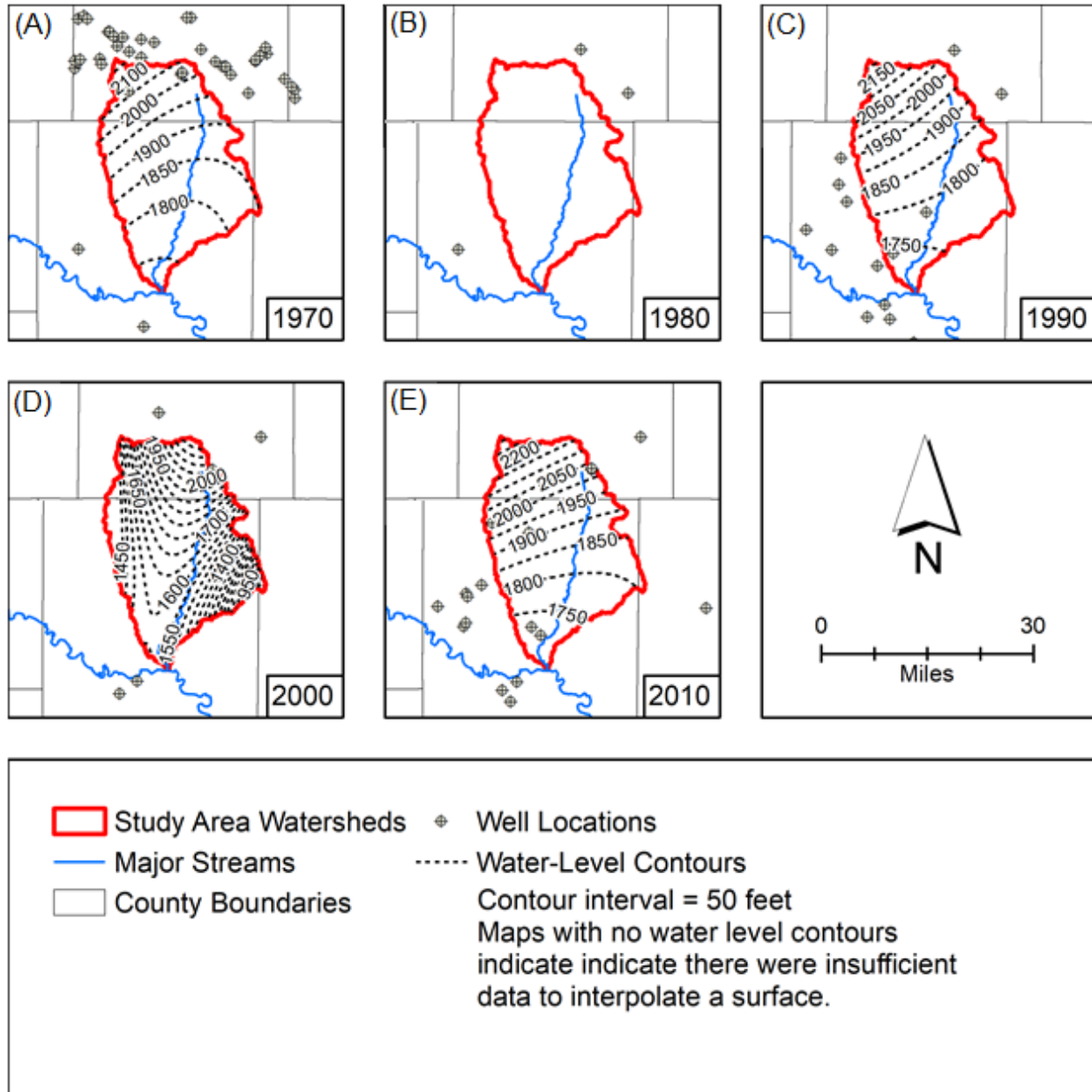


Figure 9-13 – Potentiometric surface from 1970 through 2010 for the Elm Creek watershed

For the San Saba watershed, potentiometric surfaces generated for 1990, 2000, and 2010 are fairly consistent (Figure 9-14). Results suggest stable water levels, with only slight declines indicated for the eastern portion of the watershed. In the western portion of the watershed, water levels appear to have increased between 2000 and 2010, as indicated by the change in location of the labeled 2050 ft surface contour. We consider these differences in contours, however, to stem from differences in the well locations used to generate the contours, rather than in actual differences in water levels within the groundwater system. It is not possible to discern from available data whether the local potentiometric surface is changing due to the change in actual groundwater supplies, or due to the change in well locations use to generate the potentiometric surfaces.

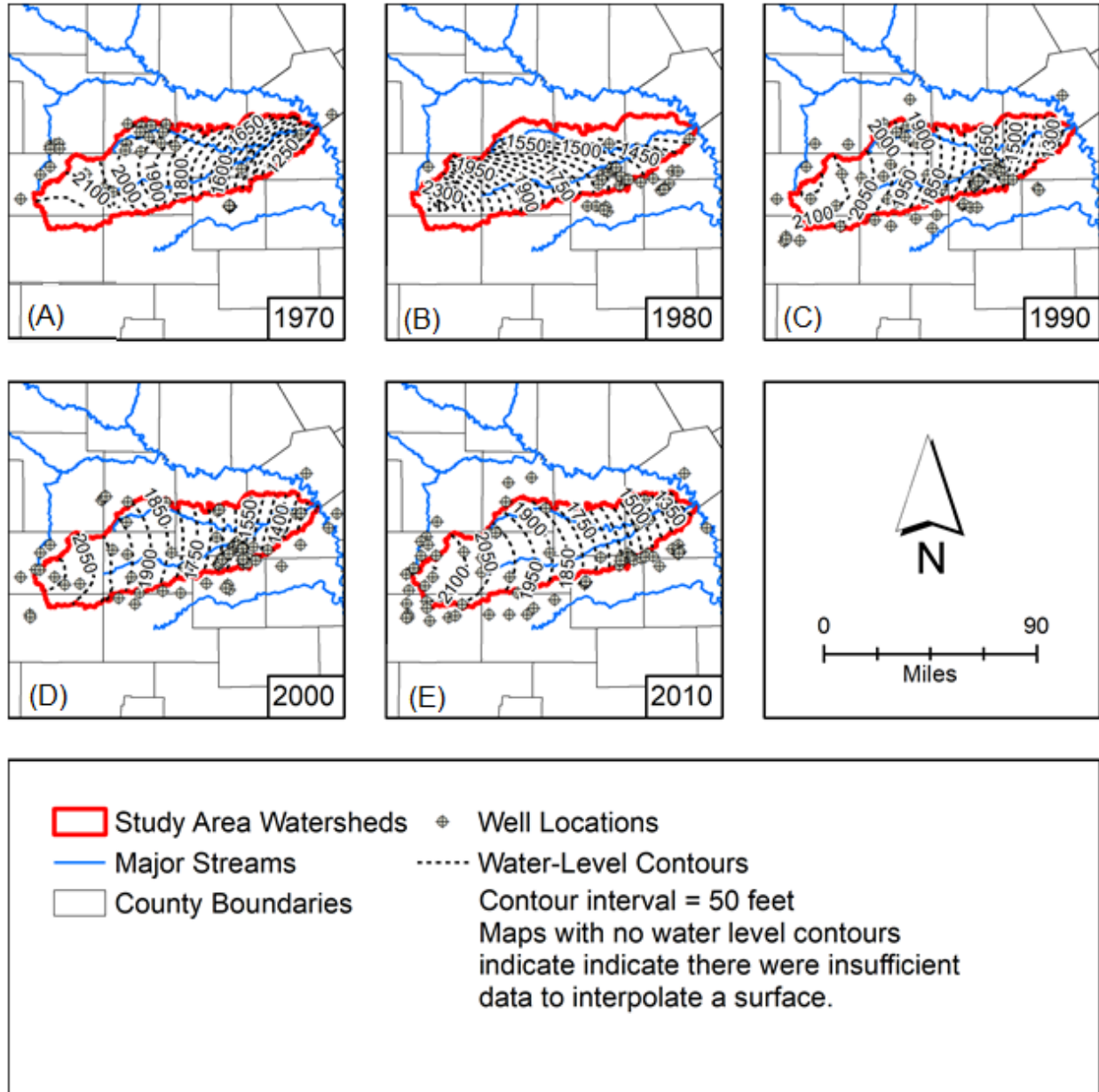


Figure 9-14 – Potentiometric surface from 1970 through 2010 for the San Saba watershed.

Similarly to results from the Elm Creek and San Saba watersheds, potentiometric surfaces generated for the South Concho watershed (Figure 9-15) seem to vary more due to well water level measurement locations, rather than due to actual changes in water levels. The water level contours for 1990 and 2010 suggest there may a small decline, but it is unclear and inconclusive. Results from 1970 data are also similar to those from 1990 data, and a large decline is suggested by comparing surfaces from 1970 and 2000. Yet this large decline is not as large when comparing 1970 and 2010 surfaces, with water levels seeming to have increased between 2000 and 2010. Definitive conclusions regarding trends in potentiometric surface elevations may not be made based on available data.

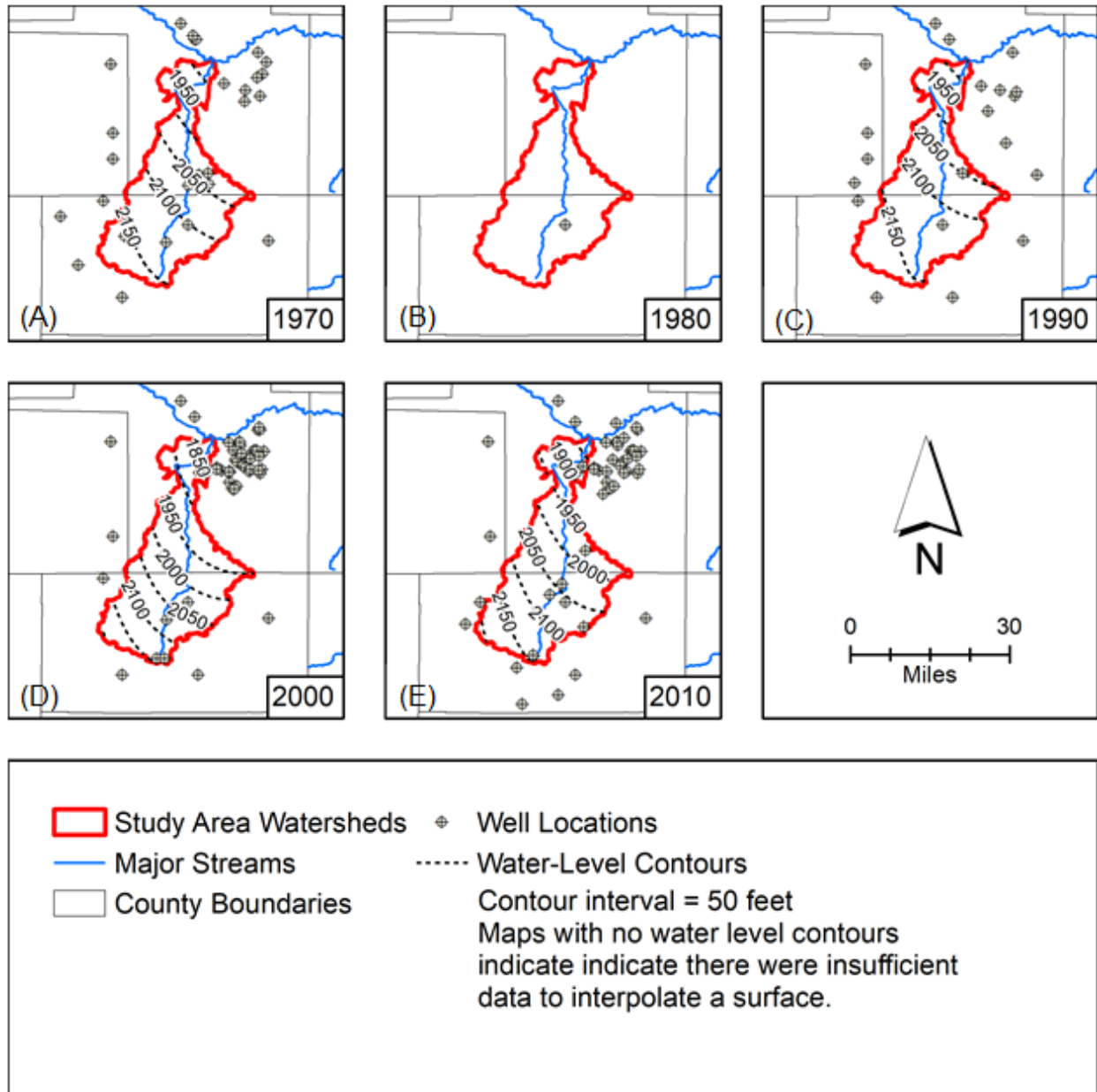


Figure 9-15 – Potentiometric surface from 1970 through 2010 for the South Concho watershed.

For the North Concho (Figure 9-16), there appears to be slight decline from 1970 to 2000 in lower part of the watershed, with a rise in water levels in the upper part of the watershed during the same period. The decline is consistent with the decline in the Lipan Aquifer discussed by Beach and others (2004). The apparent rise appears due to the number of data points in the interpolation rather than any real water level change. Water level declines are evident in the upper reaches of the watershed for the period from 2000 to 2010, with levels in the lower portion of the basin remaining stable over this time. We suspect that the declines in the upper portion of the watershed are based on the differences in the number of wells used to generate each surface, specifically wells located to the south west of the upper portion of the watershed boundary.

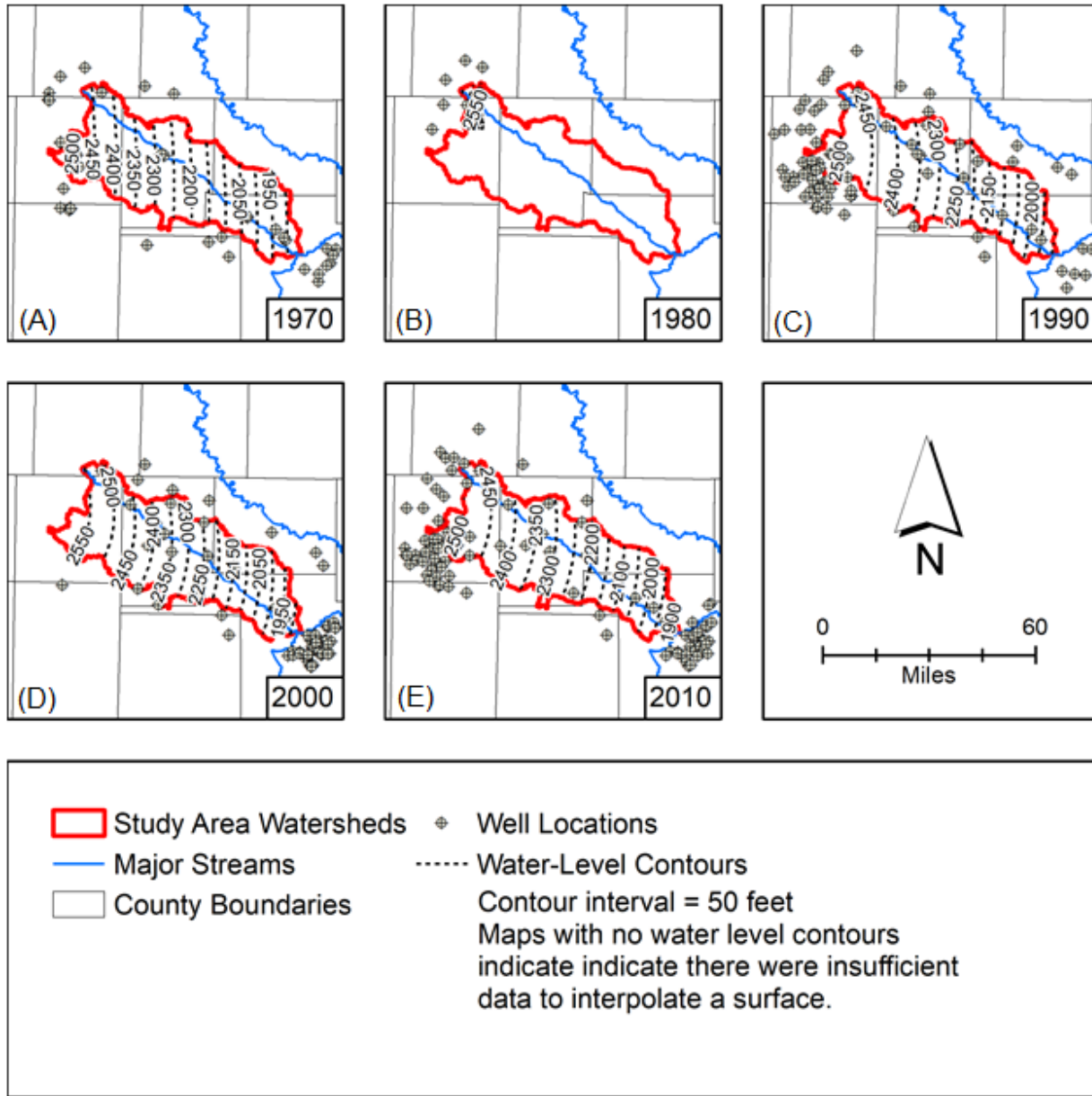


Figure 9-16 – Potentiometric surface from 1970 through 2010 for the North Concho watershed.

9.3 Baseflow Analysis

Although not required for this Phase II analysis, we decided to analyze baseflows over time for each of the subject area watersheds. Our objective was to identify if baseflows (which are typically indicative of groundwater contributions to streamflow) exhibit significant trends over the 1940-2016 project period of record. Baseflow analyses were performed using the Recursive Digital Filter method implemented in WHAT (Lim and others, 2005) available at <https://engineering.purdue.edu/mapserve/WHAT/> as of 7/1/2019.

For our analysis, we used the gage data for the six streamflow gauge locations discussed in Section 0 and shown on Figure 6-1. Baseflows were determined as daily streamflow values, from which we computed the cumulative annual baseflow at each location. The Mann-Kendall analysis technique was then used to assess trends within the annual baseflow datasets. Results of the analysis show that baseflow at four of the six gaging stations has a decreasing trend.

Along with changes in climatic conditions, an additional cause for the decreasing baseflow observed at four locations could be groundwater pumping within the watersheds. While the data are limited for assessing the amount of water-level decline near the streams, we observe in part of the North Concho watershed declines in water levels near the river that would affect baseflow (see Figure 9-10). However, water level declines in wells near streams in the San Saba watershed are less apparent, but each of gage locations in the San Saba watershed indicates a decreasing baseflow trend.

9.3.1 Elm Creek Watershed

Annual baseflow calculated from readings at site “USGS 08127000 Elm Ck at Ballinger, TX” ranged from 22 acre-feet in 2013 to over 25,000 acre-feet in 1992. As Figure 9-17 shows, there is a stable trend in annual baseflow for Elm Creek, but an increasing trend in the percent of the total flow that is attributable to baseflow. Evaluation of the seasonal results indicates an increasing trend in baseflow during the winter months and a decreasing baseflow trend for May. Table 9-1 **Error! Reference source not found.** provides results for monthly and seasonal time periods.

The Elm Creek watershed is primarily in Runnels County with the northern third of the watershed in Taylor County. **Error! Reference source not found.** illustrates the reported groundwater pumping in Runnels and Taylor counties, as reported by TWDB (2019). Total pumping from both counties is typically less than 6,000 acre-feet per year. With available data, it is not possible to link any changes in baseflow to changes in annual groundwater pumping data for the Elm Creek watershed.

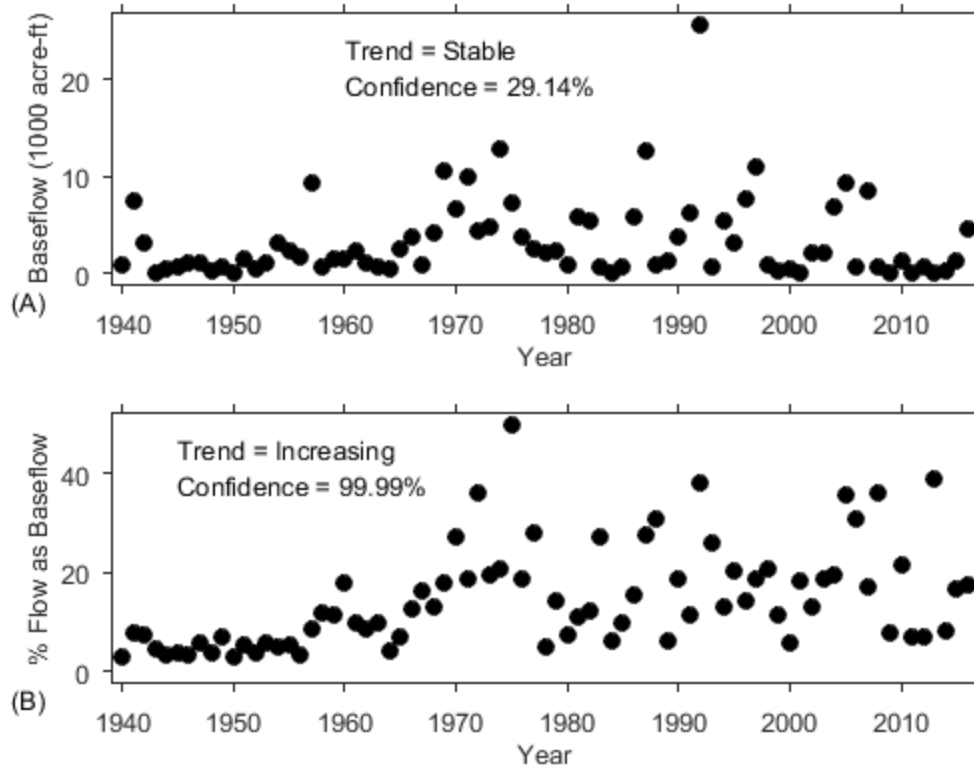


Figure 9-17 – Calculated annual baseflow in the Elm Creek watershed from USGS 0812700 Elm Ck at Ballinger, TX streamflow data.

Table 9-1 – Mann-Kendall results for baseflow trends, Elm Creek at Ballinger

<u>Time Period</u>	<u>1940-2016</u>	
	<u>Trend</u>	<u>Confidence Level</u>
January	Increasing	97.43%
February	Increasing	96.38%
March	Increasing	99.37%
April	Stable	60.83%
May	Decreasing	96.09%
June	Stable	25.19%
July	Stable	39.50%
August	Stable	29.11%
September	Stable	66.96%
October	Stable	40.02%
November	Stable	40.35%
December	Increasing	85.11%
Spring	Stable	70.28%
Summer	Stable	28.82%
Fall	Stable	40.43%
Winter	Increasing	88.93%
Annual	Stable	29.15%

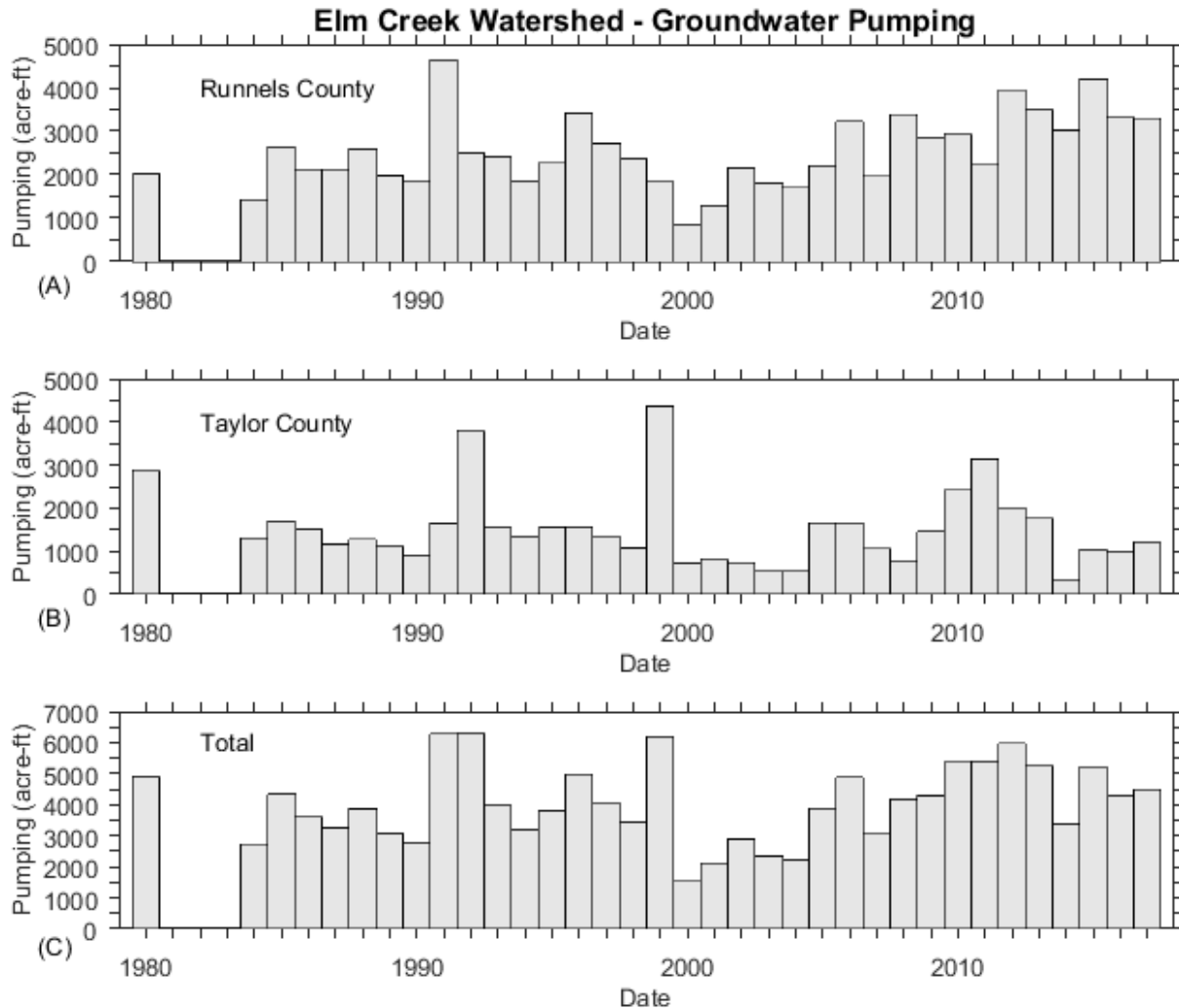


Figure 9-18 – Reported pumping in Runnels and Taylor counties (TWDB, 2019).

9.3.2 San Saba Watershed

Like the streamflow trend analysis in Section 0, we performed a baseflow analysis for each of the three gage locations in the San Saba watershed. For the groundwater pumping comparison, we collected historical pumping estimates from the four main counties covered by the watershed: McCulloch, Menard, San Saba, and Schleicher. Reported pumping from the four counties has been relatively stable since 1980. Figure 9-19 illustrates the reported pumping in the four counties.

As discussed below, all three datasets show decreasing trends in baseflow. With relatively stable pumping, the overall water balance may be changing within the watershed or the pumping is significantly greater than the aquifers can naturally recharge. While the baseflow is decreasing, the percent of streamflow that is attributable to baseflow is increasing at two locations. This increasing trend may reflect the occurrence of fewer high streamflow events and increased ability of the shallow aquifers to accept recharge.

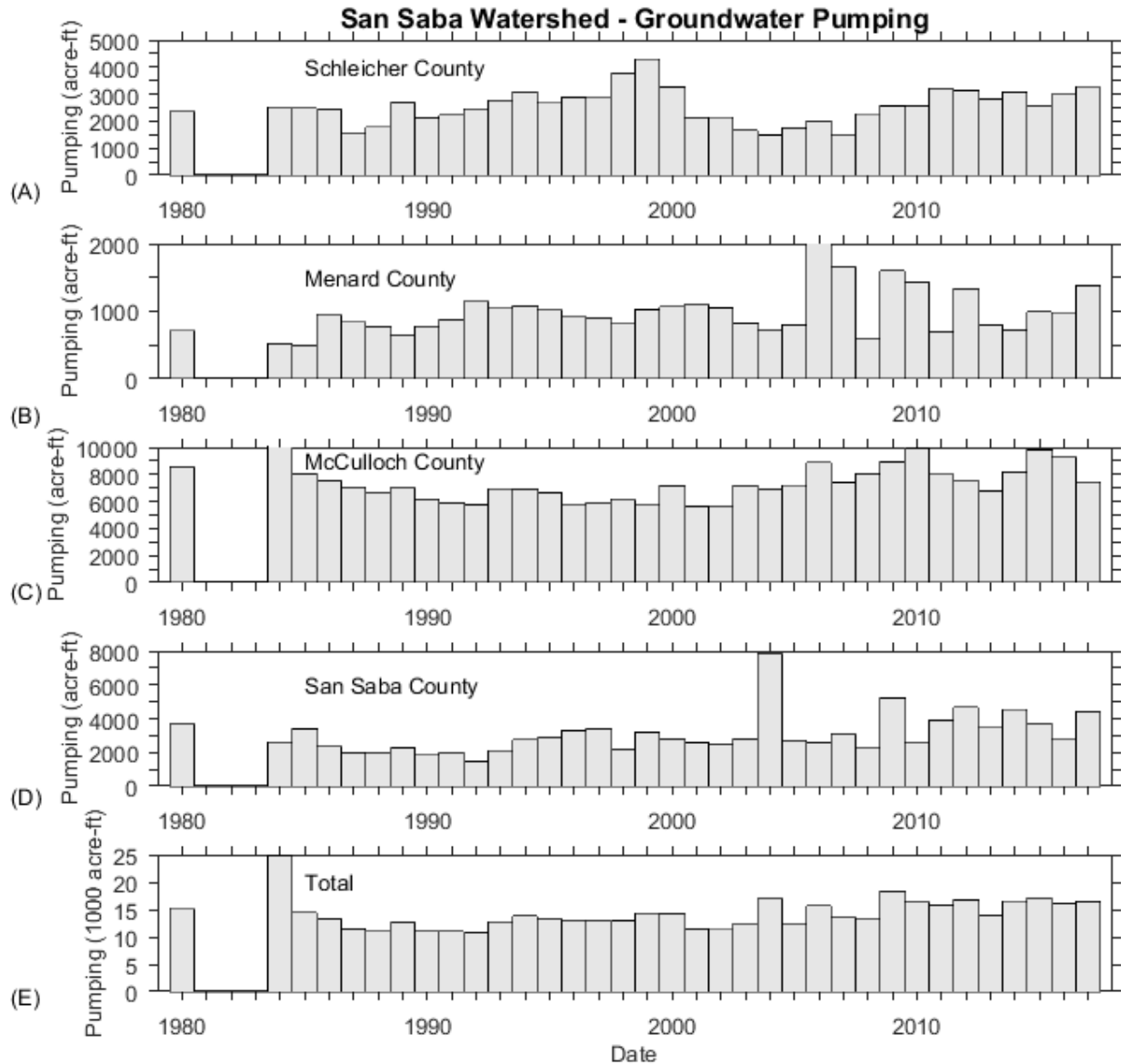


Figure 9-19 – Reported pumping in McCulloch, Menard, San Saba, and Schleicher counties (TWDB, 2019).

9.3.2.1 San Saba River at Menard

Annual baseflow calculated from readings at site “USGS 08144500 San Saba Rv at Menard, TX” ranged from about 2,000 acre-feet in 1984 to nearly 30,000 acre-feet in 1990. As Figure 9-20 shows, there is a decreasing trend in annual baseflow for San Saba River at Menard and a stable trend in the percent of streamflow that is baseflow. Table 9-2 provides results for monthly and seasonal time periods.

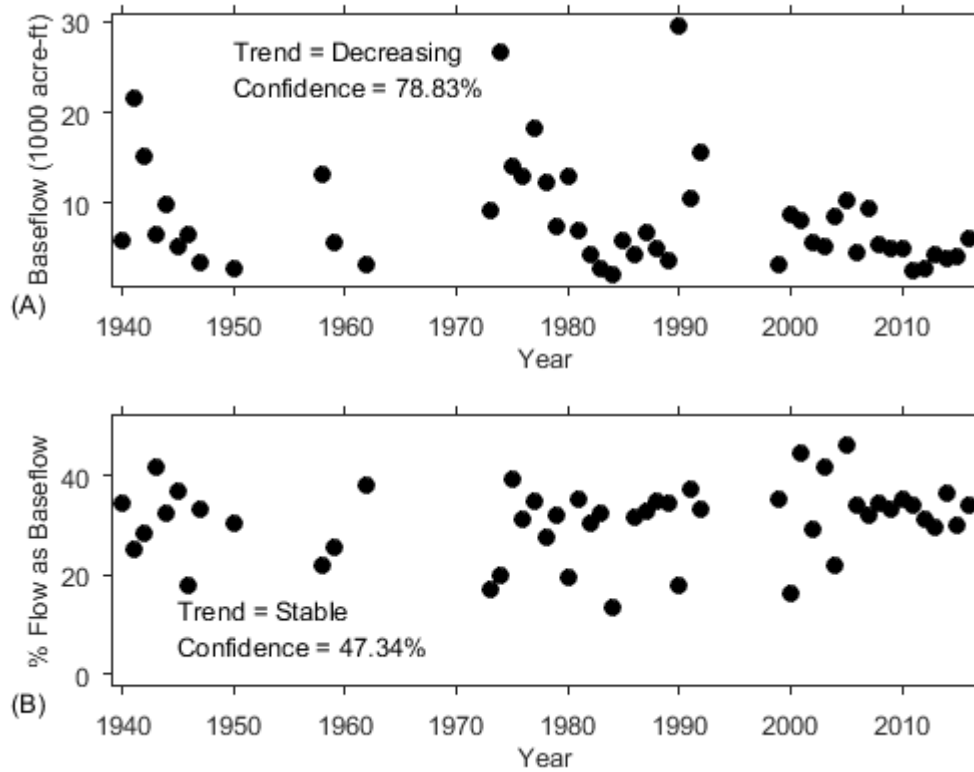


Figure 9-20 – A) Calculated annual baseflow in the San Saba watershed from USGS 08144500 San Saba Rv at Menard, TX streamflow data, and B) Percent of total streamflow that is baseflow.

Table 9-2 – Mann-Kendall results for baseflow trends, San Saba River at Menard

	<u>1940-2016</u>	
<u>Time Period</u>	<u>Trend</u>	<u>Confidence Level</u>
January	Stable	7.71%
February	Stable	37.15%
March	Stable	28.82%
April	Stable	7.01%
May	Stable	33.99%
June	Stable	13.27%
July	Stable	9.10%
August	Stable	4.56%
September	Stable	14.66%
October	Stable	50.74%
November	Stable	35.26%
December	Stable	20.14%
Spring	Stable	26.18%
Summer	Stable	15.00%
Fall	Stable	27.84%
Winter	Stable	7.01%
Annual	Decreasing	78.84%

9.3.2.2 *Brady Creek at Brady*

Annual baseflow calculated from readings at site “USGS 08145000 Brady Ck at Brady, TX” ranged from 1 acre-foot in 1963 to more than 11,000 acre-feet in 1957. As Figure 9-21 shows, there is a decreasing trend in annual baseflow for Brady Creek at Brady, but an increasing trend in the percent of streamflow that is baseflow. Table 9-3 **Error! Reference source not found.** provides results for monthly and seasonal time periods.

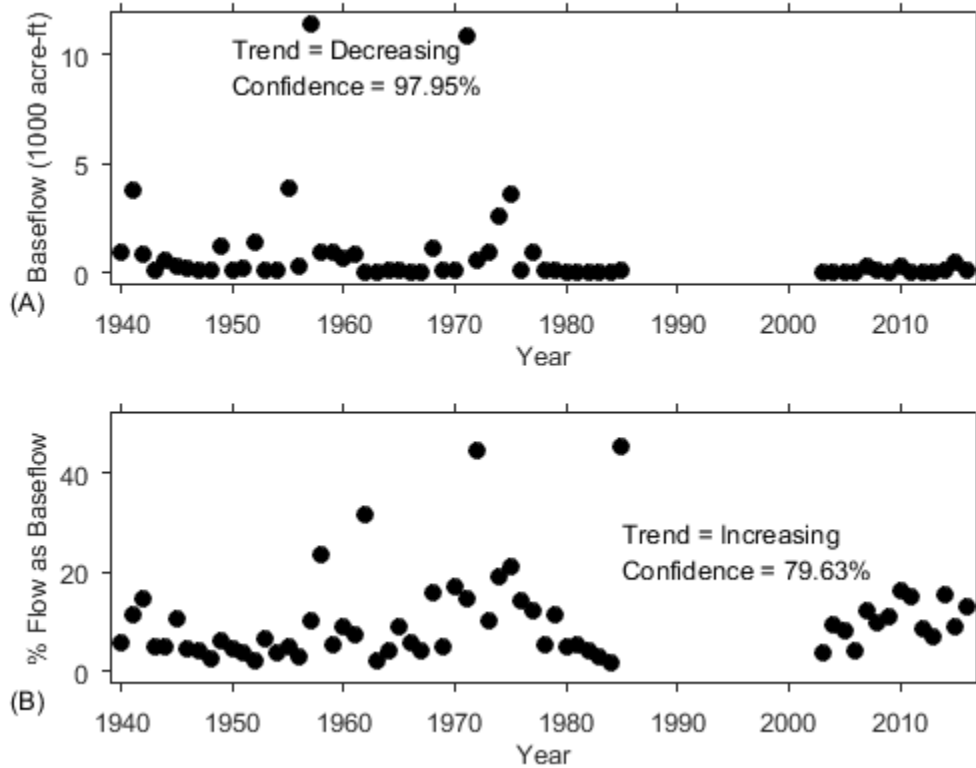


Figure 9-21 – A) Calculated annual baseflow in the San Saba watershed from USGS 08145000 Brady Ck at Brady, TX streamflow data, and B) Percent of total streamflow that is baseflow.

Table 9-3 – Mann-Kendall results for baseflow trends, Brady Creek at Brady

	<u>1940-2016</u>	
<u>Time Period</u>	<u>Trend</u>	<u>Confidence Level</u>
January	Stable	32.30%
February	Stable	47.38%
March	Stable	18.87%
April	<u>Decreasing</u>	<u>92.59%</u>
May	<u>Decreasing</u>	<u>98.69%</u>
June	<u>Decreasing</u>	<u>90.27%</u>
July	Stable	38.87%
August	Stable	26.43%
September	<u>Decreasing</u>	<u>80.44%</u>
October	Stable	49.77%
November	Stable	26.75%
December	<u>Decreasing</u>	<u>75.16%</u>
Spring	<u>Decreasing</u>	<u>99.43%</u>
Summer	<u>Decreasing</u>	<u>87.61%</u>
Fall	Stable	68.21%
Winter	Stable	64.45%
Annual	<u>Decreasing</u>	<u>97.95%</u>

9.3.2.3 San Saba River at San Saba

Annual baseflow calculated from readings at site “USGS 08146000 San Saba Rv at San Saba, TX” ranged from more than 5,500 acre-feet in 1954 to nearly 100,000 acre-feet in 1941. As Figure 9-22 shows, there is a decreasing trend in annual baseflow for San Saba River at San Saba, but an increasing trend in the percent of streamflow that is baseflow. Table 9-4 provides results for monthly and seasonal time periods.

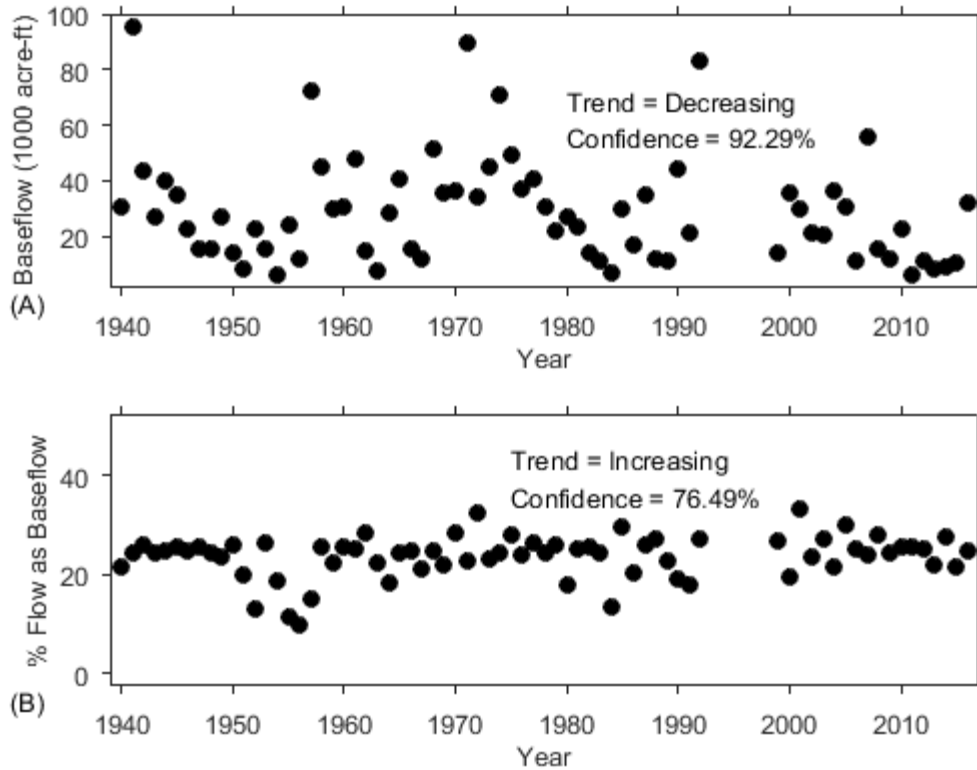


Figure 9-22 – A) Calculated annual baseflow in the San Saba watershed from USGS 08146000 San Saba Rv at San Saba, TX streamflow data, and B) Percent of total streamflow that is baseflow.

Table 9-4 – Mann-Kendall results for baseflow trends, San Saba River at San Saba

<u>Time Period</u>	<u>1940-2016</u>	
	<u>Trend</u>	<u>Confidence Level</u>
January	Stable	65.57%
February	Stable	67.76%
March	Stable	51.57%
April	Stable	73.04%
May	Decreasing	99.45%
June	Decreasing	97.91%
July	Decreasing	75.97%
August	Stable	65.12%
September	Decreasing	89.16%
October	Decreasing	95.37%
November	Decreasing	76.67%
December	Stable	59.91%
Spring	Decreasing	94.20%
Summer	Decreasing	92.51%
Fall	Decreasing	89.16%
Winter	Stable	58.92%
Annual	Decreasing	92.30%

9.3.3 South Concho Watershed

Annual baseflow calculated from readings at site “USGS 08128000 S Concho Rv at Christoval, TX” ranged from 389 acre-feet in 1954 to over 12,000 acre-feet in 1975. There is a stable trend in baseflow and the percent of streamflow that is baseflow. Figure 9-23 illustrates the calculated annual baseflow at the gage location and Table 9-5 provides results for monthly and seasonal time periods.

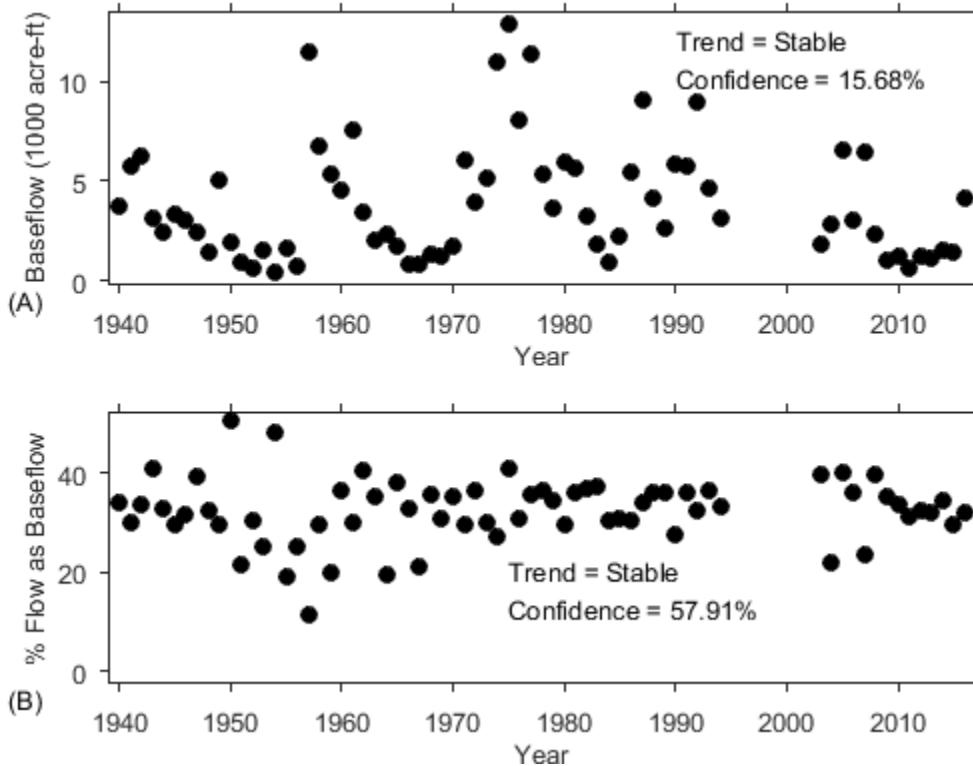


Figure 9-23 – A) Calculated annual baseflow in the South Concho watershed from USGS 0812800 S Concho Rv at Christoval, TX streamflow data, and B) Percento of total streamflow that is baseflow.

Table 9-5 – Mann-Kendall results for baseflow trends, South Concho River at Christoval

<u>1940-2016</u>					
<u>Time Period</u>	<u>Trend</u>	<u>Confidence Level</u>	<u>Time Period</u>	<u>Trend</u>	<u>Confidence Level</u>
January	Stable	37.77%	November	Stable	6.31%
February	Stable	37.77%	December	Stable	35.89%
March	Stable	3.51%			
April	Stable	30.13%	Spring	Stable	19.46%
May	Stable	28.82%	Summer	Stable	53.47%
June	Stable	43.85%	Fall	Stable	24.18%
July	Stable	73.23%	Winter	Stable	45.03%
August	Stable	43.25%	Annual	Stable	15.69%
September	Stable	18.77%			
October	Stable	41.45%			

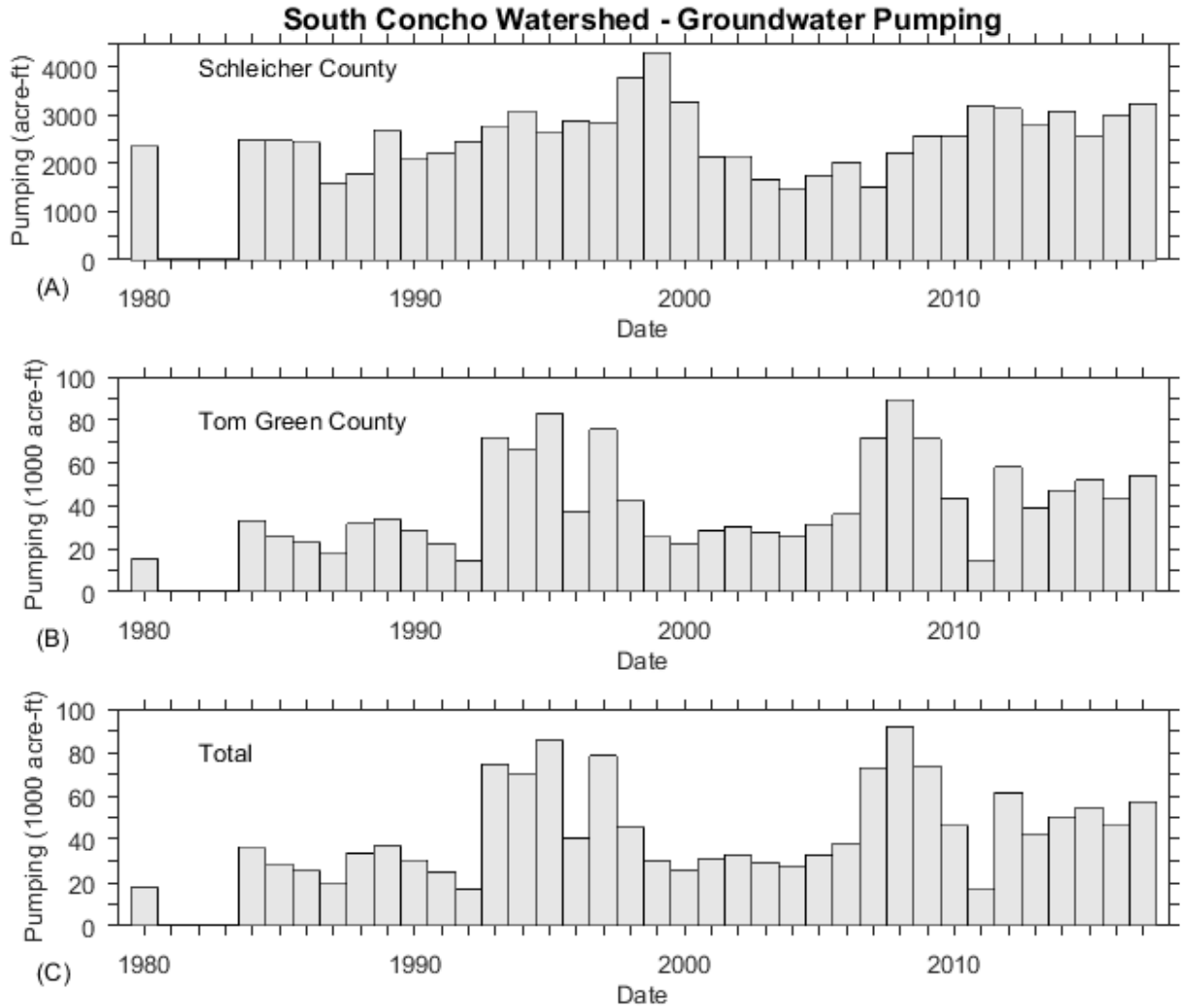


Figure 9-24 – Reported pumping in Schleicher and Tom Green counties (TWDB, 2019)

Figure 9-24 illustrates the reported pumping in Schleicher and Tom Green counties. The pumping in Tom Green County is much greater than in Schleicher County. Regional water-level declines associated with the pumping may be capturing baseflow that would otherwise occur during spring and summer months within the South Concho watershed. However, the capture of potential baseflow is not reflected in the analysis of baseflow trends, as baseflow quantities have remained stable while pumping has generally increased with time.

9.3.4 North Concho Watershed

Annual baseflow calculated from readings at site “USGS 08134000 N Concho Rv nr Carlsbad, TX” ranged from 0 acre-feet in 1970 to nearly 25,000 acre-feet in 1957. Annual baseflow is decreasing at the gage location (Figure 9-25), and similar trends were evident for all monthly and seasonal time periods (Table 9-6). While the baseflow is decreasing, the percent of streamflow that is baseflow is increasing.

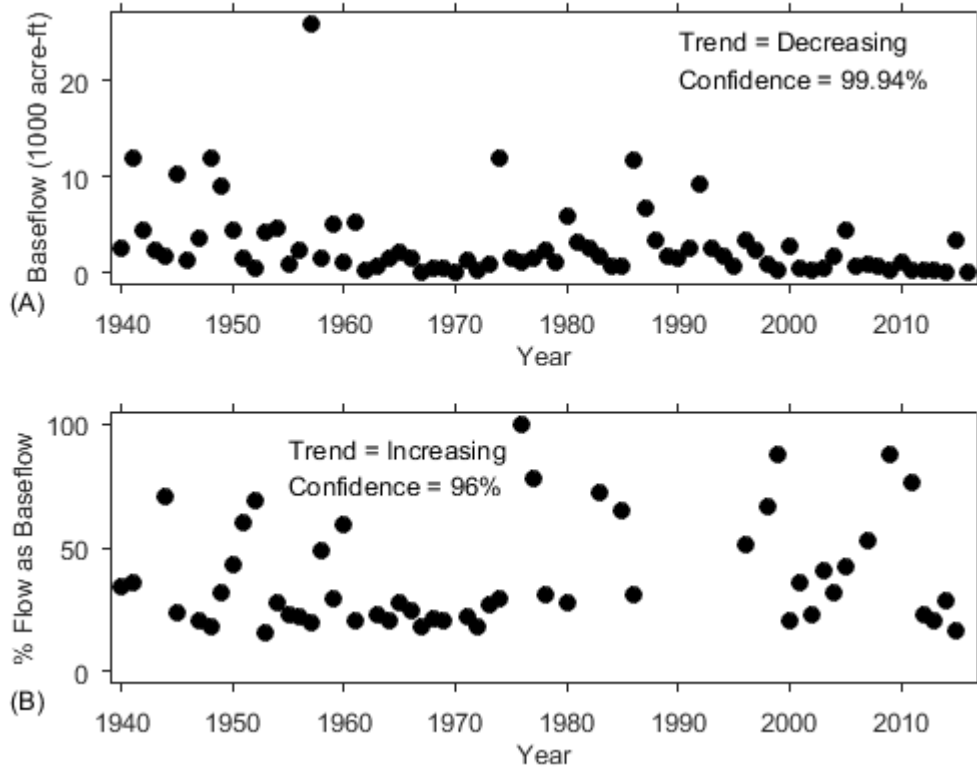


Figure 9-25 – Calculated annual baseflow in the North Concho watershed from USGS 08134000 N Concho River nr Carlsbad, TX streamflow data.

Table 9-6 – Mann-Kendall results for baseflow trends, North Concho River nr Carlsbad

	<u>1940-2016</u>				
<u>Time Period</u>	<u>Trend</u>	<u>Confidence Level</u>	<u>Time Period</u>	<u>Trend</u>	<u>Confidence Level</u>
January	Decreasing	87.80%	January	Decreasing	92.20%
February	Decreasing	90.85%	February	Decreasing	96.43%
March	Decreasing	83.54%	March		
April	Decreasing	97.11%	April	Decreasing	99.94%
May	Decreasing	99.76%	May	Decreasing	99.98%
June	Decreasing	99.70%	June	Decreasing	88.49%
July	Decreasing	99.97%	July	Decreasing	94.37%
August	Decreasing	99.62%	August	Decreasing	99.94%
September	Decreasing	99.77%	September		
October	Decreasing	85.88%	October		

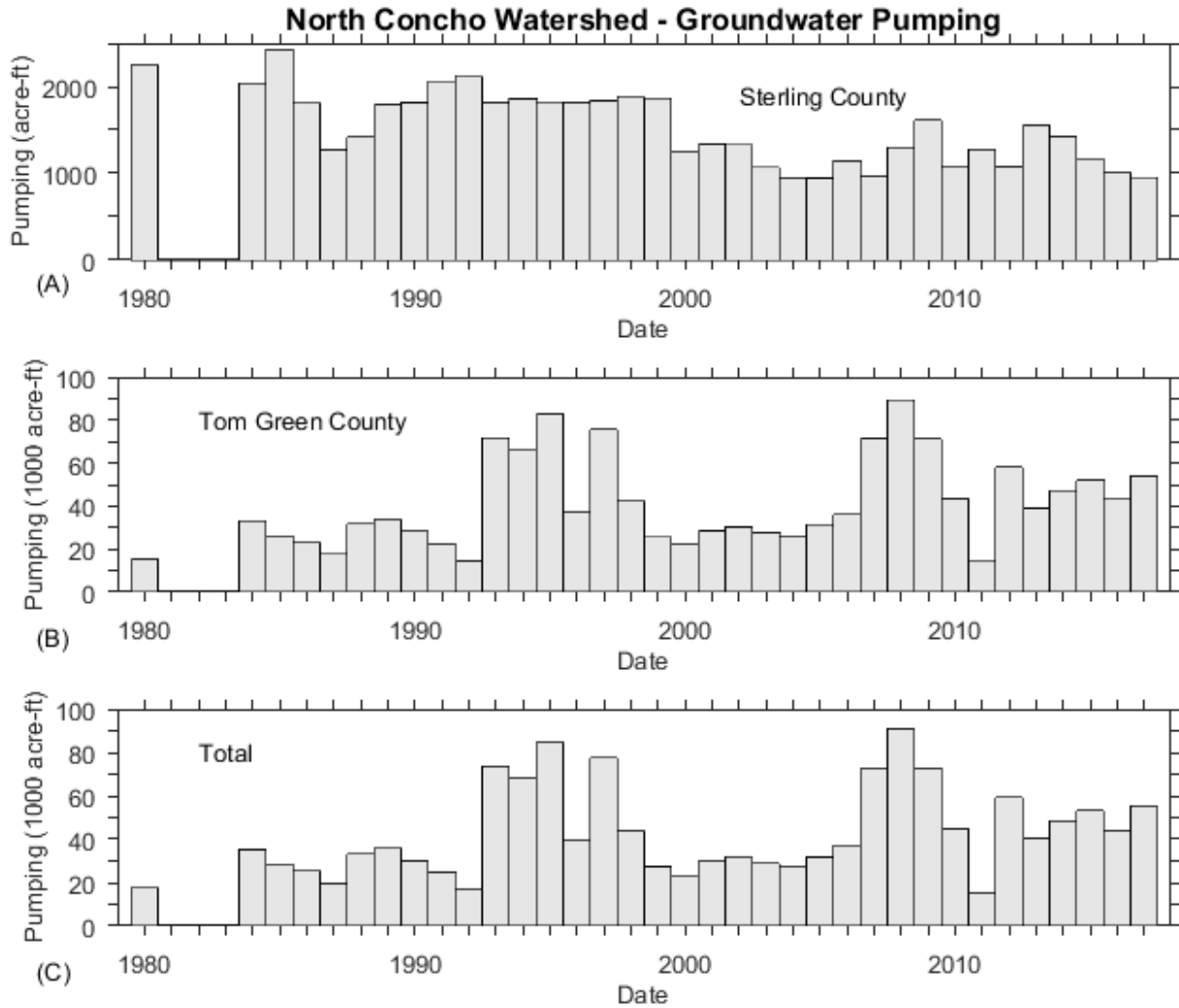


Figure 9-26 – Reported pumping in Sterling and Tom Green counties (TWDB, 2019).

The decreasing trend in baseflow within the North Concho River could be associated with declining groundwater levels near the stream. However, these water level declines were not observable in the available groundwater data. The decline in baseflow is likely a combination of many factors including a general increase in quantifiable groundwater pumping in Sterling and Tom Green counties (Figure 9-26).

Most of the reported pumping has occurred in Tom Green County. Since 2000, the TWDB has reported the estimated pumping per aquifer and the data indicate about 60 percent of the pumping in Tom Green County comes from the Lipan Aquifer. In most years since 2000, irrigation pumping is more than 90 percent of the total Lipan Aquifer pumping and based on the work by Beach and others (2004) most of the irrigation pumping is occurring east of the watershed. As Figure 9-2 illustrates, the North Concho River flows across the Lipan Aquifer and the pumping from the aquifer has likely caused a small change in regional aquifer water levels that resulted in a decrease in baseflow to the river.

9.4 Groundwater Analysis Summary

This section detailed the available groundwater data for the study area watersheds for the purpose of supporting or refuting the idea that changes in groundwater levels could impact changes in streamflow. In general, streamflow at any location is a combination of baseflow derived from the local aquifer and runoff generated by periodic rain events. Therefore changes in streamflow (Section 0) may result from changes in baseflow and/or changes in runoff.

Baseflows to streams represent water movement from the groundwater system to the surface water system, and for such movement to occur, water levels within the groundwater system must exceed those in the surface water system. Thus if groundwater levels were to decline sufficiently (over either a local or regional scale) then groundwater elevations would become lower than water elevations in the surface water system. This would reduce baseflows to zero and could possibly cause surface water to flow from the stream into the groundwater system. Both of these outcomes would reduce streamflow.

Our analysis of regional groundwater levels suggested possible declines, especially for the North Concho watershed. However these possible declines were not definitive, as insufficient data are available to fully quantify regional groundwater level changes over time.

We were able to reasonably link many changes in water levels in 7 shallow groundwater wells with variable streamflow records from nearby streamflow gages. The generally large periods of time between groundwater measurements, however, made difficult developing exact correlation between groundwater level changes and streamflow changes. In general it appears evident that water levels within groundwater wells located close to streams tended to increase around the time of large streamflow events. Insufficient data was available to determine if the well water level caused the change in streamflow, or if the streamflow caused the change in the well water level. It was also impossible to discern how local groundwater pumping may affect the streamflow, as insufficient data were available regarding groundwater pumping from wells in the vicinity of the 7 shallow wells included in this analysis.

Baseflow analyses indicated that within the San Saba and North Concho watersheds, baseflows are decreasing, while such flows remained stable within the Elm Creek and South Concho watersheds. Baseflow as a percentage of total streamflow was found to be increasing in the Elm Creek watershed, the lower portion of the San Saba watershed (encompassing Brady and San Saba), and within the North Concho watershed. Such increases tend to reflect more that runoff to the stream is decreasing and therefore reducing the total streamflow. This is supported by data from the North Concho watershed, where baseflow is declining while the percentage of streamflow as baseflow is increasing.

Based on analyses of all available data presented in this section, we determined that we could not definitively confirm or refute the potential connection between groundwater in surficial aquifers and flow in streams running through the surficial aquifers.

10 Task 8 – Demonstrating Cause and Effect Regarding Rainfall/Runoff Response

The purpose of this task is to integrate the results of all previous tasks into a mathematical model which quantifies streamflow. Comparing quantified streamflow under various modeling scenarios would therefore identify the relative importance of various model factors in controlling runoff from each study area watershed. The objective of this task is NOT to compare calculated streamflows with actual recorded streamflows; doing so would require a spatially distributed water balance model using spatially and temporally distributed input data. Available data presented herein is insufficient for the development of an accurate spatially distributed model. However such a model is possible, and was partially developed as part of the Soil-Water-Balance model developed and discussed in Section 0.

The objective of this task is to quantify the DIFFERENCE in streamflow that would theoretically result based on changes to watershed parameters.

For discussion purposes, the mathematical model developed under this task will be referred to as the “Upper Colorado Water Balance Model (UCWBM).” The UCWBM was created specifically for this project, and applies the basic principles of water accounting and mass balance to simulate water movement through the study area watersheds. The model was developed for use within the MATLAB software, and model source code is provided in the **Appendix** .

10.1 Methodology

To develop the methodology for quantifying streamflow differences resulting from modifications to watershed parameters, it is necessary to develop sound hydrologic theory as to how the parameters interact. The parameters considered in this analysis were:

1. Rainfall quantity and timing
2. Land Use/Land Cover
3. Small Ponds within each watershed
4. Soil moisture content
5. Water loss from soil and vegetation through evapotranspiration
6. Water loss from the soil through movement and diversions (pumping)

The UCWBM was originally envisioned to incorporate a water balance in both the surface water and groundwater portions of the model domain. However given the lack of knowledge regarding groundwater diversions and evapotranspiration (model parameters #5 and #6), it was determined that doing a subsurface water balance would not be fruitful.

The UCWBM, as developed under this task, considers only parameters #1-#4 within its water balance process, and is limited in scope to consider only the surface water balance. The following subsections detail how the model incorporates each parameter into the calculation process.

10.1.1 UCWBM modeling of rainfall quantity and timing

Rainfall patterns for each watershed were discussed and detailed within Section 0 of this report. Daily rainfall data is also available at various locations within each watershed. The UCWBM uses rainfall data as the direct input water source driving the model calculations. For simplicity purposes, the UCWBM uses only a single rainfall dataset for each watershed within the study area, and assumes this rainfall applies uniformly to all locations within each watershed. Rainfall values used within the UCWBM are the daily rainfall totals described in Section 0. For any modeled day when rainfall records were unavailable (i.e. assigned a value of “-1 inch” within the rainfall databases), the UCWBM model assumes zero rainfall occurred on that day.

Table 10-1 – Rainfall data sources used within the UCWBM

Watershed	Gauge Location	Period of Record	Report Section
Elm Creek	Ballinger	1900-2018	Section 7.1.1.1
San Saba	San Saba	1940-2018	Section 7.1.3.3
South Concho	Christoval	1940-2018	Section 7.1.4.2
North Concho	Sterling City	1926-2018	Section 7.1.5.3

10.1.2 UCWBM modeling of Land Use/Land Cover

To approximate the rainfall-runoff response of each watershed, the UCWBM utilizes the standard “Curve Number Method” originally developed by the Soil Conservation Service (SCS) and commonly described in all basic hydrology textbooks. The curve number method calculates runoff generated by rainfall events according to the following series of equations:

Eq. 10-1 $q = \frac{(P-I_a)^2}{(P-I_a)+S}$

Eq. 10-2 $I_a = 0.2S$

Eq. 10-3 $S = \frac{1000}{CN} - 10$

Where “q” is the resulting runoff (Units = inches), “P” is the depth of rainfall (Units = Inches), “I_a” is the initial abstractions representing the amount of rainfall lost to the land surface or canopy, and “S” is the potential maximum retention of water by the land surface and local groundwater system. The value “CN” is the curve number describing the land use/land cover of the watershed (which is also dependent upon the watershed’s hydrologic

soil group). Curve number values were annually computed for each watershed for the period 1940-2016 based on recorded land use data (Section 4.3 and Figure 4-16).

When implementing the curve number equations for computing runoff, the UCWBM first computes values for “S” and “I_a” using Eq. 10-3 and Eq. 10-2. Prior to computing runoff (“q”), the UCWBM compares values of P to the computed values of I_a, and only computes runoff if precipitation exceeds the depth of water lost to the initial abstractions. In this way runoff is only computed when there is sufficient precipitation (“P”) to reach the ground, after accounting for canopy losses. This concept was first presented in Section 7.2.

Values for “P” are the actual daily values of recorded rainfall from gages as listed in Table 10-1. Therefore through the application of Eq. 10-1 - Eq. 10-3 for every daily rainfall event, the UCWBM calculates the depth of water that will become runoff within each watershed. This water depth is converted to a volume of runoff “Q” by multiplying “q” by the watershed surface area.

The equation parameter “S” mathematically represents the portion of the rainfall that is to enter the groundwater system as recharge. In Eq. 10-3, the value for S is computed entirely based on the “CN” value as adjusted for antecedent moisture conditions. Therefore S varies based on the land use/land cover characteristics of the watershed as well as recently occurring rainfall. In UCWBM simulations, the user must specify a “watershed year” from which the watershed’s CN value will be derived. Curve numbers are then adjusted at each UCWBM daily model timestep to account for antecedent moisture conditions, prior to calculating “S” values.

10.1.2.1 Modeling Soil Moisture Effects

While the UCWBM does not explicit compute soil moisture content or adjust runoff based on computed soil moisture values, it does simulate the influence of soil moisture on runoff through the use of “antecedent moisture conditions.” Specifically, curve numbers used within the UCWMB are adjusted to account for antecedent moisture conditions based on the preceding 5-day accumulated rainfall totals and season of the year. Adjustments are made to curve numbers by first classifying the antecedent moisture condition as “I-Dry,” “II-Average,” or “III -Wet” and then adjusting the curve numbers based on the classification. Curve number adjustments for antecedent moisture conditions are provided in Table 10-2 and were also discussed in Section 7.2.

Table 10-2 – Adjustments to curve numbers based on antecedent moisture conditions

Condition	Formula	5-Day Antecedent Rainfall Criteria	
		Growing Season March 15-October 15	Dormant Season October 16-March 14
I - Dry	$CN_I = \frac{4.2CN}{10 - 0.058CN}$	RT < 1.4 in	RT < 0.5 in
II - Average	"CN" From Section 4.3	1.4 in ≤ RT ≤ 2.0 in	0.5 in ≤ RT ≤ 1.0 in
III - Wet	$CN_{III} = \frac{23CN}{10 + 0.13CN}$	RT > 2.0 in	RT > 1.0 in

RT = Total rainfall for the previous 5-days

To demonstrate the curve number adjustment process, consider a watershed with a curve number of 80 as calculated entirely based on the land use/land cover characteristics (See Section 4.3). If the previous 5-days of rainfall and the season of the year suggested the watershed would be in "I-Dry" conditions, then per Table 10-2 the adjusted curve number ("CN_I") would be calculated as:

$$CN_I = \frac{4.2CN}{10 - 0.058CN} = \frac{4.2(80)}{10 - 0.058(80)} = 62.7$$

The resulting dry condition curve number is lower than the originally computed "II-Average" condition curve number, indicating that under dry conditions a greater portion of the rainfall would be lost to recharge the groundwater system, and would not become runoff. Continuing the example, if the previous 5-days of rainfall and the season of the year suggested the watershed would be in "III-Dry" conditions, then per Table 10-2 the adjusted curve number ("CN_{III}") would be calculated as:

$$CN_{III} = \frac{23CN}{10 + 0.13CN} = \frac{23(80)}{10 + 0.13(80)} = 90.1$$

The resulting wet condition curve number is higher than the originally computed "II-Average" condition curve number, indicating that under wet conditions a lesser portion of the rainfall would be lost to recharge the groundwater system, resulting in increased runoff.

Within the UCWBM, values of "P" for the previous 5-days are summed to compute the total rainfall parameter ("RT") used in Table 10-2 to assess antecedent moisture criteria. Thus RT is computed based on the total rainfall depth over the past 5-days, and not based on the depth of precipitation that reaches the ground surface (i.e. P-I_a). The seasonal criteria listed in Table 10-2 define the "growing season" to be between March 15 and October 15, based on our experience with modeling crop irrigation water availability in the Colorado and Brazos River Basins of Texas.

10.1.3 UCWBM modeling of Small Impoundments

Once the volume of runoff is known, it is necessary to determine how much of this runoff will reach the watershed outlet, and how much will be stored within any ponds that exist within the watershed. Properties of the small ponds were identified in Section 4.1 and quantified by watershed and year in Figure 4-10 - Figure 4-13.

To determine the impacts of small ponds on streamflow, the UCWBM tracks the water content of each pond over time. Ponds may be filled by available runoff (“Q”) and rainfall landing directly on the pond surface. Any runoff used to fill a pond is removed from the volume of water computed as streamflow leaving the watershed. Ponds will not release flow downstream unless and until each pond is filled to capacity. Within the UCWBM, ponds only lose water daily due to evaporation, and no water is modeled as being lost through the pond subsurface into the groundwater system. Evaporation rate data was obtained from the TWDB gross evaporation database (downloaded on 6/1/2019 from <https://waterdatafortexas.org/lake-evaporation-rainfall>). Ideally evaporation rates from free-surface waterbodies (such as small ponds) will be functions of the air temperature and local wind speed, among other parameters. As such the temperature data detailed in Section 5 is implicitly included in the measured evaporation data published by the TWDB.

With this method of modeling the impacts of small ponds, the UCWBM treats all ponds as if they were in series and located at the outlet of the watershed. All ponds are simulated as having access to 100% of the runoff generated from the entire watershed, regardless of the physical location of the ponds within the watershed. As such, it is likely that the UCWBM is over-estimating the cumulative impact of ponds on watershed streamflow, as modeled ponds are able to receive runoff from a greater portion of the watershed than they would receive based on their physical location within the watershed. For this reason, UCWBM results with respect to the impacts of small impoundments should be considered as “worst-case” scenarios in quantifying any reductions in watershed streamflow.

10.1.4 UCWBM operation

The UCWBM operates on a daily timestep, and computes total watershed streamflow (at the outlet) for each calendar year of simulation. In running the UCWBM, the model user specifies five parameters:

- **Precipitation Year:** the year of precipitation data
- **Watershed Year:** the year for which watershed conditions (land use and small pond quantities) are simulated
- **Initial Storage:** the initial quantity of water stored in each simulated small pond
- **Storage Carry-Over:** whether or not the modeled initial pond storage at the beginning of the simulated year is set to the specified initial storage or carried over from the last day of the previously modeled year.
- **Simulation Method & Subject Watershed:** directs which watershed to be simulated, and which model functions are to be included in the simulation.

With these five parameters, the model user can direct the UCWBM to simulate the observed rainfall for any given year with watershed conditions computed for any given year. This allows for the comparison of stream flows resulting from, for example, past drought periods with current watershed conditions. The UCWBM, through the parameter “Simulation Method” allows the user to simulate only land use/land cover change, only inclusion of small ponds, or simulating both small ponds and land use/land cover change. It is also possible to adjust the land use/land cover change calculations to exclude the impact of antecedent soil moisture. These variations in model components allow for the determination of the relative importance of each component for each study area watershed.

Figure 10-1 depicts the computational process incorporated into the UCWBM, showing a simulation lasting for one calendar year. As shown, for each daily model timestep, the UCWBM first reduces the volume of water stored in ponds by a quantity determined by the current pond area and the daily evaporation rate, with the daily evaporation rate determined based on the watershed year specified by the model user. The UCWBM only tracks pond storage for ponds in existence as of the user-specified watershed year. After adjusting storage for evaporation losses, if rainfall occurred on the modeled day, storage is increased based on direct precipitation and inflows from watershed runoff. Pond storage is always limited to the maximum capacity of each pond, with any excess water passed as “inflow” to the next pond or as streamflow out of the watershed once all ponds are full. Streamflow data is output at each daily model timestep, along with water loss data due to evaporation.

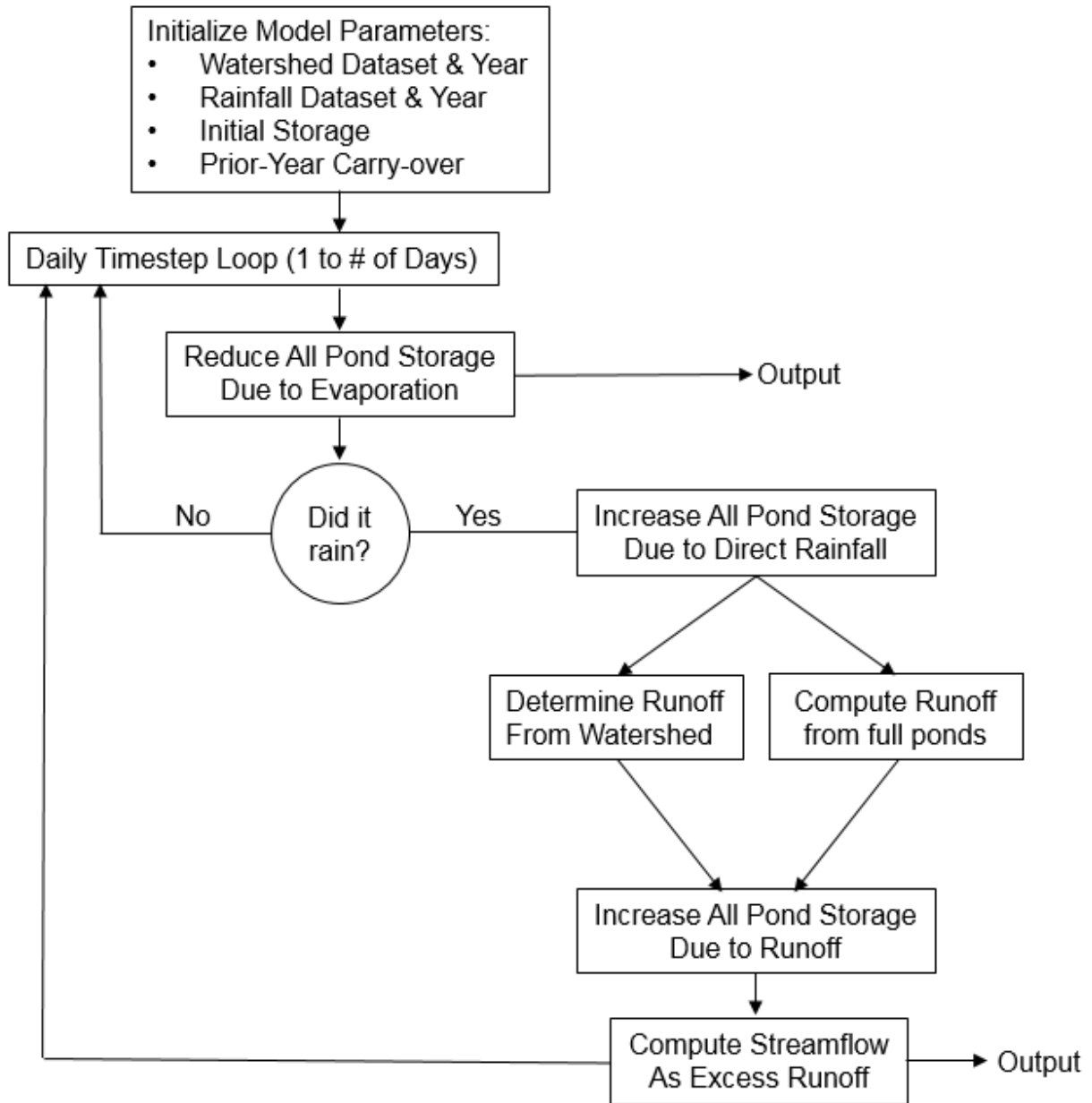


Figure 10-1 – Computational process included within the UCWBM

10.2 UCWBM Results – Full Simulation

The following sections present the UCWBM results for each watershed, tailored to depict changes over the 1940-2016 period of record used in this Phase II analysis. Results are presented as comparisons of streamflow generated for all precipitation years, using the 1940 and 2016 watershed years. Comparative results are presented as both a magnitude (acre-ft/yr) and percentage difference between modeled scenarios. The actual computed runoff (Q) should not be compared with actual measured streamflow quantities reported in Section 0.

For all results presented herein, the UCWBM was run assuming all ponds were initially 50% full on January 1 of each modeled year, without regard to carry-over from the previously modeled December 31 pond storage levels. Precipitation years were simulated for the period from 1940 to 2016. Under this setup, the UCWBM treated each model precipitation year individually, to allow for assessment of how rainfall patterns in that year, coupled with watershed changes between 1940 and 2016, lead to changes in computed streamflows.

The following sections detail UCWBM results from simulations that account for the combined effects of the following parameters:

- Small Impoundment Storage
- Changing Land-use/Land Cover
- Antecedent Moisture Conditions (Soil Moisture).

Section 10.3 discusses the relative effects of each of these parameters on resulting streamflow from each of the study area watersheds.

10.2.1 UCWBM results for the Elm Creek watershed

Figure 10-2 presents UCWBM results for the Elm Creek watershed, specifically comparing computed streamflow for all precipitation years under watershed conditions from 1940 and 2016. The curve numbers for the Elm Creek watershed ranged from 64.99 (1940) to 64.53 (2016), with a minimum value of 63.33 computed for 1962. The decrease in curve number between 1940 and 2016 suggests that the watershed should lose more surface runoff to the ground under 2016 conditions. It is also notable that the Mann-Kendall analysis on the annual dataset of Elm Creek watershed curve numbers indicates an increasing trend with a high confidence level (Figure 4-16A). The difference in curve numbers between the 1940 and 2016 conditions is, however, minimal, and the resulting change in ground infiltration rates is not expected to be significant. The main difference between 1940 and 2016 watershed conditions is the addition of over 4,000 acre-ft of storage capacity within small ponds, as well as the addition of nearly 2,000 acres of water surfaces exposed to evaporative losses when ponds are full.

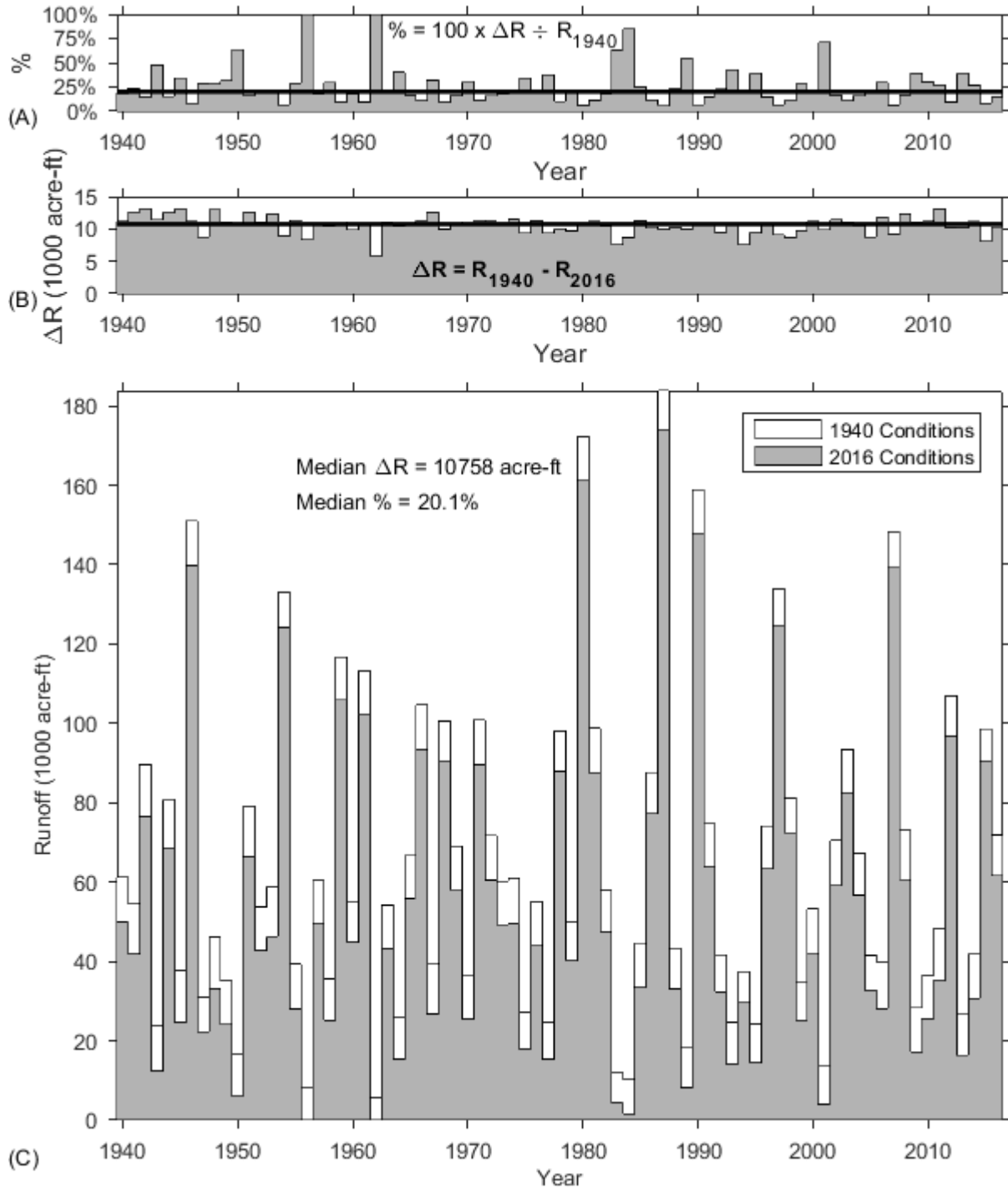


Figure 10-2 – UCWBM results for the Elm Creek watershed – (A) Percentage difference in runoff by year, (B) difference in runoff by year (in acre-ft), (C) computed runoff leaving the watershed as streamflow.

As shown in Figure 10-2, computed runoff for the 1940 watershed conditions exceeded those for the 2016 watershed conditions for all modeled precipitation years. The median difference in runoff was approximately 10,758 acre-ft/yr. The percentage difference in runoff (based on the runoff generated under 1940 conditions) ranged from 5%-100%, with

the median percentage difference equal to 20.1%. UCWMB model results therefore indicate that the existence of small ponds within the Elm Creek watershed, a slight change in watershed land use, and variations in rainfall patterns from year to year combine to result in an approximate 20% median decrease in runoff leaving the watershed as streamflow. It is also noted that rainfall trends for the Ballinger area have remained stable over the 1940-2016 time period, when considering all rainfall events (Figure 7-2) and only runoff-generating events (Figure 7-14).

10.2.2 UCWBM results for the San Saba Watershed

Figure 10-3 presents UCWBM results for the San Saba watershed, specifically comparing computed streamflow for all precipitation years under watershed conditions from 1940 and 2016. The curve numbers for the San Saba watershed ranged from 70.2 (1940) to 70.2 (2016), with the lowest value of 69.5 occurring in 1962. The slight decrease in curve numbers (from 1940 to 2016) suggests that the watershed should lose more surface runoff to the ground under 2016 conditions. Yet as the decrease is minimal, the resulting change in ground infiltration rates is not expected to be significant. . It is also notable that the Mann-Kendall analysis on the annual dataset of San Saba watershed curve numbers indicates an increasing trend with a high confidence level (Figure 4-16B). The main difference between 1940 and 2016 watershed conditions is the addition of over 17,000 acre-ft of storage capacity within small ponds, as well as the addition of over 5,600 acres of water surfaces exposed to evaporative losses when ponds are full.

As shown in Figure 10-3 – UCWBM results for the San Saba watershed, computed runoff for the 1940 watershed conditions exceeded those for the 2016 watershed conditions for all modeled precipitation years. The median difference in runoff was approximately 21,100 acre-ft/yr. The percentage difference in runoff (based on the runoff generated under 1940 conditions) ranged from 1.5-16.0%, with the median percentage difference equal to 3.41%. UCWMB model results therefore indicate that the existence of small ponds within the San Saba watershed, a slight change in watershed land use, and variations in rainfall patterns from year to year combine to result in an approximate 3% median decrease in runoff leaving the watershed as streamflow. It is also noted that rainfall trends for the San Saba area have remained stable over the 1940-2016 time period, when considering all rainfall events (Figure 7-6) and were found to be increasing when considering only runoff-generating events (Figure 7-16). Therefore data from the UCWBM detail how streamflows within the San Saba watershed may be depleted even with increasing trends in runoff-generating annual rainfall events.

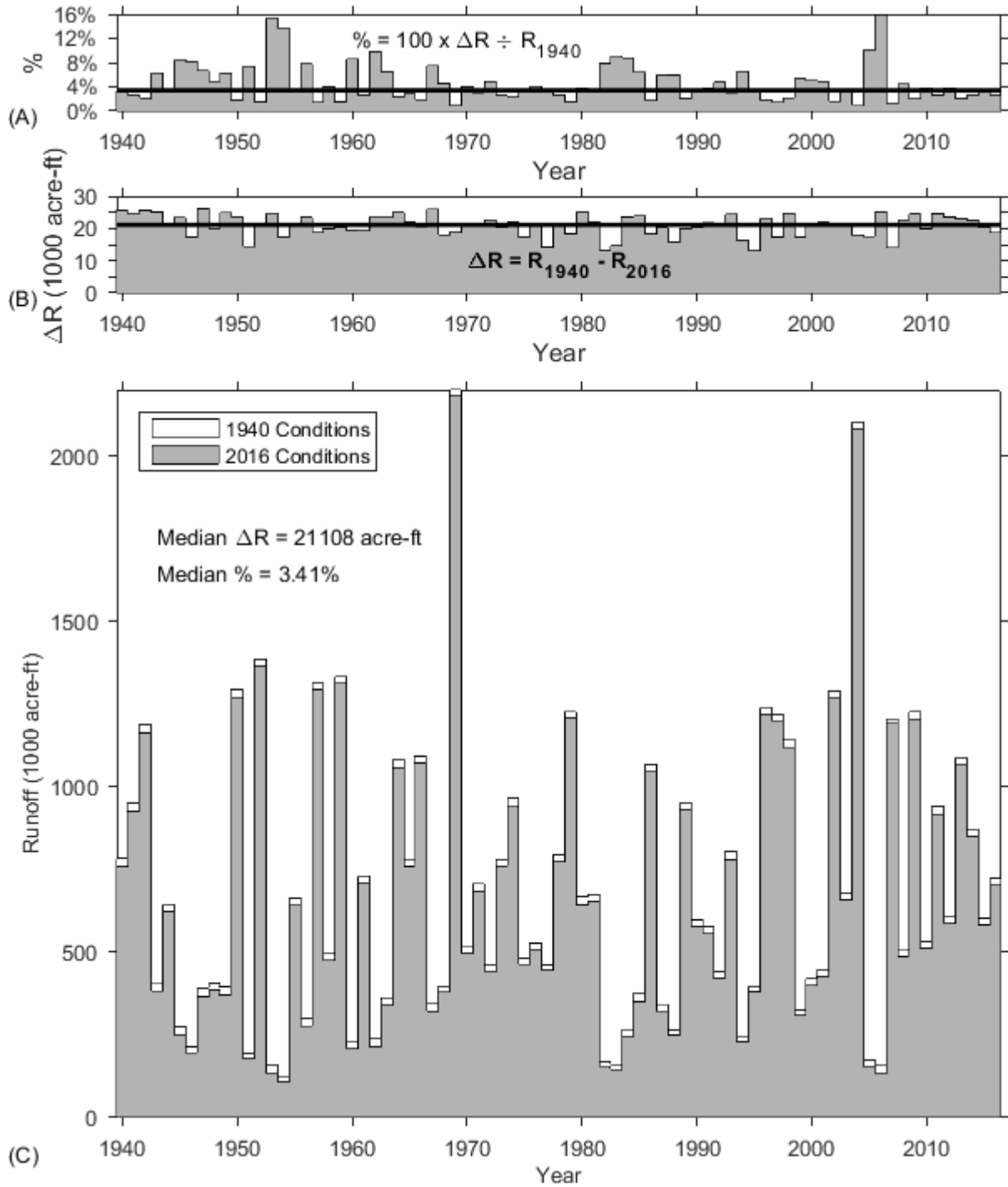


Figure 10-3 – UCWBM results for the San Saba watershed – (A) Percentage difference in runoff by year, (B) difference in runoff by year (in acre-ft), (C) computed runoff leaving the watershed as streamflow.

10.2.3 UCWBM results for the South Concho Watershed

Figure 10-4 presents UCWBM results for the South Concho watershed specifically comparing computed streamflow for all precipitation years under watershed conditions from 1940 and 2016. The curve numbers for the South Concho watershed ranged from 67.9 (1940) to 68.5 (2016), with the increase suggesting that the watershed should gain more surface runoff under 2016 conditions. It is also notable that the Mann-Kendall analysis on the annual dataset of South Concho watershed curve numbers indicates an increasing trend with a high confidence level (Figure 4-16C).

With respect to small ponds, 2016 conditions add over 3,500 acre-ft of storage capacity, as well as the addition of nearly 700 acres of water surfaces exposed to evaporative losses when ponds are full. In comparison to the Elm Creek and San Saba watersheds, the South Concho watershed has less much small pond storage capacity and open water surface areas from which water may evaporate.

As shown in Figure 10-4, computed runoff for the 1940 watershed conditions actually were often less than those computed for the 2016 watershed conditions, especially during years for which higher runoff quantities were computed. This likely reflects the importance of the increase in curve number for the watershed, resulting in more runoff in years with greater precipitation. For years with lower precipitation, the increase in runoff resulting from the increased curve number is at least partially offset by a decrease in runoff resulting from water capture and evaporation from the small ponds.

For the 77 years of simulation (1940-2016), the median difference in runoff was approximately 1,200 acre-ft/yr indicating that 2016 watershed conditions would produce increased streamflow compared to 1940 watershed conditions given identical rainfall patterns. The percentage difference in runoff (based on the runoff generated under 1940 conditions) ranged from -2%-49%, with the median percentage difference equal to approximately 2%.

For the South Concho watershed, UCWMB model results indicate that changes within the land use/land cover of the watershed (which result in curve number changes) are more controlling of computed runoff than are the inclusion of small ponds. However for years in which lower rainfall totals produce runoff, the existence of the small ponds reduces streamflow to a greater extent than the land-use/land cover change increases the streamflow. The net result ranges between -3000 acre-ft/yr and 3000 acre-ft/yr in UCWBM computed runoff.

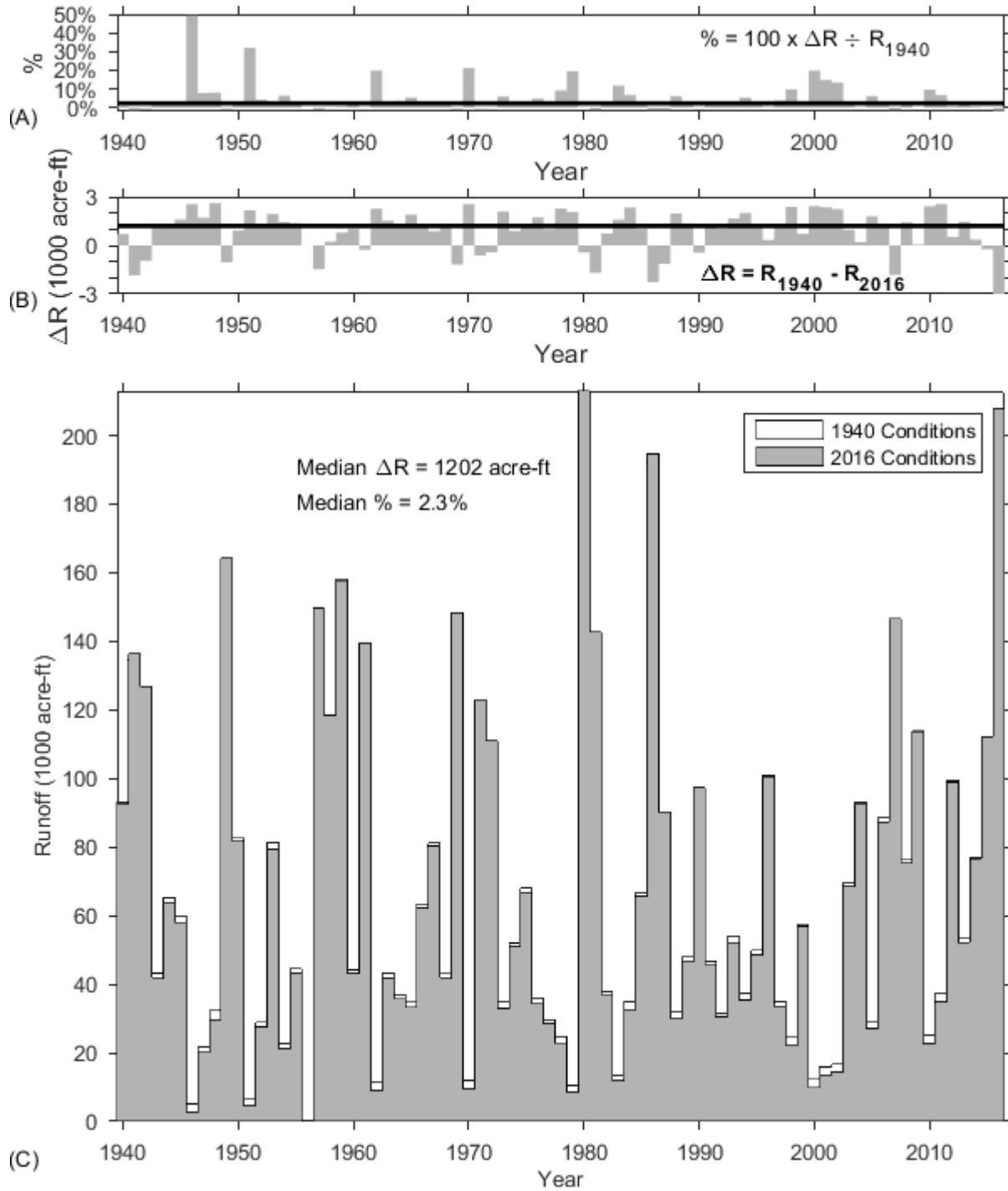


Figure 10-4 – UCWBM results for the South Concho watershed – (A) Percentage difference in runoff by year, (B) difference in runoff by year (in acre-ft), (C) computed runoff leaving the watershed as streamflow.

10.2.4 UCWBM results for the North Concho Watershed

Figure 10-5 presents UCWBM results for the North Concho watershed specifically comparing computed streamflow for all precipitation years under watershed conditions from 1940 and 2016. The curve numbers for the South Concho watershed ranged from 68.6 (1940) to 66.2 (2016), with the decrease suggesting that the watershed should lose more surface runoff under 2016 conditions. It is also notable that the Mann-Kendall analysis on the annual dataset of North Concho watershed curve numbers indicates a decreasing trend with a high confidence level (Figure 4-16D).

With respect to small ponds, 2016 conditions add over 3,500 acre-ft of storage capacity, as well as the addition of nearly 1000 acres of water surfaces exposed to evaporative losses when ponds are full. In comparison to the Elm Creek and San Saba watersheds, the North Concho watershed has less much small pond storage capacity and open water surface areas from which water may evaporate. Storage capacity and open water surface areas are similar for the South Concho and North Concho watershed ponds.

As shown in Figure 10-5, computed runoff for the 1940 watershed conditions were always greater than those computed for the 2016 watershed conditions, especially during years for which higher runoff quantities were computed. This likely reflects the importance of the decrease in curve number for the watershed, resulting in more runoff in years with greater precipitation.

For the 77 years of simulation (1940-2016), the median difference in runoff was approximately 25,200 acre-ft/yr indicating that 2016 watershed conditions would produce decreased streamflow compared to 1940 watershed conditions given identical rainfall patterns. The percentage difference in runoff (based on the runoff generated under 1940 conditions) ranged from 0%-49%, with the median percentage difference equal to approximately 15%.

For the North Concho watershed, UCWMB model results indicate that changes within the land use/land cover of the watershed (which result in curve number changes), combined with the effects of small ponds and antecedent moisture conditions result in 15% reductions in median streamflow from the watershed. Streamflow reductions ranged from 0 acre-ft/yr to 70,000 acre-ft/yr. The 0 acre-ft/yr reductions occurred in 1956 and 1986, where the rainfall gage at Sterling City did not record any events that would generate runoff (Figure 7-19). Result from 1986, however, should be discounted as data was not available until October of that year.

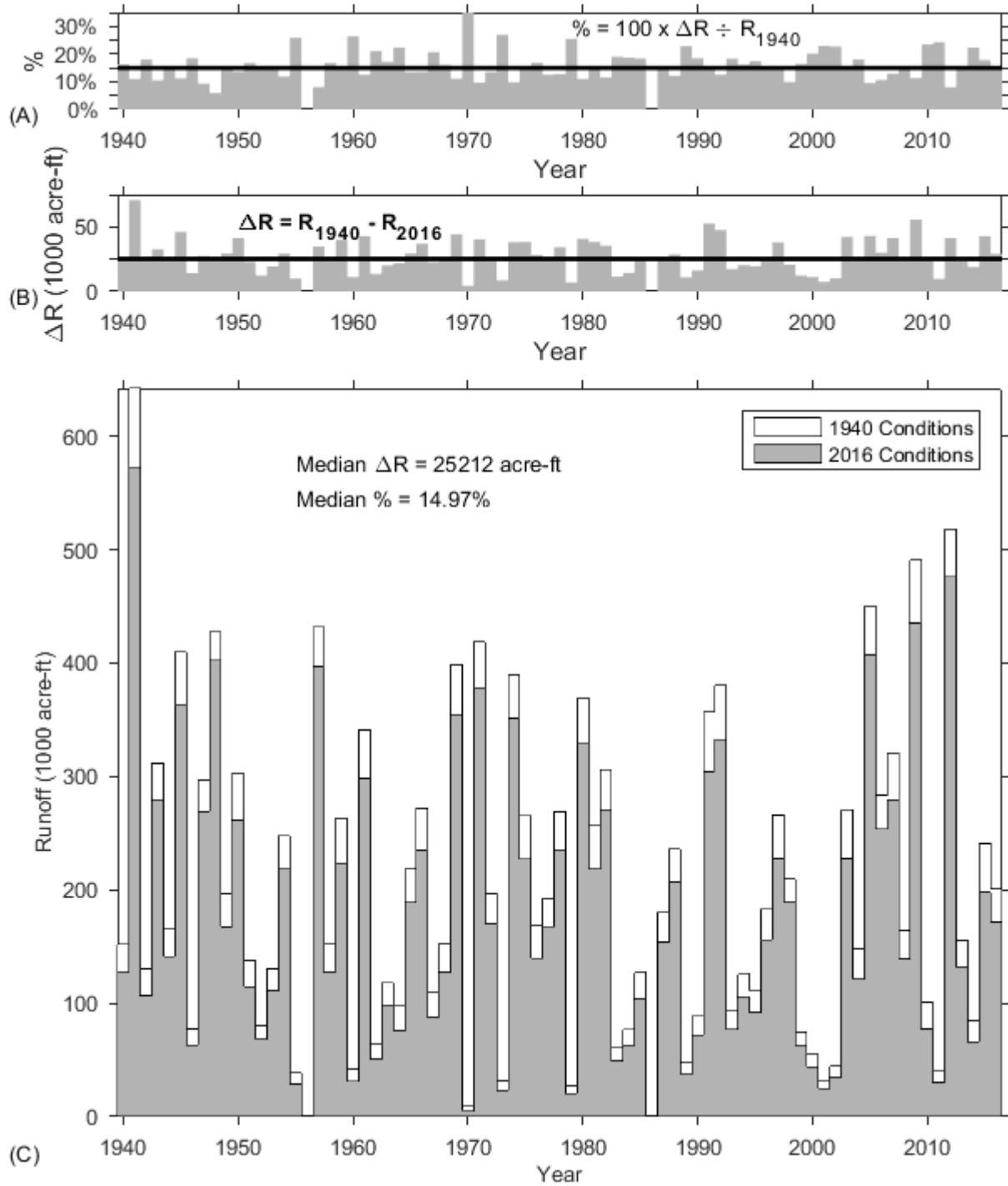


Figure 10-5 – UCWBM results for the North Concho watershed

10.3 UCWBM results – By Watershed Parameter

The following discussion details UCWBM results from simulations that account for the combined effects of combinations of two of the following three parameters:

- Small Impoundment Storage (“Ponds”)
- Changing Land-use/Land Cover (“LULC”)
- Antecedent Moisture Conditions (“AMC”)

By comparing results from simulations that exclude a single parameter, the impact of the excluded parameter may be discerned. Table 10-3 presents UCWBM results for each watershed from the full system simulations (Section 10.2) and from simulations excluding individual simulation parameters.

Table 10-3 – UCWBM results by watershed parameter, comparing 2016 and 1940 conditions

Watershed	Simulation**	Difference (1940-2016) conditions					
		Median		Maximum		Minimum	
		Acre-ft	%	Acre-ft	%	Acre-ft	%
Elm Creek	Full	10,758	20.10%	13,112	100%	5,761	5.44%
San Saba	Full	21,108	3.41%	26,111	15.90%	13,088	0.84%
South Concho	Full	1,202	2.30%	2,613	49.33%	-3,279	-1.61%
North Concho	Full	25,212	14.97%	70,617	48.34%	0	0%
Elm Creek	LULC & AMC	1,480	2.70%	3,315	4.53%	261	0.99%
San Saba	LULC & AMC	3,724	0.63%	8,389	1.01%	1,070	0.25%
South Concho	LULC & AMC	-1,970	-3.47%	0	0%	-6,046	-6.19%
North Concho	LULC & AMC	21,181	12.73%	66,214	22.32%	0	0%
Elm Creek	Ponds & AMC	9,132	19.16%	11,941	100%	4,855	3.93%
San Saba	Ponds & AMC	17,420	2.81%	23,432	15.82%	7,032	0.45%
South Concho	Ponds & AMC	3,165	6.14%	3,913	56.77%	0	0.00%
North Concho	Ponds & AMC	3,971	2.72%	5,230	38.72%	0	0%
Elm Creek	LULC & Ponds	8,864	60.27%	11,547	100%	0	0%
San Saba	LULC & Ponds	20,616	9.16%	28,986	100%	11,083	1.31%
South Concho	LULC & Ponds	1,499	14.51%	3,347	100%	-1,143	-1.90%
North Concho	LULC & Ponds	16,393	36.53%	46,302	100%	37	10.12%

**Full = LULC, Ponds, and AMC included in simulation

As indicated in Table 10-3, excluding small ponds from the simulation of the Elm Creek watershed caused the median difference between 1940 and 2016 conditions to be reduced by over 9,000 acre-ft, or 86% of the full simulation difference. In contrast, land use changes only resulted in a 1,626 acre-ft reduction (15% of the full simulation difference). Similarly eliminating the antecedent moisture conditions from the simulation resulted in a 1,894 acre-ft reduction in median difference (17% of the full simulation difference). Thus for the Elm Creek watershed, the small ponds have the largest impact on streamflow. Similar conclusions may be drawn for the San Saba watershed. In contrast, for the North Concho watershed, the exclusion of the small ponds reduces the median difference in streamflow by 15%, whereas excluding the variable LULC reduces the median streamflow difference by 84%. Thus for the North Concho watershed, LULC is the most important model parameter. The results from the South Concho watershed are notable in that the full simulation indicates 2016 watershed conditions will result in a median difference in streamflow 1,202

acre-ft less than under 1940 watershed conditions. However upon excluding the small pond impacts, results from the South Concho simulation indicate that 2016 watershed conditions would yield a median INCREASE in streamflow by 1,970 acre feet. Thus for the South Concho watershed, the small ponds have the greatest impact on streamflow (compared to the other model parameters), yet their impact is mitigated by the increased runoff expected as a result of LULC conditions within the watershed.

Table 10-4 presents a water budget analysis indicating the median percentage of total rainfall that is lost to evaporation (“E”) from ponds, is intercepted by the vegetative canopy (“C”), enters the groundwater system (“GW”) or becomes runoff and streamflow (“SW”). Results indicate that losses due to evaporation are minimal, and are non-existent under 1940 watershed conditions (when small ponds did not exist within the watersheds). The greatest portion of rainfall is lost to canopy interception “C,” with losses of up to 85% in the North Concho watershed. Canopy losses also include low-depth rainfall events that do not generate runoff (according to the curve number method), and as such would tend to be higher in areas like the North Concho watershed which has a low median rainfall depth (Figure 7-12D). Another observation drawn from Table 10-4 are that water entering the groundwater system is often twice as large a quantity than runoff entering streams, and

Table 10-4 – UCWBM results as a median percentage of total modeled rainfall

		Results as a Median Percentage of Total Modeled Rainfall							
		2016 Conditions				1940 Conditions			
Watershed	Simulation	E	C	GW	SW	E	C	GW	SW
Elm Creek	Full	1%	71%	19%	8%	0%	71%	19%	10%
San Saba	Full	0%	65%	21%	12%	0%	65%	21%	13%
South Concho	Full	0%	71%	18%	9%	0%	72%	18%	9%
North Concho	Full	0%	71%	19%	10%	0%	70%	19%	11%
Elm Creek	LULC & AMC	0%	71%	19%	10%	0%	71%	19%	10%
San Saba	LULC & AMC	0%	65%	21%	13%	0%	65%	21%	13%
South Concho	LULC & AMC	0%	71%	18%	9%	0%	72%	18%	9%
North Concho	LULC & AMC	0%	71%	19%	10%	0%	70%	19%	11%
Elm Creek	Ponds & AMC	1%	72%	18%	7%	0%	72%	18%	9%
San Saba	Ponds & AMC	0%	65%	21%	12%	0%	65%	21%	12%
South Concho	Ponds & AMC	0%	72%	18%	8%	0%	72%	18%	9%
North Concho	Ponds & AMC	0%	72%	19%	9%	0%	72%	19%	9%
Elm Creek	LULC & Ponds	1%	72%	18%	7%	0%	72%	18%	9%
San Saba	LULC & Ponds	0%	76%	19%	5%	0%	76%	19%	5%
South Concho	LULC & Ponds	0%	84%	14%	2%	0%	85%	13%	2%
North Concho	LULC & Ponds	0%	85%	13%	2%	0%	82%	15%	3%

**Full = LULC, Ponds, and AMC included in simulation

^^E = Evaporation loss, C = Canopy loss, GW = Groundwater recharge, SW = Surface water runoff

11 Summary and Conclusions

The ultimate goal of this Phase II project effort was to further identify and quantify the causes of observed reductions in the rainfall-runoff response for portions of the Upper Colorado River Basin. Statistical analyses were performed to assess trends in temperature (maximum and minimum), streamflow, precipitation, and soil moisture. Groundwater wells were reviewed to assess their potential for causing pumping-induced streamflow reductions. Efforts were undertaken to determine the number, surface area, and capacity of small impoundments not otherwise considered when assessing Texas water availability. Lastly, a water balance model was developed to assess how trends in some of the studied parameters may related to changes in streamflow.

The following are the general conclusions identified during this Phase II effort based on Mann-Kendall trend analyses applied to gage records:

1. Rainfall totals measured for the recent drought (2008-2016) exceed or are equal to totals from the 1947-1957 drought (on an average annual basis).
2. Streamflow totals measured for the recent drought (2008-2016) are below and often significantly lower than streamflow totals measured for the 1947-1957 drought.
3. All study area watersheds contained at least 100 new small impoundments that were not included in the NHD (2002 revision). These impoundments were generally small in both area and capacity.
4. Land use/Land cover changes within each watershed have resulted in decreasing curve numbers over time for the North Concho watershed, which typically causes increases in water infiltration into the groundwater system and reducing surface runoff. Curve numbers for all other study area watersheds exhibited increasing trends, indicating they should produce greater runoff per rain event.
5. Most temperature gauges throughout the study area watersheds demonstrated increasing minimum temperatures with decreasing or stable maximum daily temperatures.
6. Temperature trends are not consistent amongst all recording stations within the subject area watersheds, and trend gradients (both increasing and decreasing) are observable.
7. All precipitation recording stations experienced either increasing trends or remained stable when considering annual precipitation totals. None of the stations reported a decreasing trend for annual precipitation.
8. Some precipitation stations experienced increasing frequencies of rain events, with the number of annual rainy days increasing. Combined with generally stable total annual rainfall quantities, the resulting median rainfall depth often follows a decreasing trend.
9. Seasonal shifts and variations in precipitation data are prevalent for most stations, with many reporting increasing rainfall in March and decreasing rainfall in April. Precipitation amounts during the winter months are generally stable.
10. Soil moisture content can significantly affect the rainfall-runoff response. Soil moisture content is highly variable in time and space

11. Median annual soil moisture records (from the GLDAS datasets) indicate an increasing trends for all of the study area watersheds. This suggests that the upper soil layers throughout each watershed are filling with surface water after rain events. Soil moisture is generally being lost to migration or evapotranspiration at a slower rate than it is being replenished from rainfall.
12. Although limited data is available, water levels in shallow wells adjacent to major streams do often show changes consistent with changes in measured streamflow.
13. The lack of sufficient local groundwater pumping data prevents assessing whether pumping from such shallow, near-stream wells has effectively reduced streamflow.
14. Baseflow to streams from the alluvial groundwater system, as quantified as a percentage of annual streamflow, is increasing for sites within the North Concho, San Saba, and Elm Creek watersheds. This suggests that any future reductions in baseflow will lead to reductions in overall streamflow for these watersheds. Baseflows within the South Concho watershed have remained stable.

The following conclusions were derived from the results of the UCWBM modeling. This modeling tested the relative importance of land use/land cover changes, precipitation changes, soil moisture (antecedent moisture conditions) and changes in the small impoundment numbers within each watershed.

1. Median streamflow reductions of 20% within the Elm Creek watershed may be attributed to the impact of small ponds, land use/land cover change, and soil moisture conditions on translating the runoff into streamflow. Small ponds have the largest effect on streamflow reduction within the Elm Creek watershed (compared to land use/land cover changes).
2. Median streamflow reductions of 3% within the San Saba watershed may be attributed to the impact of small ponds, land use/land cover change, and soil moisture conditions on translating the runoff into streamflow. Small ponds have the largest effect on streamflow reduction within the San Saba watershed (compared to land use/land cover changes).
3. Within the South Concho watershed, land use/land cover changes tend to increase runoff/streamflow overtime, yet this increase is overshadowed by larger decreases in streamflow resulting from the small ponds within the watershed.
4. For the North Concho watershed, land use/land cover change from 1940-2016 is the main factor driving streamflow reductions. Total median reductions in streamflow amount to nearly 15% of the streamflow generated under 1940 watershed conditions. Small ponds have a minimum impact on streamflow within the North Concho watershed, due in part because relatively few ponds exist across this watershed.

Based on the analyses presented in this document, we offer the following theories.

1. Less intense rainfall is occurring more often, and lower intensity rainfall events will produce less runoff. Therefore while annual rainfall totals may be stable or increasing, the frequency and magnitude of runoff-generating rain events are likely better indicators of streamflow response.

2. Higher minimum temperatures may lead to an overall increase in evaporation and evapotranspiration rates.
3. As the effects of noxious brush on streamflow were deemed “not quantifiable” during this Phase II analysis, its potential for large-scale impacts on streamflow reduction cannot be discounted, and warrants further study.
4. For the North Concho watershed, land use/land cover change was identified as the most significant factor in reducing streamflow. Any reductions would be enhanced should noxious brush dominate the portions of the watershed, and the SCS curve number method does not account for the impacts of noxious brush on the rainfall-runoff response. Given the large decrease in streamflow during the 2008-2016 drought (compared to the 1947-1957 drought), and given the magnitude of streamflow reduction computed with the UCWBM, an additional cause for streamflow reductions is needed. We suspect noxious brush is the additional cause resulting in reduced streamflow within the North Concho watershed.
5. For the Elm Creek, San Saba, and South Concho watersheds, small ponds are playing a role in reducing streamflow. Improved quantification of their impacts on streamflow would yield further insight onto whether regulating such small ponds would yield beneficial increases in streamflow.
6. It is unclear how changes in patterns of rainfall distribution over the course of the year might affect the rainfall/runoff relationship. It is possible that the changing rainfall distribution may affect the types of seasonal vegetation grown on the landscape, and that various vegetation types will affect overall evapotranspiration rates. These potential connections warrant further research.

12 Recommendations

Based on the analyses and the results presented in this Phase II report, we recommend the following further actions be considered in any potential Phase III study:

1. Refinement of the UCWBM to better represent the entire Colorado River watershed. Potential refinements include:
 - a. Incorporation of additional sub-watersheds
 - b. Use of gridded input data for land use and rainfall, and application of the SWB across all subwatersheds at a HUC-6 scale or higher.
 - c. Delineating subwatersheds for all ponds, and tracking pond connectivity within the landscape
 - d. Developing a soil-water balance model to couple with the surface water portion of the current UCWBM.
 - e. Developing a better linkage between temperature and evaporation/evapotranspiration rates
 - f. Including future temperature and precipitation scenarios derived from global climate models
2. Additional analyses focusing on small ponds. These analyses could include:
 - a. Expanding the Small Pond analysis to include the entire Colorado River watershed.
 - b. Using the historical aerial images within Google Earth to better identify creation dates for all ponds
 - c. Developing a geodatabase of pond and watershed features to better track future changes in the watershed and their potential impact on streamflow.
3. Comprehensive study the relationship between noxious brush and streamflow. Such a study should include:
 - a. Defining the types of noxious brush and determining their water usage characteristics
 - b. Mapping the current extent of noxious brush, and historical extent should data be available.
 - c. Applying results of paired documented watershed studies to the entire areas where noxious brush currently exists, and quantifying the effect on streamflow assuming the noxious brush was replaced with Texas native vegetation.
4. Additional temperature and precipitation analyses with respect to periodicity and ENSO cycles as drivers for change.
5. Develop a semi- or fully- distributed rainfall/runoff model of the study area watersheds, similar to those presented in (Xia, 2012). Such a model would provide spatial variability in model input (which is not included in the UCWBM), and would be able to simulate both surface runoff and subsurface infiltration processes. The model should account for the extent and water usage properties of the noxious brush common to each watershed.

13 Acknowledgements

LRE Staff are grateful for the assistance of numerous staff members of the Texas Water Development Board for their insight and guidance through this project. Staff provided input during multiple meetings, and were always quick to respond to inquiries. Specific thanks are offered to:

Nelun Fernando, PhD – TWDB Project Manager, Surface Water Availability Section
Caimee Schoenbaechler, MEM – TWDB Team Lead, Bays and Estuaries Section

14References

- Baker, R.C. and Baum, G.H., 1965, Ground-Water Conditions in Menard County, Texas: Texas Water Commission Bulletin 6519, 92 p.
- Beach, J.A., Burton, S., and Kolarik, B., 2004, Groundwater availability model for the Lipan Aquifer in Texas: Contract report to the Texas Water Development Board, 246 p.
- Crooks, S.M.A.K.A.L., 2015, Simulation of River Flow in the Thames Over 120 Years: Evidence of Change in Rainfall-Runoff Response?: *Journal of Hydrology: Regional Studies*, v. 4, p. 172-195.
- Di Long, L.L.A.B.S., 2014, Uncertainty in evapotranspiration from land surface modeling, remote sensing, and GRACE satellites: *Water Resources Research*, v. 50, no. 2,
- Duan, K.G.S.S.G.M.P.V.C.E.C.C.S.S.H.D.A.Z.L.Z.A.Y.Z., 2017, Future shift of the relative roles of precipitation and temperature in controlling annual runoff in the conterminous United States: *Hydrology and Earth System Sciences*, v. 21, p. 5517-5529.
- Fry, J., Xian, G., Jin, S., Dewitz, J., Homer, C., Yang, L., Barnes, C., Herold, N., and Wickham, J., 2011, Completion of the 2006 National Land Cover Database for the Conterminous United States: *PE&RS*, v. 77, no. 9, p. 858-864.
- Galloway, D., Jones, D.R., and Ingebritsen, S.E., 1999, Land Subsidence in the United States: U.S. Geological Survey Circular 1182, 177 p.
- Granato, G.E., 2006, Kendall-Theil Robust Line (KTRLLine—version 1.0)—A visual basic program for calculating and graphing robust nonparametric estimates of linear-regression coefficients between two continuous variables: U.S. Geological Survey Techniques and Methods 4-A7, 31 p.
- Helsel, D.R..A.H.R.M., 2002, Statistical Methods in Water Resources US Geological Survey,
- Hoffman, J., Leake, S.A., Galloway, D.L., and Wilson, A.M., 2003, MODFLOW-2000 Ground-Water Model—User Guide to the Subsidence and Aquifer-System Compaction (SUB) Package: U.S. Geological Survey, Open-File Report 03—233, 46 p.
- Homer, C., Dewitz, J..F.J., Coan, M., Hossain, N., Larson, C., Herold, N., McKerrow, A., VanDriel, J.N., and Wickham, J., 2007, Completion of the 2001 National Land Cover Database for the Conterminous United States: *Photogrammetric Engineering and Remote Sensing*, v. 73, no. 4, p. 337-341.

Homer, C.G., Dewitz, J.A., Yang, L., Jin, S., Danielson, P., Xian, G., Coulston, J., Herold, N.D., Wickham, J.D., and Megown, K., 2015, Completion of the 2011 National Land Cover Database for the conterminous United States-Representing a decade of land cover change information: Photogrammetric Engineering and Remote Sensing, v. 81, no. 5, p. 345-354.

Houborg, R..M.R.B.L.R.R.A.B.F.Z., 2012, Drought indicators based on model-assimilated Gravity Recovery and Climate Experiment (GRACE) terrestrial water storage observations: Water Resour. Res., v. 48, no. W07525,

Kendall, M.G., 1975, Rank Correlation Methods (4th) London, Charles Griffin,

Kennedy Resource Company, 2017, Evaluation of Rainfall/Runoff Patterns in the Upper Colorado River Basin Phase I:

LCRA, 2015, Lakes Buchanan and Travis Water Management Plan and Drought Contingency Plans: Submission to the Texas Commission on Environmental Quality,

LCRA, 2019, Water Management Plan Amendment Application: Submitted to the Texas Commission on Environmental Quality,

Leake, S.A. and Galloway, D.L., 2007, MODFLOW Ground-Water Model—User Guide to the Subsidence and Aquifer-System Compaction Package (SUB-WT) for Water-Table Aquifers: U.S. Geological Survey, Techniques and Methods 6–A23, 42 p.

Lim, K.J., Engel, B.A., Tang, Z., Choi, J., Kim, K.S., Muthukrishnan, S., and Tripathy, D., 2005, Automated Web GIS Based Hydrograph Analysis Tool, WHAT: Journal of the American Water Resources Association, v. 41, no. 6, p. 1407-1416.

Mace, R.E. and Angle, E.S., 2004, Aquifers of the Edwards Plateau in Aquifers of the Edwards Plateau - Report 360 Texas Water Development Board, 1-20 p.

Mann, H.B., 1945, Non-parametric tests against trend: Econometrica, v. 13, p. 163-171.

McAfee, S.A..P.G.T..W.C.A..M.G., 2017, Application of synthetic scenarios to address water resource concerns: A management-guided case study from the Upper Colorado River Basin: Climate Services, v. 8, p. 26-35.

Meals, D.W..J.S.S.A.D.A.J.B.H., 2011, Statistical Analysis for Monotonic Trends: National Nonpoint Source Monitoring Program Tech Notes , v. 6, p. 1-23.

- Meals, D.W..J.S.S.A.D.A.J.B.H., 2011, Statistical Analysis for Monotonic Trends: National Nonpoint Source Monitoring Program Technotes 6, p. 23.
- Natural Resources Conservation Service, 1986, Urban Hydrology for Small Watersheds - TR-55 (2nd) Washington, D.C., U.S. Department of Agriculture, 164 p.
- Natural Resources Conservation Service, 2018, Web Soil Survey, <https://websoilsurvey.nrcs.usda.gov/app/WebSoilSurvey.aspx>, accessed July 2018.
- PRISM Climate Group, Oregon State University, 2018, <http://prism.oregonstate.edu/>, accessed July 2018.
- Sohl, T.L..R.R.B.M.S.K.D.J.W.S.Q.R.A.F.A., 2018, Modeled historical land use and land cover for the conterminous United States: 1938-1992:
- Terzaghi, K., 1925, Erdbaumechanik auf bodenphysikalisher Grundlage Vienna, Austria, Deuticke, 399 p.
- Thornthwaite, C.W. and Mather, J.R., 1957, Instructions and Tables for Computing Potential Evapotranspiration and the Water Balance: Publications in Climatology, v. X, no. 3, p. 185-311.
- Vogelmann, J.E., Howard, S.M., Yang, L., Larson, C.R., Wylie, B.K., and Van Driel, J.N., 2001, Completion of the 1990's National Land Cover Data Set for the conterminous United States: Photogrammetric Engineering and Remote Sensing, v. 67, p. 650-662.
- Westenbroek, S.M., Kelson, V.A., Dripps, W.R., Hunt, R.J., and Bradbury, K.R., 2010, SWB—A Modified Thornthwaite-Mather Soil-Water-Balance Code for Estimating Groundwater Recharge: 60 p.
- Willis, G.W., 1954, Ground-Water Resources of Tom Green County, Texas: Texas Board of Water Engineers Bulletin 5411, 100 p.
- Woodhouse, C.A..G.T.P.K.M.S.A.M.A.G.J.M., 2016, Increasing influence of air temperature on upper Colorado River streamflow: Geophysical Research Letters, v. 43, p. 2174-2181.
- Xia, Y.K.M.M.E.B.C.J.S.L.L.C.A.H.W.J.M.B.L.Q.D.D.L., 2012, Continental-scale water and energy flux analysis and validation for North American Land Data Assimilation System project phase 2 (NLDAS-2): 2. Validation of model-simulated streamflow: Jornal of Geophysical Research, v. 117, p. D03110.

Xia, Y.K.M.M.E.J.S.B.C.E.W.L.L.C.A.H.W.J.M.B.L.D.L.V.K.Q.D.K.M.Y.F.A.D.M., 2012, Continental-scale water and energy flux analysis and validation for the North American Land Data Assimilation System project phase 2 (NLDAS-2): 1. Intercomparison and application of model products: *Journal of Geophysical Research*, v. 117, p. D03109.

Young, S.C., Mace, R.E., and Rubinstein, C., 2018, Surface water-groundwater interaction issues in Texas: *Texas Water Journal*, v. 9, no. 1, p. 129-149.

15 Appendices

Appendix A – Tables of Land Use/Land Cover Acreage

Final Report: Evaluation of Rainfall-Runoff Trends in the Upper Colorado River Basin (Phase Two)
 TWDB Contract Number 1800012283

Table A-1 – Land-use/Land Cover Area (acres) by year & category – Elm Creek Watershed

Year	Water	Developed	Mining	Barren	Forest			Grassland	Shrubland	Cropland	Hay & Pastureland	Wetland	
					Deciduous	Evergreen	Mixed					Herbaceous	Woody
1940	872	1492	0	5165	2708	8677	160	70362	71326	133930	3420	459	114
1941	872	1492	0	5188	2708	8677	160	70959	73966	130739	3351	459	114
1942	872	1492	0	5188	2708	8677	160	71418	76951	127410	3259	436	114
1943	872	1492	0	5188	2708	8677	160	71877	79155	124931	3122	390	114
1944	872	1492	0	5188	2708	8677	160	72084	81427	122451	3122	390	114
1945	872	1492	0	5188	2708	8677	160	72130	82070	121763	3122	390	114
1946	872	1492	0	5188	2708	8677	160	72199	82598	121189	3122	367	114
1947	872	1492	0	5188	2708	8677	160	72359	83172	120477	3122	344	114
1948	872	1492	0	5188	2708	8677	160	72520	83516	119972	3122	344	114
1949	872	1492	0	5188	2708	8677	160	72589	84251	119214	3122	298	114
1950	872	1492	0	5188	2708	8677	160	72681	85009	118388	3122	275	114
1951	872	1492	0	5188	2708	8677	160	72681	85651	117745	3122	275	114
1952	872	1492	0	5188	2708	8677	160	72727	86478	116919	3122	229	114
1953	872	1492	0	5188	2708	8677	160	72819	86776	116528	3122	229	114
1954	872	1492	0	5188	2708	8677	160	72842	87098	116207	3122	229	91
1955	872	1492	0	5188	2708	8677	160	72887	87786	115472	3122	229	91
1956	872	1492	0	5188	2708	8677	160	72933	88131	115105	3122	206	91
1957	872	1492	0	5188	2708	8677	160	72979	88452	114738	3122	206	91
1958	872	1492	0	5188	2708	8677	160	73025	88911	114256	3122	183	91
1959	872	1492	0	5188	2708	8677	160	73048	89072	114049	3145	183	91
1960	872	1492	0	5188	2708	8677	160	73071	89439	113682	3145	160	91
1961	872	1492	0	5188	2708	8677	160	73209	89898	113062	3168	160	91
1962	872	1492	0	5234	2708	8677	160	73232	90426	112465	3168	160	91
1963	872	1492	0	5234	2708	8677	160	73232	88498	114393	3168	160	91
1964	872	1492	0	5234	2708	8677	160	73209	85881	117033	3168	160	91
1965	872	1492	0	5234	2708	8654	160	73186	83815	119123	3191	160	91
1966	872	1492	0	5211	2708	8654	160	73117	81152	121900	3191	137	91
1967	872	1492	0	5211	2708	8654	160	73094	79063	124035	3191	114	91
1968	872	1492	0	5211	2708	8654	160	73071	76698	126423	3191	114	91
1969	872	1492	0	5234	2708	8654	160	73370	77617	125183	3191	114	91

Final Report: Evaluation of Rainfall-Runoff Trends in the Upper Colorado River Basin (Phase Two)

TWDB Contract Number 1800012283

Table A-1 – Land-use/Land Cover Area (acres) by year & category – Elm Creek Watershed, Cont.

Year	Water	Developed	Mining	Barren	Forest			Grassland	Shrubland	Cropland	Wetland		
					Deciduous	Evergreen	Mixed				Hay & Pastureland	Herbaceous	Woody
1970	872	1492	22	5234	2708	8654	160	73668	78512	123943	3213	114	91
1971	872	1492	45	5234	2708	8654	160	73875	79247	122979	3213	114	91
1972	872	1515	45	5234	2708	8654	160	74012	79958	122107	3213	114	91
1973	872	1515	45	5234	2708	8654	160	74058	80762	121258	3213	114	91
1974	872	1515	45	5257	2708	8654	160	74150	81749	120156	3213	114	91
1975	872	1561	45	5257	2708	8654	160	74150	81496	120362	3213	114	91
1976	872	1584	45	5257	2708	8654	160	74127	81404	120454	3213	114	91
1977	872	1606	45	5257	2708	8654	160	74127	81336	120500	3213	114	91
1978	872	1652	45	5257	2708	8654	160	74127	81152	120615	3236	114	91
1979	872	1721	45	5257	2708	8654	160	74081	81106	120638	3236	114	91
1980	872	1767	68	5257	2708	8654	160	74058	81037	120661	3236	114	91
1981	987	1905	91	5188	2708	8562	229	73186	79889	122291	3420	137	91
1982	987	1905	91	5188	2708	8562	229	73140	78328	123989	3420	137	0
1983	987	1905	91	5188	2708	8494	229	73140	76813	125573	3420	137	0
1984	987	1905	91	5188	2708	8494	229	73140	75987	126423	3420	114	0
1985	1216	1905	91	5188	2685	8494	229	73002	74380	127961	3420	114	0
1986	1790	1951	137	5165	2662	8494	229	72497	72910	129315	3420	114	0
1987	1790	1951	183	5165	2662	8494	229	72543	73002	129132	3420	114	0
1988	1790	1997	229	5165	2662	8494	229	72612	73186	128787	3420	114	0
1989	1790	2020	298	5165	2662	8494	229	72704	73347	128443	3420	114	0
1990	1790	2020	390	5165	2662	8494	229	72704	73530	128168	3420	114	0
1991	1790	2020	459	5188	2662	8494	229	72796	73645	127823	3466	114	0
1992	1790	2020	482	5165	2662	8494	229	72842	73898	127525	3466	114	0
1993	1813	2020	482	5142	2662	8471	229	72842	74173	127249	3489	114	0
1994	1813	2020	482	5142	2662	8471	229	72819	74288	127112	3535	114	0
1995	1836	2020	459	5165	2662	8471	229	72773	74449	126928	3581	114	0
1996	1836	2020	436	5165	2662	8471	229	72773	74724	126629	3627	114	0
1997	1836	2020	436	5165	2662	8471	229	72773	75275	125987	3719	114	0
1998	1836	2020	482	5165	2662	8471	229	72773	75459	125734	3741	114	0
1999	1813	2020	505	5165	2662	8471	229	72773	75505	125688	3741	114	0

Final Report: Evaluation of Rainfall-Runoff Trends in the Upper Colorado River Basin (Phase Two)
 TWDB Contract Number 1800012283

Table A-1 – Land-use/Land Cover Area (acres) by year & category – Elm Creek Watershed, Cont.

Year	Water	Developed	Mining	Barren	Forest			Grassland	Shrubland	Cropland	Hay & Pastureland	Wetland	
					Deciduous	Evergreen	Mixed					Year	Water
2000	1813	2020	505	5165	2662	8471	229	72750	76101	125091	3764	114	0
2001	1813	2020	573	5165	2662	8471	229	72750	76056	125068	3764	114	0
2002	1813	2020	642	5142	2662	8471	229	72727	76056	125045	3764	114	0
2003	1813	2020	688	5142	2662	8471	229	72658	76078	125045	3764	114	0
2004	1813	2020	711	5142	2662	8471	229	72612	75895	125252	3764	114	0
2005	1813	2020	711	5142	2662	8448	229	72635	75849	125298	3764	114	0
2006	1813	2112	711	5142	2662	8448	229	72612	76308	124770	3764	114	0
2007	1813	2157	780	5073	2662	8448	229	72566	76997	124081	3764	114	0
2008	1813	2203	757	5073	2662	8448	229	72566	77479	123576	3764	114	0
2009	1813	2226	803	5027	2662	8448	229	72566	78282	122750	3764	114	0
2010	1813	2295	849	5004	2662	8448	229	72543	78764	122199	3764	114	0
2011	1767	2341	895	4958	2662	8448	229	72520	78696	122291	3764	114	0
2012	1767	2364	941	4958	2662	8402	229	72405	78351	122727	3764	114	0
2013	1767	2387	941	4958	2662	8402	229	72291	77915	123255	3764	114	0
2014	1767	2410	987	4912	2662	8356	229	72222	77479	123783	3764	114	0
2015	1767	2456	1193	4866	2662	8356	206	72176	76928	124196	3764	114	0
2016	1767	2525	1193	4866	2662	8356	206	72153	76584	124494	3764	114	0

Final Report: Evaluation of Rainfall-Runoff Trends in the Upper Colorado River Basin (Phase Two)

TWDB Contract Number 1800012283

Table A-2 – Land-use/Land Cover Area (acres) by year & category – San Saba Watershed

Year	Water	Developed	Mining	Barren	Forest			Grassland	Shrubland	Cropland	Hay & Pastureland	Wetland	
					Deciduous	Evergreen	Mixed					Herbaceous	Woody
1940	3902	7139	22	5509	17447	205762	68	395477	1190679	167676	20638	734	91
1941	3902	7139	22	5509	17447	205808	68	397337	1197979	159802	19329	711	91
1942	3971	7139	22	5509	17447	206014	68	399770	1205762	151377	17263	711	91
1943	3994	7139	22	5509	17447	206083	68	401239	1212718	144467	15656	711	91
1944	4040	7139	22	5509	17447	206244	68	403627	1220707	135674	13934	642	91
1945	4040	7139	22	5509	17447	206221	68	403627	1221740	134274	14325	642	91
1946	4040	7139	22	5509	17447	206244	68	403673	1222199	133264	14807	642	91
1947	4040	7139	22	5509	17447	206290	68	403696	1222865	132001	15358	619	91
1948	4040	7139	22	5509	17447	206290	68	403673	1223530	130785	15955	619	68
1949	4063	7139	22	5509	17447	206290	68	403535	1224426	129545	16437	596	68
1950	4063	7139	22	5509	17447	206290	68	403236	1225137	128397	17171	596	68
1951	4086	7139	22	5509	17447	206336	68	404086	1228856	123645	17309	573	68
1952	4132	7139	22	5509	17470	206359	68	404729	1231841	119949	17309	550	68
1953	4155	7162	22	5509	17493	206427	68	405716	1235537	115082	17355	550	68
1954	4155	7162	22	5509	17493	206427	68	406427	1238980	110812	17539	505	45
1955	4178	7162	22	5509	17493	206450	68	407093	1242309	106818	17584	413	45
1956	4178	7185	22	5509	17493	206542	68	407943	1246763	101331	17676	390	45
1957	4201	7185	22	5509	17493	206542	68	408218	1249380	97887	18204	390	45
1958	4201	7208	22	5509	17493	206611	68	408356	1252089	94329	18824	390	45
1959	4224	7231	22	5509	17493	206611	68	408608	1253787	91643	19536	367	45
1960	4224	7254	22	5509	17493	206611	68	408838	1255440	89118	20156	367	45
1961	4224	7254	22	5509	17493	206634	68	409182	1257323	86134	20890	367	45
1962	4224	7277	45	5509	17493	206703	68	409320	1258654	83677	21786	344	45
1963	4224	7300	45	5509	17493	206427	68	408838	1253053	89738	22061	344	45
1964	4224	7323	45	5509	17493	205853	68	408494	1245752	97750	22245	344	45
1965	4201	7346	45	5509	17493	205394	68	407713	1239623	105004	22359	344	45
1966	4178	7415	45	5509	17493	204866	68	406864	1232162	113521	22635	344	45
1967	4591	7460	45	5463	17470	204086	68	406244	1225390	121074	22865	344	45
1968	5486	7506	45	5463	17424	203122	68	405348	1218250	129063	22979	344	45
1969	5486	7529	45	5463	17424	203099	68	406014	1219513	126629	23484	344	45

Final Report: Evaluation of Rainfall-Runoff Trends in the Upper Colorado River Basin (Phase Two)

TWDB Contract Number 1800012283

Table A-2 – Land-use/Land Cover Area (acres) by year & category – San Saba Watershed, Cont.

Year	Water	Developed	Mining	Barren	Forest					Wetland			
					Deciduous	Evergreen	Mixed	Grassland	Shrubland	Cropland	Hay & Pastureland	Herbaceous	Woody
1970	5486	7575	45	5463	17424	203145	68	406359	1221051	124311	23829	344	45
1971	5486	7644	68	5463	17424	203168	68	406910	1222474	121854	24196	344	45
1972	5509	7759	68	5463	17424	203145	68	407506	1223829	119237	24747	344	45
1973	5509	7897	68	5463	17424	203191	68	408103	1225711	115932	25390	344	45
1974	5509	8034	91	5463	17424	203168	68	408792	1227226	113200	25826	344	0
1975	5509	8126	91	5463	17424	203053	68	408402	1226193	113820	26652	344	0
1976	5509	8195	91	5463	17424	202938	68	408218	1225160	114416	27318	344	0
1977	5509	8402	114	5463	17424	202846	68	408057	1223691	115197	28030	344	0
1978	5509	8539	183	5463	17424	202777	68	407874	1222566	115725	28673	344	0
1979	5509	8608	183	5463	17424	202640	68	407598	1221418	116483	29407	344	0
1980	5509	8631	183	5463	17424	202594	68	407369	1220431	116781	30348	344	0
1981	5532	8815	114	5119	17355	201928	45	407690	1220247	117607	30280	413	0
1982	5578	8884	114	5119	17355	201905	45	408356	1220730	116368	30280	413	0
1983	5578	8907	183	5119	17355	201882	45	408654	1221235	115495	30303	390	0
1984	5578	8930	183	5119	17355	201882	45	409067	1222061	114325	30211	390	0
1985	5601	8930	229	5119	17355	201882	45	409159	1222566	113774	30096	390	0
1986	5601	8953	229	5119	17355	201882	45	409550	1223553	112488	30004	367	0
1987	5601	9044	252	5119	17355	201721	45	408930	1219237	116368	31106	367	0
1988	5601	9228	298	5119	17355	201675	45	407966	1214990	120408	32093	367	0
1989	5601	9274	459	5119	17355	201629	45	407208	1210766	124678	32644	367	0
1990	5601	9343	482	5119	17355	201538	45	406359	1206267	129315	33356	367	0
1991	5601	9481	573	5119	17355	201469	45	405463	1201101	133930	34641	367	0
1992	5601	9504	642	5119	17355	201331	45	404086	1196280	138842	35973	367	0
1993	5601	9504	665	5119	17240	200849	45	404499	1198094	138108	35055	367	0
1994	5601	9504	596	5165	17194	199793	45	404912	1200665	137258	34044	367	0
1995	5601	9504	619	5142	17125	198691	45	405463	1202318	136845	33402	367	0
1996	5624	9504	688	5096	17125	198117	45	405853	1203902	136202	32598	367	0
1997	5647	9504	734	5073	17011	197451	45	405785	1205670	135583	32254	367	0
1998	5647	9504	734	5073	17011	196487	45	406427	1207575	134710	31542	367	0
1999	5624	9504	734	5050	16942	195890	45	406336	1208884	134825	30899	367	0

Final Report: Evaluation of Rainfall-Runoff Trends in the Upper Colorado River Basin (Phase Two)
 TWDB Contract Number 1800012283

Table A-2 – Land-use/Land Cover Area (acres) by year & category - San Saba Watershed, Cont.

Year	Water	Developed	Mining	Barren	Forest			Grassland	Shrubland	Cropland	Hay & Pastureland	Wetland	
					Deciduous	Evergreen	Mixed					Year	Water
2000	5624	9504	803	5050	16873	194949	45	406887	1210353	134366	30280	367	0
2001	5624	9504	780	5027	16368	193204	45	406313	1213269	134664	29935	367	0
2002	5624	9504	803	5165	16023	191230	45	406382	1215266	135169	29545	367	0
2003	5647	9550	849	5188	15679	189646	45	406382	1217079	135468	29224	367	0
2004	5670	9550	872	5394	15220	187741	45	406795	1218824	135743	28879	367	0
2005	5670	9550	826	5417	14761	186111	45	407438	1220385	135720	28810	367	0
2006	5670	9618	803	5440	14738	186065	45	407415	1221579	134802	28581	367	0
2007	5670	9641	803	5440	14715	185996	45	407415	1222681	133976	28374	367	0
2008	5670	9664	803	5440	14669	185973	45	407529	1223599	133103	28213	367	0
2009	5670	9802	780	5417	14623	185927	45	407644	1224471	132323	27984	367	0
2010	5693	9871	780	5417	14623	185950	45	407690	1225413	131313	27892	367	0
2011	5693	10078	849	5394	14577	185904	45	407552	1224196	132392	28030	367	0
2012	5693	10169	941	5371	14577	185789	45	407552	1223163	133379	28030	367	0
2013	5693	10399	964	5325	14531	185697	45	407208	1222245	134205	28397	367	0
2014	5693	10583	1056	5325	14393	185697	45	406818	1221074	135399	28627	367	0
2015	5693	10720	1033	5303	14416	185514	45	406634	1219559	136845	28994	367	0
2016	5693	11019	1033	5303	14439	185307	45	406588	1218709	137281	29315	367	0

Final Report: Evaluation of Rainfall-Runoff Trends in the Upper Colorado River Basin (Phase Two)
 TWDB Contract Number 1800012283

Table A-3 – Land-use/Land Cover Area (acres) by year & category – South Concho Watershed

Year	Water	Developed	Mining	Barren	Forest			Grassland	Shrubland	Cropland	Hay &	Wetland	
					Deciduous	Evergreen	Mixed				Pastureland	Herbaceous	Woody
1940	3696	3741	0	2525	6290	1033	0	32047	280647	24678	1974	137	0
1941	3696	3741	0	2525	6290	1033	0	32185	281680	23530	1951	137	0
1942	3696	3787	0	2525	6290	1033	0	32254	282506	22658	1928	91	0
1943	3696	4063	0	2525	6290	1033	0	32369	283310	21487	1905	91	0
1944	3696	4132	0	2525	6290	1033	0	32369	284412	20316	1905	91	0
1945	3696	4132	0	2525	6290	1033	0	32369	284504	20224	1905	91	0
1946	3696	4132	0	2525	6290	1033	0	32392	284825	19857	1928	91	0
1947	3696	4132	0	2525	6290	1033	0	32392	284963	19696	1951	91	0
1948	3696	4132	0	2525	6290	1033	0	32415	285330	19306	1951	91	0
1949	3696	4132	0	2525	6290	1033	0	32415	285606	19031	1951	91	0
1950	3696	4132	0	2525	6290	1033	0	32415	285881	18755	1951	91	0
1951	3696	4132	0	2525	6290	1033	0	32438	286179	18434	1951	91	0
1952	3696	4132	0	2525	6290	1033	0	32438	286501	18112	1951	91	0
1953	3696	4132	0	2525	6290	1033	0	32438	286822	17814	1951	68	0
1954	3696	4132	0	2525	6290	1033	0	32438	287144	17493	1951	68	0
1955	3696	4132	0	2525	6290	1033	0	32438	287373	17263	1951	68	0
1956	3696	4132	0	2525	6290	1033	0	32506	287741	16827	1951	68	0
1957	3696	4132	0	2525	6290	1033	0	32506	287924	16643	1951	68	0
1958	3696	4132	0	2525	6290	1033	0	32506	288085	16483	1951	68	0
1959	3696	4155	0	2525	6290	1033	0	32529	288131	16391	1951	68	0
1960	3696	4155	0	2525	6290	1033	0	32529	288269	16253	1951	68	0
1961	3696	4155	0	2525	6290	1033	0	32529	288406	16115	1951	68	0
1962	3696	4155	0	2525	6290	1033	0	32552	288705	15794	1951	68	0
1963	3696	4224	0	2525	6290	1033	0	32552	288383	16046	1951	68	0
1964	3696	4247	0	2525	6290	1033	0	32529	288131	16299	1951	68	0
1965	3696	4269	0	2525	6290	1010	0	32506	287786	16643	1974	68	0
1966	3696	4269	0	2525	6290	987	0	32506	287442	17011	1974	68	0
1967	4315	4292	0	2525	6290	964	0	32024	287258	17033	1997	68	0
1968	5922	4315	0	2525	6290	964	0	31450	286570	16827	1859	45	0
1969	5922	4430	0	2525	6290	964	0	31427	287419	15886	1859	45	0

Final Report: Evaluation of Rainfall-Runoff Trends in the Upper Colorado River Basin (Phase Two)

TWDB Contract Number 1800012283

Table A-3 – Land-use/Land Cover Area (acres) by year & category – South Concho Watershed, Cont.

Year	Water	Developed	Mining	Barren	Forest			Grassland	Shrubland	Cropland	Wetland		
					Deciduous	Evergreen	Mixed				Hay & Pastureland	Herbaceous	Woody
1970	5922	4476	0	2525	6290	964	0	31496	287947	15243	1859	45	0
1971	5922	4545	22	2525	6313	964	0	31450	288567	14554	1859	45	0
1972	5922	4568	22	2525	6313	964	0	31473	289095	13980	1859	45	0
1973	5922	4752	22	2525	6313	964	0	31473	290013	12878	1859	45	0
1974	5922	4820	22	2525	6313	964	0	31450	290702	12144	1859	45	0
1975	5922	5486	22	2525	6313	941	0	31198	290335	12075	1905	45	0
1976	5922	5899	22	2525	6313	918	0	30945	290243	12029	1905	45	0
1977	5922	6496	22	2525	6313	918	0	30853	289944	11822	1905	45	0
1978	5922	6910	22	2525	6313	918	0	30831	289623	11753	1905	45	0
1979	5922	7713	22	2525	6313	918	0	30716	289141	11524	1928	45	0
1980	5922	8516	22	2525	6313	918	0	30440	288911	11225	1928	45	0
1981	5853	8654	45	2157	6611	941	0	30463	289646	10537	1836	22	0
1982	5853	9113	68	2157	6611	941	0	30257	289485	10422	1836	22	0
1983	5853	9251	137	2112	6611	941	0	30165	289531	10307	1836	22	0
1984	5853	9573	183	2066	6611	941	0	30050	289485	10146	1836	22	0
1985	5853	10055	321	1928	6611	941	0	29752	289348	10101	1836	22	0
1986	5853	10560	413	1882	6611	941	0	29568	289003	10078	1836	22	0
1987	5853	10812	413	1882	6611	941	0	29476	288957	9940	1859	22	0
1988	5853	10858	505	1836	6611	941	0	29430	289026	9825	1859	22	0
1989	5853	11042	528	1813	6611	941	0	29384	289256	9435	1882	22	0
1990	5853	11202	550	1790	6611	941	0	29361	289256	9159	2020	22	0
1991	5853	11524	619	1744	6611	941	0	29178	289348	8907	2020	22	0
1992	5853	11639	688	1744	6588	941	0	29086	289393	8769	2043	22	0
1993	5853	12075	711	1744	6588	941	0	28948	288842	8976	2066	22	0
1994	5853	12465	711	1744	6588	941	0	28856	288360	9182	2043	22	0
1995	5853	12718	711	1744	6565	941	0	28879	287878	9412	2043	22	0
1996	5853	12924	757	1721	6542	895	0	28810	287534	9687	2020	22	0
1997	5876	13475	757	1721	6496	895	0	28719	287075	9687	2043	22	0
1998	5876	13934	757	1721	6427	826	0	28627	286593	9917	2066	22	0
1999	5876	14348	757	1721	6359	826	0	28489	285766	10468	2134	22	0

Final Report: Evaluation of Rainfall-Runoff Trends in the Upper Colorado River Basin (Phase Two)
 TWDB Contract Number 1800012283

Table A-3 – Land-use/Land Cover Area (acres) by year & category – South Concho Watershed, Cont.

Year	Water	Developed	Mining	Barren	Forest			Grassland	Shrubland	Cropland	Hay & Pastureland	Wetland	
					Deciduous	Evergreen	Mixed					Year	Water
2000	5876	14577	757	1721	6359	826	0	28420	285238	10789	2180	22	0
2001	5876	14738	757	1721	6313	826	0	28787	284779	10766	2180	22	0
2002	5922	15128	757	1675	6221	826	0	28719	284573	10743	2180	22	0
2003	5968	15335	780	1629	6221	826	0	28787	284205	10812	2180	22	0
2004	5991	15748	780	1561	6175	803	0	29040	283654	10812	2180	22	0
2005	5991	15817	803	1538	6129	826	0	29269	283379	10812	2180	22	0
2006	5991	16276	803	1538	6129	826	0	29132	282851	11065	2134	22	0
2007	5991	16896	849	1515	6129	780	0	29040	282231	11179	2134	22	0
2008	5991	17470	872	1492	6129	780	0	28948	281611	11317	2134	22	0
2009	5991	17998	895	1469	6129	757	0	28719	280922	11730	2134	22	0
2010	5991	18457	895	1469	6106	734	0	28673	280280	11983	2157	22	0
2011	5968	19375	895	1469	6106	711	0	28420	278305	13337	2157	22	0
2012	5968	19926	964	1400	6106	711	0	28282	276538	14692	2157	22	0
2013	5968	20408	987	1377	6083	688	0	28191	274403	16483	2157	22	0
2014	5968	20913	1078	1285	6037	688	0	28053	272222	18342	2157	22	0
2015	5968	21418	1147	1216	5968	688	0	27961	270867	19283	2226	22	0
2016	5968	22061	1170	1193	5922	688	0	27846	270270	19375	2249	22	0

Final Report: Evaluation of Rainfall-Runoff Trends in the Upper Colorado River Basin (Phase Two)
 TWDB Contract Number 1800012283

Table A-4 – Land-use/Land Cover Area (acres) by year & category – North Concho Watershed

Year	Water	Developed	Mining	Barren	Forest			Grassland	Shrubland	Cropland	Hay & Pastureland	Wetland	
					Deciduous	Evergreen	Mixed					Herbaceous	Woody
1940	459	8999	0	5394	1836	3030	0	154476	577754	205555	5004	390	780
1941	459	8999	0	5394	1836	3030	0	155647	588383	193824	4958	390	757
1942	459	8999	0	5417	1836	3030	0	157070	602157	178741	4889	390	688
1943	459	8999	0	5417	1836	3030	0	158425	615679	163957	4866	367	642
1944	459	8999	0	5417	1836	3030	0	159550	628948	149678	4843	367	550
1945	459	8999	0	5417	1836	3030	0	159733	631634	146854	4843	344	528
1946	459	8999	0	5417	1836	3030	0	159963	634641	143640	4843	321	528
1947	459	8999	0	5417	1836	3030	0	160215	638475	139554	4843	321	528
1948	459	8999	0	5417	1836	3030	0	160330	641414	136478	4889	321	505
1949	459	8999	0	5417	1836	3030	0	160651	644283	133379	4889	321	413
1950	459	8999	0	5417	1836	3030	0	160812	647589	129935	4889	321	390
1951	459	8999	0	5417	1836	3030	0	160950	649931	127456	4889	321	390
1952	459	8999	0	5417	1836	3030	0	161019	651515	125895	4889	298	321
1953	459	8999	0	5417	1836	3030	0	161202	654338	122956	4912	206	321
1954	459	8999	0	5417	1836	3030	0	161386	656290	120821	4912	206	321
1955	1354	8999	0	5417	1836	3030	0	160789	658815	118067	4912	206	252
1956	3397	9022	0	5417	1836	3030	0	159802	660973	114876	4889	183	252
1957	3397	9022	0	5417	1836	3030	0	159917	662947	112786	4889	183	252
1958	3397	9067	0	5417	1836	3030	0	159986	665518	110123	4889	183	229
1959	3397	9067	0	5417	1836	3030	0	160146	667768	107713	4889	183	229
1960	3397	9090	0	5417	1836	3030	0	160261	670661	104752	4889	160	183
1961	3397	9182	0	5417	1836	3030	0	160422	673553	101629	4889	160	160
1962	3397	9297	0	5417	1836	3030	0	160491	676744	98255	4889	160	160
1963	3397	9412	0	5417	1836	3007	0	158677	674908	101813	4889	160	160
1964	3397	9458	0	5417	1836	3007	0	156910	672956	105486	4889	160	160
1965	3397	9458	0	5417	1836	3007	0	155142	671763	108448	4889	160	160
1966	3397	9481	0	5417	1836	3007	0	153948	670936	110445	4889	160	160
1967	3397	9527	0	5417	1836	3007	0	152295	669949	113062	4889	137	160
1968	3397	9595	0	5417	1836	3007	0	151606	668457	115197	4889	114	160
1969	3397	9687	0	5417	1836	3007	0	151790	677456	105922	4889	114	160

Final Report: Evaluation of Rainfall-Runoff Trends in the Upper Colorado River Basin (Phase Two)
TWDB Contract Number 1800012283

Table A-4 – Land-use/Land Cover Area (acres) by year & category – North Concho, Cont.

Year	Water	Developed	Mining	Barren	Forest			Grassland	Shrubland	Cropland	Wetland		
					Deciduous	Evergreen	Mixed				Hay & Pastureland	Herbaceous	Woody
1970	3397	9779	0	5417	1836	3007	0	151928	686799	96349	4889	114	160
1971	3397	9894	0	5417	1836	3007	0	152180	696120	86662	4889	114	160
1972	3397	10032	0	5417	1836	3007	0	152617	706634	75573	4889	114	160
1973	3397	10101	0	5417	1836	3007	0	152731	716574	65472	4889	114	137
1974	3397	10146	0	5417	1836	3007	0	152984	727617	54132	4889	114	137
1975	3397	10422	0	5417	1836	3007	0	152915	727066	54476	4889	114	137
1976	3397	10996	0	5417	1836	3007	0	152685	726377	54820	4889	114	137
1977	3397	11524	0	5417	1836	3007	0	152594	725941	54820	4889	114	137
1978	3397	11983	0	5417	1836	3007	0	152456	724954	55486	4889	114	137
1979	3397	12672	0	5417	1836	3007	0	152318	724150	55739	4889	114	137
1980	3397	13429	0	5417	1836	3007	0	151974	723668	55808	4889	114	137
1981	3535	13452	0	5785	1836	3099	0	149655	725596	56014	4499	45	160
1982	3535	13728	0	5785	1859	3122	0	149265	725137	56611	4499	45	91
1983	3535	13797	22	5762	1859	3122	0	149081	724701	57185	4499	45	68
1984	3535	14279	45	5739	1859	3122	0	148760	724173	57575	4499	45	45
1985	3535	14531	68	5716	1859	3122	0	148484	723760	58011	4499	45	45
1986	3535	14646	68	5716	1859	3122	0	148347	723645	58195	4499	45	0
1987	3535	14761	114	5670	1836	3099	0	148347	727043	54729	4499	45	0
1988	3535	14761	183	5647	1836	3099	0	148370	730394	51308	4499	45	0
1989	3535	14761	229	5647	1836	3099	0	148370	733723	47933	4499	45	0
1990	3535	14853	229	5647	1836	3099	0	148438	737626	43870	4499	45	0
1991	3535	14876	229	5647	1836	3099	0	148461	740909	40541	4499	45	0
1992	3535	15082	252	5647	1836	3076	0	148553	744168	36983	4499	45	0
1993	3558	15426	298	5647	1836	3076	0	148507	742148	38590	4545	45	0
1994	3558	15886	298	5739	1836	3076	0	148347	740702	39600	4591	45	0
1995	3581	16551	298	5693	1836	3076	0	148232	738980	40794	4591	45	0
1996	3581	17033	436	5670	1813	3076	0	148071	736960	42355	4637	45	0
1997	3581	17470	436	5670	1813	3030	0	147979	735353	43663	4637	45	0
1998	3604	17860	436	5601	1813	2984	0	147819	733494	45362	4660	45	0
1999	3627	18434	459	5532	1813	2961	0	147566	730922	47543	4775	45	0

Final Report: Evaluation of Rainfall-Runoff Trends in the Upper Colorado River Basin (Phase Two)
 TWDB Contract Number 1800012283

Table A-4 – Land-use/Land Cover Area (acres) by year & category – North Concho Watershed, Cont.

Year	Water	Developed	Mining	Barren	Forest			Grassland	Shrubland	Cropland	Hay & Pastureland	Wetland	
					Deciduous	Evergreen	Mixed					Year	Water
2000	3627	18893	550	5440	1813	2961	0	147428	729109	49012	4797	45	0
2001	3650	19191	550	5417	1813	2961	0	147382	728696	49173	4797	45	0
2002	3650	19352	573	5463	1813	3030	0	147474	728213	49265	4797	45	0
2003	3696	19880	596	5417	1813	3053	0	147566	727502	49334	4775	45	0
2004	3719	20064	619	5417	1813	3076	0	147658	726974	49540	4752	45	0
2005	3741	20362	619	5463	1813	3076	0	147727	726331	49770	4729	45	0
2006	3741	21235	642	5463	1813	3076	0	147497	724885	50550	4729	45	0
2007	3741	21992	573	5463	1813	3076	0	147291	723393	51561	4729	45	0
2008	3741	22543	573	5440	1790	3076	0	147107	722084	52548	4729	45	0
2009	3741	23347	596	5394	1790	3076	0	146923	721005	53030	4729	45	0
2010	3741	23966	596	5280	1790	3053	0	146831	719168	54476	4729	45	0
2011	3741	25000	642	5211	1790	3053	0	146556	712075	60812	4752	45	0
2012	3741	25436	665	5165	1767	3053	0	146303	707001	65748	4752	45	0
2013	3741	26170	665	5165	1767	3007	0	146212	701285	70867	4752	45	0
2014	3741	26790	688	5165	1767	3007	0	145959	696740	75022	4752	45	0
2015	3741	27341	757	5096	1767	3007	0	145867	691207	80096	4752	45	0
2016	3741	28512	757	5073	1767	3007	0	145569	688475	81978	4752	45	0

Final Report: Evaluation of Rainfall-Runoff Trends in the Upper Colorado River Basin (Phase Two)
TWDB Contract Number 1800012283

```
if commands <=8 && commands > 4
    option = 2;
    commands = commands - 4;
end
if commands <=12 && commands > 8
    option = 3;
    commands = commands - 8;
end
if commands <=16 && commands > 12
    option = 4;
    commands = commands - 12;
end
if commands <=20 && commands > 16
    option = 5;
    commands = commands - 16;
end
if commands <=24 && commands > 20
    option = 6;
    commands = commands - 20;
end
if commands <=24 && commands > 20
    option = 6;
    commands = commands - 20;
end
if commands <=28 && commands > 24
    option = 7;
    commands = commands - 24;
end
if commands <=32 && commands > 28
    option = 8;
    commands = commands - 28;
end
if commands == 33
    option = 0;
end
%commands dictates which watershed is considered
%option dictates whether the code is performing simulations or
%displaying simulation results.

%Model Hard-Coded Options Settings:
%option = 2;

%Notes:
%Option 1 = Perform UCWBM Computations
%Option 2 = Load Previous UCWBM Results, Generate Figures
%Option 3 = Simulate only Land Use Change - Ignore ponds
%Option 4 = Output Results from Option 3
%Option 5 = Simulate only Ponds - Ignore land use change
%Option 6 = Output Results from Option 5

if option ~= 0
    %%%%%%%%%%%
    %Get Rainfall
    %%%%%%%%%%%
```

Final Report: Evaluation of Rainfall-Runoff Trends in the Upper Colorado River Basin (Phase Two)
 TWDB Contract Number 1800012283

```

if commands == 1
  load C:\Jordan\LREWater_Projects\TWDB_RainfallRunoff\Task4\BallingerRain_PoR.asc
  YEAR_Rain = BallingerRain_PoR(:,3);
  MONTH_Rain = BallingerRain_PoR(:,1);
  DAY_Rain = BallingerRain_PoR(:,2);
  RAIN = BallingerRain_PoR(:,4); %Units = inches
end
if commands == 2
  load C:\Jordan\LREWater_Projects\TWDB_RainfallRunoff\Task4\Kennedy_PoR.asc
  YEAR_Rain = Kennedy_PoR(:,1);
  MONTH_Rain = Kennedy_PoR(:,2);
  DAY_Rain = Kennedy_PoR(:,3);
  RAIN = Kennedy_PoR(:,9);
end
if commands == 3
  load C:\Jordan\LREWater_Projects\TWDB_RainfallRunoff\Task4\Kennedy_PoR.asc
  YEAR_Rain = Kennedy_PoR(:,1);
  MONTH_Rain = Kennedy_PoR(:,2);
  DAY_Rain = Kennedy_PoR(:,3);
  RAIN = Kennedy_PoR(:,5);
end
if commands == 4
  load C:\Jordan\LREWater_Projects\TWDB_RainfallRunoff\Task4\NorthConcho\SterlingCityPrecip_PoR.mat
  YEAR_Rain = YEAR_PoR;
  MONTH_Rain = MONTH_PoR;
  DAY_Rain = DAY_PoR;
  RAIN = RAIN_PoR;
end

%Exclude Missing Data from Rainfall Record
for jj = 1:1:length(RAIN)
  if RAIN(jj) == -1
    RAIN(jj) = 0;
  end
end
yrs_Rain = min(YEAR_Rain):1:max(YEAR_Rain);

%%%%%%%%%%
%Get Evaporation - Free Surface
%%%%%%%%%%
if commands == 1
  load ElmCreek_Evap.mat
  Gross_Evap = GrossEvap_Elm;
end
if commands == 2
  load SS_Evap.mat
  Gross_Evap = GrossEvap_SS;
end
if commands == 3
  load SC_Evap.mat
  Gross_Evap = GrossEvap_SC;
end
if commands == 4
  load NC_Evap.mat
  
```

Final Report: Evaluation of Rainfall-Runoff Trends in the Upper Colorado River Basin (Phase Two)
 TWDB Contract Number 1800012283

```

Gross_Evap = GrossEvap_NC;
end
MONTH_EVAP = MONTH;
YEAR_EVAP = YEAR;
%%%%%%%%%%%%%%%%%%%%%%%%%%%%%%%%%%%%%%%%%%%%%%%%%%%%%%%%%%%%%%%%%%%%%%%%
%Get Small Pond Data
%%%%%%%%%%%%%%%%%%%%%%%%%%%%%%%%%%%%%%%%%%%%%%%%%%%%%%%%%%%%%%%%%%%%%%%%
if commands == 1
  load ElmCreek_SmallPonds.mat
end
if commands == 2
  load SS_SmallPonds.mat
end
if commands == 3
  load SC_SmallPonds.mat
end
if commands == 4
  load NC_SmallPonds.mat
end
MONTH_EVAP = MONTH;
YEAR_EVAP = YEAR;

%%%%%%%%%%%%%%%%%%%%%%%%%%%%%%%%%%%%%%%%%%%%%%%%%%%%%%%%%%%%%%%%%%%%%%%%
%Get Land Use/Land Cover Data
%%%%%%%%%%%%%%%%%%%%%%%%%%%%%%%%%%%%%%%%%%%%%%%%%%%%%%%%%%%%%%%%%%%%%%%%
if commands == 1
  load ElmCreek_LandUse.mat
  WatershedArea = 298532.583378; %acres
end
if commands == 2
  load SanSaba_LandUse.mat
  WatershedArea = 2013884.39146; %acres
end
if commands == 3
  load SouthConcho_LandUse.mat
  WatershedArea = 356571.893723; %acres
end
if commands == 4
  load NorthConcho_LandUse.mat
  WatershedArea = 963909.433534; %acres
end
CN_YEAR = 1940:1:2016; %Period of Record Only Per TWDB Request

% Q = (P-ia)^2/((P-ia)+S)
% ia = 0.2S
% S = (1000/CN)-10
%
%Q = Runoff in Inches
%P = Rainfall in Inches
%ia = initial abstractions = amount that doesn't runoff (inches)
%S = potential maximum retention (in)

```

Final Report: Evaluation of Rainfall-Runoff Trends in the Upper Colorado River Basin (Phase Two)
TWDB Contract Number 1800012283

```
% Incorporate Rainfall, Ponds, Evap, and Curve Numbers
RainYears = yrs_Rain;
PondYears = min(CN_YEAR):1:max(YEARsp);

NumRainYears = length(RainYears);
NumPondYears = length(PondYears);
TotalRunoffResults = zeros(NumRainYears,NumPondYears);
TotalEvapResults = zeros(NumRainYears,NumPondYears);
TotalNonRunoffResults = zeros(NumRainYears,NumPondYears);
TotalCanopyLossResults = zeros(NumRainYears,NumPondYears);

InitialFull = 50;
CarryOver = 0;

if option == 1 || option == 3 || option == 5 || option == 7
    % Perform Simulations using UCWBM

    for oo = 1:1:NumPondYears
        disp(['Working On Watershed Year ' num2str(PondYears(oo)) ' (#' num2str(oo) ' out of '
num2str(NumPondYears) ')'])
        Pond_Year = PondYears(oo);
        if Pond_Year < min(CN_YEAR)
            cnToUse = WeightedCurveNumber(1,1);
        end
        if Pond_Year > max(CN_YEAR)
            cnToUse = WeightedCurveNumber(length(CN_YEAR),1);
        end
        if Pond_Year <= max(CN_YEAR) && Pond_Year >= min(CN_YEAR)
            is = 0; ic = 0;
            kk = 0; icc = 0;
            while kk == 0
                ic = ic + 1;
                if ic <= length(CN_YEAR)
                    if CN_YEAR(ic) == Pond_Year
                        icc = ic;
                        kk = 1;
                    end
                end
            end
            else
                kk = 1;
            end
        end
        cnToUse = WeightedCurveNumber(icc,1);
    end
    if option == 5
        cnToUse = min(squeeze(WeightedCurveNumber(:,1)));
    end

    % Define Antecedant Moisture Conditions and adjust the curve numbers
    CN(2) = cnToUse; % Antecedant Moisture Condition #2
end
```

Final Report: Evaluation of Rainfall-Runoff Trends in the Upper Colorado River Basin (Phase Two)
 TWDB Contract Number 1800012283

CN(1) = 4.2*cnToUse/(10-0.058*cnToUse); % Antecedent Moisture Condition #1
 CN(3) = 23*cnToUse/(10+0.13*cnToUse); % Antecedent Moisture Condition #1

```

PondsOn = zeros(length(YEARsp),1);
PondStorage = zeros(length(PondsOn),366);
if option == 1 || option == 5 || option == 7 %Turn of ponds for option 3
  for jj = 1:1:length(PondsOn)
    if Pond_Year >= YEARsp(jj)
      PondsOn(jj) = 1;
    else
      PondStorage(jj,1) = 0;
    end
  end
end
if oo == 1
  TotalRainYear = zeros(NumRainYears,1);
end
for yy = 1:1:NumRainYears
  Precip_Year = RainYears(yy);
  %Get Rain
  is = 0;
  kk = 0; ic = 0;
  while kk == 0
    ic = ic + 1;
    if ic <= length(YEAR_Rain)
      if YEAR_Rain(ic) == Precip_Year
        is = ic;
        kk = 1;
      end
    else
      kk = 2;
    end
  end
  isleap = rem(Precip_Year,4);
  if isleap == 0
    jj = 365;
  else
    jj = 364;
  end
  DailyRain = RAIN(is:is+jj);
  mnRain = MONTH_Rain(is:is+jj);
  DailyEvap = zeros(length(DailyRain),1);
  numdays = length(DailyRain);

  if oo == 1
    TotalRainYear(yy) = sum(DailyRain);%inches
  end
  if Precip_Year >= min(YEAR_EVAP) && Precip_Year <= max(YEAR_EVAP)
    %Find Evapotiation Data
    is = 0;
    kk = 0; ic = 0;
    while kk == 0
      ic = ic + 1;

```

Final Report: Evaluation of Rainfall-Runoff Trends in the Upper Colorado River Basin (Phase Two)
 TWDB Contract Number 1800012283

```

    if ic <= length(YEAR_EVAP)
      if YEAR_EVAP(ic) == Precip_Year
        is = ic;
        kk = 1;
      end
    else
      kk = 2;
    end
  end
else
  if Precip_Year < min(YEAR_EVAP)
    is = 1;
  end
  if Precip_Year > max(YEAR_EVAP)
    is = length(YEAR_EVAP)-11;
  end
end
EvapData = Gross_Evap(is:is+11);
for jj = 1:1:length(DailyEvap)
  mn = 31;
  if mnRain(jj) == 2 && isleap == 0
    mn = 29;
  end
  if mnRain(jj) == 2 && isleap ~= 0
    mn = 28;
  end
  if mnRain(jj) == 4 || mnRain(jj) == 6 || mnRain(jj) == 9 || mnRain(jj) == 11
    mn = 30;
  end
  dr = EvapData(mnRain(jj))/mn/12; %units = ft per day
  DailyEvap(jj) = dr;
end

%Look at Ponds
np = length(YEARsp);
if CarryOver == 1 && yy > 1
  PondStorage = zeros(np,numdays+1);
  PondStorage(:,1) = pshold;
else
  PondStart = InitialFull;
  PondStorage = zeros(np,numdays+1);
  PondStorage(:,1) = VOLUMEsp*PondStart/100;
end

PondLossToEvap = zeros(np,numdays);
NotRunoff = zeros(numdays,1);
CanopyLoss = zeros(numdays,1);
Runoff = zeros(numdays,1);
Runoff_Volume = zeros(numdays,1);

%% %MODEL TIMELOOP%% %
for jj = 1:1:numdays

```


Final Report: Evaluation of Rainfall-Runoff Trends in the Upper Colorado River Basin (Phase Two)
 TWDB Contract Number 1800012283

```

RainToday = DailyRain(jj); % Units = inches;
if option ~= 7
  if jj > 4
    Antecedent5Day = sum(DailyRain(jj-4:1:jj));
  else
    Antecedent5Day = 5*RainToday; % approximation
  end
  %Check Growing or Dormant Season
  %Growing Season = March 15-October 15
  %Ignoring Leap years
  IsDormant = 0;
  if jj > 74 %March 14th in non-leap year
    if jj < 290 %October 16th in non-leap year
      IsDormant = 1;
    end
  end
  % Adjust curve number for antecedent conditions
  if IsDormant == 1 && Antecedent5Day < 1.4 % inches
    DailyCNtoUse = CN(1); % Dry
  end
  if IsDormant == 1 && Antecedent5Day >= 1.4 && Antecedent5Day <= 2 % inches
    DailyCNtoUse = CN(2); % Average
  end
  if IsDormant == 1 && Antecedent5Day > 2 % inches
    DailyCNtoUse = CN(3); % Wet
  end
  if IsDormant == 0 && Antecedent5Day < 0.5 % inches
    DailyCNtoUse = CN(1); % Dry
  end
  if IsDormant == 0 && Antecedent5Day >= 0.5 && Antecedent5Day <= 1 % inches
    DailyCNtoUse = CN(2); % Average
  end
  if IsDormant == 1 && Antecedent5Day > 1 % inches
    DailyCNtoUse = CN(3); % Wet
  end
else
  DailyCNtoUse = CN(2); % Average
end

%Reduce Pond Volumes due to evaporation
if option ~= 3
  for kk = 1:1:np
    if PondsOn(kk) == 1 && PondStorage(kk,jj) > 0
      % Water is present - determine pond surface area
      Area = 0.911*PondStorage(kk,jj)^0.695;
      PondLossToEvap(kk,jj) = min(Area*DailyEvap(jj),PondStorage(kk,jj)); %Units acre-ft
      PondStorage(kk,jj) = PondStorage(kk,jj)-PondLossToEvap(kk,jj);
    end
  end
end
S = (1000/DailyCNtoUse)-10;
ia = 0.2*S;
extra = 0;

```

Final Report: Evaluation of Rainfall-Runoff Trends in the Upper Colorado River Basin (Phase Two)
 TWDB Contract Number 1800012283

```

if option ~= 3
  if RainToday > 0
    %Increase Pond Storage based on the direct rainfall
    %entering the pond via the pond surface - ie not runoff
    extra = 0;
    for kk = 1:1:np
      if PondsOn(kk) == 1 && PondStorage(kk,jj) > 0
        %Water is present - determine pond surface area
        Area = 0.911*PondStorage(kk,jj)^0.695;
        VolumeFromRain = RainToday/12*Area; % acre-ft
        PondStorage(kk,jj) = PondStorage(kk,jj)+VolumeFromRain;
        if PondStorage(kk,jj) > VOLUMEsp(kk)
          extra = extra+PondStorage(kk,jj)-VOLUMEsp(kk);
          PondStorage(kk,jj)=VOLUMEsp(kk);
        end
      end
    end
    %Extra is the additional streamflow spilling out of
    %full ponds as a result of direct rainfall
  end
end
if RainToday > ia %it rained enough to generate runoff

%Compute Abstractions

%  $Q = (P-ia)^2/((P-ia)+S)$ 
% ia = 0.2S
%  $S = (1000/CN)-10$ 
%
% Q = Runoff in Inches
% P = Rainfall in Inches
% ia = initial abstractions = amount that doesn't runoff (inches)
% S = potential maximum retention (in)

CanopyLoss(jj) = ia;
Runoff(jj) = (RainToday-ia)^2/((RainToday-ia)+S); %Inches
NotRunoff(jj) = (RainToday-ia)-Runoff(jj); %Inches

% Assume equal rainfall all over the basin, compute volume of runoff
Runoff_V = Runoff(jj)/12*WatershedArea + extra; %Add in spillage from full ponds

if option ~= 3
  %Now Subtract off the volume to ponds
  for kk = 1:1:np
    if PondsOn(kk) == 1 %Pond is simulated
      def = VOLUMEsp(kk)-PondStorage(kk,jj); %Storage on the previous day
      if Runoff_V >= def
        PondStorage(kk,jj+1) = PondStorage(kk,jj)+def;
        Runoff_V = Runoff_V-def;
      else
        PondStorage(kk,jj+1) = PondStorage(kk,jj)+Runoff_V;
      end
    end
  end
end

```

Final Report: Evaluation of Rainfall-Runoff Trends in the Upper Colorado River Basin (Phase Two)
 TWDB Contract Number 1800012283

```

        Runoff_V = 0;
    end
    end
    end
    end
    Runoff_Volume(jj) = Runoff_V;
else
    PondStorage(:,jj+1) = PondStorage(:,jj);
    CanopyLoss(jj) = RainToday;
end
ToCanopy = CanopyLoss(jj);
ToGround = NotRunoff(jj);
ToRunoff = Runoff;

end
pshold = PondStorage(:,size(PondStorage,2));

total_runoff = sum(Runoff_Volume);
total_evap = sum(sum(PondLossToEvap));
total_nonRunoff = sum(NotRunoff)/12*WatershedArea;
total_CanopyLoss = sum(CanopyLoss)/12*WatershedArea;
TotalRunoffResults(yy,oo) = total_runoff;
TotalEvapResults(yy,oo) = total_evap;
TotalNonRunoffResults(yy,oo) = total_nonRunoff;
TotalCanopyLossResults(yy,oo) = total_CanopyLoss;
end
end

%Save UCWBM Results
if option == 1
    if commands == 1

save('UCWBM_1_Results.mat','TotalRunoffResults','TotalEvapResults','TotalNonRunoffResults','PondYears','Rain
Years','TotalRainYear','WatershedArea','TotalCanopyLossResults')
    end
    if commands == 2

save('UCWBM_2_Results.mat','TotalRunoffResults','TotalEvapResults','TotalNonRunoffResults','PondYears','Rain
Years','TotalRainYear','WatershedArea','TotalCanopyLossResults')
    end
    if commands == 3

save('UCWBM_3_Results.mat','TotalRunoffResults','TotalEvapResults','TotalNonRunoffResults','PondYears','Rain
Years','TotalRainYear','WatershedArea','TotalCanopyLossResults')
    end
    if commands == 4

save('UCWBM_4_Results.mat','TotalRunoffResults','TotalEvapResults','TotalNonRunoffResults','PondYears','Rain
Years','TotalRainYear','WatershedArea','TotalCanopyLossResults')
    end
end
if option == 3
    if commands == 1

```

Final Report: Evaluation of Rainfall-Runoff Trends in the Upper Colorado River Basin (Phase Two)
TWDB Contract Number 1800012283

```
save('UCWBM_3_1_Results.mat','TotalRunoffResults','TotalEvapResults','TotalNonRunoffResults','PondYears','RainYears','TotalRainYear','WatershedArea','TotalCanopyLossResults')
end
if commands == 2

save('UCWBM_3_2_Results.mat','TotalRunoffResults','TotalEvapResults','TotalNonRunoffResults','PondYears','RainYears','TotalRainYear','WatershedArea','TotalCanopyLossResults')
end
if commands == 3

save('UCWBM_3_3_Results.mat','TotalRunoffResults','TotalEvapResults','TotalNonRunoffResults','PondYears','RainYears','TotalRainYear','WatershedArea','TotalCanopyLossResults')
end
if commands == 4

save('UCWBM_3_4_Results.mat','TotalRunoffResults','TotalEvapResults','TotalNonRunoffResults','PondYears','RainYears','TotalRainYear','WatershedArea','TotalCanopyLossResults')
end
if option == 5
if commands == 1

save('UCWBM_5_1_Results.mat','TotalRunoffResults','TotalEvapResults','TotalNonRunoffResults','PondYears','RainYears','TotalRainYear','WatershedArea','TotalCanopyLossResults')
end
if commands == 2

save('UCWBM_5_2_Results.mat','TotalRunoffResults','TotalEvapResults','TotalNonRunoffResults','PondYears','RainYears','TotalRainYear','WatershedArea','TotalCanopyLossResults')
end
if commands == 3

save('UCWBM_5_3_Results.mat','TotalRunoffResults','TotalEvapResults','TotalNonRunoffResults','PondYears','RainYears','TotalRainYear','WatershedArea','TotalCanopyLossResults')
end
if commands == 4

save('UCWBM_5_4_Results.mat','TotalRunoffResults','TotalEvapResults','TotalNonRunoffResults','PondYears','RainYears','TotalRainYear','WatershedArea','TotalCanopyLossResults')
end
if option == 7
if commands == 1

save('UCWBM_7_1_Results.mat','TotalRunoffResults','TotalEvapResults','TotalNonRunoffResults','PondYears','RainYears','TotalRainYear','WatershedArea','TotalCanopyLossResults')
end
if commands == 2

save('UCWBM_7_2_Results.mat','TotalRunoffResults','TotalEvapResults','TotalNonRunoffResults','PondYears','RainYears','TotalRainYear','WatershedArea','TotalCanopyLossResults')
end
if commands == 3
```

Final Report: Evaluation of Rainfall-Runoff Trends in the Upper Colorado River Basin (Phase Two)
TWDB Contract Number 1800012283

```
save('UCWBM_7_3_Results.mat','TotalRunoffResults','TotalEvapResults','TotalNonRunoffResults','PondYears','Ra  
inYears','TotalRainYear','WatershedArea','TotalCanopyLossResults')  
    end  
    if commands == 4  
  
save('UCWBM_7_4_Results.mat','TotalRunoffResults','TotalEvapResults','TotalNonRunoffResults','PondYears','Ra  
inYears','TotalRainYear','WatershedArea','TotalCanopyLossResults')  
    end  
    end  
end  
  
%%%%%%%%%
```

Appendix C -Draft Report – Review Comments from TWDB

The following comments were provided from TWDB via email on August 17, 2019. Responses to each comment are provided below, immediately after each comment. Responses are denoted in ***bold italics***. TWDB comments were organized into the following categories:

- Required Changes (13 Items)
 - Specific Draft Final Report Comments (93 Items)
 - Figures and Tables Comments (17 Items)
- Suggested Changes (10 Items)
 - Figures and Tables Comments (1 Item)

It was unclear whether TWDB intended to include the “Specific Draft Final Report Comments (93 Items)” and “Figures and Tables Comments (17 Items)” as part of the “Required Changes,” yet LRE Water reviewed all provided comments as if they were “required” in order to improve the value of the project report. LRE Water met with TWDB staff on August 21, 2019 to discuss the provided comments and finalize how the comments were to be addressed.

REQUIRED CHANGES

General Draft Final Report Comments:

1. Please add the following statement to the cover page of the final report:

Pursuant to Senate Bill 1 as approved by the 85th Texas Legislature, this study report was funded for the purpose of studying environmental flow needs for Texas rivers and estuaries as part of the adaptive management phase of the Senate Bill 3 process for environmental flows established by the 80th Texas Legislature. The views and conclusions expressed herein are those of the author(s) and do not necessarily reflect the views of the Texas Water Development Board.

Changed as requested

2. Please ensure the final report adheres to the formatting guidelines for Texas Water Development Board reports (http://www.twdb.texas.gov/about/contract_admin/index.asp; See “Helpful Contracting Documents”).

Changed as requested

3. The study characterizes and attempts to explain the temporal changes in the rainfall and runoff response in the Upper Colorado River Basin of Texas. The assessment of the trends in rainfall and streamflow is carried out using the Mann-Kendall statistic; the linkages to potential agents of changes, namely temperature, soil moisture, and land cover, are done empirically. The investigators also introduce a simple water balance model based on curve number. The study points to land cover change, in particular the increase in the number of small ponds as a possible cause for the changes in runoff.

Comment acknowledged, no change is requested or required.

4. Overall, the study is done competently, and the methods employed are mostly appropriate. However, there are several technical issues related to the data sets used, temporal consistency of the data sets, interpretation of the data sets, and the presentation that the investigators need to address.

Comment acknowledged and addressed through responses to other comments.

5. The methodology and the source of the datasets used in the study are not clearly described in all sections, which made it difficult to review the report or to replicate the results. Please describe all data pre-processing, processing, and analysis methodologies in detail for each section. If, as described in Chapters 6 and 7, data from multiple gauges were used to compile the record for one location, the IDs of all stations used, and their respective periods of record must be included in a table within the main text of the report. The methodology used to compile the data from multiple gauges into one record must also be included in the respective chapter.

Comment acknowledged and addressed through responses to other comments.

6. There is a concern that the study methodology, as described in the report, results in an over-estimation of the number of small ponds in the study area and may also overstate the impact of those ponds on streamflow. Specifically, the methodology does not distinguish between natural pools in the river and man-made impoundments and does not account for the differences in impacts on streamflow from off-channel and on-channel impoundments. Please include a discussion in the report that addresses possible implications of the methodology adopted on the over-estimation of small ponds in the study area.

Comment acknowledged and addressed.

7. In general, the periods of analysis for the various data sets are mismatched, which can lead to confusing and possibly misleading results. For example, temperature data for Ballinger, TX was analyzed over the period of record from 1900 to 2019 (Section 5.1.1). Precipitation data at this site were analyzed over the same period of record from 1900 to 2019 (Section 7.3.1). GLDAS soil moisture data for the Elm Creek watershed were analyzed over the period of record from 1948 to 2019 (Section 8.2). Although the period of record for this data set extended from 1932 to 2019, analysis for streamflow data for Elm Creek was limited to 1940 to 2018 (Section 6.3).

As noted by the authors, using the full period of record for the analysis provides “a long period of record from which to infer trends” (Section 7.3.1, 1st paragraph). However, many of the data sets exhibit trends that vary over time. Depending on the period of data chosen for analysis, a subset of data may exhibit a substantially different trend from that displayed by analysis of the entire period of record. For example, as noted by the authors (Section 5.1.1, 2nd paragraph), the number of days over 100°F for Ballinger, TX has a significantly decreasing trend when analyzed over the entire period of record, but an increasing trend when only the 1970 to 2016 data is considered. Therefore, to the extent possible, the analysis for all datasets should be conducted over one consistent time period of interest.

Because the goal for this study was to assess the impact of various changes not accounted for in the streamflow naturalization process (Section 1, 2nd paragraph), the time period of greatest interest is 1940 to 2016, which corresponds to the available period of record for naturalized flow (Section 3.3, Table 3.1). Although it is informative to see how conditions have varied outside this time period, trends within the time period of 1940 to 2016 should be the focus of the trend analysis. It is recognized that some data sets can only approximate this time period. For example, 1938 may be the closest date for approximating land use data for 1940 (Section 4.3, 3rd paragraph) and 1948 may be the earliest date possible for approximating soil moisture data (Section 8.2). However, to the extent possible, it is most informative to know the trends in temperature, precipitation, land use, soil moisture, etc. across the time period 1940 to 2016 and how each of these may relate to trends in observed and naturalized flow over the same time period.

We recommend that the authors redo the analysis, as appropriate, to identify trends in temperature, precipitation, and other factors across the period 1940 to 2016 and use those trends to assess the impact of various changes not accounted for in the streamflow naturalization process.

Comment acknowledged and addressed. The report was revised to include data only from 1940-2016 when such data is available. LRE Water does not agree with this approach, and believes that utilizing longer periods of record, when available,

provides greater insight into the processes that may be contributing to rainfall-runoff response.

8. Site #1 is referred to in the document at “North Concho River near Carlsbad” (e.g. Section 3.3, page 3-5, 1st paragraph) and as “North Concho River at Carlsbad” (e.g. Section 3.3, page 3-6, 2nd paragraph). To avoid confusion that these may be different sites, please refer to Site #1 as “North Concho River near Carlsbad” throughout the document.

Changed as requested

9. There are inconsistencies related to Figure and Table references as well as issues related to pagination in the document, which are described more specifically in the comments below.

Comment acknowledged and addressed.

10. Section 4.3, Page 4-14 and throughout: The term 'noxious brush' has no specific meaning and is presumed negative. A definition of the species or another term like 'woody cover' is needed.

Comment acknowledged but rejected as the term “noxious brush” was used in the Phase I report for this project, in the Phase II request for proposals issued by TWDB, and in the Scope of Work for Phase II.

11. Sections 5, 6, and 7, Page 5-1 to 7-79: Sensitivity analysis of the trend analysis is needed to verify that trends are not unduly influenced but the timing of the start and end dates of the data record. For example, please undertake a jackknife analysis, by omitting the first 10 or last 10 years, to verify that the trend and significance are preserved.

Comment acknowledged and not addressed. Considering a 1940-2016 period of record, there are 77 years of data typically being analyzed. The purpose of the analysis is to assess trends over this time period, not of a shortened period. The revised Mann-Kendall methodology explains our level of confidence in the presented trends.

12. Please thoroughly check the document for numerous grammar, spelling, and typographical errors, and correct these errors in the final report.

The following typos are not exclusive but are highlighted because they may cause considerable confusion when reading the report.

- a) Section 6.1 North Concho Watershed Flow Analysis, Page 6-43, 1st Paragraph, 3rd Sentence: "USGS 08314000 N Concho Rv nr Carlsbad" should be " USGS 08134000 N Concho Rv nr Carlsbad."
- b) Section 8.1 GRACE Data Analysis, Page 8-1, 2nd Paragraph, 1st Sentence: "Point of Interest #5" should be "Point of Interest #3."
- c) Section 8.1 GRACE Data Analysis, Page 8-1, 3rd Paragraph, 2nd Sentence: "a prolonged dry period in the end of 2013" should be "a prolonged dry period in the end of 2003."
- d) Section 10.2.2 UCWBM results for the San Saba Watershed, Page 10-12, 3rd paragraph, Last Sentence: "results in a median 16% decrease in runoff" should be "results in a median 29% decrease in runoff."

Comment acknowledged and addressed.

13. Please check the page numbering for each section and ensure that numbering is sequential.

Comment acknowledged and addressed.

Specific Draft Final Report Comments:

1. Section 1, Page 1-17: Please define what non-statistical investigations are and explain how such investigations were used to assess "how soil moisture fluctuations may be linked to rainfall-runoff response".

Comment acknowledged and addressed.

2. Section 1, Page 1-18:
 - 1st Paragraph on the page: Last sentence is confusing and perhaps incorrect. Likely should refer to days on which minimum temperature did not fall below 60 degrees rather than days on which it did not exceed 60 degrees.
 - Last sentence. Evaporation rates should be included in the list of hydrologic affects.

Comment acknowledged and addressed.

3. Section 1.2.2, Page 1-18: Last sentence. Please include runoff in the list of implications.

Comment acknowledged and addressed.

4. Section 1, Page 1-19: Please clarify what a "drought period" is for the purposes of the study.

Comment acknowledged and addressed.

5. Section 1, Page 1-20: Please clarify how an SCS runoff curve number for a given watershed varies with time, and also clarify the meaning of “decreasing curve number trend”.

Comment acknowledged and addressed.

6. Section 1.2.5., Page 1-20: Last sentence is contradictory to the preceding information in the paragraph and the results presented in section 4.11.

Comment acknowledged and addressed.

7. Section 1.3.4, Page 1-21, last sentence: Given the unreliability of GRACE soil moisture data, the observation should discount the data validity rather than the physically understood and well-established relationship between soil moisture and runoff.

Comment acknowledged and addressed.

8. Section 1.3.4, Page 1-21: Please change “Data from Ballinger, TX was overlain on...” to “Data from Ballinger was compared to....”

Comment acknowledged and addressed.

9. Section 1.3.4 Relating Soil Moisture Fluctuations to Runoff, p. 1-21, first paragraph: In second to last sentence, the last reference to “rainfall” likely should refer to “runoff”, if the sentence is to make sense. Please clarify and revise the sentence as needed.

Comment acknowledged and addressed

10. Section 1.4, Page 1-21: Please change “This model allows for the simulation of rainfall...” to “This models allows for the simulation of runoff...”

Comment acknowledged and addressed with clarifying text

11. Section 1.5, Page 1-22, last bullet point: Please clarify what is meant by the following statement: “...whose land use/land cover has decreased marginally...”. In particular, please address the following when clarifying the statement:
 - In what land use/land cover type has there been a decrease?
 - Has the decrease in one land use/land cover type resulted in the increase of another land use/land cover type?
 - How is “marginally” defined?

Comment acknowledged and addressed with clarifying text

12. Section 1.5, Page 1-22, last sentence. Suspicions are not supported by analysis summarized in the report. Please revise sentence to reflect actual analysis results.

Comment acknowledged and addressed with clarifying text

13. Section 1.6, Page 1-23: The five recommendations in this section do not track with the three recommendations in Section 12. Please address this discrepancy in the final report.

Comment acknowledged and addressed with clarifying text

14. Section 2, Page 2-1, first paragraph: Omit the phrase ‘into the Highland Lakes.’ The Highland Lakes are not the subject of this phase II report. Three of the four focus areas are upstream of O.H. Ivie which, is not part of the Highland Lakes chain. Please use “subject watersheds” instead.

Comment acknowledged and addressed with clarifying text

15. Section 2, Page 2-1, fourth paragraph: The phrase “upstream of the Highland Lakes is misleading and should be struck. Three of the four focus areas are upstream of O.H. Ivie, which is not part of the Highland Lakes chain. Please use “subject watersheds” instead.

Comment acknowledged and addressed.

16. Section 2, Page 2-1, last paragraph: The word “proof” is overstated. Rather these facts lead to a theory that streamflow is lower. Also, the word “much” is not a technical term but rather an unverifiable subjective qualifier. Please reword this paragraph and omit the use of “proof” and “much”.

Comment acknowledged and addressed

17. Section 2, Page 2-1, end of first paragraph. The qualifier “drastically” is not a technical term but rather an unverifiable subjective qualifier. Please reword the sentence and omit use of “drastically”.

Comment acknowledged and addressed

18. Section 2.1 and 2.2, Pages 2-1, 2-2, & 2-3: 1957 and 2016 were wet years, which did not contribute to the drawdown of the drought, and 1957 was a record flood/outlier. Please test for sensitivity of trend results to outliers by omitting these years in the analysis.

Comment acknowledged and addressed, although it was assumed to refer to Figures 2.1, 2.2, 2.3 and 2.4 rather than Section 2.1 and 2.2 (which were not defined).

19. Section 3: The literature review should not be a stand-alone chapter but should provide the rationale for why methodologies selected in the study were adopted. It needs to be more comprehensive to cover the key methodologies used in the study. Please revise this section accordingly.

Comment acknowledged and addressed

20. Section 3.1, Pages 3-1 and 3-2: Please include the following additional relevant literature:

- *Commentary on "Effect of brush control on evapotranspiration in the North Concho River watershed using the eddy covariance technique" by Saleh, et al (2009), Journal of Soil and Water Conservation, (Brad Wilcox, John Walker, James Heilman), July/August 2010.*

Saleh, et al. concluded that brush control reduces evapotranspiration, which yields more groundwater recharge and an increase in stream flow. This paper critiques the Saleh study and provides historical stream flow evidence that brush management in the North Concho watershed will not lead to increases in water flow. To date, about \$14 million was spent on clearing about 463 square miles of mesquite and cedar in a 1,200 square mile watershed. The authors found that stream flow is much lower now than before 1960 and attribute these declines to improved rangeland management, thus, smaller flood events and less runoff for a given amount of rainfall. The focus is on runoff events since it is believed that groundwater sources only provide about 10% of the North Concho's flow. The authors wrap up their paper by stating that brush control is a "vitaly important land management practice, and if done properly, can lead to improved biodiversity and even watershed protection, however, there is no compelling evidence that it is a viable strategy for increasing water supply, and in the case of the North Concho watershed, there is strong evidence that it does not increase water supply".

- *Woody plant encroachment paradox: Rivers rebound as degraded grasslands convert to woodlands, Brad Wilcox, Yun Huang, both of Texas A&M Ecosystem Science and Management, April 2010.*

This study analyzed 85 years of data on four major river basins in the Edwards Plateau region of Texas. The Frio, Guadalupe, Llano, and Nueces Rivers were evaluated from a 10-year average stream flow, base flow, and storm flow perspective. They conclude that the contribution of base flow has doubled, even though woody cover has expanded, and rainfall amounts have remained constant. They further hypothesize that it is landscape degradation (loss of vegetative cover) and not woody encroachment that leads to regional-scale declines in groundwater recharge and stream flow.

- *Effects of Selective Brush Management on Water Quantity and Quality in the Honey Creek State Natural Area, Comal County, Texas*, Philip Wright (USDA), Richard Slattery (USGS), George Ozuna (USGS), c 2009.

Based on brush management/water related studies in the 1990's that demonstrated possible benefits of woody vegetation removal correlating with increased spring flow and stream flow measured at several demonstration project sites, this study was initiated to do a side-by-side comparison of two watersheds, one with an area of 230 acres and the other 358 acres in size. Numerous stream flow, rainfall, and evapotranspiration gages were installed within this area to monitor watershed conditions.

Comment acknowledged yet not addressed. The purpose of the literature review was to guide the analysis and formulate a study methodology.

21. *Effects of Brush Management on Water Resources*, C. Allan Jones and Lucas Gregory, Texas Water Resources Institute, Texas A&M AgriLife, Texas Water Resources Institute Technical Report, November 2008.

Comment acknowledged yet not addressed.

22. *Uncertainty in evapotranspiration from land surface modeling, remote sensing, and GRACE satellites*, Di Long, Laurent Longuevergne and Bridget R. Scanlon, Water Resources Research, Volume 50, Issue 2, February 2014.
doi.org/10.1002/2013WR014581.

Comment acknowledged and addressed

23. *Untenable nonstationarity: An assessment of the fitness for purpose of trend tests in hydrology*, Francesco Serinaldi, Chris G. Kilsbya, Federico Lombardoc, *Advances in Water Resources* 111 (2018) 132–155.

Comment acknowledged and addressed

24. *A new indicator framework for quantifying the intensity of the terrestrial water cycle.* Thomas G. Huntington, Peter K. Weiskel, David M. Wolock, Gregory J. McCabe, Journal of Hydrology Volume 559, April 2018, Pages 361-372. doi.org/10.1016/j.jhydrol.2018.02.048

Comment acknowledged yet not addressed

25. Pages 3-8 to 3-11, Figures 3.3 to 3.6. The legend abbreviations are not explained.

Comment acknowledged and addressed

26. Section 3.2, Pages 3-3: The use of Mann-Kendall test in this study is commended. However, it should be noted that Mann-Kendall is a screen test and is not conclusive without finding a physical driver to the trend (Serinaldi, 2018). Furthermore, the comparison of S to 1 is not an accepted threshold rather when the absolute value of S is small, no trend is indicated. The null hypothesis of no trend is rejected when S (and therefore Kendall' τ) are significantly different from zero ([EPA 2016](#)) and ([Helsel and Hirsch, 2002](#)). Significantly different from zero can be subjective.

Comment acknowledged and addressed

27. Section 3.2. In presenting the Mann-Kendall test, it is useful to describe the null hypothesis, and the criteria for significance upfront. The statistic S depends on sample size n and use of S for depicting trend is often misleading because of this. Alternatively, the statistic Z is more commonly used. Also, it is more conventional to present the p-value than the "significance" measure. Please consider using Sen's slope to characterize the magnitude of the trend of normalized variables.

Comment acknowledged and addressed. Sen's Slope was not used for the majority of the report as quantified trends were not desired.

28. Section 3.3.3 Site #2 – South Concho at Carlsbad, Page 3-8, first paragraph: In describing Figure 3.4 on the following page, it should be noted that the large difference in cumulative observed flow and cumulative naturalized flow after 2001 is almost entirely due to a gap in the observed streamflow from 1995 to 2001. Please discuss the possible implications of the data gap on results.

Comment acknowledged and addressed

29. Section 3.3.4 Site #6 – San Saba at San Saba, Page 3-9, first paragraph: In describing Figure 3.5 on the following page, it should be noted that the large difference in cumulative observed flow and cumulative naturalized flow after 1997 is at least partially

due to a gap in the observed streamflow from 1993 to 1997. Please discuss the possible implications of the data gap on results.

Comment acknowledged and addressed

30. Section 3.4.2 Temperatures for Sterling City, TX, Page 5-35, second paragraph: The authors state “The trend is not strong, yet it does suggest a general warming of the area.” Based on Figure 5.22B, it appears the statement should be “The trend is not strong, yet it does suggest a general cooling of the area.” Please revise this section as needed.

Comment acknowledged and addressed

31. Section 3.4.2 Temperatures for Sterling City, TX, Page 5-37, third paragraph: The authors state “greater variation in year-to-year annual maximum temperatures is likely to occur.” Since forecasting of future events is beyond the scope of this study, this statement could more accurately be phrased as “greater variation in year-to-year annual maximum temperatures has occurred.” Please revise wording in this paragraph as needed.

Comment acknowledged and addressed

32. Section 4.1: It appears that the investigators relied on USGS topo maps as the basis for determining the number and total surface over the 1950s-60s. It is also stated that the maps of 1970 and 1980s were used. Please include a table of data sources be added prior to displaying Figs 4.6-4.9. In addition, can the rising trend be simply a consequence of differences in sources? Using manually made topo map along with satellite images available only from recent two decades is an inherently risky proposition. It is understood that there are perhaps no better alternatives, but the caveat must be noted in the report.

Comment acknowledged and partially addressed. Data sources were obtained from TNRIS and cited as such. 149 individual USGS quadrangle maps were reviewed, with portions of each map spanning portions of one or more of the study area watersheds. This was noted in the text, but a list of the individual map names was not provided. A caveat was included in the text, as requested.

33. Page 4-14 and Section 4.3. First sentence. Omit the phrase ‘into the Highland Lakes.’ The Highland Lakes are not the subject of this phase II report. Three of the four focus areas are upstream of O.H. Ivie, which is not part of the Highland Lakes chain. Please use “subject watersheds” instead.

Comment acknowledged and addressed

34. Section 4.1.1, National Hydrography Dataset (NHD). The “NHD_Waterbodies” dataset includes both naturally and artificially formed, as well as on-channel impoundments and some impoundments that would be considered by TCEQ to be off-channel impoundments. The text should specifically state that natural lakes/ponds were not excluded from the analysis. Further, at this point in the process, off-channel reservoirs should have been identified so they could be treated separately in the determination of any impacts from impoundments. Finally, if the Google Earth Imagery used to estimate surface area was from a very wet year, the surface area of the ponds could be overstated.

Comment acknowledged and addressed. LRE disagrees that using Google Earth Imagery from wet years leads to overstating pond surface areas. Inundation during wet years is indicative of the true storage capacity of each pond, which directly affects the pond’s impact on streamflow. This principle is clarified in the text.

35. Page 4-3, first paragraph: Include the source and the year of the base map aerial land surface image obtained from the ArcGIS system software in the text.

Comment acknowledged. The ArcGIS software does not provide a specific citation for its basemap images, yet provides a list of sources from which the images may have been obtained. It also does not provide any indication of the data on which the image was taken. The image used in Figure 4-1 and Figure 4-4 was used only for illustrative purposes, and was not used to determine creation dates of the identified small ponds. Proper citations are not available for these images, yet the source of the images (ArcGIS online basemaps) is provided.

36. Section 4.2, Small Impoundment Results, Page 4-9, first paragraph: The investigators noted that the equation used in the Colorado Basin Water Availability Model (WAM) was used to estimate the storage capacity of the small ponds. However, the multiplier coefficient used in Eq. 4-1 (0.991) is not consistent with the values used in the WAM. The correct multiplier for the storage area relationship is 0.911.

Comment acknowledged and addressed, and results were updated throughout the report.

37. Section 4.3: Please clarify what LANDSAT “terrain images” are. Also, please provide all metadata for LANDSAT images analyzed in this study. At minimum, a table with LANDSAT version, year of acquisition, and the bands analyzed must be included.

Comment acknowledged yet not addressed as requested. LANDSAT data were obtained through GEE, and were cited as such in the text. The available data showed biweekly land images from 1986-2019 and is too numerous to reference in a table.

38. Section 4.3, Noxious Brush and Land Use Analysis, Page 4-14, third paragraph: The text should describe in more detail the source(s) of the land use/land cover dataset and the processing methodology used in the study. The author noted that the gridded land use/land cover data from 1938-2017 (Sohl et al., 2018) was obtained from www.siencebase.gov. However, the referenced data source (i.e., Sohl et al., 2018) contains the “modeled historical land use and land cover for the conterminous United States: 1938 – 1992”. The link provided in the text provides another dataset entitled “Conterminous United States Land Cover Projections - 1992 to 2100”.

Comment acknowledged and addressed

39. 4.3 Noxious Brush & Land Use Analysis. Page 4-14, paragraph that carries over to next page: Text states that for computing watershed-wide runoff curve numbers, all portions of the study area were classified as part of “Soil Group D.” That classification appears consistent with Figure 4-11, on page 4-16, for two portions of the study area but inconsistent for the other two. Figure 4-11 appears to show very little Soil Group D in the Elm Creek watershed. The North Concho watershed, again from Figure 4-11, appears to show fairly large amounts of soil groups other than Group D. Perhaps, the classification is not particularly important for the results, but further discussion/justification would be helpful.

Comment acknowledged and addressed

40. Section 4.3, Noxious Brush & Land Use Analysis, Page 4-14, last paragraph: Provide some statistics or text in the report to support the assumption of choosing Soil Hydrologic Group D as the representative soil type for all study watersheds. The author noted that this assumption is well supported by soil hydrologic group data from the National Resources Conservation Service (NRCS) shown in Figure 4.11. However, Figure 4.11 shows that most of the soils within the Elm Creek watershed are Soil Hydrologic Groups B and C.

Comment acknowledged and addressed

41. Section 4.3, page 4-15: Please describe the methodology adopted to obtain a different curve number (CN) each year. CNs are typically not revised on an annual basis. Therefore, please provide the tabular data showing what these annual CNs are. Also, please provide information on which CNs, or combination of CNs, were used to represent each watershed. Please provide a table with the CNs associated with each land cover/land use type in each watershed.

Comment acknowledged and addressed

42. Section 5, Task 3 – Temperature Trend Analysis, Page 5-2, first paragraph: The investigators note that the TSTool software was used to obtain the temperature time series for this study. As described by the author, the TSTool compiles available time series from a variety of sources, such as NRCS and USGS. The report should include an appendix listing information for the weather stations used in the analysis, such as the name of the station, latitude and longitude, and a period of data availability.

Comment acknowledged and addressed

43. Section 5 and Section 7: Please provide actual data source citations instead of stating that the data were downloaded from TSTool. TsTools is just a tool, like NASA's Mirador or the IRI Data Library, which are portals for data access, manipulation, and download, but not a data source.

Comment acknowledged and addressed

44. Section 5.1.1 Temperatures for Ballinger, TX, Page 5-3, first Paragraph: Based on Figure 5.2, it appears that April should also be included with the months when daily high temperatures occasionally exceeded 100°F. It also appears that September should be removed from the list of months when daily low temperatures were occasionally below 32°F.

Comment acknowledged and addressed

45. Page 5-10 Section 5.1.2. Visual inspection of Figure 5.7 does not support the trend hypothesis. It appears that outliers may be driving the trend conclusion. The existence of a 'gradient' may be anomalous. Please check the data for the presence of outliers and remove any such outliers before undertaking the trend test.

Comment acknowledged and addressed

46. 5.3.1 Temperatures for San Angelo, TX, Page 5-25, first paragraph: The text indicates that temperature data were compiled from numerous sites in order to create a single record. Based on fairly large differences that exist periodically for temperature gages in Austin, at Camp Mabry versus Austin-Bergstrom Airport, the potential may exist for this type of compilation to skew the data enough to affect the statistical analyses undertaken. At any rate, it would be helpful to have some discussion of whether that potential has been accounted for.

Comment acknowledged and addressed

47. 5.4.1 Temperatures for Big Spring, TX, Page 5-31, first paragraph: The text indicates that temperature data were compiled from numerous sites in order to create a single record. Based on fairly large differences that exist periodically for temperature gages in Austin, at Camp Mabry versus Austin-Bergstrom Airport, the potential may exist for this type of compilation to skew the data enough to affect the statistical analyses undertaken. At any rate, it would be helpful to have some discussion of whether that potential has been accounted for.

Comment acknowledged and addressed

48. 5.4.2 Temperatures for Sterling City, TX, Page 5-35, last paragraph: The last sentence on the page references a warming trend. However, that the discussion preceding that sentence does not appear to provide any support for concluding that a warming trend is seen. In addition, the period of record at this location is much shorter than for most other locations. That may or may not be important, but seems like it would be good to acknowledge it and explain its significance, if any.

Comment acknowledged and addressed

49. Section 6.1, North Concho Watershed Flow Analysis, Page 6-43, first paragraph 1: Correct the USGS Station number from “08314000” to “08134000” in all instances that is appears in the report.

Comment acknowledged and addressed

50. Section 6.2, South Concho Watershed, Page 6-46, first paragraph: According to the “Water-Year Summary” information for USGS Gage 08128000 (available at <https://waterdata.usgs.gov/nwis/>), the streamflow measured at USGS gaging station 08128000 is affected to an unknown degree by diversions to the South Concho Irrigation Company canal 800 feet upstream from the station. The report should include text explaining how these diversions might have an impact, if any, on the streamflow trend analysis for the South Concho Watershed.

Comment acknowledged and not addressed. Streamflow data was compiled during Phase I and re-used herein.

51. Section 6.3, Elm Creek Watershed, Page 6-47, first paragraph:

- Correct the name of the USGS Gage from “Elm Ck at Ballingerl, TX” to “Elm Ck at Ballinger, TX” in all instances that is appears in the report.
- According to the “Water-Year Summary” information for USGS Gage 08127000 (available at <https://waterdata.usgs.gov/nwis/>), at least 10 percent of the

contributing drainage area has been regulated by New Lake Winters. The report should include text explaining how these diversions might have an impact, if any, on the streamflow trend analysis for the Elm Creek Watershed.

Comments acknowledged and addressed

52. Section 6.3: Elm Creek Watershed, Page 6-48, first full paragraph (immediately below Figure 6.7): The statement indicating that the Mann-Kendall analysis may be misleading because of a recent trend, raises questions about the value of the conclusions drawn from other applications of that same analysis for other data in the report. At any rate, it would be helpful to have some discussion about what needs to be considered in applying the analysis in light of varying periods-of-record, trends over time, and the like.

Comments acknowledged and addressed

53. Section 6.3, Elm Creek Watershed, Page 6-48, last paragraph: The author noted that “Figure 6.8 indicates that annual flows within Elm Creek are driven mostly by surface runoff resulting from precipitation events, yet with a groundwater contribution provided as baseflow local recharge is sufficient”. The report should include text explaining in more detail how the above statement is supported from the information provided in Figure 6.8. Specifically, describe how groundwater contribution to baseflow was inferred based on the annual flows at USGS Gage 08127000.

Comments acknowledged and addressed

54. Section 6.4.2, Brady Creek at Brady, Page 6-51: According to the “Water-Year Summary” information for USGS Gage 08145000 (available at <https://waterdata.usgs.gov/nwis>), the flow measured at this station is affected at times by discharge from the flood-detention pools of flood-retarding structures above the station. The report should include text explaining how these diversions might have an impact, if any, on the streamflow trend analysis for the San Saba Watershed.

Comment acknowledged and not addressed. Streamflow data was compiled during Phase I and re-used herein.

55. Section 6.4.2 Brady Creek at Brady, Page 6-52, first paragraph: The last sentence of the paragraph is confusing. It appears to be intended to say something like “the creek has not experienced year-round flow in any year since 1941.” Please reword the last sentence of the paragraph to clearly convey its intended meaning.

Comments acknowledged and addressed

56. Section 6.4.3, San Saba River at San Saba, Page 6-54, first paragraph: According to the “Water-Year Summary” information for USGS Gage 08146000 (available at <https://waterdata.usgs.gov/nwis>), the flow measured at this station has been affected by the Brady Creek Reservoir since 1963. The report should include text explaining how operation of Brady Creek Reservoir might have an impact, if any, on the streamflow trend analysis for the San Saba Watershed at USGS Gage 08146000.

Comments acknowledged and addressed

57. Section 7, Task 5 – Precipitation Trend Analysis: One of the objectives of the precipitation trend analysis is to identify trends and determine “change point” in time when significant precipitation changes occurred. However, no information about “change point” are provided for any of the study watersheds. The report should include more detail on the determination of the “change point”.

Comments acknowledged and not addressed – change points were not identifiable

58. Section 7, Task 5 – Precipitation Trend Analysis, Page 7-58, second paragraph: The report should include an appendix listing information for the weather stations used in the analysis, such as the name of the station, latitude and longitude, and a period of data availability.

Comments acknowledged and addressed

59. Section 7, sub-section 7.1.1. page 7-60, third paragraph: State what threshold (i.e., 0”, .01”, .05”) was used for minimum precipitation to count in days of no rain.

Comments acknowledged and addressed

60. 7.3.1 Ballinger, Page 7-71, first paragraph: This is another example of widely varying periods-of-record. Here the variation is in the precipitation record. Although the longer period likely provides additional insights, the difference in the period may confound comparisons across locations. Again, perhaps some discussion of the significance of the variations would be useful.

Comments acknowledged and addressed

61. 7.3.3 Elm Creek Watershed Precipitation Summary & Comparison, Page 7-74, first paragraph: The second sentence provides a comparison of precipitation trends at two locations with very different periods-of-record. As noted above, this would appear to raise questions about whether the difference in period could be affecting the result. In

addition, the record for the City of Abilene is compiled from multiple locations, see text on page 7-73, which also would seem to create the potential to skew the data. Some discussion of whether that potential exists would be helpful.

Comments acknowledged and addressed

62. Section 7, sub-section 7.4.3 San Saba, Page 7-78, first paragraph: The investigators statement that “the significance value computed for this trend is just under the value (1) indicating the trend is strong” could be confused to mean the trend is strong. For clarity, suggest rewording to “the significance value computed for this trend is just under the value of one (1), indicating the trend is not significant”.

Comments acknowledged and addressed

63. Section 7, sub-section 7.4.3 San Saba, Page 7-78: The second to last sentence is missing the word ‘not’ which substantially changes the meaning.

- Please revise this sentence to read as: “The Mann-Kendall analysis of the number of rainy days per year for San Saba (Figure 7.12C) indicates an increasing trend, yet the significance value computed for this trend is just under the value (1) indicating the trend is not strong.”

Comments acknowledged and addressed

64. Section 8, Task 6 – Soil Moisture Data Analysis, Page 8-80, first paragraph: Clarify the data sources used for the soil moisture trend analysis. The author noted that the soil moisture data are from two sources, including 1) The Gravity Recovery and Climate Experiment (GRACE), and 2) The North American Land Data Assimilation System. However, in Section 8.2, Page 8-1, second sentence, the author stated that the Global Land Data Assimilation System (GLDAS) was the second source for soil moisture data used in the study. According to <https://ldas.gsfc.nasa.gov/>, the GLDAS and NLDAS are two different datasets with different assumptions.

Comment acknowledged and addressed

65. Section 8.1, GRACE Data Analysis, Page 8-80, third paragraph, Sentence 2: The text should describe in more detail how the soil moisture data for Ballinger, TX, was calculated. More specifically, how were the data points shown in Figure 8.1 used to calculate the soil moisture? In Figure 8.1, there are multiple GRACE data points within the boundary of the watersheds, but it is not clear whether the average of multiple data points or a single data point was used to calculate the soil moisture data shown in Figure 8.2.

Comment acknowledged and addressed

66. Section 8.1, GRACE Data Analysis, Page 8-80 and 8-81: Per the analysis by Di Long referenced above, the GRACE data water balance for the Colorado basin is poor. Given the uncertainty in partitioning out soil moisture data from an already poor source, the analysis using GRACE data is likely spurious. Therefore, please include a discussion addressing the uncertainty inherent in soil moisture data from GRACE.

Comment acknowledged and addressed

67. Section 8.1, page 8-80: Strictly speaking, the GRACE retrieval does not characterize “soil moisture”. It is a vertically integrated measure of water content that encompasses groundwater (deep and shallow), soil moisture, and surface water storage, although one could argue that the higher frequency fluctuation is due to changes in soil moisture alone. Please note these facts in the introductory paragraphs.

Comment acknowledged and addressed

68. Section 8.2. page 8-1. The purpose of choosing the five cases (points of interest) in the time series of rainfall and GRACE “soil moisture” in Fig. 8.2 needs to be more specific. It is hard to see what the takeaways are from the cases. Moreover, some of the assertions need to be supported by literature or at least anecdotal evidence.

For example, it is stated “the lack of replenishment is that the land was so dry the surface water runoff was simply unable to penetrate into the ground prior to flowing down gradient and into Elm Creek”. Please provide the scientific basis for this statement. In the Western United States, there has been research showing that the land surface forms a thin crust after prolonged drought, and this crust slows down infiltration (Belnap 2006). However, the degree of impact on a watershed scale was never clearly demonstrated. Therefore, please provide citations to back-up assertions made or omit such statements from the final report.

Comment acknowledged and addressed

69. Section 8.2, Google Earth Engine (GEE) Analysis, Page 8-2, first paragraph: Include more information in the text describing how the GLDAS 2.0 and 2.1 databases were used in the study. Include in the discussion whether the outcome of the analysis was affected by combining data from the two datasets. According to the description of the databases (available at <https://disc.gsfc.nasa.gov/>), the GLDAS 2.0 is forced with Princeton meteorological forcing data set from 1948-2000 on a monthly basis with 0.25*0.25-degree spatial resolution. The GLDAS 2.1, however, is forced with a combination of model and observation-based forcing data from 2000 to present using the conditions from the GLDAS 2.0 simulation as the starting point.

Comment acknowledged and addressed

70. Section 8.2, Google Earth Engine (GEE) Analysis, Page 8-3, carry-over paragraph from previous page: The first full sentence references the potential for reservoir seepage to be affecting soil moisture. Because, as noted in the discussion, the reservoir levels are consistently quite low, it seems unlikely that seepage would be affecting soil moisture at the relatively shallow depths reflected in the soil moisture analyses. Please include a discussion of the likelihood of the potential mechanism driving such impacts.

Comment acknowledged and addressed

71. Section 9: This chapter has not adequately addressed Task 7 in the contracted scope of work, which states: “Groundwater Level Evaluations, *LRE will perform the following analyses, using available TWDB databases including submitted drillers reports. Activities will include: 1) mapping wells in the study area, including possible 3-D mapping of the wells, water levels, and terrain/surface water features, 2) Documenting well properties, water level elevations, and trends, and 3) compiling available data on historical and permitted pumping quantities. Efforts under this task may also be used to address the extent to which surface water and groundwater systems are connected within the study area watershed.*

Please include groundwater level maps (aka groundwater table/piezometric surface contour maps) at different times (i.e., every 10 or 20 years) to determine if there is a regional groundwater level decline (or increase). Please also include a compilation of historical groundwater pumping quantities, based on the TWDB groundwater usage record, and assess the correlation between historical groundwater pumping and streamflow, particularly base flow.

Comment acknowledged and addressed

72. Please include a discussion of why baseflow trends are not addressed in this report.

Comment acknowledged and addressed. Baseflow analysis was not included in the scope of work. LRE Water included the analysis in this final report as it provided valuable insight with regard to groundwater-surface water interaction.

73. Section 9, page 9-4, please explain why only wells within 150 feet depth were selected. Why were wells at all depths not selected? It would be good to check on the level of the groundwater table and select wells that have a hydraulic linkage to the groundwater table. If the hydraulic linkage is not known, the selected wells should be divided by aquifer. Please include a description of the geology and aquifer characteristics of the study area.

Comment acknowledged and addressed

74. Why were only wells within one mile from the flow line selected? Please include a description of the physical basis for such limited the spatial range from which wells were selected for the study. In the long term, any wells causing a drop in the groundwater table can contribute streamflow depletion, if the well taps into the same aquifer. Please refer to the Texas Aquifer Study (http://www.twdb.texas.gov/groundwater/docs/studies/TexasAquifersStudy_2016.pdf?d=1564425776903), and include a discussion from this report on whether there is a regional groundwater level decline identified for the study area over the period 2010–2015.

Comment acknowledged and addressed

75. Section 9 and Appendix 15: If the soil-water-balance (SWB) modeling effort was undertaken to complement the study, please include its findings in the main text of the report. Currently, the results from Section 8 and Appendix 15 appear to be contradictory. The discussion in Appendix 15 (pdf page 169), indicates that the groundwater recharge rate was increasing, coupled with a decrease in soil moisture. This could imply an increased loss of surface water to groundwater. Please include a discussion of how the results in SWB complement the findings of the main study and discuss why the findings report in Section 9 may seem contradictory to the findings reported in Appendix 15.

Comment acknowledged and addressed

76. Section 10.1. The mechanisms for UCWBM need to be clarified. It appears that the model is for continuous simulation. If so, what is the time step for the model run, and how is soil moisture variation accounted during dry periods? Is Curve Number allowed to vary over time? The model seems to assume no leakage of the water stored in pond to infiltration, and this needs to be explicitly stated.

Comment acknowledged and addressed

77. Page 10-12, Section 10.2.2. The last sentence incorrectly lists 16% as the decrease in runoff while elsewhere it is correctly listed as 29%. Please resolve this discrepancy.

Comment acknowledged and addressed

78. Section 10.2.3 UCWBM results for the North Concho Watershed, Page 10-14, third paragraph: The last sentence in the paragraph attributes the differences in simulated runoff as reflecting the change in curve numbers. However, as acknowledged in the

discussion that follows, that attribution seems potentially unfounded. It may be appropriate to more explicitly qualify the conclusion based on the result that seems counter to the SCS curve, unless further information is available to support it.

Comment acknowledged and addressed

79. 10.2.4 UCWBM results for the South Concho Watershed, Page 10-16, entire section: As for the previous section, the modeling result seems contrary to the SCS curve. Accordingly, it may be appropriate to more explicitly qualify the conclusion based on the result that seems counter to the SCS curve, unless further information is available to support it.

Comment acknowledged and addressed

80. Section 11, Page 11-18, Conclusion 3: None of the reported analysis appears to have been done on an event basis. This may need to be restated to agree with the work performed.

Comment acknowledged and addressed.

81. Section 11, Page 11-18, Conclusion 5: Please revise and clarify this conclusion after addressing review comment number.....

Comment acknowledged and addressed

82. Section 11 Summary and Conclusions, Page 11-18, General Conclusion 8: The referenced result appears to be intended to refer to annual precipitation and likely should be qualified accordingly.

Comment acknowledged and addressed

83. Section 11, Page 11-19, Conclusions 11 and 12 appear contradictory. Please address this discrepancy in the final report.

Comment acknowledged and addressed

84. Section 11 Summary and Conclusions, Page 11-19, General Conclusion 13: Based on the extremely limited well level data available, the conclusion statement appears to be overbroad. It does not appear that the available data are adequate to support a conclusion that groundwater withdrawals are not a significant source of flow depletion. That statement seems to go significantly beyond the discussion found on page 9-6 of the report: "therefore the true impact of these wells on the local stream system cannot accurately be deduced." It likely would be more accurate to say that the limited data

available are not sufficient to reach a conclusion on whether groundwater withdrawals are a significant source of streamflow loss.

Please replace conclusion 13 with the following text in the final report:

“The inability to identify and quantify the impacts of unregistered domestic and livestock wells in the study area made it impossible to realistically assess the potential impacts of groundwater pumping on streamflow in the study area.”

Comment acknowledged and addressed through a revised discussion of groundwater impacts on streamflow.

85. Section 11 Summary and Conclusions, Page 11-19, UCWBM modeling conclusion 4: As noted above, there appears to be significant question about the modeling results for these watersheds because of the unexplained effect of the SCS curve. Accordingly, any conclusion stated should acknowledge that uncertainty. The conclusion seems to overstate the justifiable confidence in the results.

Comment acknowledged and addressed

86. Section 11 Summary and Conclusions, Page 11-20, Theory 3: As noted in the report, the data were not sufficient to allow drawing any conclusions about the extent of noxious brush: "However we were unable to distinguish noxious brush (such as mesquite) from other vegetation." (Section 4-3 on page 4-14.) Accordingly, this theory, attributing flow reduction to noxious brush, does not appear to be supported by the data presented and likely should be qualified accordingly.

Comment acknowledged and addressed

87. Section 11 Summary and Conclusions, Page 11-20, Theory 4: Although stated with more qualification than Theory 3, this theory also seems to suffer from a lack of data showing an increase in noxious brush.

Comment acknowledged and addressed

88. Section 12, Page 12-20, Recommendation 2a. Omit the phrase “upstream of the Highland Lakes”. The Highland Lakes are not the subject of this phase II report. Three of the four focus areas are upstream of O.H. Ivie, which is not part of the Highland Lakes chain. Please use “subject watersheds” instead.

Comment acknowledged and addressed

89. Section 12, Page 12-20: Please add in the following recommendation:

“Additional analyses focusing on identifying and quantifying the potential impacts of groundwater pumping within the eight (8) groundwater conservation districts located within the study area and within Groundwater Management Area 7.”

Comment acknowledged and addressed within the revised groundwater analysis chapter.

90. The page numbering in the report should be corrected. There are inconsistencies in the page numbering format in different sections. For example:
- Section 1 (Executive Summary) starts from page 1-16 instead of 1-1 or 1.
 - In Sections 2 to 5, page numbering starts from 1 at the beginning of each section, which is different from the format used in other sections. For example:
 - i. Section 1 (Executive Summary) starts from page 1-16 instead of 1-1 or 1.
 - ii. Section 6 (Task 4- Streamflow Trend Analysis) starts from page 6-41. Also, part of the last paragraph of Section 5.5 is in the page number 6-41.
 - iii. Section 7 (Task 5- Precipitation Trend Analysis) starts from page 7-58.
 - iv. Similar comment for Sections 8, 9, 10, 11, 12, and 13.
 - Section 8 (Task 6- Soil Moisture Data Analysis) starts from 8-80. However, the page number changes to 8-1 two pages later. Moreover, there are two pages with the same number (8-1) in Section 8.

Comment acknowledged and addressed

91. Section 3, Task 1 Literature Review, Page 3-1: Please complete the sentence in this section or remove the incomplete sentence from the report.

Comment acknowledged and addressed

92. Please remove “TX” after all place names in the report (e.g., “Winters, TX” should be “Winters”).

Comment acknowledged and addressed

93. Page iv: Please sort abbreviations on from A–Z.

Comment acknowledged and addressed

Figures and Tables Comments:

1. Figures 2.1, 2.2, 2.3, and 2.4: Please provide detailed legends that are self-explanatory. Currently, it is not clear what these figures convey. Please also clarify what the “drought conditions” refer to.

Comment acknowledged and addressed

2. Figures throughout the report (e.g., All figures in Section 3.3, Pages 3- 7 through 3-10, and Section 15 Appendices): The numbering scheme used in the figure captions do not match the numbering scheme referred to in the text. Please make the appropriate corrections.

Comment acknowledged and addressed

3. There are multiple parts of the report where the text refers to a wrong Figure or Table, which makes it difficult to follow the discussion of the results. For example:
 - a. Section 3.3.5, Elm Creek @ Ballinger, Page 3-10, Paragraph 1:
 - “Figure 3” should be changed to “Figure 3.6”.
 - b. Section 5.12, Temperature for Abilene, TX, Page 5-7, There are several instances on this page where the cited figure has a combined reference, for example Figure 5.5Figure5.2.

Comment acknowledged and addressed

4. Figure 4.11, Page 4-16: Include the year of the data in the Figure caption.

Comment acknowledged and addressed

5. Figure 4.12, Page 4-17: Describe in the caption or the text what is meant by “weighted Curve Number” on the vertical axis.
 - Revise the figure so that the data and numbers are within the frame of the plot.

Comment acknowledged and addressed

6. Figure 4.13: Please change this to a line graph.

Comment acknowledged and addressed

7. Figure 5.1, Page 5-1: The figure would be clearer if a different shape was used for each station shown on the map. It is difficult to identify the location of the stations based on the colors assigned to the stations.

- Was any data from the stations with a short period of record used in the analysis? If yes, explain in the text and figure caption. If data from those stations was not used, remove them from the Figure as they were not part of the study.

Sub-Comment acknowledged and addressed. Un-used stations were not removed from the figures as they provide some insight into other available data within the study areas, and could thus prove to be a useful reference for future efforts. Text was adjusted to provide an explanation.

8. Fig 5.1 The map is cut-off from the margin. Please rescale figure.

Comment acknowledged and addressed

9. Fig 5.17, 5.20. Please expand the upper bound of y axis so that no points fall out of the window. Please explain why Fig. 5.1 follows 5.17?

Comment acknowledged and addressed

10. Table 5-6 See early comments on Mann-Kendall test. Ditto for other tables with Mann-Kendall statistics.

Comment acknowledged and addressed

11. Figure 6.1, Page 6-41: The figure would be clearer if a different shape was used for each station shown on the map. It is difficult to identify the location of the stations based on the colors assigned to the stations.

- Try to get the caption to be on the same page with the figure

Comment acknowledged and addressed

12. Figure 6.4, Page 6-45: Define what is mean by “Potential Change Point” in the Figure caption. Figures should be self-explanatory.

Comment acknowledged and addressed

13. Figure 7.1, Page 7-59: The figure would be clearer if a different shape was used for each station shown on the map. It is difficult to identify the location of the stations based on the colors assigned to the stations.

Comment acknowledged and addressed

14. Figure 8.2 has “% GW Storage”, as the label for the y-axis; whereas soil moisture is stated in the caption. Please resolve these discrepancies.

Comment acknowledged and addressed

15. Figure 9.1, Page 9-5: A different color or line type (e.g., dashed and solid) could be used to show the minor and major streams in the study area.

Comment acknowledged and not addressed. Lines are different weights

16. Figure 9.2, Page 9-6: Include the water level units (ft above MSL) on the vertical axis.

Comment acknowledged and addressed

17. Please add in sub-figure letters (e.g., a, b, c, etc.) for all figures that have multiple panels.

Comment acknowledged and addressed

SUGGESTED CHANGES

Specific Draft Final Report Comments:

1. Executive Summary, Recommendations, Page 1-23 and Section 12 Recommendations, Page 12-20: The report summary (Section 11, Page 11-19) mentions that “Further analysis on domestic and livestock wells is warranted,” but this was not a recommendation for further study. Consider including a recommendation for further investigation of surface water-groundwater interactions and potential impact of groundwater consumption from domestic and livestock wells, especially in watersheds where groundwater baseflow is expected to play an important role.

Comment acknowledged and addressed

2. Consider including a discussion on your vision as to how the Colorado-Lavaca Basin and Bay Area Stakeholder Committee could utilize the information presented in this report to validate or refine the environmental flow standards or identify strategies to achieve environmental flows.
3. It may be worth noting that jumps on the cumulative mass plot for observed and naturalized flow of the North Concho River near Carlsbad (Section 3.3.2, Figure 3.3, page 3-8) correspond to large flood events. Large jumps on the graph in 1948, 1957,

1974, 1986, and 2015 correspond to peak flows as listed by the USGS for this site (https://nwis.waterdata.usgs.gov/tx/nwis/peak?site_no=08134000&agency_cd=USGS&format=html).

Comment acknowledged and addressed

4. Unless there is some significant reason to do otherwise, we recommend discussing the watersheds/study sites in the same order in each section of the report. In the draft report, they are discussed in different orders in each section. For example, in Section 3.3.1 Revision & Updating of Phase 1 Results, they are discussed in the following order: Site #1, #2, #6, and #7. In Section 4.2 Small Impoundment Results, they are discussed in this order: Site #7, #6, #1, and #2. In Section 5 Task 3 – Temperature Trend Analysis, they are discussed in this order: Site #7, #6, #2, and #1.

Comment acknowledged and addressed

5. The rainfall datasets used for SWB differ from those used in the main analysis. On that note, the use of the PRISM rainfall dataset in the SWB analysis is commended because this is a quality-controlled dataset that is suitable for research studies. Given that the PRISM dataset is a gridded dataset, it would have been better suited for addressing spatial variability in precipitation that were mentioned in Section 7.

Comment acknowledged and addressed. PRISM is only available from 1981-Present and therefore does not cover the desired 1940-2016 period of record for this analysis.

6. Section 8.2, page 8-3: The accuracy of GLDAS soil moisture data at least for the period prior to 1980 was never substantiated in the literature. Note the GLDAS was driven by a forcing data set (Sheffield et al. 2006) partially based on the NCEP reanalysis (GFS reanalysis); the reanalysis was produced on a coarse grid mesh (2-dg) and the model did not have a full-fledged land surface component. Though the data set underwent correction using the CRU analysis, it is doubtful that the fidelity of the dataset is high enough to allow a proper depiction of trends in the precipitation and soil moisture on a watershed scale. To the credit of the authors, this is acknowledged in the report. But I suggest the authors perform comparisons between the GLDAS precipitation data set and the gauge data as shown in Fig. 7.10 to rule out the role of changing bias characteristics in the sharp expansion of range in SM as shown in Fig. 8.4.

Comment acknowledged and not addressed. The proposed analysis is outside the scope of work of this project

- Pages 10-7 to 10-12, Section 10. The novel UCWBM model should be independently reviewed. It is more common to use a dynamical model such as VIC for this sort of analysis.

Comment acknowledged and addressed. Insufficient spatially and temporally varying data is available for building VIC models of the study area watersheds for the period 1940-2016. UCWBM source code has been provided to allow for independent review.

- Page 12-19, Section 12. Recommendation 1. While evaluation with a dynamic model seems like a logical next step, if undertaken it should not be using a novel model but rather with a standardized and accepted model like VIC or HEC-HMS. However, the performance of dynamical models of rainfall-runoff and streamflow ranges from poor to modest both in general and specifically to this region. It is likely that the modest trends to be investigated are smaller than the uncertainties of the models making them inconclusive even though effort can be substantial.

Comment acknowledged

- Page 12-20 and Section 12. Additional recommendation to further the precipitation and temperature trend screening analysis to include the phases of ENSO as a potential explanatory factor similar to seasonality.

Comment acknowledged and addressed

- When looking at a longer period of record a trend like the increasing minimum temperature at Eldorado disappears. Therefore, it would likely be good to qualify all these results as “apparent” trends because the tests are not conclusive.

Comment acknowledged and addressed

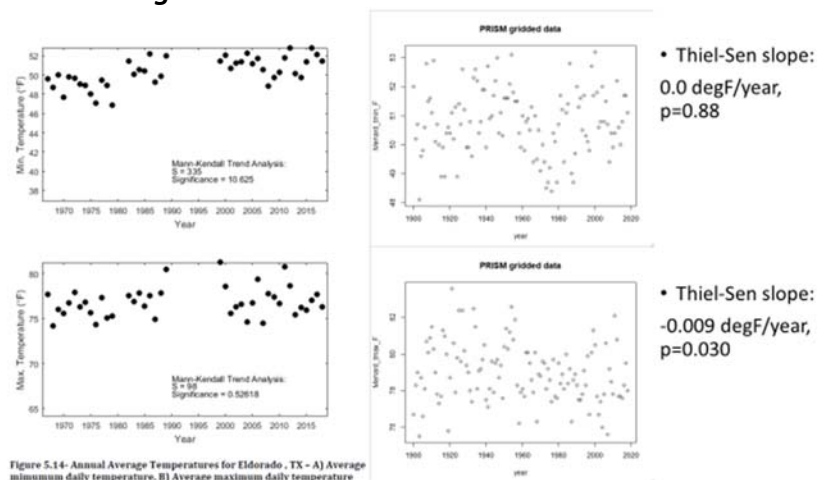


Figure 5.14- Annual Average Temperatures for Eldorado, TX - A) Average minimum daily temperature. B) Average maximum daily temperature

Comment acknowledged yet not addressed. TWDB required analyses limited to the 1940-2016 period of record if possible, and our methodology delineates the confidence we have in each trend assessment. Thiel-Sen slopes were not used as we did not attempt to quantify trends, but identify trends we consider to exist with a high degree of confidence.

Figures and Tables Comments:

1. Consider changing the shading on Figures 5.2, 5.5, 5.8, 5.12, 5-15, 5-18 and 5-21 to highlight seasons (Dec-Feb, Mar-May, Jun-Aug, Sep-Nov) used in this study rather than arbitrary blocks of three months.

Comment acknowledged and addressed